Designing broad-specificity, multi-subunit vaccines against enteric infections and studies on their immunogenicity and protective efficacy in animal models

A thesis submitted for the degree of Doctor of Philosophy (Science), of

Jadavpur University

2024

by

Risha Haldar, M.Sc.

Index No.: 75/22/Life Sc./27

Registration No. SLSBT1207522

Department of Life Science & Bio-technology
Jadavpur University
188, Raja S.C. Mallick Rd,
Kolkata - 700032.
India

CERTIFICATE FROM THE SUPERVISOR

This is to certify that the thesis entitled "**Designing broad-specificity, multi-subunit vaccines against enteric infections and studies on their immunogenicity and protective efficacy in animal models."** Submitted by ~~**Sri**~~ / Smt~~.~~ **Risha Haldar** who got ~~his~~ / her name registered on **2nd March on 2022, (Index No.: 75/22/Life Sc./27, Registration No. SLSBT1207522 Dated: 02.03.2022)** for the award of Ph. D. (Science) Degree of Jadavpur University, is absolutely based upon her own work under the supervision of **Dr. Santasabuj Das** and that neither this thesis nor any part of it has been submitted for either any degree / diploma or any other academic award anywhere before.

Santa Sabuj Das

……

Dr. Santasabuj Das
Scientist-G
Division of Clinical Medicine
ICMR-National Institute of Cholera and Enteric Diseases
Beliaghata, Kolkata-700010

सान्तासबुज दास, एस. डि.
SANTASABUJ DAS, M.D.
वैज्ञानिक (एफ) / Scientist (F)
आइ.सि.एम.आर. राष्ट्रीय कॉलरा और आंत्र रोग संस्थान
ICMR National Insurance of Cholera & Enteric Diseases
पी-३३,सी. आई. टी. रोड, स्कीम-७०एम, बेलियाघाटा, कोल-१०
P-33, CIT Road, Scheme-XM, Beliaghata, Kolkata-10
E-mail : santasabujdas@yahoo.com

DECLARATION

I do, hereby declare that the work embodied in the thesis entitled "**Designing broad-specificity, multi-subunit vaccines against enteric infections and studies on their immunogenicity and protective efficacy in animal models"** submitted for the award of Doctoral of Philosophy (Science) in Life Science and Biotechnology, is the completion of work carried put under the supervision of **Dr. Santasabuj Das, Scientist G** at the division of Clinical Medicine, ICMR-National Institute of Cholera and Enteric Diseases, Kolkata. Neither this thesis nor any part of it has been submitted for either any equivalent degree/diploma or any other academic award elsewhere.

.....

(Signature of the candidate)

Dedication

I dedicate my thesis to the almighty, my grandparents, my parents, and my family.

Acknowledgments

This work would not have been possible without the support and help of my supervisor, Ph.D. guide, Dr. Santasabuj Das. His unwavering enthusiasm, encouragement, and guidance have been my constant sources of inspiration. I am extremely thankful to Dr. Shanta Dutta, Director of the ICMR-National Institute of Cholera and Enteric Diseases (ICMR NICED), for allowing me to work at this cutting-edge research facility during my Ph.D. studies and conducting experimental research. I am very much thankful to the University Grant Commission (UGC), India, for providing me with the Ph.D. Fellowship throughout my tenure [UGC student ID-191620094970].

I would like to express my gratitude to Dr. Ashish Mukhopadhyay from ICMR NICED for his insightful advice, guidance, and support during our meetings as my research advisory committee. I am thankful to Dr. Hemanta Koley from ICMR NICED, for his immense support on animal experiments and Dr. Amlanjyoti Dhar from I3T Kolkata for his advice on protein purification techniques.

I would like to Acknowledge the Department of Biotechnology, Government of India and Japan Initiative for Global Research Network on Infectious Diseases (J-GRID), from Ministry of Education, Culture, Sport, Science and Technology in Japan and Japan Agency for Medical Research and Development (AMED), for funding my research work. I spcially thank Dr. Julian Parkhill of Welcome Trust Sangar Institute and Dr. Rupak Kumar Bhadra, CSIR-IICB for providing our lab with bacterial strains.

I am thankful to the Sabin Vaccine Institute, USA for their travel support during 13th International Conference on Typhoid & Other Invasive Salmonelloses, 2023 conferences in Kigali, Rwanda. I want to thank my past and present lab mates, namely, Dr. Pujarini Dutta, Dr, Sayan Das, Dr. Bhupesh Kumar Thakur, Dr. Rimi Chowdhury, Dr. Debayan Ganguli, Mrs. Suparna Chakraborty, Dr. Prolay Halder, Mr. Ananda Pal, Dr. Sneha Mitra, Mrs. Swarnali Chakraborty, Mr. George Banik, Mr. Sudip Dey, Mr. Sanjib Das, Dr. Soumalya Banerjee, Mr. Pritam Nandi, Dr. Jaya Verma, Dr. Lena Dhara, Mr. Udipto Sarkar, Ms. Sagarika Mali, Mr. Khokan Roy, Mr. Animesh Gope, Mrs. Sreya Banerjee, Dr. Tilti Nargis, Mr. Prosenjit Samanta, Dr. Bhaskar Mahanayak for providing all the help during my tenure. I want to thank Indian Council of Medical Research (ICMR) for providing all the facility to NICED, where I worked. I also want to thank Prof. Biswadip Das, Head of the Department (HOD), Department of Life Science and Biotechnology, Jadavpur University, for allowing me to register in the

department. I also want to thank other faculty members for delivering useful lectures in the Ph.D. course work classes.

I cannot thank enough to my mother and father for their endless love, patience, mental support, encouragement, and motivation. This venture would never have been completed without their breakthrough support and guidance.

My doctoral work has been an endeavour of passion, desire, and determination. I am immensely thankful to God for these blessings.

Date: 18.11.2024

Place: ICMR-NICED, Kolkata – 10.

Risha Haldar

UGC-Senior Research Fellow
Index No.: 75/22/Life Sc./27
Registration No. SLSBT1207522
ICMR- National Institute of Cholera and Enteric Disease
Jadavpur University

Abbreviations

µg	microgram
µL	microliter
ADH	Adipic acid dihydrazide
APC	Allophycocianin
ATCC	American Type Culture Collection
BCV	Bacteria containing vacuole
BMDC	Bone Marrow-derived Dendritic cell
Bp	Base Pair
BSA	Bovine Serum Albumin
CD	Circular Dichroism
CFU	Colony-forming units
CTAB	Cetyl Trimethyl Ammonim Bromide
CnBr	Cyanogen Bromide
DC	Dendritic Cells
DLS	Dynamic light scattering
EDAC	1-ethyl-3-(3-dimethylaminopropyl) carbodiimide hydrochloride
ELISA	Enzyme-linked immunosorbent assay
FPLC	Fast-performance liquid chromatography
FITC	Fluorescein isothiocyanate
FTIR	Fourier transform infrared spectroscopy
IFN-γ/β	Interferon gamma/ beta
IgG/A	Immunoglobulin G/A
IPTG	Isopropyl-ß-D-thiogalactopyranoside
IL	Interleukin
IM/ i.m.	Intramuscular
IN/ i.n.	Intranasal
in vitro	latin for within glass

in vivo	latin for within living
IPTG	Isopropyl β-D-Thiogalcopyranoside
Kb	Kilo base
kDa	Kilodalton
kg	Kilogram
L	Liter
LA	Luria Bertani Agar
LAL	Limulus Amebocyte Lysate
LB	Luria Bertani Broth
LD50	Lethal Dose 50%
LPS	Lipopolysaccharide
MES	2-(N-morpholino) ethanesulfonic acid
mg	milligram
mL	milliliter
NF-κB	Nuclear factor kappa-light-chain-enhancer of activated B cells
ng	nanogram
NMR	Nuclear Magnetic Resonance
NTS	Non Typhoidal Salmonella
OMP	Outer Membrane Protein
OSP	O specific polysaccharide
PAGE	Poly Acrylamide Gel Electrophoresis
PBS	Phosphate-buffered saline
PerCP	Peridinin Chlorophyll
pH	Negative logarithmic measure of hydrogen ion concentration
PVDF	Polyvinylidenedifluoride
SC/ s.c.	Subcutaneous
SCV	*Salmonella* Containing vacuole
SDS	Sodium Dodecyl Sulfate
SEM	Standard Error Mean

SPI	Salmonella Pathogenicity Island
T3SS/ TTSS	Type 3 Secretion System
TBS	Tris-Buffered Saline
TEMED	Tetra methyl ethylene diamine
Th1	Type 1 T helper
Th2	Type 2 T helper
TNF-α	Tumor necrosis factor alpha
TT	Tetanus Toxoid
Vi	Vi capsular Polysaccharide
WB	Western blot
WHO	World Health Organization

Symbols

%	Percentage
<	Less than
>	Greater than
°C	Degree Celsius
±	plus-minus
α	Alpha
β	Beta
γ	Gamma

Table of Contents

List of Figures

List of Tables

Abstract

Title of Thesis: "**Designing broad-specificity, multi-subunit vaccines against enteric infections and studies on their immunogenicity and protective efficacy in animal models**",

Submitted by: **Risha Haldar**, Index No.: **75/22/Life Sc./27**

Enteric fever poses global public health challenges due to low diagnostic yield, antibiotic resistance, and asymptomatic carrier states. Limited long-term efficacy of current typhoid vaccines, especially in smaller children, and non-availability of vaccines against other *Salmonella* serovars necessitate the development of a multivalent vaccine with wider coverage against *Salmonella* serovars. Currently licensed typhoidal vaccines include Vi-TT, Vi PS, and Ty21a, while *S.* Paratyphi, *S.* Typhimurium and *S.* Enteritidis vaccines are in clinical trials. Multivalent vaccines, such as Vi-protein conjugates co-formulated with OSP-protein conjugates are also under development. The development of multiple combined glycoconjugates is time-consuming and expensive. Here, we have developed glycoconjugates, comprising of O-specific polysaccharide (OSP) from *Salmonella* Typhimurium or Vi polysaccharide of *Citrobacter fruendii*, conjugated to outer membrane protein T2544 of *Salmonella* Typhi/ Paratyphi to provide a single vaccine formulation for typhoidal and non-typhoidal *Salmonella* serovars. We had earlier reported the immunogenicity and protective efficacy of recombinant T2544 of *Salmonella* Typhi in a mouse model, promoting robust induction of serum IgG, intestinal secretory IgA, and *Salmonella*-specific T cells and memory responses. BALB/c and C57BL/6 mice were immunized subcutaneously with the OSP-rT2544 on days 0, 14, and 28. Immunized mice were protected against *S.* Typhi, *S.* Paratyphi A and *S.* Typhimurium and cross-protected against *S.* Enteritidis. OSP-rT2544 immunization augmented serum IgG and intestinal sIgA responses, along with strong antibody recall response with higher avidity serum IgG against both OSP and T2544. Significantly raised SBA titers of both primary and recall antibodies were observed against different *Salmonella* serovars. Bacterial motility was inhibited by secretory antibodies, supporting their role in vaccine-induced protection. Finally, robust induction of T effector memory response indicates long-term efficacy of the candidate vaccine. For Vi-conjugate vaccine studies, BALB/c mice were immunized subcutaneously and intramuscularly with a single dose of Vi-rT2544 and its immunogenicity and protective efficacy were compared with Vi-TT. Vi-T2544 immunized mice protected against both *S.* Typhi and *S.* Paratyphi A, while Vi-TT was effective against *S.* Typhi alone. The candidate Vi-rT2544 vaccine elicited high titers of functional serum IgG antibodies and memory T and B cell response, underscored by the induction of higher avidity and titers of recall antibodies following a booster. Besides *Salmonella*, enteric infection of *Shigella* poses significant public health challenge in the developing world. However, lack of a widely available mouse model recapitulating human shigellosis necessitate the establishment of newer model for better understanding of disease pathogenesis and development of drugs and vaccines. To develop a *Shigella* infection model, BALB/c mice were pre-treated with streptomycin and iron ($FeCl_3$) plus desferrioxamine (chelator) intraperitoneally, followed by oral infection with *Shigella* spp. Oral challenge of mice with virulent *S. flexneri 2a* resulted in diarrhoea, body weight loss, bacterial colonization and progressive colitis with raised proinflammatory cytokines and chemokines in the large intestine. To determine if the new oral shigellosis model was useful for vaccine efficacy studies, we generated a subunit vaccine based on a recombinant protein (IpaB) from *Shigella* and delivered it intranasally. Immunized mice conferred protection against different *Shigella* serovars. Further, to protect both *Shigella* and typhoidal *Salmonella*, rIpaB was fused with rT2544 to develop a chimeric vaccine, rIpaB-T2544. Vaccinated mice mounted antigen-specific, serum IgG and IgA antibodies and a balanced Th1/Th2 response and were protected against oral challenge with *S. flexneri 2a*, *Salmonella* Typhi and *Salmonella* Paratyphi A. Overall, our vaccine candidates may be a game changer by preventing multiple enteric infections simultaneously.

Santasabuj Das

सान्तासबुज दास, एस. डि.
SANTASABUJ DAS, M.D.
वैज्ञानिक (एफ)/Scientist (F)
आइ.सि.एम.आर. राष्ट्रीय कॉलरा और आंत्र रोग संस्थान
ICMR National Insurance of Cholera & Enteric Diseases
पी-३३,सी. आई. टी. रोड, स्कीम-७०एम, बेलियाघाटा, कोल-१०
P-33, CIT Road, Scheme-XM, Beliaghata, Kolkata-10
E-mail : santasabujdas@yahoo.com

Risha Haldar
18.11.2024

Chapter 1.

Introduction & Review of Literature

1.1 General introduction

The genus *Salmonella* is a facultative anaerobic Gram-negative, non-spore-forming, rod-shaped motile bacteria with a diameter ranging from 0.5 to 1.5 micron, and a length of 2 to 5 micron and belongs to the Enterobacteriaceae family (1). *Salmonella* was initially discovered by Karl Eberth in the spleen and Peyer's patches of typhoid patients in 1880 (1). Theobald Smith believed that *Salmonella* enterica was the cause of hog cholera, hence he dubbed it "Hog-cholera bacillus" upon its discovery in 1885. In 1900, Joseph Leon Lignières coined the name *Salmonella*. There are two types of *Salmonella* enterica, which cause infection in humans. Human *Salmonella* infections can have a variety of effects that fall into two broad categories, depending on the serovar and host: (I) gastroenteritis, a self-limited infection of the terminal ileum and colon, resulting in diarrhoea and inflammation, frequently caused by the broad-range serovars Typhimurium and Enteritidis, referred to as non-Typhoidal *Salmonella* (NTS). (II) typhoid fever, a systemic infection brought on by the human-adapted serovars *Salmonella* Typhi and Paratyphi, called Typhoidal *Salmonella*. The most common way for either form of infection to spread is through contaminated food or drink (**Figure 1.1**). In healthy adults, gastroenteritis, also referred to as salmonellosis, is limited to the intestine and infrequently causes complications (2, 3). In typhoid fever, *Salmonella* spread by the lymphatic system and phagocytes, colonizing the internal organs like the liver, spleen, bone marrow, and gall bladder (4) (**Figure 1.2**). Based on host specificity, *Salmonella* serovars are categorized into three groups: ubiquitous (non-adapted), host-restricted, and host-adapted. For instance, systemic sickness in humans (5), poultry (6), and bovines (7) is caused by serovars Typhi, Galllinarum, and Abortusovis, respectively. Host-adapted serotypes are serovars that often infect a specific host species but can also cause disease in other species; for example, serovars Dublin and Choleraesuis typically colonize cattle and pigs, respectively, but have also been reported to cause disease in humans and other mammals (8, 9, 7). Numerous serovars that have reservoirs

in farm animals are strongly linked to foodborne outbreaks, including *S.* Typhimurium, *S.* Enteritidis, *S.* Newport, and *S.* Heidelberg (10).

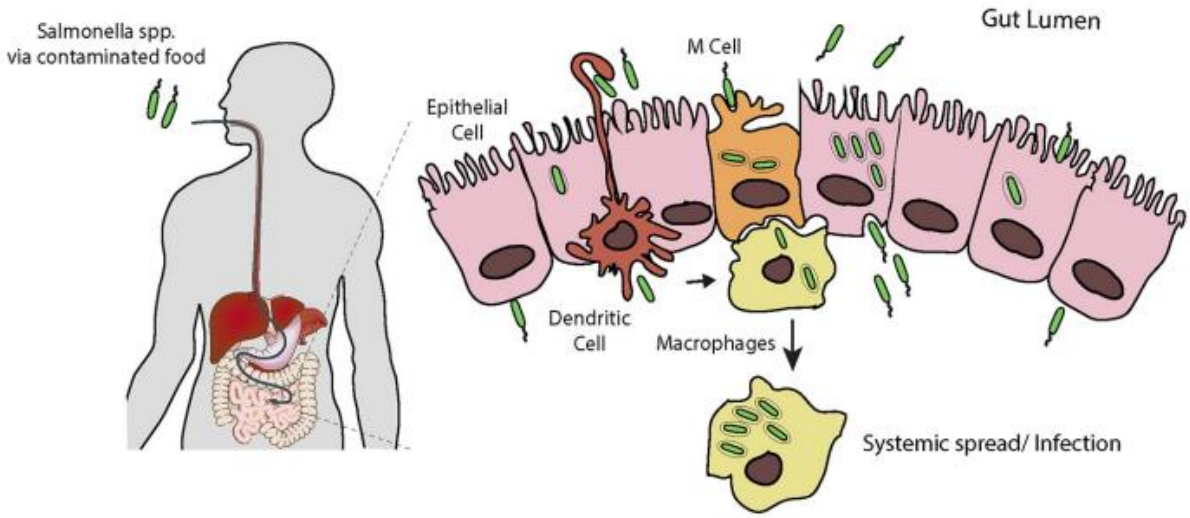

Figure 1.1. *Salmonella* infection. Salmonellae can survive in stomach acidity following consumption, and bypass the small intestine defenses to enter the epithelium. They enter M cells and are transferred to T and B lymphoid cells in Peyer's Patches. Systemic illness occurs when typhoidal *Salmonella* penetrates intestinal macrophages and spreads throughout the reticuloendothelial system. Non-typhoidal, diarrhoea-causing strains cause early local inflammation, leading to PMN infiltration. [The image is adapted from Hume PJ, Singh V, Davidson AC, Koronakis V. Swiss Army Pathogen: The Salmonella Entry Toolkit. Front Cell Infect Microbiol. 2017 Aug 9;7:348. doi: 10.3389/fcimb.2017.00348. PMID: 28848711; PMCID: PMC5552672.]

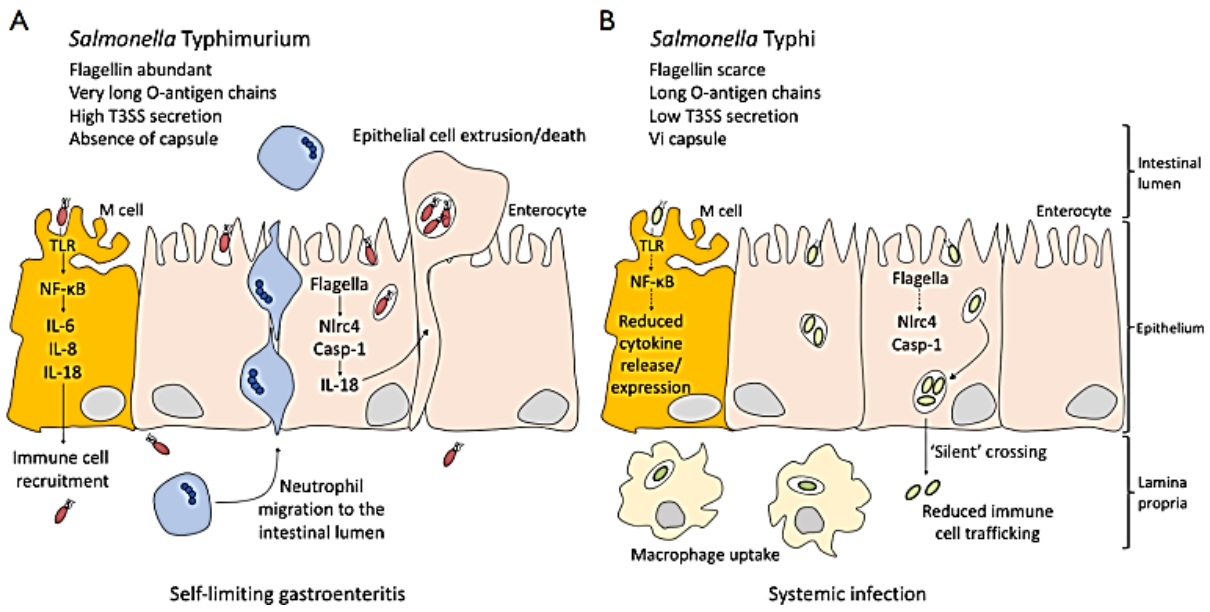

Figure 1.2. Self-limiting gastroenteritis and systemic overview of *Salmonella*. (A) *S.* Typhimurium infects a host using the flagella, LPS, O-antigen chains, and SPI-1 effectors, triggering an initial immune response that leads to self-limiting gastroenteritis. (B) *Salmonella* Typhi bypasses the host immune response by upregulating Vi capsular genes and downregulating immunogenic surface features, thus enabling itself to cross the epithelial barrier and further spread. [The image is adapted from Urdaneta V, Casadesús J. Host-pathogen interactions in typhoid fever: the model is the message. Ann Transl Med. 2018 Nov;6(Suppl 1):S38. doi: 10.21037/atm.2018.09.52. PMID: 30613613; PMCID: PMC6291556.]

Shigella species are rod-shaped, facultative anaerobic, Gram-negative, nonsporulating, nonmotile bacteria. It belongs to the Enterobacteriaceae family and infects the lower gut, causing severe recto-colitis, known as shigellosis. The isolation and characterization of *Shigella* was first reported in 1897 by Kiyoshi Shiga (11). In a majority of cases, diarrhoea occurs by bacterial colonization and invasion of small intestine and colon epithelium or by the production of an enterotoxin after bacterial colonization of the small intestine or with the preformed enterotoxins in the food (12). *Shigella* is spread by the faecal oral route (**Figure 1.3**). Only 10–

100 *Shigella* organisms can induce diarrhoea in healthy adults, making them extremely contagious and virulent (13, 12). *Shigella* normally infects humans and other primates (14), but recent reports of infections with the disease have also affected fish, chickens, piglets, rabbits, calves, and monkeys (14, 15, 16, 17, 18, 19). *Shigella* is included as a priority 3 organism on the WHO priority pathogens list due to its extremely low infectious dose and developing resistance to antibiotics (20).

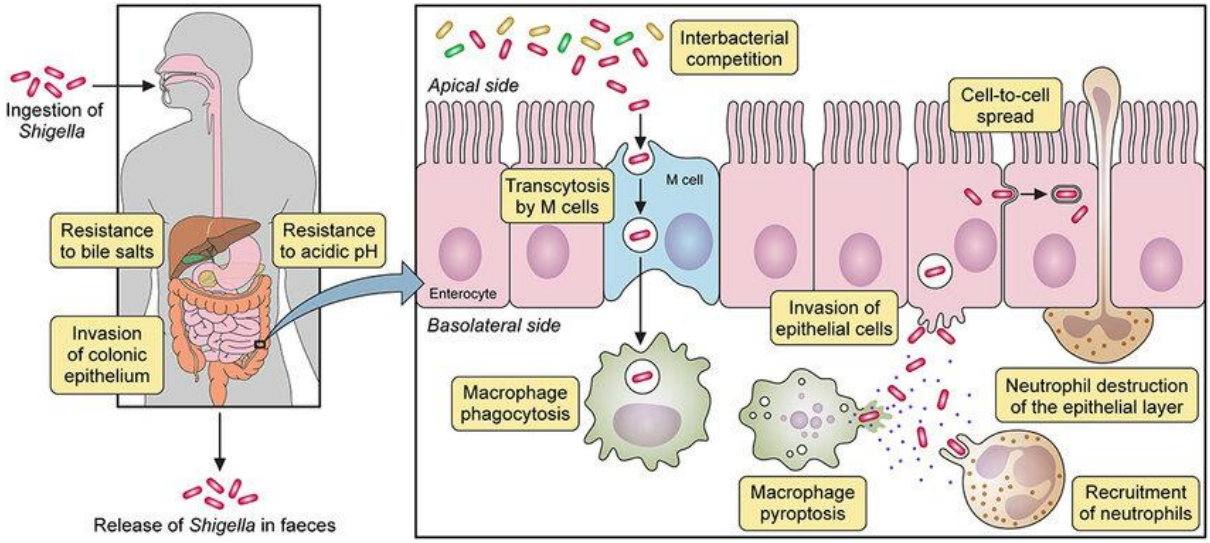

Figure 1.3. *Shigella* infection. Following ingestion and during its journey to the colon, *Shigella* needs to withstand harsh gastrointestinal conditions, such as the acidic pH of the stomach and the bactericidal effects of bile salts. It is transcytosed by M cells and internalized by macrophages. *Shigella* grows intracellularly, inhibiting immune responses and cell death. It invades the adjacent epithelial cells and is released through fecal matter. [The image is adapted from Matanza XM, Clements A. Pathogenicity and virulence of *Shigella sonnei*: A highly drug-resistant pathogen of increasing prevalence. Virulence. 2023 Dec;14(1):2280838. doi: 10.1080/21505594.2023.2280838. Epub 2023 Nov 23. PMID: 37994877; PMCID: PMC10732612.]

1.2 Taxonomy and Classification of *Salmonella* and *Shigella*

1.2.1 Classification of *Salmonella*

Gram-negative facultative intracellular anaerobes, *Salmonella* enterica can cause acute and persistent infections in a variety of hosts due to their capacity to proliferate and persist inside phagocytic dendritic cells, macrophages, and non-phagocytic epithelial cells within the host innate immune system (21, 22). These microorganisms are closely related to the genus *Escherichia* and show predominantly peritrichous motility. Based on variations in the sequence of the 16S rRNA gene, the *Salmonella* genus is classified into two species, *Salmonella* bongori and *Salmonella* enterica. Six subspecies of *Salmonella* enterica have been identified (23): enterica (I), salamae (II), arizonae (IIIa), diarizonae (IIIb), houtenae (IV), and indica (VI). In the past, *Salmonella* enterica subsp. V was regarded as bongori, however this is no longer currently in that group (**Figure 1.4**). The White-Kauffman classification scheme (24), which is based on particular patterns of agglutination reactions with antisera against two highly variable surface antigens, O (lipopolysaccharide O-antigen), H (flagellar proteins) (23, 25) and Vi (capsular polysaccharide) (26), further divides *Salmonella* isolates from the same subspecies into serovars. Over 2,500 *Salmonella* serovars have been identified, with the majority falling into the subspecies Enterica (27). *Salmonella* infections in humans are primarily caused by serovars of this subspecies, which are the only ones that habitually infect warm-blooded vertebrates (28). In contrast, serovars of *Salmonella* bongori and the other *Salmonella* enterica subspecies are typically linked to cold-blooded vertebrates (29).

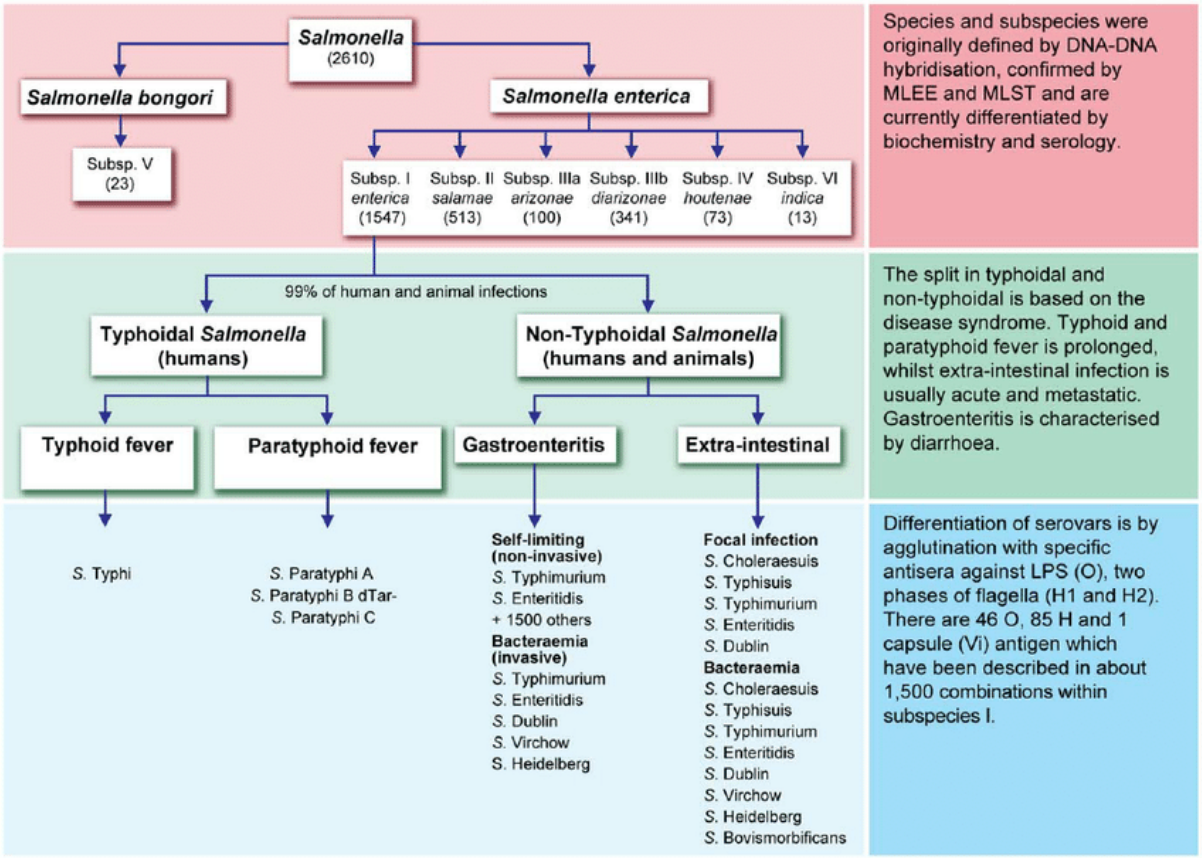

Figure 1.4. Classification of *Salmonella*. [The image is adapted from Achtman M, Wain J, Weill FX, Nair S, Zhou Z, Sangal V, Krauland MG, Hale JL, Harbottle H, Uesbeck A, Dougan G, Harrison LH, Brisse S; S. Enterica MLST Study Group. Multilocus sequence typing as a replacement for serotyping in Salmonella enterica. PLoS Pathog. 2012;8(6):e1002776. doi: 10.1371/journal.ppat.1002776. Epub 2012 Jun 21. Erratum in: PLoS Pathog. 2020 Oct 21;16(10):e1009040. doi: 10.1371/journal.ppat.1009040. PMID: 22737074; PMCID: PMC3380943.]

1.2.2 Classification of *Shigella*

Shigella was formerly known as *Bacillus coli*, as it resembled *E. coli*, and was originally given the name *Bacillus dysenteriae* (30). Afterward, they were taxonomically positioned in the genus *Shigella* in 1949 (31). Currently, four species—*S. dysenteriae*, *S. flexeneri*, *S. boydii*, and *S. sonnei*—are recognized in the genus based on their phenotypic and antigenic traits (32) (**Figure**

1.5). These species are also referred to as subgroups A, B, C, and D of *Shigella*. These subgroups are classified based on the lipopolysaccharide O-antigen repeats (33). Since the expression of flagella is deficient in all *Shigella* strains, H antigen typing cannot be developed. A crucial step in the identification and typing of *Shigella* is serotyping. Currently, there are 55 serotypes in *Shigella*. *S. sonnei* contains one serotype, while *S. boydii*, *S. dysenteriae*, and *S. flexeneri* have 20, 15, and 19 serotypes, respectively (34, 35).

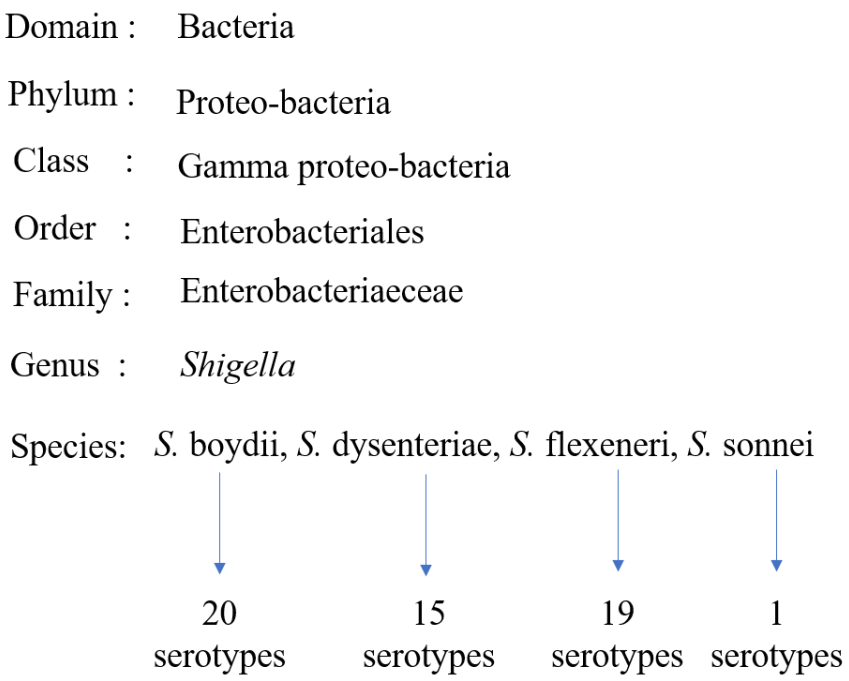

Figure 1.5. Classification of *Shigella*. (The image is created in PowerPoint)

1.3. Epidemiology of *Salmonella* and *Shigella*

1.3.1 Epidemiology of *Salmonella*

Globally, 14.3 million cases of typhoid and paratyphoid fever were reported in 2017. Of these, 10.9 million cases of typhoid fever were confirmed, resulting in 8.4 million disability-adjusted life-years (DALYs) and 116,800 fatalities. For paratyphoid infection, 3.4 million confirmed

cases, leading to 1.3 million DALYs and 19,100 fatalities were documented (36). These estimates showed that the number of confirmed cases of enteric fever, including both typhoid and paratyphoid, decreased by 44.6% from the year 1990 (25.9 million total cases). More specifically, while typhoid cases showed 46.29% decrease, paratyphoid cases declined. The number of recorded deaths in 2017 was also 38–42% lower than in 1990. The statistics progressively improved by the introduction of typhoid conjugate vaccines in endemic areas, better water, sanitation, and hygiene (WASH) practices, and subsequent health education initiatives. A global literature review of enteric fever outbreaks during 1990-2018 enumerated a total of 180,940 symptomatic infections from 303 outbreaks, including 51% of cases Asia, 15% from Africa and 14% from Oceania and remaining cases from other regions (37). By 2022, there were only 9.2 million verified cases of typhoid fever, and 110,000 fatalities (38).

India has a far greater typhoid prevalence than its neighbours, including China, Pakistan, and Indonesia, which emphasises the urgent need for efficient preventive measures (39). However, there is a shortage of data from community-based and hospital-based studies in India. A follow-up research conducted in a low-income neighbourhood of Delhi between 1995 and 1996 reported 44% of typhoid fever cases in children aged below 5 years. Typhoid incidence was 27·3 per 1000 person-years for children under five, 11·7 for those aged five to nineteen, and 1·1 in 19 to 40-years age group (40). In 2004, a community-based study was carried out in Kolkata, India, to determine risk factors for typhoid fever. Over a 12-month period, 3605 fever episodes were found in a population of 60,452. Salmonella enterica serotype Typhi was grown in blood cultures from 95 individuals. The frequency of typhoid fever was highest between the ages 5 and 10. In high-incidence areas, there were 3.7 cases of typhoid per 1000 residents annually, while in low-incidence areas, there were 0.8 cases per 1000 persons annually (41). The evaluation of typhoidal and paratyphoidal occurrences in India comes mainly from the hospital-based investigations, which might not be an accurate representation of the incidence

in the general population. A study between 2017-2020 was conducted among the age group 6 months to 14 years at three urban sites (Delhi, Kolkata, and Vellore) and one rural site (Pune) in India (42). According to hospital surveillance, the estimated incidence of typhoid fever varied between 12 and 1622 cases per 100,000 children per years for children aged 6 months to 14 years and between 108 and 970 cases per 100,000 persons per year for individuals aged 15 and above. *Salmonella* enterica serovar Paratyphi corresponded to an overall incidence of 68 cases per 100,000 children per year (43). In another study, the typhoid fever incidence across India was evaluated between 2017 and 2020 using a geospatial statistical model (42). This study found India's countrywide typhoid incidence as 360 cases per 100,000 person-years, or roughly 4.5 million cases and 8,930 fatalities per year. Significant geographic heterogeneity was also noted in this study, with higher frequency in northern urban centres and southwestern states.

Infections with *S.* Paratyphi A accounted for just 3–17% of cases in India in the early 1960s (44). Recent data, however, suggest that *S.* Paratyphi A now accounts for a sizable and possibly rising share of cases of enteric fever. *S.* Paratyphi A infections increased from 20.3% in 1999 to 30.3% in 2004, according to a retrospective research conducted in Delhi (45). Further studies conducted in rural Maharashtra showed that *S.* Paratyphi A constituted 45% of all *Salmonella* isolates in 2002 and 53% in 2003. The study shed light on the prevalence of *S.* Paratyphi A in India's rural areas, despite its small sample size (46). In India, *S.* Paratyphi A infections accounted for 38.37% of cases between 2000 and 2006 (47). According to a prospective investigation in Chandigarh, the percentage of isolates with *S.* Paratyphi A rose from 14.3% in 2003 to 40.6% in 2007 (48). A comprehensive study and meta-analysis of enteric fever cases in India between 1950 and 2015 found 377 typhoidal and 105 paratyphoidal infections for every 100,000 person-years (49). Even though the prevalence apparently decreased, typhoidal and paratyphoidal illnesses still present serious public health issues in India, particularly for young children. The absence of up-to-date population-based statistics makes it difficult to determine

whether the drop in hospitalizations for typhoid is due to better antibiotic treatment or a real drop in infection rates. Effective enteric fever prevention and management have been hampered by the lack of national disease burden estimates. Vaccination of susceptible populations of endemic areas coupled with ongoing programs to improve water, sanitation, and hygiene (WASH) are the only effective means to control the disease spread (**Figure 1.6**).

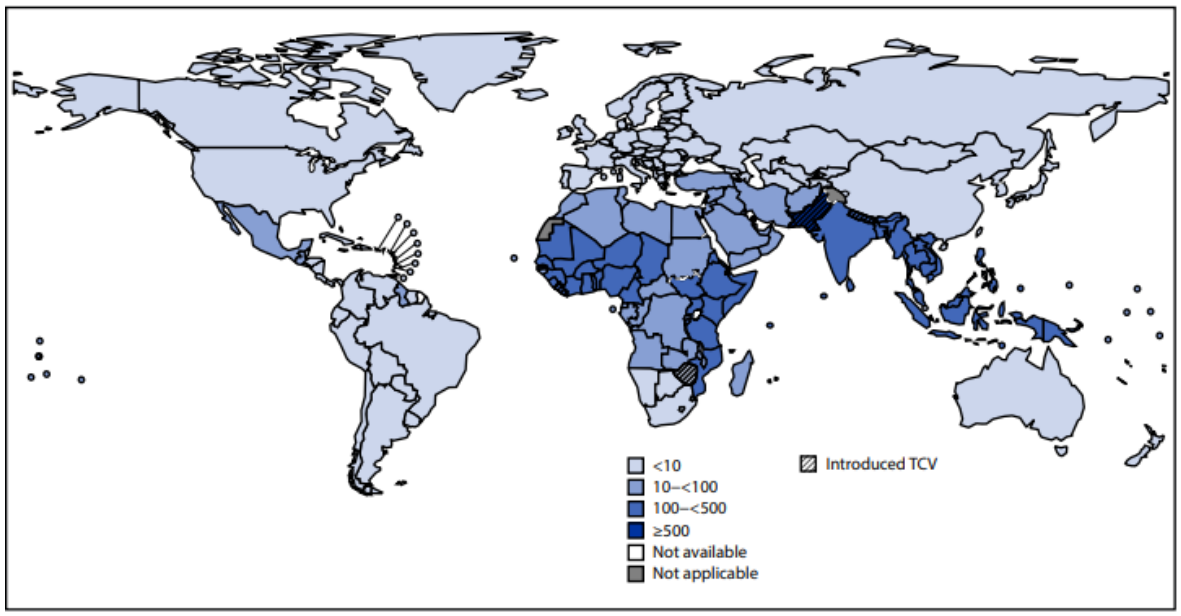

Figure 1.6. Global enteric typhoidal *Salmonella* disease Burden and introduction of typhoid conjugate vaccine, 2019-2022. [The image is adapted from Hancuh M, Walldorf J, Minta AA, Tevi-Benissan C, Christian KA, Nedelec Y, Heitzinger K, Mikoleit M, Tiffany A, Bentsi-Enchill AD, Breakwell L. Typhoid Fever Surveillance, Incidence Estimates, and Progress Toward Typhoid Conjugate Vaccine Introduction - Worldwide, 2018-2022. MMWR Morb Mortal Wkly Rep. 2023 Feb 17;72(7):171-176. doi: 10.15585/mmwr.mm7207a2. PMID: 36795626; PMCID: PMC9949843.]

Non-typhoidal *Salmonella* (NTS) infections, such as invasive non-typhoidal *Salmonella* (invasive NTS, or iNTS), have a major economic impact on society and are responsible for a considerable amount of morbidity and mortality worldwide (50, 51) (**Figure 1.7**). Approximately 6% of cases of diarrhoeal NTS develop into bloodstream infections (52-55). Particularly in sub-Saharan Africa, iNTS infection is a leading source of morbidity and mortality, with a greater fatality rate than non-invasive infection (56-58). In 2006, 93.8 million cases of NTS gastroenteritis with 155,000 fatalities were estimated globally (59). In 2010, the Global Burden of Disease (GBD) research reported that NTS was responsible for 81,300 fatalities and 4.84 million DALYs (60, 61). According to WHO estimates from the Foodborne Disease Burden Epidemiology Reference Group (FERG, 2007–2015), invasive non-typhoidal *Salmonella* enterica induces 3.9 million and non-typhoidal *Salmonella* enterica contributed 4.38 million DALYs, respectively (62). Of the 22 foodborne enteric infections worldwide, foodborne DALYs from NTS and iNTS were the most common, accounting for 4.07 million incidences (62). More recently, 594,000 cases of iNTS were reported in the GBD 2019 estimates, which led to 6.11 million DALYs and 79,000 deaths worldwide (63). Typhoid fever (17% fatalities) and paratyphoid fever (2% fatalities) were less common in children under five than NTS (36% fatalities) and iNTS (45% fatalities) (63). Sub-Saharan Africa accounts for the majority of iNTS cases with incidence rates of more than 100 cases per 100,000 person-year in the population (64). A case-fatality rate of 14.5% was reported in 2017 with higher rates among children (51). Even higher case fatality rates of 20% have been reported in Bangladesh, Vietnam, and Mali by another study (64).

NTS infections are rarely reported in India. However, in a study period between 2000-2018 from January 2000 to December 2018, 1436 NTS isolates were identified from faeces specimens obtained at the Tertiary Care Hospital in Mangalore (65). When comparing the number of NTS isolates by year, there appears to have been a sharp rise since 2009. The first

eight years (2000–2008) experienced an average of 29% NTS isolates, but the subsequent ten years had a surge in incidence to 71%. With 393 isolates (27.3%), *S.* Typhimurium was the most common serotype among the 1436 isolates. In this study area, *S.* Weltevreden and *S.* Bareilly were found to be the second and third most common serovars of NTS, accounting for 13% (182/1436) and 11% (155/1436) of the total. The predominance of *S.* Weltevreden and *S.* Bareilly was unstable but decreased over time, whereas the isolation of *S.* Typhimurium was shown to remain constant. *S.* Newport (61, 4.2%), *S.* Infantis (50, 3.4%), *S.* Enteritidis (35, 2.4%), and *S.* Cholerasius (58, 4%) are the other prevalent serovars. *S.* Lindenberg was not previously observed and was only found in 2015 (4/93), 2016 (25/95), 2017 (12/90), and 2018 (1/153). The highest frequency of NTS infection occurred in children under the age of five, accounting for an average of 19.3% of all infected individuals during that time. In another study, 320 bacterial enteric pathogens were isolated for a period from 2011–2014 in South India (66). Of which 64 (20%) were non-typhoidal *Salmonella*. Among the serogroup, O:4 (n = 26; 40.6%) was found to be the commonest followed by O:7 (n = 11; 17.1%) and O:3 (n = 11; 17.1%). In a study period of 2013–2016, samples of 27 patients from a tertiary care center in India were positive for NTS (67). Of which, *Salmonella* typhimurium was the predominant NTS isolated among 15/27 (55.5%), followed by *Salmonella* enteritidis 4/27 (14.8%). During the study period from 2016 to 2018, a total of 999 suspected NTS isolates were isolated across India (68). Most of the NTS isolates (n= 313, 58.07%) were identified from Southern India, whereas, other regions contributed between 0.37% and 18.18% of the total NTS collection. 539 NTS isolates of 999 confirmed the presence of different NTS serovars, of which the predominant serotype was *S.* Typhimurium (n=167) which constitute 30.98%. However, others include *S.* Lindenberg (n=135), *S.* Enteritidis (n=56), *S.* Weltevreden (n=44), *S.* Choleraesuis (n=41) and *S.* Mathura (n=33) which constitutes 25.05%, 10.39%, 8.16%, 7.61% and 6.12%, respectively. In another study, 26,815 clinical samples were isolated from Karnataka, India in

the time period between 2017-2019 (69). Among the 26815 samples, 24 (0.08%) showed the growth of nontyphoidal Salmonella serovars. Among these samples, five were *Salmonella* enterica subsp. enterica, three were *S.* enterica serovar Typhimurium, one was *S.* enterica subsp. diarizonae, and 15 *S.* enterica serovars could not be serologically differentiated.

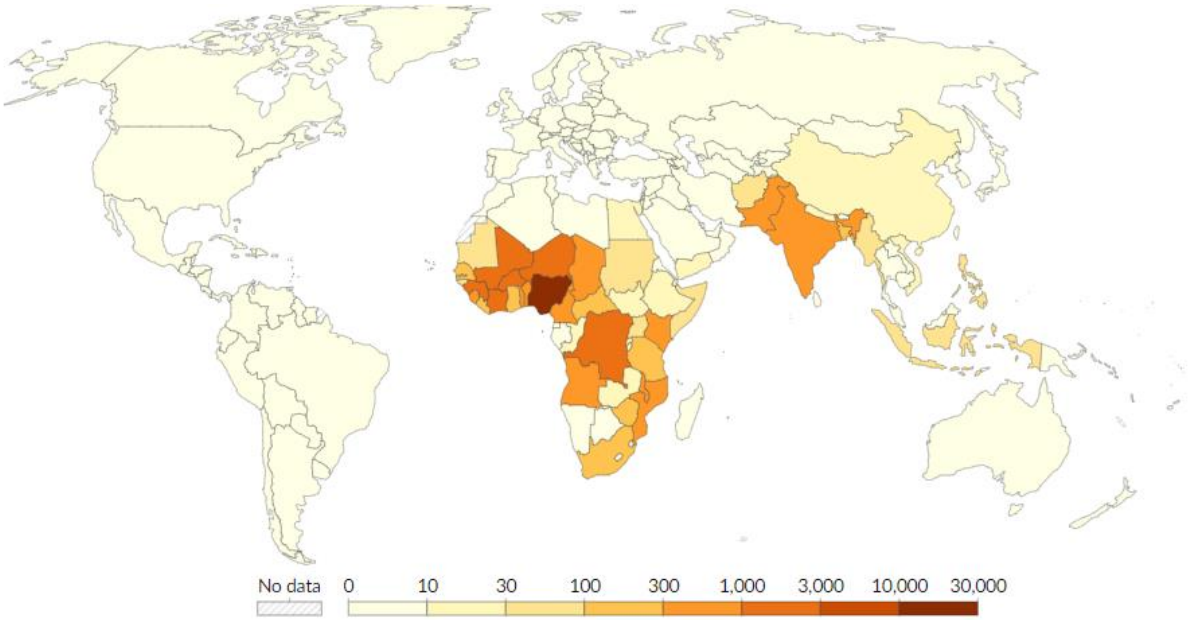

Figure 1.7. Invasive non-typhoidal *Salmonella* mortality in children below five. [The image is adapted from "Invasive non-typhoidal salmonella deaths in children under five" [dataset]. IHME, Global Burden of Disease, "Global Burden of Disease - Deaths and DALYs" [original data]. Retrieved August 19, 2024 from https://ourworldindata.org/grapher/child-deaths-from-invasive-non-typhoidal-salmonella].

1.3.2 Epidemiology of *Shigella*

Shigellosis primarily affects children between the ages of 2 and 5, and it may lead to 64,000 fatalities per year (70). The Global Enteric Multicenter Study (GEMS) in 2014 investigated the the most common diarrhoeal diseases occurring in sub-Saharan Africa and South Asia between the ages of two to five. This study investigated that, *S. flexneri 2a* (SF2a) was the most prevalent

serotype; however, *S. flexneri 6* (SF6) was found in the stools of children without diarrhoea (71). An Israeli study investigated the dynamics of shigellosis, with a focus on *S. sonnei* cycle outbreaks. Between 1998 and 2012, this study calculated that there were 2425 culture-proven cases of shigellosis per 100,000 people in Israel on average each year. Another study examined the prevalence of *S. sonnei*-mediated shigellosis in hyperendemic populations in children aged 0–59 months. From 2000 to 2013, it documented a cyclical pattern in Elad with a mean yearly incidence of 10.0 per 1000, highlighting the significance of case-control studies and providing specifics on risk factor analysis techniques (72). According to the European Surveillance System (TESSy) there were 1.7 cases per 100,000 population were attributed to Shigellosis where the highest rate was observed in children below five years of age (73). According to WHO 2021 report, an estimated 28,000 to 64,000 deaths per year were attributed to children under the age of five. Data from the Global Enteric Multicenter Study (GEMS), a 3-year, prospective, age-stratified, case/control study aimed at examining the population-based burden, aetiology, and adverse clinical consequences of acute MSD (moderate-to-severe diarrhoea) among children under 5 years old living in South Asia and sub-Saharan Africa (74). They identified *Shigella* as the most common aetiology in children between the ages of 12 and 23 months and the second most common aetiological agent among those aged 24–59 months (75). Out of the 1130 *Shigella* isolates, 65.9% and 23.7%, were *Shigella flexneri* and *S. sonnei*, 5.0% and 5.4%, were *Shigella dysenteriae* and *S. boydii*;. Out of all the *S. flexneri* serotypes, five were the most common and these were *S. flexneri 2a*, *S. flexneri 6*, *S. flexneri 3a*, *S. flexneri 2b*, and *S. flexneri 1b* (76). *Shigella* was shown to be the predominant pathogen linked to diarrhoea (attributable fraction 63.8%) and the second most prevalent pathogen linked to watery diarrhoea (attributable fraction 12.9%) (77). Two species, *Shigella flexneri* and *Shigella sonnei*, which were historically linked to developing and developed regions, respectively, are mostly responsible for the current epidemiological burden of shigellosis globally (78-80).

However, new data suggests that *S. sonnei* is spreading throughout economically transitioning regions, displacing *S. flexneri* as the primary cause of shigellosis (81). The occurrence of species replacement has been repeatedly observed in numerous Asian nations, including Bangladesh (82), Thailand (83), and Vietnam (84). The reasons for this serotype replacement are still being studied, but one theory suggests that the superior ability of *S. sonnei* to obtain antimicrobial resistance genes from commensal and pathogenic bacteria provides it with a competitive advantage over *S. flexneri*, particularly where antimicrobial use is not well regulated. Moreover, it has been documented that *S. sonnei* may grow more easily in Acanthamoeba, which is found in public water supplies (81, 85). Every year, 536 million people visit low- and middle-income countries (LMICs), and it has been calculated that *Shigella* is responsible for 2-9% of diarrhoea cases experienced by travellers (86).

Shigella species and serotypes vary in frequency among nations, with variations occurring throughout time and in correlation with economic standing. In Bangladesh, cases from both urban and rural areas showed a diverse distribution of *Shigella* serotypes (87). *S. dysenteriae*, and more especially *S. dysenteriae 1*, have been linked to numerous fatal dysentery epidemics. A decrease in disease and mortality linked to *Shigella* spp., particularly *S. dysenteriae*, has been attributed to improvements in sanitation and antimicrobial access (88, 89). Between 2001 and 2003, there was a heterogeneous distribution of *Shigella* species and serotypes in India (90). The most prevalent species was found to be *S. flexneri* (45%), followed by *S. dysenteriae* (29.4%), *S. boydii* (14.7%), and *S. sonnei* (10.2%). The same study, carried out in South India between 2003 and 2006, revealed a significant shift in the prevalence of *S. flexneri*, which remained at 45%, followed by *S. sonnei* (31%), *S. boydii* (15%), and *S. dysenteriae* (8%). It was shown that the *S. flexneri 2a* serotype predominates in the Andaman and Nicobar Islands (91). A multi-centric study from six Asian countries—China, Vietnam, Thailand, Bangladesh, Pakistan, and Indonesia—found that *S. flexneri* was the most frequently isolated species (68%)

with the exception of Thailand, where *S. sonnei* was the most common (84%). In contrast, *S. dysenteriae*, which is most frequently found in southern Asia and sub-Saharan Africa, made up only 4% of the isolates (92). From 1994 to 2002, *S. flexneri* was the most prevalent serogroup. Since 2004, the most common serogroup was the *S. flexneri* again (93). These cyclical variations have also been documented by the National Institute of Cholera and Enteric Disease (NICED), Kolkata, in eastern India, where epidemics caused by *S. dysenteriae* periodically occur after a gap of a decade or so (94). Overall, they reported that *S. flexneri* (60%) was the most common serogroup followed by *S. sonnei* (23.8%), *S. dysenteriae* (9.8%), and *S. boydii* (5.7%). According to the Global Enteric Multicenter Study, 91 samples were tested positive for shigellosiss, of which 26.4% of *flexeneri* 2a, 12.1% of 3a, 5.5% of 6, 5.5% of 4a, 5.5% of 7 and 1.1% of 1b *Shigella* were isolated from Kolkata (95). On the other hand, during the seven-year period from 2006 to 2012, *S. dysenteriae* (12%) was found to be the third most frequent in the Andaman Islands in the Bay of Bengal, after *S. flexneri* (68%) and *S. sonnei* (20%) (96). A comprehensive study was carried out from 2000 to 2022 in South Asia (Afghanistan, Bangladesh, Bhutan, India, the Maldives, Nepal, Pakistan, and Sri Lanka) (97). This study observed that the most prevalent serogroup was *Shigella flexneri* (58%) as opposed to *Shigella sonnei* (19%), *Shigella boydii* (10%), and *Shigella dysenteriae* (9%) (**Figure 1.8**). The most commonly isolated serotype of *Shigella flexneri 2a* was 36%, which was followed by 3a (12%), 6 (12%), and 1b (6%).

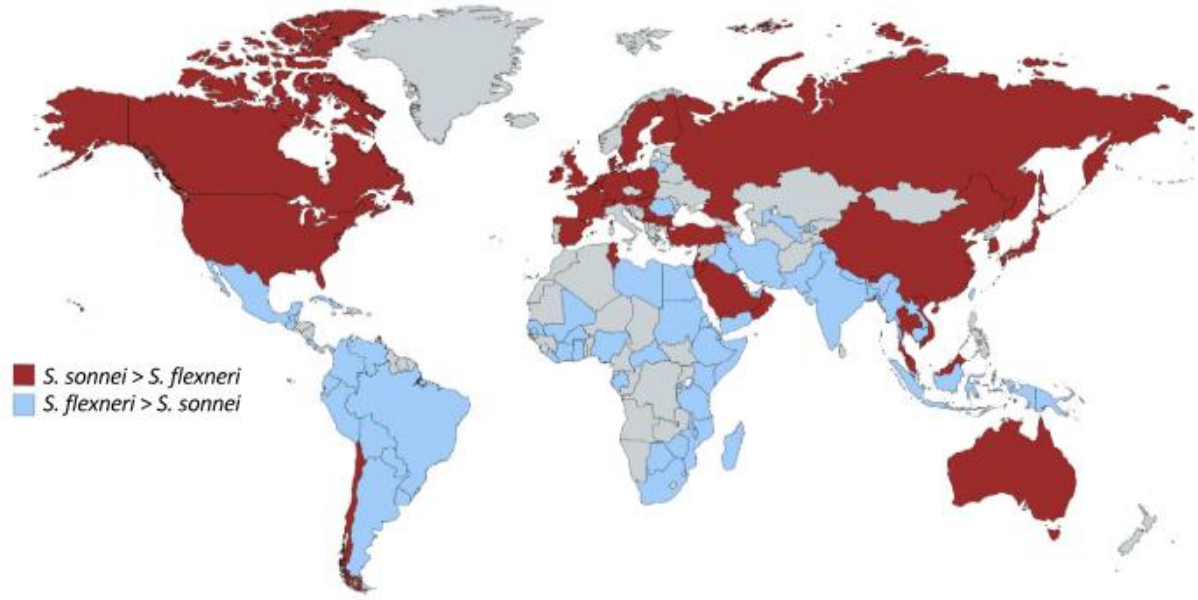

Figure 1.8. Global burden of *Shigella*. A comparative study of number of increasing cases between *S. flexeneri* and *S. sonnei*. Countries marked in blue have a larger percentage of *S. flexneri* infections whereas red color denotes the rising of *S. sonnei*. [The image adapted from Torraca V, Holt K, Mostowy S. Shigella sonnei. Trends Microbiol. 2020 Aug;28(8):696-697. doi: 10.1016/j.tim.2020.02.011. Epub 2020 Apr 8. PMID: 32663462; PMCID: PMC7611039.]

1.4. Molecular mechanism of pathogenesis of *Salmonella* and *Shigella*

1.4.1. Pathogenicity islands of *Salmonella*

Large chromosomal areas called Pathogenicity Islands (PAI) are seen in pathogenic bacteria carrying their virulence traits. The chromosomal integration of PAI has been linked to the evolution of bacterial virulence through the acquisition of novel virulence functions. The characteristics of PAI are as follows:

Table 1.1. Characteristics feature of pathogenicity island of *Salmonella*. [The table is adapted from Kombade S and Kaur N (2021) Pathogenicity Island in Salmonella. Salmonella

spp. A Global Challenge. IntechOpen. Available at: http://dx.doi.org/10.5772/intechopen.96443.]

SL No	Characteristics features of pathogenicity island
1	Possessing one or more virulence genes
2	Not seen in non-pathogenic bacteria of the same or very related species, but present in pathogenic bacteria
3	Comprise substantial genomic areas, with sizes ranging from 10 to 200 kilobases.
4	Possess DNA with a composition that is significantly different from the host genome, particularly in terms of codon use and the percentage of G+C content.
5	Frequently located next to tRNA genes
6	Frequent pairing with mobile genetic components, frequently with direct repeats on either side. Integrase gene presence at one end of the island.
7	Genetic instability that may cause the Pathogenicity Islands to disappear.

Table 1.2. The features and functions of Pathogenicity islands *Salmonella*.

SPIs	Size (Kb)	Most important genes for virulence	Function
SPI-1	40	*avrA, sprB, inv, hil, org, spt, spa, sip, iag, iac, prg, sic, sitABCD*	*Salmonella* colonization and invasion into intestinal epithelial cells, survival and proliferation inside the vacuoles
SPI-2	40	*ssr, ssaJV, sseBFG, ssc, gogAB, gtgA, pipAB, sifAB, sopD2, spiC, spvB, srfJ*	Survival and replication of *Salmonella* in phagocytes and epithelial cells, aid in *Salmonella* escape from the macrophages and plays an important regulatory role in the progression of systemic infection and intracellular pathogenesis
SPI-3	17	*MgtCB*	Helps in the survival of *Salmonella* in macrophages by enabling effective magnesium uptake in low Mg2+ environment.
SPI-4	27	*SiiABCDF*	Adhesion of *Salmonella* to epithelial cell surfaces, membrane ruffle formation and uptake of *Salmonella*
SPI-5	7	*sopB, pipABCD*	Intestinal mucosal fluid secretion and inflammatory responses
SPI-6	59	*pagN, safABCD*	Intra-macrophage survival and successful establishment of *S.* enterica in host gut during infection

SPI-7	146	*viaB*	Encodes important virulence genes, including the major Vi antigen and IVB operon, escape from phagocyte-mediated killing and modulating the innate immune responses
SPI-8	6.8	*STY3273, STY3292*	Improve bacterial fitness of typhoid serovars in gut
SPI-9	16	*spvA, spvB, spvC, spvD*	Modulation of bacterial adhesion to the epithelial cells
SPI-10	32.8	*sefB, sefC, sefR*, and *prpZ*	Regulation of chaperone protein, promoting *S.* Typhi survival in macrophages
SPI-11	15-20	*invA, invB, invC, rtsA*	Survival in macrophages
SPI-12	6.3	*rpoS, tviA, spvA, spvB*	Contributes to in vivo adaptability
SPI-13	19	*sitA, sitB, spvD*	Contributes to the virulence of *Salmonella*
SPI-14	9	*mgtC, tviA, sseD*	Enhance the ability of *Salmonella* to invade host epithelial cells
SPI-15	6.5	*sseB, sseC, spvA*	Enhances bacterium's ability to invade host tissues, manipulate host cell processes, and survive within the immune system

SPI-16	4.5	*SseK, sseJ, sseI*	Intestinal persistence of *S.* Typhimurium
SPI-17	5.1	*sifA, sifB, sifC*	These genes encode proteins that help *Salmonella* survive and replicate within host cells by manipulating host cell processes, particularly within specialized compartments called *Salmonella*-containing vacuoles (SCVs)
SPI-18	9-10	*vsgA, vsgB*	It plays a role in modulating the bacterial response to stress and in contributing to the bacteria's ability to survive and proliferate within host cells.

1.4.2. Pathogenesis of *Salmonella*

After ingestion, *Salmonella* passages through the stomach and ensures its adherence to enter the gut. The bacteria use a pH homeostasis mechanism to survive in the acidic environment of the stomach by maintaining an internal pH above 5 (98). A critical stage in pathogenesis is adhesion to host tissues: the initial close contact between the microbe and the host is necessary to initiate certain processes such as protein translocation or biofilm development, which may be followed by entrance into the host cell and subsequent systemic dispersion. According to several studies (99-101), the bacteria either invades M-cells on the Peyer's Patches or may be taken up by dendritic cells, where the bacteria will move to the mesenteric lymph nodes and underlying follicles after translocating through the epithelial barrier. After translocation across

the intestine, the bacteria spread by the reticuloendothelial system and live in the niches such as the spleen and the liver (mostly in hepatocytes) within macrophages, dendritic cells, and polymorphonuclear leukocytes (102-104) (**Figure. 1.9**).

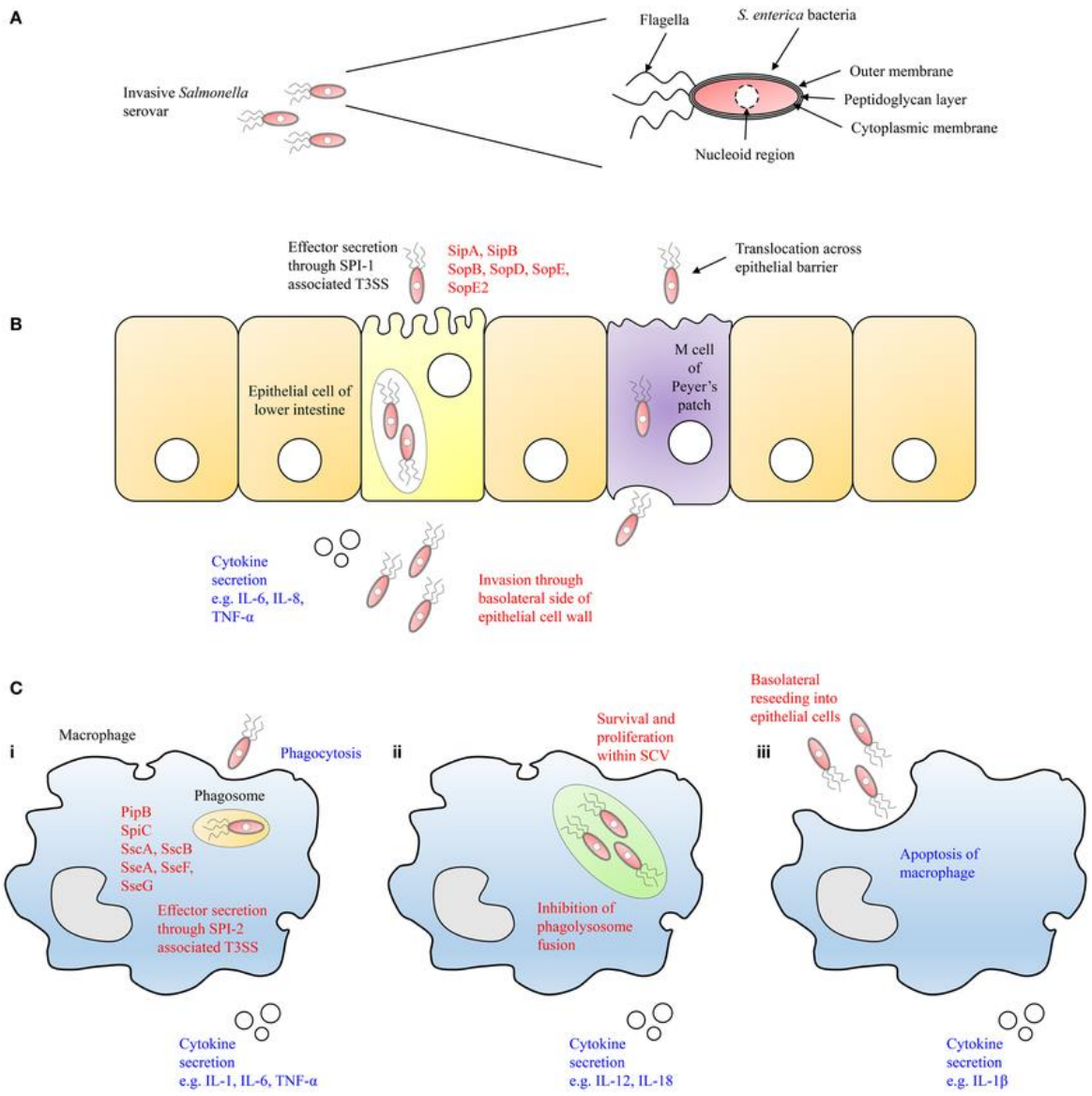

Figure 1.9. A schematic representation of the *Salmonella* infection of macrophages and lower intestine epithelial cells. (A) *Salmonella* can live until it reaches the host's epithelial cell wall in the lower intestine due to its intricate membrane structure. (B) *Salmonella* then uses the T3SS-1 gene encoded by SPI-1 to secrete effector proteins that

rapidly penetrate epithelial cells or translocate across M cells of Peyer's Patches. (C) (i) Proximal macrophages consume *Salmonella* after they have crossed the epithelial barrier. (ii) *Salmonella* will multiply within the SCV (*Salmonella* containing vacuole), causing the macrophage to secrete cytokines. (iii) subsequently, the macrophage will die, allowing *Salmonella* to break out and re-invade the host innate immune system by basolateral penetrating epithelial cells or other phagocytic cells.

[The image is adapted from Hurley D, McCusker MP, Fanning S, Martins M. Salmonella-host interactions - modulation of the host innate immune system. Front Immunol. 2014 Oct 7;5:481. doi: 10.3389/fimmu.2014.00481. PMID: 25339955; PMCID: PMC4188169.]

1.4.2.1. Adhesion to the host cell

Multiple adhesins aid in the adhesion of *Salmonella* to host cells or extracellular matrix (ECM), facilitating invasion (105). Genome analysis has identified thirteen fimbrial operons in *S.* Typhi. However, only the pil operon, which codes for the Type IVB pilus, has been shown to bind to the host surface receptor Cystic Fibrosis Transmembrane Regulator (CFTR) (106, 107). Regarding the necessity of Type IVB pilus for *S.* Typhi adhesion, there have been conflicting reports. Although a study indicated that the aforementioned pilus had no role in either adhesion or invasion (108). Other studies reported that it is necessary for invasion (109). *Salmonella* adhesins that are not fimbrile include auto-transporter adhesins (MisL, SadA, ShdA, RatB, SinH), Outer Membrane Protein (OMPs) (Rck, PagC, PagN/T2544) (110-112), and Type I secreted adhesins (SiiE and BapA), which mainly mediate attachment to different ECM proteins (113-116). Additionally, Rck but not PagC stimulates epithelial invasion (117). It has been found that MisL and ShdA bind fibronectin and aid in the intestinal colonization of *S.* Typhimurium (113, 114). The giant, non-fimbrial adhesin SiiE attaches itself to the sialic acid

and N-acetylglucosamine of the apical membrane of the intestinal epithelial cells (IECs) (118). T2544, the another adhesin protein of *S.* Typhi and *S.* Paratyphi has been shown to bind to laminin and enhance the pathogenesis of the bacteria in mouse model (112).

1.4.2.2. Entry into the host cell

Salmonella initiates its uptake by the epithelial cells after the adhesion through adhesins. The infiltration into the intestinal epithelium is essential for its survival and the development of pathogenesis since it is the first portal of entry. The two ways by which pathogens typically penetrate nonprofessional phagocytes, such as epithelial cells, are "Trigger" and "Zipper" mechanisms which vary depending on the extent of membrane remodelling that is produced (119). The "trigger" mechanism causes "membrane ruffles," or global actin cytoskeletal rearrangements throughout the cell membrane (**Figure. 1.10**). On the other hand, bacterial substances that cause localised membrane rearrangements restricted to the bacterial binding site on the host cell membrane trigger the "Zipper" process. This mechanism is also known as receptor-mediated endocytosis (**Figure. 1.10**).

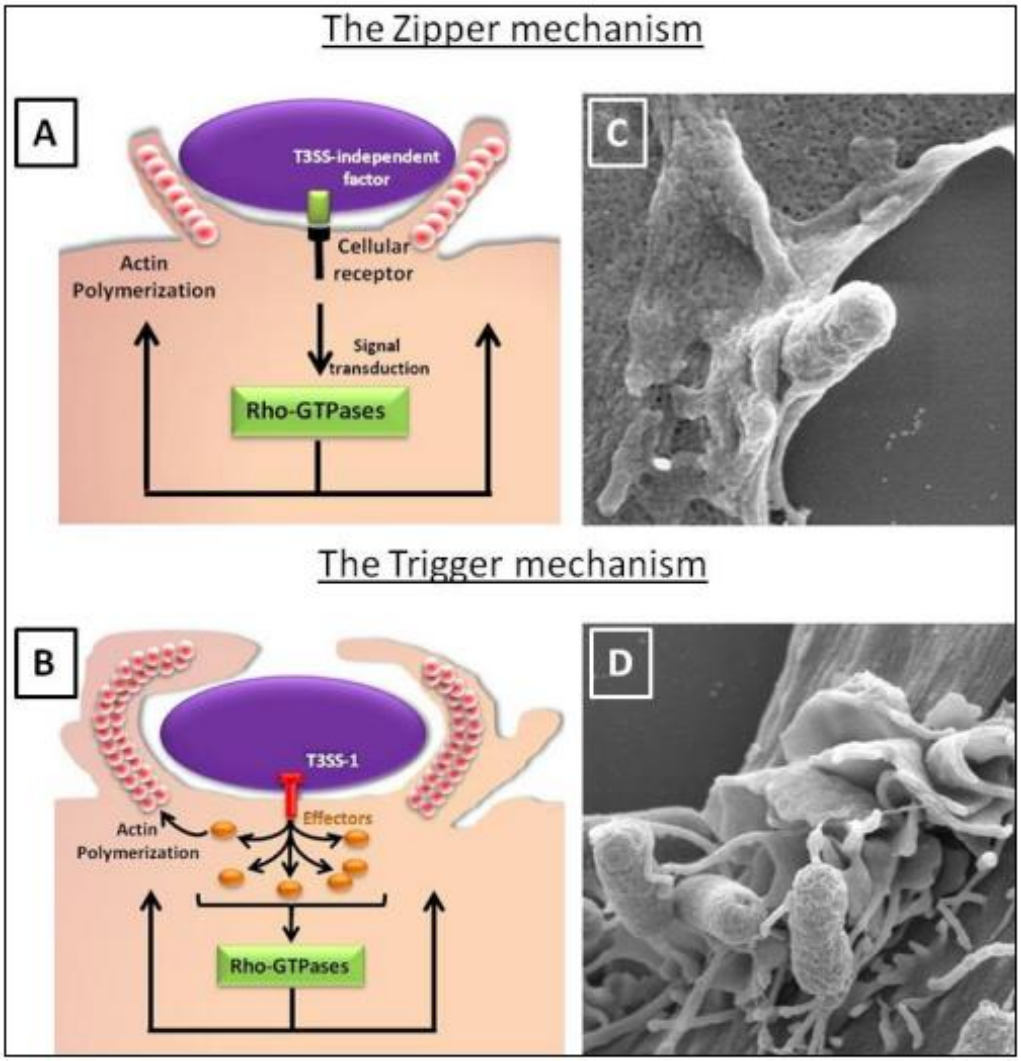

Figure 1.10. Schematic representation of the Zipper and Trigger mechanism (A, B), Scanning electron microscopy (C, D) of *Salmonella* entering into cells via a Trigger and Zipper mechanism, which is characterized by the apparition of large membrane ruffles at the bacterial entry site. [The Image adapted from Manon R, Nadia A, Fatemeh N, et al. (2012) The Different Strategies Used by Salmonella to Invade Host Cells. Salmonella - Distribution, Adaptation, Control Measures and Molecular Technologies. InTech. Available at: http://dx.doi.org/10.5772/29979.]

Another significant distinction between these pathways is that the trigger mode of entry is started by bacterial effectors that are secreted straight into the host cytoplasm by the bacterial secretion apparatus. These effectors bind to different host proteins and cause global actin ruffling. *Salmonella* Pathogenicity Island 1 (SPI-1) encodes a secretion apparatus termed T3SS-1 that is known to secrete effectors which are injected into host cells via this injectisome-like apparatus. It takes over the actin remodelling pathway and causes severe actin ruffling. However, external bacterial stimuli trigger the zipper method of entrance, mostly through attachment to certain cell-surface receptors. Both of these methods, however, work by taking control of and altering the pre-existing signalling pathways of the host cell in a way that benefits *Salmonella*. It has been found that *Salmonella* can invade host cells using both of these ways (120, 121). *Salmonella* invasion is identified by actin rearrangement at the site of entrance, which causes membrane ruffling and cytoskeletal remodelling (122-124). The Rho family of small GTPases regulates cell architecture by acting as either active or inactive GTP- or GDP-bound state, respectively. Guanine nucleotide exchange factors (GEFs) and GTPase activating proteins (GAPs), regulatory proteins that facilitate GTP loading and hydrolysis, respectively, regulate the activation state (125, 126). Generally, a pathogen can trigger these active/inactive stage switches irreversibly by covalent alterations, which frequently result in cell death, or reversibly through effectors that "mimic" the host-cell regulatory protein, thereby minimising cell damage. Similar to mammalian Rho-GEFs, SopE facilitates nucleotide exchange, which in turn activates the small GTPases of the Rho family. While SopE2 preferentially activates Cdc42, SopE stimulates both Rac1 and Cdc42 (127, 128). SopB is involved in modifying the metabolism of inositol phosphate (IP) and phosphoinositide phosphate (PIP) in the host. Studies have shown that a triple mutant of SopE, SopE2, and SopB is unable to invade eukaryotic cells (124). When *Salmonella* activates Rho GTPases, it sets off a complex signalling cascade that modifies actin dynamics and eventually results in invasion. The polymerization of monomeric

globular actin (G-actin) to filamentous actin (F-actin), which is necessary for the engulfment of bacteria, is facilitated by downstream effectors (**Figure. 1.11**). Arp2/3 complex is a probable target of Rho GTPases and can initiate actin nucleation, branching, and cross-linking (129). It has been reported that the Arp2/3 complex is recruited to membrane ruffles in cell lines that are triggered by *Salmonella* infection (130-132). Arp2/3 complex-mediated actin nucleation is facilitated by Rac1 and Cdc42. *Salmonella*-induced ruffles are formed by both WASP and Scar (131). However, bacterial entry was reduced by mutations of either or both proteins, indicating an actin rearrangement mechanism that is independent of Arp2/3. In addition to type III effector systems, *Salmonella* possesses effectors that can directly bind to actin that modify the cytoskeletal apparatus of the host (123). It has been demonstrated that SipC, has a crucial role in the translocation mechanism, and influences actin modulation. It has been demonstrated that the N-terminal and C-terminal domains of this protein are responsible for bundling of F actin and initiating actin polymerization, respectively (123). Another actin-binding protein called SipA can bind to G-actin and lower the critical actin concentration required for in vitro polymerization (133). Additionally, it has been noted that SipA makes the F-actin filament more stable and makes it easier for host actin binding proteins to bundle the filaments. SipA is thought to play a variety of roles, one of which is to modulate the placement of actin foci beneath the invasive bacteria, thus facilitating bacterial internalization. Cytoskeletal remodelling brought on by *Salmonella* invasion is usually temporary and goes away two to three hours after infection (134). SptP, a type III effector, is actively involved in this process. Tyrosine phosphatase is encoded by the C-terminus of SptP, and it is thought that the activity of this enzyme is crucial for suppressing pro-inflammatory reactions that are produced after infection (135).

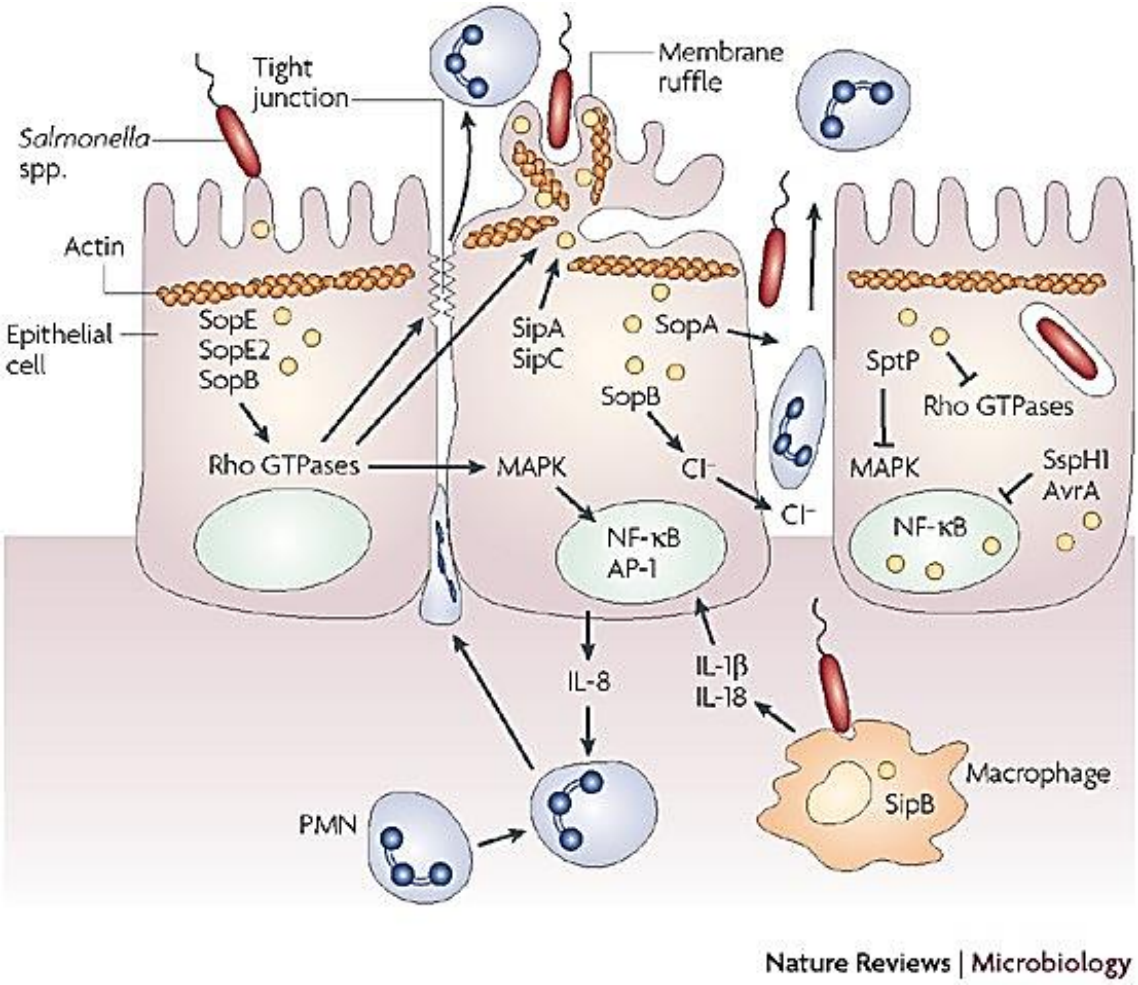

Figure 1.11. SPI1 T3SS-induced changes in host cells. Salmonellae assemble the type III secretion system (T3SS), which is encoded by *Salmonella* pathogenicity island 1 (SPI1), upon coming into contact with the epithelial cell. Translocated effectors are secreted from the type III system, released into the eukaryotic cytoplasm and initiate different changes for invasion. The image is adapted from Haraga A, Ohlson MB, Miller SI. Salmonellae interplay with host cells. Nat Rev Microbiol. 2008 Jan;6(1):53-66. doi: 10.1038/nrmicro1788. PMID: 18026123.

1.4.2.3. Intracellular survival

Following internalization, *Salmonella* releases several effectors that prevent phagosome maturation, leading to the development of specialised vacuoles known as *Salmonella*-

containing vacuoles, or SCVs, where it reproduces and survives. For survival inside macrophages, a secretion mechanism encoded by *Salmonella* Pathogenicity Island-2 (SPI-2), often referred to as T3SS-2, is crucial. One of the main characteristics of intracellular *Salmonella* pathogenesis is the formation of an actin coat around the bacteria, which promotes SCV fusion with vesicles containing actin and inhibits its fusion with other unfavourable compartments, protecting the SCV in the process (136). SopD2 prevents the fusion of SCV with the lysosomal compartment through inhibition of RILP (RAB-interacting lysosomal protein) - and FYCO1 (FYVE and coiled-coil domain containing protein 1) -mediated microtubule-based trafficking (137). After that, SCVs are transported by the microtubules to MTOC, or Microtubule Organising Centre, in the nuclear periphery (138). To maintain SCVs, it may also access membrane resources, which it uses to create a tubular network of structures known as *Salmonella*-Induced Filaments, or SIFs (**Figure 1.12**). The SPI2 effectors SifA and PipB2 control microtubule-motor accumulation on the SCV that aids in *Salmonella*-induced filament (Sif) production along microtubules (139). This facilitates the merging of SCVs within the infected cell.

Similar to GTPases, SifA has a carboxy-terminal Caax (cysteine (C)-aliphatic residue (a)-a-x) motif that is prenylated and S-acylated by host-cell enzymes. It may employ a GTPase-type mechanism for membrane localisation and Sif formation (140). In another study, it has been demonstrated that SifA binds to the host cell protein SKIP (SifA and kinesin interacting protein) (141). Studies showed that, SKIP depleted cells unable to form Sif suggesting that Sif formation requires SKIP. PipB2 can interact with SKIP (SifA and kinesin interacting protein). This interaction causes the removal of Kinesin from SCV (141). This intrusion is responsible for maintaining the integrity of SCV.

Additionally, intracellular *Salmonella* prevents the membrane trafficking of exocytic vehicles originating from the Golgi apparatus and repositions them to the SCV (142). The intracellular

replication of *Salmonella* was inhibited by inhibitors that interfere with the Golgi network, demonstrating that this phenomenon is essential for intracellular survival of *Salmonella* (138).

SseF and SseG tether SCV to the Golgi network and contributes to Sif formation and helps in the replication of *Salmonella* in SCV (142). These effectors encourage endosomal vesicle aggregation and attract Golgi-derived exocytic vesicles to the SCV implies that salmonellae can take over both endocytic and exocytic cellular transport mechanisms (143-146). It has been suggested that other effector such as, SseJ and SpvB have Sif downregulatory activities. Studies in the infection of cultured cells reported that their deletion can result in an increase in Sif production (147). Additionally, in the Nramp1-null animal model it has been observed that these effectors exhibit virulence abnormalities, suggesting that their actions contribute to systemic infection (148, 149). On the other hand, SpvB, an actin-specific ADP-ribosyl transferase promotes actin depolymerisation (148). To engage with the membrane surface, actin depolymerization may be necessary since some protein and phospholipid domains coated with polymerised actin may prevent them from binding to crucial areas of the phagosome membrane. Through the amino and carboxy termini, another effector SspH2 can interact with freshly polymerised actin, most likely by attaching to the actin binding proteins filamin and profilin. Another effector, SseI (also known as SrfH), has been demonstrated to bind to polymerised actin, most likely via filamin, and shares a high degree of similarity with the amino terminus of SspH2 (150).

During its intracellular phase, *Salmonella* evades and inhibits the innate and adaptive immune systems. PhoPQ is a two-component system that *Salmonella* uses to adapt to the intracellular environment. PhoP functions as a transcriptional regulator, whereas PhoQ is a membrane-bound protein that serves as a sensor. PhoQ detects the intracellular Mg++ and Ca++ concentrations of the host cell. PhoQ phosphorylates PhoP, causing it to become activated, when concentrations of these ions decrease. The inner and outer membrane proteins and

lipopolysaccharides of *Salmonella* are widely altered by activated PhoP (151). These changes provide resistance against antimicrobial activity by changing the surface charge density and membrane fluidity, which hinders antimicrobial peptides from penetrating the outer membrane (152). Additionally, these changes alter *Salmonella* lipopolysaccharide (LPS), making it less recognizable by the immune system and hence reduces its proinflammatory potential as indicated by the production of tumour necrosis factor (TNF-α). These offer bacteria a survival advantage in the harsh phagosome environment.

The PhoP/Q system regulates about forty genes, which are divided into two categories: PhoP repressed genes (psg) and PhoP activated genes (pag). PhoP-activated genes aid in evading the macrophage-killing process by being expressed inside the phagosome.

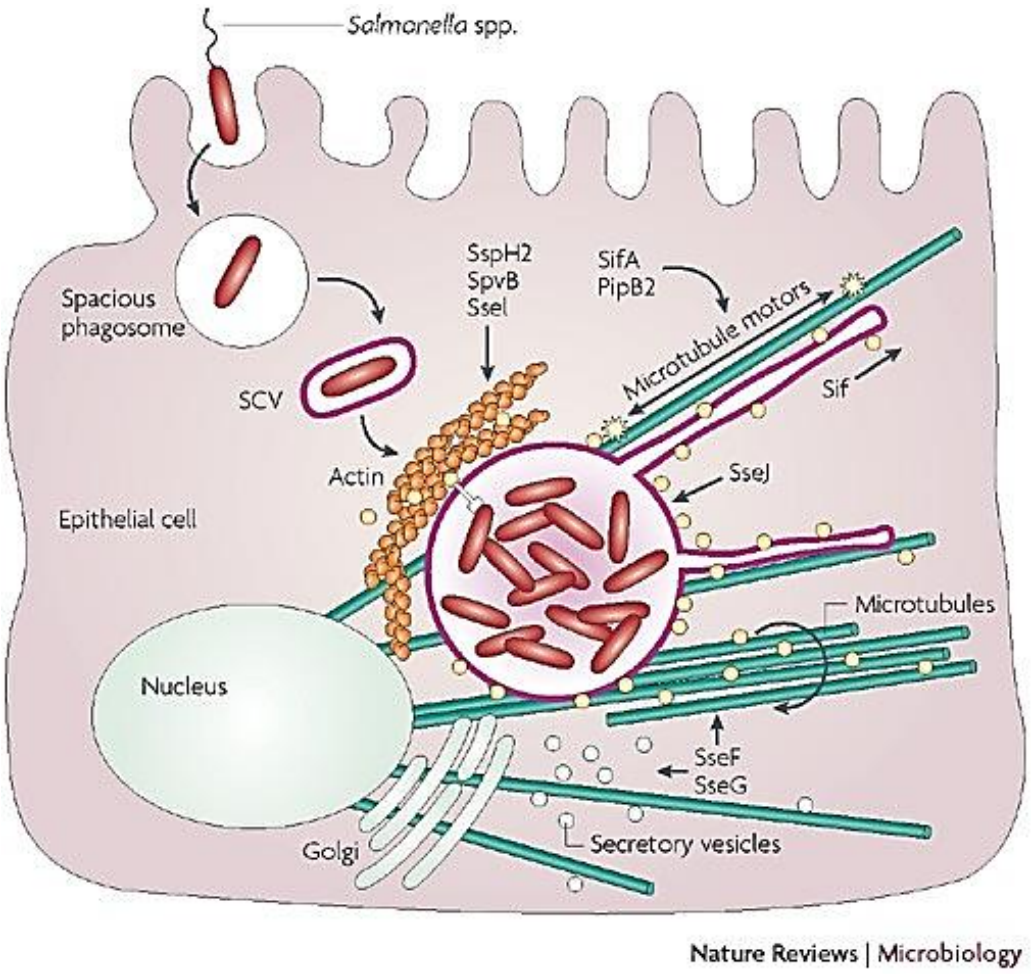

Figure 1.12. Formation of the SCV and activation of the SPI2 T3SS within the host cell. After the internalization within the host cell, *Salmonella* is engulfed within the membrane bound vesicles known as *Salmonella* containing vacuole (SCV). *Salmonella* pathogenicity island 2 (SPI2) T3SS (type III secretion system), which is generated within the SCV and helps in the survival and replication of the bacteria. [The image is adapted from Haraga A, Ohlson MB, Miller SI. Salmonellae interplay with host cells. Nat Rev Microbiol. 2008 Jan;6(1):53-66. doi: 10.1038/nrmicro1788. PMID: 18026123.]

1.4.2.4. *Salmonella* and Autophagy

Autophagy is a conserved intracellular process that transports undesired or damaged cytoplasmic components to lysosomes for degradation (153). Following invasion, the T3SS-1 system is down-regulated, which in turn triggers the T3SS-2 system because of the low pH, low $Mg2^{+}$ and $Fe3^{+}$ content, and reduced nutritional availability of the SCV (154). Although Type III secretion system T3SS-1 expression is necessary for invasion, this needle-like device may damage the SCV and have various negative effects on the pathogen. The SCV may rupture and let bacterial egress into the cytosol if the damage caused by T3SS is significant enough. Salmonella in the cytosol are quickly ubiquitin-tagged and targeted for autophagy by adaptor molecules such as p62, NDP52 (Nuclear Dot Protein 52 kDa), and OPTN (Optineurin). Autophagy receptors facilitate autophagosome formation by interacting with members of the Atg8 family, including LC3 (Microtubule-associated protein 1A/1B-light chain 3). Autophagy has the potential to target *Salmonella* that is present in damaged SCVs. Here, the altered carbohydrate structures on the SCV attract galectins, NDP-52, and ubiquitin to the membrane, designating these compartments for autophagic clearance. In contrast to antibacterial autophagy, *Salmonella* may assist to seal leaking SCVs by utilizing the autophagic apparatus.

This permits the successive acquisition of Rab5 and Rab7 to ensure T3SS-2 expression and compartment maturation, both of which promote intracellular survival (**Figure 1.13**) (155).

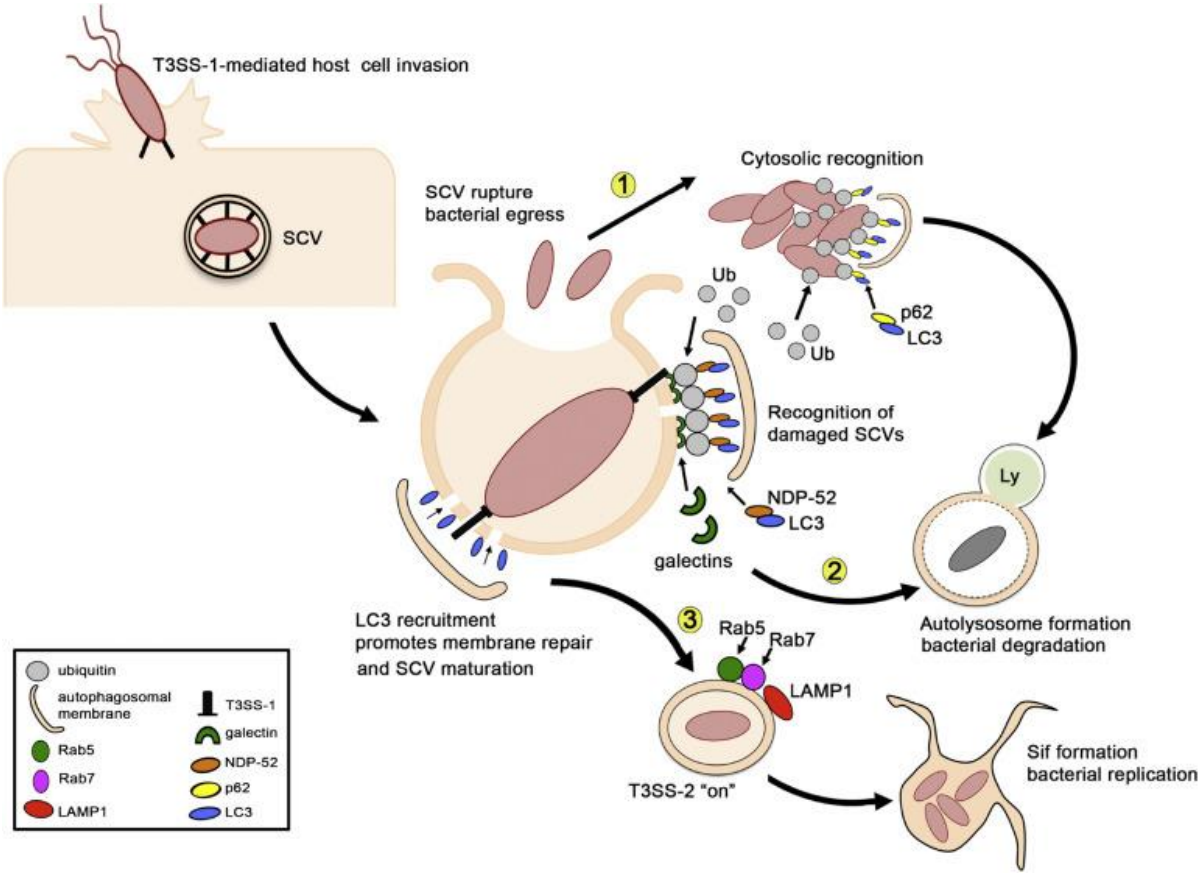

Figure 1.13. Escape of autophagy by *Salmonella*. [The image is adapted from Owen KA, Casanova JE. Salmonella Manipulates Autophagy to "Serve and Protect". Cell Host Microbe. 2015 Nov 11;18(5):517-9. doi: 10.1016/j.chom.2015.10.020. PMID: 26567504.]

Another study showed that *Salmonella* SPI-2 modulates signalling through the non-receptor tyrosine kinase FAK (focal adhesion kinase) to enhance intracellular survival in macrophages. When FAK is recruited to the surface of SCV in wild-type macrophages, more signalling via the Akt-mTOR pathway occurs, which suppresses the autophagic response. On the other hand, Akt/mTOR signalling is disturbed in FAK-deficient macrophages, which leads to the autophagic capture of intracellular bacteria and decreased bacterial survival. After an oral *S.*

Typhimurium infection, loss of FAK in macrophages led to the removal of bacteria from tissues in vivo. This study shows that the bacteria target FAK, which suppresses autophagy in macrophages and improves intracellular survival (**Figure 1.14**) (156).

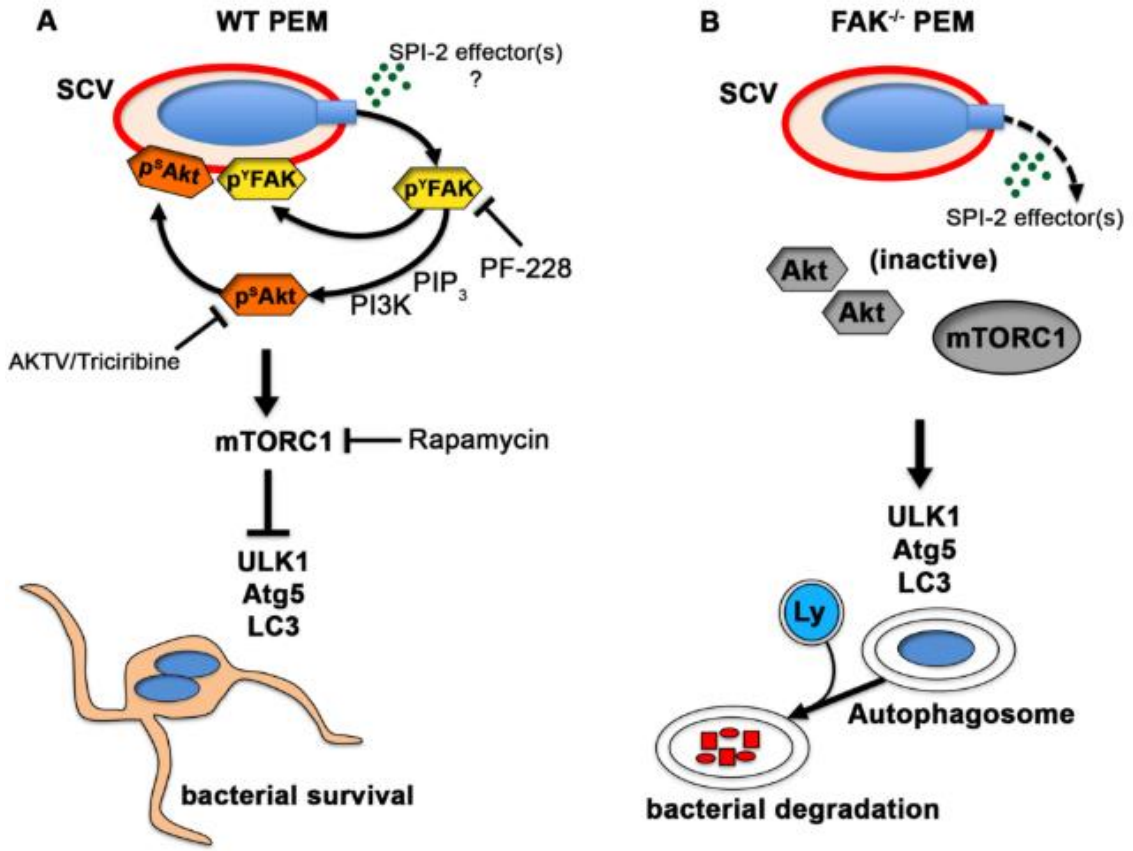

Figure 1.14. *Salmonella* SPI-2 system inhibits the autophagic uptake of intracellular *Salmonella* by initiating FAK activation. (A) SPI-2-compentent *Salmonella* in WT PEMs (Peritoneal exudate macrophages) activate and recruit to the SCV membrane via targeting FAK-Akt signalling. Strong increases in mTORC1 activation, which inhibits the autophagic response and encourages bacterial survival, coincide with increases in FAK and Akt activity. While LC3 recruitment to DinvG SCVs was decreased by pharmacological inhibition of FAK (PF-228) or Akt (AKTV/triciribine), LC3 colocalization with bacteria was boosted by mTORC1 (rapamycin) suppression, phenotyping circumstances seen in FAK-deficient macrophages. (B) When FAK is not present, Akt is dormant and cannot trigger mTORC1. LC3

is more effectively attracted to SCVs, which promotes the development of autophagosomes and improves the removal of intracellular microorganisms. [The image is adapted from Owen KA, Meyer CB, Bouton AH, Casanova JE. Activation of focal adhesion kinase by Salmonella suppresses autophagy via an Akt/mTOR signaling pathway and promotes bacterial survival in macrophages. PLoS Pathog. 2014 Jun 5;10(6):e1004159. doi: 10.1371/journal.ppat.1004159. PMID: 24901456; PMCID: PMC4047085.]

In the other study, it was found that SopF, a *Salmonella* T3SS effector can prevent autophagy. V-ATPase is recruited ATG16L1 (Autophagy-related 16-like 1) onto bacteria-containing vacuole upon bacteria-induced vacuolar damage. SopF targeted Gln124 of ATP6V0C in the V-ATPase for ADP-ribosylation. Thus, it inhibits the autophagy and facilitating *S.* Typhimurium survival in vivo (157) (**Figure 1.15**).

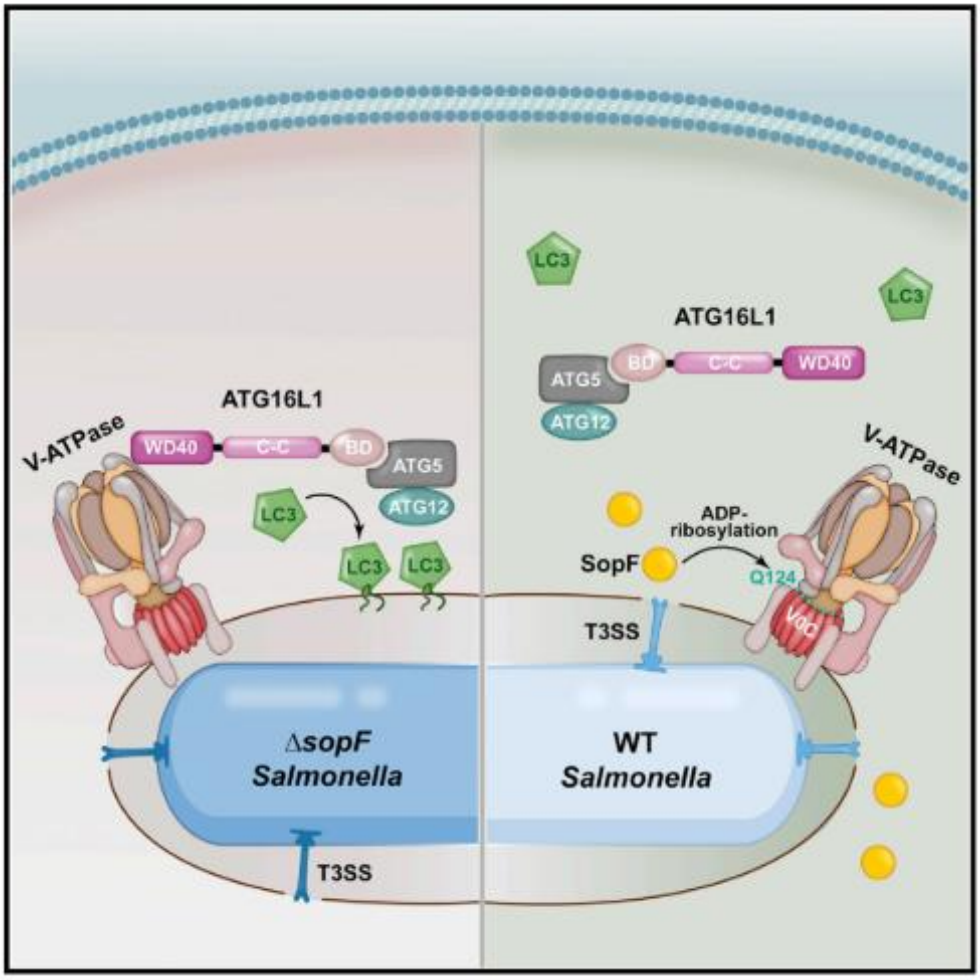

Figure 1.15. *Salmonella* escape from autophagy by effector SopE. When internalised bacteria cause damage to the resident vacuole during infection, the vacuolar ATPase detects this damage and recruits ATG16L1. However, an effector protein from pathogenic *Salmonella* blocks this defense response. [The image is adapted from Xu Y, Zhou P, Cheng S, Lu Q, Nowak K, Hopp AK, Li L, Shi X, Zhou Z, Gao W, Li D, He H, Liu X, Ding J, Hottiger MO, Shao F. A Bacterial Effector Reveals the V-ATPase-ATG16L1 Axis that Initiates Xenophagy. Cell. 2019 Jul 25;178(3):552-566.e20. doi: 10.1016/j.cell.2019.06.007. Epub 2019 Jul 18. PMID: 31327526.]

1.4.3. Pathogenicity islands of *Shigella*

Table 1.3. The features and functions of Pathogenicity islands of *Shigella*

PAIs	Size (Kb)	Genes	Function
Entry region Virulence plasmid PAIs	31	*virB*	Involved in the invasion of epithelial cells, immune evasion and cell to cell spread
		ipaB	Involved in the invasion of epithelial cells and induces apoptosis of the macrophages
		ipaCDA	Mediates endocytic uptake of bacteria
		ipgC	Molecular chaperons
		ipgA	Aids in the invasion of epithelial cells by promoting membrane ruffling and actin polymerization and facilitating intracellular spreading
		ipgB1	It is involved in altering host cell signaling pathways, which can affect cytoskeletal rearrangements and promote *Shigella* invasion and facilitating intracellular spreading
		icsB	It is involved in promoting actin-based motility and helping *Shigella* evade detection and destruction by the immune system
		ipgDEF	Modulation of Host Cell Signalling**, e**nhancement of Bacterial invasion, promotion of intracellular movement and **e**vasion of immune responses
		mxi, spa	Encode components of the Type III secretion system (T3SS), which is essential for the bacteria's ability to invade host cells and evade

			immune responses. These gene clusters work together to form a needle-like structure on the bacterial surface that injects effector proteins into host cells, manipulating cellular processes to favor bacterial invasion, survival, and spread
Chromosomal PAIs SHI-1	31	*sigA*	Intestinal fluid accumulation, cytopathic toxin
		pic	Mucus permeabilization, serum resistance, hemagglutination
		set1A, set1B	Intestinal fluid accumulation, development of watery diarrhea
SHI-2	19	*iucA to iucD, iutA*	Iron acquisition
		shiD	Colicin I and colicin V immunity
		shiA	Downregulation of inflammation by suppression of T-cell signaling
SHI-3	24	*iucA to iucD, iutA*	Iron acquisition (found only in *S. boydii*)
SHI-O	18	*gtrA, gtrB, gtrV*	Evasion of host immune response
SRL	20	*fecA to fecE, fecI, fecR*	Iron acquisition
		tetA to tetD, tetR	Tetracycline resistance
		Cat	Chloramphenicol resistance
		oxa-1	Ampicillin resistance
		aadA1	Streptomycin resistance

1.4.4. Pathogenesis of *Shigella*

Following ingestion, *Shigella* needs to withstand harsh gastrointestinal conditions, such as the acidic pH of the stomach and the bactericidal effects of bile salts during its journey to the colon. At this site, it up-regulates the acid-resistance genes, which allows it to withstand the low stomach acidity of the host (158). After consumption through the oral route, *Shigella* preferentially infiltrates the M cells covering the follicle-associated epithelium of the Peyer's patches after travelling down to the colon and rectum (159, 160) (**Figure 1.16**). Bacteria are transcytosed in the direction of the M cell pocket following their endocytosis by the M cells where they are taken up by resident macrophages. *Shigella*, however, can break down the vacuolar membranes, spread throughout the cytoplasm, and proliferate there (161). Massive inflammatory cell death is initiated by bacterial proliferation within the macrophages (162). *Shigella* released from dying macrophages then uses the basolateral surface to infiltrate the surrounding epithelium. Bacteria secretes a subset of T3SS effector proteins upon contact with epithelial cells causing actin rearrangement, which facilitates bacterial uptake (163) and subsequent processes like phagosomal escape, and cell-to-cell spread.

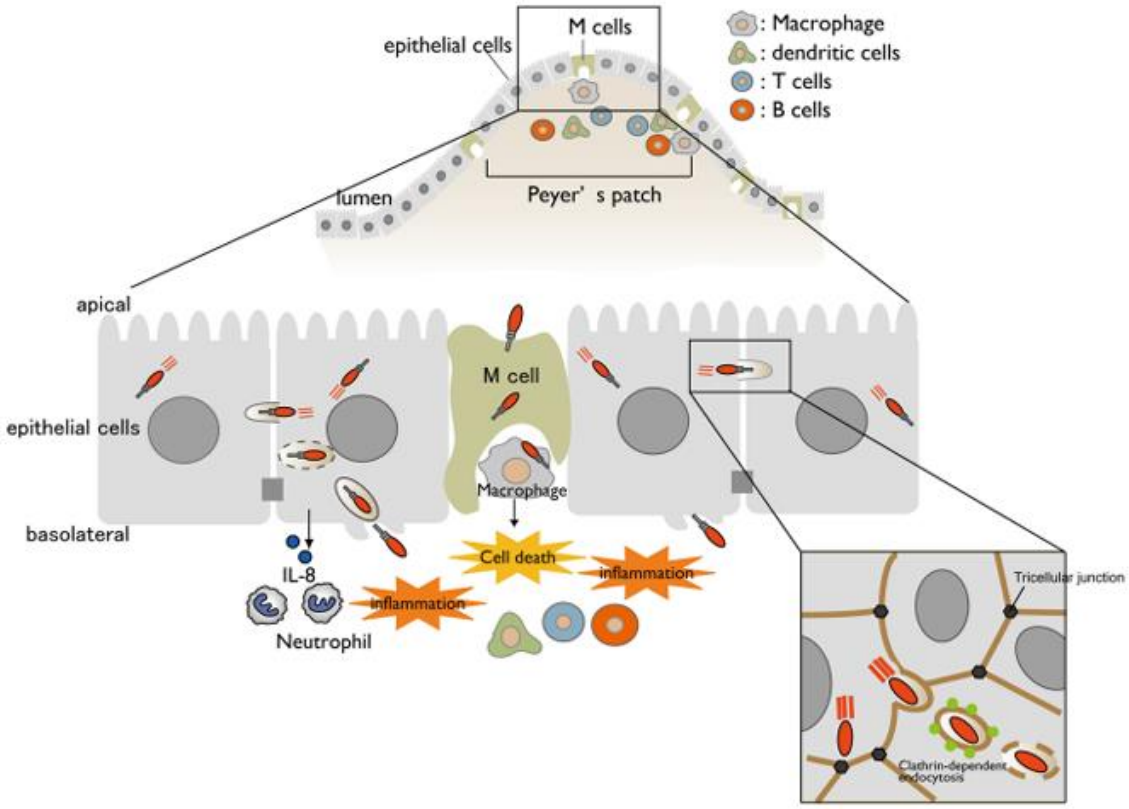

Figure 1.16. *Shigella* infection of the intestinal epithelium. Massive inflammatory colitis, also known as shigellosis, occurs due to bacterial invasion and proliferation within macrophages and epithelial cells. *Shigella* travels from cell to cell across tricellular junctions through clathrin-dependent endocytosis. [The image is adapted from Ashida H, Mimuro H, Sasakawa C. Shigella manipulates host immune responses by delivering effector proteins with specific roles. Front Immunol. 2015 May 7;6:219. doi: 10.3389/fimmu.2015.00219. PMID: 25999954; PMCID: PMC4423471.]

1.4.4.1. Entry into the host cell

The surface protein IcsA of *Shigella* first undergoes structural alterations dependent on bile salt to increase the polar adhesion to epithelial cells (164). The transcription of IcsA is temperature-dependent and is induced when *Shigella* enters the host. Bile salts also induce the translocation of the effectors, OspE1 and OspE2 which increases cellular adhesion through the OspE1/2

pathway (165). *Shigella* secretes mucins in the colon to pass through the mucus layer and onto the epithelial surface. The mucus layer acts as a physical barrier between the contents of the intestinal lumen and the immune system of the host. The thick mucus layer may limit oxygen transport, whereas the epithelium surface is rich in oxygen levels. *Shigella* detects the increased oxygen concentration at the epithelial surface and activates the Type three secretory system that enhances invasion through the epithelial cell.

Neighbouring epithelial cells are connected by tight junctions towards the apical side to create a barrier that is impermeable to fluid. *Shigella* invades polarised colonocytes on their basolateral side considerably more effectively than their apical side. The follicle-associated epithelium (FAE) of the M cells of the colon was the primary entry site of *Shigella* as observed in animal experiments and shigellosis patients (166-170). The FAE is distinguished from adjacent villus epithelial cells by lower mucus, antimicrobial peptides, and fucosylation levels. M cells are a component of the specialized epithelium that covers mucosa-associated lymphoid tissue, such as Peyer's patches of the small intestine, isolated lymphoid follicles, and cryptopatches (171) (**Figure 1.17**). M cells lack microvilli, have an apical microfold structure, and a huge pocket-like invagination on their basolateral side. These characteristics indicate that they are involved in immunosurveillance by the host (171). As a result, these cells are arranged to facilitate the deliberate extraction of bacteria from the intestinal lumen and transfer them to the basolateral side, where antigen-presenting cells like dendritic and macrophage cells are strategically positioned in or close to the M cell pocket to eliminate commensals and process antigens.

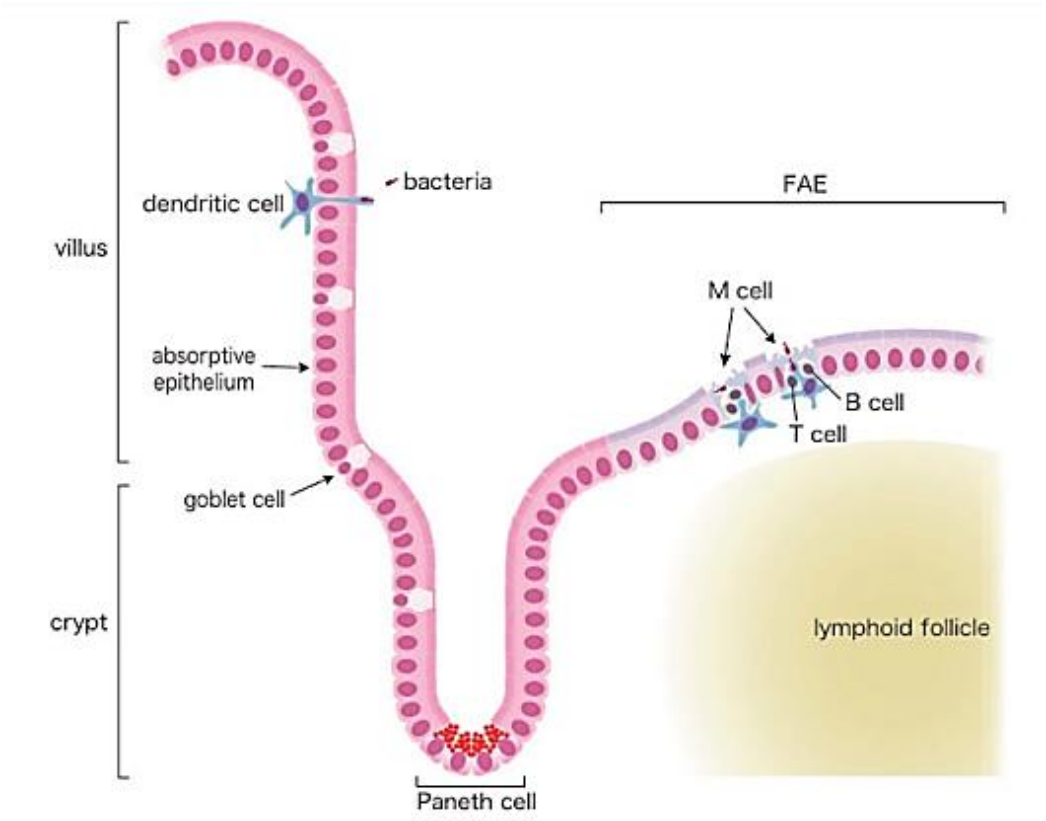

Figure 1.17. Structure of the M cell. [The image is adapted from Ohno H. Intestinal M cells. J Biochem. 2016 Feb;159(2):151-60. doi: 10.1093/jb/mvv121. Epub 2015 Dec 3. PMID: 26634447; PMCID: PMC4892784.]

As *Shigella* does not have fimbrial adhesin protein (172), the components of the needle complex, IpaB, IpaC, and IpaD, can bind α5β1 integrins as shown in Chinese hamster ovary cells, their overexpression enhances the invasion of *Shigella* in these cells (173). Furthermore, IpaB can mediate entrance via binding to the hyaluronic acid receptor CD44. These receptors are found on the basolateral side of polarised epithelial cells, suggesting a role for these receptors in the basolateral invasion of *Shigella*.

Shigella promotes ruffle formation at the cell surface through a complex containing multiple effectors, such as IpaC, IpaA, VirA, IpgD, and the guanine nucleotide exchange factors IpgB1 and IpgB2. These effectors stimulate actin cytoskeleton remodelling and actin polymerization. When IpaC is inserted into the host membrane, the C terminus faces the cytoplasm and attaches

itself directly to keratin 18 and vimentin intermediate filaments (174). The connection between vimentin and IpaC is required for *Shigella* to dock steadily with the host cell membrane and is also important for effector secretion (174). The C terminus of IpaC promotes actin remodelling through Rac1, Cdc42 and the activation of the tyrosine kinase Src (175). After Src is activated by IpaC, the actin-binding protein cortactin is phosphorylated and activated. Cortactin then interacts with the Arp2/3 complex and Src-related tyrosine kinase CrK to promote actin polymerization and actin remodelling surrounding the entry site.

Another essential effector for entrance is IpaA. IpaA promotes actin filament depolymerization, which inhibits the uncontrollably formed microspike structures caused by IpaC and controls the production of actin protrusions (176). Vinculin, a cytosolic actin-binding protein rich in focal adhesions that connects integrin adhesion molecules to the actin cytoskeleton, is directly bound by IpaA (177). Vinculin binds to the C-terminal domain of IpaA and increases the affinity for F-actin. This causes the capping of the barbed end of actin filaments and prevent monomer addition thus encouraging the F-actin depolymerization. Simultaneously, IpaA triggers actin cytoskeletal rearrangements by binding to β1 integrins and increasing the GTPase activity of RhoA, making inactivation of RhoA. This causes the disintegration of stress fibres and releases actin for the generation of membrane ruffles via the ROCK (Rho-associated protein kinase)–myosin II pathway.

Similar to IpaC, IpgB1 increases the activity of Rac1 and Cdc42 by keeping them in their GTP-bound state. This promotes the production of ruffles that is dependent on the Arp2/3 complex. Furthermore, to increase Rac1 activity, VirA may indirectly destabilize microtubules (178, 179). As opposed to IpaA, IpgB2 increases the GDP-GTP exchange of RhoA, which in turn promotes actin nucleation and stress fibre production. As a result, *Shigella* specifically targets stress fibres for disintegration and generation in a coordinated manner to facilitate bacterial entry. Additionally, the effector IpgD facilitates entry by hydrolyzing phosphatidylinositol 4,5-

bisphosphate [PI(4,5)P2]. This process facilitates actin dynamics at the invasion site by weakening the attachment between cortical actin and the membrane (180) (**Figure 1.18**).

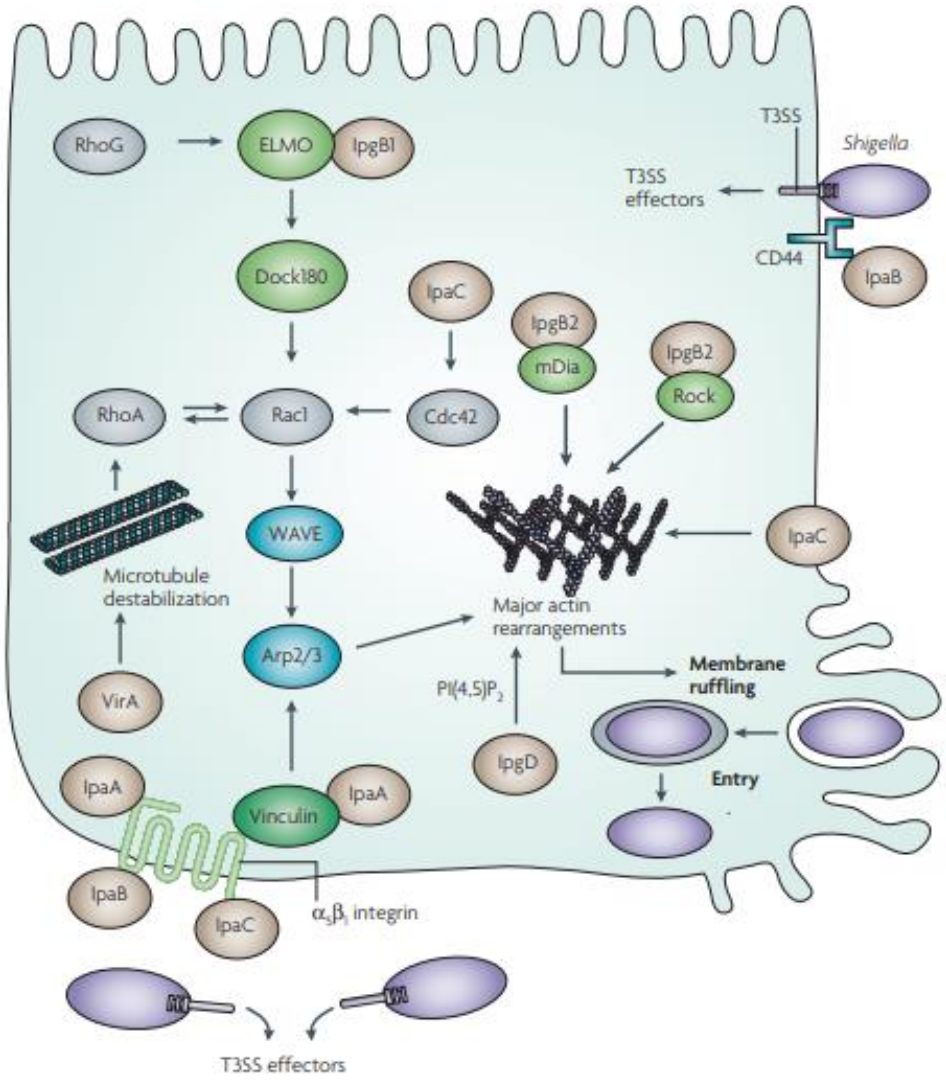

Figure 1.18. Membrane-ruffle production by *Shigella* effectors. *Shigella* distributes multiple effectors into the cytoplasm of the host cell via the type III secretion system (T3SS), which causes membrane ruffles to protrude surrounding the bacterial entrance point, by engaging with their host binding partners. [The image is adapted from Ogawa M, Handa Y, Ashida H, Suzuki M, Sasakawa C. The versatility of Shigella effectors. Nat Rev Microbiol. 2008 Jan;6(1):11-6. doi: 10.1038/nrmicro1814. PMID: 18059288.]

1.4.4.2. Phagosomal escape

Shigella invasion of epithelial cells and phagosomal escape are difficult processes to investigate because they are rapid events that last less than 15 minutes. A functional T3SS is necessary for phagosomal rupture, which is aided by *Shigella* effectors, such as IpgB1, IpgB2, and IpgD (164, 181). *Shigella* resides within a small vacuole (Bacteria containing vacuole, BCV) where the bacteria are in close contact with the phagosomal membrane, despite the tremendous ruffling that occurs after invasion. Ruffling causes macropinosomes to develop around the point of entrance. In the region of bacterial entrance, IpgD activity stimulates the development of ruffles, macropinosomes, and the recruitment of GTPase Rab11 to macropinosomes (**Figure 1.19**) (165). *Shigella* thereby triggers macropinosome formation but through the action of IpgD initiates a novel vesicular trafficking pathway that is dependent on the formation of modified macropinosomes to mediate phagosomal lysis.

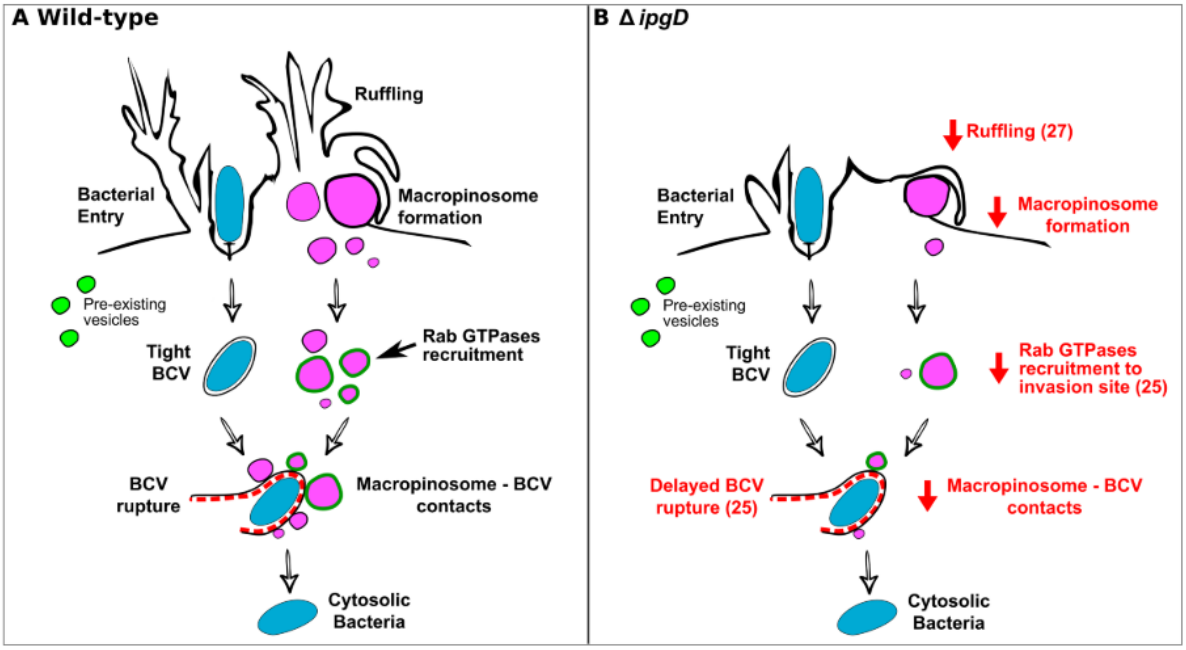

Figure 1.19. Micropinosome formation and phagosomal escape following invasion of *Shigella flexeneri*. (A) *S. flexneri* (blue) enters a tight BCV and causes membrane ruffling, which leads to the development of macropinosomes (pink). Following this, macropinosomes

are recruited by Rab GTPases (dark green). At the beginning of vacuolar rupture, macropinosomes and the BCV finally come into direct touch (dashed line), allowing the bacteria to escape into the cytosol. Endocytic vesicles that already exist (light green) are not drawn to the invasion site. (B) Vacuolar rupture is postponed due to the deletion of ipgD. [The image is adapted from Weiner A, Mellouk N, Lopez-Montero N, Chang YY, Souque C, Schmitt C, Enninga J. Macropinosomes are Key Players in Early Shigella Invasion and Vacuolar Escape in Epithelial Cells. PLoS Pathog. 2016 May 16;12(5):e1005602. doi: 10.1371/journal.ppat.1005602. PMID: 27182929; PMCID: PMC4868309.]

When *Shigella* are engulfed in phagosome/endosome, IpaB/C complex on the tip of T3SS was inserted in the membrane. Virulence factors are secreted into the cytoplasm via T3SS, triggering host cell apoptosis, cytoskeleton rearrangement etc. Secreted IpaB protein forms a tetramer complex with inserted membrane which forms the ion channel. IpaB ion channels allow positive charge inflows and outflows of small molecules then phagosome/endosome disruption occurs (182) (**Figure 1.20**).

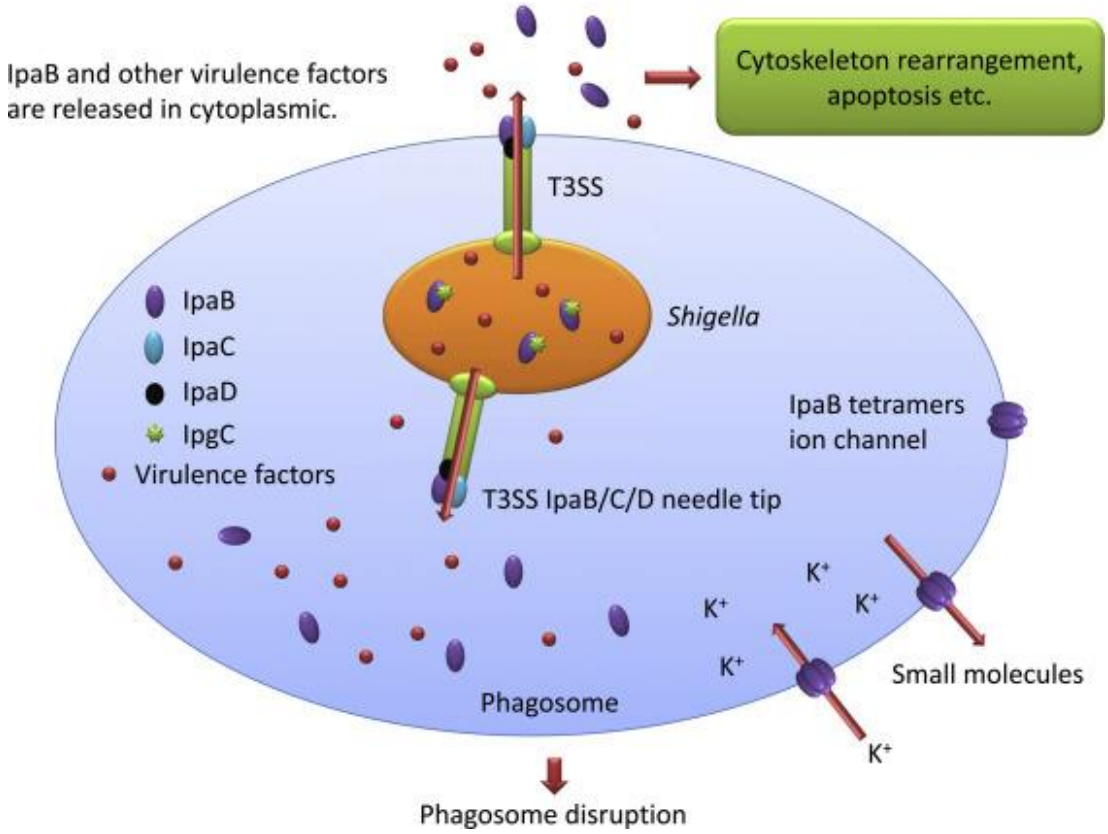

Figure 1.20. Escape of *Shigella* from phagosome/endosome. IpaB/C complex on the tip of T3SS was inserted into the membrane during *Shigella* residence into the phagosome/endosome. The phagosome/endosome is disturbed when positive charge inflows and outflows through IpaB ion channels are allowed. [The image is adapted from Yang SC, Hung CF, Aljuffali IA, Fang JY. The roles of the virulence factor IpaB in Shigella spp. in the escape from immune cells and invasion of epithelial cells. Microbiol Res. 2015 Dec;181:43-51. doi: 10.1016/j.micres.2015.08.006. Epub 2015 Sep 2. PMID: 26640051.]

1.4.4.3. *Shigella* escapes macrophages by inducing pyroptosis

Macrophages are primarily responsible for the detection, phagocytosis, and eventual death of microorganisms as well as the induction of an inflammatory response. Pathogens have developed different ways to circumvent them because of their crucial role in the bacterial elimination. *Shigella* can evade macrophages by initiating pyroptotic macrophage death.

(**Figure 1.21**) (183). Pyroptosis is a highly inflammatory form of programmed cell death that occurs when cytosolic pattern recognition receptors (PRRs) detect danger signals known as microbe-associated molecular patterns (MAMPs) and danger-associated molecular patterns (DAMPs). This detection triggers the release of proinflammatory cytokines and lytic cell death (184).

Shigella rapidly trigger pyroptotic cell death and activate the NLRP3 or NLRC4 inflammasomes, which results in the release of IL-1β and IL18, when they infiltrate and proliferate within macrophages (185-188). which bind to the IL-1 and related IL-18 receptors in a MyD88- and TRAF-dependent manner. This interaction initiates NF-κB- and mitogen-activated protein kinase (MAPK)-signaling pathways (189). Moreover, IL-1β attracts neutrophils and triggers a Th17 response, whereas IL-18 triggers the generation of gamma interferon by T and NK cells, which amplifies the antimicrobial activity of macrophages by generating nitric oxide. This results in the release of additional proinflammatory cytokines, such as IL-6 and tumour necrosis factor alpha. Members of the NAIP subfamily of NLRs, which function as direct pathogen recognition sensors and ascertain the specificity of the NLRC4-inflammasome for different bacterial ligands, are used by T3SS needle or rod components to indirectly activate NLRC4 inflammasomes. According to recent studies, *Shigella* T3SS needle protein MxiH is bound by both human and murine NAIP1 (190, 191). Furthermore, the T3SS inner rod component MxiI (186, 192) is bound by NAIP2 (**Figure 1.21**). Despite the absence of flagells in *Shigella*, some bacterial flagellins cause NAIP5 and NAIP6 to selectively activate the NLRC4-inflammasome (193-196). These NAIP proteins attach to NLRC4 after binding to their ligands, which causes pyroptosis and NLRC4-inflammasome activation. Apart from the components of bacterial T3SS, *Shigella*-induced cellular damage also sets off pyroptosis and inflammasome activation (**Figure 1.21**).

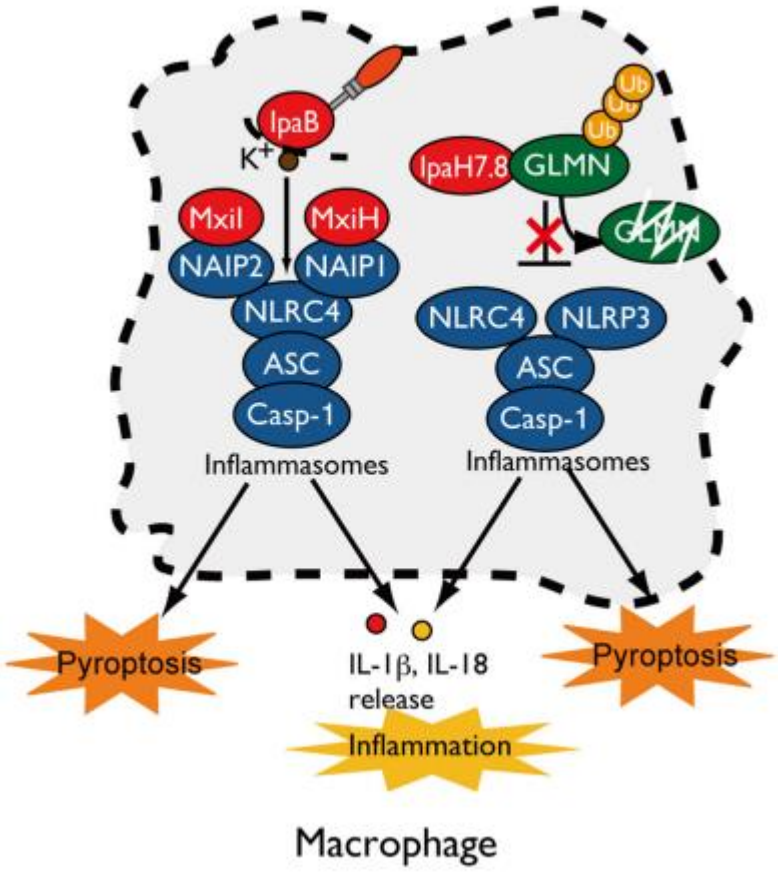

Figure 1.21. Macrophage cell death. Pyroposis or Pyonecrosis is caused by NLR inflammatory assembly and is triggered by PAMPs or DAMPs produced by *Shigella* invasion and proliferation in macrophages. [The image is adapted from [Ashida H, Mimuro H, Sasakawa C. Shigella manipulates host immune responses by delivering effector proteins with specific roles. Front Immunol. 2015 May 7;6:219. doi: 10.3389/fimmu.2015.00219. PMID: 25999954; PMCID: PMC4423471.]

IpaH7.8, a *Shigella* effector causes rapid macrophage pyroptosis by activating NLRP3- and NLRC4-dependent inflammasomes (197). *Shigella*, *Salmonella*, *Yersinia*, and *Pseudomonas* spp. are among the Gram-negative bacterial pathogens that heavily conserve IpaH family effectors, which have a new E3 ubiquitin ligase function (198). IpaH7.8 ubiquitinates the

Cullin-RING E3 ligase inhibitor GLMN (glomulin/flagellar-associated protein 68) and degrades it in a proteasome-dependent manner (**Figure 1.21**) (197). Degradation of this component causes pyroptosis and inflammasome activation because GLMN functions as a negative regulator of NLR inflammasomes. In vitro observations showed that mice intranasally infected with *Shigella* WT or ΔipaH7.8/WT complement strains exhibit more severe inflammatory responses and higher numbers of colonized bacteria compared to ΔipaH7.8 or ΔipaH7.8/CA E3 ligase-deficient mutant complemented strains (197, 198). Therefore, IpaH7.8-mediated macrophage cell death is a necessary to escape from macrophages, penetrate adjacent epithelial cells, and disseminate to neighbouring cells.

1.4.4.4. Survival of *Shigella flexneri* in epithelial cells

Shigella has developed strategies to evade host antimicrobial defences and protect the replicative niche from being destroyed. Autophagy is a key host defence mechanism that *Shigella* needs to evade to survive in the host cells (199). *Shigella* can be recognized by both canonical and noncanonical autophagy pathways; however, autophagic capture is inhibited by at least three effectors: IcsP, IcsB and VirA. When the bacterial entry site detects the *Shigella* peptidoglycan, the cytosolic sensor NOD1 recognises it, which recruits autophagic factor ATG16L1 and promotes autophagy (200). *Shigella* is prone to recognition by the complement system before invasion, resulting in the coating of bacteria with complement C3 split products (201). Surface-deposited C3 interacts directly with the autophagy marker ATG16L1, directing bacteria towards autophagy in the cytoplasm of the host cell. However, *Shigella* disrupts this process by excreting C3, partly due to the proteolytic activity of surface protease IcsP (belongs to the omptin protease family) (201) (**Figure 1.22**).

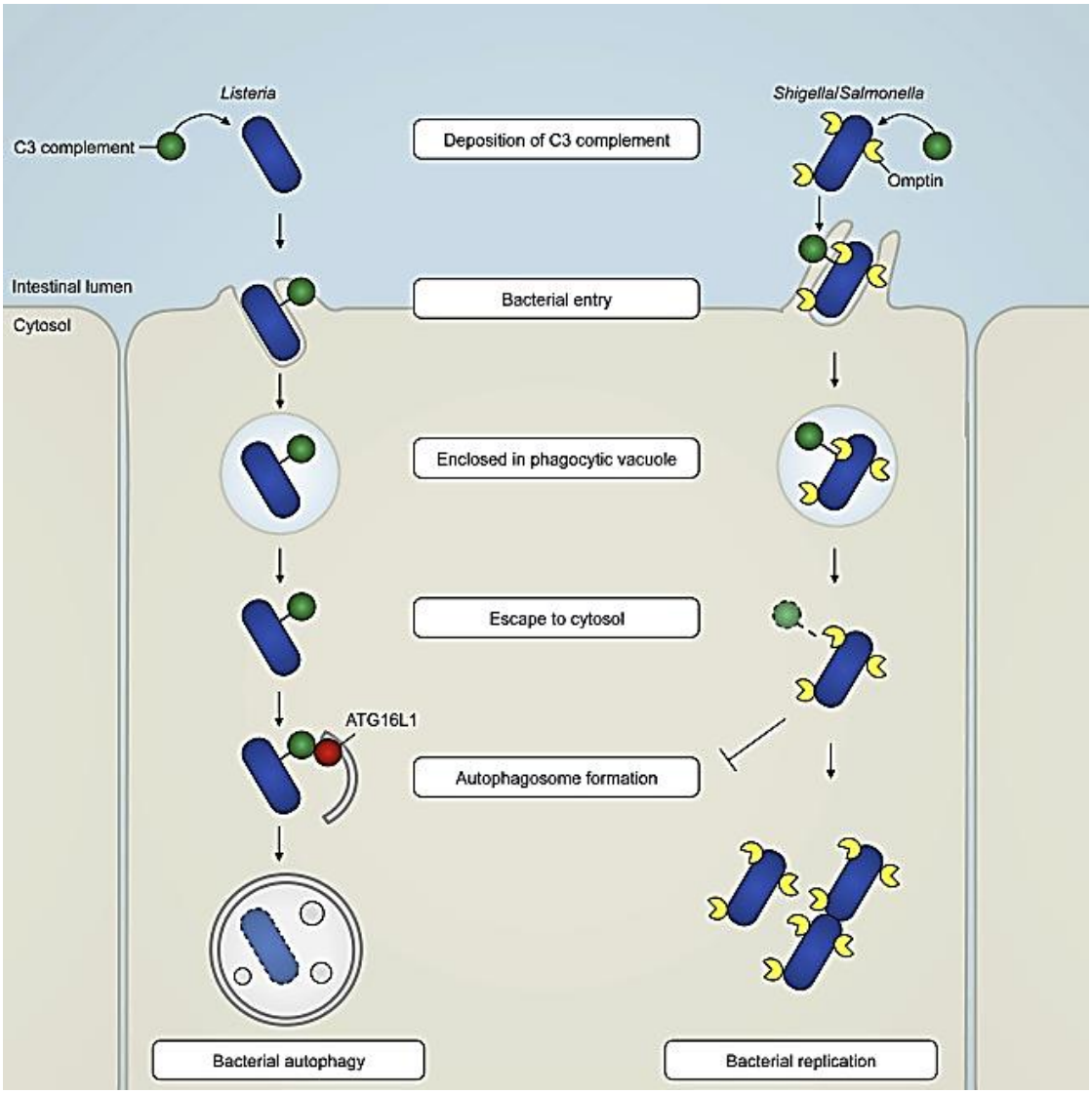

Figure 1.22. Interaction of the complement with the bacterial autophagy in the intestinal mucosa. *Shigella* express omptins, which are responsible for removing the C3 coating that prevents cytosolic bacteria from adhering to the C3-mediated autophagy limitation. [The image is adapted from Sancho-Shimizu V, Mostowy S. Bacterial Autophagy: How to Take a Complement. Cell Host Microbe. 2018 May 9;23(5):580-582. doi: 10.1016/j.chom.2018.04.010. PMID: 29746830.]

Another mechanism of the induction of *Shigella* autophagy by host using septins (202). These GTP-binding proteins can form filaments that interact with microtubules, actin filaments, and cellular membranes, making them a component of the cytoskeleton network (202). In response

to IcsA-mediated actin polymerization, septins are accumulated and form cages surrounding cytosolic *Shigella*. Septin cages limit the mobility of *Shigella* and utilise autophagic adaptors p62 and NDP52 (nuclear dot protein 52) which bind the the major autophagy marker LC3. This interaction initiates autophagosome formation and eliminate *Shigella* by autophagy (203). This process is hindered by the effector IcsB via *Shigella* actin-mediated motility (204, 205). IcsB binds to Toca-1 (transducer of CDC42-dependent actin assembly 1), a host protein required for effective actin polymerization, effectively blocking LC3 and NDP52 targeting (**Figure 1.23**). *Shigella* can enter the cell and eventually find new replicative niches in nearby cells after phagosomal lysis.

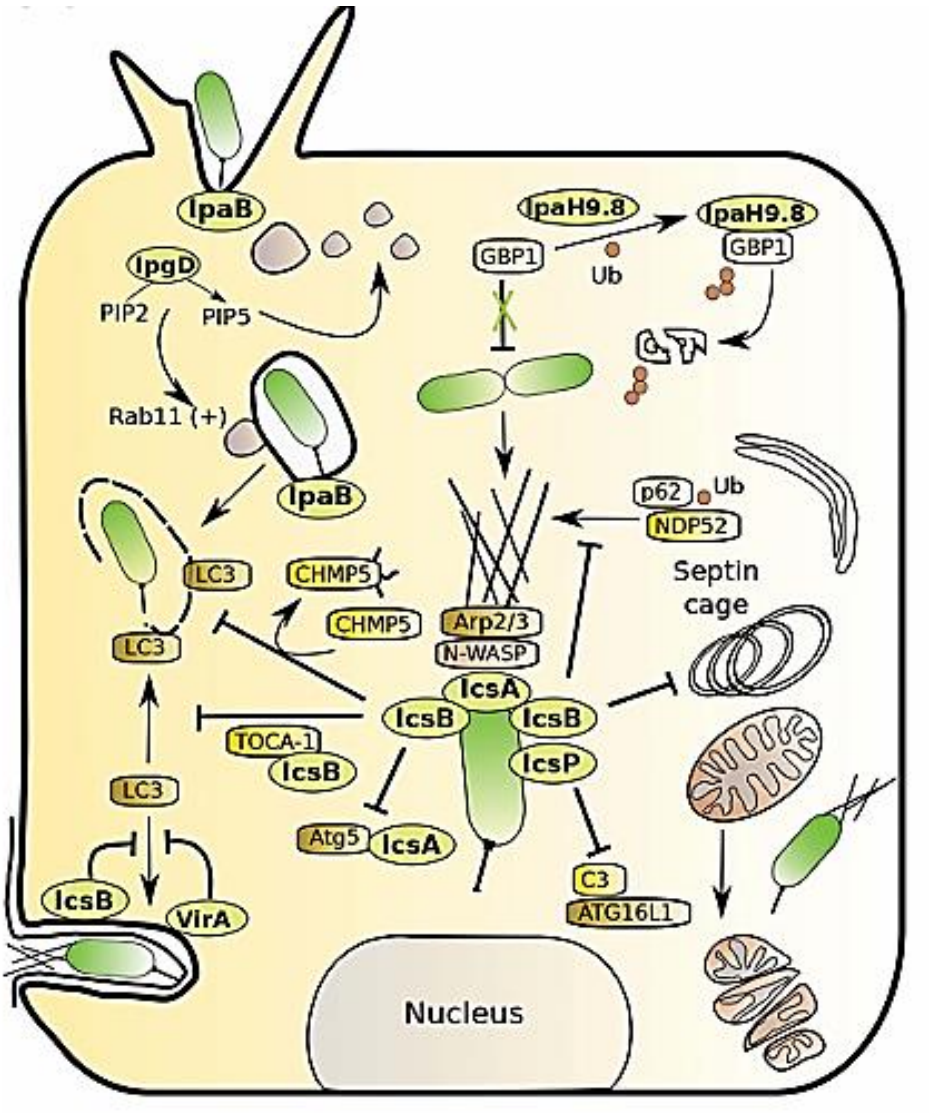

Figure 1.23. Antimicrobial defenses modulated by *Shigella*. *Shigella* actively inhibits important signalling pathways in epithelial cells to reduce the cellular proinflammatory response. [The image is adapted from Schnupf P, Sansonetti PJ. *Shigella* Pathogenesis: New Insights through Advanced Methodologies. Microbiol Spectr. 2019 Mar;7(2). doi: 10.1128/microbiolspec.BAI-0023-2019. PMID: 30953429.]

Shigella also interferes with autophagy by using the T3SS effector VirA. In addition to playing a crucial role in the entrance process (206), VirA prevents autophagosome formation by interfering with the movement of vesicles from the ER to the Golgi. VirA activates the GTPase activity of the small GTPase Rab1, rendering Rab1 inactive and unable to direct vesicle traffic from the ER to the Golgi apparatus (207, 208). Vir A in association with IcsB prevents autophagy by mediating phagosomal escape from the double membrane phagosome formed during cell-to-cell dissemination.

1.4.4.5. Maintenance of the epithelial cell cytosolic replicative niche

Shigella enters and multiplies in the cytosol, a relatively nutrient-rich environment. *Shigella* increases the expression of enzymes involved in glycolysis and mixed-acid fermentation while downregulating those involved in oxidative respiration to adapt to the low-oxygen environment of the epithelial cytosol (209). *Shigella* growth requires iron as a micronutrient, and it can obtain intracellular iron through a variety of mechanisms, such as siderophore expression and the uptake of heme or ferric and ferrous iron through specific iron transport systems, which *Shigella* upregulates in response to the low iron accessibility in the cytosolic milieu (210). The host amino acid starvation response is triggered by *Shigella* infection. This results in the activation of the sensor kinase GCN2 (general control nonderepressible 2), which in turn phosphorylates the master regulator eIF2α (eukaryotic initiation factor 2α) downstream (211). Global

translation initiation is blocked by phosphorylated eIF2α, while selective translation of the transcription factor ATF4 is enhanced. When combined with ATF3, this transcription factor increases the transcription of stress-related genes involved in amino acid metabolism and protection against oxidative damage.

Shigella reproduces intracellularly by polymerizing actin at one bacterial pole to create actin comet tails, which enable the production of protrusions carrying bacteria at the cell plasma membrane that infiltrate neighbouring cells. IcsA (VirG), the outer membrane protein of *Shigella* generates the driving force behind this intra- and intercellular dissemination (212-214). On the bacterial surface, IcsA is expressed unipolarly (215). It appears that two internal areas immediately target newly synthesised IcsA to the old pole, where it is automatically transferred to the outside membrane (216, 217). However, another protein DegP is necessary for the effective intracellular dissemination and polarised expression of IcsA (218). Besides this, N-WASP and vinculin proteins are interacting partners of IcsA at the bacterial pole (219-221). Arp 2/3 complex-mediated actin polymerization is stimulated by IcsA-specific binding of N-WASP (222, 223). The ability of *Shigella* to exploit actin-based motility may be dependent on the host cells that recognize its ligand specificity (IcsA–N-WASP) (223) (**Figure 1.24**). The actin polymerization at the bacterial pole produces a propulsive force that pushes the bacteria through the cytoplasm of the cell, where it protrudes into the adjacent epithelial cell (224). This process is dependent on myosin light chain kinase and cadherin expression of the adjacent cell (225, 226). Afterward, IpaB and IpaC are released to lyse the cellular membranes surrounding the bacteria (227). It has also been demonstrated that VacJ, another protein, is necessary for releasing *Shigella* into the cytoplasm of the subsequent cell (228). *Shigella* can therefore multiply and proliferate within the intestinal epithelial layer without coming into contact with the external environment or the immune cells that circulate in it.

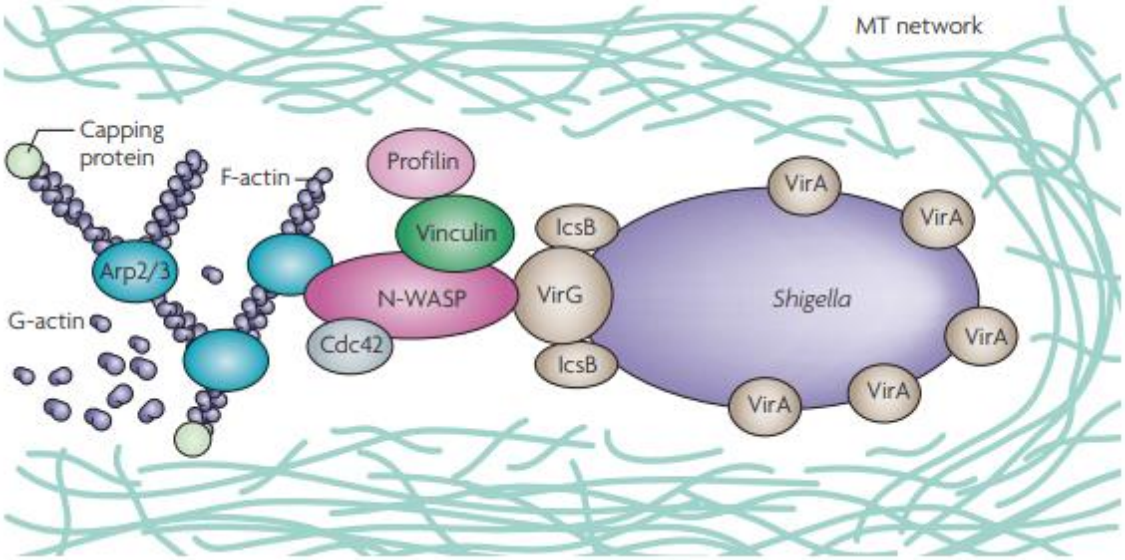

Figure 1.24. Actin polymerization and microtubule degradation enhance *Shigella* movement within the host-cell cytoplasm. Migration of *Shigella* through the polar region of epithelial cells is dependent upon the asymmetric distribution of VirG, often referred to as IcsA, on the bacterial surface. VirG interacted with N-WASP and activates the Arp2/3 complex, which facilitates the migration of bacteria. [The image is adapted from Ashida H, Mimuro H, Sasakawa C. Shigella manipulates host immune responses by delivering effector proteins with specific roles. Front Immunol. 2015 May 7;6:219. doi: 10.3389/fimmu.2015.00219. PMID: 25999954; PMCID: PMC4423471.]

1.5. Clinical presentations of *Salmonella* and *Shigella*

1.5.1. Clinical presentations of *Salmonella*

Salmonella causes two forms of the disease in humans: typhoid fever and gastroenteritis. The latter is also known as non-typhoidal salmonellosis.

1.5.1.1. Enteric Fever or Typhoid

Typhoidal *Salmonella* is mostly transmitted via tainted food or water that comes into contact with human excrement. For a week or more, people with enteric fever experience a range of symptoms, including high fever, diarrhoea, vomiting, and headaches (229). This is known as the incubation phase. A distinct fever pattern appears with enteric fever. A low-grade fever (>37.5 ◦C to 38.2 ◦C) is first observed, and in the second week, it progressively increases to a high-grade fever (>38.2 ◦C to 41.5 ◦C) (230). If the fever is not treated appropriately, it may last up to a month (231). Infected person may also have experienced frontal headache, malaise, anorexia, sore throat, dry cough, scattered abdomen pain, nausea, myalgia, bradycardia, splenomegaly (enlarged spleen), hepatomegaly (enlarged liver), and rose blotches (a blanching erythematous maculopapular rash with lesions ranging in size from 2 to 4 mm) on their chest abdomen, and occasionally the back, arms, and legs (232-234). Pancreatitis, hepatitis, and cholecystitis are among the gastrointestinal issues that affect 15% of infected people in endemic locations (235).

1.5.1.2. Enterocolitis and Diarrhoea

Human gastroenteritis which is self-limiting, is associated with non-typhoidal *Salmonella* infection. The infection typically lasts for four to seven days, with an incubation period that varies from six hours to six days. The bacteria may continue to shed through faeces for up to one month (236). Gastroenteritis is the most common human symptom, with accompanying clinical indicators such as headache, nausea, vomiting, abdominal pain, non-bloody diarrhoea, and muscle soreness (237). Immunocompromised patients and children under five years of age are among the sensitive groups where the severity of the infections increases (238). Acute illnesses such as pancreatitis, appendicitis, and cholecystitis can develop and worsen, resulting in potentially fatal disorders including sepsis and meningitis (239). Additionally, *Salmonella* infections are linked to colonic cancer development in individuals with chronic inflammatory bowel disease (IBD) (240), as well as being a risk factor for colorectal and gallbladder cancer

(241). After colonization of the bacteria at the apical epithelium of the intestine, it activates virulence factors associated with invasion. This causes inflammation, which is manifested as fluid secretion, crypt abscesses, focal and diffused PMN infiltration, epithelial necrosis, and edema (242, 243). The distinctive histological marker of inflammatory gastrointestinal illness is neutrophil recruitment to the intestinal epithelium. According to in vitro studies, the ability of *S.* enterica to draw PMNs without causing epithelial invasion is correlated with the induction of intestinal diseases in humans (244).

1.5.2. Clinical presentations of *Shigella*

Shigellosis can cause moderate watery diarrhoea or bloody mucoid diarrhoea, which can be accompanied by fever, excruciating cramping in the abdomen, and other symptoms. The most typical extraintestinal symptoms of shigellosis are neurological in nature, including fatigue, disorientation, intense headaches, and convulsions, meningitis or irritation of the meninges, encephalitis, and seizures (245). Children with seizures usually have a high temperature or abnormal blood electrolytes. Toxic megalocolon is a significant complication in newborns and young children. Other potential complications include hemolytic-uremic syndrome (HUS) and post infectious arthritis. In HUS patient, the bacterium enters the digestive tract and produces toxin that kills red blood cells. Bloody diarrhoea is a common symptom in HUS patients. HUS is only affiliated with strains of *Shigella* that produce toxins, most frequently *S. dystenteriae*. In post-infectious arthritis patients may experience chronic joint pain, eye irritation, and painful urination after an infection (246). Infections with *S. sonnei* or *S. dysenteriae* are reported to fewer cases. The rectal biopsy of a patient showed two types of colitis after *Shigella* infection, mild and moderate/severe colitis (247). In mild colitis, the histopathological observation showed flattened surface epithelium with erosions, increased cellular infiltration in the lamina

propia, and mild edema in the mucosa and submucosa. Moderate colitis was described as mucosal damage with crypt abscesses and dense infiltration of neutrophils into the lamina propia (247).

1.6. Animal models to study the *Salmonella* and *Shigella* infection

Understanding the bacterial pathogenesis is greatly aided by the use of animal models. It offers an essential platform for assessing pre-clinical safety data, immunogenicity, and efficacy. Since, *Salmonella* Typhi, *Salmonella* Paratyphi A and *Shigella* are the human-restricted pathogens, their interactions with the human host and underlying mechanism of pathogenesis study are poorly understood. Though, a few animal models, are listed in **Table 1.4** and **Table 1.5** that offer some insight into those studies.

Table 1.4. Animal models to study the *Salmonella* infection

Model	Serovars	Advantage and Disadvantage	Reference
Neonatal mice oral infection model	*S.* Typhi, *S.* Paratyphi A	This is useful for studying the intestinal pathogenesis of *Shigella* infection, but not for investigations on the immunogenicity of vaccine candidates.	(248)
Intraperitoneal infection model	*S.* Typhi, *S.* Paratyphi A	This is useful for assessing the protective efficacy study on vaccine candidates, but not for investigations on the immunogenicity of vaccine candidates.	(249)

Humanized mouse model	*S.* Typhi	It is useful in determining colonization and systemic dissemination but not in terms of vaccine efficacy.	(250)
Chimpanzee model	*S.* Typhi	Although the oral *S.* Typhi infection was established, the typhoid fever symptoms were less severe. It was challenging to define the endpoint titer for evaluating the efficacy of this model because of the larger biological variance and smaller sample size brought on by increased costs.	(251, 252)
Rabbit model	*S.* Typhi, *S.* Paratyphi A	It is useful in investigating the immunogenicity and reactogenicity of potential vaccines, however, the correlation studies with human data are complicated by a significantly raised antibody titer value.	(253)
CHIM (Control human infection	*S.* Typhi, *S.* Paratyphi A	This model is incredibly helpful for assessing the immunogenicity of vaccine candidates and offers insightful information on clinical trials involving possible vaccines.	(254, 255)

model) studies		Strict regulations and guidelines regarding the enrolment of healthy individuals from developed countries present a problem because these individuals differ from young people from disease-predisposed areas in terms of their genetic background, nutritional status and subsequent microbiome, age, and co-morbidity and co-infections linked to background immunity.	
Streptomycin mouse model	*S.* Typhimurium	This model is used to study the molecular mechanisms of enteric salmonellosis. A potential limitation of this model is the requirement for antibiotic pre-treatment, which alters the gut microbiota. This indicates that the model is not suitable to study the *Salmonella* infection in the context of microbial communities.	(256)

Table 1.5. Animal models to study the *Shigella* infection

Model	Serovars	Advantage and Disadvantage	Reference
Mouse Pulmonary Model	*S. flexneri* or *S. sonnei*	The mouse pulmonary model serves as an innovative and efficient alternative	(257)

		for studying *Shigella* infections by circumventing challenges associated with oral challenge methods. However, the approach has been hindered by the irreverent target tissue.	
Mouse Intracolonic model	*S. flexneri*	This model provides a method of studying *Shigella* infection by introducing the bacteria directly into the colon. Its practical application is greatly limited by its invasiveness, technical complexity, and differences in tissue inflammation	(258)
Xenotransplant mouse model	*S. flexneri*	This model is used to determine the role of neutrophils in limiting bacterial dissemination in human intestine. This model depended on the availability of human samples with unpredictable genetic origins, which was in addition to being technically difficult. Furthermore, B and T cells are absent in SCID mice, which makes it more difficult to investigate adaptive immunity in this situation.	(259)

NAIP-NLCR4-deficient mouse model	*S. flexneri*	This model clarifies the function of the NAIP-NLCR4 inflammasome in protecting the gastrointestinal tract from bacterial invasion, offering new insight into the host-pathogen interactions during oral *Shigella* infection. The vaccine efficacy testing has not reported using this model yet.	(260)
Zinc-Deficient mouse model	*S. flexneri*	The effects of zinc deficiency on the progression of *Shigella* infection and the host's immunological response have been investigated using the oral mouse model low in zinc. Nevertheless, the model of zinc deficiency is not able to precisely reproduce the intracellular position of *Shigella* in human infections, as the bacteria were primarily located in the extracellular space of the epithelium rather than inside epithelial cells, which highlights a limitation of this model	(261, 262)
Intraperitoneal mouse model	*S. flexneri*	This model is used to study the pathophysiology of *Shigella* and sheds light on future vaccine and treatment developments.	(262, 263)

		Rather than a localized intestinal infection, it may end in systemic pathogenesis, which can cause bacteremia or hepatitis and cause quick mortality. Furthermore, it cannot accurately duplicate the signs and symptoms of shigellosis in human.	
Streptomycin pre-treated mouse model	*S. flexneri*	This is used to study the bacteria and host interaction in the gut. Several limitations are associated with this model such as a few lesions of the epithelium cells without PMN recruitment, no histological indications of illness in the colon after oral inoculation with a high dose of *Shigella* inoculum and streptomycin treatment by feeding tube.	(264)
Guinea Pig Rectocolitis Model	*S. flexneri*	This is used to study colonic pathogenesis however infections do not fully reflect the natural infection in humans.	(265, 266)
Guinea Pig Keratoconjunctivitis Model	*S. flexneri*	This is used to characterize the virulence mechanism of *Shigella*. Nevertheless, there are obvious drawbacks to this paradigm, including	(267)

		the fact that eyes are not relevant locations of *Shigella* infection and have a different milieu than the intestine.	
Rabbit ileal loop Model	*S. flexneri*	This model is used to characterize the *Shigella* infectious cycle and to determine the pathological alterations in the intestinal mucosa that occurs during infection. But their widespread acceptance has been constrained by the difficult surgical procedures, and the unavailability of genetic modifications.	(268)
Cynomolgus Monkey Model	*Shigella dysenteriae 1*	A useful monkey model for comprehending the immunological reactions and pathophysiology of intestinal *Shigella* infections. However, the use of non-human primate models necessitates careful consideration of ethical issues and the improvement of experimental designs and costly.	(269)

Aotus Nancymaae Model	*S. flexneri*	This is another non-human primate model. With the use of this model, researchers may examine the pathogenicity of primates and gain an understanding of the disease's processes, immune responses, and possible treatments. However, the use of non-human primate models necessitates careful consideration of ethical issues and the improvement of experimental designs and costly.	(270)
Controlled Human Infection Model (CHIM)	*S. sonnei*	This is used to assess the efficacy of prospective therapies or vaccinations and provide information on human immunological response to infection. However, ethical issues and strict safety precautions are crucial to study the well-being of study participants.	(271)

1.7. Host response to *Salmonella* and *Shigella* infection

1.7.1. Host response to *Salmonella* infection

The early host response to infection by *Salmonella* is triggered by the detection of Toll-like receptors (TLRs). This activates neutrophils and mononuclear cells, which generate inflammatory cytokines such as TNF-α, IFN-γ, IL-1, IL-2, IL-6, and IL-8, which constitute the majority of the host defense mechanism against *Salmonella* (272). Toll-like receptor 5 (TLR5) has been shown to bind and become active in response to flagellin (273, 274). The recognition of flagellin by TLR5 triggers the NFκB and MAPK pathways, which in turn promotes the release of cytokines such as TNFα, IL-6, and IL-12 (275). Additionally, *Salmonella* LPS triggers the activation of TLR4 in macrophages, resulting in the production of several inflammatory cytokines, including IFN-β and IL-6 (276). It was demonstrated that TLR4 dimerises in combination with other proteins, including MD2 and CD14, after attachment to LPS and activates MAPKs and NF-κB (277). TLR4 and TLR2 are sequentially necessary for efficient macrophage function, which produces an early response to *Salmonella* infections (278). *Salmonella* lipoproteins and lipoteichoic acid are recognized by TLR2 through the use of TLR6 and TLR1 (279, 280). When TLR9 recognizes *Salmonella* DNA with unmethylated Cp motifs, it becomes activated. Upregulation of TLR1, TLR2, and TLR9 and downregulation of TLR6 was observed during *Salmonella* Typhimurium infection in rodent which is responsible for the plateau phase (control the infection in the later stages when the bacterial growth is suppressed, possibly at the adaptive phase of the immune response) (281). These findings suggest that the TLR2-TLR1 complex, TLR4 and TLR9, may be involved in the surveillance of *Salmonella* infection, particularly during the latter phases when bacterial growth is inhibited, maybe during the adaptive phase of the immune response (282).

Several biochemical signals are produced when *Salmonella* interacts with epithelial cells. This consists of the apical secretion of pathogen-elicited epithelial chemoattractant (PEEC) and the baso-lateral release of the chemokine IL-8. It has been demonstrated that intestinal epithelium secreted IL-8 in response to *S.* Typhimurium infection through an increase in intracellular

calcium, which was found to be NF-κB dependent (283). It has been shown that Type 3 Secretion System-1 (T3SS-1) is necessary for the stimulation of transmigration of polymorphonuclear neutrophils (PMN) (284). This inflammatory milieu also contains a variety of chemokines that can control the migration of neutrophils and mononuclear cells and stimulate leukocyte motility (chemokinesis). Chemokines control the movement of blood leukocytes toward the infection site by binding to CC and CXC receptors on the surface of inflammatory cells. TNF-α, which is generated by mononuclear cells and macrophages, has antibacterial properties against *Salmonella* and eliminates invasive infections in conjunction with IFN-γ, IL-2, and other cytokines.

Typhoidal *Salmonella* serotypes, such as *S.* Typhi and *S.* Paratyphi, generate a completely different host response than NTS serotypes, such as *S.* Typhimurium or *S.* Enteritidis. NTS serotypes are pyogenic and produce a traditional antibacterial host response that is characterized by neutrophilia, exudative intestinal inflammation, and occasionally bacteraemia, which results in septic shock (285) (**Figure 1.25**). However, the fact that typhoid fever does not cause neutrophilia or septic shock indicates that *S.* Typhi is an atypical bacterium that employs special pathogenicity mechanisms that limit the production of a traditional antibacterial response.

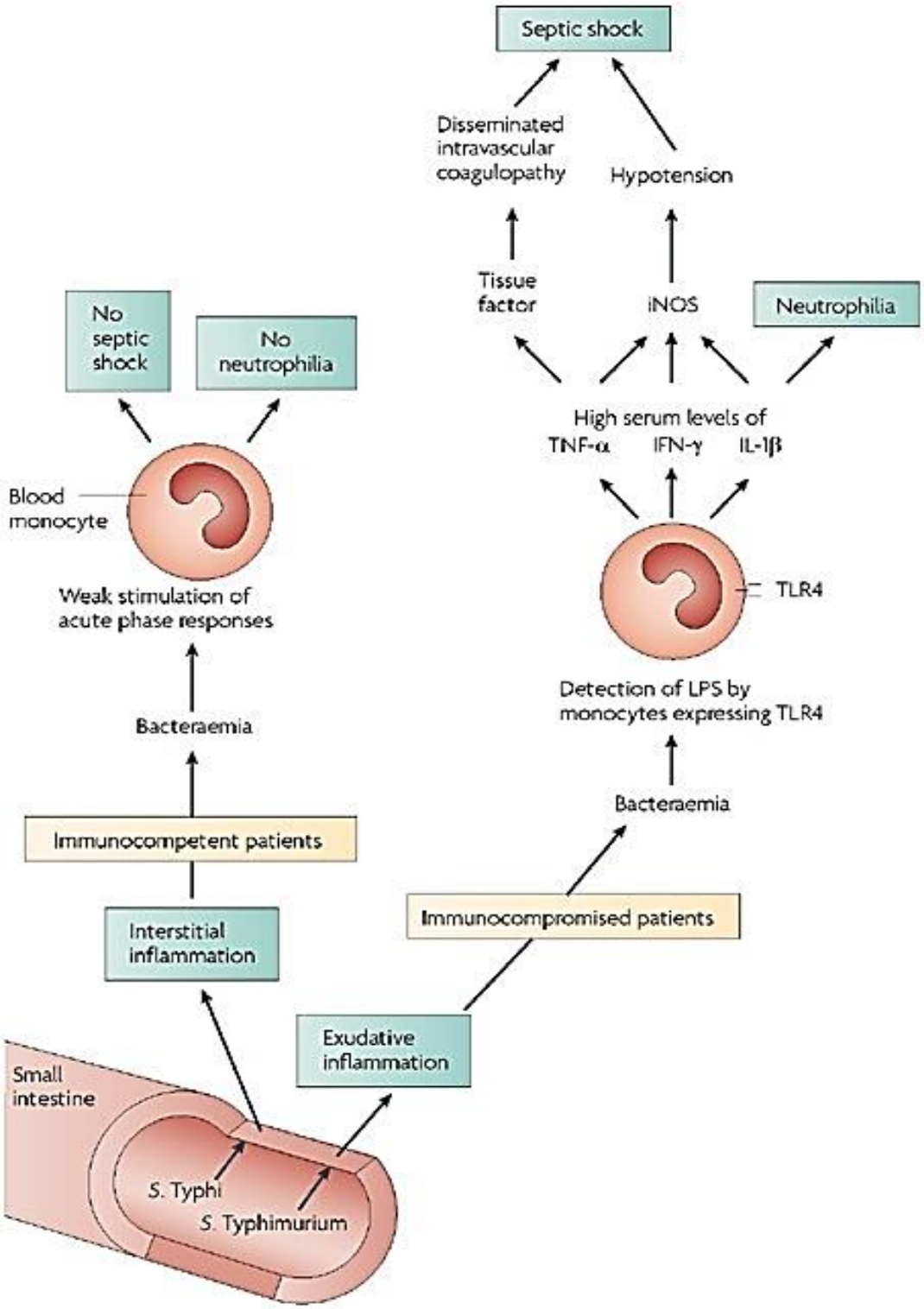

Figure 1.25. Comparison of host responses elicited by *S.* Typhi and *S.* Typhimurium. [The image is adapted from Tsolis RM, Young GM, Solnick JV, Bäumler AJ. From bench to bedside: stealth of enteroinvasive pathogens. Nat Rev Microbiol. 2008 Dec;6(12):883-92. doi: 10.1038/nrmicro2012. Epub 2008 Oct 28. PMID: 18955984.]

Both serotypes fundamentally have the same genomic components that cause acute phase reactions and exudative inflammation. For instance, both serotypes have LPS, which alone during *S.* Typhimurium infections can cause TLR4-mediated septic shock (286-289). The genomes of *Salmonella* serotypes that result in inflammatory diseases such as gastroenteritis lack *Salmonella* pathogenicity island 7 (SPI-7) (290). Human macrophages and colonic epithelial cells have been shown to produce more TNF-α and IL-8 when infected with *S.* Typhi mutants of SPI-7 (291, 292). The viaB locus, which controls the formation of Vi polysaccharides, is encoded in this region (293). Vi capsular coat is thought to block TLR4 and TLR5-mediated *S.* Typhi recognition (294). However, the mechanism is unknown. Certain level of serum anti-Vi antibodies could serve as a serologic proxy for protection against *Salmonella* infection (293). Besides this, serum antibodies were generated specific to the H-antigen, and the O-antigen of LPS following *Salmonella* infection were found protective (295-298).

The adaptive immune response to infection by *Salmonella* starts with early DC-mediated activation of pathogen-specific CD4+T cells restricted to the Peyer's patches and the mesenteric lymph nodes (299, 300). Major Histocompatibility Complex (MHC) class II genes regulate the activation of $CD4^+$T cells and T cell receptor (TCR)-αβ, which are required for the removal of pathogens from affected tissues (301, 302). Studies on the development of *Salmonella*-specific $CD4^+$ effector responses in both susceptible and resistant mice indicate that Th1 effectors are rapidly acquired by *Salmonella*-specific $CD4^+$ T cells, leading to a large expansion of these cells and increased secretion of TNF-α, IFN-γ, and IL-2 (303, 304). Tbet-expressing-, IFNγ-secreting- Th1 cells are the primary mediators of this CD4+T cell response, which is essential for clearance of pathogens from the tissues (305, 306). However, in the

absence of CD4+T cells, CD8+T cells, and NK cells release IFNγ and can regulate the bacterial burden in the early stages of the infection (307, 308).

1.7.2. Host response to *Shigella* infection

An array of humoral and cell-mediated immune responses initiates following the *Shigella* infection. Several pattern recognition receptors (PRRs), including Toll-like receptors (TLRs), detect PAMPs and DAMPs after *Shigella* invades the epithelial cell. When PRRs detect PAMPs and DAMPs, they trigger host defense signalling pathways, including those mediated by NF-kB and mitogen-activated protein kinases (MAPK). This results in the release of antimicrobial peptides, chemokines (including TNF-a and IL-8), and pro-inflammatory cytokines. These molecules stimulate the recruitment of phagocytic cells, such as neutrophils, macrophages, and dendritic cells, to the infection site that ultimately clears the intruding bacterial pathogens. It has been reported that massive neutrophil infiltration results from *Shigella* invasion causes IL-8 secretion which restricts bacterial migration (309, 310). However, *Shigella* inhibits ATP-dependent endogenous danger signalling which manipulates NF-κB pathways. It regulates the expression of certain pro-inflammatory cytokines and antimicrobial peptides to dampen inflammatory responses and promote bacterial colonization through the TTSS and its effectors (311-314). To prevent bacteria from colonizing the epithelium, intestinal mucosa releases secretory IgA (sIgA) as an additional first line of defense (315). Antibodies specific to *Shigella* lipopolysaccharide (LPS), such as serum IgG and mucosal sIgA, are secreted in response to *Shigella* infection and are crucial in preventing re-infection with the *Shigella* (316). High levels of O-specific serum IgG (mainly IgG1 and IgG2) and IgA antibodies are generated against *Shigella* 1–2 weeks after the infection (317). Studies have shown that these O-specific antibodies have protective functions against *Shigella* infection (318-320). In addition to this,

ipa proteins also contribute significant level of protection following infection (321-323). Antibodies derived from natural infection have complement-mediated bactericidal activity (324) and promote opsonophagocytic killing by mononuclear cells (325). It has been shown that Gut-derived O-specific IgA antibody secreting cells (ASCs) are believed to play a critical part in protection against *Shigella* (326, 327).

Shigella manipulates the host adaptive immune response by targeting DCs, T and B cells. *Shigella* downregulates DC recruitment during infection by decreasing production of the chemokines and cytokines such as CCL20 (328). *Shigella* effectors also mediate apoptotic death of DCs (329). *Shigella* infection has also been shown to induce cell-mediated immune responses, including upregulation of IFN-γ receptor expression and production of pro-inflammatory cytokines, such as IFN-γ (330, 331). Moreover, an expansion of T cells, particularly CD8+ and T-cell receptor (TCR) γδ+ T-cell subsets in the gut mucosa (332) has been described in the rectal mucosa of patients with shigellosis. Increased levels of activated and memory CD4+ and CD8+ T cells and expansion of defined TCR Vβ families have been reported in peripheral blood of patients with shigellosis (333, 334). T cells are essential for clearance of bacteria during primary infection, and *Shigella*-specific IL-17A secreting T cells are crucial for limiting bacterial growth during reinfection (335). Moreover, *Shigella* infection induces both primary and recall T cell expansion, predominantly of Th17 cells. Th 1 cells could limit bacterial dissemination through induction of intraepithelial lymphocytes with cytotoxic capacity.

1.8. A summary of *Salmonella* and *Shigella* vaccines

1.8.1. Summary of *Salmonella* Vaccines

Table 1.6. Vaccine pipeline for *Salmonella*

Name	Description	Composition	Developer	Stage of Development
Vaccines in development against *S.* Typhi				
Ty21a	Live attenuated	gal E mutant	Vivotif (Crucell)	Commercially available
CVD 908	Live attenuated	Deletion in the aroC and aroD	University of Maryland	Clinical trial
CVD 908 htr-A	Live attenuated	Deletion in the aroC, aroD and htr A genes	University of Maryland	Phase II study
CVD 909	Live attenuated	Continuation expression of vi polysaccharide	University of Maryland	Phase I clinical trial
Ty800	Live attenuated	Deletion in the phoP/phoQ regulatory genes	Avant Immunotherapeutics	Phase II clinical trial
M01ZH09	Live attenuated	Deletion in the aroC and ssaV genes	Emergent Biosolutions	Phase II clinical trial

Vi-PS Typhim Vi	subunit	Purified Vi-polysaccharide	Sanofi	Commercially available
Typber TCV	subunit	Vi polysaccharide conjugated with Tetanus toxoid	Bharat Biotech	Commercially available
Vi-DT	subunit	Vi polysaccharide conjugated with Diptheria toxoid	International Vaccine Institute (IVI)/ Shanta Biotech	Phase III clinical trial
Vi-CRM197	subunit	Vi polysaccharide conjugated with CRM197, nontoxic mutant of Diptheria toxoid	Novartis Vaccine Institute for Global Health (NVGH)	Phase I and II clinical trial
Vi-rEPA	subunit	Vi polysaccharide conjugated with *Pseudomonas aeruginosa* exotoxin A	National Institute for Health	Phase III clinical trial
Vaccines in development against *S.* Paratyphi				

CVD 1902	Live attenuated	deletions in the guaBA operon and the clpX operon	University of Maryland and Bharat Biotechnology	Phase II
O2:TT	Live attenuated	OSP from *S.* Paratyphi is conjugated with tetanus toxoid	Lanzhou Institute of Biological Products (LIBP)/ national Institute of Health (NIH)	Phase II
Vaccines in development against *S.* Typhi and *S.* Paratyphi				
O:2-TT + Vi-TT	Subunit	O antigen from *S.* Paratyphi A chemically conjugated with tetanus toxoid and delivered with ViTT.	NIH	phase I and II study. Technology transfer from NIH to

				Lanzhou Institute (China)
O:2-CRM197 + Vi-CRM 197	Subunit	O antigen from *S.* Paratyphi A chemically linked with CRM197, and combined with Vi-CRM197.	Pre-clinical study. Technology transferred to Biological E, India where a combination study with Vi-CRM197 was proposed	Novartis vaccine Institute for Global Health (NVGH)
O:2-DT + Vi-DT	Subunit	O antigen from *S.* Paratyphi A chemically linked with diptheria toxoid and coformulated with Vi conjugated DT	Clinical testing awaiting	IVI

The Multiple Antigen Presenting System (MAPS) Vaccine	Subunit	Affinity pair biotin- rhizavidin to formulating a complex of polysaccharide (Vi and OSP) and proteins (CRM197, rEPA of *Pseudomonas*, and a pneumococcal fusion protein SP1500-SP0785)	Pre-clinical	GSK
Vaccines in development against *S.* Typhimurium and *S.* Enteritidis				
STm + SEn GMMA	Subunit	native outer membrane vesicles (NOMVs, also termed GMMA, Generalized Modules for Membrane Antigens) of *S.* Typhimurium/*S.* Enteritidis that serve as a delivery vehicle for O-antigen, in addition to presenting a multitude of other *Salmonella* outer membrane and periplasmic protein antigens to the immune system	GVGH	Phase I

O:4+O:9-MAPS	Subunit	O:4 and O:9 antigens of *S.* Typhimurium and *S.* Enteritidis attached to carrier protein using the proprietary multiple antigen presenting system (MAPS)	BCH	Preclinical
Vaccines in development against *S.* Typhimurium, *S.* Enteritidis and *S.* Typhi				
Vi-CRM197+STm+Sen GMMA	Subunit	Vi-CRM197 conjugate is co-formulated with native outer membrane vesicles (GMMA) from *S.* Typhimurium and *S.* Enteritidis	GVGH/BioE	Phase I
Vi-TT+O:4-flagellin+O:9-flagellin	Subunit	NTS glycoconjugates consisting of O:4 and O:9 antigens coupled to the flagellin antigens of *S.* Typhimurium and *S.* Enteritidis respectively, in combination with Vi-TT conjugate	BBIL/UMD	Phase I
Vi-DT+O:4-DT+O:9-DT	Subunit	The NTS components are both glycoconjugates consisting of O:4 and O:9 coupled to DT combined with Vi-DT conjugate	IVI/SK Bioscience	Preclinical

1.8.1.1. Vaccine development against *Salmonella* Typhi

1.8.1.1.1. Live attenuated vaccine

Live bacterial vaccines are the most established, and effective vaccination methods (336). Random mutation or targeted mutagenesis are two methods for producing attenuated microorganisms. **Ty21a** was the first live attenuated oral *Salmonella* vaccine developed in both the enteric-coated capsule as well as liquid form. It was formulated by mutating the gal E, a uridine-diphosphate-galactose-4-epimerase, resulting in the inability to manufacture Vi polysaccharide and a cytoplasmic accumulation of galactose that eventually causes cell lysis (337). Three doses of oral Ty21a in enteric-coated capsules (for use in individuals ≥5 years of age) conferred 67% protection over three years and 62% protection over seven years of follow-up, whereas three doses of liquid formulation (lyophilized liquid reconstituted in buffer, for use in individuals ≥2 years of age) elicited 77% protection over three years and 78% over five years of follow-up (338, 339). This vaccine induces O-, H- specific serum and intestinal mucosal antibodies. However, no Vi-specific antibodies were generated. The strength of the initial response was mediated by IgA antibody-secreting cells and the presence of anti-O IgG antibodies (340). Long-lasting cell-mediated immunity and cytotoxic T-lymphocyte response were observed. Despite an adequate immune response and efficacy against typhoid fever, Ty21a was associated with certain drawbacks. High numbers (10^9) of bacteria are required for oral dose to obtain sufficient immunity and its use was recommended for children only above 5-6 years of age. This vaccine is highly acid-labile and hence stomach acidity has to be either neutralized or bypassed when Ty21a is to be fed orally (341). The efficacy of Ty21a is closely correlated with the specific formulation of the vaccine and the number of doses administered. (342-347).

Besides the Ty21a, several live attenuated *S.* Typhi strains have been developed for oral vaccination against typhoid fever. **CVD 908** is a mutant of *S.* typhi wild-type strain Ty2 with deletions in two genes, aroC and aroD (deletion of genes involved in aromatic amino acid synthesis (e.g., aroC and aroD)) rendering the strain nutritionally dependent on substrates (para-aminobenzoic acid (PABA) and 2,3-dihydroxybenzoate) that are not available in sufficient quantity in human tissues (348). When administered to mice, *Salmonella* aro mutants are unable to scavenge enough PABA and dihydroxybenzoate to replicate (349). Pre-clinical studies have shown that *Salmonella* aro mutants elicit robust immune responses which can protect animals against lethal challenge (350, 351). After a single oral dose of 5 × 10^7 CFU, this strain induced IgG seroconversion to *S.* Typhi lipopolysaccharide in 83% of vaccinees and stimulated specific IgA-secreting gut-derived lymphocytes in 100% of vaccinees (352). However, upon subsequent testing, CVD 908 produced bacteremia at higher doses (5 × 10^7 CFU and 5 × 10^8 CFU) (353).

A further mutation in the htrA locus of CVD 908 was performed to generate the **CVD908-htrA** vaccine strain with deletions in aroC/ aroD and htrA gene locus (341). HtrA encodes a heat shock protein in *Salmonella* (354). The resulting mutant is less virulent because of an impaired ability to survive and/or replicate in host tissues (355, 356). Single-dose oral CVD 908-htrA stimulated vigorous mucosal, humoral, and cellular immune responses, but no vaccine-induced bacteremias were detected at dose 5 × 10^7 CFU (low dose) and 4.5 × 10^8 CFU (high dose) (357, 358)**.** One drawback of the CVD 908-htrA vaccine is that it requires pre-administration of buffer to neutralize stomach acid. This is a potential delivery challenge for live attenuated vaccines.

To further improve on the live attenuated vaccine CVD 908-htrA, **CVD 909** strain was genetically engineered to constitutively express the Vi polysaccharide. The native PtviA promoter which regulates Vi expression was replaced in CVD 908-htrA with the strong

constitutive promoter Ptac to produce CVD 909 (359). Oral single dose of 10^8 – 10^9 CFU of CVD 909 induced Vi-specific IgA ASCs in 80% of volunteers (360). Although impressive ASC responses were produced, only 2 out of 32 volunteers generated anti-Vi serum IgG antibodies (361).

Another live attenuated vaccine has been developed after deletion of the global regulator PhoP/PhoQ regulon of Ty2 to generate **Ty800**. The PhoP/PhoQ regulon is a two-component regulatory system that controls the transcription of multiple genes (362-364). PhoP is a cytoplasmic transcriptional regulator and PhoQ is a membrane associated sensor kinase. This operon contributes to survival within macrophages and resistance to antimicrobial peptides (365, 366). A single dose of Oral Ty800 has been shown to stimulate IgA and anti-O serum antibody responses in volunteers (367). However, protection may wane over time, which necessitates booster doses.

Another aro-based *S.* Typhi vaccine **M01ZH09** was developed by mutating the aroC and ssaV genes of Ty2 (368, 369). This vaccine strain lacks SPI-2 structural protein SsaV, required for secretion of bacterial effectors proteins. The mutation will hinder the SPI-2 function and prevent the systemic spread. Another mutation in aroC, known as aromatic mutation prevents the bacterium from receiving essential nutrients from the mammalian host (341). The vaccine induced significant immune responses after a single oral dose (370-372). However, a single dose of M01ZH09 failed to demonstrate significant protection after a challenge with virulent *S.* Typhi (373).

1.8.1.1.2. Capsular Vi-polysaccharide based vaccine

Surface polysaccharides of many bacteria have been used as effective antigens, such as capsular polysaccharides (Vi) as in the case of Gram-negative enteric bacteria (374). The Vi capsular polysaccharide of *S.* Typhi is an important virulence factor and a protective antigen (375, 376).

A subunit vaccine consisting of a purified Vi capsular polysaccharide of *S.* Typhi strain Ty2 was developed, **Typhim Vi**, which elicited an anti-Vi antibody response in 85–95% of individuals >2 years of age with a single parenteral (intramuscular) dose (377). The vaccine efficacy for *S.* Typhi was 64–72% for 17–21 months and 55% over a period of 3 years (378). Common side effects associated with this vaccine include pain, redness, injection site induration, fever, rare allergic reactions and rashes that have been observed following vaccination and this vaccine is not effective in children below 2 years (379).

Even though both licensed live attenuated Ty21a and Vi-polysaccharide vaccines are effective, several limitations hamper their inclusion in the Expanded Programme on Immunizations (EPI) schedules of typhoid-endemic countries (341). Live attenuated vaccines are available in capsule formulation only and, hence, cannot be administered to children < 5 years of age. Multiple doses are required to complete a vaccination course, and revaccination is recommended every 5 years. This type of vaccine also requires a strict cold chain to be maintained during storage and handling, which is a major limiting factor in resource-poor settings (379). Though immunogenic, there will be a need for the pre administration of buffer to neutralize stomach acid with live attenuated vaccines, which is a potential delivery challenge. For the Vi-vaccines more fundamental immunological limitations preclude their widespread use. The Vi vaccine–induced immune response is elicited by a T cell–independent mechanism, to which children below 2 years of age respond poorly. Further, there is no development of immune memory. As a consequence, only short-term responses are generated and there is no boosting following a second vaccination that would lead to a shorter duration of protection. Revaccination is necessary every 3 years for children above 2 years (380).

1.9.1.1.3. Vi-Polysaccharide based conjugate Vaccine

In recent years, there have been major efforts to develop glycoconjugate vaccines against *S.* Typhi, which can induce effective immune responses in both infants and adults. Conjugation to a carrier protein changes the antigenic property of the polysaccharide and makes it a T cell–dependent antigen. These antigens are immunogenic in younger children and infants, elicit a booster response to subsequent immunization, and have a longer duration of protection.

Vi-rEPA, one of the earlier conjugate candidates, was developed by conjugating Vi-polysaccharide to the recombinant A subunit of Pseudomonas aeruginosa exoprotein (rEPA) which elicited strong immune responses in infants and toddlers (381-383). It induces immunologic memory, long-lived elevated titers of serum anti-Vi IgG antibody, and conferred 89% efficacy against typhoid fever over 46 months following two doses of intramuscular vaccination of preschool children (383, 384). In adults, serum anti-Vi antibody titers remained elevated for up to 10 years (383, 384). However, Vi-rEPA is associated with increased rates of fever after each vaccine dose. Swelling at the injection site was more common after the second dose (385).

The only WHO-prequalified Vi-conjugated vaccine on the market is **Vi-TT** where vi-polysaccharide is conjugated to a nontoxic tetanus toxoid carrier. Vi-TT is available in 2 formulations: Typbar-TCV (Bharat Biotech) and PedaTyph^{TM} (BioMed, India). A single dose of the intramuscular Typbar-TCV Vi-TT vaccine has a cumulative efficacy of 83% 1 to 2 years post-immunization in infants and children aged 6 months to 16 years (386). The most recent trial analysis in Malawian children aged 9 months to 12 years showed an efficacy of 78.3% in 4 years after an intramuscular single dose (387). Another formulation of Vi-TT that is licensed and marketed only in India is PedaTyph^{TM} (340). This vaccine can be administered to children of 3 months or older (388) and the efficiency of the vaccine was 94% after two doses intramuscular administration. The actual effect is uncertain due to a wide confidence interval and a lack of unclustering during statistical analysis of the study data (385).

Another Typhoid conjugate vaccine consists of the Vi polysaccharide purified from *S.* Typhi chemically conjugated to diphtheria toxoid, **Vi-DT**. A phase 3 trial in participants 6 months to 45 years old was conducted in Nepal, which confirmed the immune response is not inferior to Typbar TCV (389, 390). It has been observed that the anti-Vi IgG seroconversion rate was 99.71% in Vi-DT recipients while 99.13% in Vi-TT recipients after single dose intramuscular vaccine administration. However, significant differences were observed in the 24-month age group where lower mean GMT was observed in the Vi-DT group compared to Vi-TT (50.2 vs 73.4 EU/mL) (391). Further study is needed to elaborate on this finding.

Further, Vi-polysaccharide from *Citrobacter* was conjugated to a mutant nontoxic diphtheria toxoid carrier protein, CRM_{197} to develop **Vi-CRM_{197}**. A Phase I study was completed using a single dose of Vi-CRM197 in healthy adults, with a Vi-polysaccharide vaccine as a comparator. The GMTs were 304 and 52 EU/ml in Vi-CRM197 and Vi-polysaccharide recipients, respectively after 28 days of intramuscular vaccination. At 6 months postvaccination, the difference in antibody titers of Vi-polysaccharide and Vi-CRM197 recipients narrowed to 51 and 69, respectively, suggesting a faster decline in the antibody titers of participants with Vi-CRM197 (392). A Phase II randomized dose-ranging study (1.25 μg, 5 μg, or 12.5 μg of Vi-CRM197 or Vi-polysaccharide vaccine) conducted was found to be safe. Anti-Vi antibody responses 4 weeks after intramuscular vaccination were higher in participants receiving Vi-CRM197 (all 3 dosages) than in Vi-polysaccharide recipients. However, the response was dose-dependent, with the lowest titers found in participants receiving the 1.25 μg dose (393).

Vi- conjugated vaccines used in different clinical studies were associated with several drawbacks. First, these vaccines use non-*Salmonella* proteins. Non-specific carrier proteins used in the glycoconjugate vaccine fail to generate *Salmonella*-specific T cells, which were earlier reported to contribute overall immunity against *Salmonella* infection (394). Second, the

Vi-based conjugate vaccines are currently effective against *Salmonella* Typhi, but not *S.* Paratyphi A and B which lack Vi-polysaccharide coat.

1.8.1.2. Vaccines in development against *S.* Paratyphi

1.8.1.2.1. Live attenuated

A live attenuated *S.* Paratyphi A vaccine, **CVD 1902**, harbours deletion of clpPX and guaBA genes in the ATCC9150 parental *S.* Paratyphi A strain. The clpPX gene encodes a protease that degrades the master flagella regulator FlhD/FlhC (395, 396). The FlhD/FlhC complex is a transcriptional activator of the flagella synthesis pathway. When ClpPX is absent, FlhD/FlhC accumulates and large amounts of flagellin are produced. Which aids in the advantage of the economical purification of flagellin from recombinant *Salmonella* strains (397). This increased expression of *S.* Paratyphi A flagellar antigens may enhance the induction of antibodies, cell-mediated immunity (CMI), and innate responses via engagement of TLR5 (398-402). The guaBA operon is responsible for producing enzymes that convert hypoxanthine to guanine during guanine nucleotide biosynthesis. Mutations in the guaBA genes can affect virulence and make bacteria auxotrophic for guanine (unable to synthesize guanine needed for viability) (403, 404). Pre-clinical studies in mice showed oral CVD 1902 to be immunogenic, and protective against intraperitoneal challenge with wild type *S.* Paratyphi A. A dose-escalating phase 1 clinical trial in healthy adults showed single doses as high as 10^9 and 10^10 colony forming units (CFU) were well tolerated and elicited *S.* Paratyphi A-specific B and T cell-mediated responses (404).

1.8.1.2.2. O-specific polysaccharide based conjugate vaccine

Salmonella O-antigen (O-specific polysaccharide or OSP) is a component of the outer membrane of gram-negative bacteria which forms the distal portion of LPS. Clinical studies

have implicated it as a target for protective immunity against non-Typhi serotypes as anti-OSP antibody mediates serum bactericidal activity in healthy adults and children in the United States (405). O-Ag alone is not immunogenic in mice, but when conjugated with carrier protein can induce anti-OSP antibodies with bactericidal activity (406). O-antigen (O:2) from *S.* Paratyphi A was conjugated with tetanus toxoid to develop **O:2-TT.** A single dose of intramuscular injection of this conjugate was safe and immunogenic in phase 1 and 2 trials in adults, teenagers, and children aged 2–4 years (407). At 4 weeks after the first injection, there was more than fourfold rise in the anti-OSP serum IgG levels in the adults and teenagers, in ≥80% of the volunteers (407).

1.8.1.3. Vaccines in development against both *S.* Typhi and *S.* Paratyphi

Different combination parenteral (intramuscular) bivalent vaccines were developed for typhoid and paratyphoid fever which are under different testing stages. O:2-DT conjugate was co-formulated with the Vi-DT vaccine which is currently in a phase 1 study in India (408). Another bivalent vaccine consisting of O-antigen from *S.* Paratyphi A chemically linked with CRM197 (O:2-CRM_{197}), and combined with Vi-CRM197. Pre-clinical study Technology transferred to Biological E, and further study is under process (408). O-antigen from *S.* Paratyphi A was chemically linked with diptheria toxoid (O:2-DT) and co-formulated with Vi-DT. This vaccine is still in preclinical development (408). The Multiple Antigen Presenting System (**MAPS**) is a vaccine platform that uses the affinity pair biotin-rhizavidin to generate a complex of polysaccharides and proteins that can generate polysaccharides and proteins specific antibodies (409-412). MAPS-based vaccines induce robust, boostable and CD4+ T cell-dependent anti-polysaccharide antibody responses, as well as functional antibodies and Th1/Th17cell response to carrier proteins, which may provide additional benefits over conventional conjugate

technology. A combination of Vi and OSP bivalent MAPS vaccine generated long-lasting, and bactericidal immune responses in rabbits after two doses intramuscular immunization (413).

1.8.1.4. Vaccines in development against *S.* Typhimurium and *S.* Enteritidis

Bivalent NTS vaccines are currently being developed by the GSK Vaccines Institute for Global Health (GVGH) and consist of native outer membrane vesicles (NOMVs, also termed GMMA, Generalized Modules for Membrane Antigens) of *S.* Typhimurium/*S.* Enteritidis serve as a delivery vehicle for O-antigen, outer membrane, and periplasmic protein antigens to the immune system (414, 415). This vaccine has recently started a phase 1 trial (408). Another bivalent NTS vaccine consists of O:4 of *S.* Typhimurium and O:9 antigens of *S.* Enteritidis attached to carrier protein using the multiple antigens presenting system (MAPS) technology (408, 416, 417). This vaccine is still in preclinical development.

1.8.1.5. Vaccines in development against *S.* Typhimurium, *S.* Enteritidis and *S.* Typhi

The most advanced combination of *Salmonella* vaccine is a trivalent vaccine (418). The vaccine is composed of two NTS glycoconjugates consisting of O:4 and O:9 antigens coupled to the flagellin antigens of *S.* Typhimurium and *S.* Enteritidis respectively, in combination with Vi-TT. This vaccine has been tested in two phase 1 studies in the United States and found to be safe and immunogenic with long-lasting antibody response (419, 420).

Other vaccine formulations are under the phase I study consisting of *S.* Typhimurium and *S.* Enteritidis GMMA in combination with Vi-CRM197 (421) and pre-clinical study consisting of O:4 and O:9 coupled to DT combined with Vi-DT conjugate (408, 422).

Combination vaccine formulations with different carrier proteins chemically conjugated to different polysaccharides showed considerable promise in different trials. Despite the potential of broader protective coverage, combined glycoconjugate vaccine has several inherent limitations as it may increase the chance of carrier-specific epitope suppression (CIES) or bystander interference (421, 423, 424) which further inhibit the hapten or saccharide specific immune response. In addition, the process of creating a multi-glycoconjugate vaccination is expensive and time-consuming. This emphasises the requirement for the development of single formulations having multivalency, or multivalent vaccines, which may provide defence against a range of typhoidal and nontyphoidal *Salmonella* serovars.

The aforementioned constraints might be addressed and future vaccine formulation development made possible by the use of innovative carrier proteins. It would be ideal to have a single vaccine formulation that contains antigens unique to multiple serovars of *Salmonella*.

1.8.2. Summary of *Shigella* Vaccines

Table 1.7. Vaccine pipeline for *Shigella*

Name	Description	Composition	Developer	Stage of Development
WRSS2	Live Attenuated	Deletion in the *virG*, *senA* and *senB* genes of *S. sonnei*	WRAIR	Phase1

WRSS3	Live Attenuated	Deletion in the *virG, senA, senB* and *msBb genes of S. sonnei*	WRAIR	Phase1
ShigETEC	Live Attenuated	*S. flexneri* 2a 2457T Δ*rfbF*, *ipaBC*, and *setBA* expressing fusion protein B subunit of ETEC	EveliQure	Phase1
S4V-EPA	Subunit	Quadrivalent *S. flexneri 2a, 3a, 6* and *S. sonnei* OAg bioconjugate	LimmaTech	Phase2
Sf2a-TT15	Subunit	*S. flexneri* 2a synthetic OAg conjugate	Institute Pasteur	Phase2
ZF0901	Subunit	*S. flexneri* 2a and *S. sonnei* OAg conjugate	Beijing Zhifei Lvzhu Biopharmaceuticals	Phase3
Invaplex$_{AR}$ DETOX	Subunit	LPS from *S. flexneri 2a 2457T* Δ*msBb* and	WRAIR	Phase1

		recombinant IpaB and IpaC		
altSonflex1–2-3	Subunit	Quadrivalent *S. flexneri 1b, 2a,* 3a, and *S. sonnei* outer membrane vesicles (GMMA)	GVGH(GSK)	Phase2
OMV Sfl2a	Subunit	*S. flexneri* 2a outer membrane vesicles	Navarra University	Preclinical
Ipa DB Fusion	Recombinant protein	IpaD and IpaB protein from *S. flexneri* 2a	PATH	Preclinical
34kDa OmpA Sfl2a	Recombinant protein	Outer membrane protein A from *S. flexneri 2a*	NICED	Preclinical
PSSP-1	Recombinant protein	C-terminal half-polypeptide of IcsP from *S. flexneri 2a*	IVI	Preclinical

Several vaccine formulations against *Shigella* have been developed and are currently in different developmental stages.

1.8.2.1. Live attenuated

A series of live attenuated vaccines against *S. sonnei* has been developed using *S. sonnei* Moseley strain. A common problem with *S. sonnei* strains is the loss of the virulence plasmid.

However, the plasmid is relatively stable in the Moseley strain. Two mutated strains were developed, **WRSS2** and **WRSS3**. While both have deleted enterotoxin genes senA and senB, WRSS3 has the deletion in the msbB gene from the virulence plasmid. The removal of msbB, which encodes an acyltransferase, results in the loss of an acyl chain from the lipid A of LPS with a consequent reduction in reactogenicity (425). Both vaccines were immunogenic which elicited systemic and mucosal antibodies with functional bactericidal activity (426) and reasonably tolerated at single oral doses from 10^3-<10^7 CFU in a phase 1 trial in the US (427). However, At the 10^7 CFU dose, moderate diarrhea occurred in one WRSS2 subject while at the same dose of WRSS3, 2 subjects had moderate or severe diarrhea (427).

Another live attenuated vaccine was engineered using wild-type *S. flexneri 2a*. Here, O-antigen and Ipa antigens (targets of protective immunity), were removed through the deletion of rfbF and ipaBC genes, respectively together withthe deletion of the setAB gene to remove enterotoxins. The vaccine was engineered to express a fusion protein of labile toxin (LT) and stable toxin (ST) of enterotoxigenic E. coli (ETEC), hence the name of the vaccine is **ShigETEC**. The single oral dose of vaccine was well tolerated up to 4-time dosing with 5×10^{10} CFU and induced robust systemic immune responses, serum IgA response, and mucosal antibody responses associated with IgA in stool samples and ALS (Antibodies in Lymphocyte Supernatant). Anti- ETEC toxin responses were detected and the heat-labile toxin was associated with neutralising capacity in phase 1 trial (428). The vaccine is set to progress into phase 2 studies.

Although live attenuated vaccines with targeted genetic mutations were well tolerated in trial, balancing between acceptable levels of reactogenicity and sufficient immunogenicity remained a challenge.

1.8.2.2. Conjugate vaccine

A quadrivalent bioconjugate vaccine which carries O-antigens of *Shigella flexneri* serotypes 2a, 3a, 6 and *Shigella sonnei* bioconjugated to the EPA carrier protein to develop **S4V-EPA**. These O-antigens were chosen as they are from the most prevalent strains and will enable coverage to reach around 85% (429). According to *Shigella* incidence data from the GEMS research, such vaccination provides 64% direct coverage (430). Cross reactivity, as demonstrated preclinically with immunological sera against *Shigella* 2a and 3a serotypes, could provide an additional coverage of about 20% against *Shigella* serotypes not covered by this vaccination (431). This vaccine is currently under the phase 2 clinical trial (432).

Further synthetic conjugate vaccine, **Sf2a-TT15** was developed where *S. flexneri 2a* oligosaccharides chemically linked to tetanus toxoid (TT) carrier protein (433). Here, O-antigen consists of three pentasaccharide repeating units (giving a total of 15 saccharides). The vaccine was demonstrated to be safe and induces high titres of serum anti-SF2a LPS IgG antibodies in a phase 1 study in Israeli adults even after a single intramuscular dose (434). This conjugate is now being tested in an age-descending dose-finding phase 2 trial in Kenya and in a CHIM trial at the CDC (435).

Using more conventional glycoconjugate technology, a bivalent glycoconjugate vaccine, **ZF0901**, was developed using O-antigen from *S. sonnei* and *S. flexneri 2a* conjugated to tetanus toxoid with adipic acid dihydrazide as linker. Following a phase 1 descending age study (above 3 month) in China to show safety (436), the vaccine was tested in a phase 2 age-descending study in which it was found to be safe as no serious adverse reactions were observed and immunogenic (induces seum anti-lps IgG antibodies against both serotypes), after two doses of intramuscular immunization. Currently this vaccine is being tested in a phase 3 study (437).

1.8.2.3. Subunit vaccine

An alternative form of artificial detoxified **Invaplex (InvaplexAR-Detox)** was developed which consists of mixture of LPS with deleted msbB genes aiding in the under-acylated lipid A (making the LPS of low reactogenicity) and ipa proteins (IpaB and IpaC) extracted from Shigella flexeneri 2a. This detoxified form of LPS has allowed good safety and immunogenicity results in a recent phase 1 study after three doses of intramuscular administration (438). However, the extent of cross-protection resulting the vaccine is currently not clear. A quadrivalent vaccine, **altSonflex1-2-3**, consisting of OMV from *S. flexneri 1b, 2a* and *3a* and *S. sonnei* (with higher O-antigen expression) is currently being tested in a phase 1/2 clinical trial (439). Another vaccine composed of OMV from *S. flexeneri 2a* were encapsulated into nanoparticles which is currently being tested in preclinical level. BALB/c mice were immunized with single dose OMVs by nasal or oral route and showed 100% protection following lethal infection (440).

1.8.2.4. Recombinant vaccine

Protein-based subunit vaccine candidates are also under development. They may offer broad protection against all major serotypes but have only been tested in animals so far. Among these, the **Ipa DB** Fusion consists of a genetic fusion of the T3SS proteins IpaB and IpaD (441). Co-administration of this vaccine intradermally with double mutant Heat Labile Toxin (dmLT) from ETEC induced both mucosal and systemic immunity. A 34 kDa **OmpA** outer membrane protein developed by NICED is under the preclinical level (442). Three doses of intranasal immunization with recombinant protein induces significantly enhanced protein specific IgG and IgA Abs in both mucosal and systemic compartments and IgA secreting cells in the systemic compartment (spleen) with 100% protection against lethal bacterial challenge.

Another recombinant protein **pan-Shigella surface protein 1 (PSSP-1**) was suggested as a promising antigen against *Shigella* is under preclinical level (443). Intranasal administration with three doses of this vaccine showed cross-protection against *Shigella flexneri* serotypes 2a, 5a, and 6, *Shigella boydii*, *Shigella sonnei*, and *Shigella dysenteriae* serotype 1. It also elicited efficient local and systemic antibody responses and production of interleukin 17A and gamma interferon. Whereas, Intradermally administered PSSP-1 induced strong serum antibody responses but failed to induce protection.

Chapter 2.

Rationale of the Objectives of the study

According to WHO, high prevalence of enteric fever that occurs throughout south and south-east Asia reported in children under the age of five. To eradicate the risk of *Salmonella*, WASH strategies—safe drinking water, adequate sanitation maintenance, and food hygiene—are taken into consideration while vaccination remains the most attractive and immediate solution for the prevention of transmission of human *Salmonella* infections. However, available vaccines (Ty21a (live attenuated), Vi-polysaccharide (Vi based)) against *S.* Typhi are associated with moderate long-term efficacy and safety issues in the small children (444). Vi-polysaccharide-based glycoconjugate vaccines such as Vi-tetanus toxoid, Vi-diphtheria toxoid, Vi-rEPA, Vi-CRM197, etc have showed considerable hope; however, further research is needed to determine their long-term efficacy in typhoid-endemic areas (445). Furthermore, because intrinsic *Salmonella* proteins are absent from the current Vi-conjugate vaccines, cross-protection was absent against *S.* Paratyphi A and B and Vi-negative *S.* Typhi strains.

In contrast to the typhoid vaccines, vaccinations against *S.* Paratyphi and NTS (non-typhoidal *Salmonella*) have not yet received a licence. An ideal degree of attenuation linked with a decrease in immunogenicity in live-attenuated *S.* Paratyphi A/*S.* Typhimurium vaccination was studied in several Phase 1 studies utilizing the oral, live-attenuated vaccine (436). GMMA (Generalised Modules for Membrane Antigens) vaccines against *S.* Typhimurium and *S.* Enteritidis, on the other hand, have a significant problem in striking a balance between reactogenicity and immunogenicity (446).

Several vaccines are evaluated in preclinical studies using *Salmonella* O-antigen (O-specific polysaccharide or OSP) against *S.* Paratyphi and NTS. *Salmonella* O-antigen is a component of the outer membrane of Gram-negative bacteria which forms the distal portion of LPS that mediates serum bactericidal activity in healthy adults and children (405). Although *Salmonella* OSP molecules in their unconjugated state have limited immunogenicity, covalent attachment to proteins significantly enhances the immune response and allows their incorporation into

OSP-based vaccines (447). Several monovalent formulations [*S.* Paratyphi OSP-DT + *S.* Typhi Vi-DT, *S.* Typhimurium OSP-CRM_{197} + *S.* typhi Vi- CRM_{197} were evaluated in preclinical studies while others were tested in phase I (*S.* Typhimurium COPS-FliC + *S.* Enteritidis COPS-FliC + *S.* Typhi Vi-TT) or phase II (OSP-TT + Vi-TT) trials (448)] with different carrier proteins chemically conjugated to different polysaccharides showed considerable promise in different trials. Despite the potential of broader protective coverage, combined glycoconjugate vaccine has several inherent limitations as it may increase the chance of carrier-specific epitope suppression (CIES) or bystander interference (421, 423, 424) which further inhibit the hapten or saccharide specific immune response. In addition, the process of creating a multi-glycoconjugate vaccination is expensive and time-consuming. This emphasises the requirement for the development of single formulations having multivalency, or multivalent vaccines, which may provide defence against a range of typhoidal and nontyphoidal *Salmonella* serovars.

The aforementioned constraints might be addressed and future vaccine formulation development made possible by the use of innovative carrier proteins. It would be ideal to have a single vaccine formulation that contains antigens unique to multiple serovars of *Salmonella*. In our lab, it has been demonstrated that the outer membrane protein T2544 of *Salmonella* can produce potent, antigen-specific, opsonic antibodies and cytotoxic T lymphocytes, which protect mice against bacterial challenge (449). Therefore, in our study, we have used the T2544-protein to covalently fuse with different polysaccharides to develop two types of glycoconjugates, one is OSP-based glycoconjugate, OSP-T2544 to confer protection against typhoidal and non-typhoidal *Salmonella*, another is Vi-based glycoconjugate, Vi-T2544 to protect *Salmonella* Typhi and Paratyphi A and to compare its immunogenecity with the marketd Vi-vaccine, Vi-TT.

Mouse models to study the protective efficacy against typhoidal *Salmonella* have been established in iron overload mouse model (449, 450) whereas non-typhoidal *Salmonella* has

been reported in streptomycin-pretreated mouse model (256). However, the absence of a broadly accessible mouse model that accurately replicates human shigellosis, creates a significant barrier to a deeper comprehension of the disease pathophysiology and novel vaccinations. Iron is a crucial micronutrient for the intracellular survival and proliferation of numerous Gram-negative bacteria, such as *Shigella* and *S.* Typhi in addition to aiding in adhesion and invasion of the intestinal epithelium. It also enhances the susceptibility of mice to disease persistence (451-453). Even though the doses of iron (Fe) are toxic to bacteria (454), Fe toxicity in mice can be avoided by taking a lesser dose of iron along with the iron chelator deferoxamine (DFO), which sustains the establishment of infection as observed in *Salmonella* (455). The hexadentate chelator DFO removes free iron from the circulation and improves its excretion in the urine by binding with iron at a 1:1 molar ratio (456). As demonstrated for *Y. enterocolitica*, bacteria can bind to and absorb the ferrioxamine group of DFO via the FoxA receptor for iron utilization (457). FoxA is a TonB-dependent ferrioxamine transporter (458) and the siderophore is delivered to the periplasm via a TonB-dependent receptor. From there, it is taken to the cytosol by the PBP-dependent ABC transporter FhuBCD (459). In addition, it has also been demonstrated that streptomycin treatment can eradicate gut microbiota prior to the *Shigella* challenge (260, 261, 264). Therefore, in our study, we have developed a new oral-mouse model of Shigellosis using the combination of iron (Fe) plus chelator (desferrioxamine) with streptomycin before the oral challenge with *Shigella*.

Shigella invasion plasmid antigen B (IpaB) is largely conserved among all *Shigella* serotypes (460). IpaB-specific antibodies mediate Phagocytic activity and an IFN-γ-mediated immune response is generated (461, 462). Studies have shown that, intranasal immunization with IpaB augmented strong systemic and mucosal antibodies as well as T cell-mediated immunity and protected against *Shigella* serovars in a lethal pulmonary challenge study in mice (463, 464). Further, *Shigella* infection in CHIM (controlled human infection model) study reported that

serum IgG specific to IpaB may also function as a correlate of protection (465). Therefore, to generate a combination vaccine against *Shigella* and *Salmonella*, we have fused IpaB and T2544 to generate recombinant chimera IpaB-T2544. The effectivity of our newly developed oral mouse model was used to determine the vaccine efficacy of this chimeric fusion (IpaB-T2544) against *Shigella* and the iron overload mouse model was used to determine the vaccine efficacy against *Salmonella*.

In our study, objectives are listed as follows:

i. **Development of multi-subunit protein & polysaccharide conjugate vaccine candidate against enteric pathogens.**
ii. **Studies on the protective efficacy in animal models.**
iii. **Studies on the adaptive immune response after mucosal and systemic immunization with newly designed antigens.**

Chapter 3.

Material & Methods

3.0. Materials and methods.

3.1. Materials.

3.1.1. Bacterial strains, growth conditions and plasmid

Salmonella Typhi Ty2 and *Salmonella* Typhimurium LT2 were generous gifts from J. Parkhill, Sanger Institute, Hinxton, UK. Clinical isolates of *Salmonella* Typhimurium and *Salmonella* Enteritidis were gifted by A. Mukhopadhyay (ICMR-NICED, Kolkata, India), while *Shigella flexneri 2a* (2457 T) and clinical isolates of *Salmonella* Typhi, *Salmonella* Paratyphi A, *Shigella dysenteriae, Shigella sonnei* were received from IMTECH, Chandigarh. All *Salmonella* strains were grown in Hektoen enteric agar and *Escherichia coli* BL21, a kind gift from Dr. Rupak K. Bhadra (CSIR-IICB, Kolkata, India) was cultured in Luria–Bertani agar at 37 °C. Liquid cultures of the bacterial strains were grown in Luria Broth. Bacterial culture media and pET-28a plasmid were purchased from BD Difco and Addgene (USA), respectively. The oligonucleotides used in this study were synthesized from IDT.

3.1.2. Sources of the bacterial strains

Table 3.1. Sources of the bacterial strains used in this study

Strain	Source	Reference
Salmonella Typhi Ty2	Commercial	ATCC#700931
Salmonella Paratyphi A	Commercial	ATCC#9130
Salmonella Typhimurium LT2	Commercial	ATCC#25870
Salmonella Typhimurium C1	Clinical	Unpublished
Salmonella Typhimurium C2	Clinical	Unpublished

Salmonella Typhimurium C3	Clinical	Unpublished
Salmonella Enteritidis C1	Clinical	Unpublished
Salmonella Enteritidis C2	Clinical	Unpublished
Salmonella Enteritidis C3	Clinical	Unpublished
Shigella flexneri 2a (2457 T)	Commercial	ATCC#700930
Shigella dysenteriae	Commercial	ATCC#13313
Shigella sonnei	Commercial	ATCC#29930

3.1.3. Reagent list used for the study

Table 3.2. Chemicals.

Name	Manufacturer	Catalogue No
Trypticase soy agar (TSA)	BD Difco	211043
Trypticase soy Broth (TSB)	BD Difco	211768
Hectoen enteric agar (HEA)	BD Difco	285340
LB (Luria Bertani) Broth	BD Difco	244620
LB (Luria Bertani) Agar	BD Difco	244520
Bacto agar	Himedia	GRM026P

Terrific Broth	BD Difco	243820
Agarose	Sigma	A9539
Ferric chloride ($FeCl_3$)	LOBA Chemie	0381700500
Streptomycin sulfate	Puregene	PG-800S
Desferrioxamine (Desferal)	Novartis	2210413
Sodium bicarbonate ($NaHCO_3$)	Sigma	S5761
Gentamicin	Gibco	15710-064
Triton-X100	Sigma	T8787
Tween-20	Sigma	P2287
FBS	Gibco	10270-106
protease inhibitor cocktail	Sigma	P8340
formalin	Sigma	HT501128
Hematoxylin	Himedia	S014
Eosin	Himedia	S007
IPTG	Sigma	16758

Urea	SRL	62762
NaCl	Amresco	X190
Imidazole	Omnipur	5720
Tris	Puregene	PG-7940
SDS	Sigma	L4390
Acrylamide-Bis-acrylamide 40% solution	Sigma	A9926
Ni-NTA slurry	Qiagen	30230
Glycerol	Himedia	MB060
PVDF membrane	Millipore	IPVH00010
BSA	SRL	83803
Tween-20	Himedia	MB067
Tris	Puregene	PG-7940
PMSF	Sigma	P7626
Lysozyme	Sigma	L6876
NaOH	SRL	68151

UNO sphere Q resin	Bio-Rad	156-0101
Formalin	Sigma	F8775
Phenol	Himedia	AS022
Ethanol	Himedia	MB106
DNAse	Roche	10104159001
RNAse	Roche	10109134001
Proteinase K	Roche	03115879001
Acetic acid Glacial	Himedia	AS119
Cyanogen bromide (CnBr)	SRL	65291
Acetonitrile	Fluka	19182
ADH	Sigma	A0638
$NaHCO_3$	Sigma	S5761
EDAC	Millipore	341006
Guinea pig complement	Sigma	234395

Murine Granulocyte-Macrophage Colony Stimulating Factor (mGM-CSF)	CST	5191
Hexadecyltrimethylammonium bromide (CTAB)	SRL	66302
$CaCl_2$	Sigma	C3306
Acetone	Himedia	AS025
TMB substrate	BD OptEIA™	555214
SuperSignal West Pico	Thermo Scientific	34580
RPMI 1640 medium	Gibco	23400-021

Table 3.3. ELISA kit

Name	**Manufacturer**	**Catalogue No**
IL4	Invitrogen BD Bioscience	BMS613 555232
IL-6	Invitrogen	BMS603-2

	BD Bioscience	555240
IFN- γ	Invitrogen R&D Krishgen Biosynthesis	KMC4021 DY485-05 KB2011
IL-10	Invitrogen	BMS614
TNF-α	Invitrogen R&D	BMS607-3 DY410-05
IL-5	BD Bioscience	555236
IL-12	BD Bioscience	555256
IL-1β	R&D	DY401-05
CXCL10	R&D	DY466-05

Table 3.4. Antibodies.

Western blot		
Name	**Manufacturer**	**Catalogue No**

Rabbit Anti-Mouse His-tag antibody	Cell Signalling Technology	2365S
Rabbit Anti-Mouse IgG-HRP	Invitrogen	31450
ELISA		
Name	**Manufacturer**	**Catalogue No**
Rabbit Anti-Mouse IgG-HRP	Invitrogen	31450
Rabbit Anti-Mouse IgG1-HRP	Sigma	R136808
Rabbit Anti-Mouse IgG2a-HRP	Sigma	R124491
Goat Anti-Mouse IgA-HRP	Invitrogen	62-6720
Flow cytometry		
Name	**Manufacturer**	**Catalogue No**
Rat Anti-Mouse CD4-Percp Cy5.5	BD Bioscience	550954
Rat Anti-Mouse CD44- FITC	BD Bioscience	553133
Rat Anti-Mouse CD62L-PE Cy7	BD Bioscience	560516

Table 3.5. Oligos.

Name	Sequence	Application
T2544 FP	TTCGCCATGGAACGCCGCGGG ATCTATATCACCGGG	Cloning of T2544 in pET28a
T2544 RP	GCCCTCGAGTTAGCGGCGAAA GGCGTAAGTAATGCC	Cloning of T2544 in pET28a
T2544 fus prot FP	GCCGTCGACGGACCAGGACCA GAAGGGATCTATATCACCGGG	Cloning of T2544 in pET28a
T2544 fus prot RP	GCCCTCGAGTTAAAAGGCGTA AGTAATGCCGAG	Cloning of T2544 in pET28a
IpaB FP	CGCGGATCCGGTGGCGGTGGCTC GGATCTTACTGCTAACCAAAAT	Cloning of IpaB in pET28a
IpaB RP	CCGGAGCTC AACACAACCCATTACTCTGTTGA G	Cloning of IpaB in pET28a

3.2. Methods.

3.2.1. Cloning, expression, and purification of recombinant proteins

3.2.1.1. Cloning and expression of recombinant T2544 (rT2544)

t2544 ORF with four arginine coding sequences inserted at the NH2 terminus was PCR amplified, using *Salmonella* Typhi Ty2 genomic DNA as the template and the following forward and reverse primers:

FP-5'TTCGCCATGGAACGCCGCGGGATCTATATCACCGGG-3',

RP-5' GCCCTCGAGTTAGCGGCGAAAGGCGTAAGTAATGCC-3'.

The PCR product was cloned into pET28a at the NCoI and XhoI restriction enzymes (New England Biolabs) sites. After clone confirmation by restriction digestion, followed by sequencing (AgriGenome, India), the recombinant plasmid was transformed into *E. coli* BL21 (DE3). Transformed bacteria were inoculated into LB (BD Difco) broth (300 ml) and incubated until the OD_{600} reached 0.5. Recombinant T2544 expression was inducted by 1mM IPTG for 4h at 37°C, followed by centrifugation at 5000 g. The induction was confirmed by SDS-PAGE, stained with Coomassie Blue. To isolate the inclusion bodies, induced bacterial cells were resuspended in sonication buffer (30 ml) and subjected to 5 cycles of sonication on ice, with each cycle consisting of 5 pulses of 1 sec each followed by 1-minute incubation. The power output was designed to deliver a maximum of 30 watts at a frequency of 20 kHz. The sonicated pellet was collected following centrifugation at 15000 rpm for 20 min at 4°C, and washed (times with protein extraction wash buffer (20 ml). After centrifugation, recombinant T2544 was extracted from the inclusion bodies using protein extraction buffer [10 mM Tris-HCL (pH 12.0), 5ml] and analyzed by 12% SDS-PAGE.

3.2.1.2. Purification of recombinant T2544 (rT2544)

The extracted rT2544 was purified by ion exchange chromatography using UNO sphere Q resin (Bio-rad), according to the manufacturer's protocol. A Glass econo-column (1.0 x 10 cm, Bio-Rad) was packed 50% with the resin, followed by washing with 5 column volumes (CV) of water and equilibration with 10 CV (column volume) of equilibration buffer (1X PBS, pH 7.4).

The equilibrated resin was admixed with the recombinant protein (rT2544, 5ml) and kept for binding up to 3h at room temperature. The mixture was passed through the column and after washing with 3 CV (column volume) of ion exchange wash buffer, column-bound rT2544 was eluted using ion exchange elution buffer with Nacl gradient. Briefly, 1 ml of elution buffer containing 1M NaCl was inserted to the protein bound column that already had 40% of wash buffer and 1ml of eluted volume was collected. Eluted rT2544 was quantitated by Bradford Reagent (Sigma) and protein purity was determined by 12% SDS-PAGE. Protein extraction and IEC buffer compositions are mentioned in T**able 3.6**.

T**able 3.6**. **Composition of rT2544 extraction and purification buffer**

Protein extraction buffer from inclusion body	**Composition**
Sonication buffer	20 mM Tris-HCl, 400 mM NaCl, 1mM PMSF, lysozyme (1mg/ml), pH 8.0
Wash buffer	20 mM Tris-HCl, pH 8.0
Extraction buffer	10 mM Tris-HCl at pH 12.0
Protein purification buffer used in ion exchange chromatography	**Composition**
Equilibration buffer	10 mM Tris-HCL, pH 8.0, and 1.2 mM NaCl

Wash buffer	10 mM Tris-HCL, pH 8.0, and 1.2 mM NaCl
Elution buffer	10 mM Tris-HCL, pH 8.0, and 1M NaCl

3.2.1.3. Cloning and expression of recombinant IpaB-T2544

IpaB and *t2544* genes were cloned in tandem into the prokaryotic expression vector pET28a. We first amplified the 801 bp domain regions of *IpaB* gene by PCR using the genomic DNAs of *Shigella flexeneri 2a* strain as the template and cloned into pET28a vector using the following IpaB primers: IpaB forward primer: CGCGGATCCGGTGGCGGTGGCTCG GATCTTACTGCTAACCAAAAT and IpaB reverse primer: CCGGAGCTC AACACAACCCATTACTCTGTTGAG where BamHI and SacI were used as restriction enzymes (New England Biolabs). Later on, *t2544* along with an upstream linker sequence (GGACCAGGACCA is the gene codon of a non-furin linker containing glycine and proline amino acids) (total sequence length 663bp) was PCR amplified and the PCR product was cloned between SalI and XhoI restriction enzymes (New England Biolabs) of the pET28a-IpaB plasmid (T2544 FP: GCCGTCGACGGACCAGGACCAGAAGGGATCTATATCACCGGG and T2544 RP: GCCCTCGAGTTAAAAGGCGTAAGTAATGCCGAG). After clone confirmation by restriction digestion, followed by sequencing (Agri genome), the recombinant plasmid (rIpaB-T2544) was transformed into *E. coli* BL21 (DE3) pLysS cells. Transformed *E. coli* BL21 pLysS cells were inoculated into terrific broth (BD Difco) and incubated until the OD_{600} reached 0.5. Transformed cells were induced with 1 mM isopropylthiogalactoside (IPTG) for 4 h at 37°C, followed by centrifugation at 5000g. Protein in the induced pellet was observed by 12% SDS-PAGE.

3.2.1.4. Purification of recombinant IpaB-T2544

The resulting pellet was resuspended in lysis buffer containing 8 M urea, 200 mM NaCl, 2 mM imidazole and 50 mM Tris-HCl. Induced bacterial cells were subjected to 5 to 80 cycles of sonication on ice, with each cycle consisting of 5 pulses of 1 sec each and a 1-minute incubation period. The power output was designed to deliver a maximum of 30 watts at a frequency of 20 kHz. The sonicated sample was purified by affinity chromatography using Ni-NTA slurry according to the manufacturer's instructions (Qiagen). Briefly, the sonicated sample was centrifuged at 15000 rpm for 30 minutes at 4°C. The supernatant was collected and used for protein purification. 1ml of Ni-NTA slurry was centrifuged at 1500 × g and the supernatant were removed. The Ni-NTA beads were then mixed with equilibration buffer (20 mM Tris-HCl, 400 mM NaCl, 5 mM imidazole, 8 M urea) for 1 hour at room temperature. 4ml of protein supernatant was added to the equilibrated Ni-NTA beads and incubated at room temperature for 4 hours. The protein-Ni-NTA mixture was loaded into the column (Bio-Rad empty polypropylene column). The recombinant protein was eluted from the column using elution buffer (20 mM Tris-HCl, 300 mM NaCl, 500 mM imidazole, 8 M urea) and then renatured by gradual removal of urea by dialysis in 20 mM Tris-HCl, 150 mM NaCl, 10% glycerol, 0.5% Triton-X 100 and 2 M urea buffer using a 10 kD membrane (Millipore). The purity of the protein was determined by sodium dodecyl-sulfate polyacrylamide gel electrophoresis (SDS–PAGE).

3.2.2. Extraction and purification of polysaccharides

3.2.2.1. Extraction of polysaccharide OSP (O-specific polysaccharide)

Lipopolysaccharide (LPS) was purified from *S.* Typhimurium, using the hot phenol method as reported earlier (466). Briefly, *Salmonella* Typhimurium LT2 strain was cultured in Luria Broth (1L) at 37°C for 10h (OD 1.8). Formalin-inactivated cells were collected by centrifugation at 5000 g and washed twice with PBS. After resuspension in PBS (30 ml). 90% phenol (HiMedia) was used for 30 min at 68°C to extract crude LPS from the cell pellet. The suspension was centrifuged at 7,300 × g at 10°C for 1 h. The aqueous layer (60 ml) was precipitated with ethanol (final concentration 75%), and the precipitate was treated with DNAse (1 μg/mL), RNase (1 μg/mL) and Proteinase K (100 μg/mL) (all purchased from Roche), followed by dialysis overnight against PBS (pH 7.4) at 4°C. Extracted LPS was used to further extract O-specific polysaccharide (OSP). To this end, LPS was incubated with 1% acetic acid (HiMedia), pH 3.0, and 100 °C for 1.5 hours, followed by ultracentrifugation at 64,000 ×g for 5h at 10 °C, using a WX+ Ultra series centrifuge (Thermo Scientific). The supernatant was dialyzed for 48h against PBS (pH 7.4) and OPS was purified by size exclusion chromatography.

3.2.2.2. Purification of polysaccharide OSP by size exclusion chromatography

Size exclusion chromatography was performed as described earlier (467). Briefly, rT2544, OSP and OSP-rT2544 (conjugate) samples in normal saline (pH 7.4) were filtered through 0.22 μm syringe filters (HiMedia) and run in a Hiload 16/60 Sephacryl S300 size exclusion column (Cytiva Life Sciences) at a flow rate of 0.5 mL/min at 4°C using Biorad NGC chromatography system. The column was previously equilibrated with normal saline (pH 7.4). The buffer solution was degassed and filtered through 0.22 μm cellulose acetate membrane filters (Millipore). The polysaccharide and the protein were detected at λ =215 nm and 280 nm, respectively.

3.2.2.3. Extraction of Vi polysaccharide from *Citrobacter fruendii*

Two liter Brain Heart infusion broth cultures were inoculated at 1:100 from overnight cultures and were grown at 37 °C to an OD600 of 1.0. cells were collected by centrifugation at 10,000 rpm for 10 min. To collect Vi antigen secreted into culture supernatants, hexadecyltrimethylammonium bromide was added to the cell-free culture medium at a final concentration of 0.1% (wt/vol). The mixture was stirred for 1 h, and precipitated Vi antigen was collected by centrifugation at 10,000 rpm. The sedimented material was resuspended in 8 mL of 1-M CaCl2. Ethanol was added to a final concentration of 80% (vol/vol), and the mixture was mixed on a roter for 20 min. The precipitate was collected by centrifugation at 12,000 rpm for 20 min and was washed three times with 8 mL ethanol and once with 8 mL acetone. The Vi antigen was collected by centrifugation at 12,000 rpm for 20 min after each washing step. The pellet was resuspended in 3 mL acetone and was dried. Dried Vi antigen was resuspended in 8 mL of 20 mM Tris·HCl (pH 8.0) containing 2 mM MgCl2. DNase and RNase (Roche) were added to a final concentration of 10 μg/mL and the mixture was incubated at 37 °C for 3 h. Proteinase K (Invitrogen) was added to a final concentration of 20 μg/mL and was incubated for 2 h at 55 °C. Then 8 mL of Tris HCl-buffered phenol (pH 8.0) was added, and the mixture was inverted for 20 min at 20 °C. The mixture then was centrifuged at 12,000 rpm for 15 min, and the aqueous phase was removed and dialyzed against water for 2 days. The vi-polysaccharide was purified by size exclusion Chromatography. Vi preparations were characterized by protein content <1% (by Bradford assay), nucleic acid content <0.5% (by A_{260}) and endotoxin level <0.1 UI/ μg (by LAL).

3.2.2.4. Purification of Vi polysaccharide by size exclusion chromatography

Samples of rT2544, Vi, and Vi-rT2544 (conjugate) in normal saline (pH 7.4) were filtered using 0.22 μm syringe filters (HiMedia) before being passed down a Bio-Rad size exclusion chromatography column. Sephacryl S500 resin (120 ml) was packed 80% full in a Glass Eco-

Column (1.5 x 75 cm, Bio-Rad). This was followed by washing with 5 column volumes (CV) of water and equilibration with 10 CV (column volume) of equilibration buffer (1X PBS, pH 7.4). After degassing the buffer solution, Millipore 0.22 µm cellulose acetate membrane filters were used for filtering. Concentrated samples (500 µl) were passed through the column at a flow rate of 0.2 mL/min at 4°C. Eluted fractions were collected and concentrated. The polysaccharide and the protein were detected at λ =450 nm and 280 nm, respectively.

3.2.3. Conjugation of protein and polysaccharide

3.2.3.1. Conjugation of OSP and rT2544

Conjugation was performed as described earlier (466). Briefly, purified OSP (1.2 mg/ml in PBS, pH 8.5-9.0) was activated with an equal volume of cyanogen bromide (CnBr, SRL), prepared as 1.2 mg/ml in acetonitrile (Fluka). The reaction mixture was kept for 6 min on ice and the pH was maintained with 0.1M NaOH. The activated mixture was derivatized with 0.8M ADH (Sigma), dissolved in 5M $NaHCO_3$ (SRL). For this reaction, the pH was adjusted to 8-8.5 with 0.1M HCl. The reaction mixture was stirred at 4°C overnight and dialyzed against 1x PBS, pH 7.4 at the same temperature for 16 h. ADH derivatized OSP was then mixed with 3 ml of recombinant T2544 (1.25 mg /ml), followed by the addition of EDAC (0.05M) to the mixture and incubated for 4h on ice. The pH of this protein-polysaccharide mixture was maintained at 5.1 to 5.5 with 0.1 M HCl. Finally, the mixture was dialyzed against 1x PBS (pH 7.4) for 48 hours at 4°C.

3.2.3.2. Conjugation of Vi and rT2544

The purified Vi (1.2 mg/ml in PBS, pH 8.5-9.0) was activated with an equal volume of cyanogen bromide (CnBr, SRL), prepared as 1.2 mg/ml in acetonitrile (Fluka). The reaction

mixture was kept for 6 min on ice and the pH was maintained with 0.1M NaOH. The activated mixture was derivatized with 0.8M ADH (Sigma), dissolved in 5M NaHCO3 (SRL). For this reaction, the pH was adjusted to 8-8.5 with 0.1M HCl. The reaction mixture was stirred at 4°C overnight and dialyzed against 1x PBS, pH 7.4 at the same temperature for 16 h. ADH derivatized Vi-polysaccharide was mixed with 3 ml of recombinant T2544 (1.25 mg/ml), followed by the addition of EDAC (0.05M) to the mixture and incubated for 4h on ice. The pH of this protein-polysaccharide mixture was maintained at 5.1 to 5.5 with 0.1 M HCl. Finally, the mixture was dialyzed against 1x PBS (pH 7.4) for 48 hours at 4°C.

3.2.4. Estimation of protein and polysaccharides

3.2.4.1. Estimation of protein by Bradford reagent

Protein samples were measured by Bradford reagent according to manufacturer protocol.

3.2.4.2. Estimation of O-specific polysaccharide (OSP)

The concentration of the OSP was measured by phenol-sulphuric assay. Two hundred microlitre of 5% phenol was added to each tube containing 100 µl of sample (column fractions), vortexed followed by the addition of 2 ml of concentrated sulphuric acid. Reaction mixtures were cooled for 30 min, and OD was taken at 490 nm. The concentration of OSP was calculated using the standard curve.

3.2.4.3. Estimation of Vi polysaccharide

Vi is measured by standard ELISA using the equation $y = 0.6195x - 0.0684$

3.2.5. Circular Dichroism (CD)

Circular dichroism was performed as described earlier (468). Briefly, 1.0 ml of protein samples (rT2544, rIpaB and rIpaB-T2544, [180 µg/ml]) were filtered through a 0.45 µm pore-size filter to remove suspended particles, and taken in a 0.1 mm path-length quartz cuvette. Circular dichroism (CD) spectrum of the protein sample was captured at the wavelength range of 200 to 300 nm at 25°C on the Jasco-1500 spectrophotometer. A minimum of three spectra were recorded at 1 nm steps at a speed of 50 nm per minute. Baselines were subtracted and data was recorded as ellipticity (CD [mdeg]).

3.2.6. Fast-performance liquid chromatography (FPLC)

FPLC was performed as described earlier (467). Briefly, rT2544, OSP and OSP-rT2544 run in a Hiload 16/60 Sephacryl S300 size exclusion column (Cytiva, flow rate 0.5 mL/min at 4°C) and Vi, and Vi-rT2544 run in Sephacryl S500 size exclusion column (Bio Rad, flow rate 0.5 mL/min at 4°C) in normal saline (pH 7.4). Samples were filtered through 0.22 µm syringe filters (HiMedia) before run into the column. The buffer solution was degassed and filtered through 0.22 µm cellulose acetate membrane filters (Millipore). The polysaccharide and the protein were detected at λ =215 nm and 280 nm, respectively.

3.2.7. Dynamic light scattering (DLS)

DLS was performed as described earlier (469, 470). Briefly, 1 ml of Protein (rT2544), polysaccharide (OSP) and conjugate samples (OSP-rT2544) at a concentration of 0.8-1 mg/ml were filtered through a 0.45 µm pore-size filter to remove particles, if any prior to the measurement. Hydrodynamic sizes of the samples were calculated using ZEN 3600 Malvern Zetasizer with 5 mW HeNe laser at 25°C. The dispersed light is gathered at 173° in this system, which employs backscatter detection.

3.2.8. Fourier transform infrared spectroscopy (FTIR)

FTIR was performed as described earlier (471). Briefly, functional groups of lyophilized polysaccharides (OSP and Vi) and conjugate samples (OSP-rT2544 and Vi-rT2544) were monitored using potassium bromide (KBr) pellet method (1:100 w/w). To create translucent 1 mm pellets, potassium bromide was combined with lyophilized samples (0.8–1.0 mg) and pressed with 7500 kg for 30 seconds. Spectra were recorded using the translucent pellet in Perkin Elmer Spectrum 100 system in the spectral region of 4000–400/ cm.

3.2.9. Proton NMR

^{1}H NMR was performed as described earlier (469). Briefly, Lyophilized polysaccharide (OSP and Vi) and conjugate samples (OSP-rT2544 and Vi-rT2544), dissolved in 0.5 mL of D_2O (Sigma, 99.9%) were analyzed in a 400 MHz NMR spectrometer (JOEL 400 YH) at 25°C using NMR Pipe on Mac OS X workstation. A sodium salt, TSP-D4 (0.38%) was used as a standard. The spectrometer was arranged with a 5 mm triple-resonance z-axis gradient cryogenic probe head and four frequency channels. Initial delays in the indirect dimensions were intended to provide -180° and 90° first-order phase corrections at zero and first order, respectively. States-TPPI phase cycling was used to achieve quadrature detection in the indirect dimensions with a one-second relaxation delay.

3.2.10. Immunization of Mice

3.2.10.1. Preparation of antiserum

One group of female, inbred C57BL/6 and BALB/c mice (5-6 weeks old) were immunized subcutaneously with OSP (8µg), rT2544 (24 µg), or OSP-rT2544 (8µg of OSP and 24 µg of rT2544) at 2-weeks intervals for 3 times. Other group of BALB/c mice were immunized

subcutaneously and intramuscularly with 25 µg of the Vi in Vi-rT2544 and Vi-TT, at day 0 and another set were intranasally immunized with 40µg of rT2544, rIpaB, or rIpaB-T2544 at 2-weeks intervals for 3 times. Blood samples were taken from the immunized mice at each time point by tail snip and incubated for 30 min at 37°C. Antiserum was separated from blood by centrifugation at 1,200 × g at 4°C for 15 min and stored at −80°C.

3.2.10.2. Collection of fecal contents and intestinal washes

Fecal samples were collected before and after each immunization dose, weighed, and carefully dissolved in 100 mg/ml of PBS, containing 1% BSA (SRL), centrifuged at 15,000 × g at 4°C for 10 min, and protease inhibitor cocktails (Sigma-Aldrich) were added to the supernatants before storage at −80°C. Intestinal washes were collected after the sacrifice of the immunized mice (on day 38). To this end, the small intestine was removed and washed three times with 1 ml of PBS-1% BSA (BSA, SRL). Samples were centrifuged at 10,000 × g at 4°C for 10 min, and protease inhibitor cocktails (Sigma-Aldrich) were added to the supernatants before storage at −80°C.

3.2.11. Enzyme-Linked Immunosorbent Assay (ELISA)

3.2.11.1. Estimation of IgG/IgA antibodies by ELISA

IgG and IgA antibodies specific for protein and polysaccharides were detected by ELISA. Microtiter plates were coated with 5 µg/ml of polysaccharides (OSP or vi) and 2 µg/ml of proteins (rT2544 or rIpaB) and incubated at 4°C overnight. After rinsing with PBS-T (Phosphate buffer saline, containing 0.05% Tween 20), the wells were blocked using PBS, containing 1% BSA (SRL) for 1 hour at room temperature. Following further washes, plates were incubated with serum, feces, or intestinal lavage samples, diluted serially (1:200 to 1:

102400 for IgG and 1:20 to 1:20480 for IgA) for 2 hours at room temperature. Subsequently, Goat anti-mouse IgG (1:10000) or IgA (1:5000) antibodies conjugated to HRP were added to the wells and incubated for 1 h at room temperature. The immune complex was developed using tetramethyl benzidine (TMB) substrate (BD OptEIA^{TM}) and OD_{450} of the mixture was measured in a spectrophotometer (Shimadzu, Japan).

3.2.11.2. Avidity assay

Avidity test was performed as described earlier (472). Briefly, after overnight incubation with the respective antigens (OSP, Vi and rT2544), microtiter plates were incubated with OSP-rT2544 or Vi-rT2544 anti-sera with a dilution of 1:100 in PBS-T. To test for the avidity of serum IgG antibody, respective antigen-antibody complexes in the wells were washed (3 times) with PBS-T, containing 6M urea before the addition of HRP-conjugated anti-mouse IgG. The avidity index was calculated by multiplying the ratio of the absorbances of the wells that were washed with and without 6M urea-containing buffer by 100.

3.2.11.3. Estimation of Cytokines from serum by ELISA

Serum cytokines (IL-4, IL-6, IFN- γ, IL-10 and TNF-α) (Invitrogen, USA) as well as IFN-γ (Krishgen biosystem) in the co-culture supernatants of T cells (OSP-rT2544 and Vi-rT2544 immunized mice) and BMDCs were measured using the commercial ELISA kits following the manufacturer's protocol. Briefly, Precoated ninety-six well plates were incubated with serum samples along with biotin-conjugate for 2h at room temperature. After three subsequent washes, plates were further incubated for one hour at room temperature with streptavidin-HRP. Following the addition of the TMB substrate, colour development was evaluated using spectrophotometry at 450 nm.

3.2.11.4. Estimation of Cytokine from intestinal tissue by ELISA

Cecum and colon were isolated from mice at different post-infection time points and rinsed 5 times in PBS to remove fecal contents. Organs were then homogenized in 1 mL of 2% FBS in PBS with protease inhibitors, and spun down at 2000 g. The concentration of IL-1β, TNFα, IFNγ, and CXCL10 were measured in the supernatant using the commercial ELISA kits (R&D) following the manufacturer's protocol. Briefly, ninety-six well plates were incubated overnight with capture antibody in coating buffer. Following three subsequent washes plates were subjected for blocking for one hour at room temperature. Samples were added to the wells following wash and incubated for two hours at room temperature. After three subsequent washes, plates were further incubated for two hours at room temperature with detection antibody. After three washes plates were further incubated with streptavidin-HRP for twenty minutes at room temperature. Following three washes plates were finally incubated with substrate for thirty minutes at room temperature. The reaction was stopped with the stop solution and the color development was evaluated using spectrophotometry at 450 nm.

3.2.11.5. Estimation of Cytokine from splenocytes by ELISA

PBS and rIpaB-T2544 immunized mice were sacrificed on day 38, ten days after the last booster dose was administered; splenocytes were then collected from the spleen. 200 µl of splenocytes were cultured in RPMI 1640 medium (1×10^5 cells/well) in 96-well microtiter plates. Cells were incubated with 5µg/ml of rIpaB-T2544. After 48h, supernatants were collected and levels of cytokine secretion were measured (pg/ml). Cytokines were estimated by commercial ELISA kits (BD bioscience [IL-4, IL-5, IL-6, IL-12], R&D [IL-4, IFN-γ, TNF-α]) following the manufacturer's instructions.

3.2.12. Western blot

Western blot was performed as described earlier (449). In glycoconjugate experiments, OSP, Vi, rT2544, OSP-rT2544 and Vi-rT2544 (8 µg each), resolved in 10% SDS-PAGE and were transferred to a PVDF membrane (Millipore). After blocking with 5% BSA for 1 h at room temperature, membranes were incubated overnight at 4 °C with polyclonal anti-rT2544 antibody (1:5000 dilutions), raised in-house. In other experiments, rT2544 (5 µg), rIpaB (7µg) and rIpaB-T2544 (3 µg each) were resolved in 12% SDS-PAGE, and then transferred to a PVDF membrane (Millipore). After transfer, membrane was washed with 1X TBS for 5 min at room temperature. After blocking with 5% BSA for 1 h at room temperature, membranes were washed with 1X TBS-T [Tris Buffered Saline pH 7.5, containing 0.1% Tween-20 (v/v)] three times for 5 min at room temperature. Membranes were then incubated with mouse anti-His-tag (CST) antibody (1:1000) in 5% BSA, 1X TBS, 0.1% Tween 20 at 4°C with gentle shaking, overnight. Membranes were washed with TBS-T for 5 times and incubated with secondary anti-mouse IgG antibody (1:10000 dilutions), conjugated to horseradish peroxidase (HRP) for 1 h at room temperature. After 3 washes with TBS-T in an orbital shaker, membranes were developed by chemiluminescent reagents (SuperSignal West Pico, Thermo Fisher) and the signals were captured in ChemiDoc ^{TM} MP imaging system (Bio Rad).

3.2.13. Serum bactericidal assay (SBA)

Serum bactericidal assay was performed according to an earlier described method (473, 474). Sera collected from the immunized C57BL/6 and BALB/c mice on different post vaccination days were heat-inactivated at 56°C for 20 min and serially diluted in PBS (1:100 to 1:102400). A mixture comprising of 25µl of guinea pig complement (25% final concentration) and 15 µl of PBS, 50 µl of diluted heat-inactivated serum and 10 µl of diluted bacteria (310 CFU, T_0) was prepared. The mixture was incubated for three hours (T_{180}) at 37°C with gentle agitation (130 rpm). The mixtures were plated on LB agar and the plates were incubated overnight at

37°C. Bactericidal titer of the complement-containing antisera was expressed as the dilution of the serum required for the reduction of bacterial growth by 50% at T_{180} compared with T_0. Data was analyzed using GraphPad Prism 8.0.1.244 software.

3.2.14. Soft agar motility inhibition assay

A motility assay was performed as described earlier (475). Briefly, soft agar (LB medium with 0.4 % Bacto agar, BD Difco) was mixed with 5% intestinal lavage from the experimental mice (collected on day 38 after the first immunization dose) and left at room temperature to dry. Bacteria (1×10^6 CFU) were plated on top of the dried plates, which were incubated for 10 hours at 37 °C. Bacterial motility was measured by the diameter (mm) of the clearing zones and the data was analyzed using GraphPad Prism 8.0.1.244 software.

3.2.15. Endotoxicity measurement by LAL assay

Endotoxicity was measured by LAL assay according to the manufacturers protocol. Briefly, 50µL of sample was added in the 96 well microtiter plate. After that 50µL of LAL reagent was added to each well and incubated at 37°C for 10 minutes. After incubation, 100µL of Chromogenic Substrate solution was added and incubated at 37°C for 6 minutes. 100µL of Stop Reagent (25% acetic acid) was added and the absorbance was measured at 405-410 nm.

3.2.16. Memory T cell assay

Myeloid precursor cells from mouse bone marrow (BM) were used to generate dendritic cells as described earlier (449). Briefly, bone marrow cells from the femur and tibia of naïve C57BL/6 or BALB/c mice were cultured in RPMI 1640 medium, supplemented with murine Granulocyte-Macrophage Colony Stimulating Factor (mGM-CSF, 20 ng/mL) for 7 days. On day 7, cells were harvested and starved for 12 h in RPMI 1640 containing 1% FBS, followed

by stimulation with OSP or OSP-rT2544 or Vi-rT2544 or Vi-TT for 24h. $CD4^+$ T cells were isolated from the spleens of the immunized mice on day 120 or 172 of the first immunization using magnetic beads (BD IMag™ anti-mouse CD4 Magnetic Particles, USA). $CD4^+$ T Cells were co-cultured for 24h or 48 h at 37°C in presence of 5% CO2 with antigen-pulsed BMDCs at 1:1 ratio. IFN-γ concentration was estimated in the culture supernatants by ELISA (Krishgen biosystem), while the$CD4^+$ T cells were analyzed by flow cytometry for T-effector memory cell determination markers ($CD4^+CD62L^{low}$ $CD44^{hi}$).

3.2.17. Flow Cytometry

Cells were stained with fluorochrome-conjugated anti-mouse antibodies following the standard protocol. Briefly, $CD4^+$ T Cells co-cultured with antigen-pulsed BMDCs were harvested and subjected to F_c blocking in FACS buffer (1:50 ratio) for 20 min on ice. Following centrifugation at 1500 rpm for 5 min at 4°C, cells were stained with fluorochrome-conjugated antibodies (BD Biosciences) against specific surface markers (CD4-Percp Cy5.5, CD44- FITC, and CD62L-PE Cy7) for 30 min at 4°C in the dark. After staining, the cells were washed three times in FACS buffer and fluorescent signals were measured by FACS ARIA-II (BD Bioscience). Data were analyzed by FlowJo (version V10.8.1).

3.2.18. Protection study

3.2.18.1. Protection from *S.* Typhi and *S.* Paratyphi challenge in Iron (Fe3+) Overload Mouse Model

Iron-overload BALB/c mice were infected with *Salmonella* Typhi or *Salmonella* Paratyphi A as described earlier (473, 449). Briefly, BALB/c mice were treated with intraperitoneal injection of Fe3+ as FeCl3 (0.32 mg per gm of body weight) along with Desferoxamine (25

mg/Kg body weight) four hours prior to the bacterial challenge. Four hours later, mice were treated 5% $NaHCO_3$ to neutralize the stomach acids. After 20 minutes of the bicarbonate treatment, mice were orally infected with 5 x 10^7 CFU of *S.* Typhi or 5 x 10^5 CFU of *S.* Paratyphi A and monitored for 10 days.

3.2.18.2. Protection from *S.* Typhimurium and *S.* Enteritidis challenge in Streptomycin pre-treated mice model

Streptomycin pre-treated C57BL/6 mice were infected with *Salmonella* Typhimurium and *Salmonella* Enteritidis as described earlier (256). Briefly, C57BL/6 mice were treated with streptomycin (20 mg/mouse) orally as a beverage for 24 h. At 20 h after streptomycin treatment, water and food were withdrawn for 4 h. Four hours later, mice were treated 5% $NaHCO_3$ to neutralize the stomach acids. After 20 minutes of the bicarbonate treatment, mice were orally infected with 5 x 10^6 CFU of *S.* Typhimurium or *S.* Enteritidis and monitored for 30 days.

3.2.18.3. Protection from *Shigella* challenge in Streptomycin and iron pre-treated Mouse Model

BALB/c mice were pretreated with streptomycin sulfate and iron with desferal (desferoxamine). Mice deprived of food and water for 4–6 hr before the oral streptomycin (20 mg/mouse) treatment (256). Afterward, animals were supplied with water and food ad libitum. 20h later the streptomycin treatment, water and food were withdrawn again and mice were injected with Desferrioxamine (25 mg/Kg body weight) intraperitoneally. Fifteen minutes later the Desferrioxamine treatment, $FeCl_3$ (0.32 mg per gm of body weight) was administered the same route before 4 hours of infection (439, 463). Four hours later, mice were treated with 5%

$NaHCO_3$ to neutralize the stomach acids. After 20 minutes of bicarbonate treatment, mice were infected by oral gavage with *Shigella flexeneri 2a* (5×10^7 CFU) resuspended in PBS.

3.2.18.4. Colonization study

To enumerate intracellular CFU from the ceca and colons from un-infected, infected, and immunized mice, organs were isolated aseptically at different time points. Tissues were vigorously washed in PBS with gentamicin (50 µg/ml) and mechanically homogenized in 1x PBS followed by lysed with 1% Triton-X100. Lysates were serially diluted and plated on TSA plates containing 100 µg/ml streptomycin. Colonies were counted after overnight incubation at 37°C. Fecal pellets were collected and homogenized in 2% FBS in 1 mL of PBS containing protease inhibitors. For CFU determination serial dilutions were made in PBS and plated on TSA plates containing 100 µg/ml streptomycin.

3.2.19. Histopathology

Colon and caecum tissues were excised from mice and preserved in 10% formalin. Formalin-dissolved tissues were then embedded in paraffin blocks. Tissues fixed in paraffin were divided into 5-µm-thick sections. The sections were soaked in xylene twice for 20 minutes at 56°C to deparaffinize and were dehydrated with ethanol (twice at 100%, once at 95%, and once at 75% ethanol) for five minutes. Tissue sections were mounted on glass slides and stained with Hematoxylin and Eosin. Slides were examined under a microscope and evaluated in a blinded fashion by two independent investigators. Different magnifications of images were captured to represent different parameters. 10x - presence of swelling (edema) in the submucosal layer, 20x- degenerative changes in the epithelial lining, 40x - presence of increased infiltration of

lymphocytes in the mucosa and submucosa, loss of crypt architecture with loss of goblet cells. Slides were scored for different histological parameters as described in **Table 3.7.**

Table 3.7. Histopathological scoring system for intestinal changes (260, 449, 476-478)

SL NO.	Criteria	Score
1	Intact crypt architecture with abundant records of goblet cells, intact mucosa, and submucosa without abnormal infiltrates, without submucosal swelling and without degenerative changes in the epithelial lining	0
2.1	Loss of crypt architecture with minimal goblet cells loss (<50%)	1
2.2	loss of crypt architecture with mild goblet cells loss (50%)	2
2.3	loss of crypt architecture with moderate goblet cell loss (>50%)	3
3.1	PMN infiltration into mucosa without submucosa with degenerative changes in the epithelial lining	1

3.2	PMN infiltration into mucosa with submucosa with degenerative changes in the epithelial lining	2
3.3	PMN infiltration into mucosa with submucosa and submucosal swelling with degenerative changes in the epithelial lining	3
	Severity of parameters	**Combined score**
4.1	No inflammation	0
4.2	Minimal signs of inflammation	1-2
4.3	Mild inflammation	3-4
4.4	Moderate inflammation	5-8
4.5	Profound inflammation	9-13

3.2.20. Statistical analysis

Data related to CD, FPLC, DLS and FTIR were analyzed using ORIGIN software (2019b). NMR data were processed in MestReNova-9.0.1 -9.0.1-13254 software. Antibody titers were represented as reciprocal of the log 2 values. Statistical analysis was performed using GraphPad Prism 8.0.1.244. Comparison between two groups was calculated by student t-test (*P, 0.05, **P < 0.01, ***P < 0.001, ****P < 0.0001), while One-way ANOVA, two-way

ANOVA with Tukey's post-hoc test was performed for multiple comparisons. Statistical significance was measured at *P <0.05, **P < 0.01, ***P < 0.001, ****P < 0.0001).

Chapter 4.

Results

4.1. Objective 1.

Development of multi-subunit protein & polysaccharide conjugate vaccine candidate against enteric pathogens

4.1.1. Development of OSP-rT2544

4.1.1.1. Purification of recombinant T2544

Cloning of pET28a-*t2544* was confirmed by restriction digestion, followed by agarose gel electrophoresis of the digested product that showed migration of *t2455* amplicon along the predicted size of 663bp (**Figure 1A**). Nucleotide sequencing of the clone showed in-frame cloning and correct orientation of *t2544* gene (**Figure 1B**). Recombinant T2544 (rT2544) extracted from the inclusion bodies of *E. coli* BL21 (DE3) migrated along the size of 30 kDa in SDS-PAGE (**Figure 1C**) and ion exchange chromatography yielded a highly purified protein of the same size (**Figure 1D**). Protein extraction and IEC buffer compositions are mentioned in **Table 3.6**. Further purification by size exclusion chromatography generated a smaller peak near 104.8 ml and a major peak near 112.8 ml fractions (**Figure 1E**).

[The detailed methodologies were discussed in the materials and method section **3.2.1.1.-3.2.1.2.]**

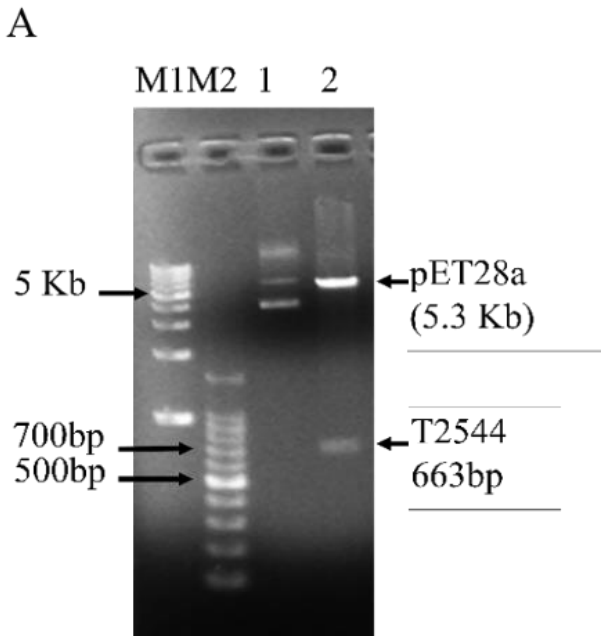

B

>ArgT2544_pET.Forward_32206-1_P4629,Raw Sequence(1126 bp)

CATGCAAGGGGGCGGAACATTCCCCTCTAGAATAATTTTGTTTAACTTTAAGAAGGAGATATACCATGGAACGCCGCGGGATCTATATCACCGGG
AAAGCGGGGACATCCGTAGTCAATGTCTATGGAATCAACTCAACCTTCAGCCAGGATGAGATAGTTAATGGTCATGCAACGTTACCTGACCGTA
CCAAAGGCGTTTTGGCGGCGGGGTTGCTATCGGTTATGACTTTTATGATCCATTCCAGCTTCCAGTACGTTTAGAACTGGATACCACTTTCAGA
GGTGAGACGGATGCTAAAGGCGGGCAGGATATTATTGCATTTGGTGATCCAGTACACATAAATGTAAAAAATCAGGTCCGAATGACCACTTACA
TGGTTAATGGCTATTATGATTTTCACAATAGTACGGCATTTACTCCCTATATCAGCGCAGGCGTTGGCCTCGCTCATGTGAAGCTAAGTAATAACA
CCATTCCTGTTGGTTTTGGTATTAATGAAACTCTGTCTGCTTCAAAAAATAACTTTGCCTGGGGCGCAGGTATCGGTGCAAAATATGCTGTAACA
GATAATATTATGATTGACGCCAGTTATAAATACATTAATGCTGGCAAAGTAAGCATTTCAAAAAATCACTATGCTGGTGATGAACATACCGCTTAT
GATGCAGACACAAAGGCTGCCTCCAATGACTTCATGCTCGGCATTACTTACGCCTTTCGCCGCTAACTCGAGCACCACCACCACCACCACTGA
GATCCGGCTGCTAACAAAGCCCGAAAGGAAGCTGAGTTGGCTGCTGCCACCGCTGAGCAATAACTAGCATAACCCCTTGGGGCCTCTAAACGG
GTCTTGAGGGGTTTTTTGCTGAAAGGAGGAACTATATCCGGATTGGCGAATGGGACGCGCCCTGTAGCGGCGCATTAAGCGCGGCGGGTGTGG
TGGTTACGCGCAGCGTGACCGCTACACTTGCCAGCGCCCTAACGCCGCTCTTTCGCTTTCTTCCCTCCTTTCTCGCACGTTCGCGGCTTCCCGTC
AGCTCTAATCGGGGCTCCCTTTAGGTTTCCGATTATGCTTACGCACTCGACCCCAAAAAACTTGATTAGGGTGATGGTTTCACTATG

>ArgT2544_pET.Reverse_32206-2_P4629,Raw Sequence(1239 bp)

TGGGAACCTTCAGACCGTTTAGAGGCCCCAAGGGGTTATGCTAGTTATTGCTCAGCGGTGGCAGCAGCCAACTCAGCTTCCTTTCGGGCTTTGT
TAGCAGCCGGATCTCAGTGGTGGTGGTGGTGGTGCTCGAGTTAGCGGCGAAAGGCGTAAGTAATGCCGAGCATGAAGTCATTGGAGGCAGCCT
TTGTGTCTGCATCATAAGCGGTATGTTCATCACCAGCATAGTGATTTTTTGAAATGCTTACTTTGCCAGCATTAATGTATTTATAACTGGCGTCAAT
CATAATATTATCTGTTACAGCATATTTTGCACCGATACCTGCGCCCCAGGCAAAGTTATTTTTTGAAGCAGACAGAGTTTCATTAATACCAAAACC
AACAGGAATGGTGTTATTACTTAGCTTCACATGAGCGAGGCCAACGCCTGCGCTGATATAGGGAGTAAATGCCGTACTATTGTGAAAATCATAAT
AGCCATTAACCATGTAAGTGGTCATTCGGACCTGATTTTTTACATTTATGTGTACTGGATCACCAAATGCAATAATATCCTGCCCGCCTTTAGCATC
CGTCTCACCTCTGAAAGTGGTATCCAGTTCTAAACGTACTGGAAGCTGGAATGGATCATAAAAGTCATAACCGATAGCAACCCCGCCGCCAAA
AACGCCTTTGGTACGGTCAGGTAACGTTGCATGACCATTAACTATCTCATCCTGGCTGAAGGTTGAGTTGATTCCATAGACATTGACTACGGATG
TCCCCGCTTTCCCGGTGATATAGATCCCGCGGCGTTTCCATGGTATATCTCCTTCTTAAAGTTAAACAAATTATTTCTAGAGGGGAATTGTTATCC
GCTCACAATTTCCCCTATAGTGAGTCGTATTAATTTCGCGGGATCGAGATCTCGATCCTCTACGCCGGACGCATCGTGGCCGGCATCACCGGCGG
CACAGTGGCGGTTGCTGGCGCCTATATCGCCGAACATCACCGATGGGGAAGATCGGGCTCGCCACTTCGGGCTCATGAGCGCTTGTTTCGGCGT
GGGGTAATGGTGCAGGCCCCGGTGCCCGGGGAACTGTGGCGGCATTTCCTGGATTGCACCATTCCTTGGCGGCGGCGTGCCCTCAACGGGCCT
CAACTTACTACTGGCTGACTCTAATTGCACGGAGTGCATTAAGGTAGGCCGTCAGAATCCCGGGACACATCGATTGGGCGCCAACCTTTCGCGG
TATGTTG

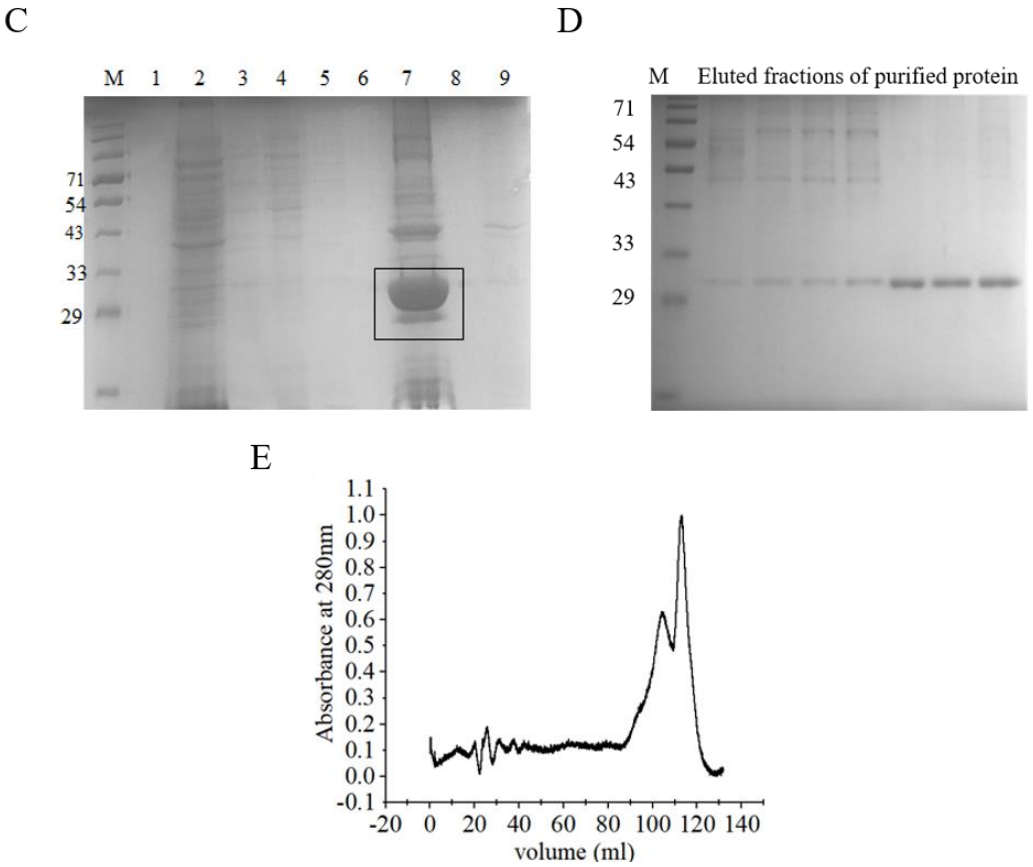

Figure 1. Purification and characterization of recombinant T2544. (A) 1% Agarose gel electrophoresis of pET28A-*t2544* after restriction digestion with XhoI and NcoI. Lane M1: 1

kb DNA ladder, M2: 100bp DNA ladder, 1: Undigested pET28A-t*2544* clone, 2: pET28A-t*2544* clone digested by XhoI and NcoI**.** (B) Sequencing of the clone using pET forward and reverse primers. The FASTA file format of the sequences is provided. Yellow and green color code for the recognition sites of the restriction enzyme NcoI and XhoI, respectively, whereas magenta and blue color code for open reading frame (ORF) and arginine nucleotide sequence, respectively. (C) 12% SDS-PAGE of recombinant T2544 (rT2544) protein expressed in *E. coli* and extracted from inclusion bodies. Lane M: Protein molecular weight marker (Prestained), Lane 1: empty lane, Lane 2: Cell lysate after sonication, Lane 3 to 4: supernatant after PBS wash, Lane 5 to 6: empty lanes, Lane 7: supernatant after re-suspension in extraction buffer, Lane 8: empty lane, Lane 9: pellet after re-suspension in extraction buffer**.** (D) 12% SDS-PAGE showing the elution profile of rT2544 (3.5 µg) after ion exchange chromatography (IEC). rT2544 extracted from the inclusion bodies of E. coli was admixed with UNO sphere Q ion-exchange resin (Bio-rad), followed by binding to the Glass econo-column, 1.0 x 10 cm (Biorad) (E) Elution profiles of rT2544 (0.8 mg/ml) from the size exclusion chromatography column (Hiload 16/60 Sephacryl S300, Cytiva), detected at 280 nm.

4.1.1.2. Characterization of recombinant T2544

The secondary structure of rT2544 detected by Far-UV CD spectra showed one negative band at 222.1 nm, indicating alpha helix, and two positive bands at 195.2 nm and 203.4 nm, suggesting β helical structures (**Figure 2A**). Dynamic light scattering measured the hydrodynamic radius of rT2544 as 22.16 nm (**Figure 2B**). [The detailed methodologies were discussed in the materials and method section **3.2.5. - 3.2.7.**]

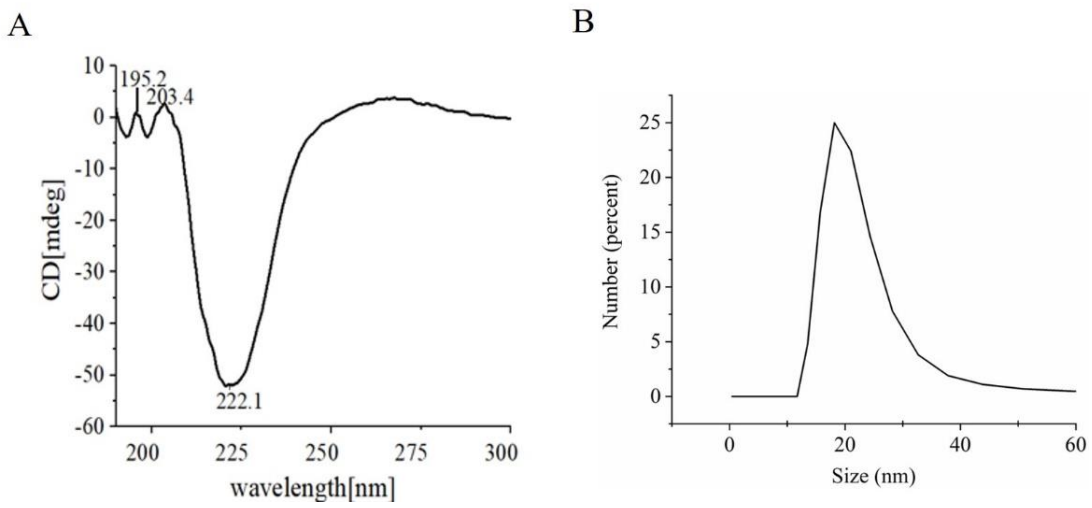

Figure 2. Characterization of recombinant T2544. (A) Far-UV circular dichroism spectra of rT2544 (180 µg/ml) captured at the wavelength range of 200 to 300 nm at 25°C in PBS (pH 7.4) on the Jasco-1500 spectrophotometer. Data presented as ellipticity (CD [mdeg]) after subtracting the baseline values. (B) Hydrodynamic radius (R_h) of rT2544 protein (0.8 mg/ml, PBS, pH 7.4) was determined by dynamic light scattering (DLS) at 25°C. For each analysis, experiment was replicated three times, and data from a representative experiment are shown.

4.1.1.3. Purification of OSP

Lipopolysaccharide extracted from *S.* Typhimurium LT2 and resolved in SDS-PAGE showed multiple higher molecular weight bands and a smear corresponding to lower molecular weights upon silver staining. Acid hydrolysis of LPS removed the smear, suggesting their origin from the lipid A component, while the core oligosaccharide bands were left behind in the gel (**Figure 3A**). The gel filtration profile of OSP showed two peaks near 109.23 ml and 117.9 ml fractions that corresponded to their average K_d values of ~ 22.75 kDa (**Figure 3B, Table 1**). [The detailed methodologies were discussed in the materials and method section **3.2.2.1., 3.2.2.2. and 3.2.6.**]

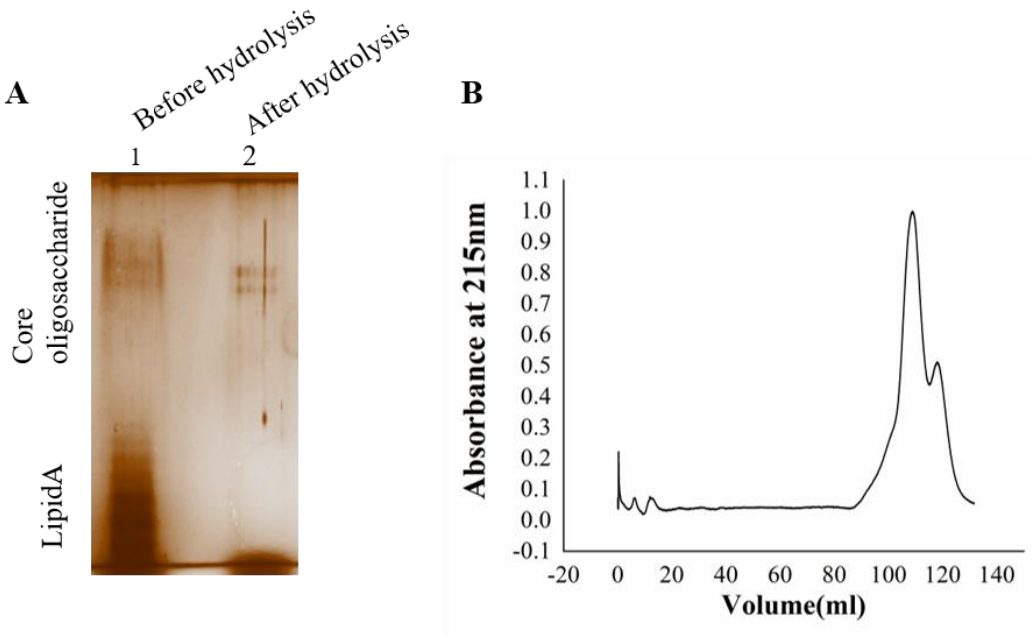

Figure 3. Extraction and purification of OSP. (A) Visualization of LPS and OSP resolved in 10% SDS-PAGE, stained by silver staining. LPS was extracted from *S.* Typhimurium LT2 strain by hot-phenol method and subjected to acid hydrolysis to isolate OSP. Lane 1: purified LPS (8 µg), Lane 2: purified OSP (8 µg). (B) Elution profiles of OSP (1mg/ml in normal saline, pH 7.4) eluted at a flow rate of 0.5 mL/min at 4°C from a size exclusion chromatography column (Hiload 16/60 Sephacryl S300, Cytiva), pre-equilibrated with normal saline, pH 7.4. The OSP was detected at λ =215 nm using Bio-Rad NGC chromatography system.

Table 1. K_d determination in OSP

Elution volume (ml)	**K_d[a]**	**MW(KDa)[b]**	**Average MW(KDa)**
109.23	0.86	26.9	22.75

117.9	0.97	18.6	

[a] K_d values were calculated following FPLC analysis on Hiload 16/60 Sephacryl-S300 column. To determine the void volume, dextran 500KDa was used and the K_d values were determined using the following formulae,

$K_d = V_e - V_0 / V_t - V_0$ where, V_e = peak elution volume (mL), V_0= void volume (mL), V_t=total elution volume (mL)

[b] Molecular weight of OSP was calculated from the dextran (20, 40, 70, 500 kDa) standard curve using the formulae y = -0.68x + 1.8386.

4.1.1.4. Characterization of OSP

^{1}H NMR analysis showed signals between 2.0 and 2.2 ppm, arising from the O-acetyl groups at C-2 of Abequose that confirmed the presence of the characteristic sugar of *S.* Typhimurium OSP. Signals between 1.79 and 1.97 ppm and 3.50 and 3.94 ppm of NMR spectra were generated from the protons bound to C-3 of Abequose and C-5 of Rhamnose and Abequose, respectively **(Figure 4A**). FTIR analysis disclosed the characteristic wave patterns of active OSP. Waves near 1650 cm^{-1} indicated carbonyl group (C=O), while those in the region of 1413-1261 cm^{-1} represented the deformation of C-H and C-OH groups. In contrast, waves near 1095 cm^{-1} and 1022 cm^{-1} corresponded to the characteristic peaks of the glycosidic linkage and the bands in the 936–800 cm^{-1} region, which is called the anomeric region, indicated the α and β configuration of the anomeric carbon **(Figure 4B**). Molecular radius of OSP was 4.42 nm, as calculated by DLS (**Figure 4C**). [The detailed methodologies were discussed in the materials and method section **3.2.7, 3.2.8. and 3.2.9.**]

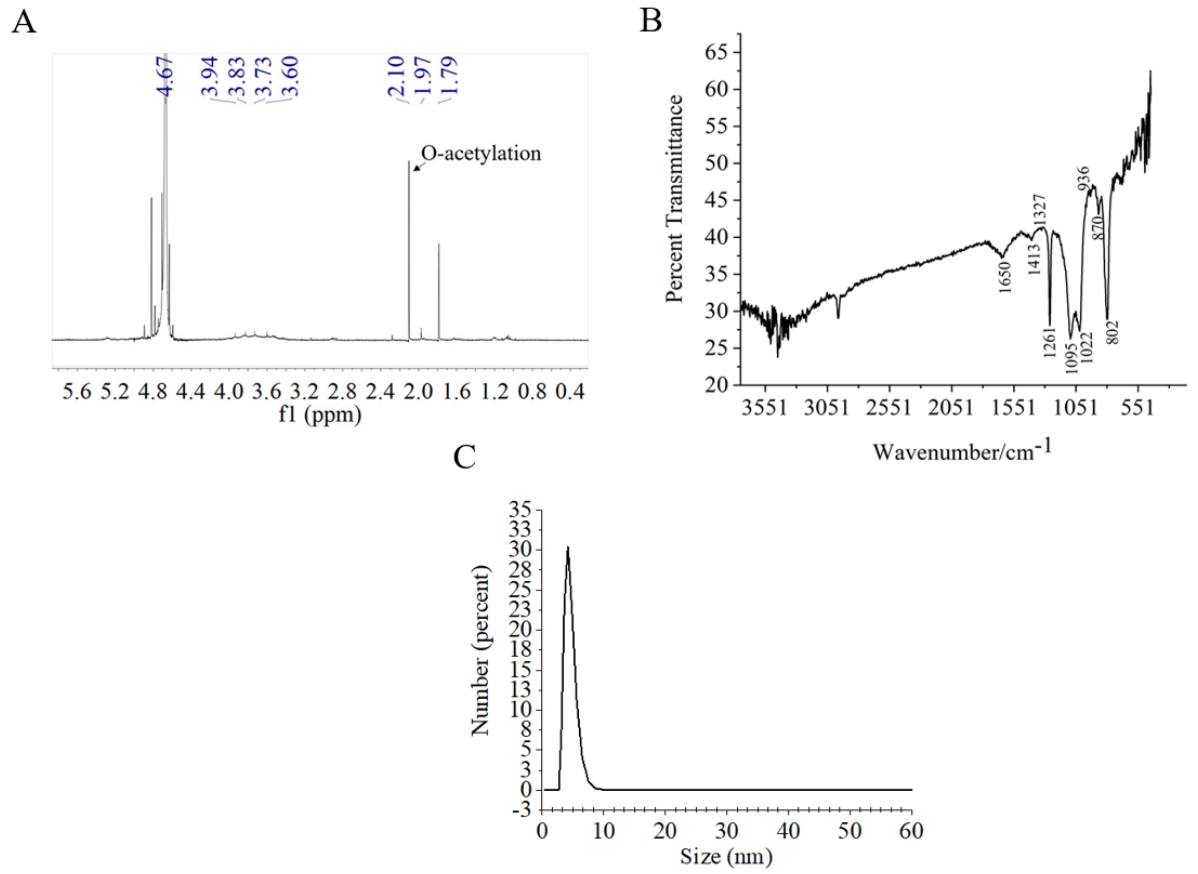

Figure 4. Characterization of OSP. (A) ^{1}H NMR of OSP showing the characteristic peak of O-acetylation associated with OSP at C-2 of Abequose at 2.1 ppm. Signals between 1.79 and 1.97 ppm were generated from the protons bound to C-3 of Abequose and 3.60 and 3.94 ppm from the protons bound to C-5 of Rhamnose and Abequose. Peak arises near 4.67 ppm indicating the D_2O solvent. (B) Fourier Transform Infrared spectrum (FTIR) showing different functional groups of O-specific polysaccharide (OSP). Waves near 1650 cm^{-1} indicated carbonyl group (C=O), while those in the region of 1413-1261cm^{-1} represented the deformation of C-H, C-OH group. In contrast, waves near 1095 cm^{-1} and 1022 cm^{-1} corresponded to the characteristic peaks of the glycosidic linkage. In addition, bands in the 936–800 cm− 1 region indicated aldehyde and ketone group. (C) Dynamic light scattering (DLS) showing hydrodynamic radius (R_h) of OSP (0.88 mg/ml, PBS, pH 7.4), determined at 25°C using ZEN 3600 Malvern Zetasizer. For each analysis, experiment was replicated three times, and data from a representative experiment are shown.

4.1.1.5. OSP and rT2544 conjugation purification and characterization of the conjugate

Conjugates of OSP and rT2544 displayed a smear tail in the western blots, probed with T2544 antibody, indicating heterogeneity of size and mass-to-charge ratios (**Figure 5**). FPLC analysis showed the major peak of OSP-r2544 elution after the calculated void volume (41.66 ml), as opposed to the elution peaks of OSP at 109.23 ml and 117.9 ml and rT2544 at 112.8 ml (**Figure 6A**). Higher hydrodynamic diameter of OSP-rT2544 (57.45 nm) compared with OSP (4.42 nm) and rT2544 (22.16 nm) suggested the formation of higher-order complex formation between the polysaccharide (OSP) and the protein (rT2544) (**Figure 6B**). However, we observed different molar ratios of OSP and rT2544 in the glycoconjugate molecules (**Table 2**). To find out the functional groups in the purified OSP-rT2544 conjugate, FTIR analysis was performed. FTIR showed one additional functional group in the conjugate (OSP-rT2544), the strong amide bond of protein at 1628 cm^{-1}, which was absent in OSP. On the other hand, similar functional groups in OSP-rT2544 and OSP corresponded to different wave lengths. Thus, carbonyl groups **(**C=O) were detected at 1673 cm-^{1}, deformation of C-H, C-OH groups appeared near region 1458-1261 cm^{-1} and glycosidic linkage emerged at 1095 cm^{-1} and 1158 cm^{-1} in OSP-T2544**.** In addition, α and β configurations of the anomeric carbon were detected near the regions 921 cm^{-1} and 800 cm^{-1} (**Figure 6C**). However, O-acetylation pattern at C-2 of Abequose between 2.0 and 2.2 ppm was similar in OSP and OSP-T2544 in ^{1}H NMR study (**Figure 6D**). But, two different peaks of the OSP-rT2544 molecule that corresponded to the aliphatic region of the protein and observed near 0.97 ppm and 2.77 ppm were absent from OSP. Total sugar and protein contents and the molecular weights of the conjugate and the un-conjugated preparations used for immunization are shown in **Table 3.** The highest molecular weight of the conjugate (398.1 KDa) was used for the immunization. [The detailed methodologies were discussed in the materials and method section **3.2.6, 3.2.7., 3.2.8., 3.2.9. and 3.2.12.**]

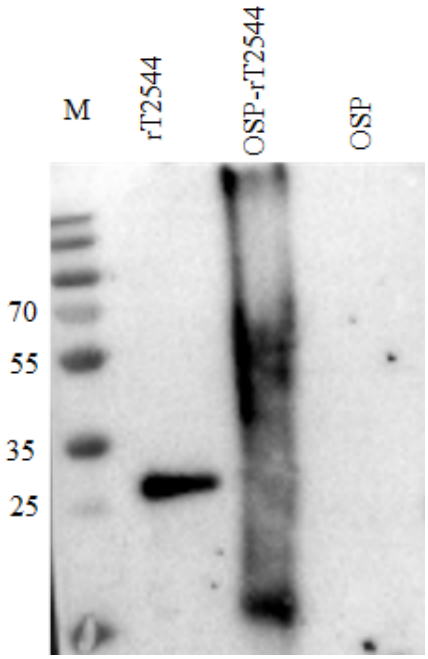

Figure 5. Western blot of OSP-rT2544 conjugate. The blot was probed with anti-rT2544 antibody after resolving the conjugated and un-conjugated samples in 10% SDS-PAGE. The experiment was repeated three times and a representative blot is shown here.

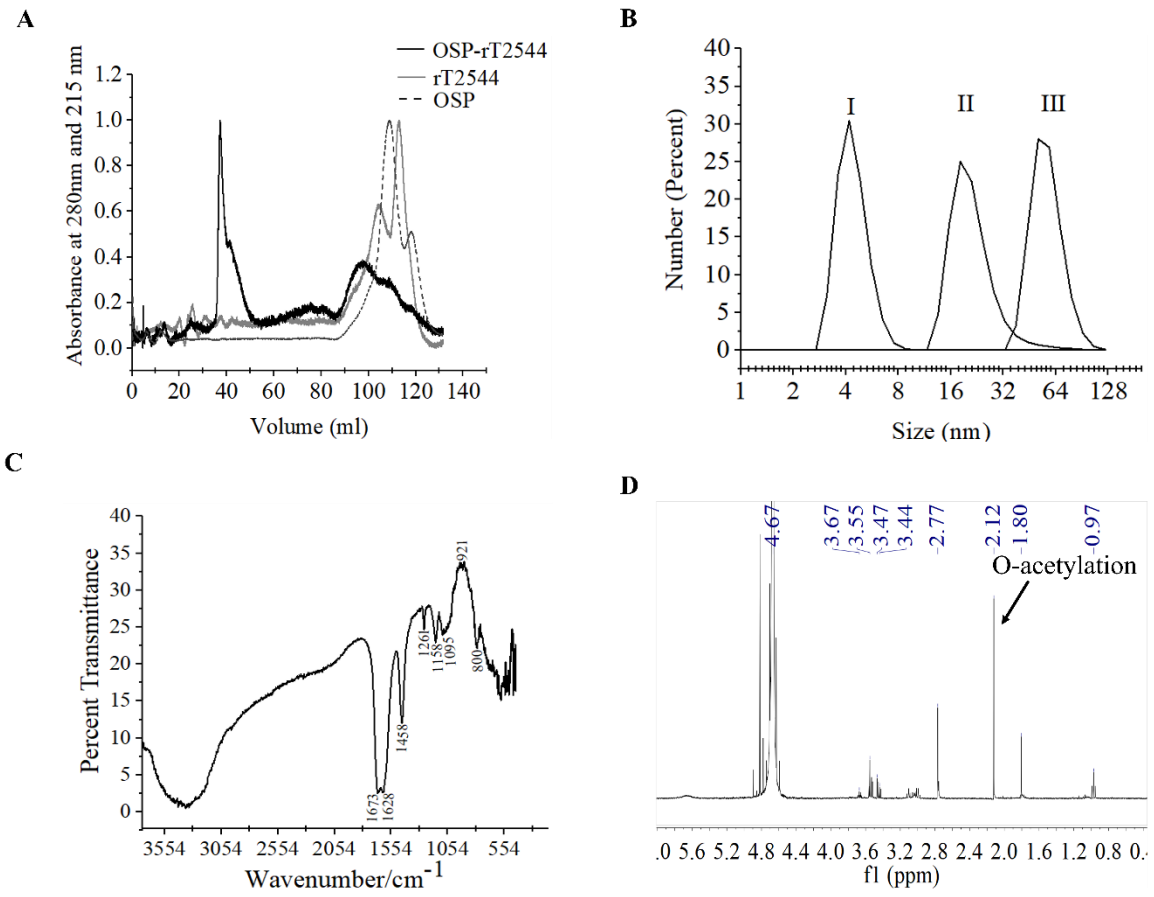

Figure 6. Characterization of OSP-rT2544 conjugate. (A) Gel filtration chromatography. OSP-rT2544 conjugate containing 1.83 mg of total protein and 0.59 mg of total sugar in normal saline (pH 7.4) was injected into Hiload 16/60 Sephacryl S300 column (Cytiva). The column was pre-equilibrated with normal saline, pH 7.4 and the flow rate was maintained at 0.5 mL/min. The conjugate (OSP-rT2544) and T2544 were observed (eluted at 41.66 ml and 112.8 ml) at 280 nm, while OSP (eluted at 109.23 ml and 117.9 ml) was observed at 215 nm at 4°C using Bio-Rad NGC chromatography system. (B) Dynamic light scattering (DLS) showing hydrodynamic radius (R_h) of (I) OSP (0.88 mg/ml); (II) rT2544 (0.8 mg/ml); (III) OSP-rT2544 (1 mg/ml), dissolved in PBS (pH 7.4) at 25 °C using ZEN 3600 Malvern Zetasizer. (C) Fourier Transform Infrared (FTIR) spectrum of the lyophilized conjugated sample (OSP-rT2544) was monitored using potassium bromide (KBr) pellet method (1:100 w/w). Spectra recorded in the Perkin Elmer Spectrum 100 system in the spectral region of 4000–400/ cm indicating different functional groups of OSP-rT2544: carbonyl group (C=O) (1673 cm^{-1}), C-H and C-OH groups (1458-1261 cm^{-1}), glycosidic linkage (1095 and 1158 cm^{-1}), aldehyde and ketone groups (921 and 800 cm^{-1}) and amide bond of the protein (1628 cm^{-1}). (D) ^1H NMR of lyophilized OSP-rT2544, dissolved in 0.5 mL of D_2O showing the characteristic peak of O-acetylation of OSP at C-2 of Abequose (2.12 ppm) in a 400 MHz NMR spectrometer (JOEL 400 YH) at 25°C. Additional peaks indicate protons bound to C-5 (3.4-3.6 ppm) and C-3 (1.8 ppm) of monosaccharides, the protein peaks (0.97 and 2.77 ppm) and the D2O solvent (4.67 ppm). For each analysis, experiment was replicated three times, and data from a representative experiment are shown.

Table 2. Determination of K_d, sugar, and protein concentration in the OSP-rT2544 conjugate sample

Sample	Elution volume (ml)	K_d (FPLC)	sugar (OSP)a (mg/ml)	protein (rT2544)b (mg/ml)	OSP to rT2544 molar ratio c (wt/wt)	MW (KDa)d
OSP-rT2544	41.66	0.02	0.3	0.6	1:1.53	398.1
	75.76	0.44	0.09	0.45	1:3.75	112.2
	97.09	0.71	0.02	0.28	1:11.2	44.6

[a] The concentration of the OSP was measured by phenol-sulphuric assay. Two hundred microlitre of 5% phenol was added to each tube containing 100 µl of sample (column fractions), vortexed followed by the addition of 2 ml of concentrated sulphuric acid. Reaction mixtures were cooled for 30 min, and OD was taken at 490 nm.

[b] Protein concentration was measured by Bradford assay.

[c] Molar ratios were calculated based on the OSP and protein molecular masses (OSP Avg. MW= 22.75 KDa, rT2544 Avg. MW= 30 KDa).

[d] Molecular weight of OSP was calculated from the dextran (20, 40, 70, 500 kDa) standard curve using the formulae $y = -0.68x + 1.8386$.

Table 3. Determination of total sugar, protein content, molecular weight (MW) and endotoxicity in different samples (OSP, rT2544, OSP-rT2544) for immunization

Sample	Total sugar (mg/ml)	Total protein (mg/ml)	MW (KDa)	Endotoxicity (a) (EU/µg)
OSP-rT2544	0.59	1.83	398.1	-0.03
OSP	1.6	-	22.75	-0.6
rT2544	-	1.2	30	-0.7

[a] Endotoxicity was measured in the samples by LAL assay using LAL assay kit (Thermo Scientific), following the standard protocol.

4.1.2. Development of Vi-rT2544

4.1.2.1. Purification and characterization of Vi

The Vi-polysaccharide (Vi PS) extracted from *Citrobacter freundii* was purified by size exclusion Chromatography. The gel filtration profile of Vi PS using the Sephacryl S500 column (120ml) revealed the characteristic peak of the vi antigen near 50 ml, 80ml and 90 ml that corresponded to their average KDa values of ~160kDa (**Figure 7A, Table 4**). The eluted fractions of the Vi was collected and the absorption was measured by ELISA at 450 nm.

Proton NMR analysis (D_2O, at 400MHz, room temperature) was used as a confirmation of the identity of the vi-polysaccharide sample (typical signals of the vi-polysaccharide chain were detected, confirming the presence of the characteristic sugars)**. Figure 7B** indicates the

presence of different patterns of characteristic sugars of vi-polysaccharides as follows- O-acetylation of C3 carbon at 1.89 ppm, H1 of αGalANAc at 4.88 ppm, H2 of αGalANAc at 4.12 ppm, H3 of αGalANAc at 5.57 ppm, H4 of αGalANAc at 4.36 ppm and H5 of αGalANAc at 4.58 ppm respectively.

FTIR analysis disclosed the characteristic wave patterns of active Vi (**Figure 7C**). Waves near 1650 cm^{-1} indicated carbonyl group (C=O), while those in the region of 1260 cm^{-1} and 1417 cm^{-1} represented the deformation of C-OH groups and carboxylate anion. In contrast, waves near 1095 cm^{-1} and 1021 cm^{-1} corresponded to the characteristic peaks of the glycosidic linkage and the bands in the 867–802cm^{-1} region, which is called the anomeric region, indicated the α and β configuration of the anomeric carbon. [The detailed methodologies were discussed in the materials and method section **3.2.2.3, 3.2.2.4., 3.2.8. and 3.2.9.**]

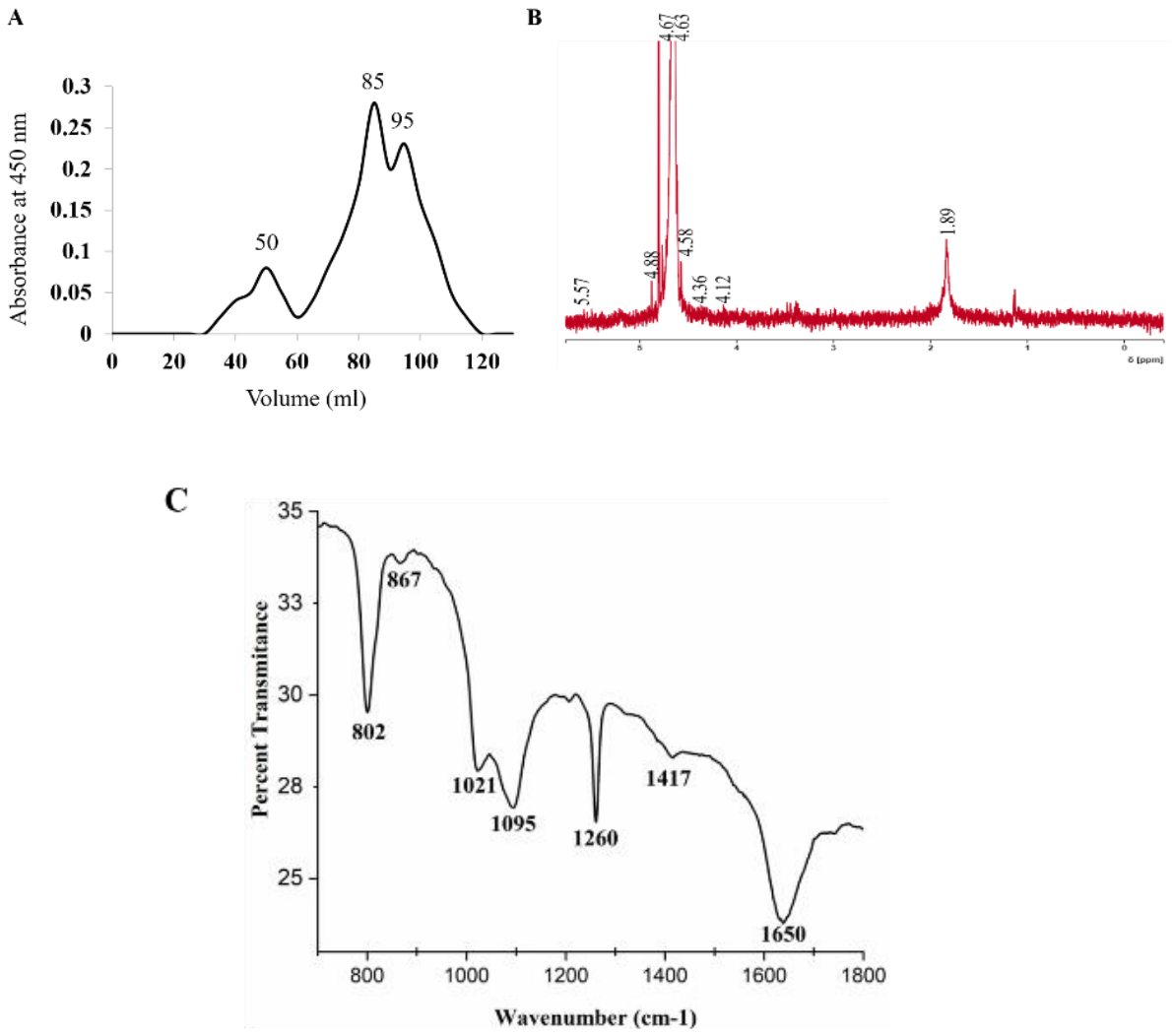

Figure 7. Purification and characterization of Vi. (A) Gel filtration chromatography. Vi containing 250µg of total sugar in normal saline (pH 7.4) was injected into Sephacryl S500 column (120ml). The column was pre-equilibrated with normal saline, pH 7.4 and the flow rate was maintained at 0.2 mL/min. Vi eluted at 50 ml, 85ml and 95 ml was observed at 450 nm at 4°C. (B) ^{1}H NMR of lyophilized vi, dissolved in 0.5 mL of D_2O showing the characteristic peak of Vi in a 400 MHz NMR spectrometer (JOEL 400 YH) at 25°C. O-acetylation of Vi was determined at C-3 of galactosaminouronic acid (1.89 ppm), protons bound to H1 of αGalANAc at 4.88 ppm, H2 of αGalANAc at 4.12-4.17 ppm, H3 of αGalANAc at 5.5-5.57 ppm, H4 of αGalANAc at 4.3-4.36 ppm and H5 of αGalANAc at 4.58 ppm Peak

near 4.63-4.67 ppm indicated the D2O solvent. For each analysis, experiment was replicated three times, and data from a representative experiment are shown. (C) Fourier Transform Infrared (FTIR) spectrum of the lyophilized unconjugated Vi was monitored using potassium bromide (KBr) pellet method (1:100 w/w). Spectra recorded in the Perkin Elmer Spectrum 100 system in the spectral region of 4000–400/ cm indicating different functional groups of Vi. carbonyl group (C=O) (1695-1650 cm^{-1}), C-OH groups (1260 cm^{-1}) and carboxylate anion (1417-1412 cm^{-1}), glycosidic linkage (1095-1023 cm^{-1}), α and β configuration of the anomeric carbon (861-802 cm^{-1}) was observed in both Vi sample.

Table 4. K_d determination in Vi

Elution volume (ml)	K_d[a]	MW(KDa)[b]	Average MW(KDa)
50	0.125	316.22	160
85	0.56	100	
95	0.625	63.09	

[a] K_d values were calculated following FPLC analysis on Sephacryl-S500 column (120ml). To determine the void volume, dextran 500KDa was used and the K_d values were determined using the following formulae,

$K_d = V_e - V_0 / V_t - V_0$ where, V_e = peak elution volume (mL), V_0= void volume (mL), V_t=total elution volume (mL)

[b] Molecular weight of Vi was calculated from the dextran (20, 40, 70, 500 kDa) standard curve using the formulae y = -0.7118x + 1.9595.

4.1.2.2. Vi and rT2544 conjugation purification and characterization of the conjugate

Conjugates of Vi and rT2544 displayed a smear tail in the western blots, probed with T2544 antibody, indicating heterogeneity of size and mass-to-charge ratios (**Figure 8**). The conjugate mixture (250 µg of Vi and 420 µg of protein) after dialysis in PBS buffer (pH7.2) was purified by size exclusion chromatography using Sephacryl S500 column (120ml). The eluent was monitored by measuring the absorption of protein at 280 nm (Bradford) and Vi at 450 nm (ELISA). The FPLC analysis of the conjugate indicates the peak of the conjugate eluted after the calculated void volume (40 ml). We collected the eluted fractions (41 ml, and 110 ml) and the major peak of Vi-rT2544 was obtained after the calculated void volume (41 ml) as opposed to the elution peaks of Vi at 50 ml and rT2544 at 110 ml (**Figure 9A**). The eluted fractions (41 ml, and 110 ml) of Vi-rT2544 were measured for the analysis of Vi and protein content in that sample. All these two regions indicated the observable polysaccharide and protein content with different molar ratios. The total sugar, protein content, and the Kd values in the conjugated sample are depicted in **Table 5**. The highest molecular weight of the conjugate (Kd 0.01, 501KDa) was used for immunization.

To characterize the conjugate, we performed the ^{1}H NMR in D_2O, at 400MHz at room temperature (**Figure 9B**). Different patterns of characteristic sugars of Vi-polysaccharide obtained from ^{1}H NMR at 1.89 ppm (O-acetylation at C3 carbon of galactosaminouronic acid), 4.88 ppm (H1 of αGalANAc), 4.17 ppm (H2 of αGalANAc), 5.5 ppm (H3 of αGalANAc), 4.3 ppm (H4 of αGalANAc) and 4.58 ppm (H5 of αGalANAc) were similar to unconjugated vi-polysaccharide. But, one different peak of the vi-T2544 molecule that corresponded to the

aliphatic region of the protein observed at 3.21 ppm was absent from the unconjugated vi-polysaccharide.

To find out the functional groups in the purified Vi-rT2544 conjugate, FTIR analysis was performed (**Figure 9C**). FTIR showed one additional functional group in the conjugate (Vi-rT2544), the amide bond of protein at 1604, 1645 and 1540 cm^{-1}, which was absent in Vi. On the other hand, similar functional groups in Vi-rT2544 and Vi corresponded to different wave lengths. Thus, carbonyl groups (C=O) were detected at 1650 cm-^{1}, deformation of C-OH groups appeared near region 1260 cm^{-1} and glycosidic linkage emerged at 1097 cm^{-1} and 1023 cm^{-1}, the region of 1412 cm^{-1} represented the carboxylate anion in Vi-rT2544. In addition, α and β configurations of the anomeric carbon were detected near the regions 861 cm^{-1} and 802 cm^{-1}. Stability of Vi-rT2544 conjugate was checked by passing the conjugate through the S-500 column (120 ml) (**Figure 9D**). The figure shows similar elution profile of the freshly prepared conjugate (Vi-rT2544) and the conjugate at the end of the stability test done at 4°C (both eluted near 40ml (0.01 K_d)). This suggests that Vi-rT2544 was stable at 4°C. [The detailed methodologies were discussed in the materials and method sections **3.2.12, 3.2.6., 3.2.8 and 3.2.9.**]

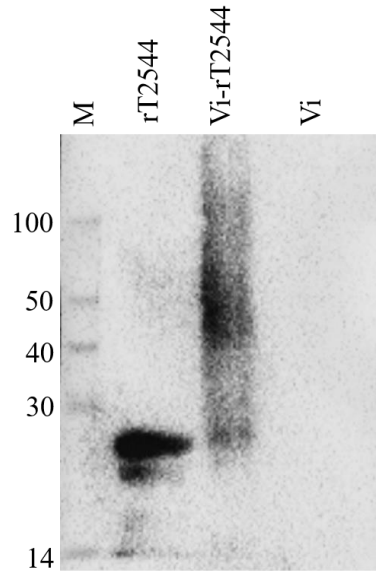

Figure 8. Western blots of Vi-rT2544 conjugate. rT2544 (8 µg), conjugate (Vi-rT2544, 8 µg), and Vi (8 µg), resolved in 10% SDS-PAGE and probed with anti-rT2544 antibody. The experiment was repeated three times and a representative blot is shown here.

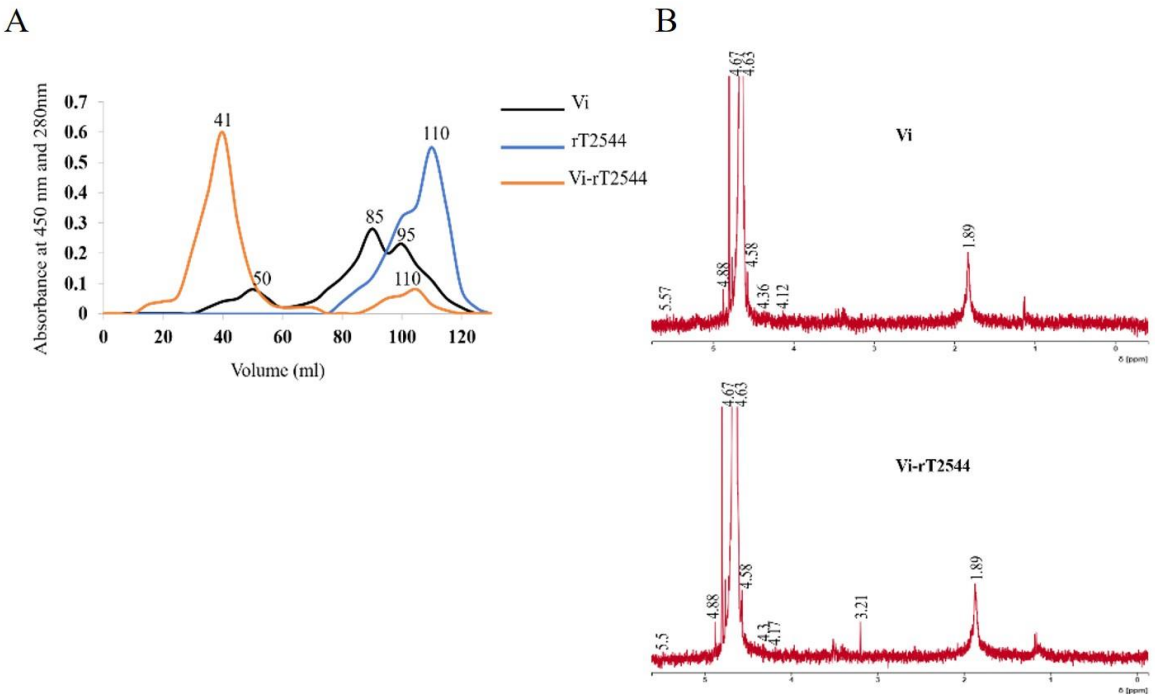

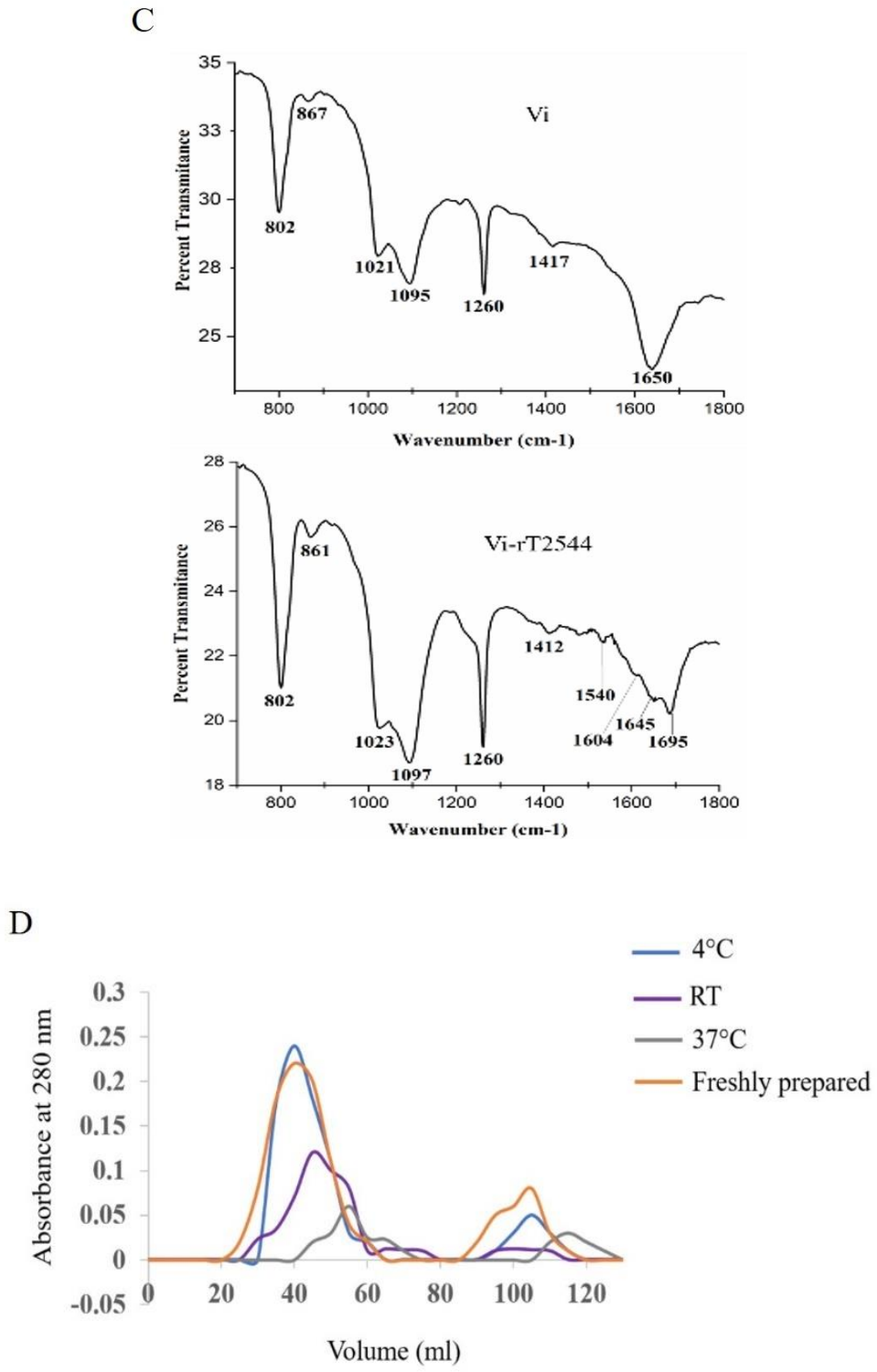

Figure 9. Characterization of Vi and Vi-rT2544 conjugate. (A) Gel filtration chromatography. Vi-rT2544 conjugate containing 250µg of total sugar and 420 µg of total protein in normal saline (pH 7.4) was injected into Sephacryl S500 column (120ml). The column was pre-equilibrated with normal saline, pH 7.4 and the flow rate was maintained at

0.2 mL/min. The conjugate (Vi-rT2544) and T2544 were observed (eluted at 41 ml and 110 ml) at 280 nm, while Vi (eluted at 50 ml, 85ml and 95 ml) was observed at 450 nm at 4°C. (B) ^{1}H NMR of lyophilized vi and Vi-rT2544, dissolved in 0.5 mL of D_2O showing the characteristic peak of Vi in a 400 MHz NMR spectrometer (JOEL 400 YH) at 25°C. O-acetylation of Vi was determined at C-3 of galactosaminouronic acid (1.89 ppm), protons bound to H1 of αGalANAc at 4.88 ppm, H2 of αGalANAc at 4.12-4.17 ppm, H3 of αGalANAc at 5.5-5.57 ppm, H4 of αGalANAc at 4.3-4.36 ppm and H5 of αGalANAc at 4.58 ppm respectively in both vi and Vi-rT2544 group. An additional peak of the protein obtained at 3.21 ppm in Vi-rT2544 group was absent in Vi. Peak near 4.63-4.67 ppm indicated the D2O solvent. For each analysis, experiment was replicated three times, and data from a representative experiment are shown. (C) Fourier Transform Infrared (FTIR) spectrum of the lyophilized conjugated Vi-rT2544 and unconjugated Vi was monitored using potassium bromide (KBr) pellet method (1:100 w/w). Spectra recorded in the Perkin Elmer Spectrum 100 system in the spectral region of 4000–400/ cm indicating different functional groups of Vi and Vi-rT2544: carbonyl group (C=O) (1695-1650 cm^{-1}), C-OH groups (1260 cm^{-1}) and carboxylate anion (1417-1412 cm^{-1}), glycosidic linkage (1095-1023 cm^{-1}), α and β configuration of the anomeric carbon (861-802 cm^{-1}) was observed in both Vi and Vi-rT2544 sample. The amide bond of protein (1604, 1645 and1540 cm^{-1}) observed in Vi-rT2544 was absent in Vi. (D) Stability of Vi-rT2544. Vi-rT2544 conjugate purified by size exclusion chromatography, containing 250µg of total sugar and 420 µg of total protein was kept for 41 days at 4°C, 37 °C and room temperature (RT). Stability of the conjugate was checked by passing through the S-500 column (120ml).

Table 5. Determination of K_d, Vi, and protein concentration and endotoxicity in the conjugate (Vi-rT2544) sample

Sample	Elution volume (ml)	K_d (FPLC)	sugar (Vi)[a] (µg/ml)	protein (rT2544)[b] (µg/ml)	Vi to rT2544 molar ratio [c] (wt/wt)	MW (KDa)[d]	Endotoxicity e (EU/µg)
Vi-rT2544	41	0.01	184	220	1:6.3	501	0.03
	110	0.8	43.3	155	1:18	32	0.06

[a]The concentration of the Vi was measured by ELISA at 450nm using the following equation.

y = 0.6195x -0.0684.

[b] Protein concentration was measured by Bradford assay.

[c] Molar ratios were calculated based on the Vi and protein molecular masses (Vi Avg. MW= 160 KDa, rT2544 Avg. MW= 30 KDa).

[d] Molecular weight was calculated from the dextran (20, 40, 70, 500 kDa) standard curve using the formulae y = -0.7118x + 1.9595.

[e]Endotoxicity was measured in the samples by LAL assay using LAL assay kit (Thermo Scientific), following the standard protocol.

4.1.3. Development of rIpaB-T2544

4.1.3.1. Purification and characterization of recombinant IpaB-T2544

we generated a recombinant protein (rIpaB-T2544)-based subunit vaccine by expressing a chimeric gene construct of *Shigella flexneri* 2a *ipab* and *Salmonella* Typhi *t2544* in-frame in *E.coli*. Clone confirmation was done by agarose gel electrophoresis of restriction digestion products (**Figure 10A**), followed by nucleotide sequencing (**Figure 10B**). The recombinant protein (rIpaB-T2544, 55 kDa) was purified from *E. coli* BL21 (DE3) PlyS by affinity chromatography using Ni-NTA agarose (**Figure 10C)** and confirmed by western blots (**Figure 10D).** Secondary structure of rIpaB-T2544 was analyzed by Far-UV CD spectra that showed one negative band, indicating alpha helix and one positive band, suggesting β helical structure at 222.5 nm and 206 nm, respectively (**Figure 10E**). [The detailed methodologies were discussed in the materials and method sections **3.2.1.3., 3.2.1.4., 3.2.12 and 3.2.5.**]

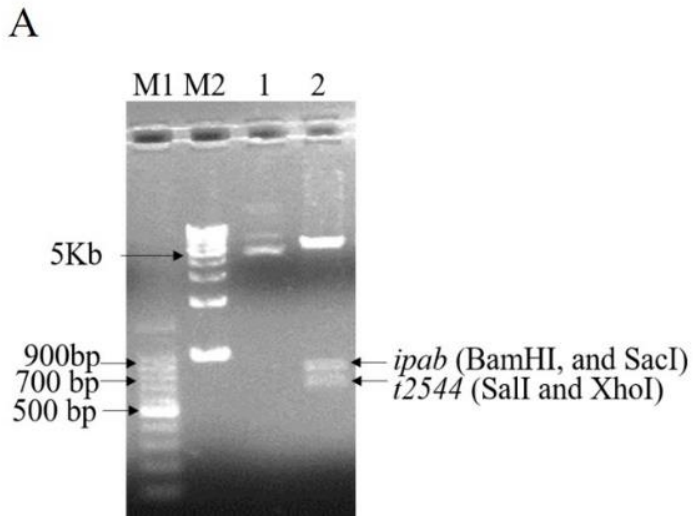

B

A. >TIC_pET.Forward_33617-1_P4815,Raw Sequence(1250 bp)

AGAAATAGATGTTGAGCGGGAACATTCCCTCTAGAATAATTTTGTTTAACTTTAAGAAGGAGATATACCATGGGCAGCAGCCATCATCA
TCATCATCACAGCAGCGGCCTGGTGCCGCGCGGCAGCCATATGACACCTCAAAATATTACTGATTTGTGTGCAGAATACCACAACACA
CAAATATATACGCTAAATGATAAGATATTTTCGTATACAGAATCTCTAGCTGGAAAAAGAGAGATGGCTATCATTACTTTTAAGAATGGT
GCAATTTTTCAAGTAGAAGTACCAGGTAGTCAACATATAGATTCACAAAAAAAAAGCGATTGAAAGGATGAAGGATACCCTGAGGATTG
CATATCTTACTGAAGCTAAAGTCGAAAAGTTATGTGTATGGAATAATAAAACGCCTCATGCGATTGCCGCAATTAGTATGGCAAATGGA
TCCGGTGGCGGTGGCTCGGATCTTACTGCTAACCAAAATATTAATACAACTAATGCACACTCAACTTCAAATATATTAATCCCTGAACTT
AAAGCACCAAAGTCATTAAATGCAAGTTCCCAACTAACGCTTTTAATTGGAAACCTTATTCAAATACTCGGTGAAAAATCTTTAACTGC
ATTAACAAATAAAATTACTGCTTGGAAGTCCCAGCAACAGGCAAGACAGCAAAAAAACCTAGAATTCTCCGATAAAATTAACACTCTT
CTATCTGAAACTGAAGGACTAACCAGAGACTATGAAAAACAAATTAATAAACTAAAAAACGCAGATTCTAAAATAAAAGACCTAGAA
AATAAAATTAACCAAATTCAAACAAGATTATCCGAACTCGACCCAGAGTCACCAGAAAAGAAAAAATTAAGCCGGGAAGAAATACAA
CTCACTATCAAAAAAGACGCAGCAGTTAAAGACAGGACATTGATTGAGCAGAAAACCCTGTCAATTCATAGCAAACTTACAGATAAA
TCAATGCAACTCGAAAAAGAAAAAGACTCTTTTTCTGCATTTTCAAACACAGCATCTGCTGAACAGCTATCAACCCAGCAGAATCATA
GCCGGACTTGCCAGTGTACCTCATGATGCACTTTATTCACTAGTGAAAAAATATGAGATCTTAAAAATGATCTGCTCTATTCAGTCCTCT
CCAGATCAGGAAAACCTGGATTGGAAAGAAAATCTGGATGAATGCTGCTGAGATACGTAAGCCGAGAACCTCACAGACATATTTGGC
CTGTGGTTTTGAC

B. >TIC_pET.Reverse_33617-4_P4815,Raw Sequence(1197 bp)

GGGAACCCTCAGGACCGTTTAGAGGCCCCAAGGGGTTATGCTAGTTATTGCTCAGCGGTGGCAGCAGCCAACTCAGCTTCCTTTCGG
GCTTTGTTAGCAGCCGGATCTCAGTGGTGGTGGTGGTGGTGCTCGAGTTAAAAGGCGTAAGTAATGCCGAGCATGAAGTCATTGGAG
GCAGCCTTTGTGTCTGCATCATAAGCGGTATGTTCATCACCAGCATAGTGATTTTTTGAAATGCTCACTTTGCCTGCATTAATGTATTTAT
AACTGGCGTCAATCATAATATTATCTGTTACAGCATATTTTGCACCGATACCTGCGCCCCAGGCAAAGTTATTTTTTGAAGCAGACAGA
GTTTCATTAATACCAAAACCAACAGGAATGGTGTTATTACTTAGCTTCACATGAGCGAGGCCAACGCCTGCGCTGATATAGGGTGTAAA
TGCCGTACTATTGTGAAAATCATAATAACCATTAACTATGTAAGTGGTCATTCGGACCTGATTTTTTACATTTATGTGTACTGGCTGACCA
AATGCAATAATATCCTGCCCGCCTTTAGCATCCGTCTCACCTCTGAAAGTGGTATCCAGTTCTAAACGTACTGGAAGCTGGAATGGATC
ATAAAAGTCATAACCGATAGCAACCCCGCCGCCAAAAACGCCTTTGGTACGGTCAGGTAACGTTGCATGACCATTGACTATCTCCTCC
TGGCTGAAGGTTGAGTTGATTCCATAGACATTGACTACGGATGTCCCCGCTTTCCCGGTGATATAGATCCCTTCTGGTCCTGGTCCGTC
GACGGAGCTCAACACAACCCATTACTCTGTTGAGTTCTTCTGCTTTACGTACTTCAGCAGCATACTCATCAGATTTTCTCTCCATTTCA
GTTTTTCTTGATTCTTGGAGAGACTGGAATAGAGCCAGATCATTTTTTAAAGATTCTTCATTATTTTTTCCACTAGTGAATAAAGGTTGC
CATCAATTGAGTAACACTGGCAAGTCCGTATGATTTCTGCTGGGATGATAGCTGTCAGCAGATGCTGTGTTTGAAATGCAGAAAGAGT
CTATTTCTTTTCGAGTTGCATTGAATTATCTGTAGTTTGCTATGATTGACGGATTTCTGGCTCAATCAATGTGCGTACTTAACTGCCTGCA
CGTTTTGATGATGATCTCGGCTAAGTTCAGTCCGGGGAA

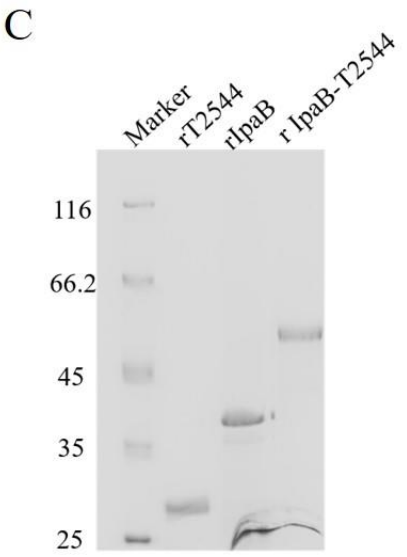

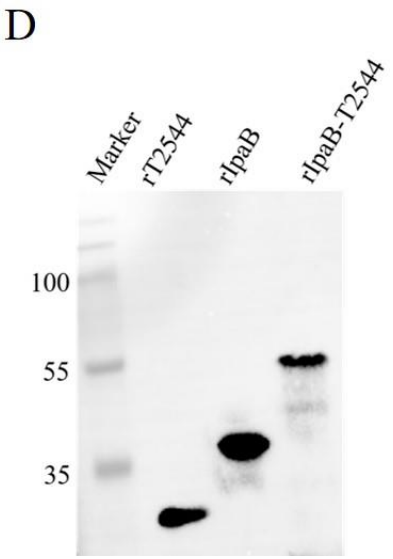

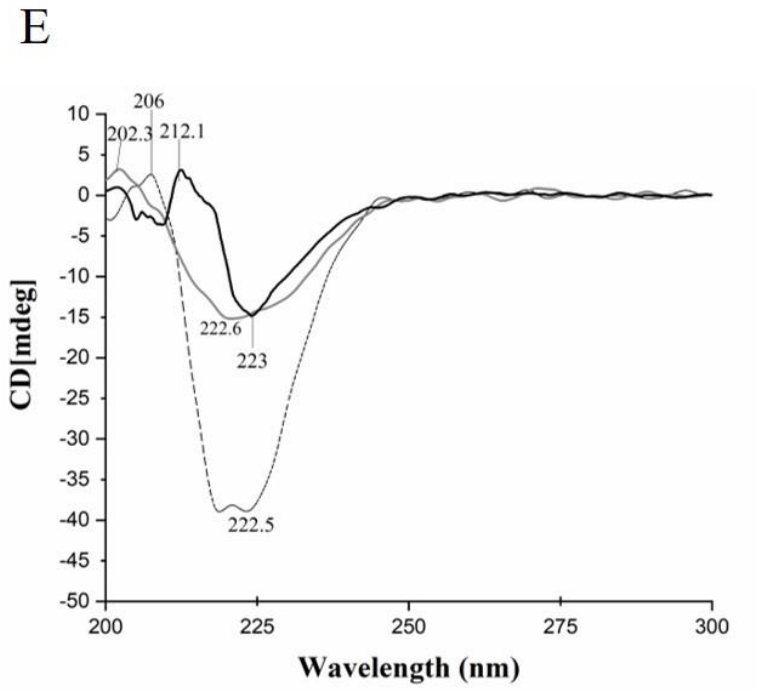

Figure 10. Cloning and purification of rIpaB-T2544. (A) 1% Agarose gel electrophoresis of pET28a-ipab-t2544 clone, after restriction digestion with BamHI, and SacI, SalI and XhoI. Lane M1: 1 kb DNA ladder, M2: 100bp DNA ladder, 1: Undigested clone, 2: Restriction enzymes digested clone. (B) Sequencing of the rIpaB-T2544 clone using pET forward and reverse primers. A, The FASTA file format of the sequences is provided. Yellow and green colors code for the recognition sites of the restriction enzyme BamHI and linker sequence (GS linker), respectively, whereas the blue color codes for the open reading frame (ORF) of IpaB. B, Yellow, sky, and red colors code for the recognition sites of the restriction enzymes XhoI, SalI and SacI. The green color codes for the linker sequence (GP linker), whereas the magenta color code for the open reading frame (ORF) of t2544 and the blue color code for the open reading frame (ORF) of IpaB. (C) 12% SDS–PAGE of recombinant purified proteins (5µg of each). Molecular mass markers (kDa) are on the left. (D) Western blot probed with anti-His antibody after resolving the recombinant purified proteins (rT2544, 5 µg, rIpaB, 7 µg, rIpaB-T2544, 3 µg) in 12% SDS-PAGE. Molecular mass markers (kDa) are on the left. The experiment was repeated three times and a representative blot is shown here. (E) Far-UV

circular dichroism spectra of protein samples (180 µg/ml) captured at the wavelength range of 200 to 350 nm at 25°C in PBS (pH 7.4) on the Jasco-1500 spectrophotometer. Data presented as ellipticity (CD [mdeg]) after subtracting the baseline values. Experiment was replicated three times, and data from a representative experiment are shown. Different lines are described as follows; upper line- rT2544, middle line-rIpaB and lower line- rIpaB-T2544. Experiment was replicated three times, and data from a representative experiment are shown.

Summary

- T2544 from *Salmonella* typhi was cloned into pET28a vector and expressed in *E. coli* after transforming into BL21 (DE3). The average molecular weight of the T2544 was nearly 30 KDa. T2544 was purified by ion exchange chromatography followed by size exclusion chromatography. The secondary structure was determined by circular dichroism (CD) spectra.
- OSP from *Salmonella* Typhimurium was extracted using hot-phenol method. The average molecular weight of the OSP was 22.75 KDa. It was purified by size exclusion chromatography. The sugar composition and the O-acetylation level was determined by FTIR and ^{1}H NMR.
- Both the OSP and T2544 were covalently linked using carbodiimide reaction and the large size of the conjugate OSP-T2544 was found to be 398.1 KDa (Figure 6A, Table 2). Conjugates of OSP and rT2544 displayed a smear tail in the western blots, probed with T2544 antibody, indicating heterogeneity of size and mass-to-charge ratios. The large OSP-rT2544 conjugate complex was eluted at the 41.66 ml while the unconjugated samples were found at 109.23 ml and 117.9 ml (OSP) and 112.8 ml (rT2544) respectively, observed by size exclusion chromatography. Small

glycoconjugates were found near 75.76 ml and 97.09 ml (Table 2). The O-acetylation level and the sugar composition of the OSP were unchanged after conjugation. However, an additional peak of protein was found in the conjugate (OSP-T2544) determined by FTIR and ^{1}H NMR absent in unconjugated OSP.

- Vi from *Citrobacter fruendii* was extracted using CTAB (Cetyl trimethyl ammonium bromide) precipitation method. The average molecular weight of Vi was 160 KDa. It was purified by size exclusion chromatography. The sugar composition and the O-acetylation level was determined by FTIR and ^{1}H NMR.
- Vi and rT2544 were covalently fused using the carbodiimide chemistry and the size of the conjugate Vi-rT2544 was found to be 500 KDa (Figure 9A, Table 5). Smear like pattern of Vi and rT2544 was visualized in the western blots, probed with T2544 antibody. Size exclusion chromatography showed different elution volumes of the Vi-rT2544 (41 ml), Vi (50 ml, 85 ml and 95 ml) and rT2544 (110 ml), displaying the large complex of Vi-rT2544 conjugate. The O-acetylation level and the sugar composition of the Vi were unchanged after conjugation. However, an additional peak of protein was found in the conjugate (Vi-rT2544) determined by FTIR and ^{1}H NMR was absent in unconjugated Vi.
- *ipab* and *t2544* genes were cloned in -frame in PET28a vector and expressed in *E. coli* after transforming into BL21 (DE3) plyS. The average molecular weight of the rIpaB-T2544 was 55 KDa. Chimeric rIpaB-T2544 was purified by Ni-NTA chromatography and the secondary structure was determined by circular dichroism (CD) spectra.

4.2. Objective 2.

Studies on the protective efficacy in animal models

4.2.1. Vaccination with OSP-rT2544 conferred a broad range of protection against typhoidal and non-typhoidal *Salmonella*

To investigate broad range efficacy of our candidate vaccine, BALB/c and C57BL/6 mice were immunized subcutaneously with three doses of OSP-rT2544, rT2544, OSP, or PBS (vehicle) at 14 days intervals (**Figure 11A, Table 6**). Protective efficacy of the vaccines was evaluated in BALB/c mice for *S.* Typhi and *S.* Paratyphi A and in C57BL/6 mice for *S.* Typhimurium and *S.* Enteritidis strains (**Table 7**). A 10xLD_{50} dose killed all the BALB/c mice within a period of 5-6 days in the vehicle- and OSP-treated groups, while 75-77% of mice that received either OSP-rT2544 or rT2544 were alive at 10 days post-infection and beyond (**Figure 11 B, C)**. On the other hand, OSP-rT2544 and OSP immunization protected 70-80% and 20 % of C57BL/6 mice, respectively against *S.* Typhimurium infection, while all the mice that received rT2544 or the vehicle only died within 25 days (**Figure 11 D)**. Interestingly, 55-60% of latter mouse strain immunized with OSP-rT2544 also survived *S.* Enteritidis challenge (**Figure 11 E)**. Protection of the immunized mice was observed for both the reference as well as clinical strains, strongly suggesting the potential of OSP-rT2544 as a candidate quadrivalent vaccine for typhoidal and non-typhoidal *Salmonella* infections. [The detailed methodologies were discussed in the materials and method sections **3.2.10.1., 3.2.18.1. and 3.2.18.2.**]

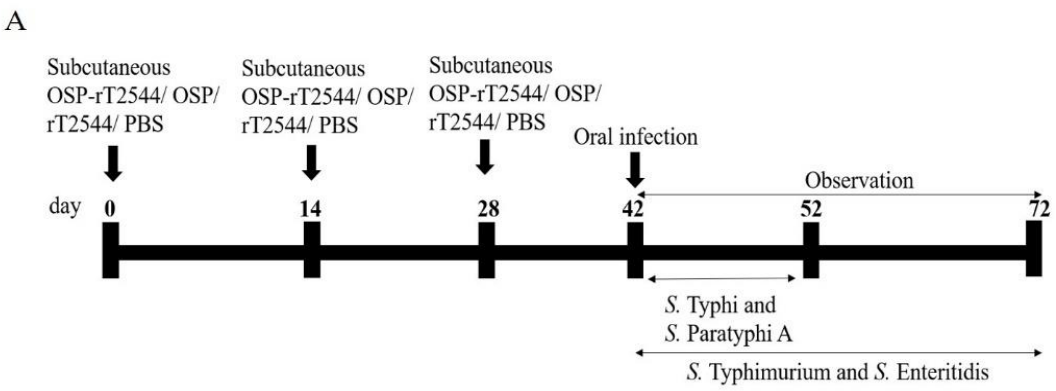

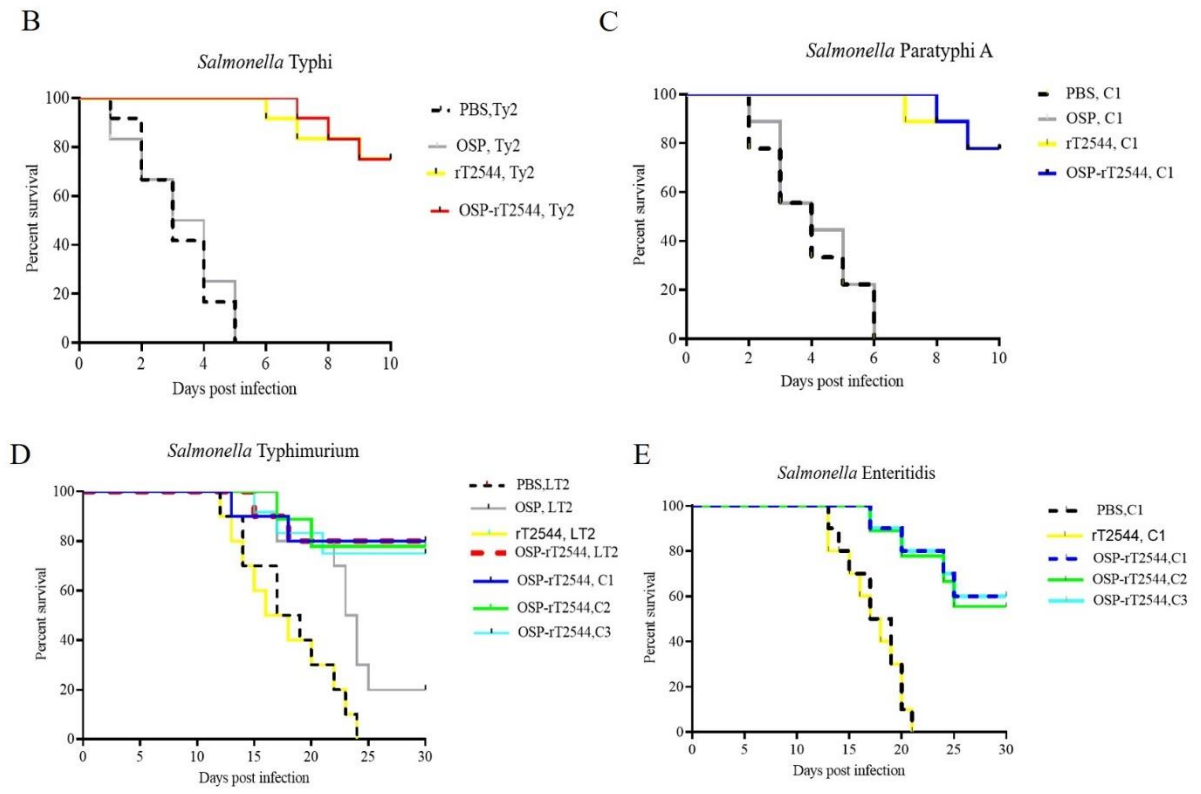

Figure 11. Protection of mice after subcutaneous immunization with OSP-rT2544. (A) Experimental scheme of mouse subcutaneous immunization with the vehicle (PBS), conjugate (OSP-rT2544) (8 µg of OSP or 24 µg of rT2544 in conjugate), or unconjugated vaccines (OSP 8 µg, rT2544 24 µg)), followed by oral bacterial challenge. (B-E) Kaplan-Meyer plot of cumulative mortality of the infected mice. BALB/c mice were orally challenged with *S.* Typhi Ty2 (5 x 10^7 CFU, n= 12) (B) or *S.* Paratyphi A (5 x 10^5 CFU, n=9) (C) and monitored for 10 days. For NTS strains, C57BL/6 mice were orally challenged with *S.* Typhimurium (5 x 10^6 CFU of the LT2 strain (n=10), clinical strain 1 (C1, n=10), clinical strain 2 (C2, n=9) and clinical strain 3 (C3, n=12)) (D) or *S.* Enteritidis (5 x 10^6 CFU of C1 (n=10), C2 (n=9) or C3 (n=10)) (E) and monitored for 30 days. The colour scheme used to mark different experimental groups are shown in **Table 8**.

Table 6. Vaccine formulation doses used for immunogenicity (OSP-rT2544) studies

Mice strain	Immunogen	Adjuvant	Dose of OSP (µg/mice)	Dose of T2544 (µg/mice)
C57BL/6	OSP-rT2544 OSP rT2544	Alum Alum Alum	8 8 -	25.5 - 25.5
BALB/c	OSP-rT2544 OSP rT2544	Alum Alum Alum	8 8 -	25.5 - 25.5

Table 7. Bacterial strains used for challenge study following OSP-rT2544 immunization

Immunogen for immunization	Challenged bacterial strain	Mouse used for challenge	Mice model used for challenge study	Routes of challenge	Dose of challenge [10X LD_{50}]
OSP-rT2544 rT2544 PBS (Vehicle)	*S.* Typhi Ty2 *S.* Typhi clinical isolates (C1, C2, C3)	BALB/c	Iron overload model	Oral	5 x 10^7 CFU

OSP-rT2544 rT2544 PBS (Vehicle)	*S.* Paratyphi Clinical isolates (C1, C2, C3)	BALB/c	Iron overload model	Oral	5 x 10^5 CFU
OSP-rT2544 OSP PBS (Vehicle)	*S.* Typhimurium WT (LT2) *S.* Typhimurium clinical isolates (C1, C2, C3)	C57BL/6	Streptomycin model	Oral	5 x 10^6 CFU
OSP-rT2544 OSP PBS (Vehicle)	*S.* Enteritidis clinical isolates (C1, C2, C3)	C57BL/6	Streptomycin model	Oral	5 x 10^6 CFU

Table 8. Colour scheme for different experimental groups (OSP, rT2544, OSP-rT2544)

Immunogen (no infection)	**Colour code**
Vehicle (PBS)	Black
OSP	Grey

rT2544	Yellow
OSP-rT2544	Orange
Immunogen (with infection)	**Colour code**
Vehicle (PBS)	Black
OSP	Grey
rT2544	Yellow
OSP-rT2544 (infection with reference strains)	Orange
OSP-rT2544 (infection with C1)	Blue
OSP-rT2544 (infection with C2)	Green
OSP-rT2544 (infection with C3)	Sky

4.2.2. Vaccination with Vi-rT2544 conferred protection against *Salmonella* Typhi and Paratyphi

To investigate the protective efficacy of our candidate vaccine following a single immunization, a comparative study was performed between Vi-T2544 and Vi-TT immunized mice using the different routes (SC, subcutaneous and IM, intramuscular) (**Figure 12A**). BALB/c mice were immunized with a single dose of Vi-rT2544, Vi-TT, or PBS (vehicle) at day 0 and challenged with 10X- LD_{50} doses of *S*. Typhi and *S*. Paratyphi A on day 122 (**Figure 12B-C**). It was found that mice subcutaneously immunized with Vi-T2544 and Vi-TT showed ~66% and ~40%

protection while intramuscular immunization showed ~66% and ~30% protection against 10X-LD_{50} doses of *S.* Typhi (**Figure 12 B, C)**. We have previously reported the protective efficacy of rT2544 immunization in mice against *S.* Paratyphi A challenge (256). In this study, ~60% protection against *S.* Paratyphi A was observed in both subcutaneous and intramuscular Vi-T2544 immunized mice (**Figure 12B, C**). However, no protection was found in Vi-TT immunized mice against *S.* Paratyphi A challenge. All the vehicle-immunized mice died in all the groups. [The detailed methodologies were discussed in the materials and method sections **3.2.10.1., and 3.2.18.1**]

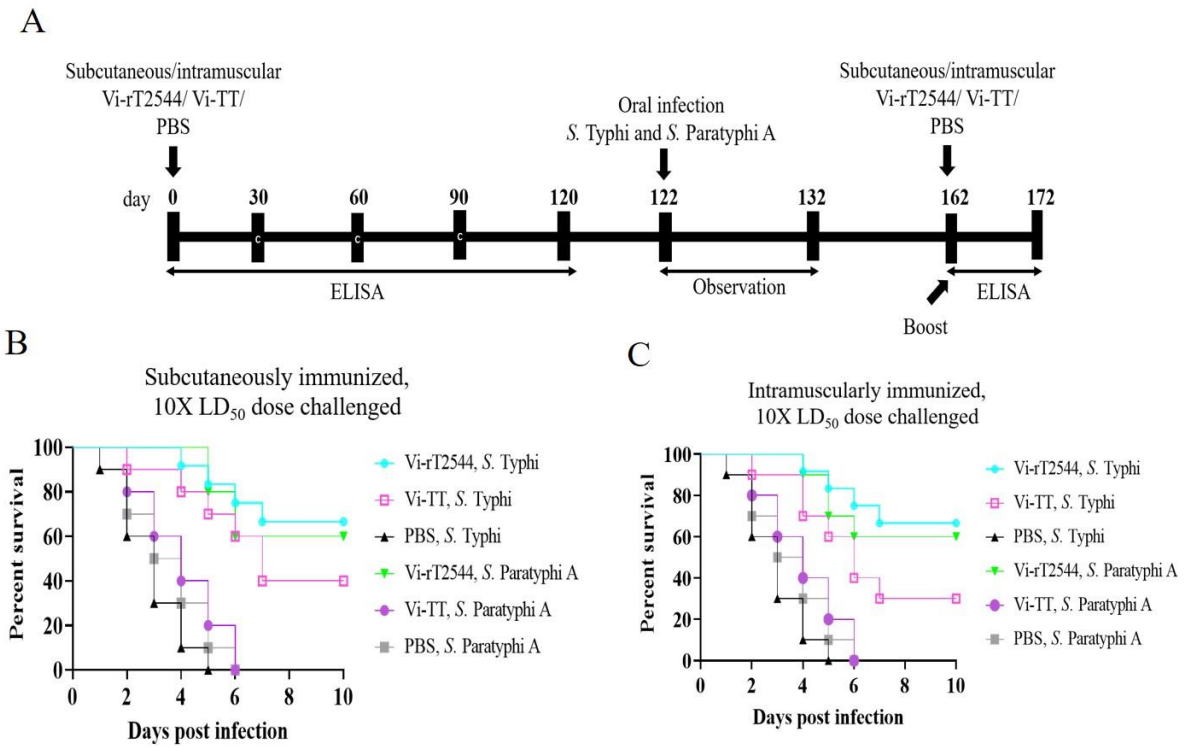

Figure 12. Single Vi-rT2544 immunization provides better protection against *Salmonella* Typhi and *Salmonella* Paratyphi A than Vi-TT. (A) Experimental scheme of mouse immunization with the vehicle (PBS) and conjugate (Vi-T2544, Vi-TT) (25 µg of Vi in conjugate), at day 0, followed by oral bacterial challenge. (B-C) Kaplan-Meyer plot of cumulative mortality of the infected mice. Immunized BALB/c mice were orally challenged on day 122 of first immunization with *S.* Typhi Ty2 (5 x 10^7 CFU, n=10) or *S.* Paratyphi A (5 x

10^5 CFU, n=10) and monitored for 10 days. The colour scheme used to mark different experimental groups is shown in **Table 9**.

Table 9. Colour scheme for different experimental groups (Vi-rT2544, Vi-TT)

Immunogen (with infection)	**Colour code**
***S.* Typhi**	
Vi-T2544	Sky blue
Vi-TT	Pink
Vehicle (PBS)	Black
***S.* Paratyphi A**	
Vi-T2544	Green
Vi-TT	Purple
Vehicle (PBS)	Gray
Immunogen (without infection)	**Colour code**
Vehicle (PBS)	Black
Vi-T2544	Orange
Vi-TT	Blue

4.2.3. Development of oral *Shigella* infection model in BALB/c mice

4.2.3.1. Combined treatment with streptomycin and iron ($FeCl_3$) renders mice susceptible to oral *Shigella* infection and disease development

To establish an oral *Shigella* infection model, different groups of BALB/c mice (10 weeks old, n=6) were pre-treated with various combinations of oral streptomycin and/or injectable iron ($FeCl_3$) plus iron chelator, desferal ($FeCl_3$/desferal) 24h and 4h, respectively before the oral gavage with different doses of virulent *Shigella flexeneri 2a* as shown in **Figure 13**. All mice that received either streptomycin or $FeCl_3$/deferral survived the bacterial challenge (**13 A-C**). In contrast, 50% and 100% of the mice that received 5×10^8 CFU (LD_{50}) and 5×10^9 CFU (LD_{100}), respectively after pre-treatment with both streptomycin and $FeCl_3$/desferal succumb to the infection (**Figure 13 E**). All the mice similarly pre-treated, but challenged with 5×10^7 CFU (sublethal dose) of *S. flexneri 2a* survived (**Figure 13E**). Overall, the findings suggested that iron plus streptomycin pre-treatment increases susceptibility of mice oral *Shigella* infection. In contrast, LD_{50} and LD_{100} doses for other *Shigella* serovars, such as *S. dysenteriae* and *S. sonnei* in streptomycin plus $FeCl_3$/desferal pre-treated mice were 1 log lower than *S. flexneri 2a* (**Figure 14**). Further, sublethal infection (5×10^7 CFU) with *S. flexneri 2a* led to diarrhoea by 24 hours (**Figure 15 A v**) and maximum body weight loss (69%) at 48h p.i. (**Figure 15 B v**) in streptomycin and iron pre-treated group. In comparison, mice from the other groups had no diarrhoea (**Figure 15 A i-iv**) and showed continued increase of body weights (**Figure 15 B i-iv**). In the infected mice, disease severity correlated with bacterial recovery from the colon and caecum lysates and the feces. We observe peak CFU at 48h p.i. that gradually decreased with time (**Figure 15 C**), indicating gradual recovery, which corroborated with the self-limiting *Shigella* gastroenteritis of humans (323). Together these results suggested that oral challenge with *Shigella spp*. readily causes colonic infection and disease in streptomycin- and iron-pre-treated mice and may be considered as a model for human shigellosis. [The detailed

methodologies were discussed in the materials and method sections **3.2.18.3., 3.2.18.4.**]

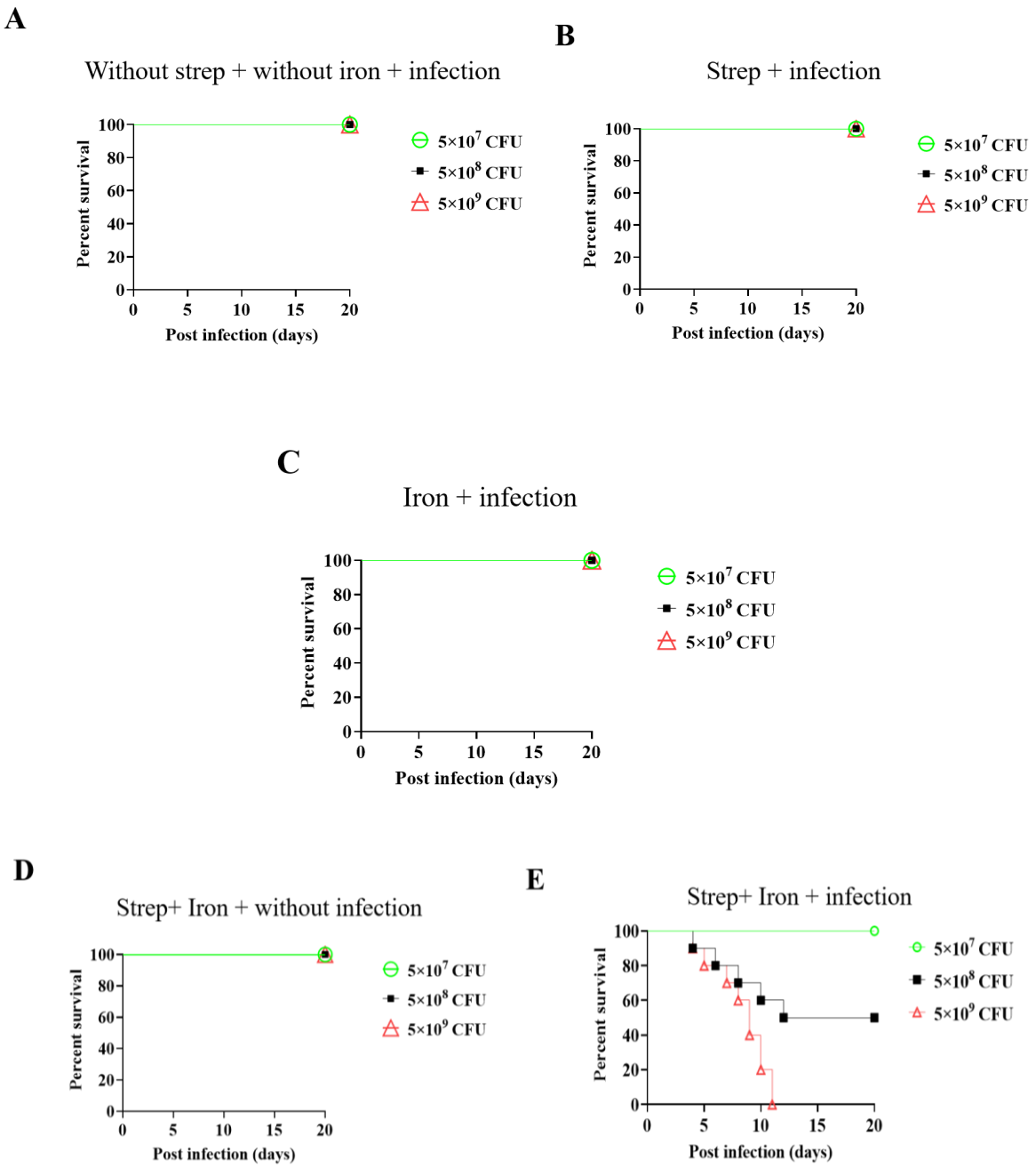

Figure 13. Survival assay with different doses of *Shigella flexeneri 2a*. Kaplan-Meyer plot of cumulative mortality of BALB/c mice (n=6). Different groups of mice were infected (A, B, C, E) with *Shigella flexeneri 2a* with different doses while one group remained uninfected (D). The mortality of mice was observed for 20 days. The color scheme used to mark different bacteria doses are as follows; green-5×10^7 CFU; black- 5×10^8 CFU; and red- 5×10^9 CFU.

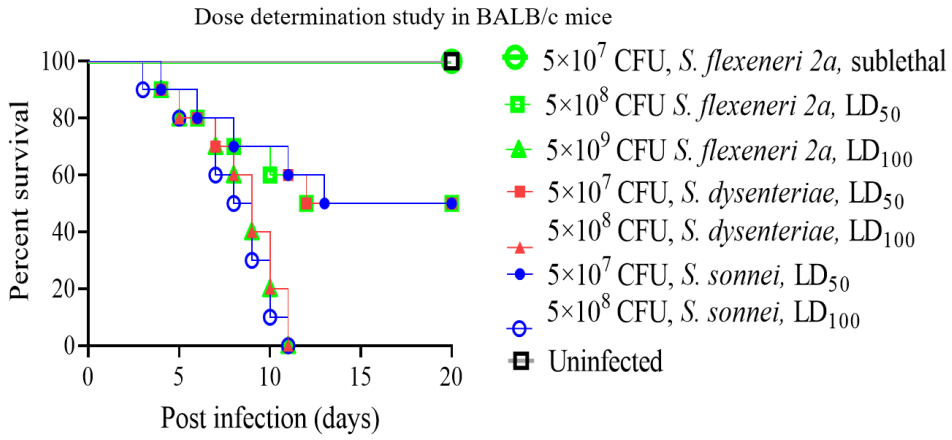

Figure 14. Survival assay against Different *Shigella* serovars. Kaplan-Meyer plot of cumulative mortality of infected mice. Streptomycin and iron pre-treated BALB/c mice (n=10) were infected with different doses of *Shigella* serovars and observed for 20 days. The colour scheme used to mark different experimental groups are as follows: uninfected-black; *Shigella flexeneri 2a*-green; *Shigella dysenteriae*-red; *Shigella sonnei*-blue.

A

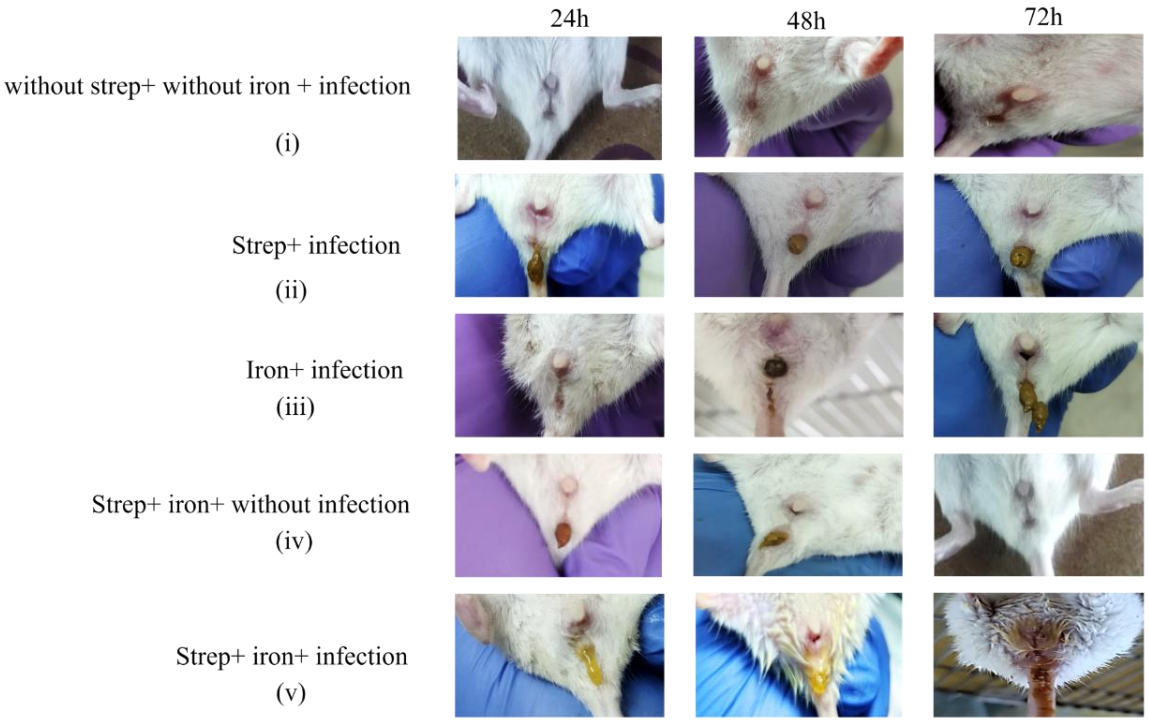
24h
48h
72h
without strep+ without iron + infection
(i)
Strep+ infection
(ii)
Iron+ infection
(iii)
Strep+ iron+ without infection
(iv)
Strep+ iron+ infection
(v)

B

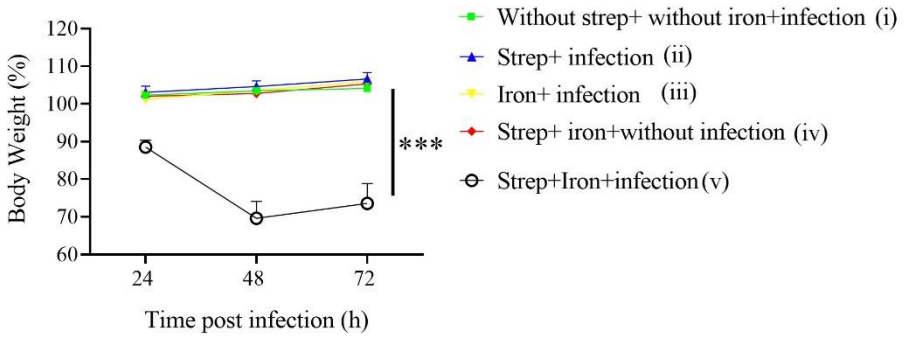
Body Weight (%)
120
110
100
90
80
70
60
24
48
72
Time post infection (h)
***
Without strep+ without iron+infection (i)
Strep+ infection (ii)
Iron+ infection (iii)
Strep+ iron+without infection (iv)
Strep+Iron+infection (v)

C

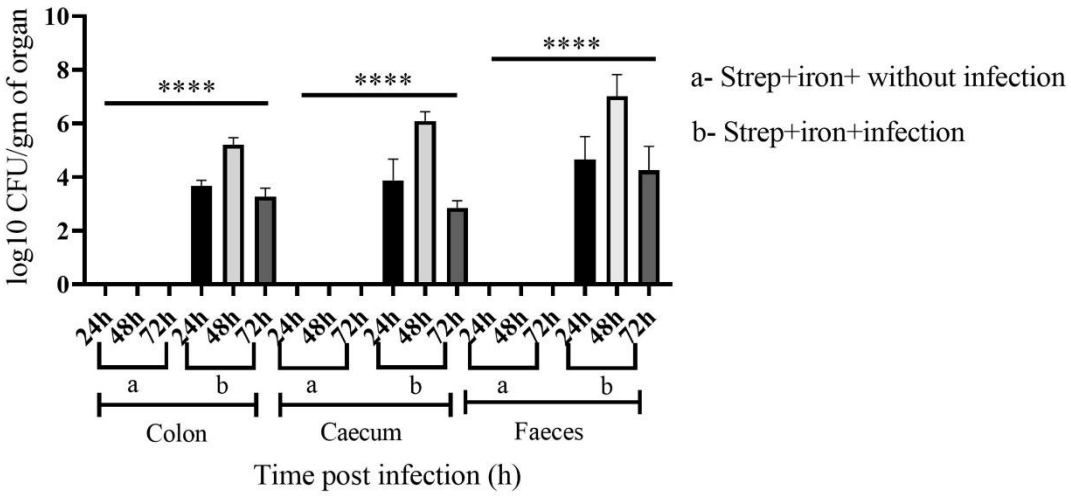
log10 CFU/gm of organ
10
8
6
4
2
0
****
****
****
24h
48h
72h
a
b
Colon
Caecum
Faeces
Time post infection (h)
a- Strep+iron+ without infection
b- Strep+iron+infection

Figure 15. Adult mice were susceptible to oral infection with *S. flexneri 2a* strain at a dose of 5×10^7. (A) Photographs of the anal region of BALB/c mice of different groups at different post-infection time points. A representative image from three independent experiments (n=4 mice per group) is shown. (B) Body weight changes post-infection. Data represent mean ± SEM values of multiple animals (n=4 mice per group) at each time point. Statistical analyses were performed by one-way ANOVA and Tukey's post-test for multiple comparisons, *P < 0.05, **P < 0.01, ***P <0.001. (C) Colony forming units (CFU) of *S. flexneri 2a* in the colon, cecum, and feces of infected and control mice. All the tissue homogenates were cultured overnight on TSA plate. Data represent mean ± SEM of the values from multiple animals (n=6 mice per group). Statistical analyses were performed by one-way ANOVA and Tukey's post-test for multiple comparisons, *P < 0.05, **P < 0.01, ***P <0.001.

4.2.3.2. Oral *S. flexneri 2a* infection of mice, pre-treated with streptomycin and iron causes colitis

Length of the colon is a widely used indicator of the severity of *Shigella* colitis. We observed maximum shortening of the colon (average length 40 mm) at 48h post-infection only in strep+iron pre-treated animals (**Figure 16 A-B v**) in comparison to >87 mm in the other groups (**Figure 16 A-B i-iv**)). Colon and caecum morphology were studied by histology of hematoxylin and eosin stained tissues after *Shigella flexeneri 2a* infection (5×10^7 CFU) (**Figure 17**). Tissue sections of the control group (**Figure 17 i-iv, Figure 18 i-iv, Figure 19, i-iv Figure 20**) showed well-organized histological features with intact intestinal epithelial lining and properly arranged crypts with abundant goblet cells. No abnormal PMN infiltrates and thickening of the mucosal and submucosal layers were observed. In contrast, streptomycin and iron/deferral pre-treated infected mice showed evidence of tissue damage, characterized by

disruption of epithelial lining, loss of crypt architecture with decreased goblet cell numbers and increased PMN infiltration into the mucosa of the colon and caecum at 24 and 72 hrs (**Figure 17 v, Figure 18 v, Figure 19 v**). A submucosal swelling (edema) with PMN infiltration was observed at 48h of infection. Resolution of these damages was visible after 72h with recovery of crypt structure and goblet cell number, decreased PMN infiltration and repair of the epithelial lining. The process of resolution and repair further progressed and the recovery of the tissue architecture was complete by 7d post-infection (**Figure 21 and Figure 22**). A blind histological scoring was performed with the infected tissue samples and plotted in a bar diagram **(Table 3.7, Table 10 and Figure 23**). In our study, visible bacteria within the cells were observed in the pathological specimens (**Figure 21 and Figure 22**, 24-72 h, white arrows, 40X magnification).

Together these data suggested that oral *Shigella* infection caused severe inflammatory damage to the colonic tissues in streptomycin- and iron-pretreated mice. The macroscopic and microscopic features of colonic and caecal inflammation were accompanied by the release of high levels of pro-inflammatory cytokines and chemokines, such as TNF-α, IL-1β, IFN-γ and CXCL10 in the supernatants of the tissue homogenates at different time points with maximum levels recorded after 48h of infection (**Figure 24 A-D**). Together the above results suggested that streptomycin and iron pre-treatment of adult mice rendered them susceptible to oral *Shigella* infection, with rapid colonization of the large intestine and the development of progressive colitis, manifested by diarrhoea, loss of body weights, shortening of the colon with tissue destruction and pro-inflammatory cytokines and chemokines production. [The detailed methodologies were discussed in the materials and method sections **3.2.18.4., 3.2.19. and 3.2.11.4.**]

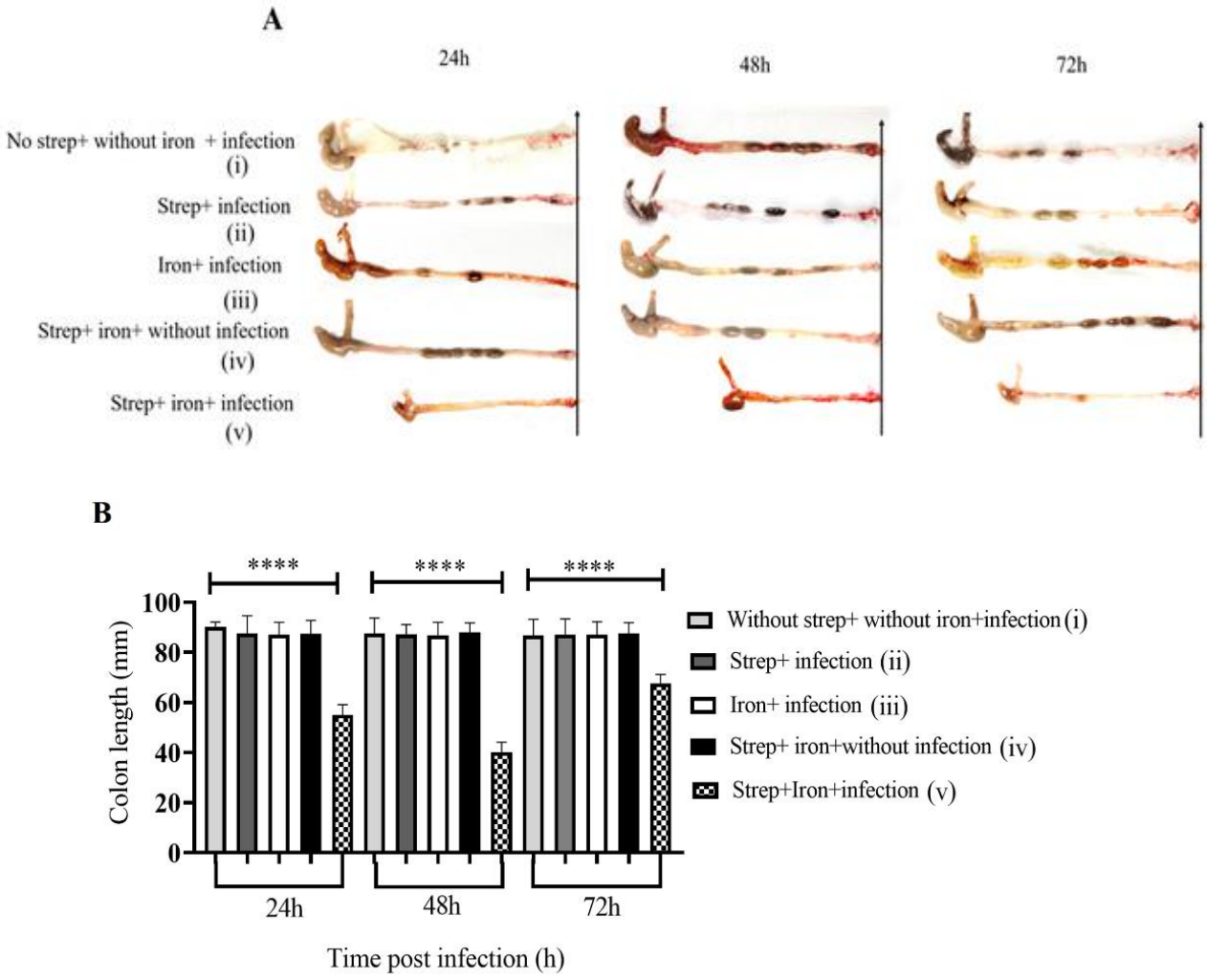

Figure 16. Susceptible adult mice showed decreased colon length after oral infection with *S. flexneri 2a* strain at a dose of 5×10^7. (A) Colonic shortening after the infection. Caecum and ascending colon isolated from the infected and uninfected mice, sacrificed at different time points post-infection. A representative image from three independent experiments (n=6 mice per group) is shown. (B) Graphical representation of Colon length. Data represent mean ± SEM of the values from multiple animals (n=6 mice per group). Statistical analyses were performed using one-way ANOVA and Tukey's post-test for multiple comparisons; *P < 0.05, **P < 0.01, ***P <0.001.

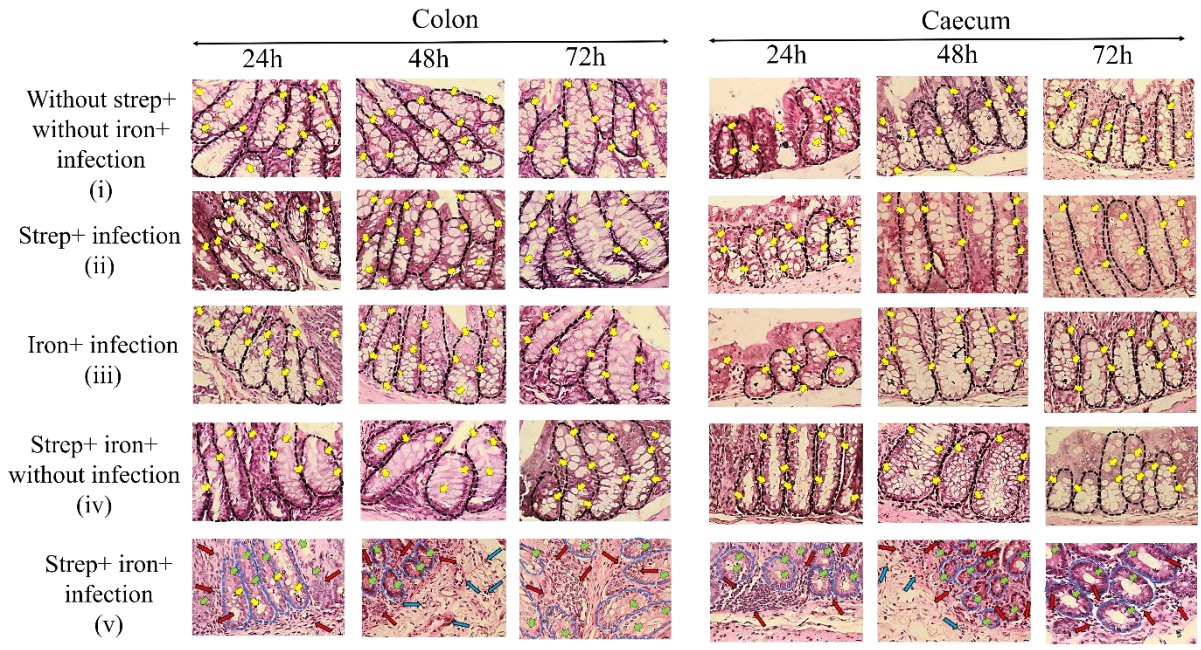

Figure 17. Histology sections (40X magnification) of the colon and caecum tissue of BALB/c mice after different treatments. Different groups of mice (n=6 mice per group) were infected with 5×10^7 CFU *Shigella flexeneri 2a* and sacrificed at the indicated time points. Colon and caecum were excised, fixed, and embedded in paraffin. Tissue sections were stained with Hematoxylin & Eosin and observed in a microscope (40x magnification, Scale bar =10 µm). The images are the magnified form of the 10X images (areas of green box) presented in Figure 18 (Colon) and Figure 19 (Caecum). Intact crypt architecture with abundant records of goblet cells, intact mucosa and submucosa without abnormal infiltrates were observed in the control group of mice (i-iv). Streptomycin-iron with infected group (v) showed loss of crypt architecture with decreased goblet cells, increased infiltration of lymphocytes in the mucosa and submucosa. Black round dotted circles represent intact crypt architecture and blue round dotted circles represent loss of crypt architecture. Different colors of arrow indicate different parameters as follows; yellow arrow- abundant goblet cells; green arrow- loss of goblet cells; red arrow- lymphocyte infiltration in the mucosa; blue arrow- lymphocyte infiltration in the submucosa.

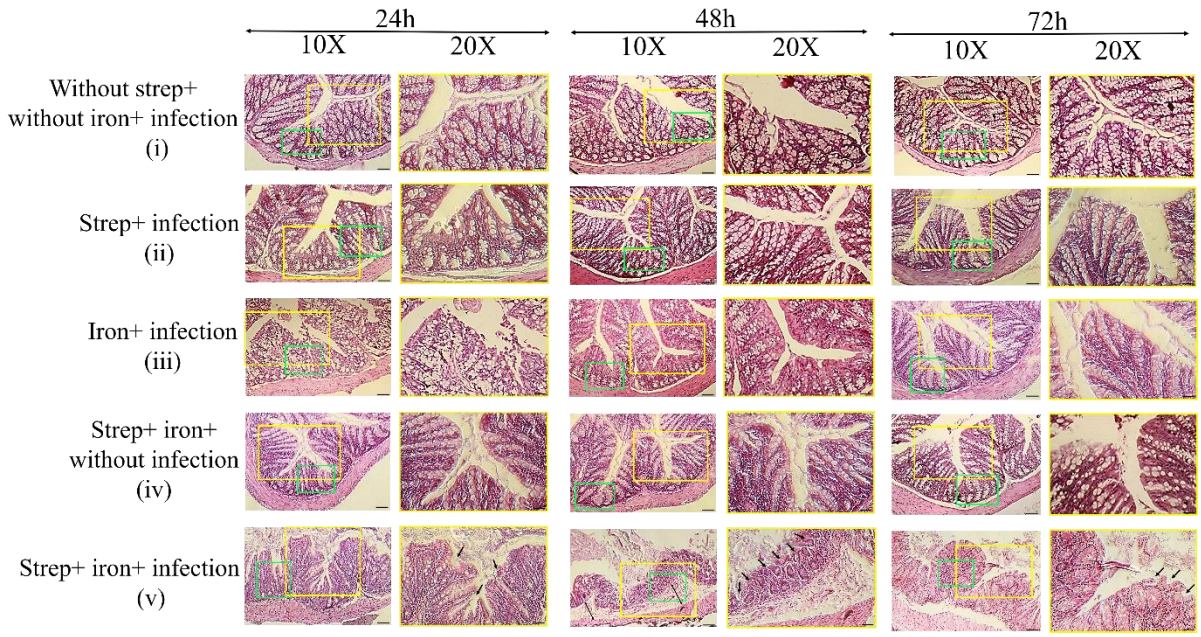

Figure 18. Histology sections (10X and 20X magnification) of the colon tissue of BALB/c mice after different treatments. Different groups of mice (n=6 mice per group) were infected with 5×10^7 CFU *Shigella flexeneri 2a* and sacrificed at the indicated time points. Colon was excised, fixed, and embedded in paraffin. Tissue sections were stained with Hematoxylin & Eosin and observed in a microscope. Intact epithelial lining was observed in the control group of mice (i-iv, 20X magnification). Streptomycin-iron with infected group (v) showed degenerative changes in the epithelial lining (20X magnification), and submucosal swelling (edema) (10X magnification). Yellow boxes represent the 20X (Scale bar =50 µm) magnification of the 10X (Scale bar =100 µm) image. Green boxes indicate the region selected for presentation in Figure 17 (colon). Double-headed black arrow indicates submucosal swelling (edema); single black arrow indicates the changes in the epithelial lining.

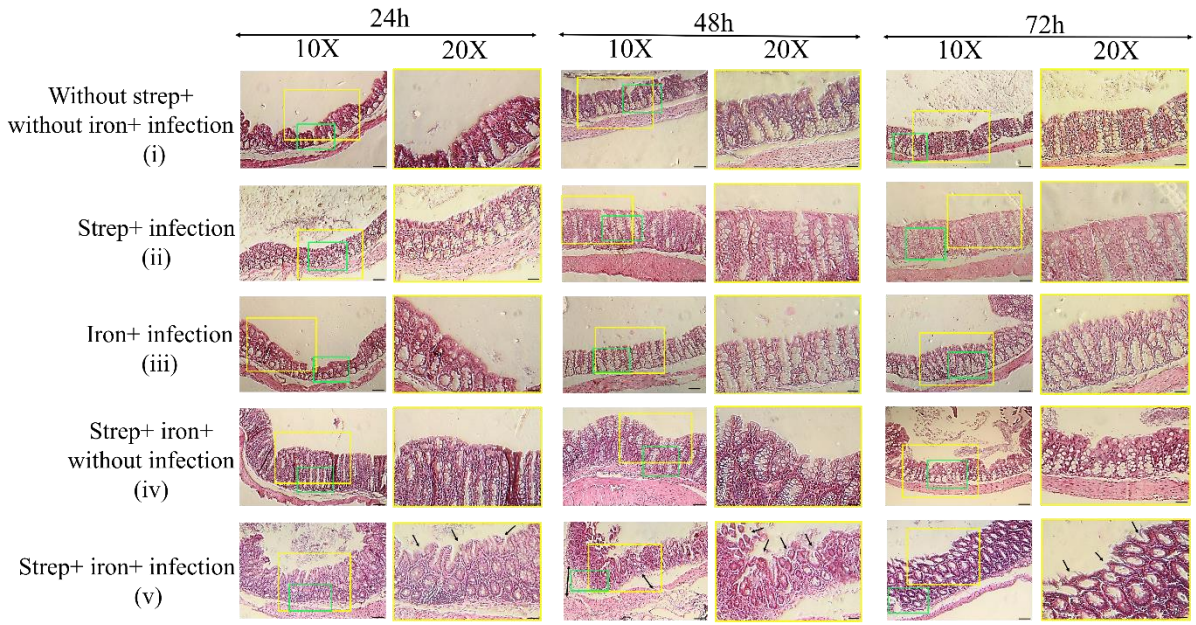

Figure 19. Histology sections (10X and 20X magnification) of the caecum tissue of BALB/c mice after different treatments. Different groups of mice (n=6 mice per group) were infected with 5×10^7 CFU *Shigella flexeneri 2a* and sacrificed at the indicated time points. Caecum was excised, fixed, and embedded in paraffin. Tissue sections were stained with Hematoxylin & Eosin and observed in a microscope. Intact epithelial lining was observed in the control group of mice (i-iv, 20X magnification). Streptomycin-iron with infected group (v) showed degenerative changes in the epithelial lining (20X magnification), and submucosal swelling (edema) (10X magnification). Yellow boxes represent the 20X (Scale bar =50 µm) magnification of the 10X (Scale bar =100 µm) image. Green boxes indicate the region selected for presentation in Figure 17 (caecum). Double-headed black arrow indicates submucosal swelling (edema); single black arrow indicates the changes in the epithelial lining.

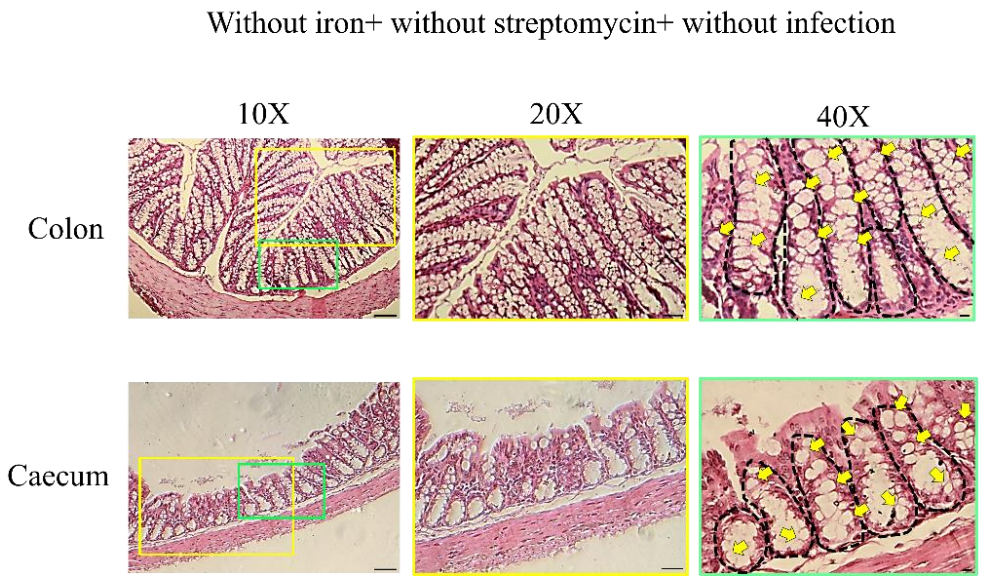

Figure 20. Histology sections of the colon and caecum tissue of uninfected and untreated BALB/c mice. Un treated (without strep+ without iron) + uninfected (without infection) mice (n=4) were sacrificed at 0h. Colon and caecum were excised, fixed, and embedded in paraffin. Tissue sections were stained with Hematoxylin & Eosin and observed in a microscope. Intact epithelial lining, intact crypt architecture with abundant records of goblet cells, intact mucosa and submucosa without abnormal infiltrates were observed in the group of mice. Yellow boxes represent the 20X (Scale bar =50 µm) and green boxes represent 40X (Scale bar =10 µm) magnification of the 10X (Scale bar =100 µm) image. Black round dotted circles represent intact crypt architecture, yellow arrow represents- abundant goblet cells.

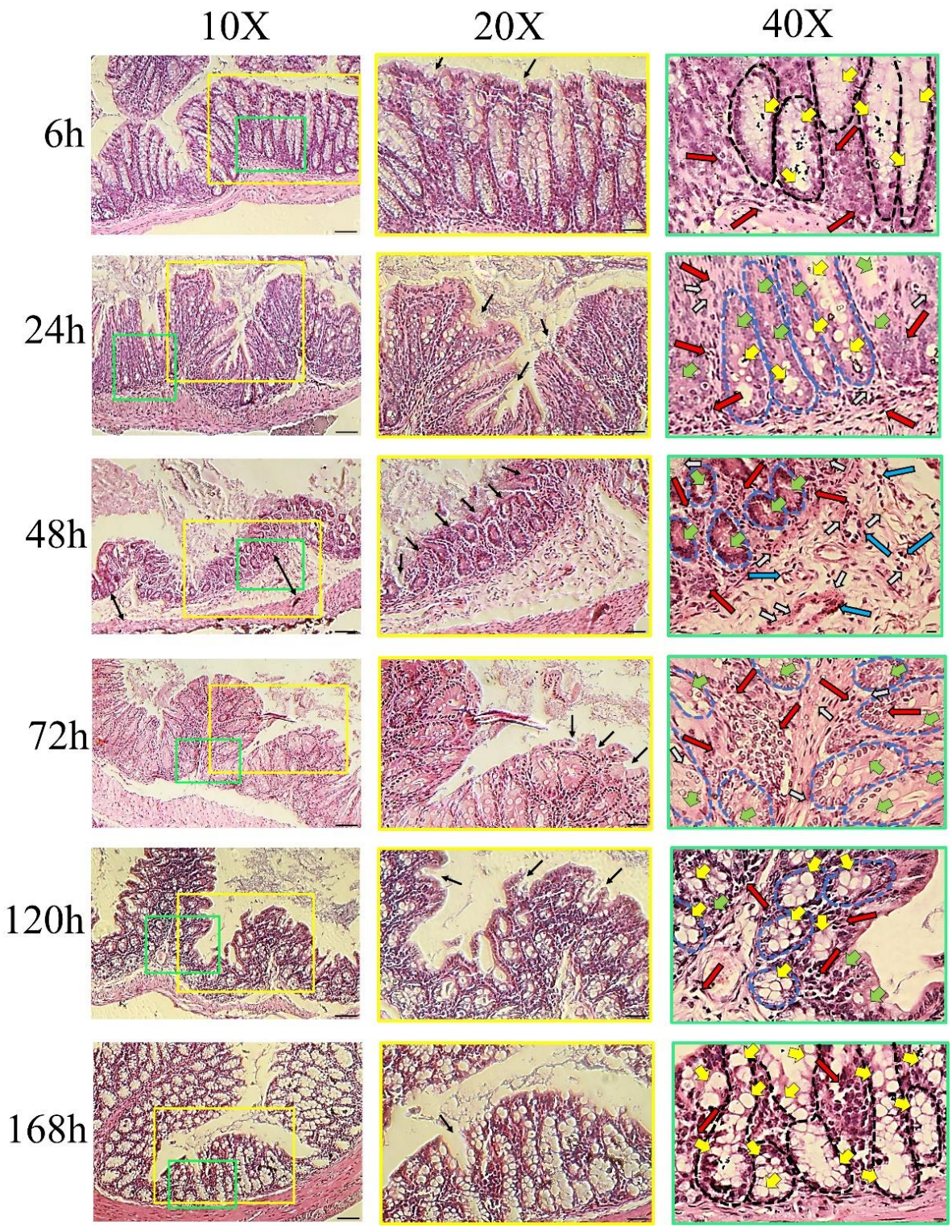

Figure 21. Histology sections of the colon tissue of BALB/c mice after infection (all time points). Mice (n=12) were pretreated with streptomycin and iron and infected with 5×10^7 CFU *Shigella flexeneri 2a.* Infected mice were sacrificed at the indicated time points. Colon was excised, fixed, and embedded in paraffin. (A) Tissue sections were stained with Hematoxylin

& Eosin, observed in a microscope and (B) histological scores were blindly assessed. Streptomycin-iron with infected group showed degenerative changes in the epithelial lining (20X magnification), loss of crypt architecture with decreased goblet cells (40X magnification), increased infiltration of lymphocytes in the mucosa and submucosa (20X magnification), and submucosal swelling (edema) (10X magnification). Yellow boxes represent the 20X (Scale bar =50 µm) and green boxes represent 40X (Scale bar =10 µm) magnification of the 10X (Scale bar =100 µm) image. Black round dotted circles represent intact crypt architecture and blue round dotted circles represent loss of crypt architecture. Different colors of arrow indicate different parameters as follows; yellow arrow- abundant goblet cells; green arrow- loss of goblet cells; red arrow- lymphocyte infiltration in the mucosa; blue arrow- lymphocyte infiltration in the submucosa; double headed black arrow- submucosal swelling (edema); single black arrow indicates the changes in the epithelial lining; white arrow-bacteria.

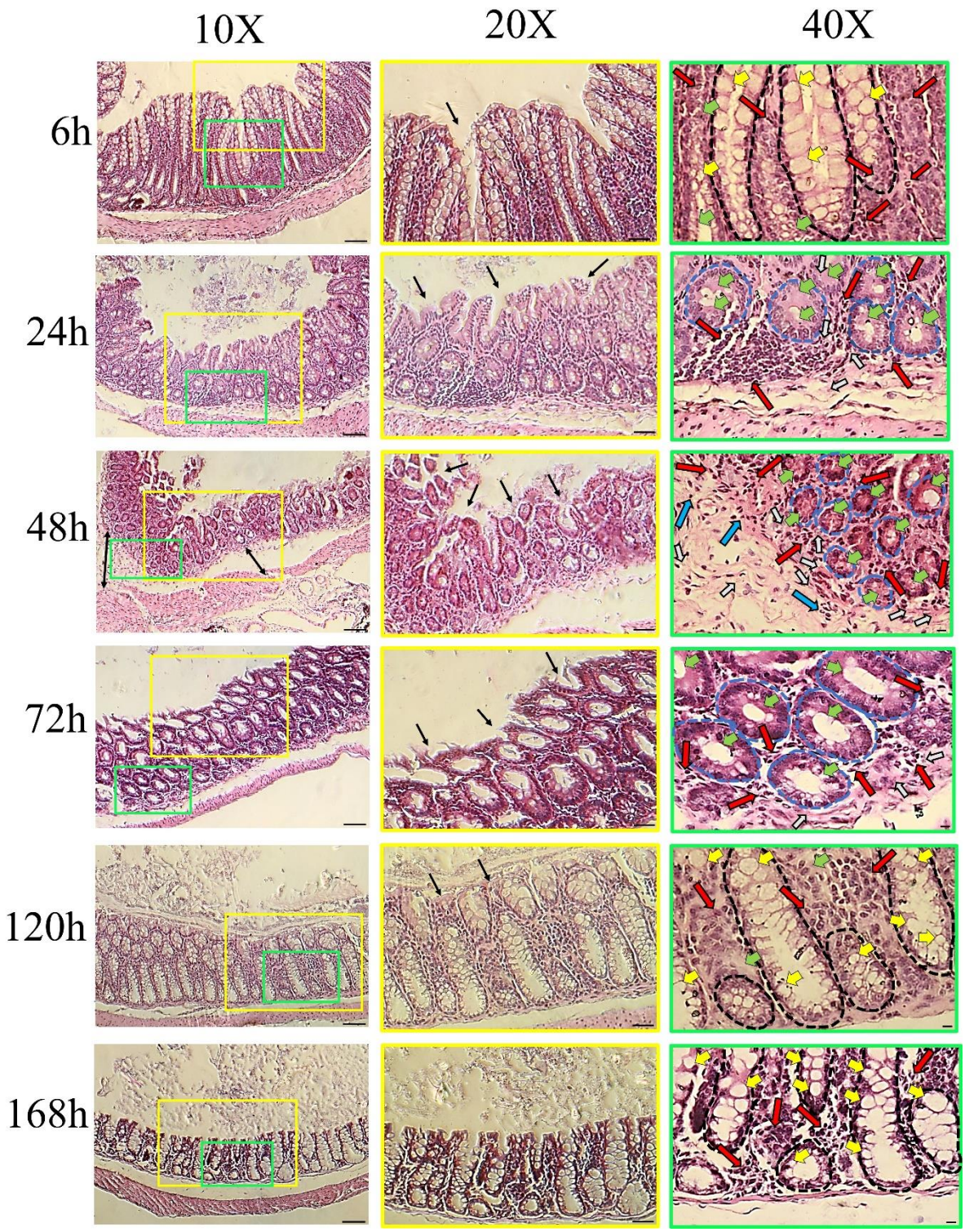

Figure 22. Histology sections of the caecum tissue of BALB/c mice after infection (all time points). Mice (n=12) were pretreated with streptomycin and iron and infected with 5×10^7 CFU *Shigella flexeneri 2a.* Infected mice were sacrificed at the indicated time points. Caecum was excised, fixed, and embedded in paraffin. Tissue sections were stained with Hematoxylin &

Eosin, observed in a microscope and (B) histological scores were blindly assessed. Streptomycin-iron with infected group showed degenerative changes in the epithelial lining (20X magnification), loss of crypt architecture with decreased goblet cells (40X magnification), increased infiltration of lymphocytes in the mucosa and submucosa (40X magnification), and submucosal swelling (edema) (10X magnification). Yellow boxes represent the 20X (Scale bar =50 µm) and green boxes represent 40X (Scale bar =10 µm) magnification of the 10X (Scale bar =100 µm) image. Black round dotted circles represent intact crypt architecture and blue round dotted circles represent loss of crypt architecture. Different colors of arrow indicate different parameters as follows; yellow arrow- abundant goblet cells; green arrow- loss of goblet cells; red arrow- lymphocyte infiltration in the mucosa; blue arrow- lymphocyte infiltration in the submucosa; double headed black arrow- submucosal swelling (edema); single black arrow indicates the changes in the epithelial lining; white arrow-bacteria.

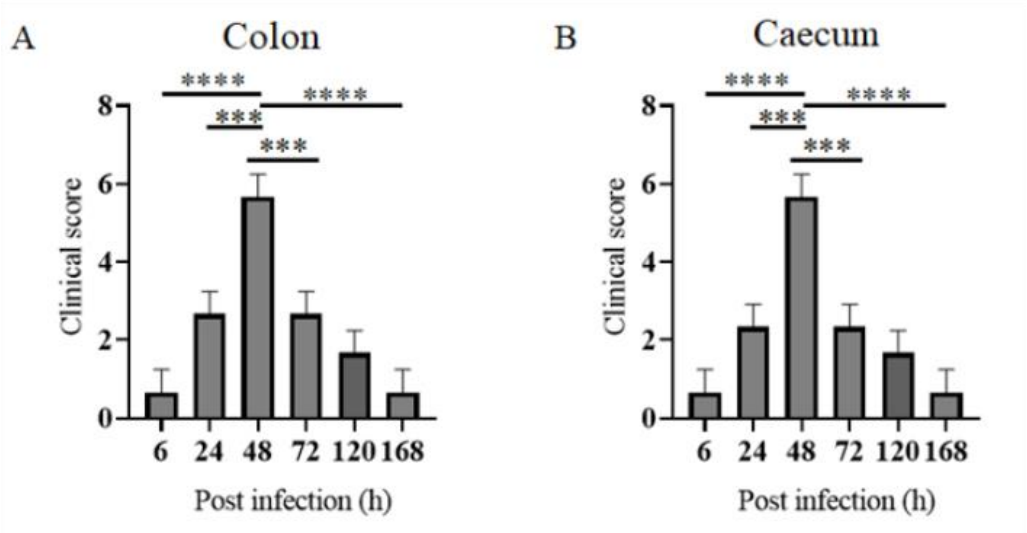

Figure 23. Histological scores of the colon and caecum tissue from BALB/c mice after different time points of infection. Mice (n=12) were pretreated with streptomycin and iron and infected with 5×10^7 CFU *Shigella flexeneri 2a*. Infected mice were sacrificed at the indicated time points. (A) Colon and (B) Caecum were excised, fixed, and embedded in

paraffin. Tissue sections were stained with Hematoxylin & Eosin and histological scores were blindly assessed. The experiment was repeated three times and one representative data is shown. The scoring parameters were mentioned in the table 3.7 and table 10.

Table 10. Histopathological scoring of colon and caecum for intestinal changes following *Shigella* challenge

		Post-infection time points					
SL NO.	Criteria	6h	24h	48h	72h	120h	168h
1	Loss of crypt architecture with minimal goblet cells loss (<50%)					1	
2	loss of crypt architecture with mild goblet cells loss (50%)		2		2		
3	loss of crypt architecture			3			

	with moderate goblet cell loss (>50%)						
4	PMN infiltration into mucosa without submucosa with degenerative changes in the epithelial lining	1	1		1	1	1
5	PMN infiltration into mucosa with submucosa with degenerative changes in						

	the epithelial lining						
6	PMN infiltration into mucosa with submucosa and submucosal swelling with degenerative changes in the epithelial lining			3			
	Combined score	1	3	6	3	2	1
	Severity of parameters	Minimal	Mild	Moderate	Mild	Minimal	Minimal

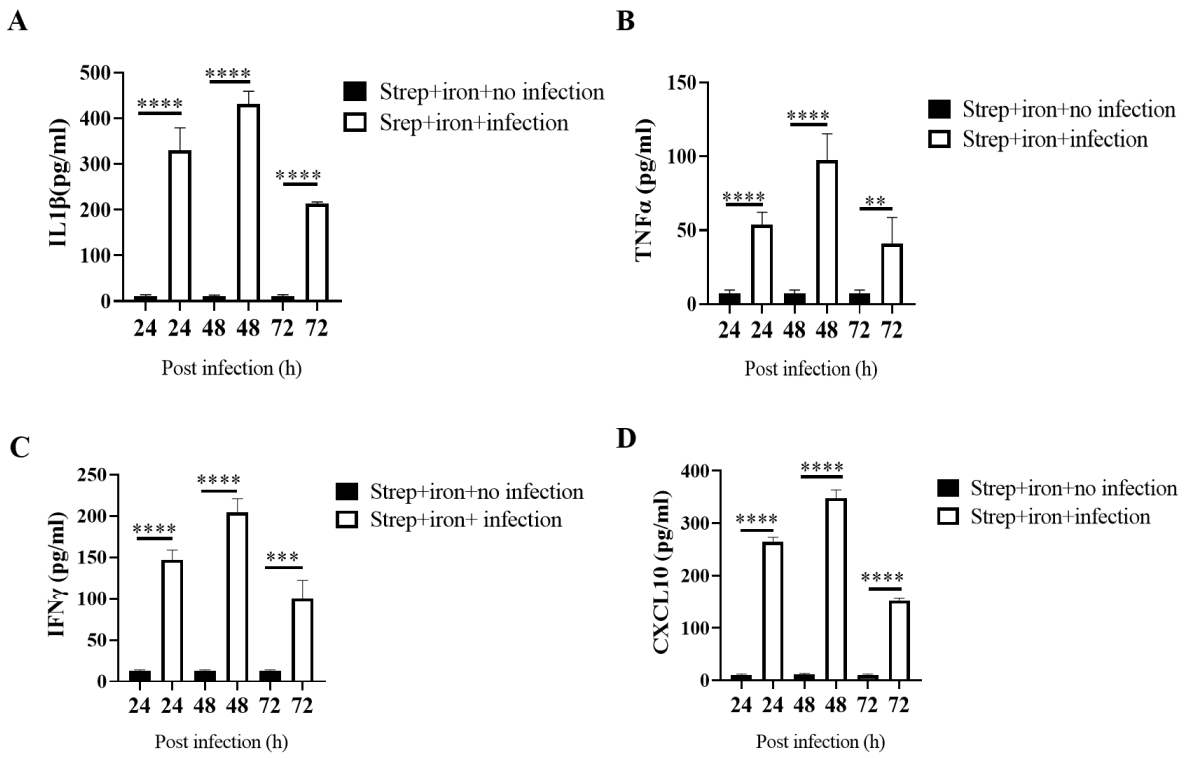

Figure 24. Proinflammatory cytokine and chemokine induction after *Shigella flexeneri 2a* infection. Streptomycin and iron pre-treated BALB/c mice (n=4) were infected with 5×10^7 CFU *Shigella flexeneri 2a*. ELISA performed with the colonic tissue homogenates for the proinflammatory cytokines (A-C) and chemokines (D). Data represent mean ± SEM values from different mice samples (n=4). Statistical analyses were performed with two-tailed Student's t-test (**P < 0.01, ***P < 0.001, ****P <0.0001) between two different groups.

4.2.4. Immunization with protein antigens conferred protection against *Shigella*

4.2.4.1. Intranasal immunization with recombinant IpaB protects mice against oral *Shigella* infections

To check for the protective efficacy of the candidate vaccine, BALB/c mice were immunized intranasally with three doses of the recombinant protein or the vehicle (PBS) at 14d intervals (**Figure 25 A)**. Oral infection with $10xLD_{50}$ dose of the *Shigella* spp. killed all the mice that

received the vehicle within 11 days of infection, whereas 80-90% of the mice immunized with rIpaB were still alive beyond 20 days (**Figure 25 B**). Collectively, the above data indicated that the newly developed oral *Shigella* infection model could be effectively used to evaluate the protective efficacy of vaccine candidates. [The detailed methodologies were discussed in the materials and method sections **3.2.10.1. and 3.2.18.3**]

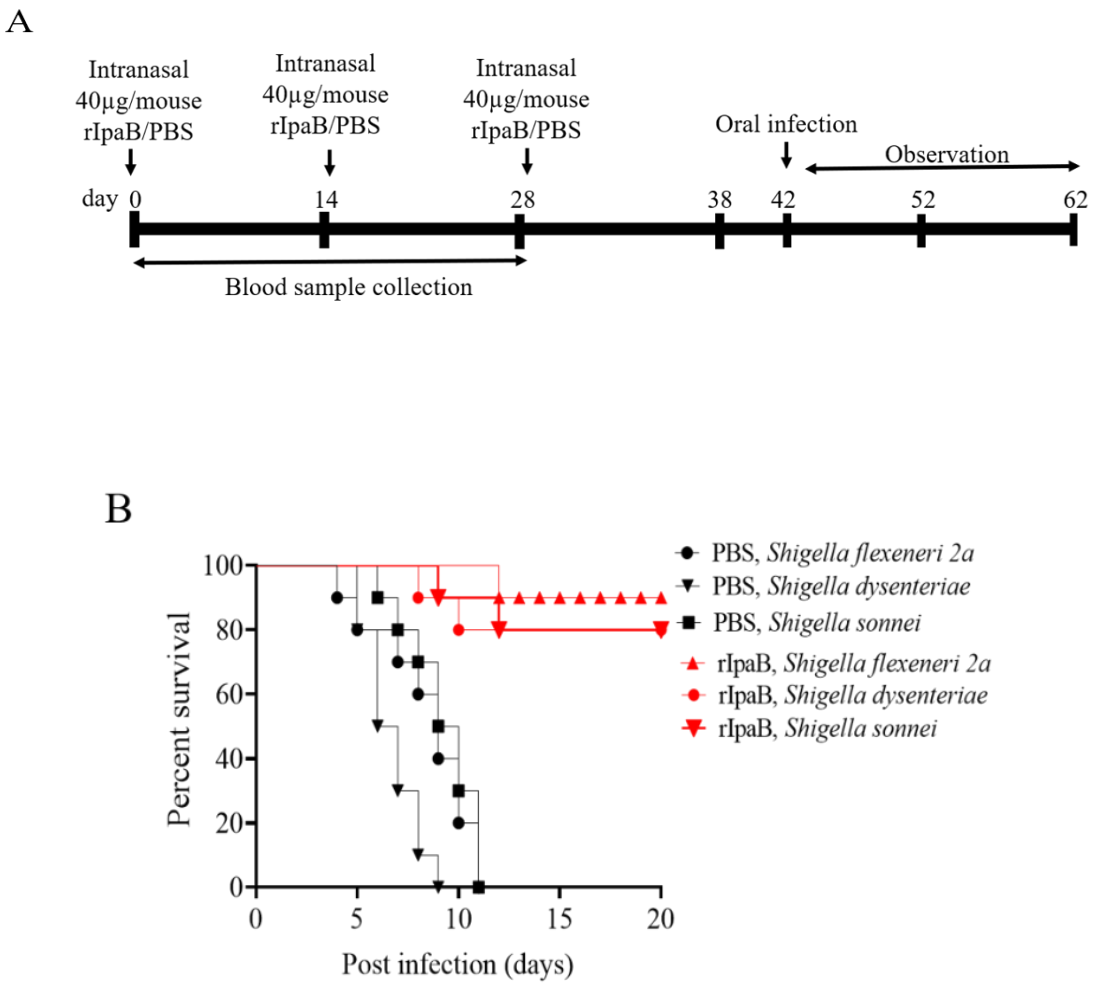

Figure 25. Intranasal immunization with recombinant IpaB augmented humoral immune response and protects mice against oral *Shigella* infections. (A) Experimental schedule of Immunization, sample collection and bacterial challenge of BALB/c mice. (B) Kaplan-Meyer plot of cumulative mortality of the mice immunized intranasally with vehicle or the recombinant protein. Ten days after the last immunization (38d), immunized mice were pre-treated with streptomycin and iron followed by oral infection with different *Shigella* spp.

(*Shigella flexeneri 2a* (5 x 10^9 CFU, n= 10), *Shigella* dysenteriae (5 x 10^8 CFU, n= 10), *Shigella* sonnei (5 x 10^8 CFU, n= 10) and monitored for 20 days. The colour scheme used to mark different experimental groups are as follows: PBS-black; rIpaB-red.

4.2.4.2. Recombinant IpaB immunization reduces colonization of the mouse large intestine by S*higella flexneri 2a* and disease manifestations after oral infection

To investigate if rIpaB could reduce the disease severity of *Shigella flexeneri 2a* infection, immunized mice were challenged orally with a sublethal dose (5×10^7 CFU) of the bacterium that was used for the model development. Vehicle-immunized mice were visibly sick with diarrhoea at 24h post-infection, while the rIpaB vaccine-immunized groups were agile and symptom-free **(Figure 26 A**). Mice immunized with rIpaB showed increased body weight as opposed to reduced body weight of the vehicle-immunized, infected group (**Figure 26 B**). Significant shortening of the colon was observed in the latter group, while rIpaB-immunized mice displayed normal colon lengths (**Figure 26 Ci-Cii)**. The above manifestations corroborated with *S. flexeneri 2a* colonization of the caecum and colon and shedding in the faeces with significant reduction of the CFU counts in rIpaB- vaccinated mice (**Figure 26 D).** Together the above results suggested that the IpaB vaccine candidate might have induced immune response in the large intestine to prevent *Shigella* infection. To further investigate if this led to reduced tissue destruction in rIpaB-vaccinated mice, histopathology of the large intestinal tissues was performed. were observed in. While mice of the unimmunized (PBS treated) group showed destruction of the epithelial lining, loss of crypt architecture with decreased number of goblet cells, increased infiltration of lymphocytes in the mucosa and submucosa, and submucosal edema, the immunized (rIpaB treated) mice had intact epithelial lining and crypt architecture with abundant goblet cells, absence of mucosal or submucosal

damage and no abnormal cellular infiltrates (**Figure 27 A-B, Figure 28 A-B).** Overall, these results suggested that intranasal immunization with rIpaB prevented *Shigella* from colonizing the large intestine after oral infection, thereby reducing tissue damage and disease manifestations. [The detailed methodologies were discussed in the materials and method sections **3.2.18.4. and 3.2.19**]

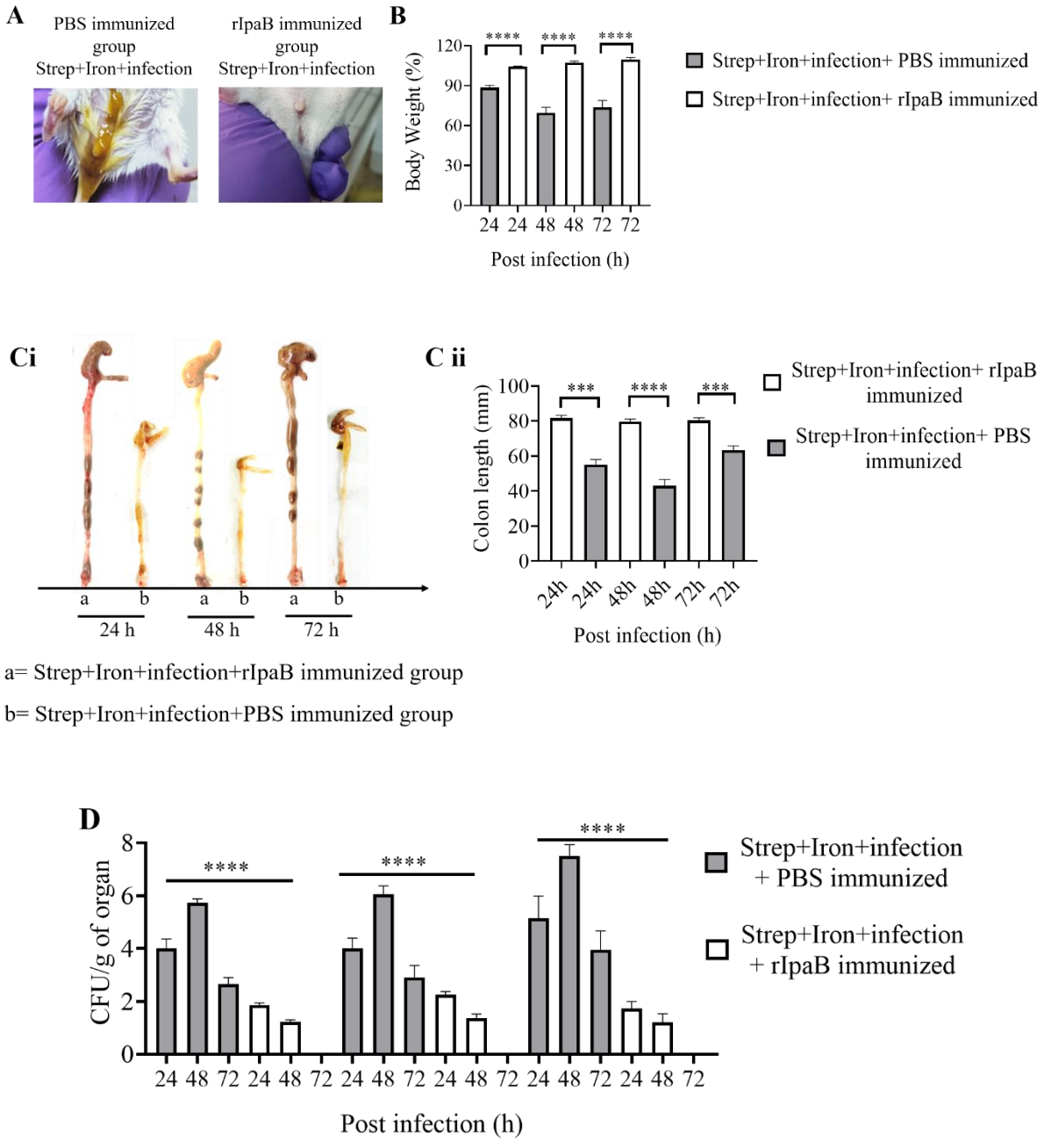

Figure 26. rIpaB immunized mice were not susceptible to infection following oral administration of *S. flexneri 2a*. BALB/c mice were immunized intranasally with Vehicle (PBS) and rIpaB (40µg/mouse) on days 0, 14, and 28. Ten days after the last immunization (38d), immunized mice were pre-treated with Streptomycin and iron followed by oral infection with 5×10^7 CFU bacteria. (A) Photos of the anal region of immunized groups at 24 hours of post-infection. Experiment was repeated three times and one image out of three independent experiments (n=6) is shown. (B) Body weight changes were monitored between infected and uninfected groups at different post-infection time points. Data represent mean ± SEM values from different mice samples (n=5). Statistical analyses were performed with two-tailed Student's t-test (****P<0.0001). (C) Mice were sacrificed at the indicated time points and the colon length of the respective groups were observed. (C i), Representative photograph of the colon length of different groups of mice. Experiment was repeated three times and one image out of three independent experiments is shown. (C ii), Bar representing the comparison of the colon length between two groups of mice. Data represent mean ± SEM values from different mice samples (n=3). Statistical analyses were performed with two-tailed Student's t-test (**P < 0.01, ***P < 0.001, ****P<0.0001). (D) Colony forming units (CFU) in homogenates of colon, cecum, and feces. Data represent mean ± SEM of the values from multiple animals (n=3). Statistical analyses were performed by one-way ANOVA and Tukey's post-test for multiple comparisons, *P < 0.05, **P < 0.01, ***P <0.001.

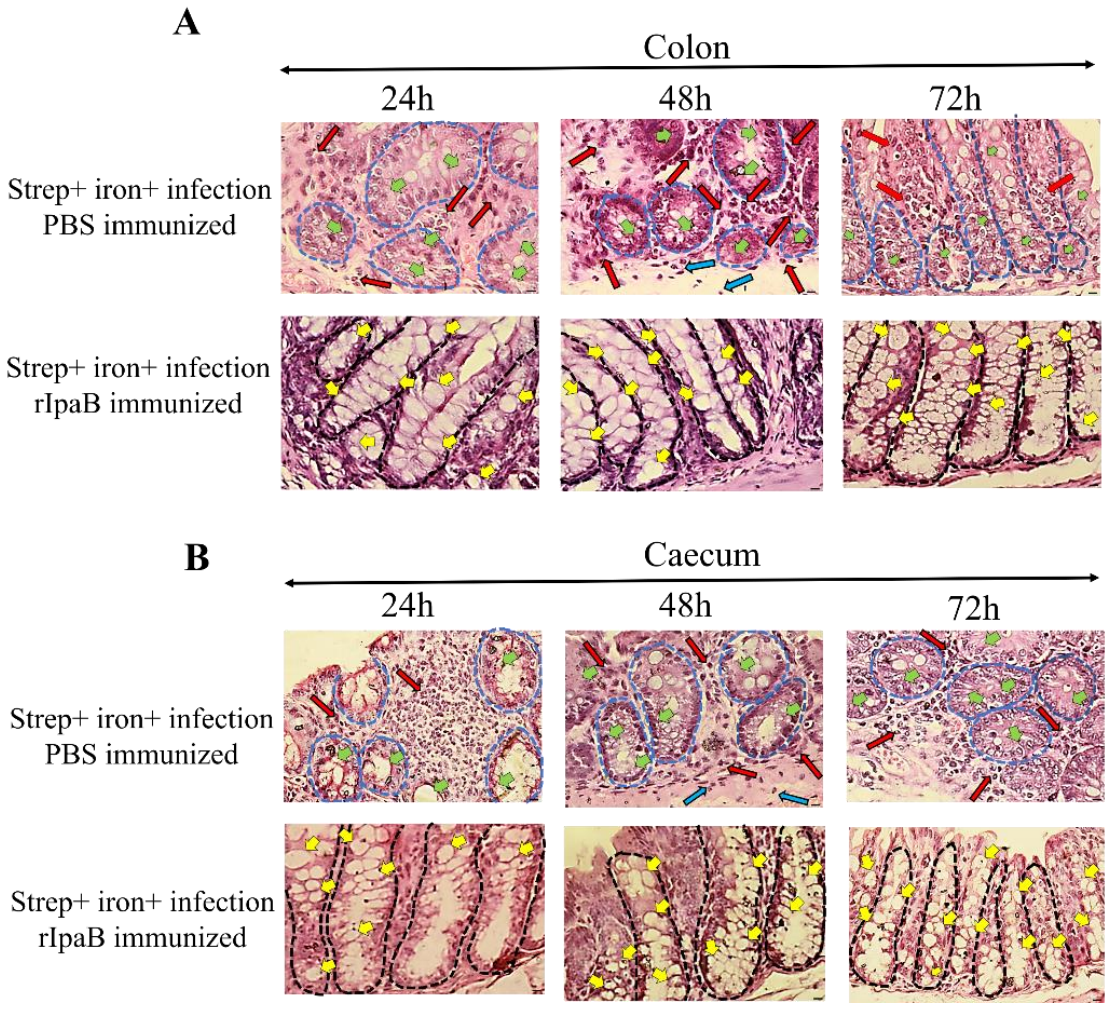

Figure 27. Histology sections (40X magnification) of colon and caecum of immunized and unimmunized BALB/c mice after infection. BALB/c mice (n=10) were immunized intranasally with Vehicle (PBS) and rIpaB (40µg/mouse) on days 0, 14, and 28. Ten days after the last immunization (38d), immunized mice were pre-treated with streptomycin and iron followed by oral infection with 5×10^7 CFU bacteria. Mice were sacrificed at the indicated time points. Colon and caecum were excised, fixed, and embedded in paraffin. Tissue sections were stained with Hematoxylin & Eosin and observed in a microscope (40x magnification, Scale bar =10 µm). The images are the magnified form of the 10X images (areas of green box) presented in Figure 28. Intact crypt architecture with abundant records of goblet cells, intact mucosa and submucosa without abnormal infiltrates were observed in the control group of mice (i-iv). Streptomycin-iron with infected group (v) showed loss of crypt architecture with decreased

goblet cells, increased infiltration of lymphocytes in the mucosa and submucosa. Black round dotted circles represent intact crypt architecture and blue round dotted circles represent loss of crypt architecture. Different colors of arrow indicate different parameters as follows; yellow arrow- abundant goblet cells; green arrow- loss of goblet cells; red arrow- lymphocyte infiltration in the mucosa; blue arrow- lymphocyte infiltration in the submucosa.

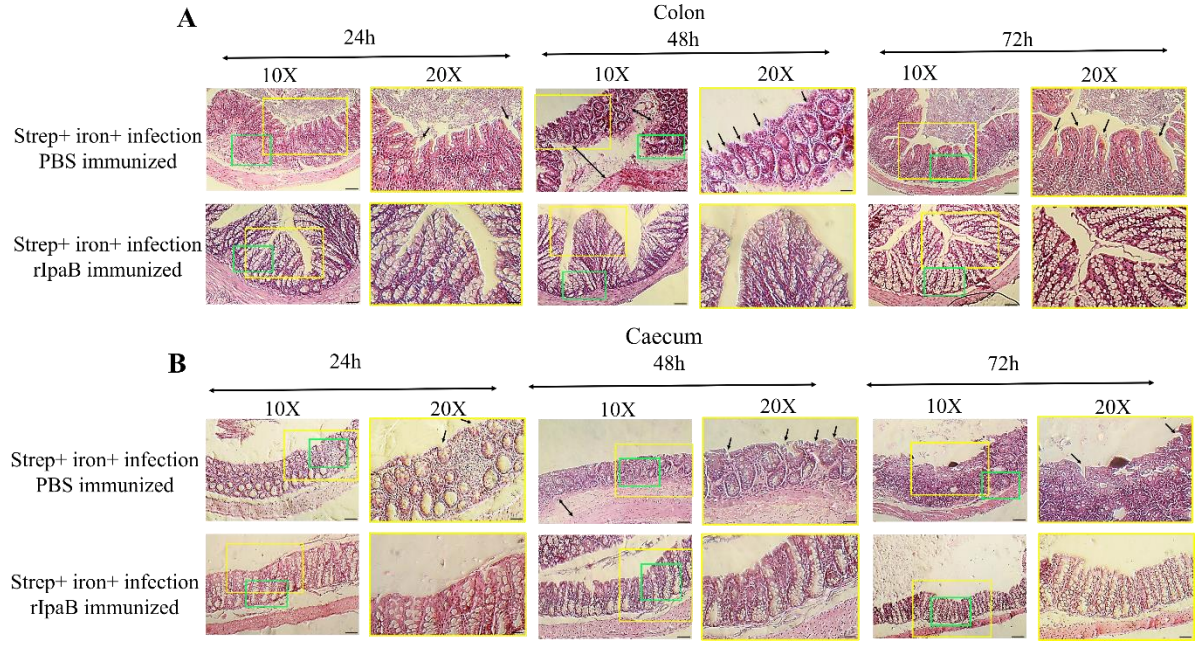

Figure 28. Histology sections (10X and 20X magnification) of colon and caecum of immunized and unimmunized BALB/c mice after infection. BALB/c mice (n=10) were immunized intranasally with Vehicle (PBS) and rIpaB (40µg/mouse) on days 0, 14, and 28. Ten days after the last immunization (38d), immunized mice were pre-treated with streptomycin and iron followed by oral infection with 5×10^7 CFU bacteria. Mice were sacrificed at the indicated time points. Colon and caecum were excised, fixed, embedded in paraffin, and tissue sections were stained with Hematoxylin & Eosin. Intact epithelial lining was observed in the control group of mice (i-iv, 20X magnification). Streptomycin-iron with infected group (v) showed degenerative changes in the epithelial lining (20X magnification),

and submucosal swelling (edema) (10X magnification). Yellow boxes represent the 20X (Scale bar =50 µm) magnification of the 10X (Scale bar =100 µm) image. Green boxes indicate the region selected for presentation in Figure 27. Double-headed black arrow indicates submucosal swelling (edema); single black arrow indicates the changes in the epithelial lining.

4.2.4.3. Intranasal immunization with recombinant chimeric protein, IpaB-T2544 protects mice against oral *Shigella* and typhoidal *Salmonella* infections

We had previously reported that a candidate vaccine formulation based on T2544, administered subcutaneously induced high levels of serum antibodies and robust effector and memory T cell response, leading to protection from *S.* Typhi challenge (449). Moreover, T2544 used as a carrier protein acted as a vaccine adjuvant and augmented the immunogenicity of *S.* Typhimurium O-specific polysaccharide (450). Hence, to develop a bivalent vaccine formulation against *Shigella* and *Salmonella* spp, a chimeric protein containing T2544 and IpaB was generated.

To check for the protective efficacy of the candidate vaccine against *Shigella* and *Salmonella*, BALB/c mice were immunized intranasally with three doses of the recombinant chimeric protein or the individual proteins that constituted the chimera or the vehicle (PBS) at 14d intervals (**Table 11, Figure 29 A)**. A 10xLD_{50} oral infection dose of *Shigella* spp. killed all the mice that received either the vehicle or rT2544 within 14 days of infection, whereas 80-90% of the mice immunized with rIpaB-T2544 or rIpaB alone were still alive beyond 20 days (**Figure 29 B-D**). Vaccine efficacy against *S.* Typhi and *S.* Paratyphi A, as evaluated in the BALB/c mouse model showed nearly 70% protection following rIpaB-T2544 immunization against 10X LD_{50} doses of *S.* Typhi (5 x 10^7 CFU) or *S.* Paratyphi (5 x 10^5 CFU), while T2544 alone was non-protective with all the immunized mice being dead within 5-6 days (**Figure 29 E-F)**. This

suggested that IpaB acted as an immune adjuvant to T2544 for intranasal vaccination. Moreover, rIpaB-T2544 is a bivalent vaccine candidate against *Shigella* spp. and *Salmonella* (*S.* Typhi and *S.* Paratyphi A), when administered through the intranasal route. [The detailed methodologies were discussed in the materials and method sections **3.2.10.1., 3.2.18.1. and 3.2.18.3**]

Table 11: Vaccine formulation doses and bacterial strains used for the immunogenicity (rIpaB, rT2544 and rIpaB-T2544) and challenged study

Mice strain	**Immunogen**	**Route of immunization**	**Adjuvant**	**Dose (µg/mice)**	**Bacterial strain for infection study**	**Infection dose**	**Infection route**	**Infection mice model**
BALB/c	rIpaB-T2544 rIpaB PBS	Intranasal	Alum Alum Alum	40 40 40	*Shigella flexeneri 2a* *Shigella dysenteriae* *Shigella sonnei*	5×10^9 CFU 5×10^8 CFU 5×10^8 CFU	Oral	Iron overload
BALB/c	rIpaB-T2544 rT2544 PBS	Intranasal	Alum Alum Alum	40 40 40	*S.* Typhi	5×10^7 CFU	Oral	Iron overload

BALB/c	rIpaB-T2544 rT2544 PBS	Intranasal	Alum Alum Alum	40 40 40	*S.* Paratyphi A	5 x 10^5 CFU	Oral	Iron overload

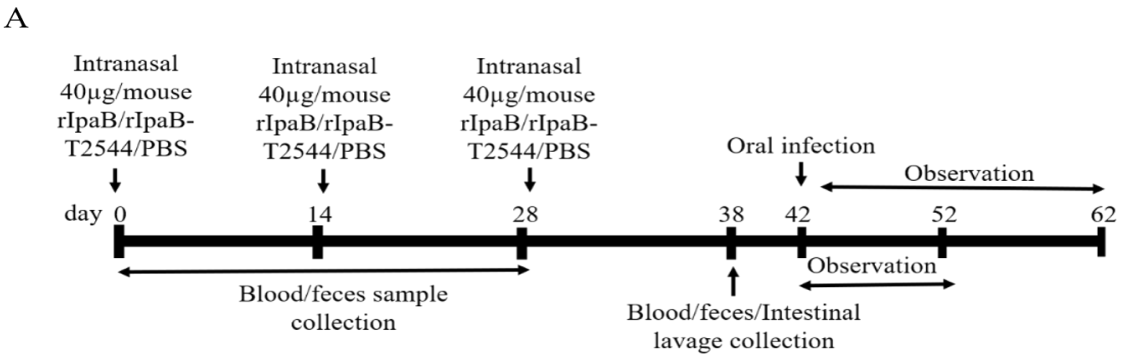

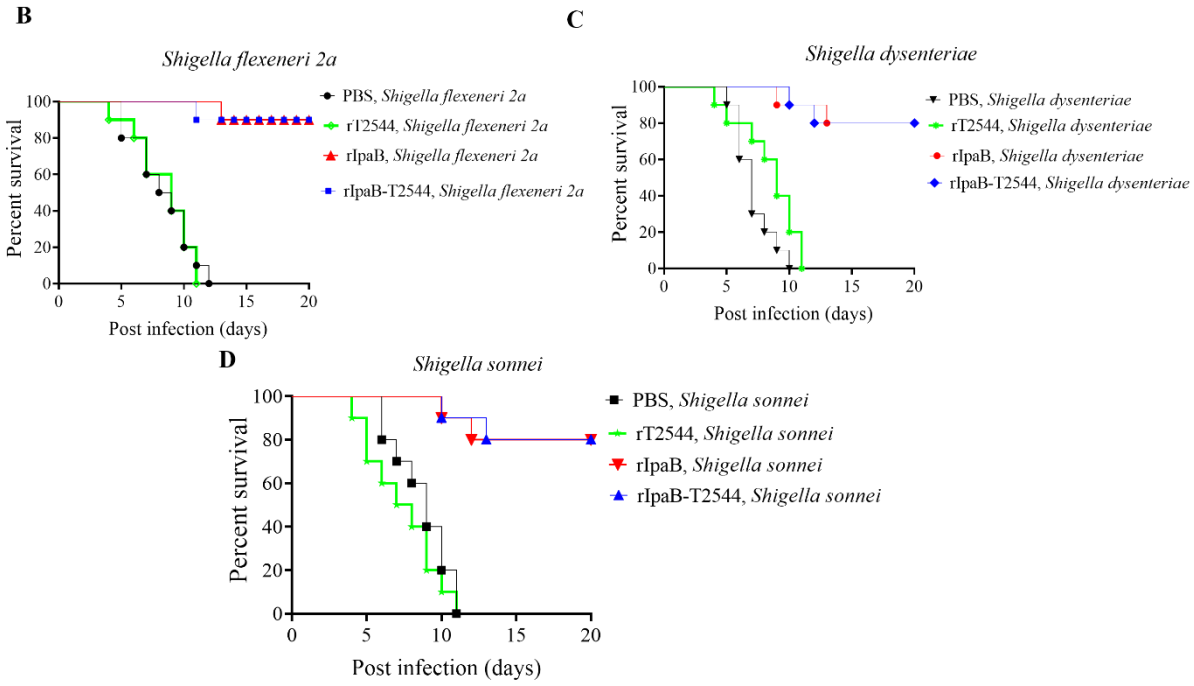

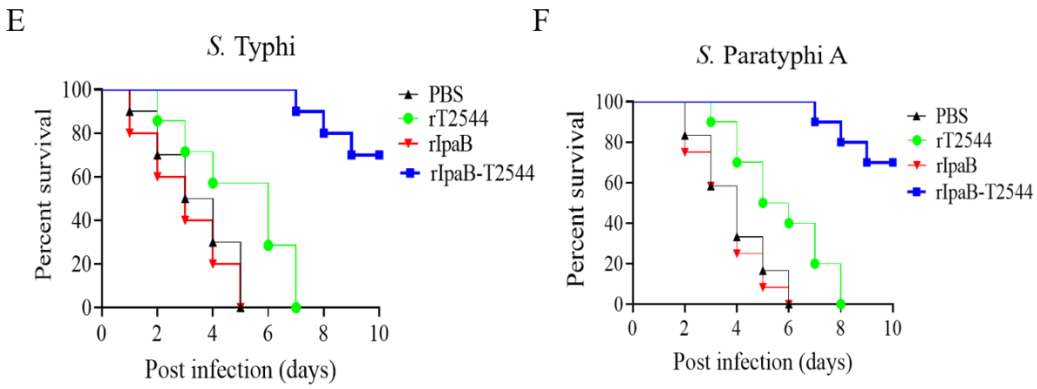

Figure 29. Intranasal immunization with recombinant chimeric protein, IpaB-T2544 protects mice against oral *Shigella* and typhoidal *Salmonella* infections. (A) Experimental schedule of Immunization, sample collection and bacterial challenge of BALB/c mice. (B-F) Kaplan-Meyer plot of cumulative mortality of the mice immunized intranasally with vehicle, chimeric (rIpaB-T2544) or the recombinant proteins (rIpaB, rT2544). One set of immunized mice were pre-treated with Streptomycin and iron followed by oral infection with *Shigella flexeneri 2a* (5 x 10^9 CFU, n= 10) (B), *Shigella dysenteriae* (5 x 10^8 CFU, n= 10) (C), *Shigella sonnei* (5 x 10^8 CFU, n= 10) (D) and monitored for 20 days. Other sets of immunized mice were pre-treated with iron followed by oral infection with *S.* Typhi (5 x 107 CFU, n= 10) (E) and *S.* Paratyphi A (5 x 105 CFU, n=10) (F) and monitored for 10 days. The colour scheme used to mark different experimental groups are as follows: PBS-black; rT2544-green; rIpaB-red; rIpaB-T2544-blue.

Summary

- Mice subcutaneously immunized with OSP-rT2544 conferred 75-77% protection against *Salmonella* Typhi and Paratyphi A; 70-80% protection against *Salmonella* Typhimurium; and 55-60% cross-protection against *Salmonella* Enteritidis.

- Single immunization with Vi-rT2544 provides better protection compared to Vi-TT against *Salmonella* Typhi and *Salmonella* Paratyphi A. It was found that mice subcutaneously immunized with Vi-T2544 and Vi-TT showed ~66% and ~40% protection while intramuscular immunization showed ~66% and ~30% protection against *S.* Typhi. Both subcutaneous and intramuscular Vi-T2544 immunized mice showed ~60% protection against *S.* Paratyphi A. However, no protection was found in Vi-TT immunized mice against *S.* Paratyphi A challenge.
- Combined administration of oral streptomycin and intraperitoneal iron plus chelator (desferrioxamine) treatment enhances the susceptibility of mice to oral *Shigella* infection and disease development. Susceptible mice showed body weight loss, decrease colon length and tissue inflammation characterized by disruption of epithelial lining, loss of crypt architecture with decreased goblet cell numbers and increased PMN infiltration into the mucosa of the colon and caecum at 24 and 72 hrs and submucosal swelling (edema) with PMN infiltration at 48h of infection. Bacterial colonization in the colon and caecum, shedding in the feces were observed at different post-infection time points. The macroscopic and microscopic features of colonic and caecal inflammation were also accompanied by the release of high levels of pro-inflammatory cytokines and chemokines, such as TNF-α, IL-1β, IFN-γ and CXCL10 in the supernatants of the tissue homogenates at different time points of infection.
- Intranasal immunization with recombinant IpaB confers 90% protection against *Shigella flexeneri 2a* and 80% protection against *Shigella dysenteriae* and *Shigella sonnei* using our newly developed oral *Shigella* mouse model.
- Recombinant IpaB immunization reduces colonization of the mouse large intestine by *Shigella flexneri 2a* and disease manifestations after oral infection. Mice immunized with rIpaB showed increased body weight, increased colon length and decreased

colonization in the colon and caecum and shedding in the feces. The immunized (rIpaB treated) mice had intact epithelial lining and crypt architecture with abundant goblet cells, absence of mucosal or submucosal damage and no abnormal cellular infiltrates.

- Intranasal immunization with recombinant chimeric protein, IpaB-T2544 conferred 80-90% protection against oral *Shigella flexeneri 2a*, *Shigella dysenteriae* and *Shigella sonnei* challenge using our newly developed *Shigella* mouse model while conferred 70% protection against oral *Salmonella* Typhi and Paratyphi A infections using iron overload *Salmonella* oral mouse model.

4.3. Objective 3.

Studies on the adaptive immune response after mucosal and systemic immunization with newly designed antigens

4.3.1. OSP-rT2544 induces protective humoral immune response against *S.* Typhi, *S.* Paratyphi A, *S.* Typhimurium and *S.* Enteritidis

We had earlier reported protective humoral response in mice against *S.* Typhi upon subcutaneous immunization with recombinant T2544 (449). To check if rT2544 present in the conjugate vaccine is equally immunogenic, serum antibody endpoint titers (The reciprocal of the titer (1/Y) at which the absorbance of the immune sera was the same as the control (PBS immunized sera)) were measured by ELISA, 10 days after completion of the primary immunization series as well as 110 days after the first immunization dose of BALB/c mice, immunized with OSP-rT2544 or the unconjugated vaccine formulations (**Figure 30 A, Table 6**). The results showed similar anti-rT2544 IgG responses at both the above time points, following vaccination with rT2544 and OSP-rT2544 (**Figure 30 B**). In contrast, anti-OSP IgG titer remained significantly elevated 110 days after immunization with OSP-rT2544 only, while it touched the baseline for the mice that received unconjugated OSP, suggesting that rT2544 acted as a vaccine adjuvant to OSP (**Figure 30 C**). Anti-rT2544 IgG was comprised of IgG1 and IgG2a isotypes, indicating the induction of both Th1 and Th2 type responses; however, IgG1 was the predominant isotype (**Figure 30 D**). To determine the functional activities of the immune sera, bactericidal assay was performed by incubating *S.* Typhi and *S.* Paratyphi A with heat-inactivated, serially-diluted sera collected from the immunized mice, supplemented with guinea pig complement. Both OSP-rT2544 and rT2544 immune sera from BALB/c mice reduced the growth of *S.* Typhi and *S.* Paratyphi A by 50% at dilutions between 1:1600 and 1:3200 and 1:6400 and 1:12800, respectively after 3h of incubation, while unconjugated OSP immune sera displayed no growth inhibition (**Figure 30 E-F, Table 11**). Similar growth inhibition of *S.* Typhi and *S.* Paratyphi A was obtained for OSP-rT2544 anti-sera collected from C57BL/6 mice as well (**Figure 31 A-B**).

Given the persistently elevated, serum anti-OSP IgG titer in BALB/c mice after immunization with OSP-rT2544, we sought to investigate antisera-mediated protection against *S.* Typhimurium in similarly-immunized C57BL/6 mice by measuring antibody endpoint titers as well as SBA titers (**Figure 32 A, Table 12**). Like the BALB/c mice, anti-OSP IgG titer was significantly higher in OSP-rT2544 antisera than OSP antisera at day 38 of immunization and remained elevated at day 110, while OSP antisera reached the baseline (**Figure 32 B**). This corroborated with correspondingly higher SBA titer of OSP-rT2544 antisera (1:6400 versus 1:200) against *S.* Typhimurium (**Figure 32 E, Table 12)**. Similar titer values were found for OSP-rT2544 antisera from BALB/c mice to induce 50% growth reduction of *S.* Typhimurium (**Figure 31)**. As expected, there was no difference in the magnitudes of serum anti-rT2544 antibodies between the animals vaccinated with OSP-rT2544 conjugate and unconjugated rT2544 (**Figure 32 C**). Markedly raised titers of OSP-specific serum IgG1 and IgG2a antibodies were observed in C57/BL6 mice immunized with OSP-rT2544, as compared with the OSP immunized mice, indicating induction of both Th1 and Th2 type responses, albeit to a significantly higher level for the later as observed for anti-rT2544 IgG isotype (**Figure 32 D**). Together the above results suggested the potential for significant protection against both typhoidal and non-typhoidal Salmonellae by OSP-rT2544 antisera.

To evaluate cross-protection against *S.* Enteritidis after immunization with OSP-rT2544 candidate vaccine, reactivity of the antisera with OSPs extracted from different *S.* Enteritidis strains was studied by measuring the titers of anti-OSP antibodies. The results showed significant cross-reactivity of OSP-rT2544 antisera with the OSPs of several clinical *S.* Enteritidis strains (**Figure 33A**). To investigate cross-protection of the antisera against *S.* Enteritidis, SBA titers were estimated as described above. The results showed 50% growth inhibition of *S.* Enteritidis by OSP-rT2544 antisera dilution of 1:800 to 1:1600 versus 1:200 dilution of OSP antisera (**Figure 33B, Table 12**). Similar result was observed for the 50%

growth reduction of *S.* Enteritidis when OSP-rT2544 antisera from BALB/c mice was used to perform serum bactericidal assay (**Figure 31)**. This result suggested broad range of protection against NTS strains after vaccination with OSP-rT2544 antigen. [The detailed methodologies were discussed in the materials and method sections **3.2.10.1., 3.2.11.1.** and **3.2.13.**]

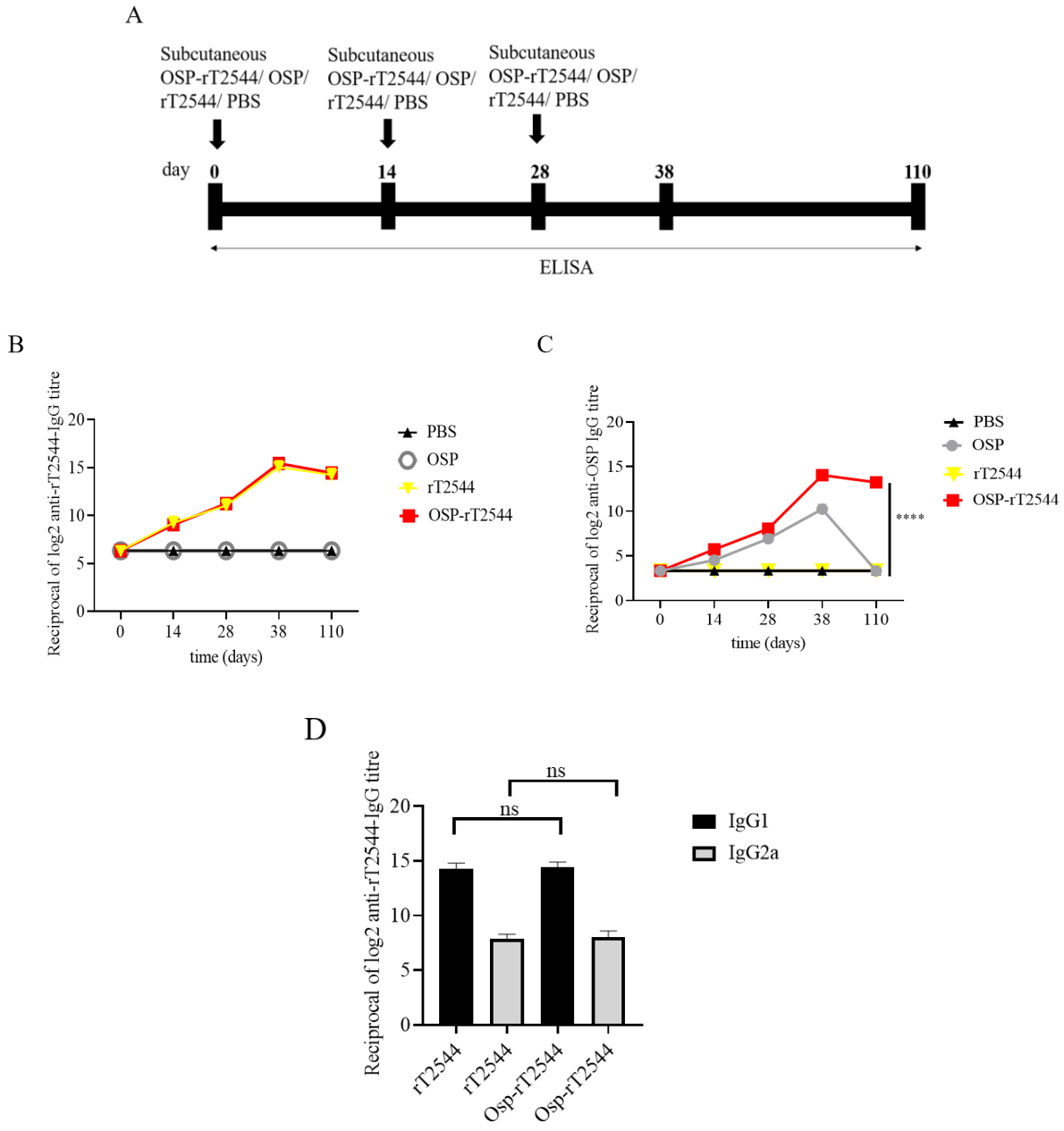

Ei

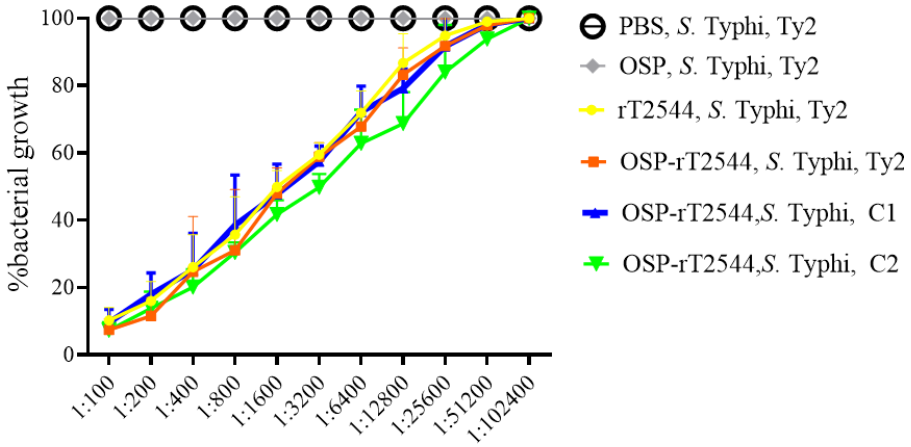
%bacterial growth
100
80
60
40
20
0
1:100
1:200
1:400
1:800
1:1600
1:3200
1:6400
1:12800
1:25600
1:51200
1:102400
PBS, S. Typhi, Ty2
OSP, S. Typhi, Ty2
rT2544, S. Typhi, Ty2
OSP-rT2544, S. Typhi, Ty2
OSP-rT2544,S. Typhi, C1
OSP-rT2544,S. Typhi, C2

Eii

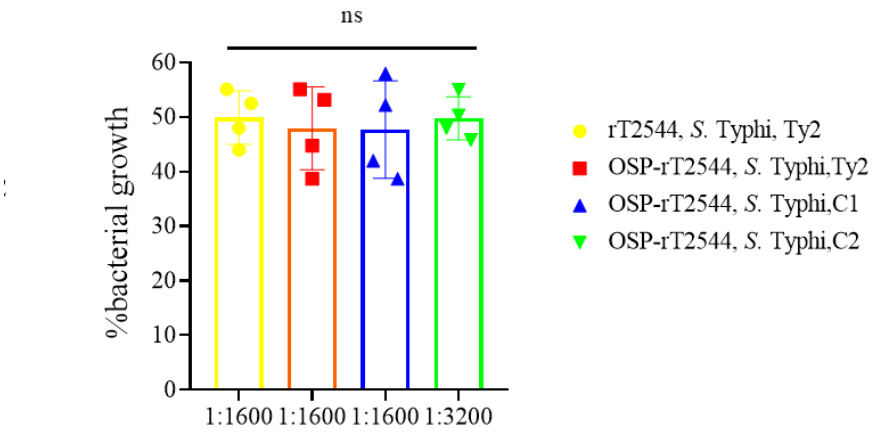
ns
%bacterial growth
60
50
40
30
20
10
0
1:1600 1:1600 1:1600 1:3200
rT2544, S. Typhi, Ty2
OSP-rT2544, S. Typhi,Ty2
OSP-rT2544, S. Typhi,C1
OSP-rT2544, S. Typhi,C2

Fi

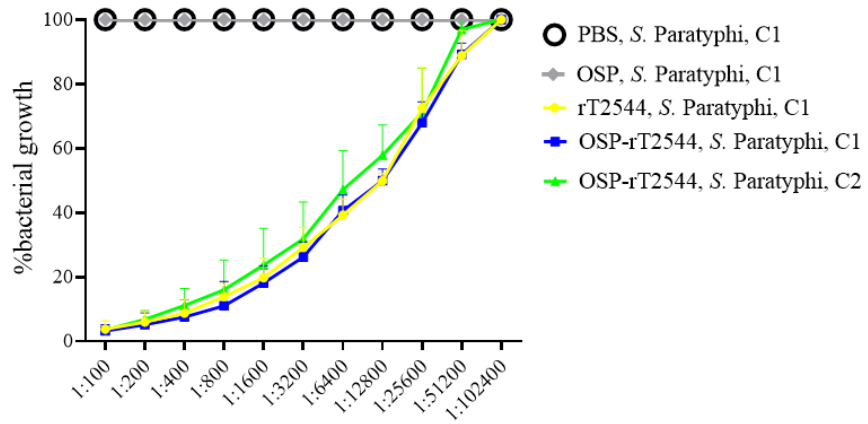
%bacterial growth
100
80
60
40
20
0
1:100
1:200
1:400
1:800
1:1600
1:3200
1:6400
1:12800
1:25600
1:51200
1:102400
PBS, S. Paratyphi, C1
OSP, S. Paratyphi, C1
rT2544, S. Paratyphi, C1
OSP-rT2544, S. Paratyphi, C1
OSP-rT2544, S. Paratyphi, C2

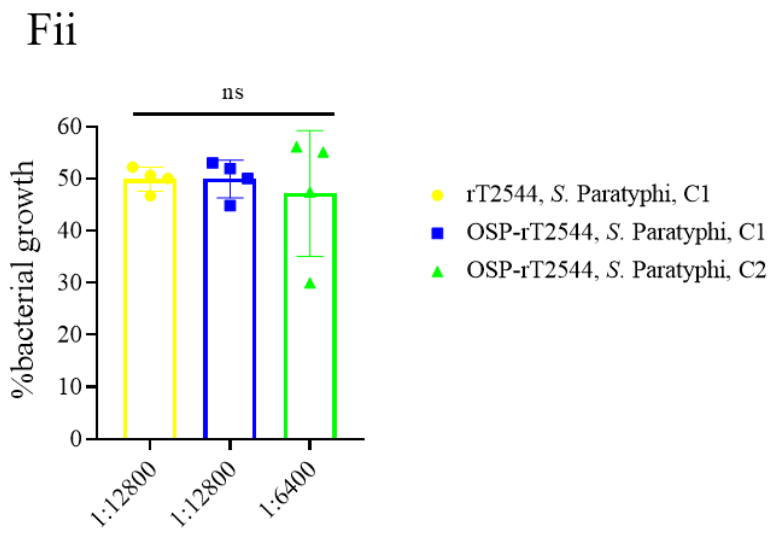

Figure 30. Protective antibody response against *S.* Typhi and *S.* Paratyphi A by OSP-rT2544 immunization. (A) Scheme of subcutaneous immunization of BALB/c mice. Mouse tissue samples were collected before each immunization dose and on day38 and day110 of the start of immunization. (B, C) Time kinetics of antigen-specific total IgG in the mouse serum as measured by ELISA. Data represent mean ± SEM values from different mice samples (n=5). X-axis indicate the time points after the start of the immunization when samples were collected. Statistical significance between the titer values from OSP-rT2544 and unconjugated OSP vaccine recipients is shown. Statistical analysis was performed using two-way ANOVA and Tukey's post-test for multiple comparisons. *P < 0.05, **P < 0.01, ***P < 0.001. (D) rT2544 specific serum IgG isotypes measured by ELISA at day 38. Data represent mean ± SEM values from different mice samples (n=5). Statistical analysis was performed using two-tailed Student's *t*-test. (E, F) Serum bactericidal assay. Serial dilutions of heat-inactivated antisera, collected from different groups of the immunized mice at 38 d of immunization were mixed with 25% guinea pig complement and incubated for 3h with the *S.* Typhi or *S.* Paratyphi A strains as indicated in the figure. Percentages of each live bacterial strain out of the original counts remaining at the end of the experiment for the individual serum dilutions are plotted (E i, F i). Bactericidal activity was expressed as the serum dilutions at which 50% of the live

bacterial loads are recovered after 3h of incubation (E ii, F ii). C1, C2 are clinical isolates; bars represent the mean percent of growth reduction ±SEM of quadruplicate samples. The clolor scheme used are described in **Table 8**.

Table 12. SBA titre using 38th day antisera (OSP-rT2544)

Anti-sera	**SBA titre (growth reduction up to 50%)**	**Bacterial strain**
SBA for *S.* Typhi		
OSP-rT2544	1:1600	Ty2
	1:1600	Clinical isolate 1
	1:3200	Clinical isolate 2
rT2544	1:1600	Ty2
OSP	No 50% reduction (50%<)	Ty2
SBA for *S.* Paratyphi A		
OSP-rT2544	1:12800	Clinical isolate 1
	1:6400	Clinical isolate 2

rT2544	1:12800	Clinical isolate 1
OSP	No 50% reduction (50%<)	Clinical isolate 1
SBA for *S.* Typhimurium		
OSP-rT2544	1:6400	LT2
	1:6400	Clinical isolate 1
	1:3200	Clinical isolate 2
	1:6400	Clinical isolate 3
OSP	1:200	LT2
rT2544	No 50% reduction (50%<)	LT2
SBA for *S.* Enteritidis		
OSP-rT2544	1:1600	Clinical isolate 1
	1:800	Clinical isolate 2
	1:800	Clinical isolate 3
OSP	1:200	Clinical isolate 1
rT2544	No 50% reduction (50%<)	Clinical isolate 1

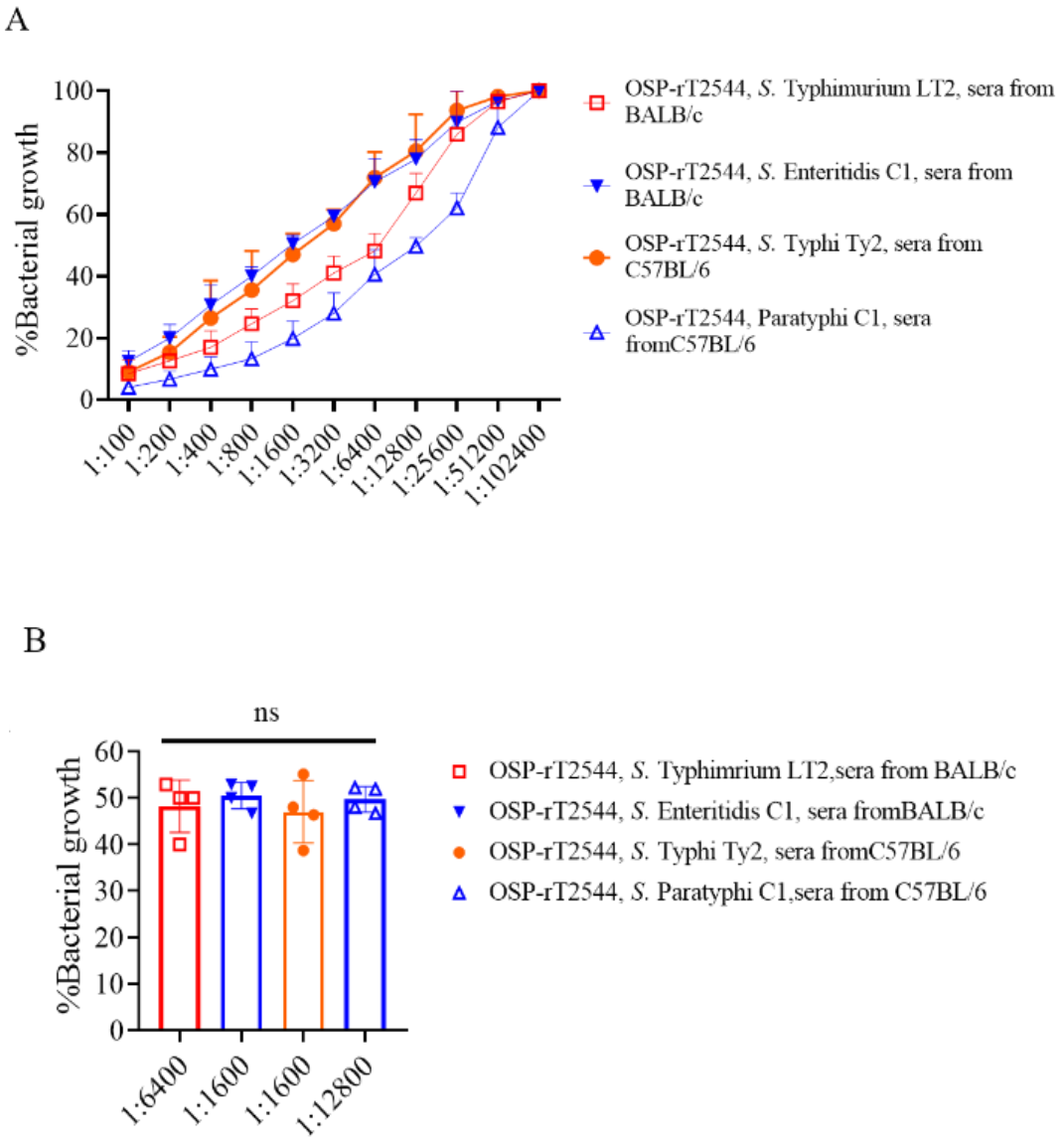

Figure 31. Serum Bactericidal assay (SBA) using OSP-rT2544 anti-sera. BALB/c (n=5) and C57BL/6 (n=5) mice were subcutaneously immunized three times with OSP-rT2544 (8 µg of OSP and 24 µg of rT2544) at days 0, 14, and 28. SBA was performed using antisera collected on day 38 after the first immunization. (A-B) Serial dilutions of heat-inactivated antisera, collected from BALB/c mice were incubated with *S.* Typhimurium LT2, or S. Enteritidis C1 strain. Similarly, C57BL/6 mice sera were incubated with *S.* Typhi or *S.* Paratyphi A strains. After adding 25% guinea pig complement, bactericidal activity was expressed as the serum dilution at which 50% growth inhibition of the bacteria was noted at T_{180} (3h time point)

compared with T_0 (A). Specific dilutions at which 50% growth reduction for different strains was observed are indicated in Figure B. C1 is the clinical isolate and values represent mean ±SEM of four independent experiments. Statistical analysis was performed using two-tailed Student's *t*-test. The clolor scheme used are described in **Table 8**.

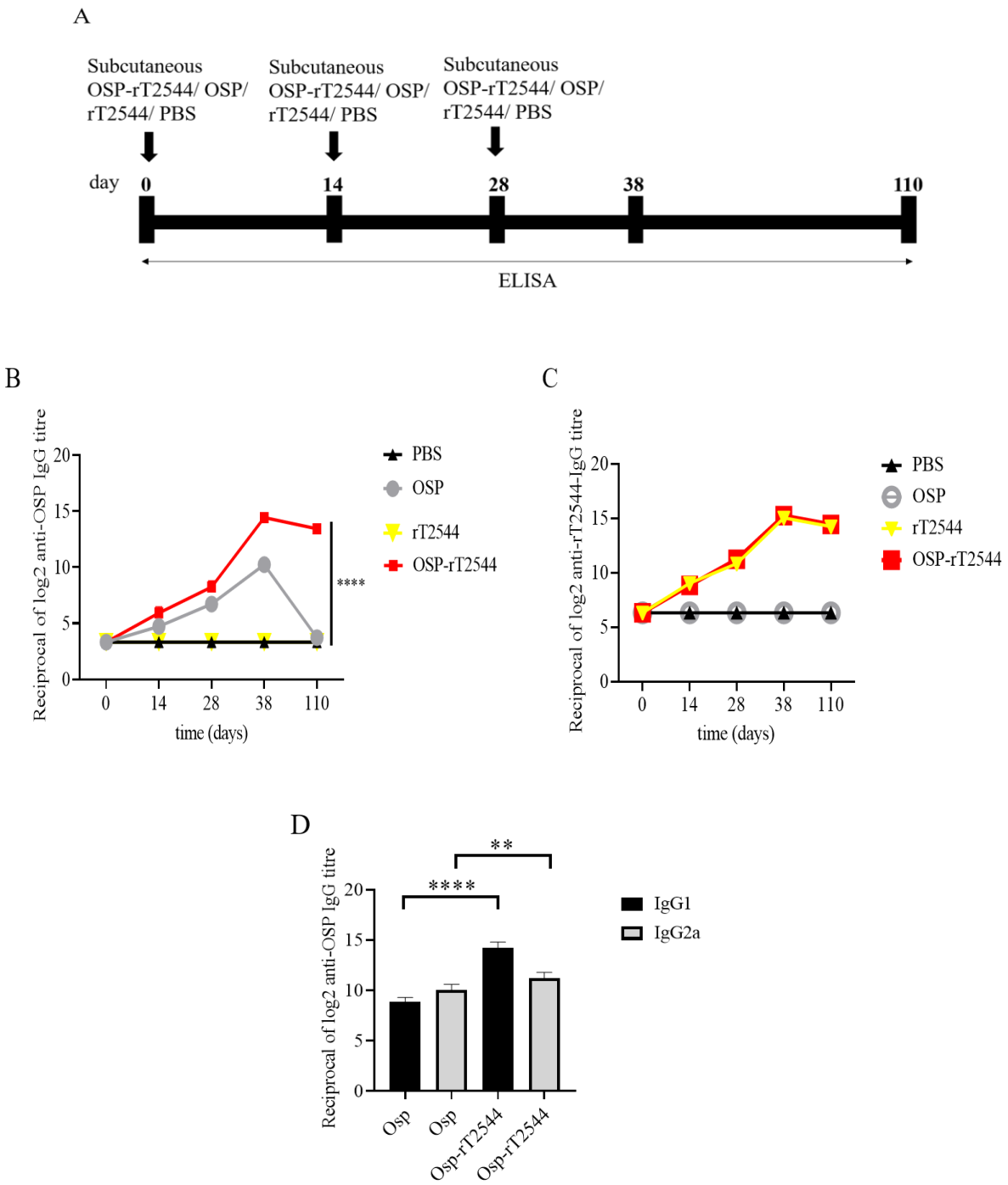

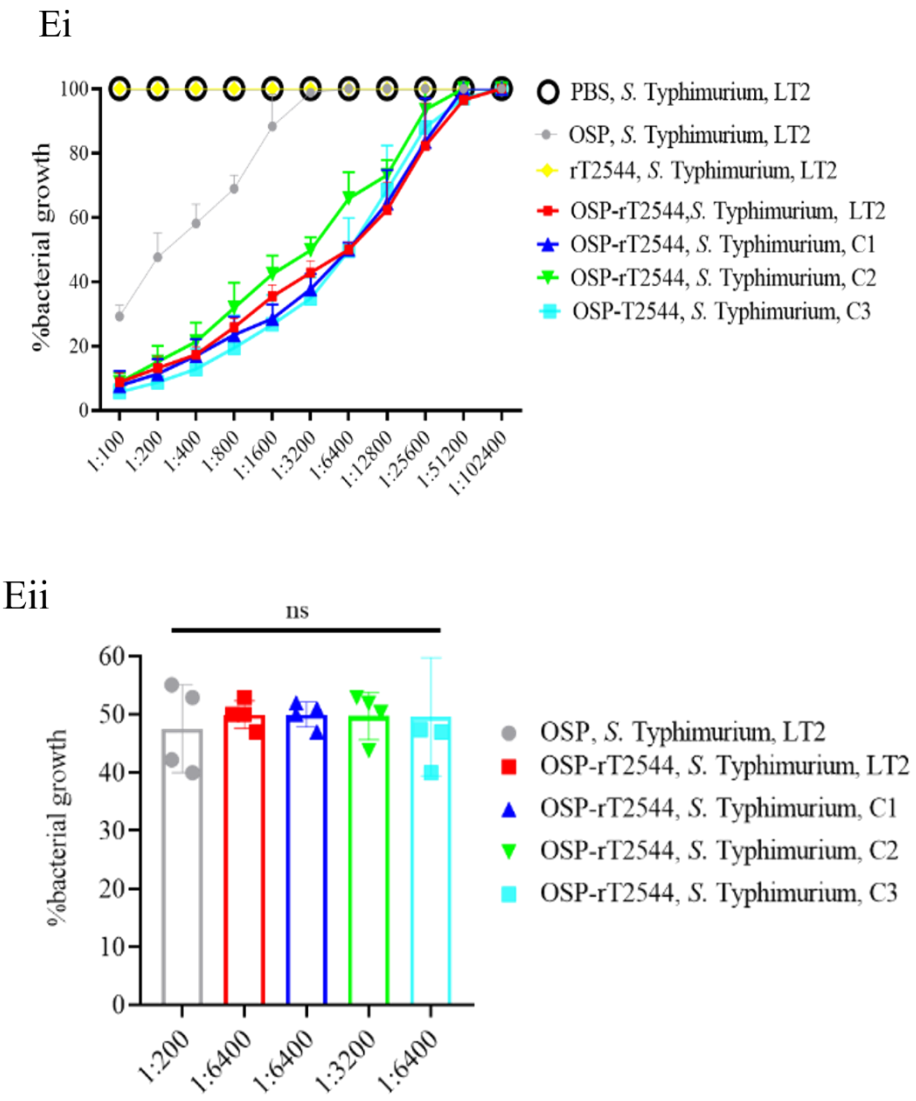

Figure 32. OSP-rT2544 immunization generates protective antibodies against *S.* Typhimurium. (A) Scheme of subcutaneous immunization of C57BL/6 mice and tissue sample collection. The scheme is similar to that described for BALB/c mice under figure 30. (B, C) Time kinetics of antigen-specific total IgG in the mouse serum as measured by ELISA. Data represent mean ± SEM values from different mice samples (n=5). X-axis indicate the time points after the start of the immunization when samples were collected. Statistical significance between the titer values from OSP-rT2544 and unconjugated OSP vaccine recipients is shown. Statistical analysis was performed using two-way ANOVA and Tukey's post-test for multiple comparisons. *P < 0.05, **P < 0.01, ***P < 0.001. (D) OSP-specific serum IgG isotypes

measured by ELISA at day 38. Data represent mean ± SEM values from different mice samples (n=5). Statistical analysis was performed using two-tailed Student's *t*-test (**P < 0.01; ****P < 0.0001). (E) Serum bactericidal assay. SBA was performed with *S.* Typhimurium, LT2 strain or the clinical isolates, as indicated in the figure, using serial dilutions of heat-inactivated antisera and guinea pig complement as described under figure 30. Bactericidal activity was expressed as above. C1, C2 and C3 are clinical isolates and bars represent the mean percent of growth reduction ± SEM of quadruplicate samples. The clolor scheme used are described in **Table 8**.

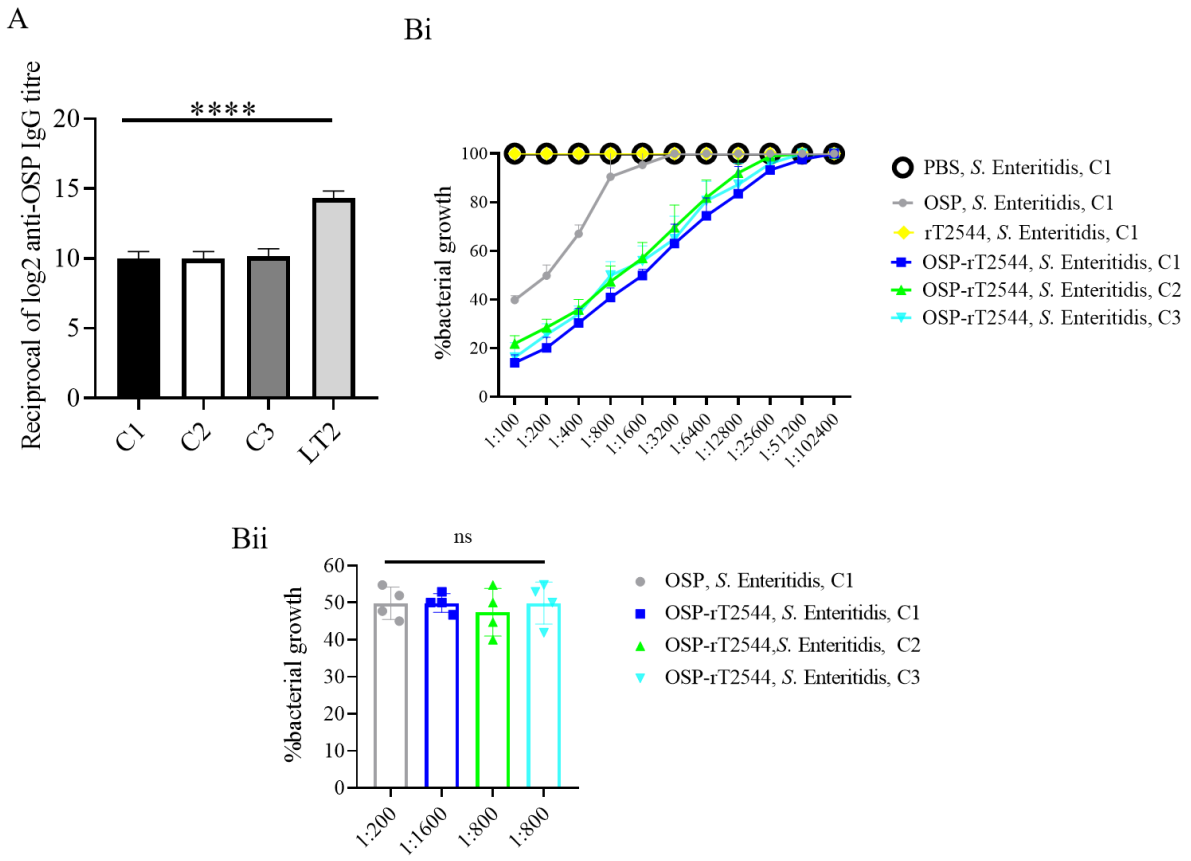

Figure 33. OSP-rT2544 immunization generates cross-protective antibodies against *S.* Enteritidis. (A) OSP was isolated from *S.* Typhimurium (LT2) and different *S.* Enteritidis (clinical isolates, C1-C3) strains and coated on the microtiter plate. Cross-reactive antibody

titer was measured in OSP-rT2544 sera (38d) by ELISA. *S.* Typhimurium (LT2) OSP was used as a positive control. Data represent mean ± SEM values from different mice samples (n=6). Statistical analysis was performed using two-tailed Student's *t*-test (**** P< 0.0001). (B) Serum bactericidal assay. Serial dilutions of heat-inactivated antisera, collected from differentially immunized mice at 38 d of immunization were mixed with 25% guinea pig complement and incubated with the *S.* Enteritidis or clinical isolates as indicated in the figure B i. Bactericidal activity was expressed as the serum dilution at which 50% growth inhibition of the bacteria was noted at T_{180} (3h incubation) compared with T_0. Specific serum dilutions showing 50% growth reduction with individual immunogens are indicated in the figure B ii. C1, C2 and C3 are clinical isolates and bars represent the mean percent of growth reduction ± SEM of quadruplicate samples. Colour scheme used is described in **Table 8**.

4.3.2. OSP-rT2544 candidate vaccine generates functional sIgA response, a hallmark of mucosal immunity

To study the mucosal immune response after OSP-rT2544 immunization, anti-OSP and anti-rT2544 sIgA antibodies were measured in the intestinal washes and fecal samples of the immunized mice and the titers were compared with the serum IgA titers (**Figure 34A)**. Anti-OSP IgA titer was increased four times in the mice immunized with the conjugate OSP-rT2544 compared with the unconjugated OSP (**Figure 34B**). On the other hand, anti-rT2544 IgA titers were comparable for the conjugated and unconjugated vaccine recipients (**Figure 34C**). To study the functionality of intestinal secretory antibodies, inhibition of bacterial motility in soft agar motility assay by intestinal lavage from the immunized mice was performed. Motility was determined by measuring the diameter of the bacterial zones after 10 hours of incubation at 37 °C (**Figure 35 A-E**). Motility inhibition of *S.* Typhi and *S.* Paratyphi A was comparable for OSP-rT2544 and rT2544 immunization. In contrast, intestinal lavage from the mice immunized

with OSP-rT2544 inhibited the motility of *S.* Typhimurium significantly more (~2.5 times) than similar samples collected from OSP-immunized mice. Similar difference was observed between the two immunization groups for soft agar motility of *S.* Enteritidis (33-36% vs 15.4% inhibition). Together these results suggested that OSP-rT2544 induced functional sIgA response in the intestine against both typhoidal and non-typhoidal *Salmonella* strains. [The detailed methodologies were discussed in the materials and method sections **3.2.10.1., 3.2.11.1.** and **3.2.14.**]

A

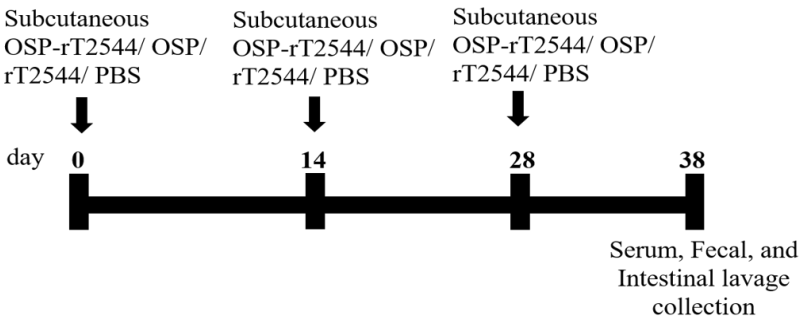

B

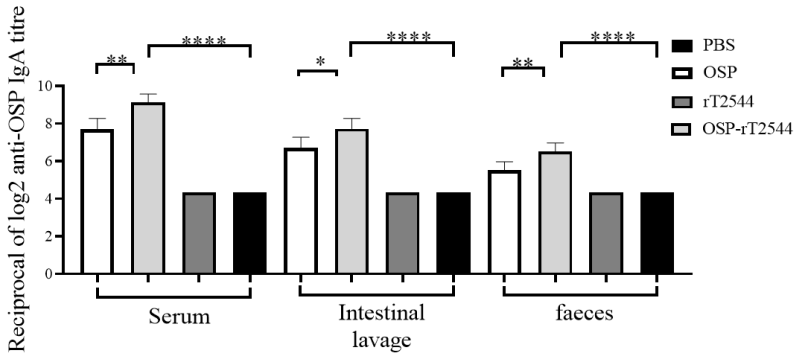

C

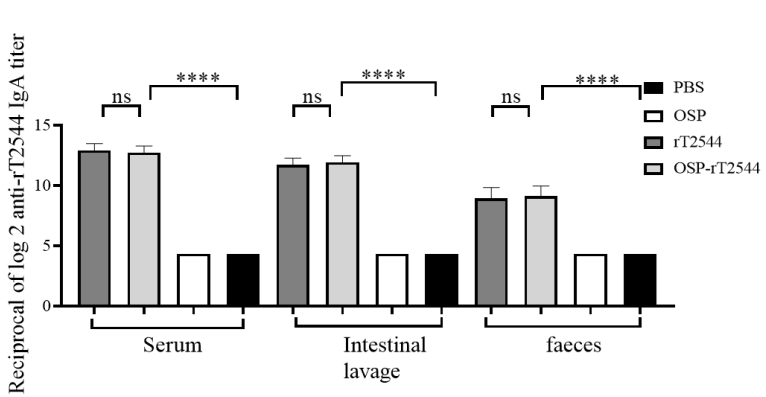

Figure 34. Induction of protective mucosal antibodies by OSP-rT2544 immunization. (A) Schedule of subcutaneous immunization of C57BL/6 mice at days 0, 14, and 28 with vehicle (PBS), conjugate (OSP-rT2544) (8µg of OSP in conjugate), or unconjugated vaccines (OSP (8 µg), rT2544 (24 µg)). Mice were sacrificed on day 38 and samples were collected. (B, C) ELISA showing OSP- and rT2544-specific serum IgA and intestinal sIgA titers in the groups of mice (n=5/ group) after immunization with different antigens. Data represent mean ± SEM values from different mice samples (n=5). Statistical analysis was performed using two-tailed Student's *t*-test (**P < 0.01; ***P < 0.001; ****P < 0.0001).

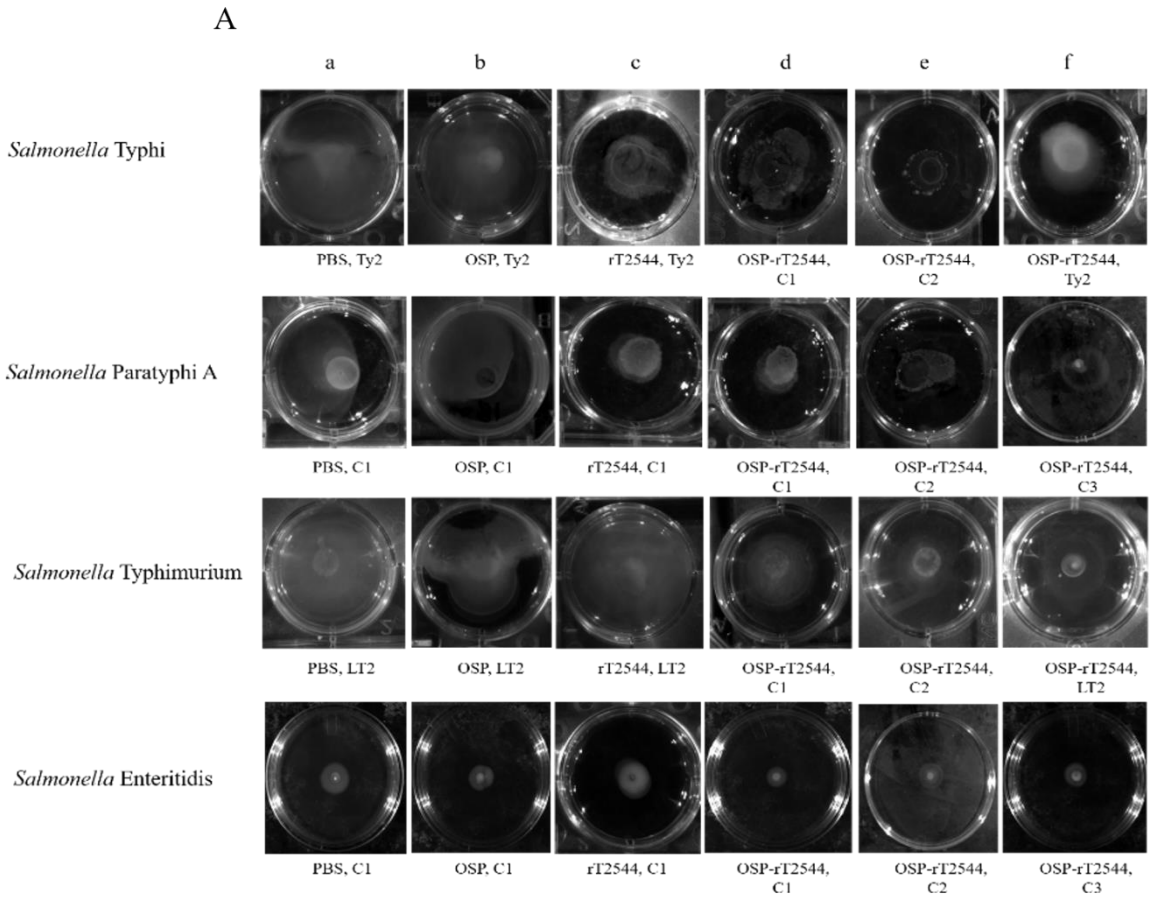

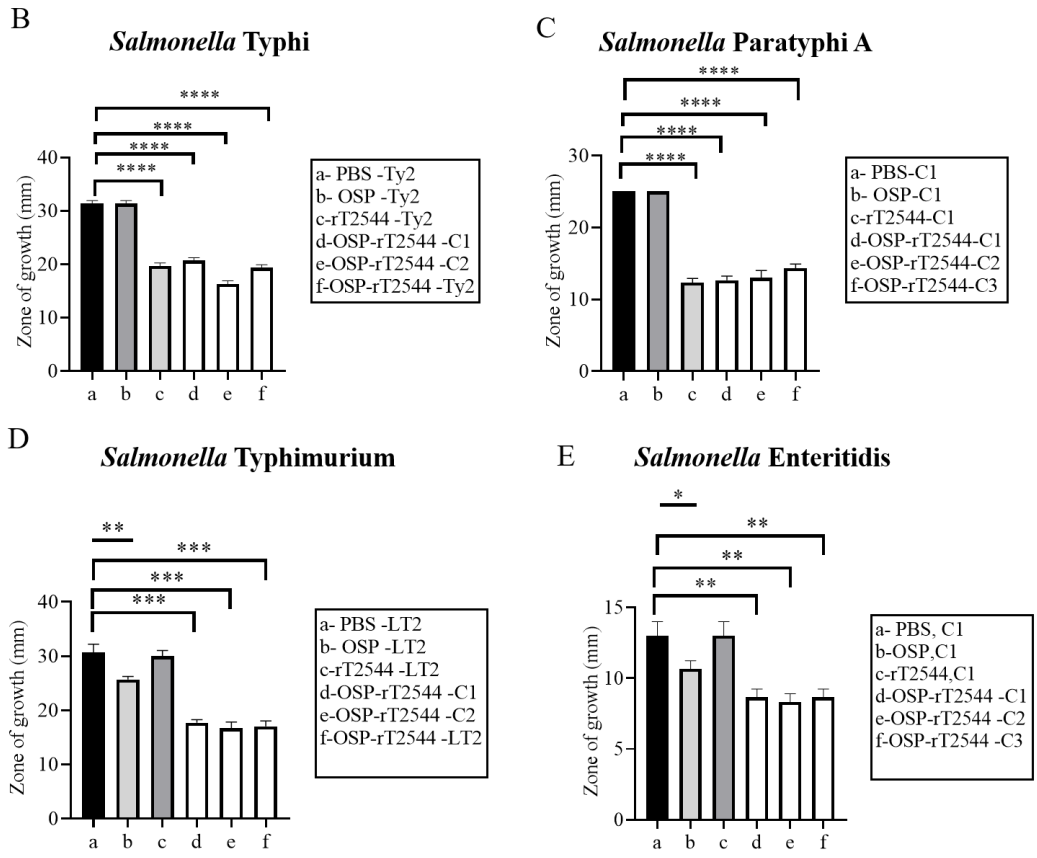

Figure 35. Soft agar motility assay. (A) Bacteria were spotted at the center of the soft agar (LB medium with 0.4 % Bacto agar) containing intestinal wash (5%) from the immunized mice collected on day 38. Bacterial migration from the inoculation point to the periphery of the plate was measured after 10h incubation at 37 °C. Experiments were repeated three times and one representative image from three independent experiments is shown. (B-E) Graphical presentation of the motility assay of Figure 34 A. Experiments were repeated three times and mean (±SEM) of the values from all three experiments were plotted. Statistical analysis was performed using two-tailed Student's *t*-test (**P < 0.01; ***P < 0.001; ****P < 0.0001).

4.3.3. OSP-rT2544 induces both Th1 and Th2 serum cytokine response

Salmonella clearance requires a Th1 response, whereas Th2 cells support the generation of

sIgA and serum antibodies. To determine the serum cytokine response, sera were collected from the OSP-rT2544 immunized C57BL/6 mice on day 38 and cytokine concentrations were measured by ELISA. We found significantly elevated, circulating pro-inflammatory/Th1 (IFNγ, TNF-α) and anti-inflammatory/Th2 (IL-4, IL-10, IL-6) cytokines in OSP-rT2544-immunized mice as opposed to only modest elevation in the comparator immunized groups (**Figure 36 A-E**). This result suggested that OSP-rT2544 immunization induces both Th1 and Th2 cytokine response in serum with the latter being predominant. [The detailed methodologies were discussed in the materials and method sections **3.2.11.3.**]

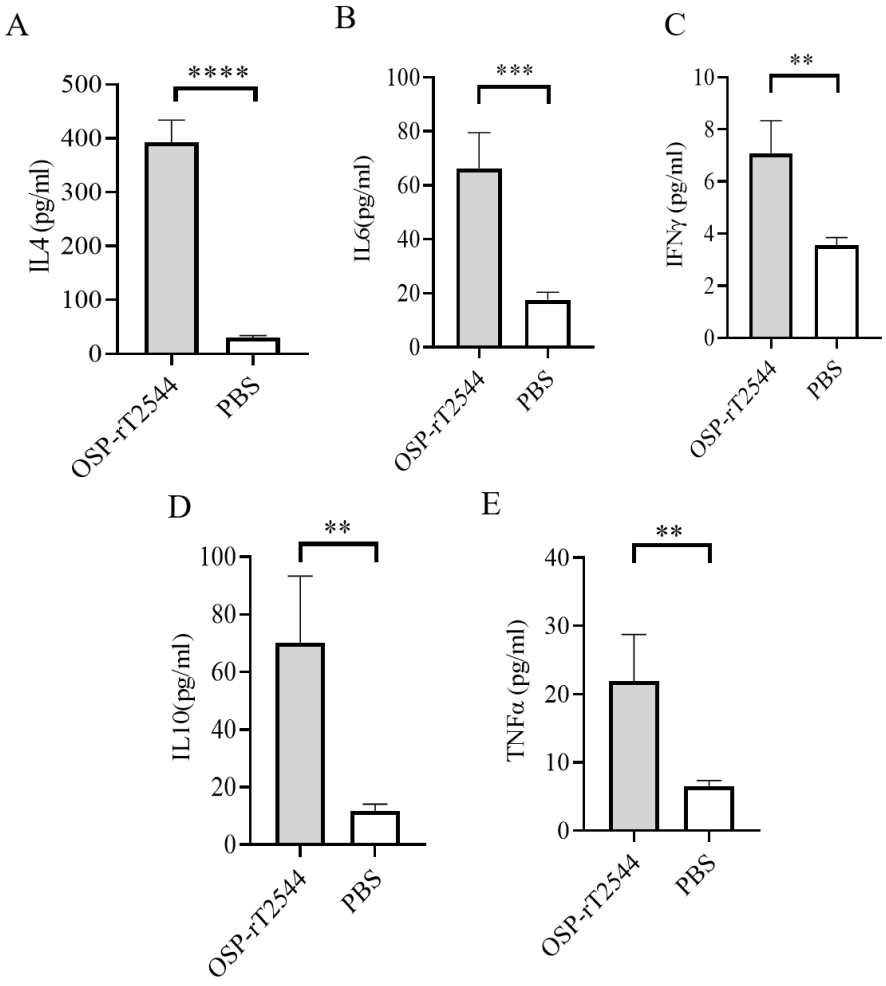

Figure 36. OSP-rT2544 induces both Th1 and Th2 serum cytokine response. C57BL/6 mice were subcutaneously immunized with OSP-rT2544 (8μg of OSP in conjugate) or PBS

(vehicle) on days 0, 14, and 28. Ten days after the last immunization (day 38), sera were collected from the immunized mice and cytokine levels in the serum were measured by ELISA. Briefly, Precoated ninety-six well plates were incubated with serum samples along with biotin-conjugate for 2h at room temperature. After three subsequent washes, plates were further incubated for one hour at room temperature with streptavidin-HRP. Following the addition of the TMB substrate, colour development was evaluated using spectrophotometry at 450 nm. Statistical analysis was performed using two-tailed Student's *t*-test (**P < 0.01; ***P < 0.001; ****P < 0.0001).

4.3.4. Immunization with OSP-rT2544 generates protective memory response

To study antigen-specific memory T cells, bone marrow derived dendritic cells (BMDCs) were isolated from the naïve C57BL/6 mice and pulsed in vitro with OSP or OSP-rT2544 antigen for 24h. Antigen-pulsed BMDCs were then co-cultured with the experimental mice splenocytes containing $CD4^+$ T cells. IFNγ release in the co-culture supernatants was estimated to be >10 folds higher for the splenocytes from OSP-rT2544 immunized mice compared with the animals that received OSP alone or left unimmunized (13.5 pg/ml), suggesting significant augmentation of T cell memory response by rT2544 when conjugated to OSP (**Figure 37A**). To determine memory T cell subsets, co-cultured $CD4^+$ T cells, as mentioned above were analyzed by flow cytometry after staining for the surface expression of 'Cluster of differentiation' (CD) markers ($CD4^+CD62L^{low}CD44^{hi}$). Cell subset analysis showed that augmented memory response was largely contributed by the effector memory T cells ($CD62L^{low}CD44^{high}$) (**Figure 37B**). Further, to analyze memory B cell response, a booster dose was administered to the immunized mice on day 110 of the first immunization and anti-OSP and anti-rT2544 serum antibodies were measured ten days later. A significantly higher

secondary antibody response (day 120) compared with the primary response (day 38) was observed (four times for anti-OSP, and eight times for anti-rT2544 antibodies) (**Figure 37 C, D**), suggesting differentiation of memory B cells into plasma cells, producing IgG at the latter time point. Given that the avidity of antibodies for the secondary response is higher than the primary response, anti-rT2544 and anti-OSP IgG immune complexes collected at days 38 and 120 were washed (3 times) with PBS-T, containing 6M urea before the addition of HRP-conjugated secondary antibodies. The avidity index was calculated by multiplying the ratio of the absorbances of the wells that were washed with and without 6M urea-containing buffer by 100. The result showed significantly high avidity indices (60-62%) of the secondary antibodies after booster immunization compared with the primary immunization (18-22%), suggesting a strong memory B cell response (**Figure 37 E, F**). To corroborate functional activities of the higher avidity antibodies, we performed serum bactericidal assay (SBA) with these antibodies and different *Salmonella* strains (**Table 13)**. The results showed 50% growth inhibition at dilutions of secondary OSP-rT2544 antisera compared with the dilutions of the primary antisera as follows, 1:3200 vs. 1:1600 for *S.* Typhi Ty2, 1:25600 vs. 1:12800 for *S.* Paratyphi A, 1:12800 vs. 1:6400 for *S.* Typhimurium LT2, 1:3200 vs. 1:1600 for *S.* Enteritidis. The result suggested that inhibition dilution of the secondary OSP-rT2544 antisera was significantly higher than inhibition accompanied by antisera collected on day 38 (**Figure. 37 G, Table 12**). These results suggested that immunization with OSP-rT2544 might elicit potent, long-lived protective immunity against *Salmonella* infection. [The detailed methodologies were discussed in the materials and method sections **3.2.11.3., 3.2.16., 3.2.11.2., 3.2.17. and 3.2.13.**]

A

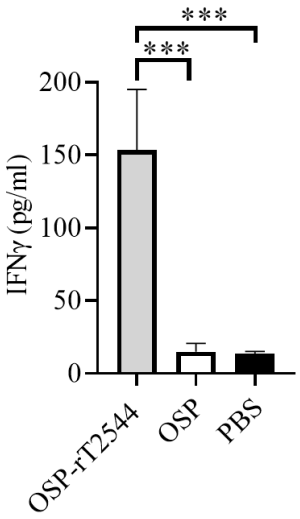
***
***
200
150
100
50
0
IFNγ (pg/ml)
OSP-rT2544
OSP
PBS

B

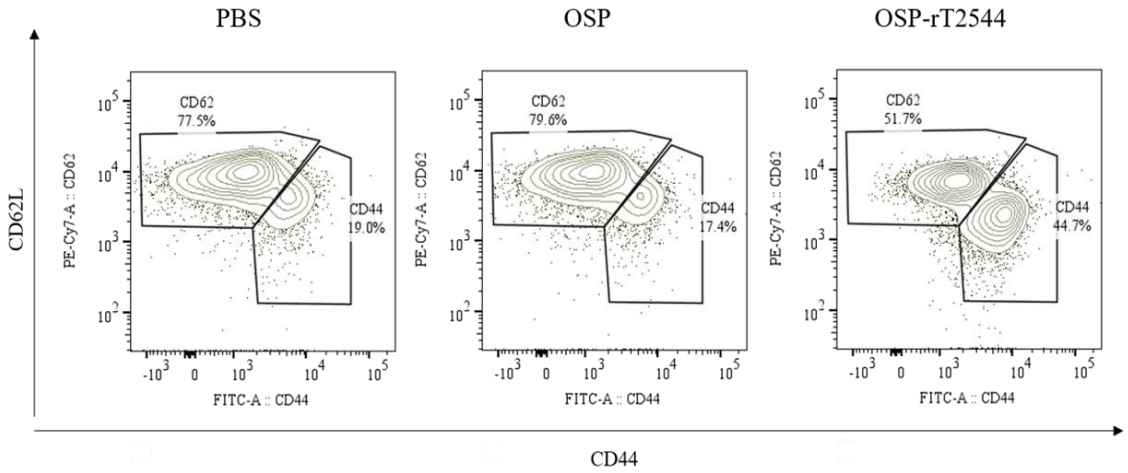
PBS
OSP
OSP-rT2544
CD62L
CD44
PE-Cy7-A :: CD62
FITC-A :: CD44
CD62
77.5%
CD44
19.0%
CD62
79.6%
CD44
17.4%
CD62
51.7%
CD44
44.7%

C

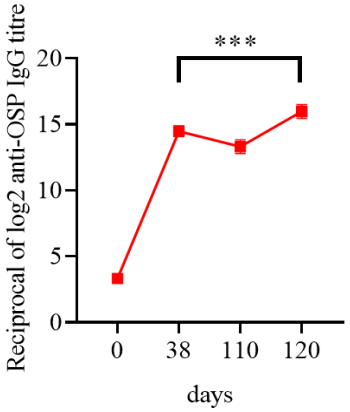
***
Reciprocal of log2 anti-OSP IgG titre
20
15
10
5
0
0
38
110
120
days

D

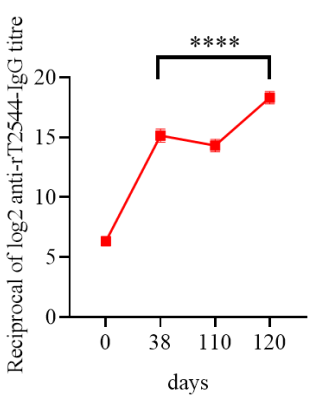
****
Reciprocal of log2 anti-rT2544 IgG titre
20
15
10
5
0
0
38
110
120
days

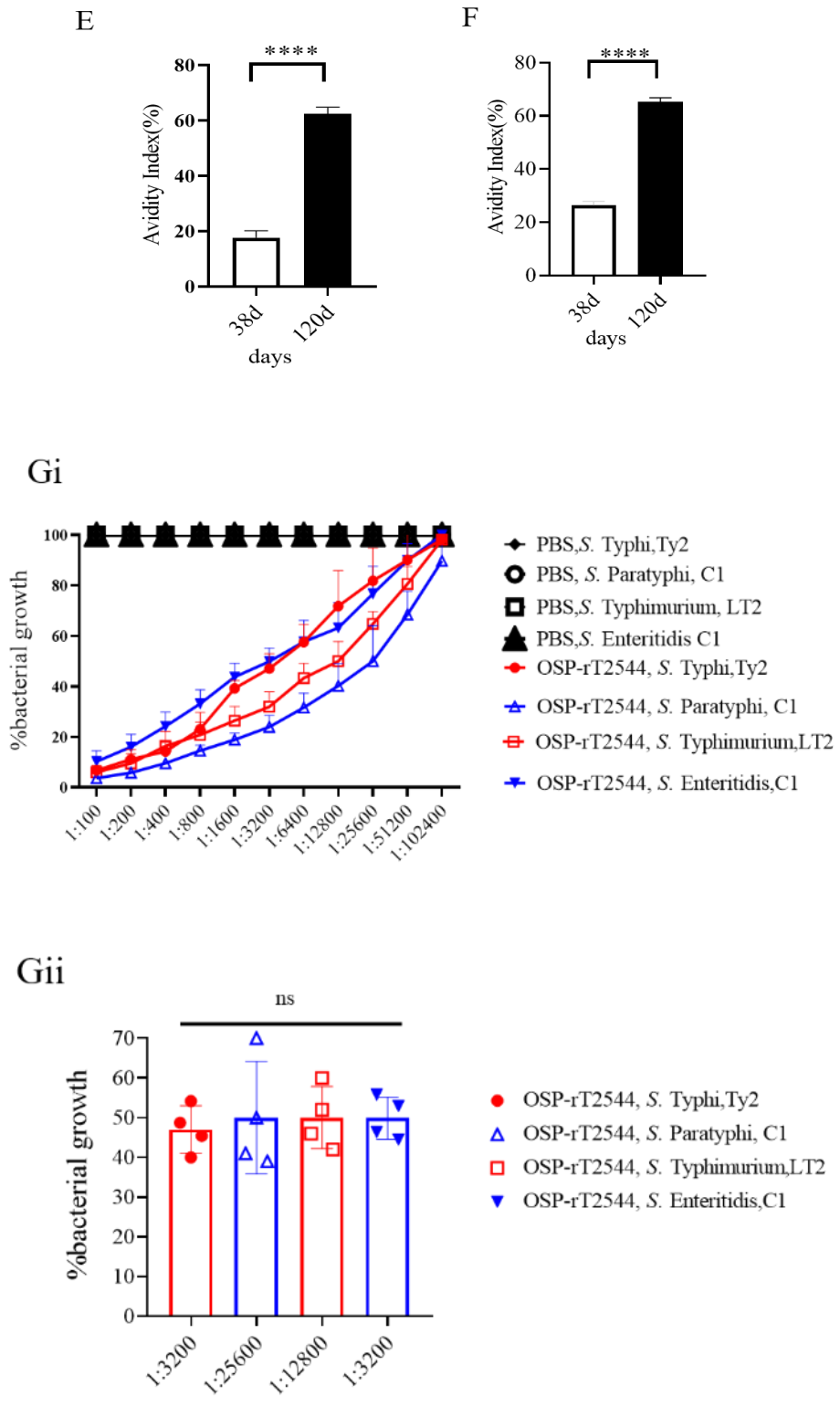

Figure 37. Induction of protective memory response following OSP-rT2544 immunization. (A) C57BL/6 mice were subcutaneously immunized with the vehicle (PBS),

conjugate (OSP-rT2544) (8 µg of OSP or 24 µg of rT2544 in conjugate), or unconjugated vaccines (OSP 8 µg, rT2544 24 µg)). Antigen-primed memory CD4+ T cells were isolated from the splenocytes of the mice 120 days of the start of the immunization. To evaluate the memory T cells response, cells were converted to effector T cells by presenting the respective antigens to them in association with MHC Class II. To this end, bone marrow derived dendritic cells (BMDCs), isolated from the naïve C57BL/6 mice were pulsed with OSP or OSP-rT2544 for 24h, followed by co-culturing of the cells with the memory T cells. Memory response was analyzed by the quantification of IFNγ released in the co-culture supernatants using ELISA. Statistical analysis was performed using two-tailed Student's *t*-test (**P < 0.01; ***P < 0.001; ****P < 0.0001). Data represents mean (±SEM) of four independent experiments. (B) $CD4^+$ T cells, co-cultured with antigen-pulsed BMDCs for 24h, as mentioned under 'Figure 37 A', were analyzed by flow cytometry after staining for the surface expression of 'Cluster of differentiation' (CD) markers for T-effector memory cell determination ($CD4^+CD62L^{low}$ $CD44^{hi}$). Representative images from one out of four experiments are shown. (C, D) C57BL/6 mice were subcutaneously immunized on days 0, 14, and 28 with OSP-rT2544 (8µg of OSP and 24 µg of rT2544 in conjugate) and a booster was given with the same antigen on day 110 (C) OSP and (D) rT2544-specific serum IgG titers were measured by ELISA at the indicated time points. Data represent mean ± SEM values from different mice samples (n=6). Statistical analysis was performed using two-tailed Student's *t*-test (***P < 0.001; ****P < 0.0001). (E, F) Antibody avidity assay. Anti-rT2544 (E) and anti-OSP (F) avidity index were determined in the OSP-rT2544 serum (diluted 1:100 in PBS-T), collected at the indicated time points after washing the immune complex with 6M urea buffer by ELISA. The avidity index was calculated by multiplying the ratio of the absorbances of the wells that were washed with and without urea-containing buffer by 100. Data represent mean ± SEM values from different mice samples (n=3). Statistical analysis was performed using two-tailed Student's *t*-test (****P < 0.0001).

(G) Serum bactericidal assay. Serial dilutions of heat-inactivated antisera, collected from differentially immunized mice at 120 d of immunization were mixed with 25% guinea pig complement and incubated with the *S.* Typhi, *S.* Paratyphi A, *S.* Typhimurium, LT2 and *S.* Enteritidis as indicated in the figure G i. Bactericidal activity was expressed as the serum dilution at which 50% growth inhibition of the bacteria was noted at T_{180} (3h incubation) compared with T_0. Immunogens that have a 50% growth reduction at a specific serum dilution are indicated in the figure G ii. Bars represent the percent mean (± SEM) of growth reduction of quadruplicate samples. Colour scheme used described in table 8.

Table 13. SBA titre using 120th day antisera (OSP-rT2544)

antisera	SBA titre (growth reduction up to 50%)	Bacterial strain
OSP-rT2544	1:3200	*S.* Typhi, Ty2
	1:25600	*S.* Paratyphi Clinical isolate 1
	1:12800	*S.* Typhimurium LT2
	1:3200	*S.* Enteritidis Clinical isolate 1

PBS	No 50% reduction (50%<)	*S.* Typhi, Ty2
	No 50% reduction (50%<)	*S.* Paratyphi Clinical isolate 1
	No 50% reduction (50%<)	*S.* Typhimurium LT2
	No 50% reduction (50%<)	*S.* Enteritidis Clinical isolate 1

4.3.5. Single dose immunization with Vi-rT2544 generates persistently higher antibody response than Vi-TT

We had earlier reported protective humoral response in mice against *S.* Typhi upon subcutaneous immunization with recombinant T2544 in the conjugate (450). To check if rT2544 present in this conjugate vaccine (Vi-rT2544) is equally immunogenic, serum antibody endpoint titers (The reciprocal of the titer (1/Y) at which the absorbance of the immune sera was the same as the control (PBS immunized sera)) were measured by ELISA up to 120 days after the first immunization dose, immunized subcutaneously and intramuscularly with Vi-rT2544, Vi-TT or vehicle (PBS). The results showed two-fold and four-fold increased anti-Vi IgG responses at the above time points, following subcutaneous and intramuscular vaccination with Vi-rT2544 compared to Vi-TT (**Figure 38 A, B**). However, no differences were observed between anti-Vi IgG titres of two Vi-rT2544 immunization routes (**Figure 39 A**). In addition to this, anti-rT2544 antibody in Vi-rT2544 conjugate was found similar to unconjugated rT2544

(**Figure 39 B**), suggesting no changes in the rT2544 specific immune response after conjugation with Vi. Markedly raised titers of Vi-specific serum IgG1 and IgG2a antibodies were observed in mice immunized with Vi-rT2544, as compared with the Vi-TT or PBS immunized mice, indicating induction of both Th1 and Th2 type responses; however, IgG1 and IgG2a was the predominant isotype following SC and IM immunization (**Figure 38 C, D**).

To study the mucosal immune response after Vi-rT2544 immunization, anti-Vi sIgA antibodies were measured in the serum, intestinal washes and fecal samples of the immunized mice. Results showed that anti-Vi IgA titer was increased two-fold in the intestinal lavage, serum and faeces in the groups of mice immunized subcutaneously and two-fold in intestinal lavage, faeces and four-fold in serum in the Vi-rT2544 group compared with the Vi-TT group (**Figure 38 E, F)**. However, no differences in anti-Vi IgA titer were observed between Subcutaneous and intramuscular immunized Vi-rT2544 group (**Figure 39 C**). All the above results indicated that Vi-rT2544 immunization induces significant higher humoral and mucosal antibody responses compared to Vi-TT. [The detailed methodologies were discussed in the materials and method sections **3.2.10.1.** and **3.2.11.1.**]

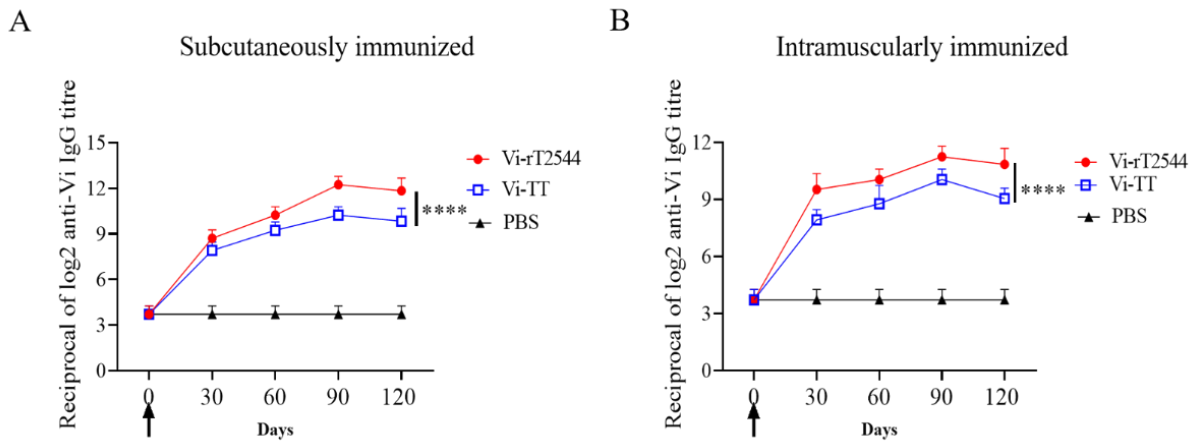

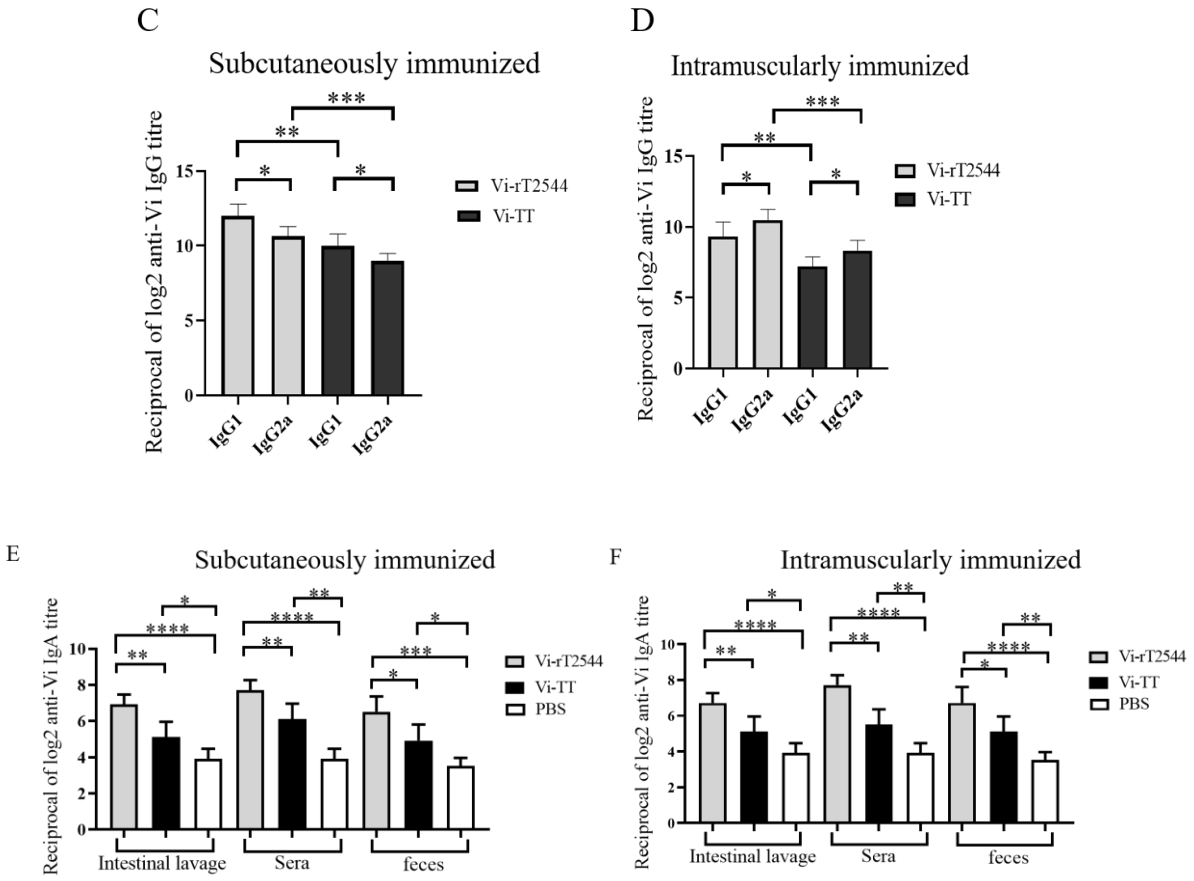

Figure 38. Parenteral immunization (Single dose) with Vi-T2544 elicit robust antibody responses compared to Vi-TT. BALB/c mice were subcutaneously and intramuscularly immunized on day 0 with Vi-T2544 or Vi-TT (25µg of Vi in conjugate). (A-B) Time kinetics of antigen-specific total IgG in the mouse serum as measured by ELISA in BALB/c mice. Data represent mean ± SEM values from different mice samples (n=5). X-axis indicate the time points after the start of the immunization when samples were collected. Statistical significance between the titer values from Vi-T2544 and Vi-TT vaccine recipients is shown. Statistical analysis was performed using two-way ANOVA and Tukey's post-test for multiple comparisons. ****P < 0.0001. Arrows indicates the immunization time points. (C, D) Vi-specific serum IgG isotypes measured by ELISA at day 120. Data represent mean ± SEM values from different mice samples (n=6). Statistical analysis was performed using two-tailed Student's *t*-test. *P < 0.05, **P < 0.01 ; ***P < 0.001. (E, F) ELISA showing Vi-specific serum

IgA and intestinal sIgA titers in the groups of BALB/c (n=5) mice. Immunized mice were sacrificed on day 120 of first immunization and samples were collected. Data represents mean ± SEM values from different mice samples (n=5). Statistical analysis was performed using two-tailed Student's *t*-test (*P < 0.05 ; **P < 0.01; ***P < 0.001; ****P < 0.0001).

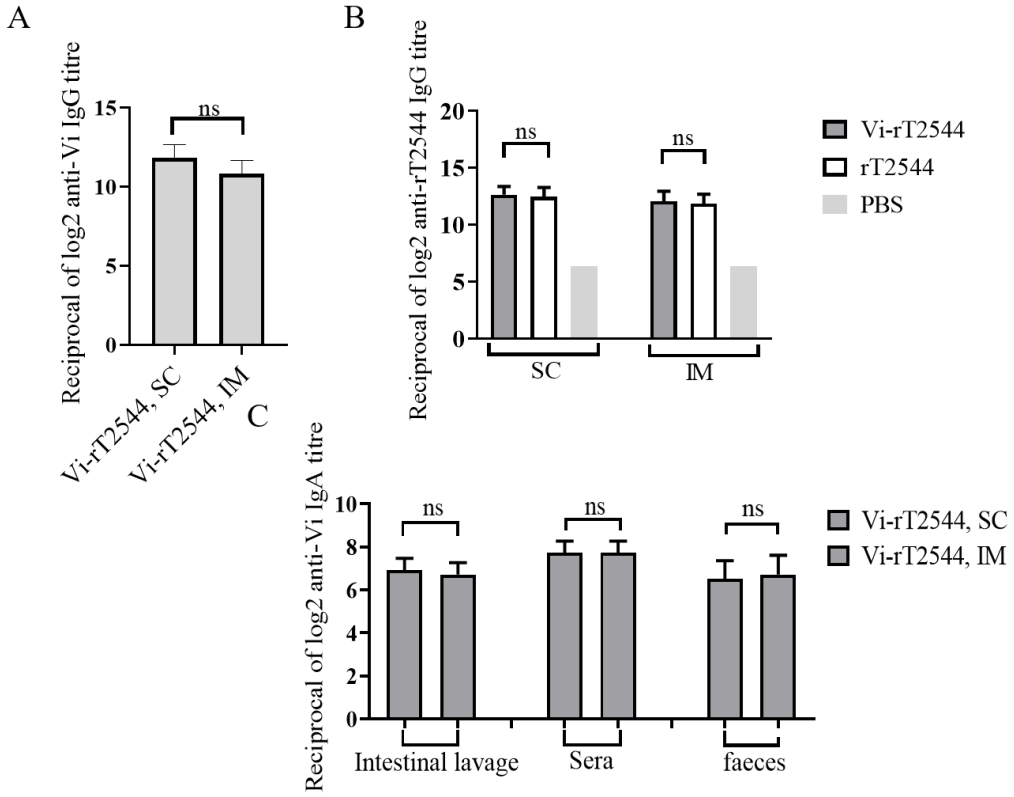

Figure 39. Comparative immunization study between different immunization routes following single immunization with Vi-T2544 or rT2544. BALB/c mice were subcutaneously and intramuscularly immunized on day 0 with Vi-T2544 or rT2544 (25µg of Vi or 29 µg of rT2544 in conjugate). (A) Vi-specific total IgG in the mouse serum was measured by ELISA at day 120 in Vi-T2544 immunized mice. Data represent mean ± SEM values from different mice samples (n=5). (B) rT2544-specific serum IgG in the mouse serum measured by ELISA at day 120. Data represent mean ± SEM values from different mice samples (n=5). (C) ELISA showing Vi-specific IgA titers in the groups of Vi-rT2544 immunized mice. Immunized mice were sacrificed on day 120 of first immunization and

samples were collected. Data represents mean ± SEM values from different mice samples (n=5). Abbreviations; SC- subcutaneous; IM- intramuscular.

4.3.6. Single Vi-rT2544 immunization induces both Th1 and Th2 serum cytokine response

To evaluate the impact of Vi-rT2544 and Vi-TT formulations on cytokine expression, various cytokines were assessed. Four different cytokines, namely, Interleukin (IL) 4, IL 10, and Interferon (IFN)-γ were targeted for measurement due to their roles in the maturation of plasma cell and production of antibody. To determine the serum cytokine response, sera were collected from the Vi-rT2544 immunized BALB/c mice on day 122 and cytokine concentrations were measured by ELISA. We found significantly elevated, circulating pro-inflammatory/Th1 (IFNγ) and anti-inflammatory/Th2 (IL-4 and IL-10) cytokines in Vi-rT2544-immunized mice compared to Vi-TT immunized group (**Figure 40 A-F**). This result indicating the induction of both Th1 and Th2 type responses; however, Th2 and Th1 was the predominant isotype following subcutaneous (SC) and intramuscular (IM) immunization. [The detailed methodologies were discussed in the materials and method sections **3.2.11.3.**]

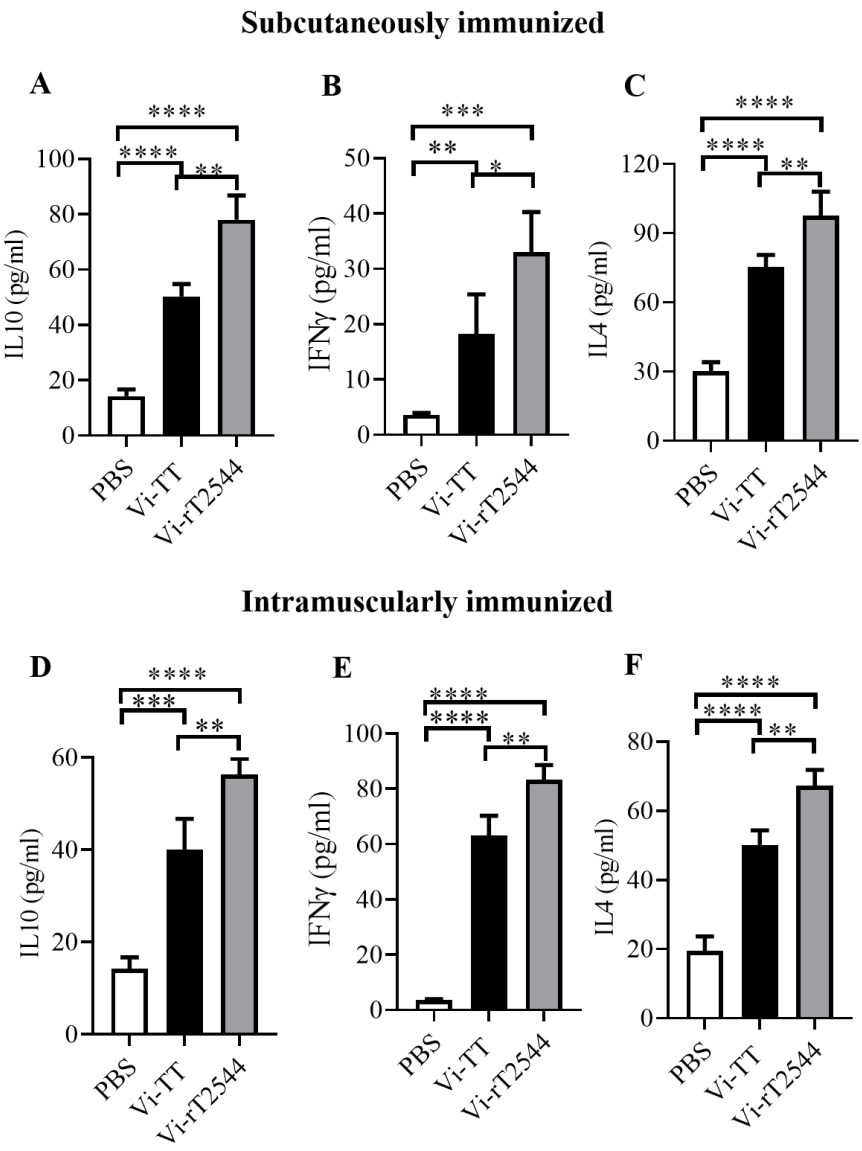

Figure 40. Single Vi-rT2544 immunization induces both Th1 and Th2 serum cytokine response. BALB/c mice were subcutaneously and intramuscularly immunized with on day 0 with Vi-T2544 or Vi-TT (25µg of Vi in conjugate) as described in figure 12. Sera were collected from the immunized mice on day 120 and cytokine levels in the serum were measured by ELISA. Briefly, Precoated ninety-six well plates were incubated with serum samples along with biotin-conjugate for 2h at room temperature. After three subsequent washes, plates were further incubated for one hour at room temperature with streptavidin-HRP. Following the addition of the TMB substrate, colour development was evaluated using spectrophotometry at

450 nm. Statistical analysis was performed using two-tailed Student's *t*-test (*P < 0.05; **P < 0.01; ***P < 0.001; ****P < 0.0001).

4.3.7. Single dose immunization with Vi-rT2544 generates greater magnitude of memory response than Vi-TT

To study antigen-specific memory T cells following single immunization dose, $CD4^+$ T cells isolated form splenocytes (on day 172) of immunized mice co-cultured with antigen-pulsed bone marrow-derived dendritic cells (BMDCs) as described above. IFNγ release in the co-culture supernatants was estimated to be >1.2 folds (SC) and >1.4 folds (IM) higher for the splenocytes from Vi-rT2544 immunized mice compared with the animals that received Vi-TT, suggesting significant augmentation of T cell memory response by rT2544 when conjugated to Vi (**Figure 41 A, E**). To determine memory T cell subsets, co-cultured $CD4^+$ T cells, as mentioned above were analyzed by flow cytometry after staining for the CD markers ($CD4^+CD62L^{low}CD44^{hi}$). Cell subset analysis showed that Vi-rT2544 augmented 10.8 % (SC) and 14.1% (IM) higher memory response than Vi-TT was largely contributed by the effector memory T cells ($CD62L^{low}CD44^{high}$) (**Figure 41 B, F**). Further, to analyze memory B cell response, a booster dose was administered to the immunized mice on day 162 of the first immunization, and anti-Vi serum antibodies were measured ten days later. A significantly higher secondary anti-Vi antibody response on day 172 compared with day 120 was observed (SC, Vi-rT2544, 4 times, Vi-TT, 2 times; IM, Vi-rT2544, 4 times, Vi-TT, 2 times). However, the induction of Vi-specific secondary antibodies (day 172) were comparatively higher in Vi-rT2544 (for SC and IM, 8 times higher) group compared to Vi-TT immunized group (**Figure 41 C, G**), suggesting differentiation of higher memory B cells into plasma cells, producing IgG at the latter time point in the former group.

The avidity index was calculated as described above. The result showed significantly high avidity indices of the secondary antibodies (SC, Vi-rT2544, 57%; Vi-TT, 43.7%; IM, Vi-rT2544, 39.6%; Vi-TT, 27.6%) after booster immunization compared with the primary immunization (SC, Vi-rT2544, 32%; Vi-TT, 22.4%; IM, Vi-rT2544, 22.5%; Vi-TT, 17.1%), suggesting a strong memory B cell response (**Figure 41 D, H**). The result also indicated that Vi-rT2544 induces significantly higher secondary avidity indices (SC, Vi-rT2544, 1.3-fold and IM, Vi-rT2544, 1.4-fold) than Vi-TT. [The detailed methodologies were discussed in the materials and method sections **3.2.11.3., 3.2.16., 3.2.17.** and **3.2.11.2.**]

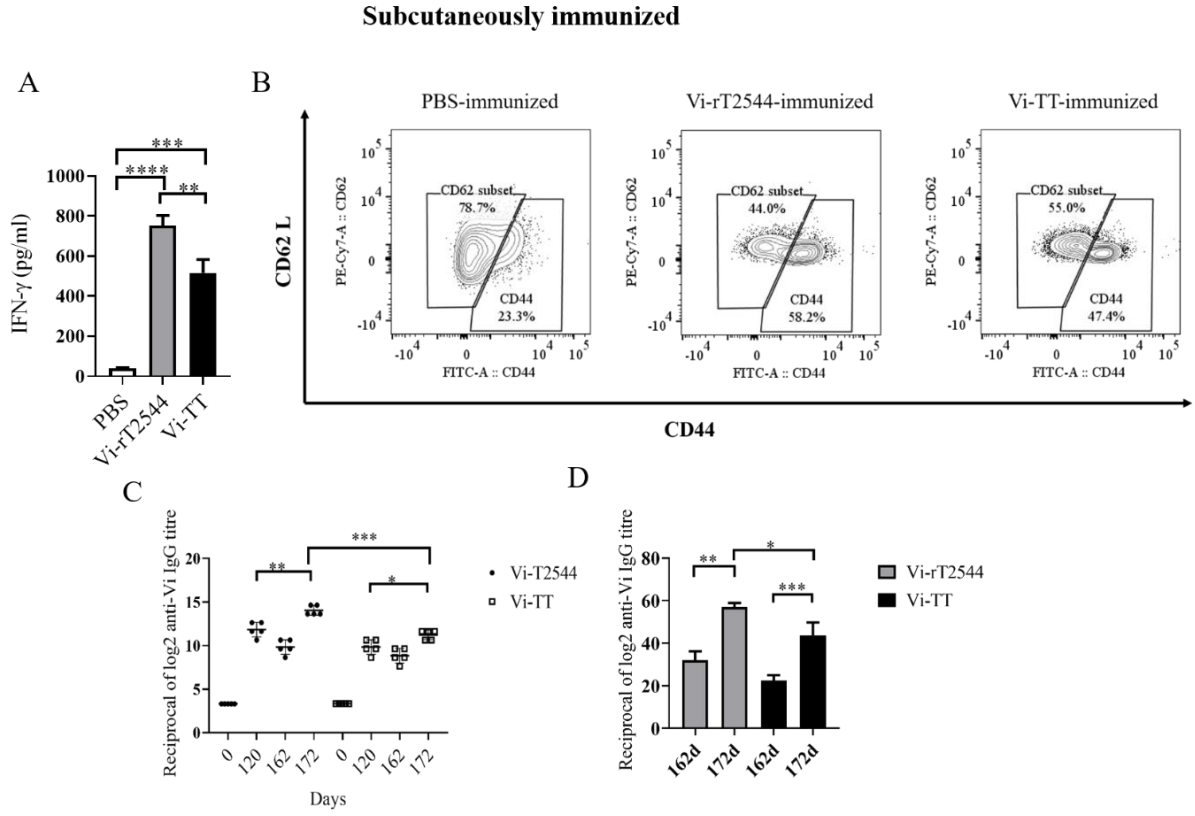

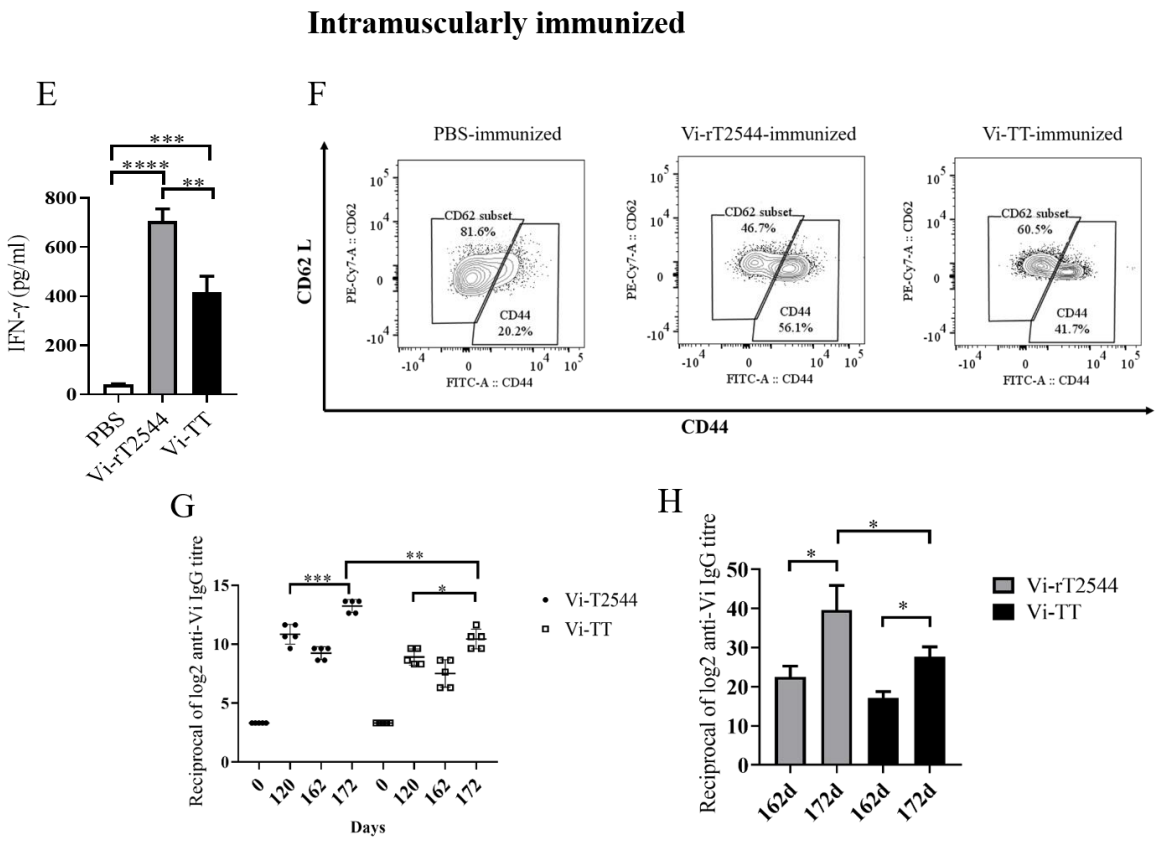

Figure 41. Induction of memory response following single Vi-rT2544 immunization. (A, E) BALB/c mice were subcutaneously and intramuscularly immunized on day 0 with Vi-T2544 or Vi-TT (25µg of Vi in conjugate). Antigen-primed memory CD4+ T cells were isolated from the splenocytes of the mice 172 days of the start of the immunization. To evaluate the memory T cells response, cells were converted to effector T cells by presenting the respective antigens to them in association with MHC Class II. To this end, bone marrow derived dendritic cells (BMDCs), isolated from the naïve BALB/c mice were pulsed with Vi-T2544 or Vi-TT for 48h, followed by co-culturing of the cells with the memory T cells. Memory response was analyzed by the quantification of IFNγ released in the co-culture supernatants using ELISA. Statistical analysis was performed using two-tailed Student's t-test (**P < 0.01 ; ***P < 0.001; ****P < 0.0001). Data represents mean (±SEM) of three independent experiments. (B, F) CD4+ T cells, co-cultured with antigen-pulsed BMDCs for 48h, as mentioned under 'Figure 41 A, E', were analyzed by flow cytometry after staining for the surface expression of 'Cluster of

differentiation' (CD) markers for T-effector memory cell determination (CD4+CD62Llow CD44hi). Representative images from one out of three experiments are shown. (C, G) BALB/c mice were subcutaneously and intramuscularly immunized on days 0 with Vi-T2544 or Vi-TT (25µg of Vi in conjugate) and a booster was given with the same antigen on day 162. Vi specific serum IgG titers were measured by ELISA at the indicated time points. Data represent mean ± SEM values from different mice samples (n=5). Statistical analysis was performed using two-tailed Student's t-test (*P < 0.05 ; **P < 0.01; ***P < 0.001; ****P < 0.0001). (D, H) Antibody avidity assay. Anti-Vi avidity index were determined in the Vi-rT2544 and Vi TT serum (diluted 1:100 in PBS-T), collected at the indicated time points after washing the immune complex with 6M urea buffer by ELISA. The avidity index was calculated by multiplying the ratio of the absorbances of the wells that were washed with and without urea containing buffer by 100. Data represent mean ± SEM values from different mice samples (n=3). Statistical analysis was performed using two-tailed Student's t-test (*P < 0.05 ; **P < 0.01; ***P < 0.001).

4.3.8. Single immunization with Vi-rT2544 elicited protective memory response higher than Vi-TT

To determine the functional activities of the immune sera, bactericidal assay was performed by incubating *S.* Typhi and *S.* Paratyphi A with heat-inactivated, serially-diluted sera collected from the different immunized mice, supplemented with guinea pig complement. The results showed 50% growth inhibition at dilutions of secondary Vi-rT2544 antisera (day 172) compared with the dilutions of the primary antisera (day 120) as follows, 1:1600 vs. 1:800 (SC) and 1:800 vs 1: 1400 (IM) for *S.* Typhi Ty2, 1:12800 vs. 1:6400 (SC) and 1:6400 vs 1:3200 (IM) for *S.* Paratyphi A; secondary Vi-TT antisera compared with the dilutions of the primary antisera as follows, 1:400 vs 1:200 (SC) and 1:200 vs 1:100 (IM) for *S.* Typhi (**Figure 42 A-**

B). However, no growth inhibition was observed for *S.* Paratyphi A using Vi-TT sera. The result suggested that inhibition dilution of the secondary Vi-rT2544 antisera (day 172) was significantly higher than inhibition accompanied by antisera collected on day 120 and also higher than the Vi-TT. These results also suggested that single-dose immunization with Vi-rT2544 elicits long-lived protective memory antibodies with higher bactericidal activity against both *Salmonella* Typhi and *Salmonella* Paratyphi A infection. [The detailed methodologies were discussed in the materials and method sections **3.2.13.**]

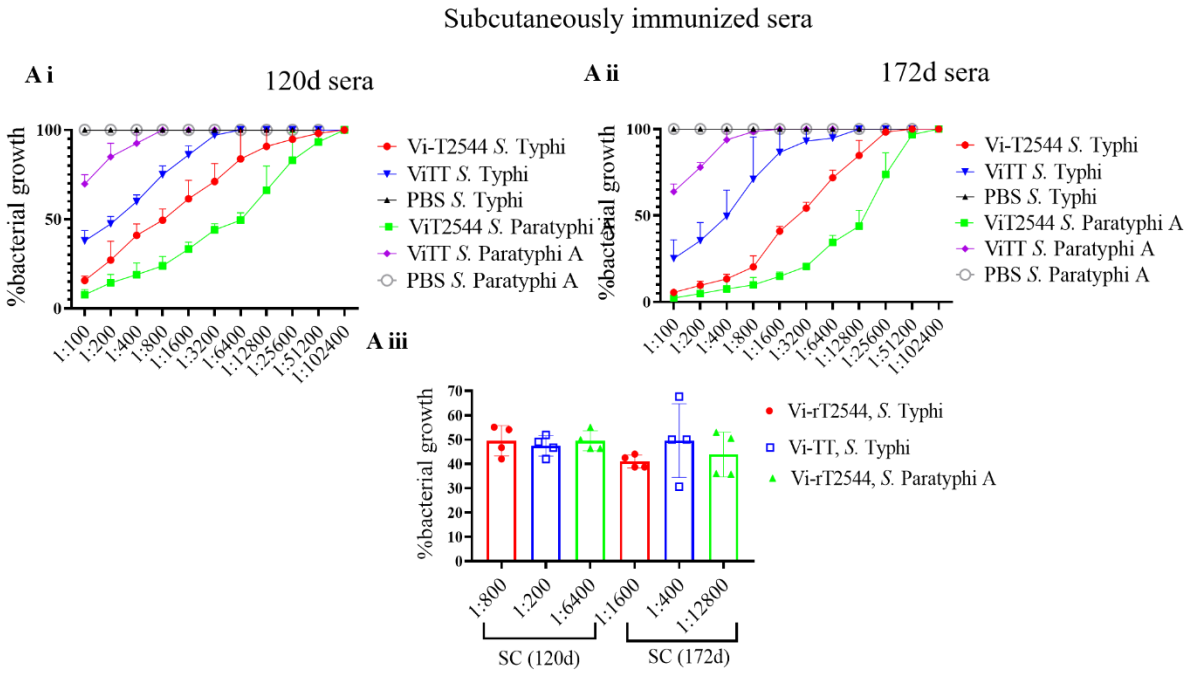

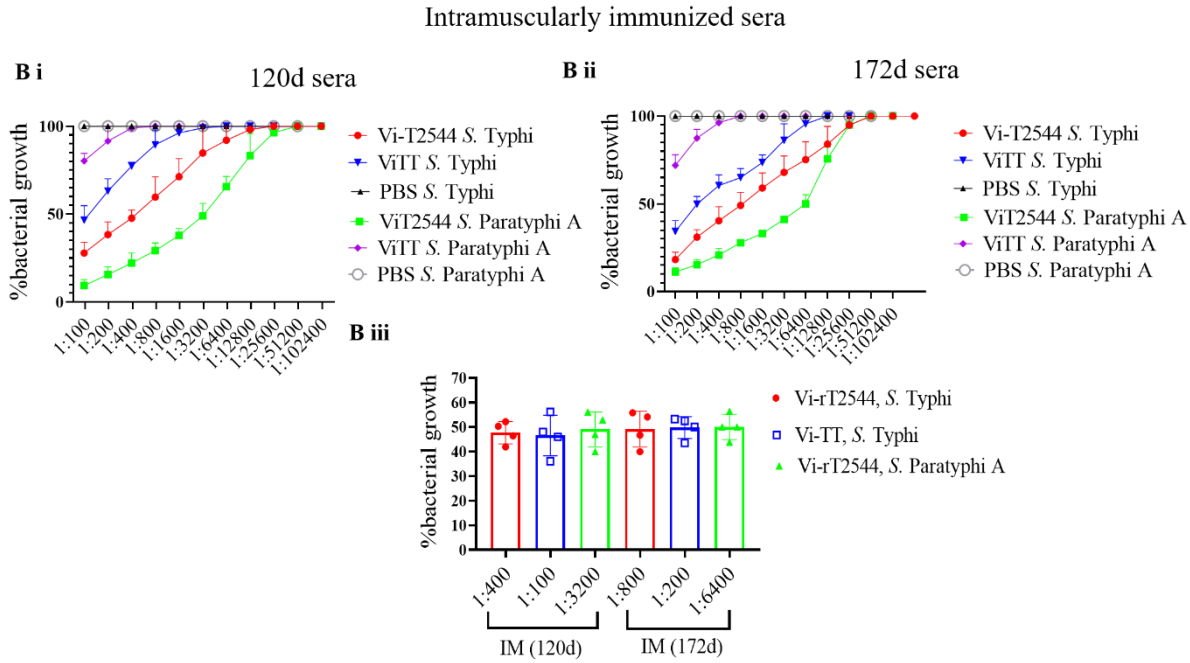

Figure 42. Single immunization with Vi-rT2544 elicited functional antibodies with higher bactericidal activity compared to Vi-TT. Serum bactericidal assay. BALB/c mice were subcutaneously and intramuscularly immunized on day 0 with Vi-T2544 or Vi-TT (25µg of Vi in conjugate). A booster dose was administered to the immunized mice on day 162 of the first immunization. Serial dilutions of heat-inactivated antisera, collected from differentially immunized mice at days 120 and 172 of immunization were mixed with 25% guinea pig complement and incubated with the *S.* Typhi and *S.* Paratyphi A. (A i-A ii, B i- B ii) Bactericidal activity was expressed as the serum dilution at which 50% growth inhibition of the bacteria was noted at T_{180} (3h incubation) compared with T_0. (A iii, B iii) Bactericidal activity was expressed as the serum dilution at which 50% growth inhibition of the bacteria was noted. Bars represent the percent mean (± SEM) of growth reduction of quadruplicate samples.

4.3.9. IpaB in the chimeric vaccine candidate functions as an adjuvant to T2544 to improve the serum and mucosal antibody response

Analysis of serum antibody endpoint titers showed that immunization with rIpaB and rIpaB-T2544 induced similar magnitudes of the IpaB-specific IgG, while T2544-specific IgG titers were significantly higher for the chimeric vaccine (**Figure 43 Ai-Aii).** The IgG isotypes comprised of IgG1 and IgG2a, indicating induction of both type 1 and type 2 responses, although latter was predominant (**Figure 43 Bi-Bii).** Serum and intestinal secretory IgA titers followed the same pattern as serum IgG, with identical anti-IpaB titers for rIpaB and rIpaB-T2544 immunizations, but significantly higher anti-T2544 IgA titers for the chimeric-protein vaccine (**Figure 43 Ci-Cii**). Collectively these results suggested that rIpaB-T2544 was strongly immunogenic and IpaB acted as an immune adjuvant to T2544, significantly boosting the antibody titers in the serum and intestinal secretions. [The detailed methodologies were discussed in the materials and method sections **3.2.10.1.** and **3.2.11.1.**]

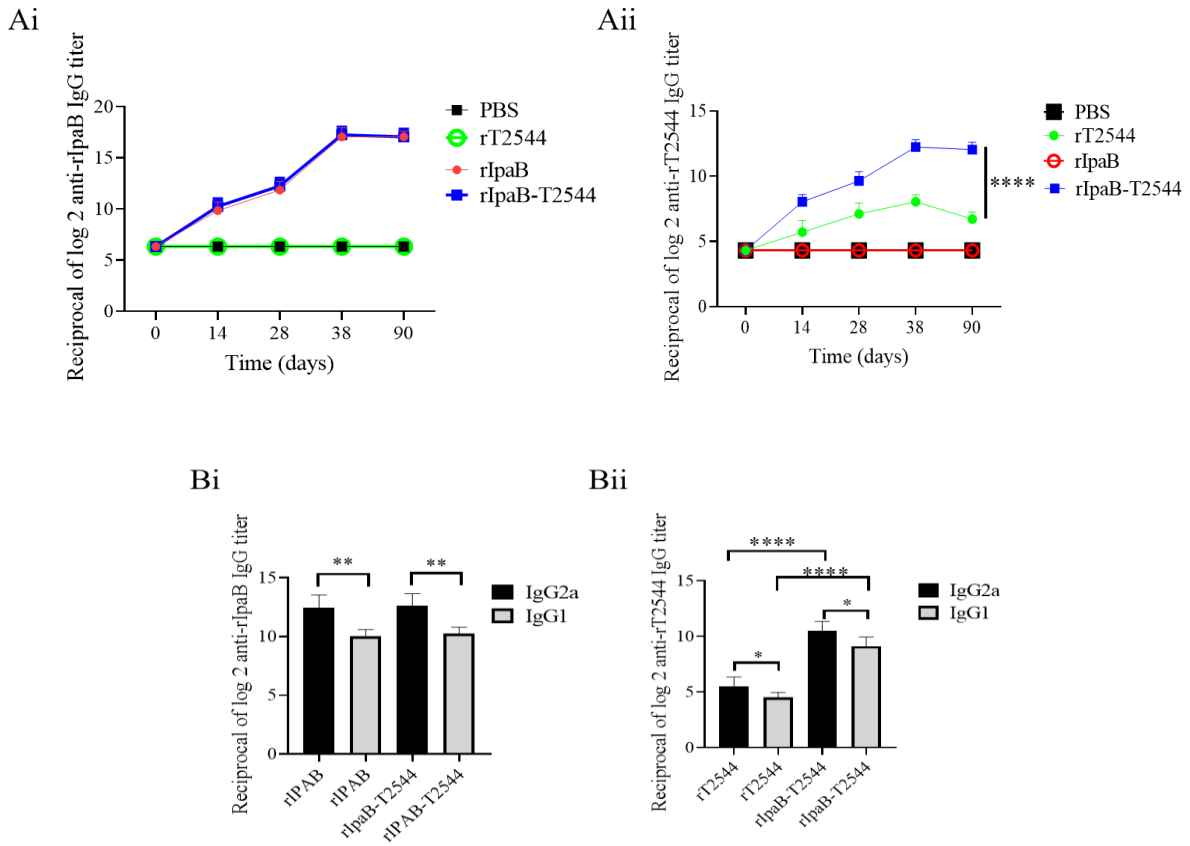

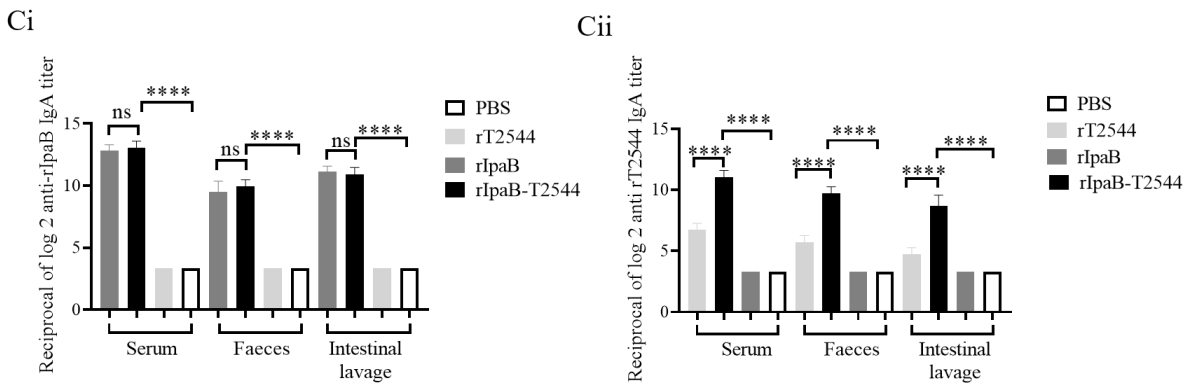

Figure 43. Humoral and mucosal adjuvanticity of rIpaB in intranasal rIpaB-T2544 immunized mice. (A) BALB/c mice were immunized intranasally with 40µg of rIpaB, rIpaB-T2544 and PBS (vehicle) on days 0, 14 and 28. Time kinetics of antigen-specific total IgG in the mouse serum as measured by ELISA. Data represent mean ± SEM values from different mice samples (n=5). X-axis indicate the time points after the start of the immunization when samples were collected. Statistical significance between the titer values from rIpaB-T2544 and rT2544 vaccine recipients is shown. Statistical analysis was performed using two-way ANOVA and Tukey's post-test for multiple comparisons, ****P < 0.0001. The colour scheme used to mark different experimental groups are as follows: PBS-black; rT2544-green; rIpaB-red; rIpaB-T2544-blue. (B) Serum IgG isotypes measured by ELISA at day 38. Data represent mean ± SEM values from different mice samples (n=5). Statistical analysis was performed using two-tailed Student's t-test. ****P < 0.0001. (C) ELISA showing serum IgA and intestinal sIgA titers after immunization with different antigens. Mice were sacrificed on day 38 and samples were collected. Data represent mean ± SEM values from different mice samples (n=5). Statistical analysis was performed using two tailed Student's t-test. ****P < 0.0001.

4.3.10. Recombinant IpaB-T2544 induces a balanced T helper cell response

Cell-mediated immune responses may significantly contribute to vaccine-induced protection, with Th1 response being required to clear intracellular pathogens and Th2 cells promoting serum antibodies and sIgA production. To assess the cellular immune responses induced by our candidate vaccine, splenocytes isolated from the immunized mice were subjected to mixed leukocyte reaction (MLR) and cultured for 48 h with antigen stimulation. Both Th1 (IL12, IFNγ, TNFα, IL-2) and Th2 (IL-4, IL-5) cytokines, as measured in the culture supernatants were significantly elevated in rIpaB-T2544-immunized mice, as opposed to minimal rise in the vehicle-immunized group (**Figure 44 A-B**). These results suggested a balanced T-cell response after immunization with rIpaB-T2544. [The detailed methodologies were discussed in the materials and method sections **3.2.11.5.**]

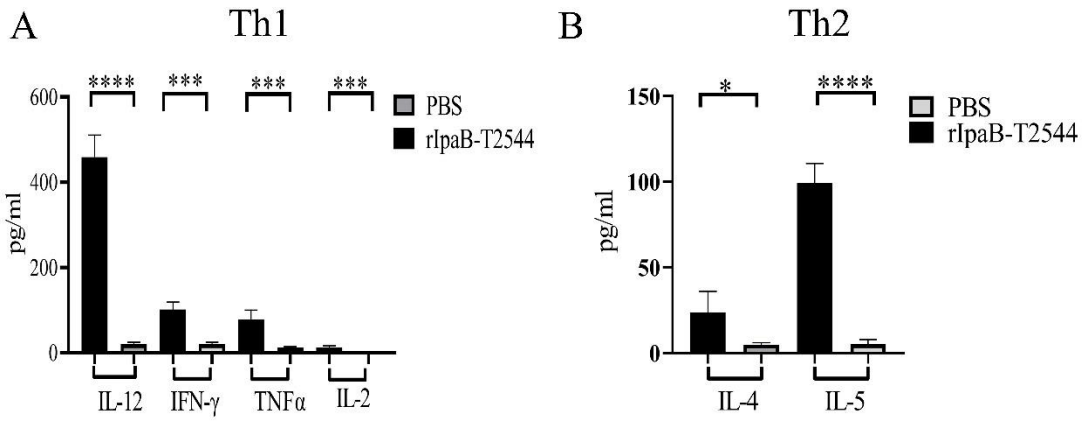

Figure 44. Balanced Th1 and Th2 cytokine production from splenocytes of intranasal rIpaB-T2544 immunized mice. BALB/c mice were immunized intranasally with 40µg of rIpaB-T2544 and PBS (vehicle) on days 0, 14 and 28. Immunized mice were sacrificed on day 38 and splenocytes were isolated and cultured in the presence of antigen stimulation for 48 h. (A-B), T cell cytokines were measured from the culture supernatants by ELISA. Data represent mean ± SEM values from different mice samples (n=4). Experiment was replicated three times, and data from a representative experiment are shown. Statistical analysis was performed using two tailed Student's t-test (*P < 0.05; ***P < 0.001; ****P < 0.0001).

Summary

- Recombinant T2544 functions as an adjuvant to increase the serum anti-OSP antibody titer by 32 times after subcutaneous immunization of mice with OSP-rT2544, keeping the levels of anti-T2544 antibodies unchanged.
- OSP-rT2544 conjugate induced anti-OSP IgG1 and IgG2a compared with unconjugated OSP where the former is the predominant. We also found increased IL4 concentrations in the conjugate antisera corroborated with the IgG subclass data. IL-4 plays an important role in humoral immunity by inducing differentiation of Th0 into Th2 cells and mediating IgG1 antibody release.
- We measured protective efficacy of vaccine antigen-specific antibodies by serum bactericidal assay (SBA) titer and soft agar motility inhibition assay using intestinal sIgA. OSP-rT2544 antisera displayed SBA titer of 1:1600 against *S.* Typhi and *S.* Enteritidis, while titers for *S.* Paratyphi A and *S.* Typhimurium attained the values of 1:12800 and 1:6400, respectively. OSP-rT2544 immunized group showed 2-fold increased secretory antibody titres compared to OSP. We found significant inhibition of bacterial motility in soft agar by intestinal secretory antibodies from OSP-rT2544 compared to unconjugated OSP.
- Following vaccination with OSP-rT2544, sustained OSP- and rT2544-specific primary antibody response was observed at day 110, which further increased after the administration of a booster dose on day 110 with the production of recall antibodies with higher avidity, is a marker for T-cell dependent affinity maturation. To further corroborate the antibody recall response, we checked for $CD4^+$ effector memory T cells producing IFN-γ in the OSP-rT2544 immunized mice. Elevated levels (15-fold higher) of IFN-γ production were found following antigen restimulation of mouse splenocytes

in the recipients of OSP-rT2544 compared with unconjugated OSP. The percentage of $CD4^+$ effector memory T cells was found 2.6 times higher in OSP-rT2544 immunized mice compared to unconjugated OSP group, determined from the FACS analysis.

- **Overall, from the OSP-rT2544 immunization study, we can conclude that-**
  - **OSP-rT2544 induces protective humoral immune response against *S.* Typhi and *S.* Paratyphi A, S. Typhimurium and *S.* Enteritidis**
  - **OSP-rT2544 generates functional sIgA response, a hallmark of mucosal immunity**
  - **OSP-rT2544 induces both Th1 and Th2 serum cytokine response.**
  - **OSP-rT2544 generates protective memory response**
- Mouse immunized with single dose of Vi-rT2544 showed two-fold and four-fold increased anti-Vi IgG antibodies, following subcutaneous (SC) and intramuscular (IM) vaccination compared to Vi-TT.
- Markedly raised titers of Vi-specific serum IgG1 and IgG2a antibodies were observed in mice immunized with Vi-rT2544, as compared with the Vi-TT immunized mice, indicating induction of both Th1 and Th2 type responses; however, IgG1 and IgG2a was the predominant isotype following SC and IM immunization. Anti-Vi IgA titer was increased two-four -fold in the intestinal lavage, serum and faeces in the groups of mice immunized with Vi-rT2544 compared to Vi-TT following SC and IM immunization.
- We found significantly elevated, circulating pro-inflammatory/Th1 (IFNγ) and anti-inflammatory/Th2 (IL-4 and IL-10) cytokines in Vi-rT2544-immunized mice compared to Vi-TT immunized group. This result indicates the induction of both Th1 and Th2 type responses; however, Th2 and Th1 were the predominant isotype following SC and IM immunization.

- To study antigen-specific memory T cells following single Vi-rT2544 immunization dose, $CD4^+$ T cells isolated from splenocytes (on day 172) of immunized mice co-cultured with antigen-pulsed bone marrow-derived dendritic cells (BMDCs) from naïve mice. IFNγ release in the co-culture supernatants was estimated to be >1.2 folds (SC) and >1.4 folds (IM) higher for the splenocytes from Vi-rT2544 immunized mice compared with the animals that received Vi-TT, suggesting significant augmentation of T cell memory response by rT2544 when conjugated to Vi. Cell subset analysis showed that Vi-rT2544 augmented 10.8 % (SC) and 14.1% (IM) higher memory response than Vi-TT was largely contributed by the effector memory T cells.
- Further, to analyze memory B cell response, a booster dose was administered to the immunized mice on day 162 of the first immunization, and anti-Vi serum antibodies were measured ten days later. A significantly higher secondary anti-Vi antibody response on day 172 compared with day 120 (primary antibody) was observed (SC, Vi-rT2544, 4 times, Vi-TT, 2 times; IM, Vi-rT2544, 4 times, Vi-TT, 2 times). However, the induction of Vi-specific recall antibodies (day 172) was comparatively higher in Vi-rT2544 (for SC and IM, 8 times higher) group compared to Vi-TT immunized group, suggesting differentiation of higher memory B cells into plasma cells, producing IgG at the latter time point in the former group. Vi-rT2544 induces significantly higher recall antibodies with higher avidity (SC, Vi-rT2544, 1.3-fold and IM, Vi-rT2544, 1.4-fold) compared to Vi-TT.
- Serum Bactericidal Assay (SBA) suggested that inhibition dilution of the Vi-rT2544 antisera (day 172) was significantly higher than inhibition accompanied by antisera collected on day 120 and also higher than the Vi-TT.
- **Overall, from the Vi-rT2544 immunization study we can conclude that-**
    - **Vi-rT2544 elicits robust antibody responses compared to Vi-TT**

- **Vi-rT2544 induces both Th1 and Th2 serum cytokine response**
- **Vi-rT2544 elicited protective memory response higher than Vi-TT**
- **Vi-rT2544 elicited functional antibodies with higher bactericidal activity compared to Vi-TT**

- Analysis of serum antibody endpoint titers showed that mice immunized with rIpaB induced 2560 times higher IpaB-specific IgG compared with the vehicle (PBS) immunization. Analysis of serum antibody endpoint titers showed that immunization with rIpaB and rIpaB-T2544 induced similar magnitudes of IpaB-specific IgG, while T2544-specific IgG titers were 32- times higher for the chimeric vaccine compared to unfused rT2544.
- The IgG isotypes comprised of IgG1 and IgG2a, indicating induction of both type 1 and type 2 responses, although the latter response was predominant.
- rIpaB-specific serum and intestinal secretory IgA titers were identical to rIpaB-T2544 immunizations, but 15-20 times higher anti-T2544 IgA titers were observed for the chimeric protein vaccine (rIpaB-T2544).
- Both Th1 (IL12, IFNγ, TNFα, IL-2) and Th2 (IL-4, IL-5) cytokines, as measured in the culture supernatants from the splenocytes were significantly elevated in rIpaB-T2544-immunized mice, as opposed to minimal rise in the vehicle-immunized group.
- **Overall, from the IpaB-rT2544 immunization study we can conclude that-**
    - **Recombinant IpaB specific humoral and mucosal antibody response was unaltered before and after chimeric fusion.**
    - **IpaB in the chimeric vaccine candidate augmented increased humoral and mucosal antibody response to T2544**
    - **rIpaB in the chimera acts as adjuvant to rT2544**
    - **rIpaB-T2544 induced a balanced T helper cell response**

Chapter 5.

General discussion

In our first study, we describe the development of a multivalent glycoconjugate that contains the outer membrane protein (T2544) of *S.* Typhi/*S.* Paratyphi and O-specific polysaccharide (OSP) from *S.* Typhimurium. This glycoconjugate showed strong potential as a multivalent vaccine against both typhoidal and non-typhoidal *Salmonella* serovars. Subcutaneous immunization of mice with OSP-rT2544 induced rapid seroconversion with high titers of protective antibodies in the serum and intestinal secretions, along with memory B and T cell response.

S. Typhimurium type 3 secretion system tip and translocator proteins, as well as their chimaera, have been shown to provide serotype independent protection against NTS (non-typhoidal *Salmonella*). Nevertheless, the level of protection was only moderate at best in contrast to 80% protective effectiveness of OSP-rT2544 (479). Many of the currently available vaccines are made of bacterial surface polysaccharides, which makes them appealing candidates for vaccine development. Since polysaccharides are T-independent antigens, they are not immunogenic and do not elicit immunological memory; nevertheless, they can be effectively coupled with carrier proteins to increase their immunogenicity (480). There are several reports on the synthesis of glycoconjugate vaccines employing various conjugation chemistries and covalent link between the saccharide and carrier protein molecules (481-484). The conjugation methods used can be divided into two primary groups: "selective attachment" at the polysaccharide (PS) terminus and "random linkage" along the polysaccharide (PS) chain. Random chemistry produces heterogeneous structures with high molecular weight (MW), that are cross-linked and often undefined, while selective chemistry produces better-defined structures without modifying the saccharide chain chemically (481, 485, 486, 487). The conjugation chemistry of glycoconjugate vaccines has a major impact on their immunogenicity. Studies utilizing various linkers and chemical techniques to couple OSP to multiple carrier proteins from various *Salmonella* strains revealed that when polysaccharides are directly attached to the carrier

protein, significant antigenic epitopes might be sterically protected by the bulky protein (488). Alternatively, when a linker binds the polysaccharide to a carrier protein, steric shielding might be reduced and the polysaccharide could be externally delivered to the immune cells. This increases the quantity of antigenic epitopes that are available to activate antigen-presenting cells (488). We have generated OSP-rT2544 conjugate in this study using the random linking method—which involves randomly activating hydroxyl groups along the saccharide using CnBr (cyanogen bromide) (489-492). For polysaccharide-protein conjugation, cyclanylation is a tried-and-true technique that works well. It has been previously applied to OSP-TT (404), Hib-protein conjugate (492), *V. cholerae* O:1 serotype Inaba (493), *V. cholerae* O:1 serotype Ogawa (484), and *Francisella tularensis* (495). After the cyanylation reaction, 1-ethyl-3-(3-dimethy laminopropyl) carbodiimide (EDC)-mediated condensation results in the formation of cyanate esters, which then react with the hydroxyl groups to produce cyclic imidocarbonates that can couple to the carboxyl groups of the carrier proteins (496). Instead of CnBr, different chemical like CDAP was also used to activate polysaccharides has been reported for a number of different glycoconjugates (404, 497). The formation of isourea linkages between the cyanoesters on the activated carbohydrate and the lysine residues on the carrier protein is the main mechanism of CDAP-mediated activation (491, 494). On the other hand, over-crosslinking, which causes the carbohydrates and peptides to gel and diminish the immunogenicity of the glycoconjugates, is a significant disadvantage of CDAP chemistry (488). During the manufacture of vaccines, ADH linker is frequently used in conjunction with CnBr. In glycoconjugate vaccine for meningococcal serogroup X, conjugation chemistry employing an ADH linker was found more reactive because of a shorter reaction time and a higher derivatization yield (498).

Like OSP-TT (31), Vi-CRM197 (484), and Hib-protein (492) conjugates, we employed ADH linker to form a covalent bond via carbodiimide chemistry between OSP and rT2544.

The molar ratio of the sugar to the carrier protein and the molecular weight (MW) of the conjugate are two factors that affect vaccine immunogenicity. Due to numerous activation sites within OSP and several linkage spots on the protein (T2544), a very large molecular weight, crosslinked conjugate with a partition coefficient (kd) of 0.02 was generated in our study. Higher MW glycoconjugate immunization has been shown to elicit a stronger anti-PS antibody response. It has been observed that greater anti-Vi and anti-saccharide IgG responses were produced by larger and more cross-linked Vi-DT and GBS type III-TT conjugate vaccines, respectively (499, 500). The immunogenicity of glycoconjugates is directly correlated with the saccharide-to-protein ratio; higher ratios enhance cross-linking and activate B cells that are specific to saccharides and increase polysaccharide loading. OSP-rT2544 (PS to protein molar ratio of 1.53) conjugate generated using ADH linker by random activation produced noticeably higher anti-OSP antibodies than unconjugated OSP after three subsequent immunizations in mice. These characteristics align with the *Salmonella* Typhimurium OSP-TT conjugate, which is generated by random activation using ADH linker where the saccharide to protein ratio was 0.6. Compared to the molecule produced via selective chemistry with a saccharide to protein ratio (w/w) of 0.1, this conjugation was found more immunogenic (497).

Furthermore, when Vi polysaccharide coupled to recombinant *Pseudomonas aeruginosa* exotoxin A (rEPA) by random chemistry, the immunogenicity of *Salmonella* Typhi Vi conjugates was boosted by ADH linker rather than using cystamine or SPDP linker (501). Comparable outcomes were seen when *S. aureus* type 8 capsular PS was connected to rEPA or DT via random chemistry; in these cases, the PS to protein ratio was larger when the ADH linker was used as opposed to cystamine or SPDP (502, 503). In a study utilizing cholera toxin (CT) and deacylated lipopolysaccharides (LPS) from *Vibrio cholerae* O1 serotype Inaba, it was found that conjugates with LPS to CT ratios of 0.8 were produced by random chemistry using

ADH linker, whereas the ratio was 0.72 for single-point attachment using SPDP linker, with the former being more immunogenic (504). On the other hand, *Salmonella* Enteritidis OSP directly conjugated to flagellin monomers, polymers, or CRM197 by random activation without linkers or with selective aminooxyoxime thioether chemistry using diaminooxy cysteamine and N-(γ-maleimidobutyloxy)- sulfosuccinimide ester linker induced similar IgG response and confers protection against bacterial challenge in mice (501, 505).

The immune response specific to the carrier proteins used in the glycoconjugate preparations is generally unaltered, however, the immunogenicity against the covalently attached polysaccharides is enhanced. Following subcutaneous immunization of mice, T2544 acts as an adjuvant to raise the serum anti-OSP antibody titer by 32 times while maintaining the levels of anti-T2544 antibodies unaltered. After three intramuscular immunization doses, mice treated with flagellin in a conjugate formulation containing *Salmonella* Enteritidis OSP showed a ten-fold increase in anti-OSP antibody titers. However, the anti-flagellin antibody response against the conjugation was comparable to that of unconjugated flagellin (505). Similar outcomes were found when OSP from *Salmonella* Typhimurium was conjugated to FliC or CRM197 via random chemistry (506, 507), despite the conjugation producing a 100-fold increase in the anti-CRM197 antibody titer. Interestingly, conjugation utilizing selective chemistry resulted in a substantially increased anti-OSP antibody response described here. This contrasts with the majority of earlier research (497, 501, 504) that found that glycoconjugates produced via random chemistry produced a stronger antibody response. Following three doses of intraperitoneal immunization with *S.* Typhimurium OSP-porin conjugate, anti-OSP and anti-porin end-point titers were found to be 1/600 and 1/8500, respectively (508). In comparison, the anti-OSP and anti-T2544 end-point titers in our study were 1/25600 and 1/51200, respectively.

The majority of *Salmonella* conjugate vaccines, both those with licenses and those in the advanced stages of clinical testing, are monovalent and only target a single strain of *Salmonella*. In India, Vi-TT conjugate vaccination locally has been licenced against *Salmonella* Typhi infection (509, 510, 511). OSP-FliC, OSP-CRM197, and OSP-porin conjugates (506, 508) provided 90–100% protection against reference and clinical strains of *S.* Typhimurium. On the other hand, the OSP-rT2544 candidate vaccine provided 75–80% protection against *S.* Typhi, *S.* Paratyphi A, and *S.* Typhimurium and 55–60% cross-protection against *S.* Enteritidis. Although the exact reason for the cross-reactivity to *S.* Enteritidis is still unknown, the most plausible explanation is antibodies against shared core regions or common O-Ag epitopes such as O:1 and O:12. IgG1 and IgG2a subclasses were present in serum antibodies specific to OSP and rT2544. It has been reported that in the absence of T cell interaction, polysaccharide antigens induce an IgG2 class transition (512). Conversely, T cell-dependent (TD) protein antigens elicit IgG1 antibodies. After conjugation to a carrier protein, anti-polysaccharide antibodies in mice moved towards the IgG1 subclass (513, 514). Comparing conjugated OSP-rT2544 to unconjugated OSP, anti-OSP IgG1 was comparatively higher than IgG2a. This supports the findings of the earlier published research (507, 515) that showed the conjugate immunized group primarily had IgG1 antibodies specific to OSP. The concept that two forms of the saccharide may activate separate regulatory mechanisms or select B cell clones with different isotype-specificity is supported by the higher IgG1 response in conjugate compared to unconjugated form (449). We also found increased IL4 concentrations in the conjugate antisera that was previously reported for other glycoconjugate vaccines (407). IL-4 plays a significant role in humoral immunity by inducing Th0 cells to differentiate into Th2 cells and facilitating the generation of IgG1 antibodies, which may activate the classical complement system and offer long-term protection.

We evaluated the protective effectiveness of vaccine antigen-specific antibodies by employing intestinal sIgA in the soft agar motility inhibition experiment and the serum bactericidal assay (SBA). SBA is recognized as a reliable in vitro indicator of vaccine immunogenicity. A 50% reduction in the number of bacteria was observed when *Salmonella*-specific antibodies were assessed for complement-mediated bacterial killing using SBA. SBA titers of 1:1600 were shown by OSP-rT2544 antisera against *S.* Typhi and *S.* Enteritidis, whereas titers of 1:12800 and 1:6400 were obtained by *S.* Paratyphi A and *S.* Typhimurium, respectively. Serum bactericidal titers for OSP-TT (anti-*S.* Typhi) and OSP-CRM197 (anti-*S.* Typhimurium and *S.* Enteritidis) were found to be significantly lower in published investigations. Although intestinal secretory antibodies significantly inhibited bacterial mobility in soft agar, we were unable to locate any comparable research with other glycoconjugate vaccines in the published literature. Nonetheless, in contrast to the 2-fold increase after OSP-rT2544 immunization in our current study, 3-fold elevated sIgA titers were observed following immunization with OSP-CRM197 (507). This could be related to the reduced motility of *Salmonella* when pre-incubated with the intestinal wash from vaccinated mice, as was previously noted for *S.* Typhi and *S.* Paratyphi A ghost cell-based bivalent vaccine candidate (516). In certain studies, conjugate sera were passively transferred into mice to conduct functional tests. OSP-TT antisera given intraperitoneally provided passive protection against *S.* Typhimurium (497), with passively transferred IgM (80–100%) providing greater protection than IgG (20–30%). However, when passive rabbit antisera of OSP-porin conjugate was injected intravenously, mice were fully protected against an intraperitoneal challenge with *S.* Typhimurium (508). In different studies, opsonophagocytosis was used to assess the functionality of conjugate antisera. When antisera from COPS-FliC conjugate were pre-incubated with the *S.* Enteritidis, opsonophagocytosis increased by 5% as compared to the vehicle immune sera (505). Nevertheless, we did not use the opsonophagocytosis assay or passive immunization to assess the OSP-rT2544 antisera.

A successful vaccine must be able to produce a strong and long-lasting immunological memory in order to have the desired effect on public health. Tetrasaccharide-CRM197 conjugate was used to show an antibody recall response following a booster on day 260, when the initial antibody response was twice as low as the titers attained during the third dose of immunization (day 36) (517). On the other hand, in our study, after administration of OSP-rT2544 vaccination, a sustained primary antibody response specific to OSP and rT2544 was seen at day 110. This response was further enhanced with the administration of a booster dose, resulting in the production of higher avidity antibodies, a marker for T-cell dependent affinity maturation. Following the administration of a conjugate vaccine comprising *Vibrio cholerae* O1 Inaba and tetanus toxoid to human volunteers, a different investigation assessed the memory response of B cells using the ELISPOT assay. The results showed that, there were 3.5 OSP-specific and 5 carrier protein-specific IgG spots per 10^5 splenocytes at day 56 (518). In the OSP-rT2544 immunized mice, we looked for CD4+ effector memory cells that were generating IFN-γ in order to further support the antibody recall response. Our lab previously reported the generation of recombinant T2544-specific CD4+ T cells (449). After antigen restimulation of mouse splenocytes in OSP-rT2544 recipients, higher levels of IFN-γ production were observed. Nevertheless, comparable research on glycoconjugate vaccines containing OSP was not previously published.

This study has significant limitations, despite the fact that it effectively demonstrated the activation of various immune system arms with protective serum and mucosal antibody response, conferring broad spectrum protection against both typhoidal and non-typhoidal *Salmonella* serovars. The immunogenicity of prospective glycoconjugate vaccines that were developed with various conjugation chemistries and different linker molecules between OSP and T2544 was not compared. T2544 is an intrinsic *Salmonella* protein, therefore comparing it side by side with a different preparation that contains OSP attached to a non-*Salmonella* protein

might shed further light on the processes behind the activation of the immune system in response to glycoconjugate vaccinations. It would be more precise to characterise the immune response if the T cell response was further elaborated, encompassing the activation of various CD4+ T cell subsets (Th9, Th17, follicular helper T cell, resident memory, and central memory T cells) as well as cytotoxic T cells (central and effector memory cells). Lastly, studies outlining the relative roles of the cellular, mucosal, and humoral immune system compartments will aid in the development of more advanced vaccines with higher efficacies.

In our second study, we have synthesized a bivalent glycoconjugate comprising the outer membrane protein (T2544) of *S.* Typhi/*S.* Paratyphi and Vi from *Citrobacter freundii*. We furthermore evaluated a comparative immunogenicity between the licensed Vi-TT vaccine with that of Vi-rT2544 in BALB/c mice. A bivalent conjugate vaccine against both *S.* Typhi and *S.* paratyphi would be an appealing approach to combat the frequent co-endemicity of these serogroups, as Vi-TT is only effective against *S.* Typhi. The first World Health Organisation (WHO) prequalified glycoconjugate vaccine, Typbar TCV (Vi PS conjugated to tetanus toxoid), is safe and produces an enduring antibody response in infants and young children with 80% efficacy in typhoid endemic areas, such as Malawi, Bangladesh, and Nepal (509, 510, 511). In our previous studies, we demonstrated that in adult mice, O-specific polysaccharide (OSP) conjugated to the carrier protein (rT2544) using random chemistry with an ADH linker generated a strong immunological response in addition to a protective efficacy response with a ratio of ≥1 (450). A few reports for Vi-polysaccharide-based conjugates have been made; they report that a comparable conjugation strategy between Vi and CRM197 produced more antibodies when Vi to CRM197 had a weight-to-weight ratio of 0.9 and 2.1 than a ratio of 10 (510). Using identical conjugate chemistry, the anti-Vi antibody reaction gradually increased with increasing DT to PS content in Vi-DT conjugates (519). This supports the findings of our current investigation, in which the identical linker was used to conduct Vi-rT2544 conjugation

utilizing random chemistry. A wt/wt ratio of 1.6 for the Vi-rT2544 conjugation results in increased levels of anti-Vi antibodies. The immunogenicity of glycoconjugates is directly correlated with the saccharide-to-protein ratio; higher ratios enhance cross-linking and activate B cells that are specific to saccharides and increase polysaccharide loading.

Vi-rT2544 had been evaluated as a potential vaccine against *S.* Typhi and *S.* ParatyphiA in mice using immunogenicity tests and bacterial challenge trials. Mice received a single injection of 25µg of Vi were compared to the comparator group Vi-TT. The majority of *Salmonella* conjugate vaccines, including those with licenses, are monovalent and only work against single serovar of the *Salmonella*. Children aged 2 to 5 participated in clinical trials of Vi-rEPA vaccination in Vietnam received 89% protection against *S.* Typhi during a 46-month period (382, 383), Whereas children (>3 months) showed 100% vaccine effectiveness with Vi-TT vaccination (520). The Vi-DT typhoid conjugate was found both immunogenic and safe in Nepal (391). The protective efficacy of our study indicates that BALB/c mice immunized with Vi-rT2544 showed 60% protection against both *Salmonella* Typhi and *Salmonella* Paratyphi A, whereas Vi-TT alone only showed 30-40% protection against *Salmonella* Typhi after a single dose of immunization. However, no protection against *S.* Paratyphi A was observed after Vi-TT vaccination.

In our study, T2544 serves as an adjuvant, to raise the serum anti-Vi antibody titer by 320 (SC) and 160 (IM) times after immunization, while maintaining the same levels of anti-T2544 antibodies, as demonstrated by the OSP-rT2544 conjugate (450). Mice receiving three subcutaneous immunization doses showed a 100-fold increase in anti-Vi antibody titers when administered in a conjugate formulation (2.5 mg vi in conjugation) containing Vi from *Salmonella* Typhi (484). After two intramuscular immunizations, the Vi-FliC nanoconjugate group exhibited 1.5 times stronger anti-Vi IgG antibodies (521), but after three subcutaneous injections, the Vi-OMPC conjugate group developed 10-fold greater anti-Vi antibodies than the

unconjugated Vi (522) group. In contrast to Vi-TT, mice immunized with Vi-rT2544 produce anti-Vi IgG antibodies that are 2-fold (SC) and 4-fold (IM) higher. Moreover, the latter group showed a 2-4-fold (intramuscular, subcutaneous) increase in Vi-specific sIgA response. There are only fewer reports are available regarding the Vi-specific IgA response. After two subcutaneous immunizations in mice, a Vi-specific IgA response was found in Vi-CRM197 conjugate; however, the response was not statistically significant when compared to unconjugated Vi (523).

We determined both IgG1 and IgG2a subclasses in the serum antibodies specific to Vi. Typically, both isotypes are generated in comparatively small amounts in a 1:1 ratio in T-independent antigens (polysaccharides) (524). When a T-dependent antigen is encountered, IgGl is the most dominant subclass produced in both humans and mice (525). After subcutaneous immunization, both conjugate Vi-rT2544 and Vi-TT elevated anti-Vi IgG1 titers more than IgG2a. However, a much higher level of IgG2a was detected following intramuscular immunization. The results corroborated with our cytokine data, where both Th1 and Th2 was elevated in both the Vi-rT2544 and Vi-TT immunized groups. However, Th2 was predominant after subcutaneous immunization whereas Th1 was predominant after intramuscular immunization. Similar results were noted in a few studies when mice received two intramuscular doses of Vi-TT (526).

With "assistance" from carrier-specific CD4+ T cells, conjugated vaccinations create a pool of long-lasting memory B cells that are crucial for the preservation of protective serological memory. A second dose of antigen triggers memory B cells to activate and respond quickly, which shifts the secondary antibody response to a higher proportion of IgG than in the first and increases its overall size (526). After a single immunization, the induction of effector memory T-cells was shown to be 10.8%–14.1% higher in Vi-rT2544 group compared to Vi-TT. A persistent Vi-specific primary antibody response following vaccination with Vi-rT2544 was

observed at day 162, and this response was further enhanced by the generation of greater avidity antibodies following the administration of a booster dose. Following a booster dose on day 162 of primary immunization, eight times stronger secondary antibody responses was exhibited in Vi-rT2544 group on day 172d when compared to Vi-TT. This outcome was consistent with our earlier research, which found that after receiving a booster dosage on day 110, secondary antibodies with greater avidity were produced on day 120 (450). Different studies assessed the B cell memory response following the administration of a combination vaccine containing MenC and CRM197 to human volunteers, using the ELISPOT assay and found 12.5 MenC-specific IgG spots per 2×105 splenocytes at day 30 (527). Furthermore, increases in antibody avidity following Vi-rT2544 immunization were 1.3–1.4 times greater than following Vi-TT immunization, indicating T-cell-dependent affinity maturation was higher for the former. We evaluated the production of IFN-γ by CD4+ effector memory cells to further corroborate the antibody recall response in the Vi-rT2544 and Vi-TT immunized group. Vi-rT2544 recipients showed higher levels of IFN-γ production (1.2-fold (SC) and 1.4-fold (IM)) after antigen restimulation in comparison to Vi-TT. Nevertheless, comparable research on glycoconjugate vaccinations incorporating Vi was not previously published.

Serum bactericidal assay (SBA) was implemented to assess the functional activities of the increased avidity antibodies of Vi-rT2544. The secondary antisera Vi-rT2544 showed an SBA titer with a higher dilution of 1:1600 (SC), 1:800 (IM) than the comparable values for Vi-TT, which were 1:400 (SC), 1:200 (IM) against *S.* Typhi. However, no inhibition was found for Vi-TT sera against *S.* Paratyphi A, whereas SBA titers reached the values of 1:12800 (SC) and 1:6400 (IM) for Vi-rT2544 sera. We found significant inhibition of bacterial growth by bactericidal assay corresponding to our previous work (440). Similar serum bactericidal titers (1:6400) for *S.* Typhi and lower values (1:3200) for S. Paratyphi C are reported by published investigations (528). Overall, we developed a bivalent glycoconjugate vaccine against *S.* Typhi

and *S.* Paratyphi and directly compared it to the Vi-TT vaccine. We have shown that Vi-rT2544 conjugate improved protective efficacy and immunogenicity in mice in comparison to the available Vi-TT glycoconjugate.

In our next study, we present the first-ever murine model of oral *Shigella* infection in a wild-type mouse. Iron overload BALB/c mice that had received streptomycin prior to infection were vulnerable to *S. flexneri 2a* infection of the large intestine, which resulted in shortening of the colon length, neutrophil infiltration, erosions of the crypt and villus, severe diarrhoea and weight loss, and increased secretion of inflammatory cytokines and chemokines.

The human-restricted characteristics of *Shigella* has always made the development of an animal model of infection difficult. The earliest known model, keratoconjunctivitis guinea pig model (278, 529), was helpful in distinguishing between a virulent and non-virulent strain of *Shigella* and revealed the function of T3SS as a virulence determinant of *Shigella* infection. However, due to the irrelevant target tissue, it was not useful for host-pathogen interaction studies. Further insights into human shigellosis were provided by later models, such as the rabbit ileal loop (268) and rabbit (530) or guinea pig rectal (265) infection model. Especially, the infant rabbit model closely recapitulated the human, commonly observed with *S. dysenteriae* type I infection (rarely found nowadays) and manifested by severe inflammation, massive ulceration of the colonic mucosa, bloody diarrhoea, and marked weight loss, although the authors used more frequently isolated *S. flexneri 2a* for infection (530). Notwithstanding, the above models remained non-physiological due to a different portal of entry for the bacteria. These models are not very helpful for studying protective host immune responses or developing novel vaccinations, despite their great potential to aid in the creation of new drugs. Additionally, efforts were undertaken to create a *Shigella* infection model by modifying the genetic background or intestinal environment of mice. It has been reported that *Shigella* infection was established in C57BL/6 mice by eliminating their gut microbiota with an antibiotic cocktail

both before and after the oral challenge (261); nonetheless, the bacteria remained non-invasive, preventing investigations of host-pathogen interactions. Although pre-treatment of mice with a single oral dose of streptomycin was effective in modeling colitis caused by *S.* Typhimurium (256), similar attempts were exhibited to induce oral *Shigella* infection (264), particularly with *S. sonnei*, which resulted primarily in small intestinal infection with few epithelial lesions and minimal PMN infiltration. Nevertheless, mice with a genetic deficiency in the NAIP-NLRC4 inflammasome showed a marked increase in susceptibility to shigellosis (*S. flexneri*), resulting in disease manifestations subsequent to human infection. This model was utilized to illustrate the host-protective role of inflammasomes in intestinal epithelial cells (260).

After entering the host cell, *Shigella* has to quickly adapt to a new environment in which it must obtain certain nutrients or metabolic cofactors like oxygen, carbon sources, and iron that are controlled by the host. The host has developed a number of defense mechanisms in response to the inherent toxicity of free iron, including the production of iron-binding proteins to lower intracellular iron concentrations. Nonetheless, *Shigella* generate molecules such as siderophores, heme transporters, and ferric and ferrous iron transport systems that are capable of absorbing internal iron (210). *Shigella* require iron for a number of vital processes, such as DNA replication and respiration (531). The significant increase of the iron acquisition systems (Iut, Sit, FhuA, and Feo) and the stress-associated Suf protein in response to intracellular bacteria starving for iron highlights the significance of iron in *Shigella* pathogenesis (532). Feo provides iron in low-oxygen conditions, such as the gut lumen. The Sit system is expressed in the presence of oxygen and contains ferrous iron and provides iron to the bacteria growing inside the host cells (533). The iutA gene encodes the outer membrane receptor required for the import of aerobactin, a *Shigella* siderophore. Aerobactin loaded with iron can cross the outer membrane and then enter the cell by the universal hydroxamate transport system FhuBCD (534). By combining iron with streptomycin, we were able to develop a model of *S. flexneri*

infection in the wild-type mouse. In our study, the pathogenic lesions in the infected large intestine of infected mice healed by day seven, which reflected the average disease persistence in humans (535). Some animal models, however, reported a quicker recovery and a quicker removal of the bacteria. The histological characteristics of the human samples in our study were more akin to mild colitis. Effectiveness of our model against several pathogenic *Shigella* species was another strength of our model. Other mouse models reported are less useful because of the absence of intestinal disease in some cases (257) and the requirement of technical expertise in others (259). These factors make the other models less effective. Compared to the genetically-deficient mouse model of *Shigella* infection, our approach is much more straightforward, less expensive, and more physiologically accurate.

The development of the *Shigella* vaccine has been severely hampered by the lack of an appropriate animal model, which is urgently needed for the developing world. Here, we report the development of a subunit vaccine based on the invasin protein IpaB, conserved among the pathogenic *Shigella* species (*S. flexeneri 2a*, *S. dysenteriae*, and *S. sonnei*) and has been included in several vaccine formulations previously (441, 463). Additionally, we have developed a chimera of IpaB from *Shigella* and *Salmonella* Typhi/Paratyphi A conserved outer membrane protein T2544. T2544 was previously reported to protect against several *Salmonella* serotypes imparted by s.c. immunization with recombinant T2544 and a glycoconjugate of T2544 and *S.* Typhimurium OSP (450). Serum anti-IpaB endpoint IgG titre (1/204800) reported in this study was comparable while serum and faecal IgA titre (1/12800 and 1/1280) were much higher than in earlier findings. After three doses of intranasal immunization with a combination of IpaB and IpaD, IpaB-specific serum IgG and faecal IgA endpoint titres were found to be 1/1000000 and 1/1000, respectively (463). The chimeric ipaB-IpaD immunization, in conjunction with dmlt, resulted in the following outcomes: 1/1000000 for IgG specific serum and 1/100 for faecal IgA endpoint titre (441). According to another study, the addition of

adjuvant rGroEL to rIpaB resulted in a rise in IgG and IgA antibody titers that were 1.5 and 1.3 times higher, respectively, than rIpaB alone (536). IpaB/IpaD combination demonstrated 90% and 30% protection against *Shigella flexeneri 2a* at the 11- and 24-median LD50 dose, and 80% and 50% protection against *Shigella sonnei* at the 5- and 9-median LD50 dose (463). Immunization of mice against lethal doses of S. *flexeneri*, *S. sonnei*, and *S. dysenteriae* using IpaB-IpaD fusion protein containing double mutant LT (dmLT) provides 70%, 100%, and 40% protection against these serovars (441). Conversely, mice received rIpaB+GroEL vaccination provides 80% protection against the lethal dose of *S. flexeneri*, *S. sonnei*, and *S. boydii* (536). The vaccine chimaera, rIpaB-T2544, had comparable efficacy with 90% protection for *S. flexeneri* and 80% protection for *S. sonnei* and *S. dysenteriae* at 10X LD50 dose. These results are consistent with the protection observed in the lung infection model (463, 536). There was a 16-fold rise in T2544-specific IgG antibody titres following immunization with rIpaB-T2544 chimera compared to T2544 alone, which is an intriguing finding for our investigation. Furthermore, the IgA titre specific to T2544 was found to be 40 times higher in the serum and 16 times higher in the intestinal and faecal washes. This result indicates the adjuvanticity of rIpaB to rT2544.

IFNγ production is required for the protection of mice against *Shigella* infection (537). *Shigella* replicates intracellularly and multiplies further when IFNγ is not present, indicating that an IFNγ-mediated mechanism is in place to limit infection (538). Peripheral blood mononuclear cells (PBMCs) from infected patients (539) or other vaccine candidates (441, 463, 536) were used to demonstrate production of IFNγ-in response to IpaB. Th1 cell activation was demonstrated in our work by the increased production of IFNγ and other cytokines (IL-12, TNF-α, and IL-2) in mice immunized with rIpaB-T2544.

The requirement for antibiotic pre-treatment, which modifies the gut flora, may be a drawback of our mouse model. Iron modifies the local microbial population even further. This suggests

that using the model to investigate *Shigella* infection within the framework of microbial communities is not appropriate. Since the *Shigella flexneri* strain is the most common type worldwide, other strains of *Shigella* were not utilized in our study for model establishment. The virulent *Shigella flexneri 2a* strain was used in our study of disease outcomes in mice; no mutant avirulent or non-*Shigella* strain was used. Numerous virulence factors that allow *Shigella* to infiltrate and multiply within colonic epithelial cells while eluding host immune responses are responsible for *Shigella* pathogenesis. A large (200-kbp) virulence plasmid encodes the majority of Shigella's known virulence components, which are necessary for *Shigella* pathogenicity (530, 540, 541). The positive Congo Red stain indicated that the virulence plasmid was present in every strain we utilized in our investigation. Numerous *Shigella* virulence factors, including IcsA/VirG, are necessary for pathogenesis and make the mutants avirulent. It would be interesting to investigate if the virulence factors that play a non-redundant function in human and certain other animal infections (269, 265) are likewise essential for pathogenesis in our new mouse model. This is out of the scope of our current study.

We did not investigate the pathophysiology of *Shigella* in relation to cell-to-cell transmission or vacuolar escape in the intestinal epithelium. We did not repeat the protective efficacy study for IpaB in the mouse lung model, since IpaB is a known immunogenic protein and has been explored as a potential vaccine testing in a lethal pulmonary animal model. The immune cell populations triggered by rIpaB and rIpaB-T2544 were not compared. Rather, the effectiveness of rIpaB and rIpaB-T2544 as vaccines against *Shigella* spp. was found. Therefore, we did not assess the protective effectiveness of rIpaB-T2544 in additional models, such as the Guinea Pig Sereny or the newborn rabbit models.

In our preclinical study, we have used the intranasal route of immunization, since intranasal delivery of IpaB and IpaD were reported to confer better protection in comparison with the intradermal delivery in mice (542). Another possible drawback was the lack of protection in a

CHIM study (543) was observed after intranasal immunization of rIpaB, despite phase 1 studies showing that intranasal immunization with native invaplex was immunogenic and well tolerated (544, 545).

In conclusion, we have developed different protein and polysaccharide glycoconjugate and chimeric combinations which may be used as promising vaccine candidates against different enteric pathogens (*Salmonella* Typhi, *Salmonella* Paratyphi, *Salmonella* Typhimurium, *Salmonella* Enteritidis, *Shigella flexeneri 2a*, *Shigella sonnei* and *Shigella dysenteriae*) in future. Furthermore, a novel mouse model was developed, which will be employed to examine the efficacy of the vaccine candidates against various strains of *Shigella*.

Chapter 6.

Conclusion

1. Here in our study, we have developed a glycoconjugate vaccine candidate **OSP-rT2544** (**Figure 45**) that broadly protects *Salmonella* Typhi, *Salmonella* Paratyphi A, *Salmonella* Typhimurium and *Salmonella* Enteritidis. This vaccine candidate is composed of OSP (O-specific polysaccharide) from *Salmonella* Typhimurium and outer membrane protein T2544 from *Salmonella* Typhi. Subcutaneous immunization with this conjugate augmented different aspects of immune responses compared to unconjugated polysaccharide (OSP) in mice (**Figure 46**).
    - Increased functional IgG antibodies (32 times higher) in serum showed inhibition of bacterial growth in vitro.
    - Increased sIgA antibodies (2-fold increased) in the intestine can inhibit bacterial motility in vitro.
    - Generated balanced Th1 and Th2 responses in serum, while the former is the predominant.
    - Generated affinity matured functional secondary antibodies (B-memory response) with persistent, long-term memory T cell (2.6-times higher) response.

    As there is no single vaccine available to protect against typhoidal and non-typhoidal *Salmonella* serovars, we are aiming to develop this multivalent vaccine against these serovars. All these results indicated that OSP-rT2544 is a promising candidate for the development of a broad-spectrum multivalent glycoconjugate against typhoidal and non-typhoidal *Salmonella* infections.

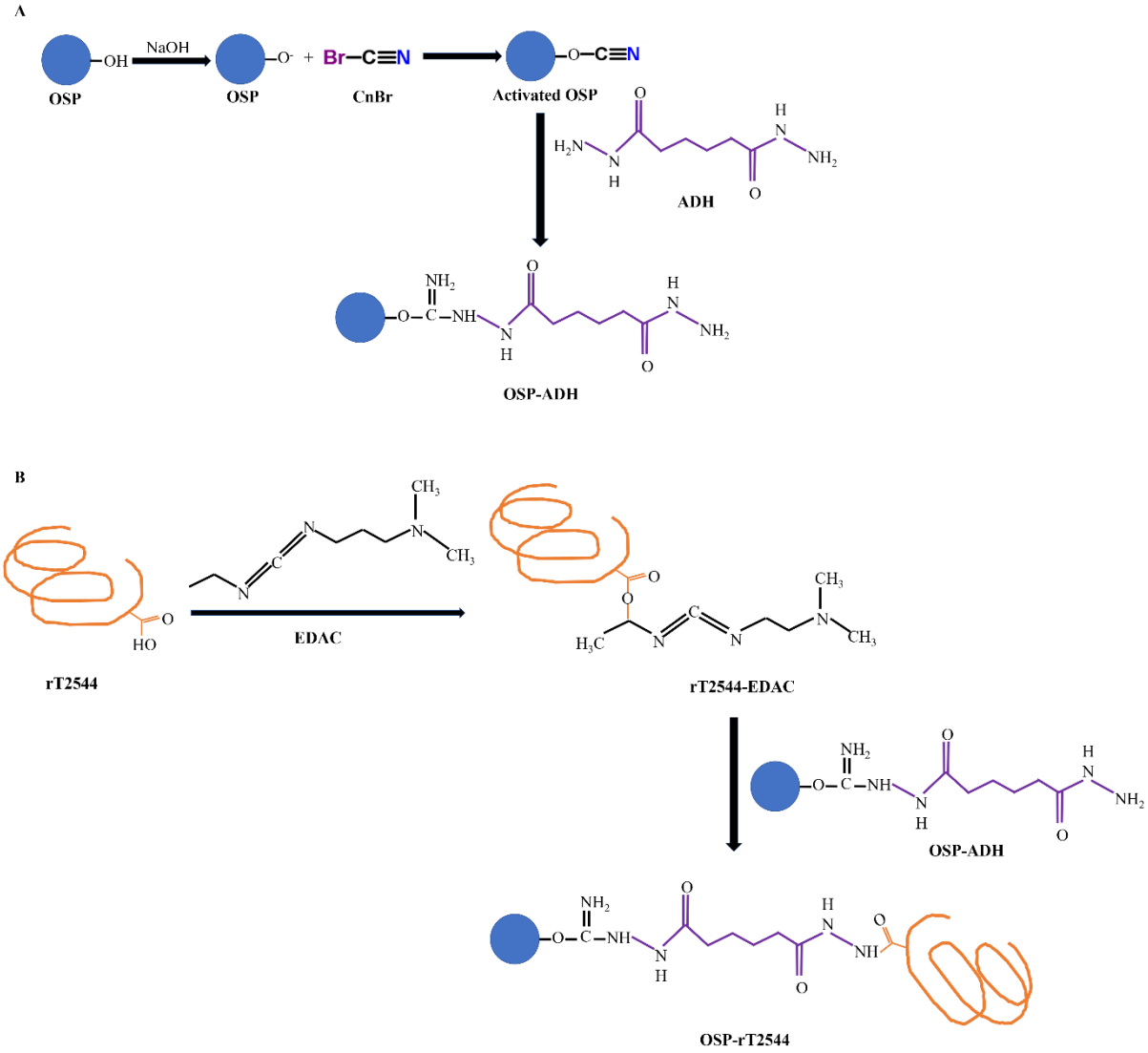

Figure 45. Summary Image 1. Schematic representation of the Summary of OSP-rT2544 conjugation chemistry. (A) OSP was derivatized with ADH after activated with CnBr. (B) rT2544 was conjugated with OSP-ADH. [The image is created using Power Point]

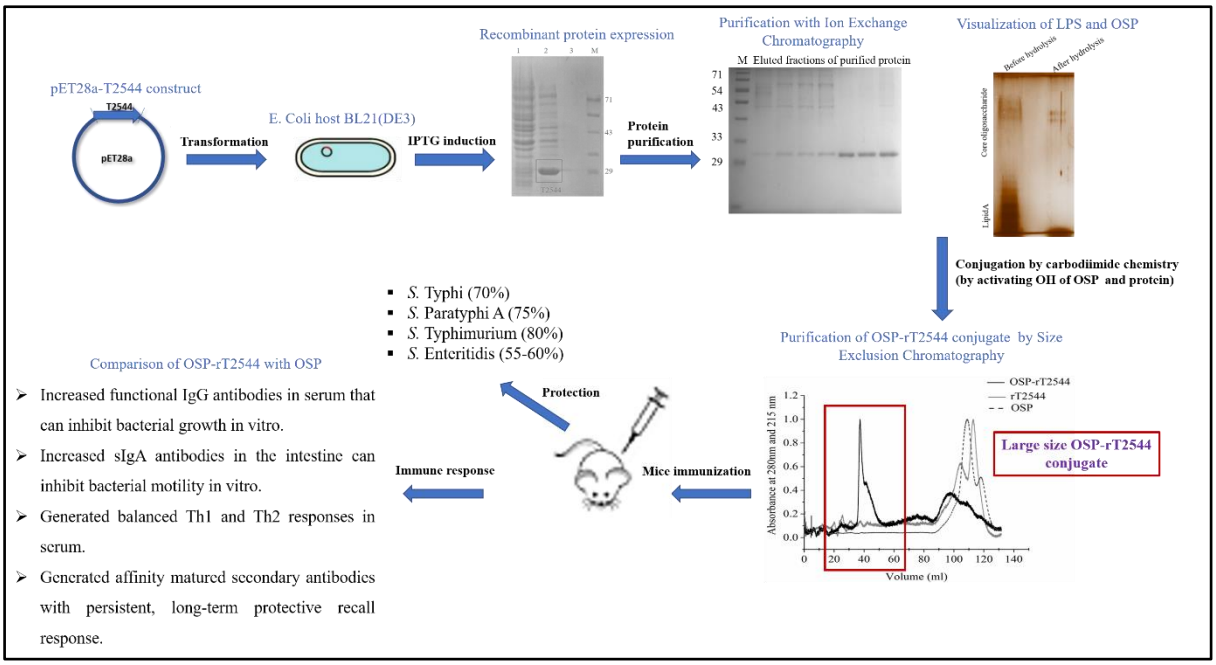

Figure 46. Summary Image 2. Summary of OSP-rT2544 immunization study.

2. We have developed a second glycoconjugate vaccine candidate, **Vi-rT2544** (**Figure 47**) that confers protection against *Salmonella* Typhi and *Salmonella* Paratyphi A. This vaccine candidate is composed of Vi (Vi polysaccharide) from *Citrobacter fruendii* and outer membrane protein T2544 from *Salmonella* Typhi. Single dose immunization with Vi-rT2544 through subcutaneous and intramuscular routes augmented the following immune responses in mice, which was compared with the response to the marketed vaccine Vi-TT(**Figure 48**).
    - Increased functional IgG antibodies (two-fold and four-fold higher following SC and IM immunization) in serum that showed inhibition of bacterial growth in vitro.
    - Increased sIgA antibodies (2-4 -fold higher) in the serum, intestine and feces.
    - Generated balanced Th1 and Th2 responses in serum while the former is the predominant.

- Generated affinity matured functional secondary antibodies (B-memory response) (8 times higher following SC and IM immunization) with persistent, long-term T memory response (10.8 % - 14.1% higher following SC and IM immunization).

As available Vi-TT vaccine is monovalent, protects only against *Salmonella* Typhi, not against *Salmonella* Paratyphi A, we are aiming to develop a bivalent Vi-based bivalent vaccine that could protect both these serovars. All these results indicated that Vi-rT2544 is a promising candidate for the development of a bivalent glycoconjugate against *Salmonella* Typhi and *Salmonella* Paratyphi A infections.

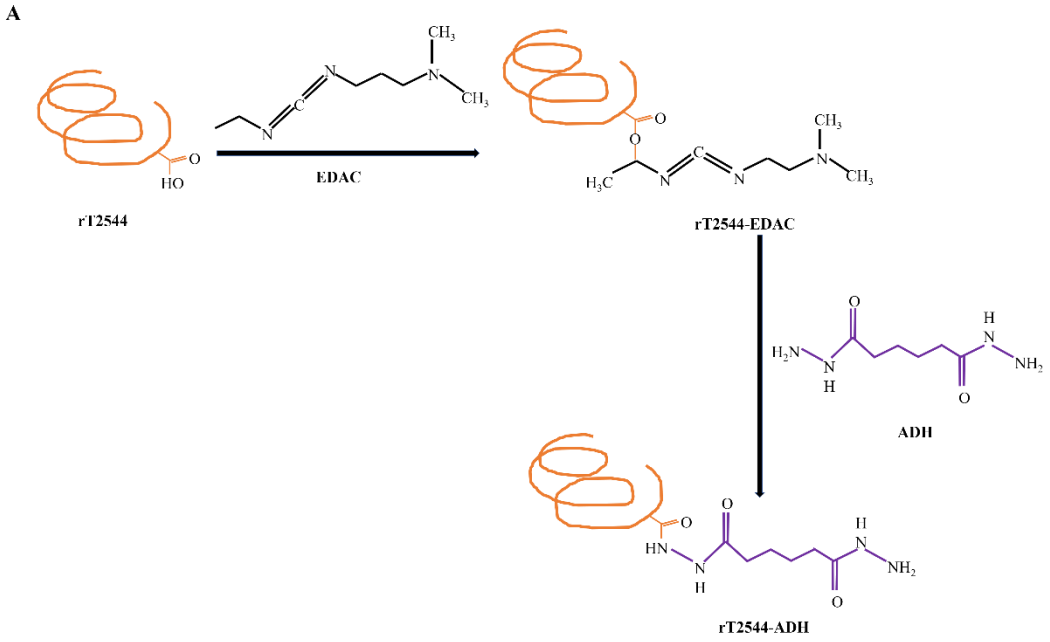

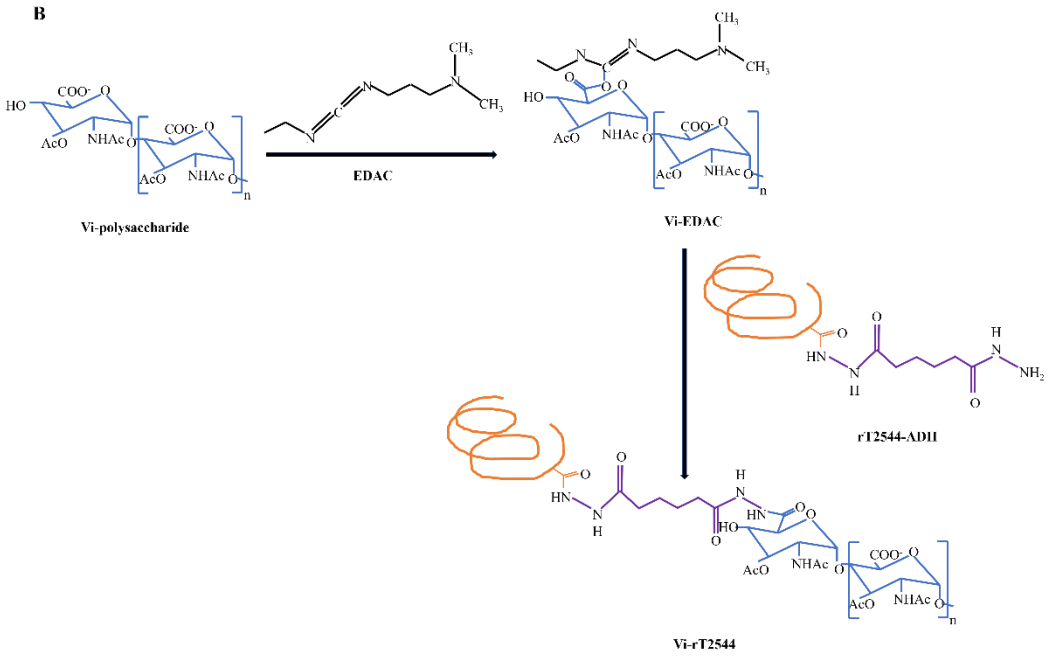

Figure 47. Summary Image 3. Schematic representation of the Summary of Vi-rT2544 conjugation chemistry. (A) rT2544 was derivatized with EDAC/ ADH. (B) Vi polysaccharide was conjugated with rT2544-ADH. [The image is created using Power Point]

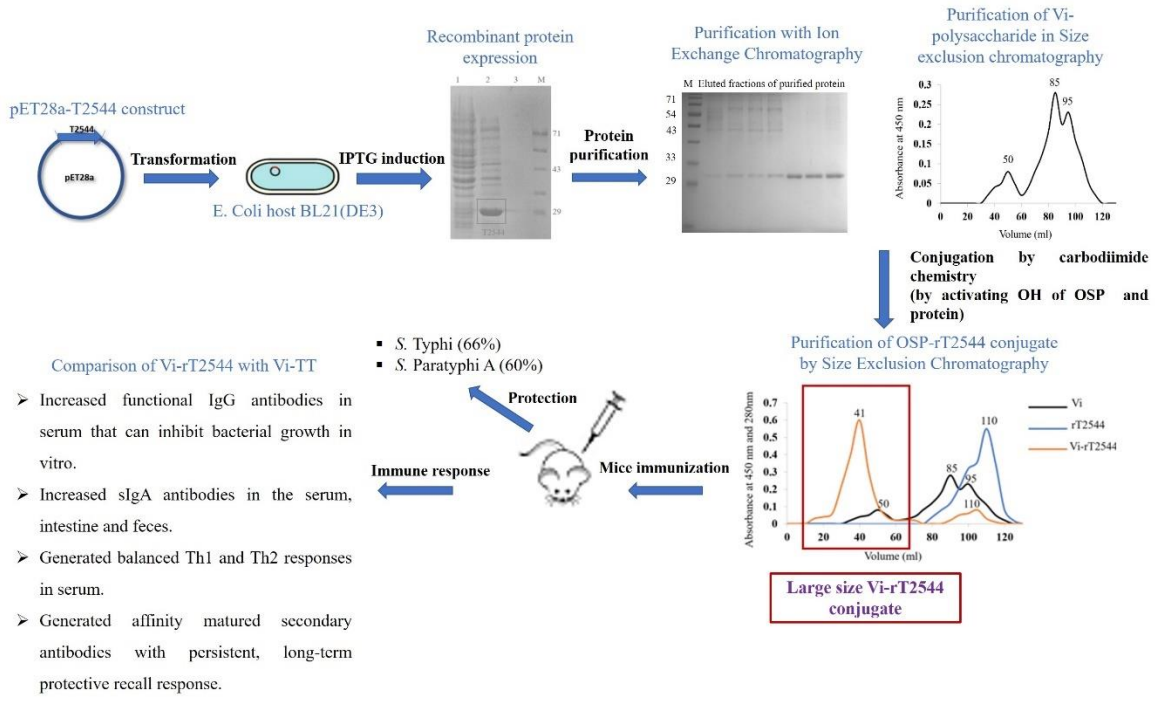

Figure 48. Summary Image 4. Summary of Vi-rT2544 immunization study.

3. We successfully established a ***Shigella*** **infection model** through oral route in adult BALB/c mice following pre-treatment of streptomycin and iron.
    - Infected mice showed diarrhoea, loss of body weight, bacterial colonization in the colon, caecum and faeces and progressive colitis characterized by shortening of the colon length, disruption of epithelial lining, loss of crypt architecture with goblet cell depletion, increased PMN infiltration into the mucosa, submucosal swelling (edema) and raised proinflammatory cytokines and chemokines in the large intestine.
    - To evaluate the usefulness of the model for vaccine efficacy studies, mice were immunized intranasally with a recombinant protein vaccine containing *Shigella* invasion protein IpaB. Vaccinated mice conferred 80-90 % protection against *Shigella flexeneri 2a*, *S. dysenteriae*, and *S. sonnei* indicating that the model is suitable for testing of vaccine candidates.
    - To protect both *Shigella* and *Salmonella*, a chimeric recombinant vaccine (**rIpaB-T2544**) was developed by fusing IpaB with *Salmonella* outer membrane protein T2544 (**Figure 49**). Vaccinated mice developed antigen-specific, serum IgG (2560 times higher IpaB-specific IgG compared with the unimmunized) and IgA antibodies (128 times, 256 times and 1280 times higher in the stool, intestinal lavage and serum compared to unimmunized) and a balanced Th1/Th2 response and were protected (80-90%) against oral challenge with *Shigella* (*S. flexneri 2a*, *S. dysenteriae*, *S. sonnei*) using our present mouse model and *Salmonella* (*Salmonella* Typhi and Paratyphi A) (60% protection) using iron overload mouse model. Additionally, it has been observed that rT2544-specific IgG (32- times higher anti-T2544 IgG) and IgA (15-20 times higher anti-T2544

IgA) antibodies were enhanced after rIpaB-T2544 immunization. This provides additional findings of the adjuvanticity of rIpaB to rT254.

No oral adult mouse model has been reported with longer disease persistence and severe inflammation so far. A Streptomycin pre-treated oral adult mouse model has been reported which is associated with shorter duration and very few PMN infiltration while another Streptomycin pre-treated oral mouse model has been reported in genetically deficient mouse to study the *Shigella* pathogenesis. Therefore, we are aiming to develop an oral *Shigella* infection in wild type mouse model to study the vaccine effectiveness. In our study, we have successfully developed this oral infection *Shigella* model in mice and vaccine efficacy of candidate vaccines showed 80-90% protection against different *Shigella* serovars was observed using our newly developed model. Therefore, this model is useful for vaccine testing studies against *Shigella* infection and the vaccine candidate rIpaB-T2544 may be used to prevent both the *Shigella* and *Salmonella* infection.

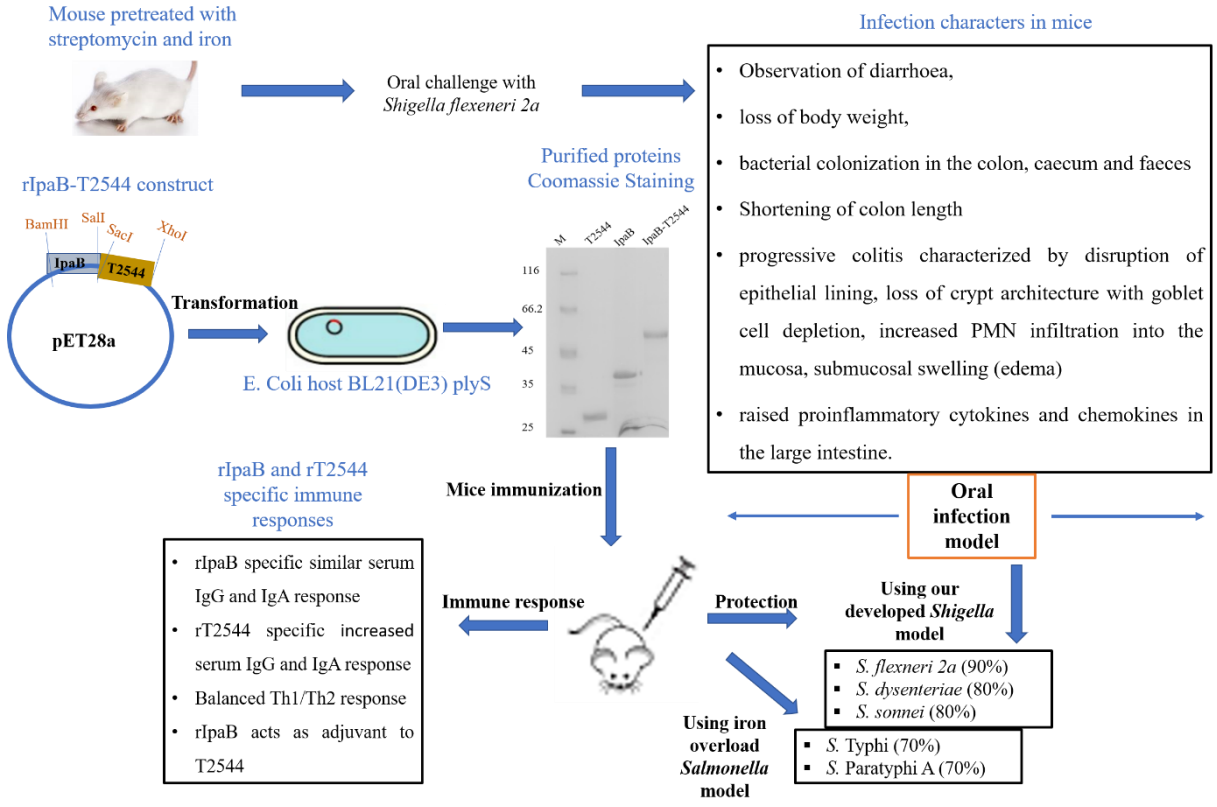

Figure 49. Summary Image 5. *Shigella* model development and rIpaB-T2544 immunization study.

Chapter 7.

Highlights of the study – salient findings.

- A multivalent glycoconjugate, **OSP-rT2544** has been developed by carbodiimide chemistry and characterized. OSP-rT2544 conferred a broad range of protection against typhoidal and non-typhoidal *Salmonella* and induces protective humoral and functional sIgA response and generates long lived protective memory (B memory and T memory) response.

- A bivalent glycoconjugate **Vi-rT2544** has been developed by carbodiimide chemistry and characterized. Vi-rT2544 conferred protection against *Salmonella* Typhi and *Salmonella* Paratyphi A and induces Vi-specific significantly higher IgG, IgA responses, secondary antibodies with higher avidity with B-memory and effector memory T cells compared to Vi-TT.

- Both OSP-rT2544 and Vi-rT2544 generates balanced Th1 and Th2 serum cytokine response.

- An oral mouse model of shigellosis was successfully established. Oral infection with *Shigella flexneri 2a* caused weight loss, shortening of the colon, bacterial colonization with severe tissue destruction, and inflammation in the large intestine (colon and caecum) of adult BALB/c mice.

- Recombinant IpaB protects mice against different *Shigella* serovars and validate this model for vaccine efficacy study against *Shigella* infection.

- Intranasal immunization with recombinant IpaB-T2544 chimera protects mice against different serovars of *Shigella* challenge using our established oral *Shigella* mouse model. IpaB-T2544 chimera also protects mice from oral challenge of *Salmonella* Typhi and Paratyphi A using iron overload mouse model. Humoral and mucosal adjuvanticity of rIpaB and balanced Th1 and Th2 cytokines from splenocytes was observed from rIpaB-T2544 immunized mice.

Chapter 8.

Bibliography

1. Andino A, Hanning I. Salmonella enterica: survival, colonization, and virulence differences among serovars. ScientificWorldJournal. 2015;2015:520179. doi: 10.1155/2015/520179. Epub 2015 Jan 13. PMID: 25664339; PMCID: PMC4310208
2. Crum-Cianflone NF. Salmonellosis and the gastrointestinal tract: more than just peanut butter. Curr Gastroenterol Rep. 2008 Aug;10(4):424-31. doi: 10.1007/s11894-008-0079-7. PMID: 18627657; PMCID: PMC2753534.
3. Lamichhane, B.; Mawad, A.M.M.; Saleh, M.; Kelley, W.G.; Harrington, P.J., II; Lovestad, C.W.; Amezcua, J.; Sarhan, M.M.; El Zowalaty, M.E.; Ramadan, H.; et al. Salmonellosis: An Overview of Epidemiology, Pathogenesis, and Innovative Approaches to Mitigate the Antimicrobial Resistant Infections. *Antibiotics* **2024**, *13*, 76. https://doi.org/10.3390/antibiotics13010076
4. Dougan G, Baker S. Salmonella enterica serovar Typhi and the pathogenesis of typhoid fever. Annu Rev Microbiol 2014;68:317-36.
5. Edsall, G., Gaines, S., Landy, M., Tigertt, W.D., Sprinz, H., Trapani, R.J., Mandel, A.D., and Benenson, A.S. (1960). Studies on infection and immunity in experimental typhoid fever. I. Typhoid fever in chimpanzees orally infected with Salmonella typhosa. The Journal of experimental medicine 112, 143-166.
6. Barrow, P.A., Huggins, M.B., and Lovell, M.A. (1994). Host specificity of Salmonella infection in chickens and mice is expressed in vivo primarily at the level of the reticuloendothelial system. Infection and immunity 62, 4602-4610.
7. Wray, C., and Sojka, W.J. (1977). Reviews of the progress of dairy science: bovine salmonellosis. The Journal of dairy research 44, 383-425.
8. Nnalue, N.A. (1991). Relevance of inoculation route to virulence of three Salmonella spp. strains in mice. Microbial pathogenesis 11, 11-18.
9. Smith, H.W., and Jones, J.E. (1967). Observations on experimental oral infection with Salmonella dublin in calves and Salmonella choleraesuis in pigs. The Journal of pathology and bacteriology 93, 141-156.
10. A. Rodriguez, P. Pangloli, H. A. Richards, J. R. Mount, and F. A. Draughon, "Prevalence of Salmonella in diverse environmental farm samples," Journal of Food Protection, vol. 69, no. 11, pp. 2576–2580, 2006., W. Rabsch, H. Tschape, and A. J. B ¨ aumler, "Non-typhoidal ¨ salmonellosis: emerging problems," Microbes and Infection, vol. 3, no. 3, pp. 237–247, 2001
11. DuPont, H.L., Levine, M.M., Hornick, R.B. and Formal, S.B. (1989) Inoculum size in shigellosis and implications for expected mode of transmission. J. Infect. Dis. 159, 1126–1127.
12. Small P, Blankenhorn D, Welty D, Zinser E, Slonczewski JL. Acid and base resistance in Escherichia coli and Shigella flexneri: role of rpoS and growth pH. J Bacteriol. 1994 Mar;176(6):1729-37. doi: 10.1128/jb.176.6.1729-1737.1994. PMID: 8132468; PMCID: PMC205261.
13. Philpott DJ, Edgeworth JD, Sansonetti PJ. The pathogenesis of Shigella flexneri infection: lessons from in vitro and in vivo studies. Philos Trans R Soc Lond B Biol Sci. 2000 May 29;355(1397):575-86. doi: 10.1098/rstb.2000.0599. PMID: 10874731; PMCID: PMC1692768.
14. Sansonetti PJ. War and peace at mucosal surfaces. Nat Rev Immunol. 2004 Dec;4(12):953-64. doi: 10.1038/nri1499. PMID: 15573130.

15. Sansonetti PJ, Arondel J, Cantey JR, Prévost MC, Huerre M. Infection of rabbit Peyer's patches by Shigella flexneri: effect of adhesive or invasive bacterial phenotypes on follicle-associated epithelium. Infect Immun. 1996 Jul;64(7):2752-64. doi: 10.1128/iai.64.7.2752-2764.1996. PMID: 8698505; PMCID: PMC174136.
16. Wassef JS, Keren DF, Mailloux JL. Role of M cells in initial antigen uptake and in ulcer formation in the rabbit intestinal loop model of shigellosis. Infect Immun. 1989 Mar;57(3):858-63. doi: 10.1128/iai.57.3.858-863.1989. PMID: 2645214; PMCID: PMC313189.
17. Man AL, Prieto-Garcia ME, Nicoletti C. Improving M cell mediated transport across mucosal barriers: do certain bacteria hold the keys? Immunology. 2004 Sep;113(1):15-22. doi: 10.1111/j.1365-2567.2004.01964.x. PMID: 15312131; PMCID: PMC1782554.
18. Phalipon A, Sansonetti PJ. Shigella's ways of manipulating the host intestinal innate and adaptive immune system: a tool box for survival? Immunol Cell Biol. 2007 Feb-Mar;85(2):119-29. doi: 10.1038/sj.icb7100025. Epub 2007 Jan 9. PMID: 17213832.
19. Martino MC, Rossi G, Martini I, Tattoli I, Chiavolini D, Phalipon A, Sansonetti PJ, Bernardini ML. 2005. Mucosal lymphoid infiltrate domi nates colonic pathological changes in murine experimental shigellosis. J Infect Dis 192:136–148 http://dx.doi.org/10.1086/430740.
20. Faherty CS, Redman JC, Rasko DA, Barry EM, Nataro JP. 2012. Shigella flexneri effectors OspE1 and OspE2 mediate induced adherence to the colonic epithelium following bile salts exposure. Mol Microbiol 85: 107–121 http://dx.doi.org/10.1111/j.1365-2958.2012.08092.x.
21. Richter-Dahlfors A, Buchan AMJ, Finlay BB. Murine Salmonellosis studied by confocal microscopy: Salmonella Typhimurium resides intracellularly inside macrophages and exerts a cytotoxic effect on phagocytes in vivo. J Exp Med (1997) 186(4):569–80. doi:10.1084/jem.186.4.569
22. Yrlid U, Svensson M, Håkansson A, Chambers BJ, Ljunggren HG, Wick MJ. In vivo activation of dendritic cells and T cells during Salmonella enterica serovar Typhimurium infection. Infect Immun (2001) 69(9):5726–35. doi:10.1128/IAI. 69.9.5726-5735.2001
23. Grimont PAD, Weill F-X. Antigenic formulae of the Salmonellae serovars. WHO Collab Cent Ref Res Salmonella. 2007;9th ed Ins.
24. Popoff MY, Le Minor L. Antigenic formulas of the Salmonella serovars. 8th revision. WHO Collab Cent Ref Res Salmonella Paris, Inst Pasteur. 2001
25. McQuiston JR, Parrenas R, Ortiz-Rivera M, Gheesling L, Brenner F, Fields PI. Sequencing and comparative analysis of flagellin genes fliC, fljB, and flpA from Salmonella. J Clin Microbiol. 2004;42: 1923–1932.
26. Fierer J, Guiney DG. Diverse virulence traits underlying different clinical outcomes of Salmonella infection. J Clin Invest (2001) 107(7):775–80. doi:10.1172/ JCI12561
27. Popoff MY, Bockemuhl J, Gheesling LL, Bockemühl J, Gheesling LL. Supplement 2002 (no. 46) to the Kauffmann-White scheme. Res Microbiol. 2004;155: 568–570.
28. McClelland M, Sanderson KE, Spieth J, Clifton SW, Latreille P, Courtney L, et al. Complete genome sequence of Salmonella enterica serovar Typhimurium LT2. Nature. 2001;413: 852–856.
29. Baumler AJ, Tsolis RM, Ficht TA, Adams LG. Evolution of host adaptation in Salmonella enterica. Infect Immun. 1998;66: 4579–4587.

30. Shiga K. Observations on the epidemiology of dysentery in Japan. Philippine J Sci 1906;1:485 500.
31. Ewing WH. Shigella nomenclature. J Bacteriol 1949;57:633 8.
32. Ewing WH. Edwards and Ewing's Identification of the Enterobacteriaceae. 4th ed. Amsterdam: Elsevier Science Publishers; 1986.
33. Jacob, J.J., Solaimalai, D., Muthuirulandi Sethuvel, D.P. et al. A nineteen-year report of serotype and antimicrobial susceptibility of enteric non-typhoidal Salmonella from humans in Southern India: changing facades of taxonomy and resistance trend. Gut Pathog 12, 49 (2020). https://doi.org/10.1186/s13099-020-00388-z
34. Grimont F, Lejay-Collin M, Talukder KA, Carle I, Issenhuth S, Le Roux K, et al. Identification of a group of Shigella-like isolates as Shigella boydii 20. J Med Microbiol 2007;56:749 54.
35. Luo X, Sun Q, Lan R, Wang J, Li Z, Xia S, et al. Emergence of a novel Shigella flexneri serotype 1d in China. Diagn Microbiol Infect Dis 2012;74:316 9.
36. Typhoid, G.B.D. and C. Paratyphoid, The global burden of typhoid and paratyphoid fevers: a systematic analysis for the Global Burden of Disease Study 2017. Lancet Infect Dis, 2019. **19**(4): p. 369-381.
37. Kim, S., et al., Spatial and Temporal Patterns of Typhoid and Paratyphoid Fever Outbreaks: A Worldwide Review, 1990-2018. Clin Infect Dis, 2019. **69**(Suppl 6): p. S499-S509.
38. Hancuh, M., et al., Typhoid Fever Surveillance, Incidence Estimates, and Progress Toward Typhoid Conjugate Vaccine Introduction - Worldwide, 2018-2022. MMWR Morb Mortal Wkly Rep, 2023. **72**(7): p. 171-176.
39. Ochiai, R.L., et al., A study of typhoid fever in five Asian countries: disease burden and implications for controls. Bull World Health Organ, 2008. **86**(4): p. 260-8.
40. Sinha, A., et al., Typhoid fever in children aged less than 5 years. Lancet, 1999. **354**(9180): p. 734-7.
41. Sur, D., et al., The malaria and typhoid fever burden in the slums of Kolkata, India: data from a prospective community-based study. Trans R Soc Trop Med Hyg, 2006. **100**(8): p. 725-33.
42. Cao, Y., et al., Geographic Pattern of Typhoid Fever in India: A Model-Based Estimate of Cohort and Surveillance Data. J Infect Dis, 2021. **224**(224 Supple 5): p. S475-S483.
43. John, J., et al., Burden of Typhoid and Paratyphoid Fever in India. N Engl J Med, 2023. **388**(16): p. 1491-1500.
44. Saxena, S.N. and R. Sen, Salmonella paratyphi A infection in India: incidence and phage types. Trans R Soc Trop Med Hyg, 1966. **60**(3): p. 409-11.
45. Mohanty, S., et al., Antibiogram pattern and seasonality of Salmonella serotypes in a North Indian tertiary care hospital. Epidemiol Infect, 2006. **134**(5): p. 961-6.
46. Mendiratta, D.K., et al., Enteric fever due to S. paratyphia - an emerging problem. Indian J Med Microbiol, 2004. **22**(3): p. 196.
47. Verma, S., et al., Emerging Salmonella Paratyphi A enteric fever and changing trends in antimicrobial resistance pattern of salmonella in Shimla. Indian J Med Microbiol, 2010. **28**(1): p. 51-3.
48. Gupta, V., J. Kaur, and J. Chander, An increase in enteric fever cases due to Salmonella Paratyphi A in & around Chandigarh. Indian J Med Res, 2009. **129**(1): p. 95-8.
49. John, J., C.J. Van Aart, and N.C. Grassly, The Burden of Typhoid and Paratyphoid in India: Systematic Review and Meta-analysis. PLoS Negl Trop Dis, 2016. **10**(4): p. e0004616.

50. Balasubramanian, R.; Im, J.; Lee, J.S.; Jeon, H.J.; Mogeni, O.D.; Kim, J.H.; Rakotozandrindrainy, R.; Baker, S.; Marks, F. The global burden and epidemiology of invasive non-typhoidal Salmonella infections. Hum. Vaccin. Immunother. 2019, 15, 1421–1426.
51. Stanaway, J.D.; Parisi, A.; Sarkar, K.; Blacker, B.F.; Reiner, R.C.; Hay, S.I.; Nixon, M.R.; Dolecek, C.; James, S.L.; Mokdad, A.H. The global burden of non-typhoidal Salmonella invasive disease: A systematic analysis for the Global Burden of Disease Study 2017. Lancet Infect. Dis. 2019, 19, 1312–1324.
52. Kennedy, M.; Villar, R.; Vugia, D.J.; Rabatsky-Ehr, T.; Farley, M.M.; Pass, M.; Smith, K.; Smith, P.; Cieslak, P.R.; Imhoff, B.; et al. Hospitalizations and deaths due to Salmonella infections, FoodNet, 1996–1999. Clin. Infect. Dis. 2004, 38 (Suppl. 3), S142–S148.
53. Varma, J.K.; Molbak, K.; Barrett, T.J.; Beebe, J.L.; Jones, T.F.; Rabatsky-Ehr, T.; Smith, K.E.; Vugia, D.J.; Chang, H.G.; Angulo, F.J. Antimicrobial-resistant nontyphoidal Salmonella is associated with excess bloodstream infections and hospitalizations. J. Infect. Dis. 2005, 191, 554–561.
54. Parry, C.M.; Thomas, S.; Aspinall, E.J.; Cooke, R.P.; Rogerson, S.J.; Harries, A.D.; Beeching, N.J. A retrospective study of secondary bacteraemia in hospitalised adults with community acquired non-typhoidal Salmonella gastroenteritis. BMC Infect. Dis. 2013, 13, 107.
55. Crump, J.A.; Sjölund-Karlsson, M.; Gordon, M.A.; Parry, C.M. Epidemiology, Clinical Presentation, Laboratory Diagnosis, Antimicrobial Resistance, and Antimicrobial Management of Invasive Salmonella Infections. Clin. Microbiol. Rev. 2015, 28, 901–937.
56. Stanaway, J.D.; Parisi, A.; Sarkar, K.; Blacker, B.F.; Reiner, R.C.; Hay, S.I.; Nixon, M.R.; Dolecek, C.; James, S.L.; Mokdad, A.H. The global burden of non-typhoidal Salmonella invasive disease: A systematic analysis for the Global Burden of Disease Study 2017. Lancet Infect. Dis. 2019, 19, 1312–1324.
57. Uche, I.V.; MacLennan, C.A.; Saul, A. A Systematic Review of the Incidence, Risk Factors and Case Fatality Rates of Invasive Nontyphoidal Salmonella (iNTS) Disease in Africa (1966 to 2014). PLoS Negl. Trop. Dis. 2017, 11, e0005118.
58. Gilchrist, J.J.; MacLennan, C.A. Invasive Nontyphoidal Salmonella Disease in Africa. EcoSal Plus 2019, 8, 10–1128.
59. Majowicz, S.E.; Musto, J.; Scallan, E.; Angulo, F.J.; Kirk, M.; O'Brien, S.J.; Jones, T.F.; Fazil, A.; Hoekstra, R.M. The global burden of nontyphoidal Salmonella gastroenteritis. Clin. Infect. Dis. 2010, 50, 882–889.
60. Murray, C.J.; Vos, T.; Lozano, R.; Naghavi, M.; Flaxman, A.D.; Michaud, C.; Ezzati, M.; Shibuya, K.; Salomon, J.A.; Abdalla, S.; et al. Disability-adjusted life years (DALYs) for 291 diseases and injuries in 21 regions, 1990–2010: A systematic analysis for the Global Burden of Disease Study 2010. Lancet 2012, 380, 2197–2223.
61. Lozano, R.P.; Naghavi, M.P.; Lim, S.P.; Aboyans, V.P.; Abraham, J.M.P.H.; Adair, T.P.; Ahn, S.Y.M.P.H.; AlMazroa, M.A.M.D.; Anderson, H.R.P.; Anderson, L.M.P.; et al. Global and regional mortality from 235 causes of death for 20 age groups in 1990 and 2010: A systematic analysis for the Global Burden of Disease Study 2010. Lancet 2012, 380, 2095–2128.

62. World Health Organization. WHO Estimates of the Global Burden of Foodborne Diseases: Foodborne Disease Burden Epidemiology Reference Group 2007–2015; World Health Organization: Geneva, Switzerland, 2015.
63. WordBank. Global Burden of Disease Study 2019 (GBD 2019) Cause, REI, and Location Hierarchies; Institute for Health Metrics and Evaluation (IHME): Seattle, WA, USA, 2020.
64. Marchello, C.S.; Birkhold, M.; Crump, J.A.; Martin, L.B.; Ansah, M.O.; Breghi, G.; Canals, R.; Fiorino, F.; Gordon, M.A.; Kim, J.-H.; et al. Complications and mortality of non-typhoidal Salmonella invasive disease: A global systematic review and meta-analysis. Lancet Infect. Dis. 2022, 22, 692–705.
65. Jacob JJ, Solaimalai D, Muthuirulandi Sethuvel DP, Rachel T, Jeslin P, Anandan S, Veeraraghavan B. A nineteen-year report of serotype and antimicrobial susceptibility of enteric non-typhoidal *Salmonella* from humans in Southern India: changing facades of taxonomy and resistance trend. Gut Pathog. 2020 Oct 23;12:49. doi: 10.1186/s13099-020-00388-z. PMID: 33110449; PMCID: PMC7585187.
66. Ballal M, Devadas SM, Shetty V, Bangera SR, Ramamurthy T, Sarkar A. Emergence and serovar profiling of non-typhoidal Salmonellae (NTS) isolated from gastroenteritis cases-A study from South India. Infect Dis (Lond). 2016 Nov-Dec;48(11-12):847-51. doi: 10.3109/23744235.2016.1169553. Epub 2016 Jun 14. PMID: 27300440.
67. Sudhaharan S, Kanne P, Vemu L, Bhaskara A. Extraintestinal infections caused by nontyphoidal *Salmonella* from a tertiary care center in India. J Lab Physicians. 2018 Oct-Dec;10(4):401-405. doi: 10.4103/JLP.JLP_79_18. PMID: 30498311; PMCID: PMC6210840.
68. Kumar S, Kumar Y, Kumar G, Kumar G, Tahlan AK. Non-typhoidal *Salmonella* infections across India: emergence of a neglected group of enteric pathogens. J Taibah Univ Med Sci. 2022 Mar 7;17(5):747-754. doi: 10.1016/j.jtumed.2022.02.011. PMID: 36050954; PMCID: PMC9396057.
69. Dhanashree B, Shenoy S. Clinical-Microbiological Study of Nontyphoidal Salmonella Infections from Karnataka, India. Scientifica (Cairo). 2024 Jul 16;2024:6620871. doi: 10.1155/2024/6620871. PMID: 39045390; PMCID: PMC11265940.
70. Libby, T.E.; Delawalla, M.L.; Al-Shimari, F.; MacLennan, C.A.; Vannice, K.S.; Pavlinac, P.B. Consequences of Shigella infection in young children: A systematic review. *Int. J. Infect. Dis.* **2023**, *129*, 78–95.
71. Livio, S.; Strockbine, N.A.; Panchalingam, S.; Tennant, S.M.; Barry, E.M.; Marohn, M.E.; Antonio, M.; Hossain, A.; Mandomando, I.; Ochieng, J.B.; et al. Shigella Isolates From the Global Enteric Multicenter Study Inform Vaccine Development. *Clin. Infect. Dis.* **2014**, *59*, 933–941.
72. Cohen, D.; Korin, H.; Bassal, R.; Markovich, M.P.; Sivan, Y.; Goren, S.; Muhsen, K. Burden and risk factors of Shigella sonnei shigellosis among children aged 0–59 months in hyperendemic communities in Israel. *Int. J. Infect. Dis.* **2019**, *82*, 117–123.
73. European Centre for Disease Prevention and Control. Shigellosis. In: ECDC. Annual epidemiological report for 2017. Stockholm: ECDC; 2020.
74. Khalil, I.A.; Troeger, C.; Blacker, B.F.; Rao, P.C.; Brown, A.; Atherly, D.E.; Brewer, T.G.; Engmann, C.M.; Houpt, E.R.; Kang, G.; et al. Morbidity and mortality due to shigella and enterotoxigenic

Escherichia coli diarrhoea: The Global Burden of Disease Study 1990–2016. Lancet Infect. Dis. 2018, 18, 1229–1240.

75. Kotloff, K.L.; Nataro, J.P.; Blackwelder, W.C.; Nasrin, D.; Farag, T.H.; Panchalingam, S.; Wu, Y.; Sow, S.O.; Sur, D.; Breiman, R.F.; et al. Burden and aetiology of diarrhoeal disease in infants and young children in developing countries (the Global Enteric Multicenter Study, GEMS): A prospective, case-control study. Lancet 2013, 382, 209–222.
76. Livio, S.; Strockbine, N.A.; Panchalingam, S.; Tennant, S.M.; Barry, E.M.; Marohn, M.E.; Antonio, M.; Hossain, A.; Mandomando, I.; Ochieng, J.B.; et al. Shigella Isolates from the Global Enteric Multicenter Study Inform Vaccine Development. Clin. Infect. Dis. 2014, 59, 933–941.
77. Liu, J.; Platts-Mills, J.A.; Juma, J.; Kabir, F.; Nkeze, J.; Okoi, C.; Operario, D.J.; Uddin, J.; Ahmed, S.; Alonso, P.L.; et al. Use of quantitative molecular diagnostic methods to identify causes of diarrhoea in children: A reanalysis of the GEMS case-control study. Lancet 2016, 388, 1291–1301.
78. Kahsay, A.G.; Muthupandian, S. A review on Sero diversity and antimicrobial resistance patterns of Shigella species in Africa, Asia and South America, 2001–2014. BMC Res Notes 2016, 9, 422.
79. Puzari, M.; Sharma, M.; Chetia, P. Emergence of antibiotic resistant Shigella species: A matter of concern. J. Infect. Public Health 2018, 11, 451–454.
80. 35. Qu,F.; Bao, C.; Chen, S.; Cui, E.; Guo, T.; Wang, H.; Zhang, J.; Wang, H.; Tang, Y.W.; Mao, Y. Genotypes and antimicrobial profiles of Shigella sonnei isolates from diarrheal patients circulating in Beijing between 2002 and 2007. Diagn. Microbiol. Infect. Dis. 2012, 74, 166–170.
81. Thompson, C.N.; Duy, P.T.; Baker, S. The Rising Dominance of Shigella sonnei: An Intercontinental Shift in the Etiology of Bacillary Dysentery. PLoS Negl. Trop. Dis. 2015, 9, e0003708.
82. Ud-Din, A.I.; Wahid, S.U.; Latif, H.A.; Shahnaij, M.; Akter, M.; Azmi, I.J.; Hasan, T.N.; Ahmed, D.; Hossain, M.A.; Faruque, A.S.; et al. Changing trends in the prevalence of Shigella species: Emergence of multi-drug resistant Shigella sonnei biotype g in Bangladesh. PLoS ONE 2013, 8, e82601.
83. Bangtrakulnonth, A.; Vieira, A.R.; Lo Fo Wong, D.M.A.; Pornreongwong, S.; Pulsrikarn, S.; Sawanpanyalert, P.; Hendriksen, R.S.; Aarestrup, F.M. Shigella from Humans in Thailand During 1993 to 2006: Spatial-Time Trends in Species and Serotype Distribution. Foodborne Pathog. Dis. 2008, 5, 773–784.
84. Vinh, H.; Nhu, N.T.; Nga, T.V.; Duy, P.T.; Campbell, J.I.; Hoang, N.V.; Boni, M.F.; My, P.V.; Parry, C.; Nga, T.T.; et al. A changing picture of shigellosis in southern Vietnam: Shifting species dominance, antimicrobial susceptibility and clinical presentation. BMCInfect. Dis. 2009, 9, 204.
85. Zarei, M.; Ghahfarokhi, M.E.; Fazlara, A.; Bahrami, S. Effect of the bacterial growth phase and coculture conditions on the interaction of Acanthamoeba castellanii with Shigella dysenteriae, Shigella flexneri, and Shigella sonnei. J. Basic Microbiol. 2019, 59, 735–743.
86. Shah, N.; DuPont, H.L.; Ramsey, D.J. Global Etiology of Travelers' Diarrhea: Systematic Review from 1973 to the Present Am. J. Trop. Med. Hyg. 2009, 4, 609–614.
87. Mani,S.; Wierzba, T.; Walker, R.I. Status of vaccine research and development for Shigella. Vaccine 2016, 34, 2887–2894.
88. Bardhan, P.; Faruque, A.S.; Naheed, A.; Sack, D.A. Decrease in shigellosis-related deaths without Shigella spp.-specific interven tions, Asia. Emerg. Infect. Dis. 2010, 16, 1718–1723.

89. Gu,B.; Cao, Y.; Pan, S.; Zhuang, L.; Yu, R.; Peng, Z.; Qian, H.; Wei, Y.; Zhao, L.; Liu, G.; et al. Comparison of the prevalence and changing resistance to nalidixic acid and ciprofloxacin of Shigella between Europe-America and Asia-Africa from 1998 to 2009. Int. J. Antimicrob. Agents 2012, 40, 9–17.
90. Taneja, N.; Mewara, A. Shigellosis: Epidemiology in India. Indian J. Med. Res. 2016, 143, 565–576.
91. Muthuirulandi Sethuvel, D.P.; Devanga Ragupathi, N.K.; Anandan, S.; Veeraraghavan, B. Update on: Shigella new serogroups/serotypes and their antimicrobial resistance. Lett. Appl. Microbiol. 2017, 64, 8–18.
92. von Seidlein L, Kim DR, Ali M, Hyejon Lee H, Wang X, Thiem VD, et al. A multicentre study of Shigella diarrhoea in six Asian countries: disease burden, clinical manifestations, and microbiology. PLoS Med 2006; 3 : e353.
93. Taneja N, Khurana S, Verma AD, Sharma M. Changing trends in shigellosis at a tertiary care centre. Indian J Pathol Microbiol 2003; 46 : 280-1.
94. Pazhani GP, Ramamurthy T, Mitra U, Bhattacharya SK, Niyogi SK. Species diversity and antimicrobial resistance of Shigella spp. isolated between 2001 and 2004 from hospitalized children with diarrhoea in Kolkata (Calcutta), India. Epidemiol Infect 2005; 133 : 1089-95.
95. Livio S, Strockbine NA, Panchalingam S, Tennant SM, Barry EM, Marohn ME, et al. Shigella isolates from the Global Enteric Multicenter Study Inform Vaccine Development. Clin Infect Dis 2014; 59 : 933-41.
96. Bhattacharya D, Bhattacharya H, Thamizhmani R, Sayi DS, Reesu R, Anwesh M, et al. Shigellosis in Bay of Bengal Islands, India: clinical and seasonal patterns, surveillance of antibiotic susceptibility patterns, and molecular characterization of multidrug-resistant Shigella strains isolated during a 6-year period from 2006 to 2011. Eur J Clin Microbiol Infect Dis 2014; 33 : 157-70.
97. Basilua Andre Muzembo, Kei Kitahara, Debmalya Mitra, Ayumu Ohno, Januka Khatiwada, Shanta Dutta, Shin-Ichi Miyoshi, Burden of *Shigella* in South Asia: a systematic review and meta-analysis, *Journal of Travel Medicine*, Volume 30, Issue 1, January 2023, taac132, https://doi.org/10.1093/jtm/taac132
98. Foster JW, Hall HK. Inducible pH homeostasis and the acid tolerance response of Salmonella typhimurium. J Bacteriol. (1991) 173:5129– 35. doi: 10.1128/JB.173.16.5129-5135.1991
99. Jones, B.D., Ghori, N., and Falkow, S. (1994). Salmonella typhimurium initiates murine infection by penetrating and destroying the specialized epithelial M cells of the Peyer's patches. The Journal of experimental medicine 180, 15-23.
100. Rescigno, M., Urbano, M., Valzasina, B., Francolini, M., Rotta, G., Bonasio, R., Granucci, F., Kraehenbuhl, J.P., and Ricciardi-Castagnoli, P. (2001). Dendritic cells express tight junction proteins and penetrate gut epithelial monolayers to sample bacteria. Nature immunology 2, 361-367.
101. Vazquez-Torres, A., Jones-Carson, J., Baumler, A.J., Falkow, S., Valdivia, R., Brown, W., Le, M., Berggren, R., Parks, W.T., and Fang, F.C. (1999). Extraintestinal dissemination of Salmonella by CD18-expressing phagocytes. Nature 401, 804-808.
102. Nakoneczna, I., and Hsu, H.S. (1980). The comparative histopathology of primary and secondary lesions in murine salmonellosis. British journal of experimental pathology 61, 76-84.

103. Richter-Dahlfors, A., Buchan, A.M., and Finlay, B.B. (1997). Murine salmonellosis studied by confocal microscopy: Salmonella typhimurium resides intracellularly inside macrophages and exerts a cytotoxic effect on phagocytes in vivo. The Journal of experimental medicine 186, 569-580.
104. Yrlid, U., Svensson, M., Hakansson, A., Chambers, B.J., Ljunggren, H.G., and Wick, M.J. (2001). In vivo activation of dendritic cells and T cells during Salmonella enterica serovar Typhimurium infection. Infection and immunity 69, 5726-5735.
105. Mellouk N, Weiner A, Aulner N, Schmitt C, Elbaum M, Shorte SL, Danckaert A, Enninga J. 2014. Shigella subverts the host recycling com partment to rupture its vacuole. Cell Host Microbe 16:517–530 http://dx .doi.org/10.1016/j.chom.2014.09.005.
106. Niebuhr K, Giuriato S, Pedron T, Philpott DJ, Gaits F, Sable J, Sheetz MP, Parsot C, Sansonetti PJ, Payrastre B. 2002. Conversion of PtdIns(4,5)P (2) into PtdIns(5)P by the S.flexneri effector IpgD reorganizes host cell mor phology. EMBO J 21:5069–5078 http://dx.doi.org/10.1093/emboj/cdf522.
107. Zhang XL, Tsui IS, Yip CM, Fung AW, Wong DK, Dai X, Yang Y, Hackett J, Morris C. Salmonella enterica serovar typhi uses type IVB pili to enter human intestinal epithelial cells. Infect Immun. 2000 Jun;68(6):3067-73. doi: 10.1128/IAI.68.6.3067-3073.2000. PMID: 10816445; PMCID: PMC97533.
108. Bishop A, House D, Perkins T, Baker S, Kingsley RA, Dougan G. Interaction of Salmonella enterica serovar Typhi with cultured epithelial cells: roles of surface structures in adhesion and invasion. Microbiology (Reading). 2008 Jul;154(Pt 7):1914-1926. doi: 10.1099/mic.0.2008/016998-0. PMID: 18599820; PMCID: PMC2652038.
109. Bravo D, Blondel CJ, Hoare A, Leyton L, Valvano MA, Contreras I. Type IV(B) pili are required for invasion but not for adhesion of Salmonella enterica serovar Typhi into BHK epithelial cells in a cystic fibrosis transmembrane conductance regulator-independent manner. Microb Pathog. 2011 Nov;51(5):373-7. doi: 10.1016/j.micpath.2011.07.005. Epub 2011 Jul 18. PMID: 21782926.
110. Crago AM, Koronakis V. Binding of extracellular matrix laminin to Escherichia coli expressing the Salmonella outer membrane proteins Rck and PagC. FEMS Microbiol Lett. 1999 Jul 15;176(2):495-501. doi: 10.1111/j.1574-6968.1999.tb13703.x. PMID: 10427733.
111. Lambert MA, Smith SG. The PagN protein mediates invasion via interaction with proteoglycan. FEMS Microbiol Lett. 2009 Aug;297(2):209-16. doi: 10.1111/j.1574-6968.2009.01666.x. Epub 2009 Jun 3. PMID: 19552707.
112. Ghosh S, Chakraborty K, Nagaraja T, Basak S, Koley H, Dutta S, Mitra U, Das S. An adhesion protein of Salmonella enterica serovar Typhi is required for pathogenesis and potential target for vaccine development. Proc Natl Acad Sci U S A. 2011 Feb 22;108(8):3348-53. doi: 10.1073/pnas.1016180108. Epub 2011 Feb 7. PMID: 21300870; PMCID: PMC3044360.
113. Dorsey CW, Laarakker MC, Humphries AD, Weening EH, Bäumler AJ. Salmonella enterica serotype Typhimurium MisL is an intestinal colonization factor that binds fibronectin. Mol Microbiol. 2005 Jul;57(1):196-211. doi: 10.1111/j.1365-2958.2005.04666.x. PMID: 15948960.
114. Kingsley RA, Santos RL, Keestra AM, Adams LG, Bäumler AJ. Salmonella enterica serotype Typhimurium ShdA is an outer membrane fibronectin-binding protein that is expressed in the intestine. Mol Microbiol. 2002 Feb;43(4):895-905. doi: 10.1046/j.1365-2958.2002.02805.x. PMID: 11929540.

115. Gerlach RG, Jäckel D, Stecher B, Wagner C, Lupas A, Hardt WD, Hensel M. Salmonella Pathogenicity Island 4 encodes a giant non-fimbrial adhesin and the cognate type 1 secretion system. Cell Microbiol. 2007 Jul;9(7):1834-50. doi: 10.1111/j.1462-5822.2007.00919.x. Epub 2007 Mar 26. PMID: 17388786.
116. Velge P, Wiedemann A, Rosselin M, Abed N, Boumart Z, Chaussé AM, Grépinet O, Namdari F, Roche SM, Rossignol A, Virlogeux-Payant I. Multiplicity of Salmonella entry mechanisms, a new paradigm for Salmonella pathogenesis. Microbiologyopen. 2012 Sep;1(3):243-58. doi: 10.1002/mbo3.28. Epub 2012 Jun 18. PMID: 23170225; PMCID: PMC3496970.
117. Cirillo DM, Heffernan EJ, Wu L, Harwood J, Fierer J, Guiney DG. Identification of a domain in Rck, a product of the Salmonella typhimurium virulence plasmid, required for both serum resistance and cell invasion. Infect Immun. 1996 Jun;64(6):2019-23. doi: 10.1128/iai.64.6.2019-2023.1996. PMID: 8675302; PMCID: PMC174031.
118. Wagner C, Barlag B, Gerlach RG, Deiwick J, Hensel M. The Salmonella enterica giant adhesin SiiE binds to polarized epithelial cells in a lectin-like manner. Cell Microbiol. 2014 Jun;16(6):962-75. doi: 10.1111/cmi.12253. Epub 2014 Jan 13. PMID: 24345213.
119. Manon R, Nadia A, Fatemeh N, et al. (2012) The Different Strategies Used by Salmonella to Invade Host Cells. Salmonella - Distribution, Adaptation, Control Measures and Molecular Technologies. InTech. Available at: http://dx.doi.org/10.5772/29979.
120. Chowdhury, R., Mandal, R.S., Ta, A., and Das, S. (2015). An AIL family protein promotes type three secretion system-1-independent invasion and pathogenesis of Salmonella enterica serovar Typhi. Cellular microbiology 17, 486-503.
121. Rosselin, M., Virlogeux-Payant, I., Roy, C., Bottreau, E., Sizaret, P.Y., Mijouin, L., Germon, P., Caron, E., Velge, P., and Wiedemann, A. (2010). Rck of Salmonella enterica, subspecies enterica serovar enteritidis, mediates zipper-like internalization. Cell research 20, 647-664.
122. Galán, J.E., and Zhou, D. (2000). Striking a balance: Modulation of the actin cytoskeleton by Salmonella. Proceedings of the National Academy of Sciences 97, 8754-8761.
123. Hayward, R.D., and Koronakiss, V. (2002). Direct modulation of the host cell cytoskeleton by Salmonella actin-binding proteins. Trends in Cell Biology 12, 15-20.
124. Zhou, D. (2001). Collective efforts to modulate the host actin cytoskeleton by Salmonella type III-secreted effector proteins. Trends in microbiology 9, 567-569.
125. Moon, S.Y., and Zheng, Y. (2003). Rho GTPase-activating proteins in cell regulation. Trends in Cell Biology 13, 13-22.
126. Schmidt, A., and Hall, A. (2002). Guanine nucleotide exchange factors for Rho GTPases: turning on the switch. Genes & Development 16, 1587-1609.
127. Friebel, A., Ilchmann, H., Aepfelbacher, M., Ehrbar, K., Machleidt, W., and Hardt, W.-D. (2001). SopE and SopE2 from Salmonella typhimurium Activate Different Sets of RhoGTPases of the Host Cell. Journal of Biological Chemistry 276, 34035-34040.
128. Hardt, W.-D., Chen, L.-M., Schuebel, K.E., Bustelo, X.R., and Galán, J.E. (1998). S. typhimurium Encodes an Activator of Rho GTPases that Induces Membrane Ruffling and Nuclear Responses in Host Cells. Cell 93, 815-826.

129. Welch, M.D., and Mullins, R.D. (2002). Cellular Control of Actin Nucleation. Annual Review of Cell and Developmental Biology 18, 247-288.
130. Stender, S., Friebel, A., Linder, S., Rohde, M., Mirold, S., and Hardt, W.D. (2000). Identification of SopE2 from Salmonella typhimurium, a conserved guanine nucleotide exchange factor for Cdc42 of the host cell. Molecular microbiology 36, 1206-1221.
131. Unsworth, K.E., Way, M., McNiven, M., Machesky, L., and Holden, D.W. (2004). Analysis of the mechanisms of Salmonella-induced actin assembly during invasion of host cells and intracellular replication. Cellular microbiology 6, 1041-1055.
132. Swanson, J., Bushnell, A., and Silverstein, S.C. (1987). Tubular lysosome morphology and distribution within macrophages depend on the integrity of cytoplasmic microtubules. Proceedings of the National Academy of Sciences 84, 1921-1925.
133. Zhou, D., Mooseker, M.S., and Galán, J.E. (1999). Role of the S. typhimurium Actin-Binding Protein SipA in Bacterial Internalization. Science 283, 2092.
134. Fu, Y., and Galan, J.E. (1999). A salmonella protein antagonizes Rac-1 and Cdc42 to mediate host-cell recovery after bacterial invasion. Nature 401, 293-297
135. Murli, S., Watson, R.O., and Galán, J.E. (2001). Role of tyrosine kinases and the tyrosine phosphatase SptP in the interaction of Salmonella with host cells. Cellular microbiology 3, 795-810
136. Gruenheid, S., and Finlay, B.B. (2003). Microbial pathogenesis and cytoskeletal function. Nature 422, 775-781.
137. D'Costa, V. M., Braun, V., Landekic, M., Shi, R., Proteau, A., McDonald, L., et al. (2015). Salmonella disrupts host endocytic trafficking by SopD2-mediated inhibition of Rab7. Cell Rep. 12, 1508–1518. doi: 10.1016/j.celrep.2015. 07.063
138. Kuhle, V., and Hensel, M. (2004). Cellular microbiology of intracellular Salmonella enterica: functions of the type III secretion system encoded by Salmonella pathogenicity island 2. Cellular and molecular life sciences : CMLS 61, 2812-2826.
139. Haraga A, Ohlson MB, Miller SI. Salmonellae interplay with host cells. Nat Rev Microbiol. 2008 Jan;6(1):53-66. doi: 10.1038/nrmicro1788. PMID: 18026123.
140. Reinicke, A. T. et al. A Salmonella typhimurium effector protein SifA is modified by host cell prenylation and S-acylation machinery. J. Biol. Chem. 280, 14620–14627 (2005).
141. Boucrot, E., Henry, T., Borg, J. P., Gorvel, J. P. & Meresse, S. The intracellular fate of Salmonella depends on the recruitment of kinesin. Science 308, 1174–1178 (2005).
142. Wang M, Qazi IH, Wang L, Zhou G, Han H. *Salmonella* Virulence and Immune Escape. Microorganisms. 2020 Mar 13;8(3):407. doi: 10.3390/microorganisms8030407. PMID: 32183199; PMCID: PMC7143636.
143. Hansen-Wester, I., Stecher, B. & Hensel, M. Type III secretion of Salmonella enterica serovar Typhimurium translocated effectors and SseFG. Infect. Immun. 70, 1403–1409 (2002).
144. Kuhle, V. & Hensel, M. SseF and SseG are translocated effectors of the type III secretion system of Salmonella pathogenicity island 2 that modulate aggregation of endosomal compartments. Cell. Microbiol. 4, 813–824 (2002).

145. Abrahams, G. L., Muller, P. & Hensel, M. Functional dissection of SseF, a type III effector protein involved in positioning the Salmonella-containing vacuole. Traffic 7, 950–965 (2006).
146. Kuhle, V., Abrahams, G. L. & Hensel, M. Intracellular Salmonella enterica redirect exocytic transport processes in a Salmonella pathogenicity island 2-dependent manner. Traffic 7, 716–730 (2006).
147. Birmingham, C. L., Jiang, X., Ohlson, M. B., Miller, S. I. & Brumell, J. H. Salmonella-induced filament formation is a dynamic phenotype induced by rapidly replicating Salmonella enterica serovar Typhimurium in epithelial cells. Infect. Immun. 73, 1204–1208 (2005).
148. Lesnick, M. L., Reiner, N. E., Fierer, J. & Guiney, D. G. The Salmonella spvB virulence gene encodes an enzyme that ADP-ribosylates actin and destabilizes the cytoskeleton of eukaryotic cells. Mol. Microbiol. 39, 1464–1470 (2001).
149. Hensel, M., Nikolaus, T. & Egelseer, C. Molecular and functional analysis indicates a mosaic structure of Salmonella pathogenicity island 2. Mol. Microbiol. 31, 489–498 (1999).
150. Haraga A, Ohlson MB, Miller SI. Salmonellae interplay with host cells. Nat Rev Microbiol. 2008 Jan;6(1):53-66. doi: 10.1038/nrmicro1788. PMID: 18026123.
151. Prost, L.R., and Miller, S.I. (2008). The Salmonellae PhoQ sensor: mechanisms of detection of phagosome signals. Cellular microbiology 10, 576-582.
152. Bader, M.W., Sanowar, S., Daley, M.E., Schneider, A.R., Cho, U., Xu, W., Klevit, R.E., Le Moual, H., and Miller, S.I. (2005). Recognition of antimicrobial peptides by a bacterial sensor kinase. Cell 122, 461-472.
153. Mostowy, S. (2013). Autophagy and bacterial clearance: a not so clear picture. Cellular microbiology 15, 395-402.
154. Yoshida S, Handa Y, Suzuki T, Ogawa M, Suzuki M, Tamai A, Abe A, Katayama E, Sasakawa C. 2006. Microtubule-severing activity of Shigella is pivotal for intercellular spreading. Science 314:985–989 http:// dx.doi.org/10.1126/science.1133174.
155. Owen KA, Casanova JE. Salmonella Manipulates Autophagy to "Serve and Protect". Cell Host Microbe. 2015 Nov 11;18(5):517-9. doi: 10.1016/j.chom.2015.10.020. PMID: 26567504.
156. Owen KA, Meyer CB, Bouton AH, Casanova JE. Activation of focal adhesion kinase by Salmonella suppresses autophagy via an Akt/mTOR signaling pathway and promotes bacterial survival in macrophages. PLoS Pathog. 2014 Jun 5;10(6):e1004159. doi: 10.1371/journal.ppat.1004159. PMID: 24901456; PMCID: PMC4047085.
157. Xu Y, Zhou P, Cheng S, Lu Q, Nowak K, Hopp AK, Li L, Shi X, Zhou Z, Gao W, Li D, He H, Liu X, Ding J, Hottiger MO, Shao F. A Bacterial Effector Reveals the V-ATPase-ATG16L1 Axis that Initiates Xenophagy. Cell. 2019 Jul 25;178(3):552-566.e20. doi: 10.1016/j.cell.2019.06.007. Epub 2019 Jul 18. PMID: 31327526.
158. Small P, Blankenhorn D, Welty D, Zinser E, Slonczewski JL. Acid and base resistance in Escherichia coli and Shigella flexneri: role of rpoS and growth pH. J Bacteriol. 1994 Mar;176(6):1729-37. doi: 10.1128/jb.176.6.1729-1737.1994. PMID: 8132468; PMCID: PMC205261.
159. WassefJS,KerenDF,MaillouxJL.RoleofMcellsininitialantigenuptakeandin ulcer formation in the rabbit intestinal loop model of shigellosis. Infect Immun (1989) 57:858–63.

160. Perdomo OJ, Cavaillon JM, Huerre M, Ohayon H, Gounon P, Sansonetti PJ. Acute inflammation causes epithelial invasion and mucosal destruction in experimental shigellosis. J Exp Med (1994) 180:1307–19. doi:10.1084/jem.180. 4.1307

161. High N, Mounier J, Prévost MC, Sansonetti PJ. IpaB of Shigella flexneri causes entry into epithelial cells and escape from the phagocytic vacuole. EMBO J (1992) 11:1991–9.

162. Zychlinsky A, Prevost MC, Sansonetti PJ. Shigella flexneri induces apoptosis in infected macrophages. Nature (1992) 358:167–9. doi:10.1038/358167a0

163. Carayol N, Tran Van Nhieu G. Tips and tricks about Shigella invasion of epithelial cells. Current Opin Microbiol (2013) 16:1–6. doi:10.1016/j.mib.2012. 11.010.

164. High N, Mounier J, Prévost MC, Sansonetti PJ. IpaB of Shigella flexneri causes entry into epithelial cells and escape from the phagocytic vacuole. EMBO J. 1992 May;11(5):1991-9. doi: 10.1002/j.1460-2075.1992.tb05253.x. PMID: 1582426; PMCID: PMC556659.

165. Mellouk N, Weiner A, Aulner N, Schmitt C, Elbaum M, Shorte SL, Danckaert A, Enninga J. 2014. Shigella subverts the host recycling com partment to rupture its vacuole. Cell Host Microbe 16:517–530 http://dx .doi.org/10.1016/j.chom.2014.09.005.

166. Sansonetti PJ, Arondel J, Fontaine A, d'Hauteville H, Bernardini ML. 1991. OmpB (osmo-regulation) and icsA (cell-to-cell spread) mutants of Shigella flexneri: vaccine candidates and probes to study the pathogenesis of shigellosis. Vaccine 9:416–422 http://dx.doi.org/10.1016/0264-410X (91)90128-S.

167. Mathan MM, Mathan VI. 1991. Morphology of rectal mucosa of patients with shigellosis. Rev Infect Dis 13(Suppl 4):S314–S318 http://dx .doi.org/10.1093/clinids/13.Supplement_4.S314.

168. Sansonetti PJ, Arondel J, Cantey JR, Prévost MC, Huerre M. 1996. Infection of rabbit Peyer's patches by Shigella flexneri: effect of adhesive or invasive bacterial phenotypes on follicle-associated epithelium. Infect Immun 64:2752–2764.

169. Wassef JS, Keren DF, Mailloux JL. 1989. Role of M cells in initial antigen uptake and in ulcer formation in the rabbit intestinal loop model of shigellosis. Infect Immun 57:858–863.

170. Perdomo OJ, Cavaillon JM, Huerre M, Ohayon H, Gounon P, Sansonetti PJ. 1994. Acute inflammation causes epithelial invasion and mucosal destruction in experimental shigellosis. J Exp Med 180:1307 1319 http://dx.doi.org/10.1084/jem.180.4.1307.

171. Miller H, Zhang J, Kuolee R, Patel GB, Chen W. 2007. Intestinal M cells: the fallible sentinels? World J Gastroenterol 13:1477–1486 http:// dx.doi.org/10.3748/wjg.v13.i10.1477.

172. Ashida H, Mimuro H, Sasakawa C. Shigella manipulates host immune responses by delivering effector proteins with specific roles. Front Immunol. 2015 May 7;6:219. doi: 10.3389/fimmu.2015.00219. PMID: 25999954; PMCID: PMC4423471

173. Watarai M, Funato S, Sasakawa C. 1996. Interaction of Ipa proteins of Shigella flexneri with α5β1 integrin promotes entry of the bacteria into mammalian cells. J Exp Med 183:991–999 http://dx.doi.org/10.1084/jem .183.3.991.

174. Russo BC, Stamm LM, Raaben M, Kim CM, Kahoud E, Robinson LR, Bose S, Queiroz AL, Herrera BB, Baxt LA, Mor-Vaknin N, Fu Y, Molina G, Markovitz DM, Whelan SP, Goldberg MB. 2016. Interme diate filaments enable pathogen docking to trigger type 3 effector trans location. Nat Microbiol 1:16025 http://dx.doi.org/10.1038/nmicrobiol .2016.25.

175. Tran Van Nhieu G, Caron E, Hall A, Sansonetti PJ. 1999. IpaC induces actin polymerization and filopodia formation during Shigella en try into epithelial cells. EMBO J 18:3249–3262 http://dx.doi.org/10.1093 /emboj/18.12.3249.
176. Tran Van Nhieu G, Ben-Ze'ev A, Sansonetti PJ. 1997. Modulation of bacterial entry into epithelial cells by association between vinculin and the Shigella IpaA invasin. EMBO J 16:2717–2729 http://dx.doi.org/10.1093 /emboj/16.10.2717.
177. Izard T, Tran Van Nhieu G, Bois PRJ. 2006. Shigella applies molec ular mimicry to subvert vinculin and invade host cells. J Cell Biol 175: 465–475 http://dx.doi.org/10.1083/jcb.200605091.
178. Yoshida S, Handa Y, Suzuki T, Ogawa M, Suzuki M, Tamai A, Abe A, Katayama E, Sasakawa C. 2006. Microtubule-severing activity of Shigella is pivotal for intercellular spreading. Science 314:985–989 http:// dx.doi.org/10.1126/science.1133174.
179. Germane KL, Ohi R, Goldberg MB, Spiller BW. 2008. Structural and functional studies indicate that Shigella VirA is not a protease and does not directly destabilize microtubules. Biochemistry 47:10241–10243 http:// dx.doi.org/10.1021/bi801533k.
180. Niebuhr K, Giuriato S, Pedron T, Philpott DJ, Gaits F, Sable J, Sheetz MP, Parsot C, Sansonetti PJ, Payrastre B. 2002. Conversion of PtdIns(4,5)P (2) into PtdIns(5)P by the S.flexneri effector IpgD reorganizes host cell mor phology. EMBO J 21:5069–5078 http://dx.doi.org/10.1093/emboj/cdf522
181. Weiner A, Mellouk N, Lopez-Montero N, Chang Y-Y, Souque C, Schmitt C, Enninga J. 2016. Macropinosomes are key players in early Shigella invasion and vacuolar escape in epithelial cells. PLoS Pathog 12: e1005602 http://dx.doi.org/10.1371/journal.ppat.1005602.
182. Yang SC, Hung CF, Aljuffali IA, Fang JY. The roles of the virulence factor IpaB in Shigella spp. in the escape from immune cells and invasion of epithelial cells. Microbiol Res. 2015 Dec;181:43-51. doi: 10.1016/j.micres.2015.08.006. Epub 2015 Sep 2. PMID: 26640051.
183. Ashida H, Kim M, Sasakawa C. 2014. Manipulation of the host cell death pathway by Shigella. Cell Microbiol 16:1757–1766 http://dx.doi .org/10.1111/cmi.12367.
184. 48. Jorgensen I, Miao EA. 2015. Pyroptotic cell death defends against intracellular pathogens. Immunol Rev 265:130–142 http://dx.doi.org/10 .1111/imr.12287.
185. Willingham SB, Bergstralh DT, O'Connor W, Morrison AC, Taxman DJ, Duncan JA, et al. Microbial pathogen-induced necrotic cell death mediated by the inflammasome components CIAS1/cryopyrin/NLRP3 and ASC. Cell Host Microbe (2007) 2:147–59. doi:10.1016/j.chom.2007.07.009
186. Miao EA, Mao DP, Yudkovsky N, Bonneau R, Lorang CG, Warren SE, et al. Innate immune detection of the type III secretion apparatus through the NLRC4 inflammasome. Proc Natl Acad Sci U S A(2010) 107:3076–80. doi:10.1073/pnas. 0913087107
187. Suzuki T, Franchi L, Toma C, Ashida H, Ogawa M, Yoshikawa Y, et al. Differential regulation of caspase-1 activation, pyroptosis, and autophagy via Ipaf and ASC in Shigella-infected macrophages. PLoS Pathog (2007) 3:e111. doi:10.1371/journal.ppat.0030111
188. Davis BK, Roberts RA, Huang MT, Willingham SB, Conti BJ, Brickey WJ, et al. Cutting edge: NLRC5-dependent activation of the inflammasome. J Immunol (2011) 186:1333–7. doi:10.4049/jimmunol.1003111

189. Schnupf P.Sansonetti PJ.2019.Shigella Pathogenesis: New Insights through Advanced Methodologies. Microbiol Spectr7:10.1128/microbiolspec.bai-0023-2019.https://doi.org/10.1128/microbiolspec.bai-0023-2019
190. Rayamajhi M, Zak DE, Chavarria-Smith J, Vance RE, Miao EA. Cutting edge: mouse NAIP1 detects the type III secretion system needle protein. J Immunol (2013) 191:3986–9. doi:10.4049/jimmunol.1301549
191. Yang J, Zhao Y, Shi J, Shao F. Human NAIP and mouse NAIP1 recognize bacterial type III secretion needle protein for inflammasome activation. Proc Natl Acad Sci U S A (2013) 110:14408–13. doi:10.1073/pnas.1306376110
192. Suzuki S, Franchi L, He Y, Muñoz-Planillo R, Mimuro H, Suzuki T, et al. Shigella type III secretion protein MxiI is recognized by Naip2 to induce Nlrc4 inflammasome activation independently of Pkcδ. PLoS Pathog (2014) 10:e1003926. doi:10.1371/journal.ppat.1003926
193. Lightfield KL, Persson J, Brubaker SW, Witte CE, von Moltke J, Dunipace EA, et al. Critical function for Naip5 in inflammasome activation by a conserved carboxy-terminal domain of flagellin. Nat Immunol (2008) 9:1171–8. doi:10. 1038/ni.1646
194. Kofoed EM, Vance RE. Innate immune recognition of bacterial ligands by NAIPs determines inflammasome specificity. Nature (2011) 477:592–5. doi:10. 1038/nature10394
195. Zhao Y, Yang J, Shi J, Gong YN, Lu Q, Xu H, et al. The NLRC4 inflammasome receptors for bacterial flagellin and type III secretion apparatus. Nature (2011) 477:596–600. doi:10.1038/nature10510
196. Tenthorey JL, Kofoed EM, Daugherty MD, Malik HS, Vance RE. Molecular basis for specific recognition of bacterial ligands by NAIP/NLRC4 inflammasomes. Mol Cell (2014) 54:17–29. doi:10.1016/j.molcel.2014.02.018
197. Suzuki S, Mimuro H, Kim M, Ogawa M, Ashida H, Toyotome T, et al. Shigella IpaH7.8 E3 ubiquitin ligase targets glomulin and activates inflammasomes to demolish macrophages. Proc Natl Acad Sci U S A (2014) 111:E4254–63. doi:10. 1073/pnas.1324021111
198. Rohde JR, Breitkreutz A, Chenal A, Sansonetti PJ, Parsot C. Type III secretion effectors of the IpaH family are E3 ubiquitin ligase. Cell Host Microbe (2007) 1:77–83. doi:10.1016/j.chom.2007.02.002
199. KrokowskiS, MostowyS.2016.Interactions between Shigella flexneri and the autophagy machinery. Front Cell Infect Microbiol 6:17 http://dx .doi.org/10.3389/fcimb.2016.00017.
200. Travassos LH, Carneiro LAM, Ramjeet M, Hussey S, Kim Y-G, Magalhães JG, Yuan L, Soares F, Chea E, Le Bourhis L, Boneca IG, Allaoui A, Jones NL, Nuñez G, Girardin SE, Philpott DJ. 2010. Nod1 and Nod2 direct autophagy by recruiting ATG16L1 to the plasma membrane at the site of bacterial entry. Nat Immunol 11:55–62 .1038/ni.1823. http://dx.doi.org/10
201. Sorbara MT, Foerster EG, Tsalikis J, Abdel-Nour M, Mangiapane J, Sirluck-Schroeder I, Tattoli I, van Dalen R, Isenman DE, Rohde JR, Girardin SE, Philpott DJ. 2018. Complement C3 drives autophagy dependent restriction of cyto-invasive bacteria. Cell Host Microbe 23: 644–652.e5 http://dx.doi.org/10.1016/j.chom.2018.04.008.
202. Torraca V, Mostowy S. 2016. Septins and bacterial infection. Front Cell Dev Biol 4:127 http://dx.doi.org/10.3389/fcell.2016.00127.

203. Mostowy S, Sancho-Shimizu V, Hamon MA, Simeone R, Brosch R, Johansen T, Cossart P. 2011. p62 and NDP52 proteins target intracyto solic Shigella and Listeria to different autophagy pathways. J Biol Chem 286:26987–26995 http://dx.doi.org/10.1074/jbc.M111.223610.

204. Sirianni A, Krokowski S, Lobato-Márquez D, Buranyi S, Pfanzelter J, Galea D,Willis A, CulleyS, Henriques R, Larrouy-MaumusG,Hollinshead M, Sancho-Shimizu V, Way M, Mostowy S. 2016. Mitochondria mediate septin cage assembly to promote autophagy of Shigella. EMBO Rep 17: 1029–1043 http://dx.doi.org/10.15252/embr.201541832.

205. Ogawa M,YoshimoriT,Suzuki T, Sagara H, Mizushima N, Sasakawa C. 2005. Escape of intracellular Shigella from autophagy. Science 307:727 731 http://dx.doi.org/10.1126/science.1106036.

206. Uchiya K, Tobe T, Komatsu K, Suzuki T, Watarai M, Fukuda I, YoshikawaM,SasakawaC.1995.Identificationof anovelvirulence gene, virA, on the large plasmid of Shigella, involved in invasion and intercel lular spreading. Mol Microbiol 17:241–250 http://dx.doi.org/10.1111/j .1365-2958.1995.mmi_17020241.x.

207. Huang J, Brumell JH. 2014. Bacteria-autophagy interplay: a battle for survival. Nat Rev Microbiol 12:101–114 http://dx.doi.org/10.1038 /nrmicro3160.

208. Dong N, Zhu Y, Lu Q, Hu L, Zheng Y, Shao F. 2012. Structurally distinct bacterial TBC-like GAPs link Arf GTPase to Rab1 inactivation to counteract host defenses. Cell 150:1029–1041 http://dx.doi.org/10.1016 /j.cell.2012.06.050.

209. Pieper R, Fisher CR, Suh M-J, Huang S-T, Parmar P, Payne SM. 2013. Analysis of the proteome of intracellular Shigella flexneri reveals pathways important for intracellular growth. Infect Immun 81:4635 4648 http://dx.doi.org/10.1128/IAI.00975-13.

210. Payne SM, Wyckoff EE, Murphy ER, Oglesby AG, Boulette ML, Davies NML. 2006. Iron and pathogenesis of Shigella: iron acquisition in the intracellular environment. Biometals 19:173–180 http://dx.doi.org/10 .1007/s10534-005-4577-x.

211. Tattoli I, Sorbara MT, Vuckovic D, Ling A, Soares F, Carneiro LAM, Yang C, Emili A, Philpott DJ, Girardin SE. 2012. Amino acid starvation induced by invasive bacterial pathogens triggers an innate host defense program. Cell Host Microbe 11:563–575 http://dx.doi.org/10.1016/j.chom .2012.04.012.

212. Bernardini ML, Mounier J, d'Hauteville H, Coquis-Rondon M, Sansonetti PJ. Identification of icsA, a plasmid locus of Shigella flexneri that governs bacterial intra- and intercellular spread through interaction with F-actin. Proc Natl Acad Sci U S A. 1989 May;86(10):3867-71. doi: 10.1073/pnas.86.10.3867. PMID: 2542950; PMCID: PMC287242.

213. Lett MC, Sasakawa C, Okada N, et al. virG, a plasmid-coded virulence gene of Shigella flexneri: identification of the virG protein and determination of the complete coding sequence. Journal of Bacteriology. 1989 Jan;171(1):353-359. DOI: 10.1128/jb.171.1.353-359.1989. PMID: 2644195; PMCID: PMC209595.

214. Sansonetti PJ, Arondel J, Fontaine A, d'Hauteville H, Bernardini ML. OmpB (osmo-regulation) and icsA (cell-to-cell spread) mutants of Shigella flexneri: vaccine candidates and probes to study the pathogenesis of shigellosis. Vaccine. 1991 Jun;9(6):416-22. doi: 10.1016/0264-410x(91)90128-s. PMID: 1887672.

215. Goldberg MB, Bârzu O, Parsot C, Sansonetti PJ. Unipolar localization and ATPase activity of IcsA, a Shigella flexneri protein involved in intracellular movement. J Bacteriol. 1993 Apr;175(8):2189-96. doi: 10.1128/jb.175.8.2189-2196.1993. PMID: 8468279; PMCID: PMC204503.
216. Steinhauer J, Agha R, Pham T, Varga AW, Goldberg MB. The unipolar Shigella surface protein IcsA is targeted directly to the bacterial old pole: IcsP cleavage of IcsA occurs over the entire bacterial surface. Mol Microbiol. 1999 Apr;32(2):367-77. doi: 10.1046/j.1365-2958.1999.01356.x. PMID: 10231492.
217. Charles M, Pérez M, Kobil JH, Goldberg MB. Polar targeting of Shigella virulence factor IcsA in Enterobacteriacae and Vibrio. Proc Natl Acad Sci U S A. 2001 Aug 14;98(17):9871-6. doi: 10.1073/pnas.171310498. Epub 2001 Jul 31. PMID: 11481451; PMCID: PMC55545.
218. Purdy GE, Hong M, Payne SM. Shigella flexneri DegP facilitates IcsA surface expression and is required for efficient intercellular spread. Infect Immun. 2002 Nov;70(11):6355-64. doi: 10.1128/IAI.70.11.6355-6364.2002. PMID: 12379715; PMCID: PMC130383.
219. Suzuki T, Miki H, Takenawa T, Sasakawa C. Neural Wiskott-Aldrich syndrome protein is implicated in the actin-based motility of Shigella flexneri. EMBO J. 1998 May 15;17(10):2767-76. doi: 10.1093/emboj/17.10.2767. PMID: 9582270; PMCID: PMC1170617.
220. Goldberg MB. Shigella actin-based motility in the absence of vinculin. Cell Motil Cytoskeleton. 1997;37(1):44-53. doi: 10.1002/(SICI)1097-0169(1997)37:1<44::AID-CM5>3.0.CO;2-H. PMID: 9142438.
221. Suzuki T, Saga S, Sasakawa C. Functional analysis of Shigella VirG domains essential for interaction with vinculin and actin-based motility. J Biol Chem. 1996 Sep 6;271(36):21878-85. doi: 10.1074/jbc.271.36.21878. PMID: 8702989.
222. Egile C, Loisel TP, Laurent V, Li R, Pantaloni D, Sansonetti PJ, Carlier MF. Activation of the CDC42 effector N-WASP by the Shigella flexneri IcsA protein promotes actin nucleation by Arp2/3 complex and bacterial actin-based motility. J Cell Biol. 1999 Sep 20;146(6):1319-32. doi: 10.1083/jcb.146.6.1319. PMID: 10491394; PMCID: PMC2156126.
223. Suzuki T, Mimuro H, Suetsugu S, Miki H, Takenawa T, Sasakawa C. Neural Wiskott-Aldrich syndrome protein (N-WASP) is the specific ligand for Shigella VirG among the WASP family and determines the host cell type allowing actin-based spreading. Cell Microbiol. 2002 Apr;4(4):223-33. doi: 10.1046/j.1462-5822.2002.00185.x. PMID: 11952639.
224. Monack DM, Theriot JA. Actin-based motility is sufficient for bacterial membrane protrusion formation and host cell uptake. Cell Microbiol. 2001 Sep;3(9):633-47. doi: 10.1046/j.1462-5822.2001.00143.x. PMID: 11553015.
225. Rathman, M., de Lanerolle, P., Ohayon, H., Gounon, P. and Sansonetti, P.J. (2000) Myosin light chain kinase plays an essential role in S. flexneri dissemination. J. Cell Sci. 113, 3375 3386.
226. Sansonetti, P.J., Mounier, J., Prevost, M.C. and Mege, R.M. (1994) Cadherin expression is required for the spread of Shigella f lexneri between epithelial cells. Cell 76, 829–839.
227. Page AL, Ohayon H, Sansonetti PJ, Parsot C. The secreted IpaB and IpaC invasins and their cytoplasmic chaperone IpgC are required for intercellular dissemination of Shigella flexneri. Cell Microbiol. 1999 Sep;1(2):183-93. doi: 10.1046/j.1462-5822.1999.00019.x. PMID: 11207551.

228. Suzuki T, Murai T, Fukuda I, Tobe T, Yoshikawa M, Sasakawa C. Identification and characterization of a chromosomal virulence gene, vacJ, required for intercellular spreading of Shigella flexneri. Mol Microbiol. 1994 Jan;11(1):31-41. doi: 10.1111/j.1365-2958.1994.tb00287.x. PMID: 8145644.
229. Thakur, R.; Suri, C.R.; Rishi, P. Contribution of typhoid toxin in the pathogenesis of Salmonella Typhi. Microb. Pathog. 2022, 164, 105444.
230. Patel, T.A.; Armstrong, M.; Morris-Jones, S.D.; Wright, S.G.; Doherty, T. Imported enteric fever: Case series from the hospital for tropical diseases, London, United Kingdom. Am. J. Trop. Med. Hyg. 2010, 82, 1121–1126.
231. Kuvandik, C.; Karaoglan, I.; Namiduru, M.; Baydar, I. Predictive value of clinical and laboratory findings in the diagnosis of the enteric fever. New Microbiol. 2009, 32, 25–30.
232. Maskey, A.P., Basnyat, B., Thwaites, G.E., Campbell, J.I., Farrar, J.J., and Zimmerman, M.D. (2008). Emerging trends in enteric fever in Nepal: 9124 cases confirmed by blood culture 1993-2003. Trans R Soc Trop Med Hyg 102, 91-95.
233. Stuart, B.M., and Pullen, R.L. (1946). Typhoid: Clinical analysis of three hundred and sixty cases. Archives of Internal Medicine 78, 629-661.
234.. Galán, J.E. Typhoid toxin provides a window into typhoid fever and the biology of Salmonella Typhi. Proc. Natl. Acad. Sci. USA 2016, 113, 6338–6344.
235. Pulford, C.V.; Perez-Sepulveda, B.M.; Canals, R.; Bevington, J.A.; Bengtsson, R.J.; Wenner, N.; Rodwell, E.V.; Kumwenda, B.; Zhu, X.; Bennett, R.J.; et al. Stepwise evolution of Salmonella Typhimurium ST313 causing bloodstream infection in Africa. Nat. Microbiol. 2021, 6, 327–338
236. Acheson, D.; Hohmann, E.L. Nontyphoidal Salmonellosis. Clin. Infect. Dis. 2001, 32, 263–269
237. Scallan, E.; Hoekstra, R.M.; Angulo, F.J.; Tauxe, R.V.; Widdowson, M.A.; Roy, S.L.; Jones, J.L.; Griffin, P.M. Foodborne illness acquired in the United States—Major pathogens. Emerg. Infect. Dis. 2011, 17, 7–15
238. Ajene, A.N.; Fischer Walker, C.L.; Black, R.E. Enteric pathogens and reactive arthritis: A systematic review of Campylobacter, salmonella and Shigella-associated reactive arthritis. J. Health Popul. Nutr. 2013, 31, 299–307.
239. Tsuchiya, Y.; Loza, E.; Villa-Gomez, G.; Trujillo, C.C.; Baez, S.; Asai, T.; Ikoma, T.; Endoh, K.; Nakamura, K. Metagenomics of microbial communities in gallbladder bile from patients with gallbladder cancer or cholelithiasis. Asian Pac. J. Cancer Prev. 2018, 19, 961.
240. Zha, L.; Garrett, S.; Sun, J. Salmonella infection in chronic inflammation and gastrointestinal cancer. Diseases 2019, 7, 28.
241. Clarke, R.C., and Gyles, C.L. (1987). Virulence of wild and mutant strains of Salmonella typhimurium in ligated intestinal segments of calves, pigs, and rabbits. American journal of veterinary research 48, 504-510.
242. Finlay, B.B., Heffron, F., and Falkow, S. (1989). Epithelial cell surfaces induce Salmonella proteins required for bacterial adherence and invasion. Science 243, 940-943.
243. McCormick, B.A., Miller, S.I., Carnes, D., and Madara, J.L. (1995). Transepithelial signaling to neutrophils by salmonellae: a novel virulence mechanism for gastroenteritis. Infection and immunity 63, 2302-2309.

244. Bennish, M.L., Wojtyniak, B.J. (1991). Mortality due to shigellosis: community and hospital d Rev Infect Dis. 13 Suppl 4:S245-51.
245. Hale TL, Keusch GT. Shigella. In: Baron S, editor. Medical Microbiology. 4th edition. Galveston (TX): University of Texas Medical Branch at Galveston; 1996. Chapter 22. Available from: https://www.ncbi.nlm.nih.gov/books/NBK8038/
246. Hale TL, Keusch GT. Shigella. In: Baron S, editor. Medical Microbiology. 4th edition. Galveston (TX): University of Texas Medical Branch at Galveston; 1996. Chapter 22. Available from: https://www.ncbi.nlm.nih.gov/books/NBK8038/
247. Anand BS, Malhotra V, Bhattacharya SK, Datta P, Datta D, Sen D, Bhattacharya MK, Mukherjee PP, Pal SC. Rectal histology in acute bacillary dysentery. Gastroenterology. 1986 Mar;90(3):654-60. doi: 10.1016/0016-5085(86)91120-0. PMID: 3510937.
248. Santander J, Curtiss R 3rd. Salmonella enterica Serovars Typhi and Paratyphi A are avirulent in newborn and infant mice even when expressing virulence plasmid genes of Salmonella Typhimurium. J Infect Dev Ctries. 2010 Nov 24;4(11):723-31. doi: 10.3855/jidc.1218. PMID: 21252450; PMCID: PMC4059606.
249. Zhu C, Xiong K, Chen Z, Hu X, Li J, Wang Y, Rao X, Cong Y. Construction of an attenuated Salmonella enterica serovar Paratyphi A vaccine strain harboring defined mutations in htrA and yncD. Microbiol Immunol. 2015 Aug;59(8):443-51. doi: 10.1111/1348-0421.12276. PMID: 26084199.
250. Song J, Willinger T, Rongvaux A, Eynon EE, Stevens S, Manz MG, Flavell RA, Galán JE. A mouse model for the human pathogen Salmonella typhi. Cell Host Microbe. 2010 Oct 21;8(4):369-76. doi: 10.1016/j.chom.2010.09.003. PMID: 20951970; PMCID: PMC2972545.
251. EDSALL G, GAINES S, LANDY M, TIGERTT WD, SPRINZ H, TRAPANI RJ, MANDEL AD, BENENSON AS. Studies on infection and immunity in experimental typhoid fever. I. Typhoid fever in chimpanzees orally infected with Salmonella typhosa. J Exp Med. 1960 Jul 1;112(1):143-66. doi: 10.1084/jem.112.1.143. PMID: 13725751; PMCID: PMC2137207.
252. Higginson EE, Simon R, Tennant SM. Animal Models for Salmonellosis: Applications in Vaccine Research. Clin Vaccine Immunol. 2016 Sep 6;23(9):746-56. doi: 10.1128/CVI.00258-16. PMID: 27413068; PMCID: PMC5014920.
253. Roland KL, Tinge SA, Kochi SK, Thomas LJ, Killeen KP. Reactogenicity and immunogenicity of live attenuated Salmonella enterica serovar Paratyphi A enteric fever vaccine candidates. Vaccine. 2010 May 7;28(21):3679-87. doi: 10.1016/j.vaccine.2010.03.019. Epub 2010 Mar 23. PMID: 20338215.
254. Sztein MB, Booth JS. Controlled human infectious models, a path forward in uncovering immunological correlates of protection: Lessons from enteric fevers studies. Front Microbiol. 2022 Sep 20;13:983403. doi: 10.3389/fmicb.2022.983403. PMID: 36204615; PMCID: PMC9530043.
255. Raymond M, Gibani MM, Day NPJ, Cheah PY. Typhoidal Salmonella human challenge studies: ethical and practical challenges and considerations for low-resource settings. Trials. 2019; 20(S2). https://doi.org/10.1186/s13063-019-3844-z PMID: 31852488
256. Barthel M, Hapfelmeier S, Quintanilla-Martínez L, Kremer M, Rohde M, Hogardt M, Pfeffer K, Rüssmann H, Hardt WD. Pretreatment of mice with streptomycin provides a Salmonella enterica serovar Typhimurium colitis model that allows analysis of both pathogen and host. Infect Immun. 2003 May;71(5):2839-58. doi: 10.1128/IAI.71.5.2839-2858.2003. PMID: 12704158; PMCID: PMC153285.

257. Mallett CP, VanDeVerg L, Collins HH, Hale TL: Evaluation of Shigella vaccine safety and efficacy in an intranasally challenged mouse model. Vaccine 1993, 11:190-196.
258. Singer M, Sansonetti PJ: IL-8 is a key chemokine regulating neutrophil recruitment in a new mouse model of Shigellainduced colitis. J Immunol 2004, 173:4197-4206.
259. Seydel KB, Li E, Swanson PE, Stanley SL: Human intestinal epithelial cells produce proinflammatory cytokines in response to infection in a SCID mouse-human intestinal xenograft model of amebiasis. Infect Immun 1997, 65:1631-1639.
260. Mitchell, P.S.; Roncaioli, J.L.; A Turcotte, E.; Goers, L.; A Chavez, R.; Lee, A.Y.; Lesser, C.F.; Rauch, I.; E Vance, R. NAIP–NLRC4- deficient mice are susceptible to shigellosis. eLife 2020, 9.
261. Medeiros, P.H.Q.S.; Ledwaba, S.E.; Bolick, D.T.; Giallourou, N.; Yum, L.K.; Costa, D.V.S.; Oriá, R.B.; Barry, E.M.; Swann, J.R.; Lima, A.Â.M.; et al. A murine model of diarrhea, growth impairment and metabolic disturbances with Shigella flexneri infection and the role of zinc deficiency. Gut Microbes 2019, 1–16.
262. Alphonse, N.; Odendall, C. Animal models of shigellosis: A historical overview. Curr. Opin. Immunol. 2023, 85, 102399.
263. Yang, J.-Y.; Lee, S.-N.; Chang, S.-Y.; Ko, H.-J.; Ryu, S.; Kweon, M.-N. A Mouse Model of Shigellosis by Intraperitoneal Infection. J. Infect. Dis. 2013, 209, 203–215
264. Martino MC, Rossi G, Martini I, Tattoli I, Chiavolini D, Phalipon A, Sansonetti PJ, Bernardini ML: Mucosal lymphoid infiltrate dominates colonic pathological changes in murine experimental Shigellosis. J Infect Dis 2005, 192:136-148
265. Shim DH, Suzuki T, Chang SY, Park SM, Sansonetti PJ, Sasakawa C, Kweon MN. New animal model of shigellosis in the Guinea pig: its usefulness for protective efficacy studies. J Immunol. 2007 Feb 15;178(4):2476-82. doi: 10.4049/jimmunol.178.4.2476. PMID: 17277155.
266. Wenzel H, Kaminski RW, Clarkson KA, Maciel M Jr, Smith MA, Zhang W, Oaks EV. Improving chances for successful clinical outcomes with better preclinical models. Vaccine. 2017 Dec 14;35(49 Pt A):6798-6802. doi: 10.1016/j.vaccine.2017.08.030. Epub 2017 Sep 7. PMID: 28890194.
267. Sereny, B. Experimental shigella keratoconjunctivitis; a preliminary report. Acta Microbiol. Acad. Sci. Hung. 1955, 2, 293–296.
268. Arm HG, Floyd TM, Faber JE, Hayes JR: Use of ligated segments of rabbit small intestine in experimental shigellosis. J Bacteriol 1965, 89:803-809.
269. Shipley, S.T.; Panda, A.; Khan, A.Q.; Kriel, E.H.; Maciel, M.; Livio, S.; Nataro, J.P.; Levine, M.M.; Sztein, M.B.; DeTolla, L.J. A challenge model for Shigella dysenteriae 1 in cynomolgus monkeys (Macaca fascicularis). Comp. Med. 2010, 60, 54–61.
270. Gregory, M.; Kaminski, R.W.; Lugo-Roman, L.A.; Galvez Carrillo, H.; Tilley, D.H.; Baldeviano, C.; Simons, M.P.; Reynolds, N.D.; Ranallo, R.T.; Suvarnapunya, A.E.; et al. Development of an Aotus nancymaae Model for Shigella Vaccine Immunogenicity and Efficacy Studies. Infect. Immun. 2014, 82, 2027–2036
271. Frenck, R.W.; Dickey, M.; Suvarnapunya, A.E.; Chandrasekaran, L.; Kaminski, R.W.; Clarkson, K.A.; McNeal, M.; Lynen, A.; Parker, S.; Hoeper, A.; et al. Establishment of a Controlled Human Infection Model with a Lyophilized Strain of Shigella sonnei 53G. mSphere 2020, 5.

272. Rydström A, Wick MJ. Monocyte recruitment, activation, and function in the gut-associated lymphoid tissue during oral Salmonella infection. J Immunol. (2007) 178:5789–801. doi: 10.4049/jimmunol.178.9.5789
273. Hayashi, F., Smith, K.D., Ozinsky, A., Hawn, T.R., Yi, E.C., Goodlett, D.R., Eng, J.K., Akira, S., Underhill, D.M., and Aderem, A. (2001). The innate immune response to bacterial flagellin is mediated by Toll-like receptor 5. Nature 410, 1099-1103.
274. Steiner, T.S. (2007). How flagellin and toll-like receptor 5 contribute to enteric infection. Infection and immunity 75, 545-552.
275. Franchi, L., Amer, A., Body-Malapel, M., Kanneganti, T.-D., Özören, N., Jagirdar, R., Inohara, N., Vandenabeele, P., Bertin, J., Coyle, A., et al. (2006). Cytosolic flagellin requires Ipaf for activation of caspase-1 and interleukin 1β in salmonella-infected macrophages. Nature Immunology 7, 576.
276. Takeuchi, O., Hoshino, K., Kawai, T., Sanjo, H., Takada, H., Ogawa, T., Takeda, K., and Akira, S. (1999). Differential roles of TLR2 and TLR4 in recognition of gram-negative and gram-positive bacterial cell wall components. Immunity 11, 443-451.
277. Mahieu, T., and Libert, C. (2007). Should we inhibit type I interferons in sepsis? Infection and immunity 75, 22-29.
278. Weiss, D.S., Raupach, B., Takeda, K., Akira, S., and Zychlinsky, A. (2004). Toll-like receptors are temporally involved in host defense. Journal of immunology 172, 4463-4469.
279. Hemmi, H., Takeuchi, O., Kawai, T., Kaisho, T., Sato, S., Sanjo, H., Matsumoto, M., Hoshino, K., Wagner, H., Takeda, K., et al. (2000). A Toll-like receptor recognizes bacterial DNA. Nature 408, 740-745.
280. Takeuchi, O., Kawai, T., Muhlradt, P.F., Morr, M., Radolf, J.D., Zychlinsky, A., Takeda, K., and Akira, S. (2001). Discrimination of bacterial lipoproteins by Toll-like receptor 6. International immunology 13, 933-940.
281. Totemeyer, S., Kaiser, P., Maskell, D.J., and Bryant, C.E. (2005). Sublethal infection of C57BL/6 mice with Salmonella enterica Serovar Typhimurium leads to an increase in levels of Toll-like receptor 1 (TLR1), TLR2, and TLR9 mRNA as well as a decrease in levels of TLR6 mRNA in infected organs. Infection and immunity 73, 1873-1878.
282. Zhang, X.L., Jeza, V.T., and Pan, Q. (2008). Salmonella typhi: from a human pathogen to a vaccine vector. Cellular & molecular immunology 5, 91-97.
283. Kaur, J., and Jain, S.K. (2012). Role of antigens and virulence factors of Salmonella enterica serovar Typhi in its pathogenesis. Microbiological research 167, 199-210.
284. Coburn B, Sekirov I, Finlay BB. Type III secretion systems and disease. Clin Microbiol Rev. 2007 Oct;20(4):535-49. doi: 10.1128/CMR.00013-07. PMID: 17934073; PMCID: PMC2176049.
285. Tsolis RM, Young GM, Solnick JV, Bäumler AJ. From bench to bedside: stealth of enteroinvasive pathogens. Nat Rev Microbiol. 2008 Dec;6(12):883-92. doi: 10.1038/nrmicro2012. Epub 2008 Oct 28. PMID: 18955984.
286. Dharmana, E., Keuter, M., Netea, M.G., Verschueren, I.C., and Kullberg, B.J. (2002). Divergent effects of tumor necrosis factor-alpha and lymphotoxin-alpha on lethal endotoxemia and infection with live Salmonella typhimurium in mice. European cytokine network 13, 104-109.

287. Engelberts, I., von Asmuth, E.J., van der Linden, C.J., and Buurman, W.A. (1991). The interrelation between TNF, IL-6, and PAF secretion induced by LPS in an in vivo and in vitro murine model. Lymphokine and cytokine research 10, 127-131.

288. Khan, S.A., Everest, P., Servos, S., Foxwell, N., Zahringer, U., Brade, H., Rietschel, E.T., Dougan, G., Charles, I.G., and Maskell, D.J. (1998). A lethal role for lipid A in Salmonella infections. Molecular microbiology 29, 571-579.

289. Wilson, R.P., Raffatellu, M., Chessa, D., Winter, S.E., Tukel, C., and Baumler, A.J. (2008). The Vi-capsule prevents Toll-like receptor 4 recognition of Salmonella. Cellular microbiology 10, 876-890.

290. Parkhill, J., Dougan, G., James, K.D., Thomson, N.R., Pickard, D., Wain, J., Churcher, C., Mungall, K.L., Bentley, S.D., Holden, M.T., et al. (2001). Complete genome sequence of a multiple drug resistant Salmonella enterica serovar Typhi CT18. Nature 413, 848-852.

291. Hirose, K., Ezaki, T., Miyake, M., Li, T., Khan, A.Q., Kawamura, Y., Yokoyama, H., and Takami, T. (1997). Survival of Vi-capsulated and Vi-deleted Salmonella typhi strains in cultured macrophage expressing different levels of CD14 antigen. FEMS microbiology letters 147, 259-265.

292. Sharma, A., and Qadri, A. (2004). Vi polysaccharide of Salmonella typhi targets the prohibitin family of molecules in intestinal epithelial cells and suppresses early inflammatory responses. Proceedings of the National Academy of Sciences of the United States of America 101, 17492-17497.

293. Szu SC, Klugman KP, Hunt S. Re-examination of immune response and estimation of anti-Vi IgG protective threshold against typhoid fever-based on the efficacy trial of Vi conjugate in young children.Vaccine (2014) 32(20):2359–63. doi:10.1016/j.vaccine.2014.02.050

294. Raffatellu, M., Chessa, D., Wilson, R.P., Dusold, R., Rubino, S., and Baumler, A.J. (2005). The Vi capsular antigen of Salmonella enterica serotype Typhi reduces Toll like receptor-dependent interleukin-8 expression in the intestinal mucosa. Infection and immunity 73, 3367-3374.

295. Kintz E, Heiss C, Black I, Donohue N, Brown N, Davies MR, Azadi P, Baker S, Kaye PM, van der Woude M. Salmonella enterica Serovar Typhi Lipopolysaccharide O-Antigen Modification Impact on Serum Resistance and Antibody Recognition. Infect Immun. 2017 Mar 23;85(4):e01021-16. doi: 10.1128/IAI.01021-16. PMID: 28167670; PMCID: PMC5364305.

296. Tacket CO, Galen J, Sztein MB, Losonsky G, Wyant TL, Nataro J, et al. Safety and immune responses to attenuated Salmonella enterica serovar Typhi oral live vector vaccines expressing tetanus toxin fragment C. Clin Immunol (2000) 97(2):146–53. doi:10.1006/clim.2000.4924

297. Tacket CO, Pasetti MF, Sztein MB, Livio S, Levine MM. Immune responses to an oral typhoid vaccine strain that is modified to constitutively express Vi capsular polysaccharide. J Infect Dis (2004) 190(3):565–70. doi:10.1086/421469

298. Hohmann EL, Oletta CA, Killeen KP, Miller SI. phoP/phoQ-deleted Salmonella typhi (Ty800) is a safe and immunogenic single-dose typhoid fever vaccine in volunteers. J Infect Dis (1996) 173(6):1408–14. doi:10.1093/infdis/173. 6.1408

299. Salazar-Gonzalez RM, Niess JH, Zammit DJ, Ravindran R, Srinivasan A, Maxwell JR, et al. CCR6-mediated dendritic cell activation of pathogen-specific T cells in Peyer's patches. Immunity. (2006) 24:623 32. doi: 10.1016/j.immuni.2006.02.015

300. McSorley SJ, Asch S, Costalonga M, Reinhardt RL, Jenkins MK. Tracking Salmonella-specific CD4T cells in vivo reveals a local mucosal response to a disseminated infection. Immunity. (2002) 16:365–77. doi: 10.1016/S1074-7613(02)00289-3

301. Hess, J., Ladel, C., Miko, D., and Kaufmann, S.H. (1996). Salmonella typhimuriumaroA- infection in gene-targeted immunodeficient mice: major role of CD4+ TCR alpha beta cells and IFN-gamma in bacterial clearance independent of intracellular location. Journal of immunology 156, 3321-3326.

302. McSorley, S.J., and Jenkins, M.K. (2000). Antibody is required for protection against virulent but not attenuated Salmonella enterica serovar typhimurium. Infection and immunity 68, 3344-3348.

303. Griffin, A.J., and McSorley, S.J. (2011). Development of protective immunity to Salmonella, a mucosal pathogen with a systemic agenda. Mucosal immunology 4, 371-382.

304. Johanns, T.M., Ertelt, J.M., Rowe, J.H., and Way, S.S. (2010). Regulatory T cell suppressive potency dictates the balance between bacterial proliferation and clearance during persistent Salmonella infection. PLoS pathogens 6, e1001043.

305. Hess J, Ladel C, Miko D, Kaufmann S. Salmonella typhimurium aroA infection in gene-targeted immunodeficient mice: major role of CD4+ TCR alpha beta cells and IFN-gamma in bacterial clearance independent of intracellular location. J Immunol. (1996) 156:3321–6.

306. Ravindran R, Foley J, Stoklasek T, Glimcher LH, McSorley SJ. Expression of T-bet by CD4T cells is essential for resistance to Salmonella infection. J Immunol. (2005) 175:4603–10. doi: 10.4049/jimmunol.175.7.4603

307. Lee S-J, Dunmire S, McSorley SJ. MHC class-I-restricted CD8T cells play a protective role during primary Salmonella infection. Immunol Lett. (2012) 148:138–43. doi: 10.1016/j.imlet.2012.10.009

308. Kupz A, Bedoui S, Strugnell RA. Cellular requirements for systemic control of Salmonella enterica serovar Typhimurium infections in mice. Infect Immun. (2014) 82:4997–5004. doi: 10.1128/IAI.02192-14

309. Jones BD, Ghori N, Falkow S. Salmonella typhimurium initiates murine infection by penetrating and destroying the specialized epithelial M cells of the Peyer's patches. J Exp Med. (1994) 180:15–23. doi: 10.1084/jem.180.1.15

310. Labrec EH, Schneider H, Magnani TJ, Formal SB. Epithelial cell penetration as an essential step in the pathogenesis of bacillary dysentery. J Bacteriol. (1964) 88:1503–18. doi: 10.1128/JB.88.5.1503-1518.1964

311. Mabbott NA, Donaldson DS, Ohno H, Williams IR, Mahajan A. Microfold (M) cells: important immunosurveillance posts in the intestinal epithelium. Mucosal Immunol. (2013) 6:666–77. doi: 10.1038/mi.2013.30

312. Sansonetti PJ, Di Santo JP. Debugging how bacteria manipulate the immune response. Immunity. (2007) 26:149–61. doi: 10.1016/j.immuni.2007.02.004

313. Gutzeit C, Magri G, Cerutti A. Intestinal IgA production and its role in host-microbe interaction. Immunol Rev. (2014) 260:76–85. doi: 10.1111/imr.12189 9

314. Zimmermann K, Haas A, Oxenius A. Systemic antibody responses to gut microbes in health and disease. Gut Microbes. (2012) 3:42 7. doi: 10.4161/gmic.19344

315. Takahashi I, Nochi T, Yuki Y, Kiyono H: New horizon of mucosal immunity and vaccines. Curr Opin Immunol 2009, 21:352-358
316. Levine MM, Kotloff KL, Barry EM, Pasetti MF, Sztein MB: Clinical trials of Shigella vaccines: two steps forward and one step back on a long, hard road. Nat Rev Microbiol 2007, 5:540-553
317. Robin, G. et al. Characterization and quantitative analysis of serum IgG class and subclass response to Shigella sonnei and Shigella flexneri 2a lipopolysaccharide following natural Shigella infection. J. Infect. Dis. 175, 1128–1133 (1997).
318. Cohen, D., Green, M. S., Block, C., Rouach, T. & Ofek, I. Serum antibodies to lipopolysaccharide and natural immunity to shigellosis in an Israeli military population. J. Infect. Dis. 157, 1068–1071 (1988).
319. Cohen, D., Green, M. S., Block, C., Slepon, R. & Ofek, I. Prospective study of the association between serum antibodies to lipopolysaccharide O antigen and the attack rate of shigellosis. J. Clin. Microbiol. 29, 386–389 (1991).
320. Van De Verg, L. L., Herrington, D. A., Boslego, J., Lindberg, A. A. & Levine, M. M. Age-specific prevalence of serum antibodies to the invasion plasmid and lipopolysaccharide antigens of Shigella species in Chilean and North American populations. J. Infect. Dis. 166, 158–161 (1992).
321. Li, A., Zhao, C. R., Ekwall, E. & Lindberg, A. A. Serum IgG antibody responses to Shigella invasion plasmid-coded antigens detected by immunoblot. Scand. J. Infect. Dis. 26, 435–445 (1994).
322. Oaks, E. V., Hale, T. L. & Formal, S. B. Serum immune response to Shigella protein antigens in rhesus monkeys and humans infected with Shigella spp. Infect. Immun. 53, 57–63 (1986).
323. Oberhelman, R. A. et al. Prospective study of systemic and mucosal immune responses in dysenteric patients to specific Shigella invasion plasmid antigens and lipopolysaccharides. Infect. Immun. 59, 2341–2350 (1991).
324. Sayem, M. A. et al. Differential host immune responses to epidemic and endemic strains of Shigella dysenteriae type I. J. Health Popul. Nutr. 29, 429–437 (2011).
325. Lowell, G. H. et al. Antibody-dependent cell mediated antibacterial activity: K lymphocytes, monocytes, and granulocytes are effective against Shigella. J. Immunol. 125, 2778–2784 (1980).
326. Kotloff, K. L. et al. Safety, immunogenicity, and transmissibility in humans of CVD 1203, a live oral Shigella flexneri 2a vaccine candidate attenuated by deletions in aroA and virG. Infect. Immun. 64, 4542–4548 (1996).
327. Coster, T. S. et al. Vaccination against shigellosis with attenuated Shigella flexneri 2a strain SC602. Infect. Immun. 67, 3437–3443 (1999).
328. Sperandio B, Regnault B, Guo J, Zhang Z, Stanley Jr SL, Sansonetti PJ, et al. Virulent Shigella flexneri subverts the host innate immune response through manipulation of antimicrobial peptide gene expression. J Exp Med. (2008) 205:1121–32. doi: 10.1084/jem.20071698
329. Kim DW, Chu H, Joo DH, Jang MS, Choi JH, Park S-M, et al. OspF directly attenuates the activity of extracellular signal-regulated kinase during invasion by Shigella flexneri in human dendritic cells. Mol Immunol. (2008) 45:3295–301. doi: 10.1016/j.molimm.2008.02.013
330. Ng SC, Kamm MA, Stagg AJ, Knight SC. Intestinal dendritic cells: their role in bacterial recognition, lymphocyte homing, and intestinal inflammation. Inflamm Bowel Dis. 2010; 16:1787–1807. [PubMed: 20222140]

331. Joffre OP, Segura E, Savina A, Amigorena S. Cross-presentation by dendritic cells. Nat Rev Immunol. 2012; 12:557–569. [PubMed: 22790179]
332. Noriega FR, Liao FM, Formal SB, Fasano A, Levine MM. Prevalence of Shigella enterotoxin 1 among Shigella clinical isolates of diverse serotypes. J Infect Dis. 1995; 172:1408–1410. [PubMed: 7594690]
333. Benjelloun-Touimi Z, Sansonetti PJ, Parsot C. SepA, the major extracellular protein of Shigella flexneri: autonomous secretion and involvement in tissue invasion. Mol Microbiol. 1995; 17:123–135. [PubMed: 7476198]
334. Wu T, Grassel C, Levine MM, Barry EM. Live attenuated Shigella dysenteriae type 1 vaccine strains overexpressing shiga toxin B subunit. Infect Immun. 2011; 79:4912–4922. [PubMed: 21969003]
335. Sellge G, Magalhaes JG, Konradt C, Fritz JH, Salgado-Pabon W, Eberl G, et al. Th17 cells are the dominant T cell subtype primed by Shigella flexneri mediating protective immunity. J Immunol. (2010) 184:2076– 85. doi: 10.4049/jimmunol.0900978.
336. Tennant SM, Levine MM. Live attenuated vaccines for invasive Salmonella infections. Vaccine. 2015 Jun 19;33 Suppl 3(0 3):C36-41. doi: 10.1016/j.vaccine.2015.04.029. Epub 2015 Apr 19. PMID: 25902362; PMCID: PMC4469493.
337. Tennant SM, Levine MM. Live attenuated vaccines for invasive Salmonella infections. Vaccine. 2015 Jun 19;33 Suppl 3(0 3):C36-41. doi: 10.1016/j.vaccine.2015.04.029. Epub 2015 Apr 19. PMID: 25902362; PMCID: PMC4469493.
338. Sanz, I., Wei, C., Lee, F. E. & Anolik, J. Phenotypic and functional heterogeneity of human memory B cells. Semin. Immunol. 20, 67–82 (2008).
339. Syed KA, Saluja T, Cho H, Hsiao A, Shaikh H, Wartel TA, Mogasale V, Lynch J, Kim JH, Excler JL, Sahastrabuddhe S. Review on the Recent Advances on Typhoid Vaccine Development and Challenges Ahead. Clin Infect Dis. 2020 Jul 29;71(Suppl 2):S141-S150. doi: 10.1093/cid/ciaa504. PMID: 32725225; PMCID: PMC7388714.
340. World Health Organization Typhoid vaccines: WHO position paper, March 2018 - Recommendations. Vaccine. 2019 Jan 07;37(2):214-216.
341. Marathe SA, Lahiri A, Negi VD, Chakravortty D. Typhoid fever & vaccine development: a partially answered question. Indian J Med Res. 2012;135(2):161-9. PMID: 22446857; PMCID: PMC3336846.
342. Chilean Typhoid Committee, Levine MM, Ferreccio C, Black RE, Germanier R. Large-scale ®eld trial of Ty21a live oral typhoid vaccine in enteric-coated capsule formulation. Lancet 1987;1:1049±52
343. Chilean Typhoid Committee, Black RE, Levine MM, Ferreccio C, Clements ML, Lanata C, Rooney J, Germanier R. E• cacy of one or two doses of Ty21a Salmonella typhi vaccine in enteric-coated capsules in a controlled ®eld trial. Vaccine 1990;8:81±4.
344. Ferreccio C, Levine MM, Rodriguez H, Contreras R. Comparative efficacy of two, three, or four doses of Ty21a live oral typhoid vaccine in enteric-coated capsules: a ®eld trial in an endemic area. J Infect Dis 1989;159:766±9.
345. Levine MM, Ferreccio C, Cryz S, Ortiz E. Comparison of enteric-coated capsules and liquid formulation of Ty21a typhoid vaccine in randomised controlled ®eld trial. Lancet 1990;336:891±4.

346. Simanjuntak C, Paleologo F, Punjabi N, Darmowitogo R, Soeprawato, Totosudirjo H, Haryanto P, Suprijanto E, Witham N, Ho€ man SL, Oral immunisation against typhoid fever in Indonesia with Ty21a vaccine. Lancet 1991;338:1055±59.
347. Levine MM, Taylor DN, Ferreccio C. Typhoid vaccines come of age. Pediatr Infect Dis J 1989;8:374±81
348. Levine MM, Galen J, Barry E, Noriega F, Chatfield S, Sztein M, Dougan G, Tacket C. Attenuated Salmonella as live oral vaccines against typhoid fever and as live vectors. J Biotechnol. 1996 Jan 26;44(1-3):193-6. doi: 10.1016/0168-1656(95)00094-1. PMID: 8717403
349. Hoiseth SK, Stocker BA. Aromatic-dependent Salmonella typhimurium are non-virulent and effective as live vaccines. Nature. 1981; 291:238–239.
350. Eisenstein TK, Killar LM, Stocker BA, Sultzer BM. Cellular immunity induced by avirulent Salmonella in LPS-defective C3H/HeJ mice. J Immunol. 1984; 133:958–961.
351. Harrison JA, Villarreal-Ramos B, Mastroeni P, Demarco de Hormaeche R, Hormaeche CE. Correlates of protection induced by live Aro- Salmonella typhimurium vaccines in the murine typhoid model. Immunology. 1997; 90:618–625.
352. Tacket CO, Hone DM, Losonsky GA, Guers L, Edelman R, Levine MM. Clinical acceptability and immunogenicity of CVD 908 Salmonella typhi vaccine strain. Vaccine. 1992;10(7):443-6. doi: 10.1016/0264-410x(92)90392-w. PMID: 1609547
353. Levine MM, Galen J, Barry E, Noriega F, Chatfield S, Sztein M, Dougan G, Tacket C. Attenuated Salmonella as live oral vaccines against typhoid fever and as live vectors. J Biotechnol. 1996 Jan 26;44(1-3):193-6. doi: 10.1016/0168-1656(95)00094-1. PMID: 8717403.
354. Tacket CO, Sztein MB, Wasserman SS, Losonsky G, Kotloff KL, Wyant TL, Nataro JP, Edelman R, Perry J, Bedford P, Brown D, Chatfield S, Dougan G, Levine MM. Phase 2 clinical trial of attenuated Salmonella enterica serovar typhi oral live vector vaccine CVD 908-htrA in U.S. volunteers. Infect Immun. 2000 Mar;68(3):1196-201. doi: 10.1128/IAI.68.3.1196-1201.2000. PMID: 10678926; PMCID: PMC97267.
355. Johnson, K., I. Charles, G. Dougan, D. Pickard, P. O'Gaora, G. Costa, T. Ali, I. Miller, and C. Hormaeche. 1991. The role of a stress-response protein in Salmonella typhimurium virulence. Mol. Microbiol. 5:401–407
356. Lowe, D. C., T. C. Savidge, D. Pickard, L. Eckmann, M. F. Kagnoff, G. Dougan, and S. N. Chatfield. 1999. Characterization of candidate live oral Salmonella typhi vaccine strains harboring defined mutations in aroA, aroC, and htrA. Infect. Immun. 67:700–707.
357. Black R, Levine MM, Young C, et al. Immunogenicity of Ty21a attenuated Salmonella typhi given with sodium bicarbonate or in enteric coated capsules. Dev Biol Stand 1983; 53:9–14.
358. Tacket CO, Sztein MB, Losonsky GA, et al. Safety and immune response in humans of live oral Salmonella typhi vaccine strains deleted in htrA and aroC aroD. Infect Immun 1997; 65:452–6.
359. Wang JY, Noriega FR, Galen JE, Barry E, Levine MM. Constitutive expression of the Vi polysaccharide capsular antigen in attenuated Salmonella enterica serovar Typhi oral vaccine strain CVD 909. Infect Immun. 2000; 68:4647–4652.
360. Tacket CO, Pasetti MF, Sztein MB, Livio S, Levine MM. Immune responses to an oral typhoid vaccine strain that is modified to constitutively express Vi capsular polysaccharide. J Infect Dis. 2004; 190:565–570. [PubMed: 15243933]

361. Tennant SM, Levine MM. Live attenuated vaccines for invasive Salmonella infections. Vaccine. 2015 Jun 19;33 Suppl 3(0 3):C36-41. doi: 10.1016/j.vaccine.2015.04.029. Epub 2015 Apr 19. PMID: 25902362; PMCID: PMC4469493.
362. Miller SI, Kukral AM, Mekalanos JJ. A two-component regulatory system (phoP phoQ) controls Salmonella typhimurium virulence. Proc Natl Acad Sci U S A. 1989; 86:5054–5058. [PubMed: 2544889]
363. Groisman EA, Chiao E, Lipps CJ, Heffron F. Salmonella typhimurium phoP virulence gene is a transcriptional regulator. Proc Natl Acad Sci U S A. 1989; 86:7077–7081. [PubMed: 2674945]
364. Belden WJ, Miller SI. Further characterization of the PhoP regulon: identification of new PhoPactivated virulence loci. Infect Immun. 1994; 62:5095–5101. [PubMed: 7927792].
365. Miller SI, Kukral AM, Mekalanos JJ. A two-component regulatory system (phoP phoQ) controls Salmonella typhimurium virulence. Proc Natl Acad Sci U S A. 1989; 86:5054–5058. [PubMed: 2544889]
366. Fields PI, Groisman EA, Heffron F. A Salmonella locus that controls resistance to microbicidal proteins from phagocytic cells. Science. 1989; 243:1059–1062. [PubMed: 2646710]
367. Hohmann EL, Oletta CA, Killeen KP, Miller SI. phoP/phoQ-deleted Salmonella typhi (Ty800) is a safe and immunogenic single-dose typhoid fever vaccine in volunteers. J Infect Dis. 1996; 173:1408–1414. [PubMed: 8648213]
368. Kirkpatrick BD, McKenzie R, O'Neill JP, Larsson CJ, Bourgeois AL, Shimko J, Bentley M, Makin J, Chatfield S, Hindle Z, Fidler C, Robinson BE, Ventrone CH, Bansal N, Carpenter CM, Kutzko D, Hamlet S, LaPointe C, Taylor DN. Evaluation of Salmonella enterica serovar Typhi (Ty2 aroC-ssaV-) M01ZH09, with a defined mutation in the Salmonella pathogenicity island 2, as a live, oral typhoid vaccine in human volunteers. Vaccine. 2006 Jan 12;24(2):116-23. doi: 10.1016/j.vaccine.2005.08.008. Epub 2005 Aug 18. PMID: 16140433.
369. Tran TH, Nguyen TD, Nguyen TT, Ninh TT, Tran NB, Nguyen VM, Tran TT, Cao TT, Pham VM, Nguyen TC, Tran TD, Pham VT, To SD, Campbell JI, Stockwell E, Schultsz C, Simmons CP, Glover C, Lam W, Marques F, May JP, Upton A, Budhram R, Dougan G, Farrar J, Nguyen VV, Dolecek C. A randomised trial evaluating the safety and immunogenicity of the novel single oral dose typhoid vaccine M01ZH09 in healthy Vietnamese children. PLoS One. 2010 Jul 26;5(7):e11778. doi: 10.1371/journal.pone.0011778. PMID: 20668668; PMCID: PMC2909895.
370. Tran TH, Nguyen TD, Nguyen TT, Ninh TT, Tran NB, Nguyen VM, et al. A randomised trial evaluating the safety and immunogenicity of the novel single oral dose typhoid vaccine M01ZH09 in healthy Vietnamese children. PLoS One. 2010; 5:e11778. [PubMed: 20668668]
371. Lyon CE, Sadigh KS, Carmolli MP, Harro C, Sheldon E, Lindow JC, et al. In a randomized, double-blinded, placebo-controlled trial, the single oral dose typhoid vaccine, M01ZH09, is safe and immunogenic at doses up to 1.7 × 10(10) colony-forming units. Vaccine. 2010; 28:3602– 3608. [PubMed: 20188175]
372. Kirkpatrick BD, Tenney KM, Larsson CJ, O'Neill JP, Ventrone C, Bentley M, et al. The novel oral typhoid vaccine M01ZH09 is well tolerated and highly immunogenic in 2 vaccine presentations. J Infect Dis. 2005; 192:360–366. [PubMed: 15995948]

373. Darton TC, Jones C, Blohmke CJ, et al. Using a human challenge model of infection to measure vaccine efficacy: a randomised, controlled trial comparing the typhoid vaccines M01ZH09 with placebo and Ty21a. PLOS Negl Trop Dis 2016; 10:e0004926.
374. Micoli, F.; Costantino, P.; Adamo, R. Potential targets for next generation antimicrobial glycoconjugate vaccines. FEMS Microbiol. Rev. 2018, 42, 388–423. [CrossRef]
375. Robbins, J.D.; Robbins, J.B. Reexamination of the protective role of the capsular polysaccharide (Vi antigen) of Salmonella typhi. J. Infect. Dis. 1984, 150, 436–449, Raffatellu, M.; Chessa, D.; Wilson, R.P.; Tukel, C.; Akcelik, M.; Baumler, A.J. Capsule-mediated immune evasion: A new hypothesis explaining aspects of typhoid fever pathogenesis. Infect. Immun. 2006, 74, 19–27.
376. Wilson, R.P.; Winter, S.E.; Spees, A.M.; Winter, M.G.; Nishimori, J.H.; Sanchez, J.F.; Nuccio, S.P.; Crawford, R.W.; Tukel, C.; Baumler, A.J. The Vi capsular polysaccharide prevents complement receptor 3-mediated clearance of Salmonella enterica serotype Typhi. Infect. Immun. 2010, 79, 830–837
377. World Health Organization. Typhoid vaccines: WHO position paper. Wkly Epidemiol Rec 2008; 83:49–60
378. Ivanoff B, Levine MM, Lambert PH. Vaccination against typhoid fever: present status. Bull World Health Organ 1994; 72:957–71
379. World Health Organization. Typhoid vaccines: WHO position paper. Wkly Epidemiol Rec 2008; 83:49–60
380. Zhou WZ, Koo HW, Wang XY, et al. Revaccination with locally-produced Vi typhoid polysaccharide vaccine among Chinese school-aged children: safety and immunogenicity findings. Pediatr Infect Dis J 2007; 26:1001–5.
381. Thiem VD, Lin FY, Canh do G, et al. The Vi conjugate typhoid vaccine is safe, elicits protective levels of IgG anti-Vi, and is compatible with routine infant vaccines. Clin Vaccine Immunol 2011; 18:730–5.
382. Canh DG, Lin FY, Thiem VD, et al. Effect of dosage on immunogenicity of a Vi conjugate vaccine injected twice into 2- to 5-year-old Vietnamese children. Infect Immun 2004; 72:6586–8
383. Lin FY, Ho VA, Khiem HB, et al. The efficacy of a Salmonella Typhi Vi conjugate vaccine in two-to-five-year-old children. N Engl J Med 2001; 344:1263–9.
384. Mai NL, Phan VB, Vo AH, et al. Persistent efficacy of Vi conjugate vaccine against typhoid fever in young children. N Engl J Med 2003; 349:1390–1.
385. Milligan R, Paul M, Richardson M, Neuberger A. Vaccines for preventing typhoid fever. Cochrane Database Syst Rev. 2018 May 31;5(5):CD001261.
386. Batool R, Qamar ZH, Salam RA, Yousafzai MT, Ashorn P, Qamar FN. Efficacy of typhoid vaccines against culture-confirmed Salmonella Typhi in typhoid endemic countries: a systematic review and meta-analysis. Lancet Glob Health. 2024 Apr;12(4):e589-e598.
387. Patel PD, Liang Y, Meiring JE, Chasweka N, Patel P, Misiri T, Mwakiseghile F, Wachepa R, Banda HC, Shumba F, Kawalazira G, Dube Q, Nampota-Nkomba N, Nyirenda OM, Girmay T, Datta S, Jamka LP, Tracy JK, Laurens MB, Heyderman RS, Neuzil KM, Gordon MA., TyVAC team. Efficacy of typhoid conjugate vaccine: final analysis of a 4-year, phase 3, randomised controlled trial in Malawian children. Lancet. 2024 Feb 03;403(10425):459-468.

388. Gloeck NR, Leong T, Iwu-Jaja CJ, Katoto PDM, Kredo T, Wiysonge CS. Typhoid conjugate vaccines for preventing typhoid fever (enteric fever). Cochrane Database Syst Rev. 2023 Jun 14;2023(6):CD015746. doi: 10.1002/14651858.CD015746. PMCID: PMC10266125.

389. International Vaccine Institute. IVI-SK's new typhoid conjugate vaccine meets primary endpoints in phase III study in Nepal. https://www.ivi.int/ivi-sks-new-typhoidconjugate-vaccine-meets-primary-endpoints-in-phase-iiistudy-in-nepal/. Accessed 15 April 2021.

390. Zhicheng Dai, Jiafeng Zhang, Zhengbo Tao, Rui Gao & Qinghua Zhao. (2024) Adverse events associated with teriparatide: a real-world disproportionality analysis of the FDA adverse event reporting system (FAERS). *Expert Opinion on Drug Safety* 0:0, pages 1-9.

391. Kumar Rai G, Saluja T, Chaudhary S, Tamrakar D, Kanodia P, Giri BR, Shrestha R, Uranw S, Kim DR, Yang JS, Park IY, Kyung SE, Vemula S, Reddy E J, Kim B, Gupta BP, Jo SK, Ryu JH, Park HK, Shin JH, Lee Y, Kim H, Kim JH, Mojares ZR, Wartel TA, Sahastrabuddhe S. Safety and immunogenicity of the Vi-DT typhoid conjugate vaccine in healthy volunteers in Nepal: an observer-blind, active-controlled, randomised, non-inferiority, phase 3 trial. Lancet Infect Dis. 2022 Apr;22(4):529-540.

392. van Damme P, Kafeja F, Anemona A, Basile V, Hilbert AK, De Coster I, Rondini S, Micoli F, Qasim Khan RM, Marchetti E, Di Cioccio V, Saul A, Martin LB, Podda A. Safety, immunogenicity and dose ranging of a new Vi-CRM_{197} conjugate vaccine against typhoid fever: randomized clinical testing in healthy adults. PLoS One. 2011;6(9):e25398. doi: 10.1371/journal.pone.0025398. Epub 2011 Sep 30. PMID: 21980445; PMCID: PMC3184126.

393. Bhutta ZA, Capeding MR, Bavdekar A, Marchetti E, Ariff S, Soofi SB, Anemona A, Habib MA, Alberto E, Juvekar S, Khan RM, Marhaba R, Ali N, Malubay N, Kawade A, Saul A, Martin LB, Podda A. Immunogenicity and safety of the Vi-CRM197 conjugate vaccine against typhoid fever in adults, children, and infants in south and southeast Asia: results from two randomised, observer-blind, age de-escalation, phase 2 trials. Lancet Infect Dis. 2014 Feb;14(2):119-29. doi: 10.1016/S1473-3099(13)70241-X. Epub 2013 Nov 28. PMID: 24290843.

394. Pham OH, McSorley SJ. Protective host immune responses to Salmonella infection. Future Microbiol. 2015;10(1):101-10. doi: 10.2217/fmb.14.98. PMID: 25598340; PMCID: PMC4323267.

395. Tomoyasu T, Ohkishi T, Ukyo Y, Tokumitsu A, Takaya A, Suzuki M, et al. The ClpXP ATPdependent protease regulates flagellum synthesis in Salmonella enterica serovar typhimurium. J Bacteriol. 2002; 184:645–653. [PubMed: 11790733]

396. Tomoyasu T, Takaya A, Isogai E, Yamamoto T. Turnover of FlhD and FlhC, master regulator proteins for Salmonella flagellum biogenesis, by the ATP-dependent ClpXP protease. Mol Microbiol. 2003; 48:443–452. [PubMed: 12675803]

397. Tennant SM, Wang JY, Galen JE, Simon R, Pasetti MF, Gat O, et al. Engineering and preclinical evaluation of attenuated nontyphoidal Salmonella strains serving as live oral vaccines and as reagent strains. Infect Immun. 2011; 79:4175–4185. [PubMed: 21807911]

398. Gewirtz AT, Navas TA, Lyons S, Godowski PJ, Madara JL, Cutting edge: bacterial flagellin activates basolaterally expressed TLR5 to induce epithelial proinflammatory gene expression, J. Immunol 167 (2001) 1882–1885. [PubMed: 11489966]

399. Gat O, Galen JE, Tennant S, Simon R, Blackwelder WC, Silverman DJ, Pasetti MF, Levine MM, Cell-associated flagella enhance the protection conferred by mucosally-administered attenuated Salmonella Paratyphi A vaccines, PLoS Negl. Trop. Dis 5 (2011) e1373. [PubMed: 22069504]
400. Sztein MB, Wasserman SS, Tacket CO, Edelman R, Hone D, Lindberg AA, Levine MM, Cytokine production patterns and lymphoproliferative responses in volunteers orally immunized with attenuated vaccine strains of Salmonella typhi, J. Infect. Dis 170 (1994) 1508–1517. [PubMed: 7995991]
401. Wyant TL, Tanner MK, Sztein MB, Salmonella typhi flagella are potent inducers of proinflammatory cytokine secretion by human monocytes, Infect. Immun 67 (1999) 3619–3624. [PubMed: 10377147]
402. Wyant TL, Tanner MK, Sztein MB, Potent immunoregulatory effects of Salmonella typhi flagella on antigenic stimulation of human peripheral blood mononuclear cells, Infect. Immun 67 (1999) 1338–1346. [PubMed: 10024580]
403. Oyston PC, Mellado-Sanchez G, Pasetti MF, Nataro JP, Titball RW, Atkins HS. A Yersinia pestis guaBA mutant is attenuated in virulence and provides protection against plague in a mouse model of infection. Microb Pathog. 2010 May;48(5):191-5. doi: 10.1016/j.micpath.2010.01.005. Epub 2010 Jan 22. PMID: 20096773; PMCID: PMC2857377.
404. Wahid R, Kotloff KL, Levine MM, Sztein MB. Cell mediated immune responses elicited in volunteers following immunization with candidate live oral Salmonella enterica serovar Paratyphi A attenuated vaccine strain CVD 1902. Clin Immunol. 2019 Apr;201:61-69. doi: 10.1016/j.clim.2019.03.003. Epub 2019 Mar 5. PMID: 30849494; PMCID: PMC6959129.
405. Trebicka E, Jacob S, Pirzai W, Hurley BP, Cherayil BJ. Role of antilipopolysaccharide antibodies in serum bactericidal activity against Salmonella enterica serovar Typhimurium in healthy adults and children in the United States. Clin Vaccine Immunol. 2013 Oct;20(10):1491-8. doi: 10.1128/CVI.00289-13. Epub 2013 Jun 26. PMID: 23803904; PMCID: PMC3807195.
406. Konadu E, Shiloach J, Bryla DA, Robbins JB, Szu SC (1996) Synthesis, characterization, and immunological properties in mice of conjugates composed of detoxified lipopolysaccharide of Salmonella paratyphi A bound to tetanus toxoid with emphasis on the role of O acetyls. Infect Immun 64: 2709–2715.
407. Konadu EY, Lin FY, Ho VA, et al. Phase 1 and phase 2 studies of Salmonella enterica serovar paratyphi A O-specific polysaccharide-tetanus toxoid conjugates in adults, teenagers, and 2- to 4-year-old children in Vietnam. Infect Immun 2000; 68:1529–34
408. MacLennan CA, Stanaway J, Grow S, Vannice K, Steele AD. *Salmonella* Combination Vaccines: Moving Beyond Typhoid. Open Forum Infect Dis. 2023 Jun 2;10(Suppl 1):S58-S66. doi: 10.1093/ofid/ofad041. PMID: 37274529; PMCID: PMC10236507.
409. Zhang, F.; Thompson, C.; Ma, N.; Lu, Y.J.; Malley, R. Carrier Proteins Facilitate the Generation of Antipolysaccharide Immunity via Multiple Mechanisms. mBio 2022, 13, e03790-21
410. Zhang, F.; Ledue, O.; Jun, M.; Goulart, C.; Malley, R.; Lu, Y.J. Protection against Staphylococcus aureus Colonization and Infection by B- and T-Cell-Mediated Mechanisms. mBio 2018, 9, e01949-18.
411. van Sorge, N.M.; Cole, J.N.; Kuipers, K.; Henningham, A.; Aziz, R.K.; Kasirer-Friede, A.; Lin, L.; Berends, E.T.M.; Davies, M.R.; Dougan, G.; et al. The classical lancefield antigen of group a Streptococcus is a virulence determinant with implications for vaccine design. Cell Host Microbe 2014, 15, 729–740.

412. Zhang, F.; Lu, Y.J.; Malley, R. Multiple antigen-presenting system (MAPS) to induce comprehensive B- and T-cell immunity. Proc. Natl. Acad. Sci. USA 2013, 110, 13564–13569.
413. Zhang F, Boerth EM, Gong J, Ma N, Lucas K, Ledue O, Malley R, Lu YJ. A Bivalent MAPS Vaccine Induces Protective Antibody Responses against Salmonella Typhi and Paratyphi A. Vaccines (Basel). 2022 Dec 30;11(1):91. doi: 10.3390/vaccines11010091. PMID: 36679935; PMCID: PMC9865949.
414. Micoli F, MacLennan CA. Outer membrane vesicle vaccines. Semin Immunol 2020; 50:101433., Fiorino F, Rondini S, Micoli F, et al. Immunogenicity of a bivalent adjuvanted gly coconjugate vaccine against Salmonella Typhimurium and Salmonella Enteritidis. Front Immunol 2017; 8:168.
415. Micoli F, Rondini S, Alfini R, et al. Comparative immunogenicity and efficacy of equivalent outer membrane vesicle and glycoconjugate vaccines against nonty phoidal Salmonella. Proc Natl Acad Sci U S A 2018; 115:10428–33.
416. Zhang F, Lu YJ, Malley R. Multiple antigen-presenting system (MAPS) to induce comprehensive B- and T-cell immunity. Proc Natl Acad Sci U S A 2013; 110: 13564–9.
417. Zhang F, Lu YJ, Malley R. Multiple antigen-presenting system (MAPS) to induce comprehensive B- and T-cell immunity. Proc Natl Acad Sci U S A 2013; 110: 13564–9.
418. Baliban SM, Allen JC, Curtis B, et al. Immunogenicity and induction of functional antibodies in rabbits immunized with a trivalent typhoid-invasive nontyphoidal Salmonella glycoconjugate formulation. Molecules 2018; 23:1749.
419. University of Maryland. NCT03981952 Salmonella conjugates CVD 1000: study of responses to vaccination with trivalent invasive Salmonella disease vac cine. 2021. https://clinicaltrials.gov/ct2/show/NCT03981952?cond=salmonella +typhimurium&draw=2&rank=8. Accessed 6 November 2022.
420. University of Maryland. NCT05525546 Salmonella conjugates CVD 2000: study of responses to vaccination with trivalent Salmonella conjugate vaccine to prevent invasive Salmonella disease. 2022. https://clinicaltrials.gov/ct2/show/ NCT05525546?cond=salmonella+typhimurium&draw=2&rank=9. Accessed 6 November 2022.
421. Borrow R, Dagan R, Zepp F, Hallander H, Poolman J. Glycoconjugate vaccines and immune interactions, and implications for vaccination schedules. Expert Rev Vaccines. 2011 Nov;10(11):1621-31. doi: 10.1586/erv.11.142. PMID: 22043960
422. International Vaccine Institute. Vaccines for a safer future. 2020. https://www.ivi. int/wp-content/uploads/2021/05/IVI-Annual-Report-2020-vf.pdf. Accessed 6 November 2022.
423. Findlow H, Borrow R. Interactions of conjugate vaccines and co-administered vaccines. Hum Vaccin Immunother. 2016;12(1):226-30. doi: 10.1080/21645515.2015.1091908. PMID: 26619353; PMCID: PMC4962715.
424. Dagan R, Poolman J, Siegrist CA. Glycoconjugate vaccines and immune interference: a review. Vaccine 2010;28:5513–23.
425. Barnoy, S.; Jeong, K.I.; Helm, R.F.; Suvarnapunya, A.E.; Ranallo, R.T.; Tzipori, S.; Venkatesan, M.M. Characterization of WRSs2 and WRSs3, new second-generation virG(icsA)-based Shigella sonnei vaccine candidates with the potential for reduced reactogenicity. Vaccine 2010, 28, 1642–1654.

426. Shrivastava S, Agnememel AB, Ndungo E, Islam D, Liang Y, Frenck RW Jr, Pasetti MF. Oral immunization with *Shigella sonnei* WRSs2 and WRSs3 vaccine strains elicits systemic and mucosal antibodies with functional anti-microbial activity. mSphere. 2024 Jan 30;9(1):e0041923. doi: 10.1128/msphere.00419-23. Epub 2023 Dec 22. PMID: 38132716; PMCID: PMC10826362.
427. Frenck, R.W., Jr.; Baqar, S.; Alexander, W.; Dickey, M.; McNeal, M.; El-Khorazaty, J.; Baughman, H.; Hoeper, A.; Barnoy, S.; Suvarnapunya, A.E.; et al. A Phase I trial to evaluate the safety and immunogenicity of WRSs2 and WRSs3; two live oral candidate vaccines against Shigella sonnei. Vaccine 2018, 36, 4880–4889.
428. Girardi, P.; Harutyunyan, S.; Neuhauser, I.; Glaninger, K.; Korda, O.; Nagy, G.; Nagy, E.; Szijarto, V.; Pall, D.; Szarka, K.; et al. Evaluation of the Safety, Tolerability and Immunogenicity of ShigETEC, an Oral Live Attenuated Shigella-ETEC Vaccine in Placebo-Controlled Randomized Phase 1 Trial. Vaccines 2022, 10, 340.
429. Noriega, F.R.; Liao, F.M.; Maneval, D.R.; Ren, S.; Formal, S.B.; Levine, M.M. Strategy for cross-protection among Shigella flexneri serotypes. Infect. Immun. 1999, 67, 782–788.
430. Kotloff, K.L.; Nataro, J.P.; Blackwelder, W.C.; Nasrin, D.; Farag, T.H.; Panchalingam, S.; Wu, Y.; Sow, S.O.; Sur, D.; Breiman, R.F.; et al. Burden and aetiology of diarrhoeal disease in infants and young children in developing countries (the Global Enteric Multicenter Study, GEMS): A prospective, case-control study. Lancet 2013, 382, 209–222.
431. Livio, S.; Strockbine, N.A.; Panchalingam, S.; Tennant, S.M.; Barry, E.M.; Marohn, M.E.; Antonio, M.; Hossain, A.; Mandomando, I.; Ochieng, J.B.; et al. Shigella isolates from the global enteric multicenter study inform vaccine development. Clin. Infect. Dis. 2014, 59, 933–941.
432. Martin, P.; Alaimo, C. The Ongoing Journey of a Shigella Bioconjugate Vaccine. Vaccines 2022
433. Barel, L.A.; Mulard, L.A. Classical and novel strategies to develop a Shigella glycoconjugate vaccine: From concept to efficacy in human. Hum. Vaccin. Immunother. 2019, 15, 1338–1356.
434. Cohen, D.; Atsmon, J.; Artaud, C.; Meron-Sudai, S.; Gougeon, M.-L.; Bialik, A.; Goren, S.; Asato, V.; Ariel-Cohen, O.; Reizis, A.; et al. Safety and immunogenicity of a synthetic carbohydrate conjugate vaccine against Shigella flexneri 2a in healthy adult volunteers: A phase 1, dose-escalating, single-blind, randomised, placebo-controlled study. Lancet Infect. Dis. 2020, 21, 546–558.
435. Phalipon, A.; Mulard, L.A. Toward a Multivalent Synthetic Oligosaccharide-Based Conjugate Vaccine against Shigella: State-of the-Art for a Monovalent Prototype and Challenges. Vaccines 2022, 10, 403.
436. Beijing Zhifei Lvzhu Biopharmaceutical Co., Ltd. Safety Study of S.Flexneriza-S.Sonnei Bivalent Conjugate Vaccine in Healthy Volunteers Aged Above 3 Months. Available online: https://clinicaltrials.gov/ct2/show/NCT03561181 (accessed on 19 June 2022).
437. Mo, Y.; Fang, W.; Li, H.; Chen, J.; Hu, X.; Wang, B.; Feng, Z.; Shi, H.; He, Y.; Huang, D.; et al. Safety and Immunogenicity of a Shigella Bivalent Conjugate Vaccine (ZF0901) in 3-Month- to 5-Year-Old Children in China. Vaccines 2021, 10, 33.
438. Turbyfill KR, Clarkson KA, Oaks EV, Kaminski RW. From Concept to Clinical Product: A Brief History of the Novel *Shigella* Invaplex Vaccine's Refinement and Evolution. Vaccines (Basel). 2022 Apr 1;10(4):548. doi: 10.3390/vaccines10040548. PMID: 35455297; PMCID: PMC9025769.

439. Maggiore, L.; Yu, L.; Omasits, U.; Rossi, O.; Dougan, G.; Thomson, N.R.; Saul, A.; Choudhary, J.S.; Gerke, C. Quantitative proteomic analysis of Shigella flexneri and Shigella sonnei Generalized Modules for Membrane Antigens (GMMA) reveals highly pure preparations. Int. J. Med. Microbiol. 2016, 306, 99–108.
440. Camacho, A.I.; Irache, J.M.; de Souza, J.; Sanchez-Gomez, S.; Gamazo, C. Nanoparticle-based vaccine for mucosal protection against Shigella flexneri in mice. Vaccine 2013, 31, 3288–3294.
441. Martinez-Becerra, F.J.; Chen, X.; Dickenson, N.E.; Choudhari, S.P.; Harrison, K.; Clements, J.D.; Picking, W.D.; Van De Verg, L.L.; Walker, R.I.; Picking, W.L. Characterization of a novel fusion protein from IpaB and IpaD of Shigella spp. and its potential as a pan-Shigella vaccine. Infect. Immun. 2013, 81, 4470–4477.
442. Chakravortty, D.; Pore, D.; Mahata, N.; Pal, A.; Chakrabarti, M.K. Outer Membrane Protein A (OmpA) of Shigella flexneri 2a, Induces Protective Immune Response in a Mouse Model. PLoS ONE 2011, 6, e22663.
443. Kim, J.O.; Rho, S.; Kim, S.H.; Kim, H.; Song, H.J.; Kim, E.J.; Kim, R.Y.; Kim, E.H.; Sinha, A.; Dey, A.; et al. Shigella outer membrane protein PSSP-1 is broadly protective against Shigella infection. Clin. Vaccine Immunol. 2015, 22, 381–388.
444. Patel PD, Patel P, Liang Y, Meiring JE, Misiri T, Mwakiseghile F, Tracy JK, Masesa C, Msuku H, Banda D, Mbewe M, Henrion M, Adetunji F, Simiyu K, Rotrosen E, Birkhold M, Nampota N, Nyirenda OM, Kotloff K, Gmeiner M, Dube Q, Kawalazira G, Laurens MB, Heyderman RS, Gordon MA, Neuzil KM; TyVAC Malawi Team. Safety and Efficacy of a Typhoid Conjugate Vaccine in Malawian Children. N Engl J Med. 2021 Sep 16;385(12):1104-1115. doi: 10.1056/NEJMoa2035916. PMID: 34525285; PMCID: PMC8202713.
445. 5. Qadri F, Khanam F, Liu X, Theiss-Nyland K, Biswas PK, Bhuiyan AI, Ahmmed F, Colin-Jones R, Smith N, Tonks S, Voysey M, Mujadidi YF, Mazur O, Rajib NH, Hossen MI, Ahmed SU, Khan A, Rahman N, Babu G, Greenland M, Kelly S, Ireen M, Islam K, O'Reilly P, Scherrer KS, Pitzer VE, Neuzil KM, Zaman K, Pollard AJ, Clemens JD. Protection by vaccination of children against typhoid fever with a Vi-tetanus toxoid conjugate vaccine in urban Bangladesh: a cluster-randomised trial. Lancet. 2021 Aug 21;398(10301):675-684. doi: 10.1016/S0140-6736(21)01124-7. Epub 2021 Aug 9. PMID: 34384540; PMCID: PMC8387974.
446. MacLennan CA, Martin LB, Micoli F. Vaccines against invasive Salmonella disease: current status and future directions. Hum Vaccin Immunother. 2014;10(6):1478-93. doi: 10.4161/hv.29054. Epub 2014 May 7. PMID: 24804797; PMCID: PMC4185946.
447. Simon R, Levine MM. Glycoconjugate vaccine strategies for protection against invasive Salmonella infections. Hum Vaccin Immunother. 2012 Apr;8(4):494-8. doi: 10.4161/hv.19158. Epub 2012 Feb 28. PMID: 22370510; PMCID: PMC3426074.
448. Calman A MacLennan, Jeffrey Stanaway, Stephanie Grow, Kirsten Vannice, A Duncan Steele, *Salmonella* Combination Vaccines: Moving Beyond Typhoid, *Open Forum Infectious Diseases*, Volume 10, Issue Supplement_1, May 2023, Pages S58–S66, https://doi.org/10.1093/ofid/ofad041

449. Das S, Chowdhury R, Ghosh S, Das S. A recombinant protein of Salmonella Typhi induces humoral and cell-mediated immune responses including memory responses. Vaccine. 2017 Aug 16;35(35 Pt B):4523-4531. doi: 10.1016/j.vaccine.2017.07.035. Epub 2017 Jul 21. PMID: 28739115.
450. Haldar R, Dhar A, Ganguli D, Chakraborty S, Pal A, Banik G, Miyoshi SI, Das S. A candidate glycoconjugate vaccine induces protective antibodies in the serum and intestinal secretions, antibody recall response and memory T cells and protects against both typhoidal and non-typhoidal Salmonella serovars. Front Immunol. 2024 Jan 9;14:1304170. doi: 10.3389/fimmu.2023.1304170. PMID: 38264668; PMCID: PMC10804610.
451. Abbas M, Hayirli Z, Drakesmith H, Andrews SC and Lewis MC (2022) Effects of iron deficiency and iron supplementation at the host-microbiota interface: Could a piglet model unravel complexities of the underlying mechanisms? Front. Nutr. 9:927754. doi: 10.3389/fnut.2022.927754.
452. Kortman GA, Boleij A, Swinkels DW, Tjalsma H. Iron availability increases the pathogenic potential of Salmonella typhimurium and other enteric pathogens at the intestinal epithelial interface. PLoS One. 2012;7(1):e29968. doi: 10.1371/journal.pone.0029968. Epub 2012 Jan 17. PMID: 22272265; PMCID: PMC3260200.
453. Cork SC, Marshall RB, Fenwick SG. The effect of parenteral iron dextran, with or without desferrioxamine, on the development of experimental pseudotuberculosis in the domestic chicken. Avian Pathol. 1998;27(4):394-9. doi: 10.1080/03079459808419357. PMID: 18484018.
454. James A. Imlay et al. Toxic DNA Damage by Hydrogen Peroxide Through the Fenton Reaction in Vivo and in Vitro.Science240,640-642(1988).DOI:10.1126/science.2834821
455. JONES, R., PETERSON, C., GRADY, R. et al. Effects of iron chelators and iron overload on Salmonella infection. Nature 267, 63–65 (1977). https://doi.org/10.1038/267063a0
456. Mobarra N, Shanaki M, Ehteram H, Nasiri H, Sahmani M, Saeidi M, Goudarzi M, Pourkarim H, Azad M. A. Review on Iron Chelators in Treatment of Iron Overload Syndromes. Int J Hematol Oncol Stem Cell Res. 2016 Oct 1;10(4):239-247. PMID: 27928480; PMCID: PMC5139945.
457. Autenrieth IB, Bohn E, Ewald JH, Heesemann J. Deferoxamine B but not deferoxamine G1 inhibits cytokine production in murine bone marrow macrophages. J Infect Dis. 1995 Aug;172(2):490-6. doi: 10.1093/infdis/172.2.490. PMID: 7622893.
458. Saldaña-Ahuactzi Z, Knodler LA. FoxR is an AraC-like transcriptional regulator of ferrioxamine uptake in Salmonella enterica. Mol Microbiol. 2022 Oct;118(4):369-386. doi: 10.1111/mmi.14970. Epub 2022 Aug 15. PMID: 35970762; PMCID: PMC9804782.
459. Mey AR, Gómez-Garzón C, Payne SM. Iron Transport and Metabolism in Escherichia, Shigella, and Salmonella. EcoSal Plus. 2021 Dec 15;9(2):eESP00342020. doi: 10.1128/ecosalplus.ESP-0034-2020. Epub 2021 Dec 13. PMID: 34910574; PMCID: PMC8865473.
460. Muthuramalingam M, Whittier SK, Picking WL, Picking WD. The Shigella Type III Secretion System: An Overview from Top to Bottom. Microorganisms. 2021 Feb 22;9(2):451. doi: 10.3390/microorganisms9020451. PMID: 33671545; PMCID: PMC7926512.
461. Shimanovich AA, Buskirk AD, Heine SJ, Blackwelder WC, Wahid R, Kotloff KL, Pasetti MF. Functional and Antigen-Specific Serum Antibody Levels as Correlates of Protection against Shigellosis in a

Controlled Human Challenge Study. Clin Vaccine Immunol. 2017 Feb 6;24(2):e00412-16. doi: 10.1128/CVI.00412-16. PMID: 27927680; PMCID: PMC5299116.

462. Bernshtein B, Ndungo E, Cizmeci D, Xu P, Kovác P, Kelly M, Islam D, Ryan ET, Kotloff KL, Pasetti MF, Alter G. 2022. Systems approach to define humoral correlates of immunity to Shigella. Cell Rep 40:111216. https://doi .org/10.1016/j.celrep.2022.111216.

463. Martinez-Becerra FJ, Kissmann JM, Diaz-McNair J, Choudhari SP, Quick AM, Mellado-Sanchez G, Clements JD, Pasetti MF, Picking WL. Broadly protective Shigella vaccine based on type III secretion apparatus proteins. Infect Immun. 2012 Mar;80(3):1222-31. doi: 10.1128/IAI.06174-11. Epub 2011 Dec 27. PMID: 22202122; PMCID: PMC3294653.

464. Heine SJ, Diaz-McNair J, Martinez-Becerra FJ, Choudhari SP, Clements JD, Picking WL, Pasetti MF. Evaluation of immunogenicity and protective efficacy of orally delivered Shigella type III secretion system proteins IpaB and IpaD. Vaccine. 2013 Jun 19;31(28):2919-29. doi: 10.1016/j.vaccine.2013.04.045. Epub 2013 May 2. PMID: 23644075; PMCID: PMC3718310.

465. Ndungo E, Randall A, Hazen TH, Kania DA, Trappl-Kimmons K, Liang X, Barry EM, Kotloff KL, Chakraborty S, Mani S, Rasko DA, Pasetti MF. A Novel Shigella Proteome Microarray Discriminates Targets of Human Antibody Reactivity following Oral Vaccination and Experimental Challenge. mSphere. 2018 Aug 1;3(4):e00260-18. doi: 10.1128/mSphere.00260-18. PMID: 30068560; PMCID: PMC6070737.

466. Konadu E, Shiloach J, Bryla DA, Robbins JB, Szu SC. Synthesis, characterization, and immunological properties in mice of conjugates composed of detoxified lipopolysaccharide of Salmonella Paratyphi A bound to tetanus toxoid with emphasis on the role of O acetyls. Infect Immun. 1996 Jul;64(7):2709-15. doi: 10.1128/iai.64.7.2709-2715.1996. PMID: 8698499; PMCID: PMC174130.

467. Micoli F, Rondini S, Gavini M, Lanzilao L, Medaglini D, Saul A, Martin LB. O:2-CRM(197) conjugates against Salmonella Paratyphi A. PLoS One. 2012;7(11):e47039. doi: 10.1371/journal.pone.0047039. Epub 2012 Nov 7. PMID: 23144798; PMCID: PMC3492368.

468. Bastos RC, Corrêa MB, de Souza IM, da Silva MN, da Silva Gomes Pereira D, Martins FO, da Silva Faria C, Ano Bom APD, de Lourdes Leal M, Jessouroun E, da Silva JG Jr, de Andrade Medronho R, da Silveira IAFB. Brazilian meningococcal C conjugate vaccine: physicochemical, immunological, and thermal stability characteristics. Glycoconj J. 2018 Feb;35(1):3-13. doi: 10.1007/s10719-017-9787-2. Epub 2017 Sep 19. PMID: 28929266.

469. He W, Mazzuca P, Yuan W, Varney K, Bugatti A, Cagnotto A, Giagulli C, Rusnati M, Marsico S, Diomede L, Salmona M, Caruso A, Lu W, Caccuri F. Identification of amino acid residues critical for the B cell growth-promoting activity of HIV-1 matrix protein p17 variants. Biochim Biophys Acta Gen Subj. 2019 Jan;1863(1):13-24. doi: 10.1016/j.bbagen.2018.09.016. Epub 2018 Sep 21. PMID: 30248376.

470. Nguyen TK, Selvanayagam R, Ho KKK, Chen R, Kutty SK, Rice SA, Kumar N, Barraud N, Duong HTT, Boyer C. Co-delivery of nitric oxide and antibiotic using polymeric nanoparticles. Chem Sci. 2016 Feb 1;7(2):1016-1027. doi: 10.1039/c5sc02769a. Epub 2015 Nov 10. PMID: 28808526; PMCID: PMC5531038.

471. Satpute SK, Banpurkar AG, Dhakephalkar PK, Banat IM, Chopade BA. Methods for investigating

biosurfactants and bioemulsifiers: a review. Crit Rev Biotechnol. 2010 Jun;30(2):127-44. doi: 10.3109/07388550903427280. PMID: 20210700.

472. Hedman K, Rousseau SA. Measurement of avidity of specific IgG for verification of recent primary rubella. J Med Virol. 1989;27:288–92.

473. Ghosh S, Chakraborty K, Nagaraja T, Basak S, Koley H, Dutta S, Mitra U, Das S. An adhesion protein of Salmonella enterica serovar Typhi is required for pathogenesis and potential target for vaccine development. Proc Natl Acad Sci U S A. 2011 Feb 22;108(8):3348-53. doi: 10.1073/pnas.1016180108. Epub 2011 Feb 7. PMID: 21300870; PMCID: PMC3044360.

474. Fiorino F, Rondini S, Micoli F, Lanzilao L, Alfini R, Mancini F, MacLennan CA and Medaglini D (2017) Immunogenicity of a Bivalent Adjuvanted Glycoconjugate Vaccine against Salmonella Typhimurium and Salmonella Enteritidis. Front. Immunol. 8:168. doi: 10.3389/fimmu.2017.00168

475. Shippy DC, Eakley NM, Mikheil DM, Fadl AA. Role of StdA in adhesion of Salmonella enterica serovar Enteritidis phage type 8 to host intestinal epithelial cells. Gut Pathog. 2013 Dec 24;5(1):43. doi: 10.1186/1757-4749-5-43. PMID: 24367906; PMCID: PMC3877977.

476. Erben U, Loddenkemper C, Doerfel K, Spieckermann S, Haller D, Heimesaat MM, Zeitz M, Siegmund B, Kühl AA. A guide to histomorphological evaluation of intestinal inflammation in mouse models. Int J Clin Exp Pathol. 2014 Jul 15;7(8):4557-76. PMID: 25197329; PMCID: PMC4152019.

477. Koelink PJ, Wildenberg ME, Stitt LW, Feagan BG, Koldijk M, van 't Wout AB, Atreya R, Vieth M, Brandse JF, Duijst S, Te Velde AA, D'Haens GRAM, Levesque BG, van den Brink GR. Development of Reliable, Valid and Responsive Scoring Systems for Endoscopy and Histology in Animal Models for Inflammatory Bowel Disease. J Crohns Colitis. 2018 Jun 28;12(7):794-803. doi: 10.1093/ecco-jcc/jjy035. PMID: 29608662; PMCID: PMC6022651.

478. Okada K, Itoh H, Ikemoto M. Circulating S100A8/A9 is potentially a biomarker that could reflect the severity of experimental colitis in rats. Heliyon. 2020 Feb 29;6(2):e03470. doi: 10.1016/j.heliyon.2020.e03470. PMID: 32140589; PMCID: PMC7052069.

479. Martinez-Becerra FJ, Kumar P, Vishwakarma V, Kim JH, Arizmendi O, Middaugh CR, Picking WD, Picking WL. Characterization and Protective Efficacy of Type III Secretion Proteins as a Broadly Protective Subunit Vaccine against Salmonella enterica Serotypes. Infect Immun. 2018 Feb 20;86(3):e00473-17. doi: 10.1128/IAI.00473-17. PMID: 29311233; PMCID: PMC5820934.

480. Calman A MacLennan, Laura B Martin & Francesca Micoli (2014) Vaccines against invasive Salmonella disease, Human Vaccines & Immunotherapeutics, 10:6, 1478-1493, DOI: 10.4161/hv.29054

481. Pozsgay V. Oligosaccharide-protein conjugates as vaccine candidates against bacteria. Adv Carbohydr Chem Biochem. 2000;56:153-99. doi: 10.1016/s0065-2318(01)56004-7. PMID: 11039111.

482. Frasch CE. Preparation of bacterial polysaccharide-protein conjugates: analytical and manufacturing challenges. Vaccine. 2009 Oct 30;27(46):6468-70. doi: 10.1016/j.vaccine.2009.06.013. Epub 2009 Jun 24. PMID: 19555714.

483. Costantino P, Rappuoli R, Berti F. The design of semi-synthetic and synthetic glycoconjugate vaccines. Expert Opin Drug Discov. 2011 Oct;6(10):1045-66. doi: 10.1517/17460441.2011.609554. Epub 2011 Sep 6. PMID: 22646863.

484. Micoli, F., Rondini, S., Pisoni, I., Proietti, D., Berti, F., Costantino, P., et al. (2011). Vi-CRM 197 as a new conjugate vaccine against Salmonella Typhi. Vaccine 29, 712–720. doi:10.1016/j.vaccine.2010.11.022

485. Wang JY, Chang AH, Guttormsen HK, Rosas AL, Kasper DL. Construction of designer glycoconjugate vaccines with size-specific oligosaccharide antigens and site-controlled coupling. Vaccine. 2003 Mar 7;21(11-12):1112-7. doi: 10.1016/s0264-410x(02)00625-4. PMID: 12559788.

486. Jones, C. (2005). Vaccines based on the cell surface carbohydrates of pathogenic bacteria. Acad Bras Cienc 77, 293–324. doi:10.1590/s0001-37652005000200009

487. Lucas AH, Apicella MA, Taylor CE. Carbohydrate moieties as vaccine candidates. Clin Infect Dis. 2005 Sep 1;41(5):705-12. doi: 10.1086/432582. Epub 2005 Jul 25. PMID: 16080094; PMCID: PMC7107877.

488. Bröker M, Berti F, Costantino P. Factors contributing to the immunogenicity of meningococcal conjugate vaccines. Hum Vaccin Immunother. 2016 Jul 2;12(7):1808-24. doi: 10.1080/21645515.2016.1153206. Epub 2016 Mar 2. PMID: 26934310; PMCID: PMC4964817.

489. Chu C, Schneerson R, Robbins JB, Rastogi SC. Further studies on the immunogenicity of Haemophilus influenzae type b and pneumococcal type 6A polysaccharide-protein conjugates. Infect Immun. 1983 Apr;40(1):245-56. doi: 10.1128/iai.40.1.245-256.1983. PMID: 6601061; PMCID: PMC264842.

490. Lees, A., Nelson, B. L., and Mond, J. J. (1996). Activation of soluble polysaccharides with 1 cyano-4-dimethylaminopyridinium tetrafluoroborate for use in proteinpolysaccharide conjugate vaccines and immunological reagents. Vaccine 14, 190–198. doi:10.1016/0264-410x(95)00195-7

491. Shafer DE, Toll B, Schuman RF, Nelson BL, Mond JJ, Lees A. Activation of soluble polysaccharides with 1-cyano-4-dimethylaminopyridinium tetrafluoroborate (CDAP) for use in protein-polysaccharide conjugate vaccines and immunological reagents. II. Selective crosslinking of proteins to CDAP-activated polysaccharides. Vaccine. 2000 Jan 18;18(13):1273-81. doi: 10.1016/s0264-410x(99)00370-9. PMID: 10649629.

492. Schneerson R, Barrera O, Sutton A, Robbins JB. Preparation, characterization, and immunogenicity of Haemophilus influenzae type b polysaccharide-protein conjugates. J Exp Med. 1980 Aug 1;152(2):361-76. doi: 10.1084/jem.152.2.361. PMID: 6967514; PMCID: PMC2185954.

493. Grandjean C, Wade TK, Ropartz D, Ernst L, Wade WF. Acid-detoxified Inaba lipopolysaccharide (pmLPS) is a superior cholera conjugate vaccine immunogen than hydrazine-detoxified lipopolysaccharide and induces vibriocidal and protective antibodies. Pathog Dis. 2013 Mar;67(2):136-58. doi: 10.1111/2049-632X.12022. Epub 2013 Feb 25. PMID: 23620159.

494. Ftacek P, Nelson V, Szu SC. Immunochemical characterization of synthetic hexa-, octa- and decasaccharide conjugate vaccines for Vibrio cholerae O:1 serotype Ogawa with emphasis on antigenic density and chain length. Glycoconj J. 2013 Dec;30(9):871-80. doi: 10.1007/s10719-013-9491-9. Epub 2013 Aug 17. PMID: 23955520; PMCID: PMC3839634.

495. Stefanetti G, Okan N, Fink A, Gardner E, Kasper DL. Glycoconjugate vaccine using a genetically modified O antigen induces protective antibodies to *Francisella tularensis*. Proc Natl Acad Sci U S A. 2019 Apr 2;116(14):7062-7070. doi: 10.1073/pnas.1900144116. Epub 2019 Mar 14. PMID: 30872471; PMCID: PMC6452683.

496. Henderson Zhu, Christine S. Rollier & Andrew J. Pollard (2021) Recent advances in lipopolysaccharide-based glycoconjugate vaccines, Expert Review of Vaccines, 20:12, 1515-1538, DOI: 10.1080/14760584.2021.1984889
497. Watson DC, Robbins JB, Szu SC. Protection of mice against Salmonella typhimurium with an O-specific polysaccharide-protein conjugate vaccine. Infect Immun. 1992 Nov;60(11):4679-86. doi: 10.1128/iai.60.11.4679-4686.1992. PMID: 1383154; PMCID: PMC258218.
498. Micoli F, Romano MR, Tontini M, Cappelletti E, Gavini M, Proietti D, Rondini S, Swennen E, Santini L, Filippini S, Balocchi C, Adamo R, Pluschke G, Norheim G, Pollard A, Saul A, Rappuoli R, MacLennan CA, Berti F, Costantino P. Development of a glycoconjugate vaccine to prevent meningitis in Africa caused by meningococcal serogroup X. Proc Natl Acad Sci U S A. 2013 Nov 19;110(47):19077-82. doi: 10.1073/pnas.1314476110. Epub 2013 Nov 4. PMID: 24191022; PMCID: PMC3839747.
499. An SJ, Yoon YK, Kothari S, Kothari N, Kim JA, Lee E, et al. Physico-chemical properties of Salmonella typhi Vi polysaccharide-diphtheria toxoid conjugate vaccines affect immunogenicity. Vaccine. 2011; 29 (44):7618–23. Epub 2011/08/17. https://doi.org/10.1016/j.vaccine.2011.08.019 PMID: 21843575.
500. Wessels MR, Paoletti LC, Guttormsen HK, Michon F, D'Ambra AJ, Kasper DL. Structural properties of group B streptococcal type III polysaccharide conjugate vaccines that influence immunogenicity and efficacy. Infect Immun. 1998; 66(5):2186–92. Epub 1998/05/09. PMID: 9573106; PubMed Central PMCID: PMCPMC108180.
501. Kossaczka Z, Lin FY, Ho VA, Thuy NT, Van Bay P, Thanh TC, Khiem HB, Trach DD, Karpas A, Hunt S, Bryla DA, Schneerson R, Robbins JB, Szu SC. Safety and immunogenicity of Vi conjugate vaccines for typhoid fever in adults, teenagers, and 2- to 4-year-old children in Vietnam. Infect Immun. 1999 Nov;67(11):5806-10. doi: 10.1128/IAI.67.11.5806-5810.1999. PMID: 10531232; PMCID: PMC96958.
502. Fattom A, Shiloach J, Bryla D, Fitzgerald D, Pastan I, Karakawa WW, Robbins JB, Schneerson R. Comparative immunogenicity of conjugates composed of the Staphylococcus aureus type 8 capsular polysaccharide bound to carrier proteins by adipic acid dihydrazide or N-succinimidyl-3-(2-pyridyldithio)propionate. Infect Immun. 1992 Feb;60(2):584-9. doi: 10.1128/iai.60.2.584-589.1992. PMID: 1730492; PMCID: PMC257668.
503. Fattom, A., Li, X., Cho, Y. H., Burns, A., Hawwari, A., Shepherd, S. E., et al. (1995). Effect of conjugation methodology, carrier protein, and adjuvants on the immune response to Staphylococcus aureus capsular polysaccharides. Vaccine 13, 1288–1293. doi:10.1016/0264-410x(95)00052-3
504. Gupta RK, Szu SC, Finkelstein RA, Robbins JB. Synthesis, characterization, and some immunological properties of conjugates composed of the detoxified lipopolysaccharide of Vibrio cholerae O1 serotype Inaba bound to cholera toxin. Infect Immun. 1992 Aug;60(8):3201-8. doi: 10.1128/iai.60.8.3201-3208.1992. PMID: 1639490; PMCID: PMC257302.
505. Simon R, Tennant SM, Wang JY, Schmidlein PJ, Lees A, Ernst RK, Pasetti MF, Galen JE, Levine MM. Salmonella enterica serovar enteritidis core O polysaccharide conjugated to H:g,m flagellin as a candidate vaccine for protection against invasive infection with S. enteritidis. Infect Immun. 2011 Oct;79(10):4240-9. doi: 10.1128/IAI.05484-11. Epub 2011 Aug 1. PMID: 21807909; PMCID: PMC3187246.
506. Baliban SM, Yang M, Ramachandran G, Curtis B, Shridhar S, Laufer RS, Wang JY, Van Druff J, Higginson EE, Hegerle N, Varney KM, Galen JE, Tennant SM, Lees A, MacKerell AD Jr, Levine MM,

Simon R. Development of a glycoconjugate vaccine to prevent invasive Salmonella Typhimurium infections in sub-Saharan Africa. PLoS Negl Trop Dis. 2017 Apr 7;11(4):e0005493. doi: 10.1371/journal.pntd.0005493. PMID: 28388624; PMCID: PMC5397072.

507. Fiorino F, Rondini S, Micoli F, Lanzilao L, Alfini R, Mancini F, MacLennan CA and Medaglini D (2017) Immunogenicity of a Bivalent Adjuvanted Glycoconjugate Vaccine against Salmonella Typhimurium and Salmonella Enteritidis. Front. Immunol. 8:168. doi: 10.3389/fimmu.2017.00168
508. Svenson SB, Nurminen M, Lindberg AA. Artificial Salmonella vaccines: O-antigenic oligosaccharide-protein conjugates induce protection against infection with Salmonella typhimurium. Infect Immun. 1979 Sep;25(3):863-72. doi: 10.1128/iai.25.3.863-872.1979. PMID: 387597; PMCID: PMC414528.
509. Patel PD, Patel P, Liang Y, Meiring JE, Misiri T, Mwakiseghile F, Tracy JK, Masesa C, Msuku H, Banda D, Mbewe M, Henrion M, Adetunji F, Simiyu K, Rotrosen E, Birkhold M, Nampota N, Nyirenda OM, Kotloff K, Gmeiner M, Dube Q, Kawalazira G, Laurens MB, Heyderman RS, Gordon MA, Neuzil KM; TyVAC Malawi Team. Safety and Efficacy of a Typhoid Conjugate Vaccine in Malawian Children. N Engl J Med. 2021 Sep 16;385(12):1104-1115. doi: 10.1056/NEJMoa2035916. PMID: 34525285; PMCID: PMC8202713.
510. Rondini S, Micoli F, Lanzilao L, Hale C, Saul AJ, Martin LB. Evaluation of the immunogenicity and biological activity of the Citrobacter freundii Vi-CRM197 conjugate herrer KS, Pitzer VE, Neuzil KM, Zaman K, Pollard AJ, Clemens JD. Protection by vaccination of children against typhoid fever with a Vi-tetanus toxoid conjugate vaccine in urban Bangladesh: a cluster-randomised trial. Lancet. 2021 Aug 21;398(10301):675-684. doi: 10.1016/S0140-6736(21)01124-7. Epub 2021 Aug 9. PMID: 34384540; PMCID: PMC8387974.
511. Shakya M et al. Efficacy of typhoid conjugate vaccine in Nepal: final results of a phase 3, randomised, controlled trial. Lancet Glob Health 2021;9(11):e1561–e1568.
512. Vidarsson G, Dekkers G, Rispens T. IgG subclasses and allotypes: from structure to effector functions. Front Immunol. 2014 Oct 20;5:520. doi: 10.3389/fimmu.2014.00520. PMID: 25368619; PMCID: PMC4202688.
513. Mäkelä O, Péterfy F, Outschoorn IG, Richter AW, Seppälä I. Immunogenic properties of alpha (1----6) dextran, its protein conjugates, and conjugates of its breakdown products in mice. Scand J Immunol. 1984 Jun;19(6):541-50. doi: 10.1111/j.1365-3083.1984.tb00965.x. PMID: 6204375.
514. Seppälä I, Pelkonen J, Mäkelä O. Isotypes of antibodies induced by plain dextran or a dextran-protein conjugate. Eur J Immunol. 1985 Aug;15(8):827-33. doi: 10.1002/eji.1830150816. PMID: 2411572.
515. Sun P, Pan C, Zeng M, Liu B, Liang H, Wang D, Liu X, Wang B, Lyu Y, Wu J, Zhu L, Wang H. Design and production of conjugate vaccines against S. Paratyphi A using an O-linked glycosylation system in vivo. NPJ Vaccines. 2018 Feb 5;3:4. doi: 10.1038/s41541-017-0037-1. PMID: 29423317; PMCID: PMC5799188.
516. Halder P, Maiti S, Banerjee S, Das S, Dutta M, Dutta S, Koley H. Bacterial ghost cell based bivalent candidate vaccine against Salmonella Typhi and Salmonella Paratyphi A: A prophylactic study in BALB/c mice. Vaccine. 2023 Sep 22;41(41):5994-6007. doi: 10.1016/j.vaccine.2023.08.049. Epub 2023 Aug 23. PMID: 37625993.

517. Reinhardt A, Yang Y, Claus H, Pereira CL, Cox AD, Vogel U, Anish C, Seeberger PH. Antigenic potential of a highly conserved Neisseria meningitidis lipopolysaccharide inner core structure defined by chemical synthesis. Chem Biol. 2015 Jan 22;22(1):38-49. doi: 10.1016/j.chembiol.2014.11.016. Epub 2015 Jan 15. PMID: 25601073.

518. Sayeed MA, Bufano MK, Xu P, Eckhoff G, Charles RC, Alam MM, Sultana T, Rashu MR, Berger A, Gonzalez-Escobedo G, Mandlik A, Bhuiyan TR, Leung DT, LaRocque RC, Harris JB, Calderwood SB, Qadri F, Vann WF, Kováč P, Ryan ET. A Cholera Conjugate Vaccine Containing O-specific Polysaccharide (OSP) of V. cholerae O1 Inaba and Recombinant Fragment of Tetanus Toxin Heavy Chain (OSP:rTTHc) Induces Serum, Memory and Lamina Proprial Responses against OSP and Is Protective in Mice. PLoS Negl Trop Dis. 2015 Jul 8;9(7):e0003881. doi: 10.1371/journal.pntd.0003881. PMID: 26154421; PMCID: PMC4495926.

519. An, S. J., Yoon, Y. K., Kothari, S., Kothari, N., Kim, J. A., Lee, E., et al. (2011). Physicochemical properties of Salmonella typhi Vi polysaccharide-diphtheria toxoid conjugate vaccines affect immunogenicity. Vaccine 29, 7618–7623. doi:10.1016/j.vaccine.2011. 08.019.

520. Mitra M, Shah N, Ghosh A, Chatterjee S, Kaur I, Bhattacharya N, Basu S. Efficacy and safety of vi-tetanus toxoid conjugated typhoid vaccine (PedaTyph™) in Indian children: School based cluster randomized study. Hum Vaccin Immunother. 2016 Apr 2;12(4):939-45. doi: 10.1080/21645515.2015.1117715. Epub 2016 Feb 22. PMID: 26901576; PMCID: PMC4962969.

521. J. Meena, R. Kumar, M. Singh, A. Ahmed, A. Kumar Panda, Modulation of immune response and enhanced clearance of Salmonella typhi by delivery of Vi polysaccharide conjugate using PLA nanoparticles, European Journal of Pharmaceutics and Biopharmaceutics (2020), doi: https://doi.org/10.1016/ j.ejpb.2020.05.023.

522. Haque S, Sengupta S, Gupta D, Bhan MK, Kumar R, Khan A, Jailkhani B. S.Typhi derived OmpC peptide conjugated with Vi-polysaccharide evokes better immune response than free Vi-polysaccharide in mice. Biologicals. 2019 Nov;62:50-56. doi: 10.1016/j.biologicals.2019.10.001. Epub 2019 Oct 9. PMID: 31606267.

523. Fiorino F, Ciabattini A, Rondini S, Pozzi G, Martin LB, Medaglini D. Immunization with the conjugate vaccine Vi-CRM_{197} against Salmonella typhi induces Vi-specific mucosal and systemic immune responses in mice. Vaccine. 2012 Sep 21;30(43):6111-4. doi: 10.1016/j.vaccine.2012.05.081. Epub 2012 Jun 15. PMID: 22705173.

524. Stein KE, Zopf DA, Johnson BM, Miller CB, Paul WE. The immune response to an isomaltohexosyl-protein conjugate, a thymus-dependent analogue of alpha(1 replaced by 6) dextran. J Immunol. 1982 Mar;128(3):1350-4. PMID: 6173433.

525. Stein KE. Thymus-independent and thymus-dependent responses to polysaccharide antigens. J Infect Dis. 1992 Jun;165 Suppl 1:S49-52. doi: 10.1093/infdis/165-supplement_1-s49. PMID: 1588177.

526. Tritama E, Riani C, Rudiansyah I, Hidayat A, Kharisnaeni SA, Retnoningrum DS. Evaluation of alum-based adjuvant on the immunogenicity of salmonella enterica serovar typhi conjugates vaccines. Hum Vaccin Immunother. 2018 Jun 3;14(6):1524-1529. doi: 10.1080/21645515.2018.1431599. Epub 2018 Feb 21. PMID: 29359991; PMCID: PMC6037457.

527. Kelly DF, Snape MD, Clutterbuck EA, Green S, Snowden C, Diggle L, Yu LM, Borkowski A, Moxon ER, Pollard AJ. CRM197-conjugated serogroup C meningococcal capsular polysaccharide, but not the native polysaccharide, induces persistent antigen-specific memory B cells. Blood. 2006 Oct 15;108(8):2642-7. doi: 10.1182/blood-2006-01-009282. Epub 2006 May 4. Erratum in: Blood. 2007 Mar 1;109(5):1849. Cutterbuck, Elizabeth A [corrected to Clutterbuck, Elizabeth A]. PMID: 16675705.

528. Li P, Liu Q, Luo H, Liang K, Han Y, Roland KL, Curtiss R 3rd, Kong Q. Bi-valent polysaccharides of Vi capsular and O9 O-antigen in attenuated *Salmonella* Typhimurium induce strong immune responses against these two antigens. NPJ Vaccines. 2018 Jan 9;3:1. doi: 10.1038/s41541-017-0041-5. PMID: 29354293; PMCID: PMC5760606.

529. Mackel Dc, Langley Lf, Venice La. The use of the guinea-pig conjunctivae as an experimental model for the study of virulence of Shigella organisms. Am J Hyg. 1961 Mar;73:219-23. doi: 10.1093/oxfordjournals.aje.a120179. PMID: 13764890.

530. Yum LK, Byndloss MX, Feldman SH, Agaisse H. Critical role of bacterial dissemination in an infant rabbit model of bacillary dysentery. Nat Commun. 2019 Apr 23;10(1):1826. doi: 10.1038/s41467-019-09808-4. PMID: 31015451; PMCID: PMC6478941.

531. Wei Y, Murphy ER. Shigella Iron Acquisition Systems and their Regulation. Front Cell Infect Microbiol. 2016 Feb 9;6:18. doi: 10.3389/fcimb.2016.00018. PMID: 26904516; PMCID: PMC4746246.

532. Killackey SA, Sorbara MT and Girardin SE (2016) Cellular Aspects of Shigella Pathogenesis: Focus on the Manipulation of Host Cell Processes. Front. Cell. Infect. Microbiol. 6:38. doi: 10.3389/fcimb.2016.00038.

533. Mey AR, Gómez-Garzón C, Payne SM. Iron Transport and Metabolism in Escherichia, Shigella, and Salmonella. EcoSal Plus. 2021 Dec 15;9(2):eESP00342020. doi: 10.1128/ecosalplus.ESP-0034-2020. Epub 2021 Dec 13. PMID: 34910574; PMCID: PMC8865473.

534. Fecker L, Braun V.1983.Cloning and expression of the fhu genes involved in iron(III)-hydroxamate uptake by Escherichia coli. J Bacteriol156:.https://doi.org/10.1128/jb.156.3.1301-1314.1983

535. Clements D, Ellis CJ, Allan RN. Persistent shigellosis. Gut. 1988 Sep;29(9):1277-8. doi: 10.1136/gut.29.9.1277. PMID: 3058558; PMCID: PMC1434353.

536. Chitradevi, S., Kaur, G., Uppalapati, S. et al. Co-administration of rIpaB domain of Shigella with rGroEL of S. Typhi enhances the immune responses and protective efficacy against Shigella infection. Cell Mol Immunol 12, 757–767 (2015). https://doi.org/10.1038/cmi.2014.86.

537. Le-Barillec K, Magalhaes JG, Corcuff E, Thuizat A, Sansonetti PJ, Phalipon A, Di Santo JP. Roles for T and NK cells in the innate immune response to Shigella flexneri. J Immunol. 2005 Aug 1;175(3):1735-40. doi: 10.4049/jimmunol.175.3.1735. PMID: 16034114.

538. Raqib R, Qadri F, SarkEr P, Mia SM, Sansonnetti PJ, Albert MJ, Andersson J. Delayed and reduced adaptive humoral immune responses in children with shigellosis compared with in adults. Scand J Immunol. 2002 Apr;55(4):414-23. doi: 10.1046/j.1365-3083.2002.01079.x. PMID: 11967124.

539. Way SS, Borczuk AC, Dominitz R, Goldberg MB. An essential role for gamma interferon in innate resistance to Shigella flexneri infection. Infect Immun. 1998 Apr;66(4):1342-8. doi: 10.1128/IAI.66.4.1342-1348.1998. PMID: 9529051; PMCID: PMC108058.

540. Phalipon A, Kaufmann M, Michetti P, Cavaillon JM, Huerre M, Sansonetti P, Kraehenbuhl JP. Monoclonal immunoglobulin A antibody directed against serotype-specific epitope of Shigella flexneri lipopolysaccharide protects against murine experimental shigellosis. J Exp Med. 1995 Sep 1;182(3):769-78. doi: 10.1084/jem.182.3.769. PMID: 7544397; PMCID: PMC2192169.

541. Sansonetti PJ, Phalipon A, Arondel J, Thirumalai K, Banerjee S, Akira S, Takeda K, Zychlinsky A. Caspase-1 activation of IL-1beta and IL-18 are essential for Shigella flexneri-induced inflammation. Immunity. 2000 May;12(5):581-90. doi: 10.1016/s1074-7613(00)80209-5. PMID: 10843390.

542. Heine SJ, Diaz-McNair J, Andar AU, Drachenberg CB, van de Verg L, Walker R, Picking WL, Pasetti MF. Intradermal delivery of Shigella IpaB and IpaD type III secretion proteins: kinetics of cell recruitment and antigen uptake, mucosal and systemic immunity, and protection across serotypes. J Immunol. 2014 Feb 15;192(4):1630-40. doi: 10.4049/jimmunol.1302743. Epub 2014 Jan 22. PMID: 24453241; PMCID: PMC3998105.

543. Harro, C.R.; Riddle, M.S.; Kaminski, R.; Turbyfill, K.R.; Gormley, R.; Porter, C.; Ranallo, R.T.; Kordis, A.; Buck, M.; Jones, A. Shigella flexneri 2a Invaplex 50 intranasal vaccine phase 2b challenge study. In Proceedings of the Vaccines for Enteric Diseases, Malaga, Spain, 9–11 September 2009.

544. Tribble D, Kaminski R, Cantrell J, Nelson M, Porter C, Baqar S, Williams C, Arora R, Saunders J, Ananthakrishnan M, Sanders J, Zaucha G, Turbyfill R, Oaks E. Safety and immunogenicity of a Shigella flexneri 2a Invaplex 50 intranasal vaccine in adult volunteers. Vaccine. 2010 Aug 23;28(37):6076-85. doi: 10.1016/j.vaccine.2010.06.086. Epub 2010 Jul 7. PMID: 20619378.

545. Riddle MS, Kaminski RW, Williams C, Porter C, Baqar S, Kordis A, Gilliland T, Lapa J, Coughlin M, Soltis C, Jones E, Saunders J, Keiser PB, Ranallo RT, Gormley R, Nelson M, Turbyfill KR, Tribble D, Oaks EV. Safety and immunogenicity of an intranasal Shigella flexneri 2a Invaplex 50 vaccine. Vaccine. 2011 Sep 16;29(40):7009-19. doi: 10.1016/j.vaccine.2011.07.033. Epub 2011 Jul 23. PMID: 21787825.

Chapter 9.

List of original publications

PUBLICATIONS

1. **Haldar, R**., Dhar, A., Ganguli, D., Chakraborty, S., Pal, A., Banik, G., Miyoshi, S. I., & Das, S. (2024). "A candidate glycoconjugate vaccine induces protective antibodies in the serum and intestinal secretions, antibody recall response and memory T cells and protects against both typhoidal and non-typhoidal Salmonella serovars." Frontiers in immunology, 14, 1304170. **https://doi.org/10.3389/fimmu.2023.1304170**

2. "A newly-developed oral infection mouse model of shigellosis for immunogenicity and protective efficacy studies of a candidate vaccine" by **Risha Haldar**, Prolay Halder, Hemanta Koley, SHIN-ICHI MIYOSHI, and Santasabuj Das. Manuscript ID is #IAI00346, Infection and Immunity. The manuscript is **accepted**.

3. Manuscript entitled "Comparative immunogenicity and protective efficacy of typhoid vaccine candidates, Vi-TT and a newly developed glycoconjugate, Vi-rT2544, in BALB/c mice" by **Risha Haldar**, Amlanjyoti Dhar, Sayan Das, Santasabuj Das, is ready to communicate.

4. Manuscript entitled 'Development of a mouse model of *S.* Paratyphi A infection and study of protective efficacy of a novel candidate vaccine' is ready to communicate. (As a co-Author)

Chapter 10.

List of oral/poster presentations in National/international conferences

International Conference:

1. **Oral presentation** on 'Preventive strategy to reduce shigellosis in a newly developed oral infection mouse model using a recombinant protein to combat Shigella sp.', organised by 23rd Annual Congress of Korean Society for Parenteral and Enteral Nutrition (**KSPEN-2024**), June 21-22, 2024, **Seoul, South Korea**.
    - **Authors: Risha Haldar**, Prolay Halder, Hemanta Koley, Shin-ichi Miyoshi, Santasabuj Das.
    - **Award:** Selected for the Travel award from 23rd Annual Congress of Korean Society for Parenteral and Enteral Nutrition (**KSPEN**), June 21-22, 2024.
2. **Poster presentation** on 'A glycoconjugate vaccine against typhoidal and non-typhoidal Salmonella'; Coalition against typhoid (**CAT-2023**), 13th International Conference on Typhoid & Other Invasive Salmonelloses held on 5-7th December, 2023, **Kigali, Rwanda**.
    - **Authors: Risha Haldar**, Suparna Chakraborty, Amlanjyoti Dhar, Ananda Pal, Santasabuj Das.
    - **Award: Travel award** from **Sabin Vaccine Institute** to attend the 13th international conference on Typhoid and other invasive Salmonellosis from 5th -7th Dec, 2023 at Kigali, Rwanda.
3. **Poster presentation** on 'Development of a broad specificity glycoconjugate vaccine against Salmonella Typhi, Salmonella Paratyphi and non-typhoidal Salmonella infections' at 16th Asian Conference on Diarrhoeal Disease and Nutrition (**ASCODD-2022**) November 11-13, 2022, Kolkata, India.
    - **Authors: Risha Haldar**, Suparna Chakraborty, Amlanjyoti Dhar, Ananda Pal, Santasabuj Das**.**

National Conference:

4. **Poster presentation** on 'Immunogenicity of a trivalent glycoconjugate vaccine against Salmonella Typhi, Salmonella Paratyphi and Salmonella Typhimurium' at the Frontiers in Disease Biology (**FIDB) 2024** organized by IISER Kolkata from March 27-30, 2024 at Kalimpong, West Bengal, India.
    - **Authors: Risha Haldar**, Amlanjyoti Dhar, Suparna Chakraborty, Santasabuj Das.
    - **Award: Best Poster Presentation AWARD** from **Frontiers in Modern Biology (FIDB) (**March 27-30, 2024 at Kalimpong, India).
5. **Poster presentation** on 'Immunogenicity and long-term protective efficacy of a trivalent glycoconjugate vaccine (Osp-rT2544) against typhoidal and non-typhoidal infection' at the **IMMUNOCON-50**, Golden Jubilee Conference of Indian Immunology Society from 5-8th October, 2023, AIIMS, New Delhi, India.
    - **Authors: Risha Haldar**, Suparna Chakraborty, Amlanjyoti Dhar, Santasabuj Das.
    - **Award: Travel award** from **Immunocon 50** to attend the Golden Jubilee Conference of Indian Immunology Society from 5^{th} – 8^{th} Oct, 2023 at AIIMS, New Delhi.
6. **Poster presentation** on 'A glycoconjugate vaccine induces protective immunity against Typhoidal and non-Typhoidal Salmonella' at 7th symposium of Frontiers in Modern Biology (**FIMB) 2023** January 20-22, IISER Kolkata, India.
    - Authors: **Risha Haldar**, Suparna Chakraborty, Amlanjyoti Dhar, Ananda Pal, Santasabuj Das.

Chapter 11.

Patents applied for

PATENTS

1. Patent entitled "**A glycoconjugate vaccine composition against *Salmonella sp.***". (Patent application number is 202311070211 and the invention was filed on 10th October, 2023).

2. Patent entitled "**A glycoconjugate vaccine composition against *Salmonella* Typhi and *Salmonella* Paratyphi**." (Patent application number is 202411074276 and the invention was filed on October 01, 2024).

frontiers | Frontiers in Immunology

TYPE Original Research
PUBLISHED 09 January 2024
DOI 10.3389/fimmu.2023.1304170

OPEN ACCESS

EDITED BY
Malick Mahdi Gibani,
Imperial College London, United Kingdom

REVIEWED BY
Ugo D'Oro,
GlaxoSmithKline, Italy
Prashant Kumar,
University of Kansas, United States

*CORRESPONDENCE
Santasabuj Das
santasabujdas@yahoo.com;
dasss.niced@gov.in

RECEIVED 29 September 2023
ACCEPTED 18 December 2023
PUBLISHED 09 January 2024

CITATION
Haldar R, Dhar A, Ganguli D, Chakraborty S, Pal A, Banik G, Miyoshi S-i and Das S (2024) A candidate glycoconjugate vaccine induces protective antibodies in the serum and intestinal secretions, antibody recall response and memory T cells and protects against both typhoidal and non-typhoidal *Salmonella* serovars. *Front. Immunol.* 14:1304170. doi: 10.3389/fimmu.2023.1304170

A candidate glycoconjugate vaccine induces protective antibodies in the serum and intestinal secretions, antibody recall response and memory T cells and protects against both typhoidal and non-typhoidal *Salmonella* serovars

Risha Haldar[1], Amlanjyoti Dhar[2], Debayan Ganguli[3], Suparna Chakraborty[1], Ananda Pal[1], George Banik[4], Shin-ichi Miyoshi[5] and Santasabuj Das[1,6]*

[1]Division of Clinical Medicine, Indian Council of Medical Research (ICMR)-National Institute of Cholera and Enteric Diseases, Kolkata, India, [2]Division of Molecular Biology and Genomics, International Institute of Innovation and Technology (I3T), Kolkata, India, [3]Department of Infectious Diseases, Washington University School of Medicine at St. Louis, St. Louis, MO, United States, [4]BD Biosciences, Kolkata, India, [5]Division of Medicine, Dentistry and Pharmaceutical Sciences, Graduate School of Medicine, Dentistry and Pharmaceutical Sciences, Okayama University, Okayama, Japan, [6]Division of Biological Science, Indian Council of Medical Research (ICMR)-National Institute of Occupational Health, Ahmedabad, India

Human *Salmonella* infections pose significant public health challenges globally, primarily due to low diagnostic yield of systemic infections, emerging and expanding antibiotic resistance of both the typhoidal and non-typhoidal *Salmonella* strains and the development of asymptomatic carrier state that functions as a reservoir of infection in the community. The limited long-term efficacy of the currently licensed typhoid vaccines, especially in smaller children and non-availability of vaccines against other *Salmonella* serovars necessitate active research towards developing a multivalent vaccine with wider coverage of protection against pathogenic *Salmonella* serovars. We had earlier reported immunogenicity and protective efficacy of a subunit vaccine containing a recombinant outer membrane protein (T2544) of *Salmonella* Typhi in a mouse model. This was achieved through the robust induction of serum IgG, mucosal secretory IgA and *Salmonella*-specific cytotoxic T cells as well as memory B and T cell response. Here, we report the development of a glycoconjugate vaccine, containing high molecular weight complexes of *Salmonella* Typhimurium O-specific polysaccharide (OSP) and recombinant T2544 that conferred simultaneous protection against *S.* Typhi, *S.* Paratyphi, *S.* Typhimurium and cross-protection against *S.* enteritidis in mice. Our findings corroborate with the published studies that suggested the potential of *Salmonella* OSP as a vaccine antigen. The role of serum antibodies in vaccine-mediated protection is suggested by rapid seroconversion with high titers of serum IgG and IgA, persistently elevated titers after primary immunization along with a strong

10.3389/fimmu.2023.1304170

antibody recall response with higher avidity serum IgG against both OSP and T2544 and significantly raised SBA titers of both primary and secondary antibodies against different *Salmonella* serovars. Elevated intestinal secretory IgA and bacterial motility inhibition by the secretory antibodies supported their role as well in vaccine-induced protection. Finally, robust induction of T effector memory response indicates long term efficacy of the candidate vaccine. The above findings coupled with protection of vaccinated animals against multiple clinical isolates confirm the suitability of OSP-rT2544 as a broad-spectrum candidate subunit vaccine against human infection due to typhoidal and non-typhoidal *Salmonella* serovars.

KEYWORDS

glycoconjugate vaccine, O-specific polysaccharide (OSP), typhoidal and non-typhoidal *Salmonella* serovars, secretory IgA (sIgA), serum bactericidal assay (SBA), soft agar motility inhibition assay, antibody avidity, memory response

Introduction

Gram-negative enteric pathogen *Salmonella* is a significant contributor to infectious disease-associated morbidity and mortality of the populations around the world. Among different serovars that cause human infections; enteric fever, manifested by an acute febrile illness with mild to moderate gastrointestinal symptoms is caused by the typhoidal *Salmonella* strains, such as *S.* Typhi and *S.* Paratyphi and is more common in South-East Asia (1). *Salmonella* Typhimurium and *Salmonella* Enteritidis, in particular, are among the most common non-typhoidal *Salmonella* (NTS) strains causes gastroenteritis without spread of the bacteria to the blood or visceral organs in other parts of the world, such as US, UK and Africa. However, invasive NTS (non-typhoidal *Salmonella*) disease is not uncommon, especially among immunocompromised individuals with case fatality rate reaching as high as 15% (2). On the other hand, around 20% of untreated enteric fever patients die of complications like intestinal perforation or encephalopathy (2). According to estimates from the Global Burden of Disease (GBD) 2019 report by the Institute of Health Metrics and Evaluation, typhoid, paratyphoid and invasive non-typhoidal infection were responsible for 40%, 9%, and 29% of all *Salmonella* mortality with 17%, 2% and 45% deaths, respectively in under 5 children (3). Further, gallstone disease has shown an association with *Salmonella* carriage that may lead to adenocarcinoma of the gall bladder.

Vaccination remains the most attractive and immediate solution for the prevention of transmission of human *Salmonella* infections. A live attenuated (*S.* Typhi Ty21a strain) and a subunit (Vi-polysaccharide) vaccine against *S.* Typhi are globally available in different countries. However, available vaccines are of only modest efficacy in the long run, while safety and efficacy remain major concerns for the live and Vi-based vaccines, respectively in the small children (4). Recent development of Vi-polysaccharide based glycoconjugate vaccines (Vi-tetanus toxoid, Vi-diphtheria toxoid, Vi-rEPA, Vi-CRM197 etc) has generated considerable hope, but their long-term efficacy in typhoid endemic areas need further proof (5). Moreover, protection induced by the available Vi-conjugate vaccines would still depend on systemic anti-Vi antibodies (6) due to the absence of intrinsic *Salmonella* proteins and would confer little protection against *S.* Paratyphi A and B and Vi-negative *S.* Typhi strains. However, cross-protection against *S.* Paratyphi B was reported with the live typhoid vaccine (7).

In contrast to the available typhoid vaccines, no vaccine against *S.* Paratyphi and NTS (non-typhoidal *Salmonella*) infections has been licensed so far. Phase 1 studies were conducted to investigate the effectiveness of the oral, live-attenuated *S.* Paratyphi A vaccine (CVD 1902), while preclinical studies evaluated oral vaccines against *S.* Typhimurium (CVD 1921 and CVD 1941) (8). Phase 1 trial with the live vaccine WT05 against iNTS resulted in prolonged stool shedding in volunteers, leading to its abandonment. The major challenge in the development of live-attenuated vaccines is the optimal degree of attenuation without reducing the immunogenicity. While the GMMA (Generalized Modules for Membrane Antigens) vaccines against *S.* Typhimurium and *S.* Enteritidis are safer than the live vaccines and induced *Salmonella*-specific B and T cell immunity, an optimal balance between the reactogenicity and immunogenicity in humans is yet to be established (8).

Recombinant *Salmonella* proteins like flagellin and outer membrane proteins (Omp C, F, and D) were examined in the vaccination strategy that generated *Salmonella*-specific B and T cells. However, proteins having multiple membrane-spanning domains have problems maintaining their structure, leading to the induction of antibodies with poor functions. Further, such vaccines are not always accessible to simple production methods and may require a laborious procedure associated with increased risk of contamination, particularly with lipopolysaccharide (LPS) (9). In addition, FliC was reported by other studies to cause significant toxicities in mice, such as liver injury, acute cardiac

dysfunction, pro-apoptotic signaling and sepsis-like systemic inflammatory response (10–12). Few published reports suggested the conserved type 3 secretion system tip and translocator proteins of NTS (non-typhoidal *Salmonella*) and their chimera as vaccine candidates for serotype-independent protection (13). In contrast, several other protein subunit vaccines provided limited protection only against the homologous NTS (non-typhoidal *Salmonella*) serovar. Overall, subunit vaccines developed against the NTS (non-typhoidal *Salmonella*) strains to-date are at best modestly efficacious, for other (14, 15).

Bacterial membrane polysaccharides have been successfully incorporated in different candidate vaccines against different pathogenic strains (16–18). *Salmonella* O-antigen (O-specific polysaccharide or OSP) is a component of the outer membrane of Gram-negative bacteria which forms the distal portion of LPS. Clinical studies have implicated it as a target for protective immunity against non-Typhi serotypes as anti-OSP antibody was able to mediate serum bactericidal activity in healthy adults and children in the United States (19). Other studies showed that OSP-specific antibodies were found to kill *Salmonella in vivo* by lowering the bacterial loads in blood, liver, and spleen following passive immunization in mice and *in vitro* studies showed complement-mediated and phagocytosis mediated bacterial killing (20). Although *Salmonella* OSP molecules in their unconjugated state have limited immunogenicity, covalent attachment to proteins significantly enhances the immune response and allows their incorporation into OSP-based vaccines (21). Several formulations with different carrier proteins (TT, DT, CRM197, FliC), chemically conjugated to OSP showed considerable promise in mouse experiments. However, the side chains attached to the common backbone of the O-antigens from different serovars make them antigenically unique (22, 23). For example, O:2 antigen is characteristic of *S.* Paratyphi A, whereas O:4 and O:4,5 is for *S.* Typhimurium. *S.* Enteritidis and *S.* Typhi share the O:9 antigen (24). As a result, different monovalent glycoconjugate vaccine formulations were combined for wider vaccine coverage against multiple serovars. For example, *S.* Paratyphi OSP-DT + *S.* Typhi Vi-DT, *S.* Typhimurium OSP-CRM_{197} + *S.* typhi Vi- CRM_{197} were evaluated in preclinical studies (25) while others were tested in phase I (*S.* Typhimurium COPS-FliC + *S.* Enteritidis COPS-FliC + *S.* Typhi Vi-TT) or phase II (OSP-TT + Vi-TT) trials (3). Despite the potential of broader protective coverage, combined glycoconjugate vaccine has several inherent limitations. Administration of multiple conjugate vaccine formulations with the same or different carrier proteins may increase the chance of carrier-specific epitope suppression (CIES) or bystander interference, as reviewed by various authors (26–28). The mechanisms related to the CIES describe the pre-existing immunity to a Carrier protein may inhibit the hapten or saccharide specific immune response connected to the same carrier. However, monovalent combination of OSP-TT examined in phase 2 study against *Salmonella* Paratyphi A showed significantly increased antibody titer against OSP (3-4-fold rise at day 180) (29). Besides this, preparation of a multi-glycoconjugate vaccine is time-consuming and costly. This underscores the need for the development of single formulation carrying multivalency (multivalent vaccines) that could offer protection against a variety of *Salmonella* serovars, both typhoidal and nontyphoidal.

Use of novel carrier proteins could overcome the limitations mentioned above and enable further development of vaccine formulations. A single vaccine formulation of *Salmonella*-specific antigens that covers different *Salmonella* serovars would be preferred. We report here the development of a glycoconjugate candidate vaccine where OSP from *S.* Typhimurium is chemically linked to the recombinant outer membrane protein rT2544 from *S.* Typhi. Previous studies from our laboratory reported strong immunogenic potential of rT2544, generating antigen-specific, opsonic antibodies and cytotoxic T cells that led to protection from bacterial challenge in mice (30). In addition to antigenicity of rT2544 and its protective efficacy against *S.* Typhi and *S.* Paratyphi, we observed strong adjuvanticity to OSP, leading to augmented anti-OSP antibody response. Thus, this study creates an opportunity to use rT2544 as a carrier protein in the glycoconjugate platform. Given that no vaccines with combined protective efficacies against typhoidal and non-typhoidal *Salmonella* are currently under clinical trials, development of an OSP-based trivalent vaccine containing rT2544 as the carrier protein could be a key step forward toward the development of a broad-specificity as well as safe and effective glycoconjugate vaccine.

Materials and methods

Bacterial strains, growth conditions and plasmid

Salmonella Typhi Ty2 and *Salmonella* Typhimirium LT2 were generous gifts from J. Parkhill, Sanger Institute, Hinxton, UK. Clinical isolates of *Salmonella* Typhimurium and *Salmonella* Enteritidis were gifted by A. Mukhopadhyay (ICMR-NICED, Kolkata, India), while clinical isolates of *Salmonella* Typhi and *Salmonella* Paratyphi A were received from IMTECH, Chandigarh. All *Salmonella* strains were grown in Hektoen enteric agar and *Escherichia coli* BL21, a kind gift from Dr. Rupak K. Bhadra (CSIR-IICB, Kolkata, India) was cultured in Luria–Bertani agar at 37°C. Liquid cultures of the bacterial strains were grown in Luria Broth. Bacterial culture media and pET-28a plasmid were purchased from BD Difco and Addgene (USA), respectively. The oligonucleotides used in this study were synthesized from IDT.

Cloning and expression, of recombinant T2544

t2544 ORF with four arginine coding sequences inserted at the NH2 terminus was PCR amplified, using *Salmonella* Typhi Ty2 genomic DNA as the template and the following forward and reverse primers:

FP-5'TTCGCCATGGAACGCCGCGGGATCTATATCACCGGG-3',

RP-5' GCCCTCGAGTTAGCGGCGAAAGGCGTAAGTAATGCC-3'.

The PCR product was cloned into pET28a at the NCoI and XhoI restriction enzymes (New England Biolabs) sites. After clone confirmation by restriction digestion, followed by sequencing (AgriGenome, India), the recombinant plasmid was transformed into *E. coli* BL21 (DE3). Transformed bacteria were inoculated into LB (BD Difco) broth (300 ml) and incubated until the OD_{600} reached 0.5. Recombinant T2544 expression was inducted by 1mM IPTG for 4h at 37°C, followed by centrifugation at 5000 g. The induction was confirmed by SDS-PAGE, stained with Coomassie Blue.

Extraction of rT2544 from bacterial inclusion bodies and purification by ion exchange chromatography

To isolate the inclusion bodies, induced bacterial cells were resuspended in sonication buffer (30 ml) and subjected to 5 cycles of sonication on ice, with each cycle consisting of 5 pulses of 1 sec each followed by 1-minute incubation. The power output was designed to deliver a maximum of 30 watts at a frequency of 20 kHz. The sonicated pellet was collected following centrifugation at 15000 rpm for 20 min at 4°C, and washed three times with protein extraction wash buffer (20 ml). After centrifugation, recombinant T2544 was extracted from the inclusion bodies using protein extraction buffer [10 mM Tris-HCL (pH 12.0), 5ml] and analyzed by 12% SDS-PAGE. The extracted rT2544 was purified by ion exchange chromatography using UNO sphere Q resin (Bio-rad), according to the manufacturer's protocol. A Glass econo-column (1.0 x 10 cm, Bio-Rad) was packed 50% with the resin, followed by washing with 5 column volumes (CV) of water and equilibration with 10 CV (column volume) of equilibration buffer (1X PBS, pH 7.4). The equilibrated resin was admixed with the recombinant protein (rT2544, 5ml) and kept for binding up to 3h at room temperature. The mixture was passed through the column and after washing with 3 CV (column volume) of ion exchange wash buffer, column-bound rT2544 was eluted using ion exchange elution buffer with Nacl gradient. Briefly, 1 ml of elution buffer containing 1M NaCl was inserted to the protein bound column that already had 40% of wash buffer and 1ml of eluted volume was collected. Eluted rT2544 was quantitated by Bradford Reagent (Sigma) and protein purity was determined by 12% SDS-PAGE. Protein extraction and IEC buffer compositions are mentioned in Supplementary Table 1.

Extraction and purification of OSP

Lipopolysaccharide (LPS) was purified from *S.* Typhimurium, using the hot phenol method as reported earlier (31). Briefly, *Salmonella* Typhimurium LT2 strain was cultured in Luria Broth (1L) at 37°C for 10h (OD 1.8). Formalin-inactivated cells were collected by centrifugation at 5000 g and washed twice with PBS. After resuspension in PBS (30 ml), 90% phenol (HiMedia) was used for 30 min at 68°C to extract crude LPS from the cell pellet. The suspension was centrifuged at 7,300 × g at 10°C for 1 h. The aqueous layer (60 ml) was precipitated with ethanol (final concentration 75%), and the precipitate was treated with DNAse (1 µg/mL), RNase (1 µg/mL) and Proteinase K (100 µg/mL) (all purchased from Roche), followed by dialysis overnight against PBS (pH 7.4) at 4°C. Extracted LPS was used to further extract O-specific polysaccharide (OSP). to this end, LPS was incubated with 1% acetic acid (HiMedia), pH 3.0, and 100°C for 1.5 hours, followed by ultracentrifugation at 64,000 ×g for 5h at 10°C, using a WX+ Ultra series centrifuge (Thermo Scientific). The supernatant was dialyzed for 48h against PBS (pH 7.4) and OSP was purified by size exclusion chromatography.

Conjugation of OSP and rT2544

Conjugation was performed as described earlier (31). Briefly, purified OSP (1.2 mg/ml in PBS, pH 8.5-9.0) was activated with an equal volume of cyanogen bromide (CnBr, SRL), prepared as 1.2 mg/ml in acetonitrile (Fluka). The reaction mixture was kept for 6 min on ice and the pH was maintained with 0.1M NaOH. The activated mixture was derivatized with 0.8M ADH (Sigma), dissolved in 5M $NaHCO_3$ (SRL). For this reaction, the pH was adjusted to 8-8.5 with 0.1M HCl. The reaction mixture was stirred at 4°C overnight and dialyzed against 1x PBS, pH 7.4 at the same temperature for 16 h. ADH derivatized OSP was then mixed with 3 ml of recombinant T2544 (1.25 mg/ml), followed by the addition of EDAC (0.05M) to the mixture and incubated for 4h on ice. The pH of this protein-polysaccharide mixture was maintained at 5.1 to 5.5 with 0.1 M HCl. Finally, the mixture was dialyzed against 1x PBS (pH 7.4) for 48 hours at 4°C.

Circular dichroism

Circular dichroism was performed as described earlier (32). Briefly, 1.0 ml of rT2544 (180 µg/ml) was filtered through a 0.45 µm pore-size filter to remove suspended particles, and taken in a 0.1 mm path-length quartz cuvette. Circular dichroism (CD) spectrum of the protein sample was captured at the wavelength range of 200 to 300 nm at 25°C on the Jasco-1500 spectrophotometer. A minimum of three spectra were recorded at 1 nm steps at a speed of 50 nm per minute. Baselines were subtracted and data was recorded as ellipticity (CD [mdeg]).

Fast-performance liquid chromatography

FPLC was performed as described earlier (33). Briefly, rT2544, OSP and OSP-rT2544 (conjugate) samples in normal saline (pH 7.4) were filtered through 0.22 µm syringe filters (HiMedia) and run in a Hiload 16/60 Sephacryl S300 size exclusion column (Cytiva Life Sciences) at a flow rate of 0.5 mL/min at 4°C using Biorad NGC chromatography system. The column was previously equilibrated with normal saline (pH 7.4). The buffer solution was degassed and filtered through 0.22 µm cellulose acetate membrane filters (Millipore). The polysaccharide and the protein were detected at λ =215 nm and 280 nm, respectively.

Dynamic light scattering

DLS was performed as described earlier (34, 35). Briefly, 1 ml of Protein, polysaccharide and conjugate samples at a concentration of 0.8-1 mg/ml were filtered through a 0.45 µm pore-size filter to remove particles, if any prior to the measurement. Hydrodynamic sizes of the samples were calculated using ZEN 3600 Malvern Zetasizer with 5 mW HeNe laser at 25°C. The dispersed light is gathered at 173° in this system, which employs backscatter detection.

Fourier transform infrared spectroscopy

FTIR was performed as described earlier (36). Briefly, functional groups of lyophilized samples were monitored using potassium bromide (KBr) pellet method (1:100 w/w). To create translucent 1 mm pellets, potassium bromide was combined with lyophilized samples (0.8–1.0 mg) and pressed with 7500 kg for 30 seconds. Spectra were recorded using the translucent pellet in Perkin Elmer Spectrum 100 system in the spectral region of 4000–400/cm.

Proton NMR

^{1}H NMR was performed as described earlier (34). Briefly, Lyophilized samples, dissolved in 0.5 mL of D_2O (Sigma, 99.9%) were analyzed in a 400 MHz NMR spectrometer (JOEL 400 YH) at 25°C using NMR Pipe on Mac OS X workstation. A sodium salt, TSP-D4 (0.38%) was used as a standard. The spectrometer was arranged with a 5 mm triple-resonance z-axis gradient cryogenic probe head and four frequency channels. Initial delays in the indirect dimensions were intended to provide -180° and 90° first-order phase corrections at zero and first order, respectively. States-TPPI phase cycling was used to achieve quadrature detection in the indirect dimensions with a one-second relaxation delay.

Western blot

Western blot was performed as described earlier (37). Briefly, OSP, rT2544 and OSP-rT2544 (8 µg each), resolved in 10% SDS-PAGE were transferred to a PVDF membrane (Millipore). After blocking with 5% BSA for 1 h at room temperature, membranes were incubated overnight at 4°C with polyclonal anti-rT2544 antibody (1:5000 dilutions), raised in-house. Membranes were washed with TBS-T [Tris Buffered Saline pH 7.5, containing 0.1% Tween-20 (v/v)] for 5 times and incubated with goat anti-mouse IgG antibody (1:10000 dilutions), conjugated to horseradish peroxidase (HRP) for 1 h at room temperature. After 3 washes with TBS-T in an orbital shaker, membranes were developed by chemiluminescent reagents(SuperSignal West Pico, Thermo Fisher) and the signals were captured in ChemiDoc ^{TM} MP imaging system (Bio Rad).

Animal breeding, immunization, and infection

Animal breeding and experimentation were approved by the institutional animal ethical committee (PRO/192/-June 2022-25). Female, inbred C57BL/6 and BALB/c mice (5-6 weeks old) were immunized subcutaneously with OSP (8µg), rT2544 (24 µg), or OSP-rT2544 (8µg of OSP and 24 µg of rT2544) at 2-weeks intervals for 3 times. Blood samples were taken from the immunized mice on days 0, 14, 28, 38, 110, and 120 by tail snip and incubated for 30 min at 37°C and centrifuged at 1,200 × g at 4°C for 15 min and stored at −80°C. Fecal samples were collected on days 0, 14, 28, and 38, weighed, and carefully dissolved in 100 mg/ml of PBS, containing 1% BSA (SRL), centrifuged at 15,000 × g at 4°C for 10 min, and protease inhibitor cocktails (Sigma-Aldrich) were added to the supernatants before storage at −80°C. Intestinal washes were collected after sacrifice of the C57BL/6 mice (on day 38). To this end, the small intestine was removed and washed three times with 1 ml of PBS-1% BSA (BSA, SRL). Samples were centrifuged at 10,000 × g at 4°C for 10 min, and protease inhibitor cocktails (Sigma-Aldrich) were added to the supernatants before storage at −80°C. Fourteen days after the last immunization (day 42), iron-overload BALB/c mice were infected with *Salmonella* Typhi or *Salmonella* Paratyphi A, while streptomycin pre-treated C57BL/6 mice were infected with *Salmonella* Typhimurium and *Salmonella* Enteritidis as described earlier (37–39). Briefly, BALB/c mice were treated with intraperitoneal injection of $Fe3^{+}$ as $FeCl_3$ in 10^{-4} N HCl (0.32 mg per gm of body weight) along with Desferoxamine (25 mg/Kg body weight) four hours prior to the bacterial challenge. Mice were orally infected with 5 x 10^7 CFU of *S.* Typhi or 5 x 10^5 CFU of *S.* Paratyphi A and monitored for 10 days. C57BL/6 mice were treated with streptomycin (20 mg/mouse) orally as a beverage for 24 h. At 20 h after streptomycin treatment, water and food were withdrawn for 4 h before the mice were infected orally with 5 x 10^6 CFU of *S.* Typhimurium or *S.* Enteritidis and monitored for 30 days.

Enzyme-linked immunosorbent assay

ELISA was performed as described earlier (37, 40). Microtiter plates were coated with 5 µg/ml of OSP or 2 µg/ml of rT2544 and incubated at 4°C overnight. After rinsing with PBS-T (Phosphate buffer saline, containing 0.05% Tween 20), the wells were blocked using PBS, containing 1% BSA (SRL) for 1 hour at room temperature. Following further washes, plates were incubated with serum, feces, or intestinal lavage samples, diluted serially (1:200 to 1: 102400 for IgG and 1:20 to 1:20480 for IgA) for 2 hours at room temperature. Subsequently, Goat anti-mouse IgG (1:10000) or IgA (1:5000) antibodies conjugated to HRP were added to the wells and incubated for 1 h at room temperature. The immune complex was developed using tetramethyl benzidine (TMB) substrate (BD OptEIA^{TM}) and OD_{450} of the mixture was measured in a spectrophotometer (Shimadzu, Japan).

Avidity test was performed as described earlier (41). Briefly, after overnight incubation with the respective antigens (OSP, rT2544), microtiter plates were incubated with OSP-rT2544 antisera with a dilution of 1:100 in PBS-T. To test for the avidity of serum IgG antibody, respective antigen-antibody complexes in the wells were washed (3 times) with PBS-T, containing 6M urea before the addition of HRP-conjugated anti-mouse IgG. The avidity index was calculated by multiplying the ratio of the absorbances of the wells that were washed with and without 6M urea-containing buffer by 100.

Serum cytokines (IL-4, IL-6, IFN- γ, IL-10 and TNF-α) (Invitrogen, USA) as well as IFN-γ (Krishgen biosystem) in the co-culture supernatants of T cells and BMDCs were measured using the commercial ELISA kits following the manufacturer's protocol.

Serum bactericidal assay

Serum bactericidal assay was performed according to an earlier described method (38, 42). Sera collected from the immunized C57BL/6 and BALB/c mice on day 38 of first immunization were heat-inactivated at 56°C for 20 min and serially diluted in PBS (1:100 to 1:102400). A mixture comprising of 25µl of guinea pig complement (25% final concentration) and 15 µl of PBS, 50 µl of diluted heat-inactivated serum and 10 µl of diluted bacteria (310 CFU, T_0) was prepared. The mixture was incubated for three hours (T_{180}) at 37°C with gentle agitation (130 rpm). The mixtures were plated on LB agar and the plates were incubated overnight at 37°C. Bactericidal titer of the complement-containing antisera was expressed as the dilution of the serum required for the reduction of bacterial growth by 50% at T_{180} compared with T_0. Data was analyzed using GraphPad Prism 8.0.1.244 software.

Soft agar motility inhibition assay

A motility assay was performed as described earlier (43). Briefly, soft agar (LB medium with 0.4% Bacto agar, BD Difco) was mixed with 5% intestinal lavage from the experimental mice (collected on day 38 after the first immunization dose) and left at room temperature to dry. Bacteria (1×10^6 CFU) were plated on top of the dried plates, which were incubated for 10 hours at 37°C. Bacterial motility was measured by the diameter (mm) of the clearing zones and the data was analyzed using GraphPad Prism 8.0.1.244 software.

Memory T cell assay

Myeloid precursor cells from mouse bone marrow (BM) were used to generate dendritic cells as described earlier (30). Briefly, bone marrow cells from the femur and tibia of naïve C57BL/6 mice were cultured in RPMI 1640 medium, supplemented with murine Granulocyte-Macrophage Colony Stimulating Factor (mGM-CSF, 20 ng/mL) for 7 days. On day 7, cells were harvested and starved for 12 h in RPMI 1640 containing 1% FBS, followed by stimulation with OSP or OSP-rT2544 for 24h. $CD4^+$ T cells were isolated from the spleens of the immunized mice on day 120 of the first immunization using magnetic beads (BD IMag™ anti-mouse CD4 Magnetic Particles, USA). $CD4^+$ T Cells were co-cultured for 24h at 37°C in presence of 5% CO2 with antigen-pulsed BMDCs at 1:1 ratio. IFN-γ concentration was estimated in the culture supernatants by ELISA (Krishgen biosystem), while the$CD4^+$ T cells were analyzed by flow cytometry for T-effector memory cell determination markers ($CD4^+CD62L^{low}$ $CD44^{hi}$).

Flow cytometry

Cells were stained with fluorochrome-conjugated anti-mouse antibodies following the standard protocol. Briefly, $CD4^+$ T Cells co-cultured with antigen-pulsed BMDCs were harvested and subjected to F_c blocking in FACS buffer (1:50 ratio) for 20 min on ice. Following centrifugation at 1500 rpm for 5 min at 4°C, cells were stained with fluorochrome-conjugated antibodies (BD Biosciences) against specific surface markers (CD4-Percp Cy5.5, CD44- FITC, and CD62L-PE Cy7) for 30 min at 4°C in the dark. After staining, the cells were washed three times in FACS buffer and fluorescent signals were measured by FACS ARIA-II (BD Bioscience). Data were analyzed by FlowJo (version V10.8.1).

Data analysis

Data related to CD, FPLC, DLS and FTIR were analyzed using ORIGIN software (2019b). NMR data were processed in MestReNova -9.0.1-13254 software. Antibody titers were represented as reciprocal of the log 2 values. Statistical analysis was performed using GraphPad Prism 8.0.1.244. Comparison between two groups was calculated by student t-test, while two-way ANOVA with Tukey's *post-hoc* test was performed for multiple comparisons. Statistical significance was measured at *P <0.05, **P < 0.01, ***P < 0.001, ****P < 0.0001).

Results

Purification and characterization of recombinant T2544

Cloning of pET28a-*t2544* was confirmed by restriction digestion, followed by agarose gel electrophoresis of the digested product that showed migration of *t2455* amplicon along the predicted size of 663bp (Figure 1A). Nucleotide sequencing of the clone showed in-frame cloning and correct orientation of *t2544* gene (Supplementary Figure 1A). Recombinant T2544 (rT2544) extracted from the inclusion bodies of *E. coli* BL21 (DE3) migrated along the size of 30 kDa in SDS-PAGE (Supplementary Figure 1B) and ion exchange chromatography yielded a highly purified protein of the same size (Figure 1B). Further purification by size exclusion chromatography generated a smaller peak near 104.8 ml and a major peak near 112.8 ml fractions (Figure 1C). The secondary

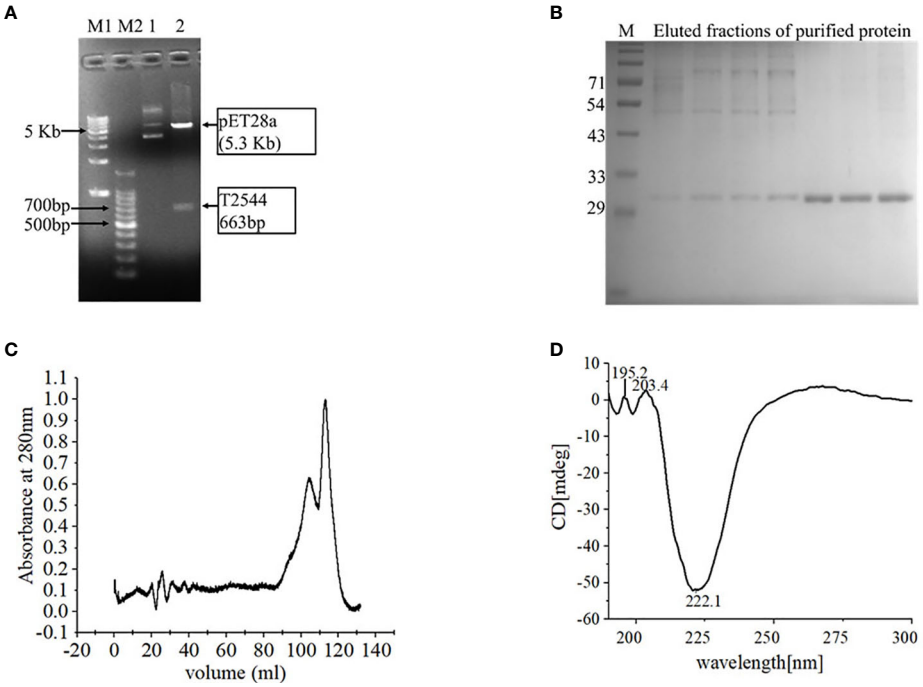

FIGURE 1
Purification and characterization of recombinant T2544. **(A)** 1% Agarose gel electrophoresis of pET28A-*t2544* after restriction digestion with XhoI and NcoI. Lane M1: 1 kb DNA ladder, M2: 100bp DNA ladder, 1: Undigested pET28A-*t2544* clone, 2: pET28A-*t2544* clone digested by XhoI and NcoI. **(B)** 12% SDS-PAGE showing the elution profile of rT2544 (3.5 µg) after ion exchange chromatography (IEC). rT2544 extracted from the inclusion bodies of E.coli was admixed with UNO sphere Q ion-exchange resin (Bio-rad), followed by binding to the Glass econo-column, 1.0 x 10 cm (Biorad) **(C)** Elution profiles of rT2544 (0.8 mg/ml) from the size exclusion chromatography column (Hiload 16/60 Sephacryl S300, Cytiva), detected at 280 nm. **(D)** Far-UV circular dichroism spectra of rT2544 (180 µg/ml) captured at the wavelength range of 200 to 300 nm at 25°C in PBS (pH 7.4) on the Jasco-1500 spectrophotometer. Data presented as ellipticity (CD [mdeg]) after subtracting the baseline values. For each analysis, experiment was replicated three times, and data from a representative experiment are shown.

structure of rT2544 detected by Far-UV CD spectra showed one negative band at 222.1 nm, indicating alpha helix, and two positive bands at 195.2 nm and 203.4 nm, suggesting β helical structures (Figure 1D). Dynamic light scattering measured the hydrodynamic radius of rT2544 as 22.16 nm (Supplementary Figure 1C).

Purification and characterization of OSP

Lipopolysaccharide extracted from *S.* Typhimurium LT2 and resolved in SDS-PAGE showed multiple higher molecular weight bands and a smear corresponding to lower molecular weights upon silver staining. Acid hydrolysis of LPS removed the smear, suggesting their origin from the lipid A component, while the core oligosaccharide bands were left behind in the gel (Figure 2A). The gel filtration profile of OSP showed two peaks near 109.23 ml and 117.9 ml fractions that corresponded to their average K_d values of ~ 22.75 kDa (Figure 2B; Supplementary Table 2). ^{1}H NMR analysis showed signals between 2.0 and 2.2 ppm, arising from the O-acetyl groups at C-2 of Abequose that confirmed the presence of the characteristic sugar of *S.* Typhimurium OSP. Signals between 1.79 and 1.97 ppm and 3.50 and 3.94 ppm of NMR spectra were generated from the protons bound to C-3 of Abequose and C-5 of Rhamnose and Abequose, respectively (Supplementary Figure 2A). Molecular radius of OSP was 4.42 nm, as calculated by DLS (Figure 2C). FTIR analysis disclosed the characteristic wave patterns of active OSP. Waves near 1650 cm^{-1} indicated carbonyl group (C=O), while those in the region of 1413-1261 cm^{-1} represented the deformation of C-H and C-OH groups. In contrast, waves near 1095 cm^{-1} and 1022 cm^{-1} corresponded to the characteristic peaks of the glycosidic linkage and the bands in the 936–800 cm^{-1} region, which is called the anomeric region, indicated the α and β configuration of the anomeric carbon (Supplementary Figure 2B).

OSP and rT2544 conjugation, purification and characterization of the conjugate

Conjugates of OSP and rT2544 displayed a smear tail in the western blots, probed with T2544 antibody, indicating heterogeneity of size and mass-to-charge ratios (Supplementary Figure 3). FPLC analysis showed the major peak of OSP-r2544 elution after the calculated void volume (41.66 ml), as opposed to the elution peaks of OSP at 109.23 ml and 117.9 ml and rT2544 at 112.8 ml (Figure 3A). Higher hydrodynamic diameter of OSP-rT2544 (57.45 nm) compared with OSP (4.42 nm) and rT2544 (22.16 nm) suggested the formation of higher-order complex formation between the polysaccharide (OSP) and the protein (rT2544) (Figure 3B). However, we observed different molar

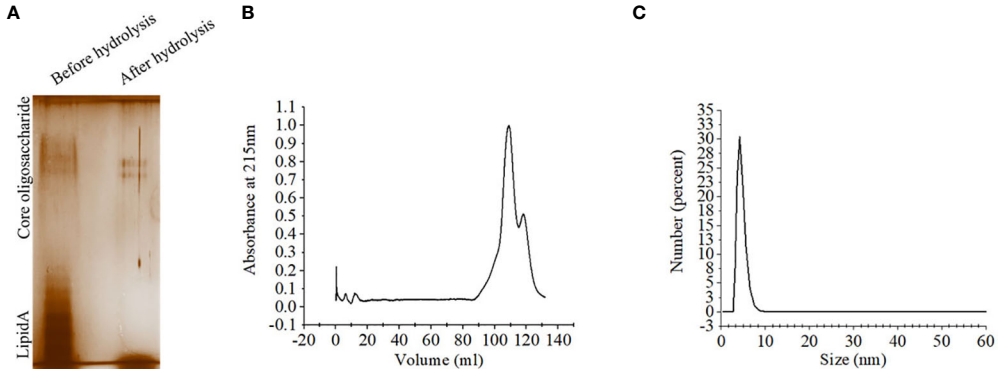

FIGURE 2
Extraction and purification of OSP. **(A)** Visualization of LPS and OSP resolved in 10% SDS-PAGE, stained by silver staining. LPS was extracted from *S.* Typhimurium LT2 strain by hot-phenol method and subjected to acid hydrolysis to isolate OSP. Lane 1: purified LPS (8 µg), Lane 2: purified OSP (8 µg). **(B)** Elution profiles of OSP (1mg/ml in normal saline, pH 7.4) eluted at a flow rate of 0.5 mL/min at 4°C from a size exclusion chromatography column (Hiload 16/60 Sephacryl S300, Cytiva), pre-equilibrated with normal saline, pH 7.4. The OSP was detected at λ =215 nm using Bio-Rad NGC chromatography system. **(C)** Dynamic light scattering (DLS) showing hydrodynamic radius (R_h) of OSP (0.88 mg/ml, PBS, pH 7.4), determined at 25°C using ZEN 3600 Malvern Zetasizer. For each analysis, experiment was replicated three times, and data from a representative experiment are shown.

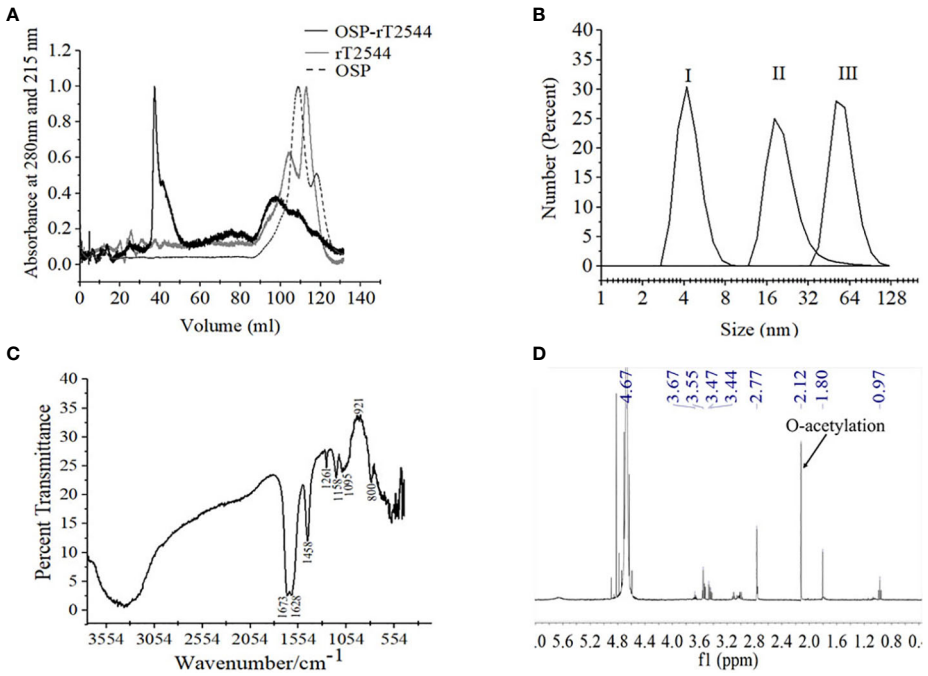

FIGURE 3
Characterization of OSP-rT2544 conjugate. **(A)** Gel filtration chromatography. OSP-rT2544 conjugate containing 1.83 mg of total protein and 0.59 mg of total sugar in normal saline (pH 7.4) was injected into Hiload 16/60 Sephacryl S300 column (Cytiva). The column was pre-equilibrated with normal saline, pH 7.4 and the flow rate was maintained at 0.5 mL/min. The conjugate (OSP-rT2544) and T2544 were observed (eluted at 41.66 ml and 112.8 ml) at 280 nm, while OSP (eluted at 109.23 ml and 117.9 ml) was observed at 215 nm at 4°C using Bio-Rad NGC chromatography system. **(B)** Dynamic light scattering (DLS) showing hydrodynamic radius (R_h) of (I) OSP (0.88 mg/ml); (II) rT2544 (0.8 mg/ml); (III) OSP-rT2544 (1 mg/ml), dissolved in PBS (pH 7.4) at 25°C using ZEN 3600 Malvern Zetasizer. **(C)** Fourier Transform Infrared (FTIR) spectrum of the lyophilized conjugated sample (OSP-rT2544) was monitored using potassium bromide (KBr) pellet method (1:100 w/w). Spectra recorded in the Perkin Elmer Spectrum 100 system in the spectral region of 4000–400/cm indicating different functional groups of OSP-rT2544: carbonyl group (C=O) (1673 cm^{-1}), C-H and C-OH groups (1458-1261 cm^{-1}), glycosidic linkage (1095 and 1158 cm^{-1}), aldehyde and ketone groups (921 and 800 cm^{-1}) and amide bond of the protein (1628 cm^{-1}). **(D)** ^{1}H NMR of lyophilized OSP-rT2544, dissolved in 0.5 mL of D_2O showing the characteristic peak of O-acetylation of OSP at C-2 of Abequose (2.12 ppm) in a 400 MHz NMR spectrometer (JOEL 400 YH) at 25°C. Additional peaks indicate protons bound to C-5 (3.4-3.6 ppm) and C-3 (1.8 ppm) of monosaccharides, the protein peaks (0.97 and 2.77 ppm) and the D2O solvent (4.67 ppm). For each analysis, experiment was replicated three times, and data from a representative experiment are shown.

ratios of OSP and rT2544 in the glycoconjugate molecules (Supplementary Table 3). To find out the functional groups in the purified OSP-rT2544 conjugate, FTIR analysis was performed. FTIR showed one additional functional group in the conjugate (OSP-rT2544), the strong amide bond of protein at 1628 cm^{-1}, which was absent in OSP. On the other hand, similar functional groups in OSP-rT2544 and OSP corresponded to different wave lengths. Thus, carbonyl groups (C=O) were detected at 1673 cm-^{1}, deformation of C-H, C-OH groups appeared near region 1458-1261 cm^{-1} and glycosidic linkage emerged at 1095 cm^{-1} and 1158 cm^{-1} in OSP-T2544. In addition, α and β configurations of the anomeric carbon were detected near the regions 921 cm^{-1} and 800 cm^{-1} (Figure 3C). However, O-acetylation pattern at C-2 of Abequose between 2.0 and 2.2 ppm was similar in OSP and OSP-T2544 in ^{1}H NMR study (Figure 3D). But, two different peaks of the OSP-rT2544 molecule that corresponded to the aliphatic region of the protein and observed near 0.97 ppm and 2.77 ppm were absent from OSP. Total sugar and protein contents and the molecular weights of the conjugate and the un-conjugated preparations used for immunization are shown in Supplementary Table 4.

Vaccination with OSP-rT2544 conferred a broad range of protection against typhoidal and non-typhoidal *Salmonella*

To investigate broad range efficacy of our candidate vaccine, BALB/c and C57BL/6 mice were immunized s.c. with three doses of OSP-rT2544, rT2544, OSP, or PBS (vehicle) at 14 days intervals (Figure 4A; Supplementary Table 5). Protective efficacy of the vaccines was evaluated in BALB/c mice for *S.* Typhi and *S.* Paratyphi A and in C57BL/6 mice for *S.* Typhimurium and *S.* Enteritidis strains, as mentioned under Materials and Methods (Supplementary Table 6). A 10xLD_{50} dose killed all the BALB/c mice within a period of 5-6 days in the vehicle- and OSP-treated groups, while 75-77% of mice that received either OSP-rT2544 or rT2544 were alive at 10 days post-infection and beyond (Figures 4B, C). On the other hand, OSP-rT2544 and OSP immunization protected 70-80% and 20% of C57BL/6 mice, respectively against *S.* Typhimurium infection, while all the mice that received rT2544 or the vehicle only died within 25 days (Figure 4D). Interestingly, 55-60% of latter mouse strain immunized with OSP-rT2544 also survived *S.* Enteritidis challenge (Figure 4E). Protection of the immunized mice was observed for both the reference as well as clinical strains, strongly suggesting the potential of OSP-rT2544 as a candidate quadrivalent vaccine for typhoidal and non-typhoidal *Salmonella* infections.

OSP-rT2544 induces protective humoral immune response against *S.* Typhi and *S.* Paratyphi A

We had earlier reported protective humoral response in mice against *S.* Typhi upon s.c. immunization with recombinant T2544. To check if rT2544 present in the conjugate vaccine is equally immunogenic, serum antibody endpoint titers (The reciprocal of the titer (1/Y) at which the absorbance of the immune sera was the same as the control (PBS immunized sera)) were measured by ELISA, 10 days after completion of the primary immunization series as well as 110 days after the first immunization dose of BALB/c mice, immunized with OSP-rT2544 or the unconjugated vaccine formulations (Figure 5A; Supplementary Table 5). The results

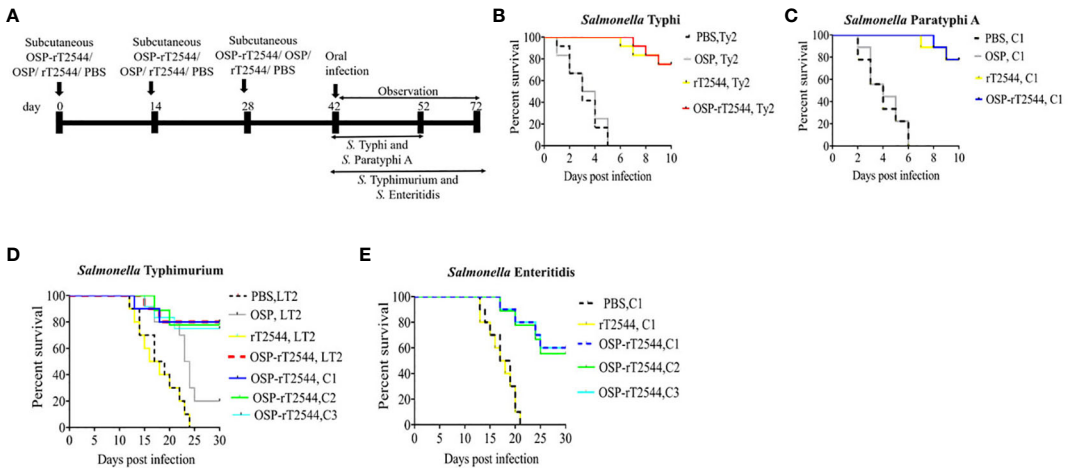

FIGURE 4
Protection of mice after subcutaneous immunization with OSP-rT2544. **(A)** Experimental scheme of mouse subcutaneous immunization with the vehicle (PBS), conjugate (OSP-rT2544) (8 µg of OSP or 24 µg of rT2544 in conjugate), or unconjugated vaccines (OSP 8 µg, rT2544 24 µg)), followed by oral bacterial challenge. **(B–E)** Kaplan-Meyer plot of cumulative mortality of the infected mice. BALB/c mice were orally challenged with *S.* Typhi Ty2 (5 x 10^{7} CFU, n= 12) **(B)** or *S.* Paratyphi A (5 x 10^{5} CFU, n=9) **(C)** and monitored for 10 days. For NTS strains, C57BL/6 mice were orally challenged with *S.* Typhimurium (5 x 10^{6} CFU of the LT2 strain (n=10), clinical strain 1 (C1, n=10), clinical strain 2 (C2, n=9) and clinical strain 3 (C3, n=12)) **(D)** or *S.* Enteritidis (5 x 10^{6} CFU of C1 (n=10), C2 (n=9) or C3 (n=10)) **(E)** and monitored for 30 days. The color scheme used to mark different experimental groups are shown in Table 1.

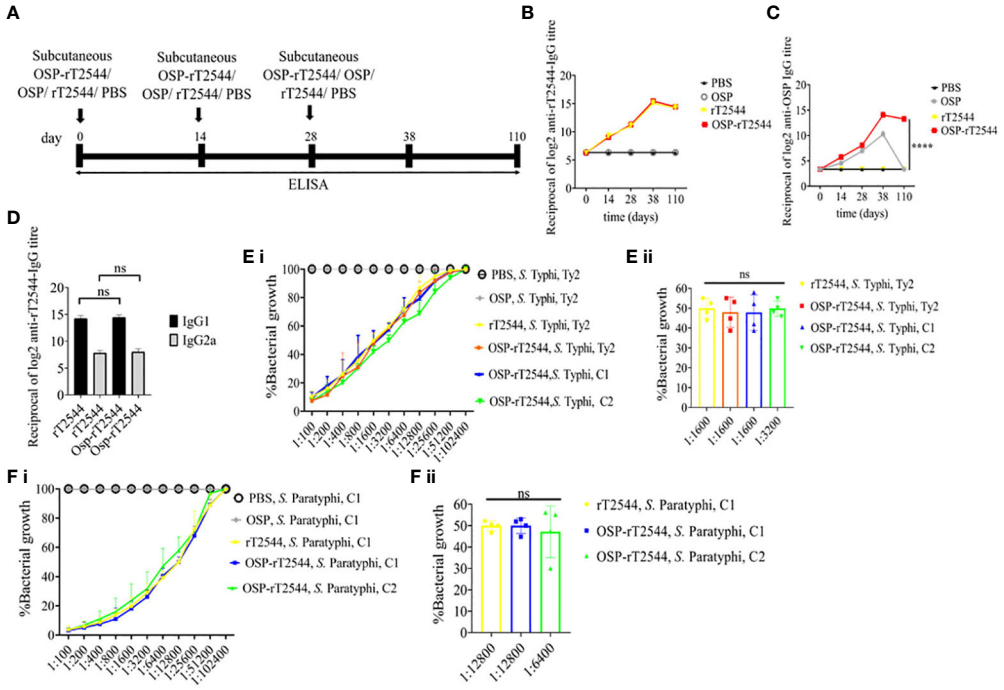

FIGURE 5
Protective antibody response against *S.* Typhi and *S.* Paratyphi A by OSP-rT2544 immunization. **(A)** Scheme of subcutaneous immunization of BALB/c mice as described under Figure 4. Mouse tissue samples were collected before each immunization dose and on day38 and day110 of the start of immunization. **(B, C)** Time kinetics of antigen-specific total IgG in the mouse serum as measured by ELISA. Data represent mean ± SEM values from different mice samples (n=5). X-axis indicate the time points after the start of the immunization when samples were collected. Statistical significance between the titer values from OSP-rT2544 and unconjugated OSP vaccine recipients is shown. Statistical analysis was performed using two-way ANOVA and Tukey's post-test for multiple comparisons. *P < 0.05, **P < 0.01, ***P < 0.001. **(D)** rT2544 specific serum IgG isotypes measured by ELISA at day 38. Data represent mean ± SEM values from different mice samples (n=5). Statistical analysis was performed using two-tailed Student's *t*-test. **(E, F)** Serum bactericidal assay. Serial dilutions of heat-inactivated antisera, collected from different groups of the immunized mice at 38 d of immunization were mixed with 25% guinea pig complement and incubated for 3h with the *S.* Typhi or *S.* Paratyphi A strains as indicated in the figure. Percentages of each live bacterial strain out of the original counts remaining at the end of the experiment for the individual serum dilutions are plotted **(E i, F i)**. Bactericidal activity was expressed as the serum dilutions at which 50% of the live bacterial loads are recovered after 3h of incubation **(E ii, F ii)**. C1, C2 are clinical isolates; bars represent the mean percent of growth reduction ± SEM of quadruplicate samples. The color scheme used are the same as above.

TABLE 1 Color scheme for different experimental groups.

Immunogen (no infection)	Color code
Vehicle (PBS)	**Black**
OSP	**Grey**
rT2544	**Yellow**
OSP-rT2544	**Orange**
Immunogen (with infection)	**Color code**
Vehicle (PBS)	**Black**
OSP	**Grey**
rT2544	**Yellow**
OSP-rT2544 (infection with reference strains)	**Orange**
OSP-rT2544 (infection with C1)	**Blue**
OSP-rT2544 (infection with C2)	**Green**
OSP-rT2544 (infection with C3)	**Sky**

showed similar anti-rT2544 IgG responses at both the above time points, following vaccination with rT2544 and OSP-rT2544 (Figure 5B). In contrast, anti-OSP IgG titer remained significantly elevated 110 days after immunization with OSP-rT2544 only, while it touched the baseline for the mice that received unconjugated OSP, suggesting that rT2544 acted as a vaccine adjuvant to OSP (Figure 5C). Anti-rT2544 IgG was comprised of IgG1 and IgG2a isotypes, indicating the induction of both Th1 and Th2 type responses; however, IgG1 was the predominant isotype (Figure 5D). To determine the functional activities of the immune sera, bactericidal assay was performed by incubating *S.* Typhi and *S.* Paratyphi A with heat-inactivated, serially-diluted sera collected from the immunized mice, supplemented with guinea pig complement. Both OSP-rT2544 and rT2544 immune sera from BALB/c mice reduced the growth of *S.* Typhi and *S.* Paratyphi A by 50% at dilutions between 1:1600 and 1:3200 and 1:6400 and 1:12800, respectively after 3h of incubation, while unconjugated OSP immune sera displayed no growth inhibition (Figures 5E, F; Supplementary Table 7). Similar growth inhibition of *S.* Typhi and *S.* Paratyphi A was obtained for OSP-rT2544 anti-sera collected from C57BL/6 mice as well (Supplementary Figure 4).

Protective humoral immune response against *S.* Typhimurium by OSP-rT2544 immunization

Given the persistently elevated, serum anti-OSP IgG titer in BALB/c mice after immunization with OSP-rT2544, we sought to investigate antisera-mediated protection against *S.* Typhimurium in similarly-immunized C57BL/6 mice by measuring antibody endpoint titers as well as SBA titers (Figure 6A; Supplementary Table 5). Like the BALB/c mice, anti-OSP IgG titer was significantly higher in OSP-rT2544 antisera than OSP antisera at day 38 of immunization and remained elevated at day 110, while OSP antisera reached the baseline (Figure 6B). This corroborated with correspondingly higher SBA titer of OSP-rT2544 antisera (1:6400 versus 1:200) against *S.* Typhimurium (Figure 6E; Supplementary Table 7). Similar titer values were found for OSP-rT2544 antisera from BALB/c mice to induce 50% growth reduction of *S.* Typhimurium (Supplementary Figure 4). As expected, there was no difference in the magnitudes of serum anti-rT2544 antibodies between the animals vaccinated with OSP-rT2544 conjugate and unconjugated rT2544 (Figure 6C). Markedly raised titers of OSP-specific serum IgG1 and IgG2a antibodies were observed in C57BL/6 mice immunized with OSP-rT2544, as compared with the OSP immunized mice, indicating induction of both Th1 and Th2 type responses, albeit to a significantly higher level for the later as observed for anti-rT2544 IgG isotype (Figure 6D). Together the above results suggested the potential for significant protection against both typhoidal and non-typhoidal Salmonellae by OSP-rT2544 antisera.

OSP-rT2544 provides cross-protection against *S.* Enteritidis

To evaluate cross-protection against *S.* Enteritidis after immunization with OSP-rT2544 candidate vaccine, reactivity of the antisera with OSPs extracted from different *S.* Enteritidis strains was studied by measuring the titers of anti-OSP antibodies. The results showed significant cross-reactivity of OSP-rT2544 antisera with the OSPs of several clinical *S.* Enteritidis strains (Figure 7A). To investigate cross-protection of the antisera against *S.* Enteritidis, SBA titers were estimated as described above. The results showed 50% growth inhibition of *S.* Enteritidis by OSP-rT2544 antisera dilution of 1:800 to 1:1600 versus 1:200 dilution of OSP antisera (Figure 7B; Supplementary Table 7). Similar result was observed for the 50% growth reduction of *S.* Enteritidis when OSP-rT2544 antisera from BALB/c mice was used to perform serum bactericidal assay (Supplementary Figure 4). This result suggested broad range of protection against NTS strains after vaccination with OSP-rT2544 antigen.

OSP-rT2544 candidate vaccine generates functional sIgA response, a hallmark of mucosal immunity

To study the mucosal immune response after OSP-rT2544 immunization, anti-OSP and anti-rT2544 sIgA antibodies were measured in the intestinal washes and fecal samples of the immunized mice and the titers were compared with the serum

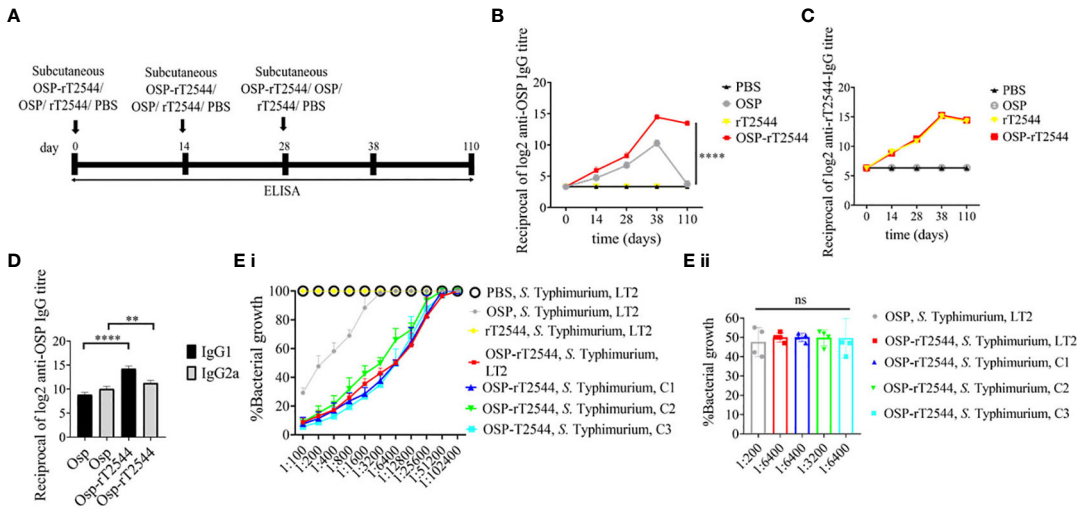

FIGURE 6
OSP-rT2544 immunization generates protective antibodies against *S.* Typhimurium. **(A)** Scheme of subcutaneous immunization of C57BL/6 mice and tissue sample collection. The scheme is similar to that described for BALB/c mice under Figure 5. **(B, C)** Time kinetics of antigen-specific total IgG in the mouse serum as measured by ELISA. Data presented and statistical significance calculated as under Figure 5. **(D)** OSP-specific serum IgG isotypes measured by ELISA at day 38. Data represent mean ± SEM values from different mice samples (n=5). Statistical analysis was performed using two-tailed Student's *t*-test (**P < 0.01; ****P < 0.0001). **(E)** Serum bactericidal assay. SBA was performed with *S.* Typhimurium, LT2 strain or the clinical isolates, as indicated in the figure, using serial dilutions of heat-inactivated antisera and guinea pig complement as described under Figure 5. Bactericidal activity was expressed as above. C1, C2 and C3 are clinical isolates and bars represent the mean percent of growth reduction ± SEM of quadruplicate samples. The color scheme used are the same as above.

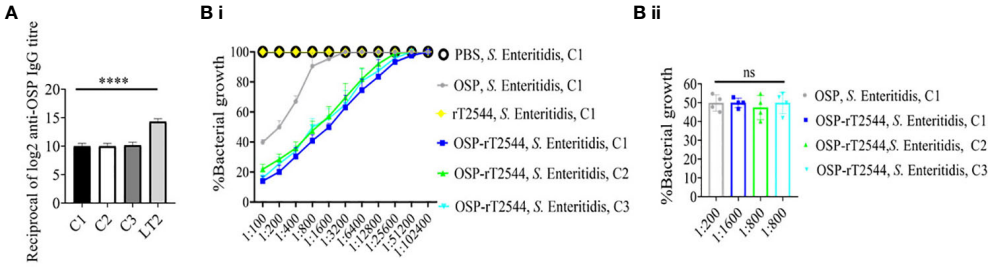

FIGURE 7
OSP-rT2544 immunization generates cross-protective antibodies against *S.* Enteritidis. **(A)** OSP was isolated from *S.* Typhimurium (LT2) and different *S.* Enteritidis (clinical isolates, C1-C3) strains and coated on the microtiter plate. Cross-reactive antibody titer was measured in OSP-rT2544 sera (38d) by ELISA. *S.* Typhimurium (LT2) OSP was used as a positive control. Data represent mean ± SEM values from different mice samples (n=6). Statistical analysis was performed using two-tailed Student's *t*-test (****P< 0.0001). **(B)** Serum bactericidal assay. Serial dilutions of heat-inactivated antisera, collected from differentially immunized mice at 38 d of immunization were mixed with 25% guinea pig complement and incubated with the *S.* Enteritidis or clinical isolates as indicated in the figure **(B i)** Bactericidal activity was expressed as the serum dilution at which 50% growth inhibition of the bacteria was noted at T_{180} (3h incubation) compared with T_0. Specific serum dilutions showing 50% growth reduction with individual immunogens are indicated in the figure **(B ii)**. C1, C2 and C3 are clinical isolates and bars represent the mean percent of growth reduction ± SEM of quadruplicate samples. Color scheme used is same as above.

IgA titers (Figure 8A). Anti-OSP IgA titer was increased four times in the mice immunized with the conjugate OSP-rT2544 compared with the unconjugated OSP (Figure 8B). On the other hand, anti-rT2544 IgA titers were comparable for the conjugated and unconjugated vaccine recipients (Figure 8C). To study the functionality of intestinal secretory antibodies, inhibition of bacterial motility in soft agar motility assay by intestinal lavage from the immunized mice was performed. Motility was determined by measuring the diameter of the bacterial zones after 10 hours of incubation at 37°C (Figures 8D–G; Supplementary Figure 5). Motility inhibition of *S.* Typhi and *S.* Paratyphi A was comparable for OSP-rT2544 and rT2544 immunization. In contrast, intestinal lavage from the mice immunized with OSP-rT2544 inhibited the motility of *S.* Typhimurium significantly more (~2.5 times) than similar samples collected from OSP-immunized mice. Similar difference was observed between the two immunization groups for soft agar motility of *S.* Enteritidis (33-36% vs 15.4% inhibition). Together these results suggested that OSP-rT2544 induced functional sIgA response in the intestine against both typhoidal and non-typhoidal *Salmonella* strains.

OSP-rT2544 induces both Th1 and Th2 serum cytokine response

Salmonella clearance requires a Th1 response, whereas Th2 cells support the generation of sIgA and serum antibodies. To determine the serum cytokine response, sera were collected from the OSP-rT2544 immunized C57BL/6 mice on day 38 and cytokine

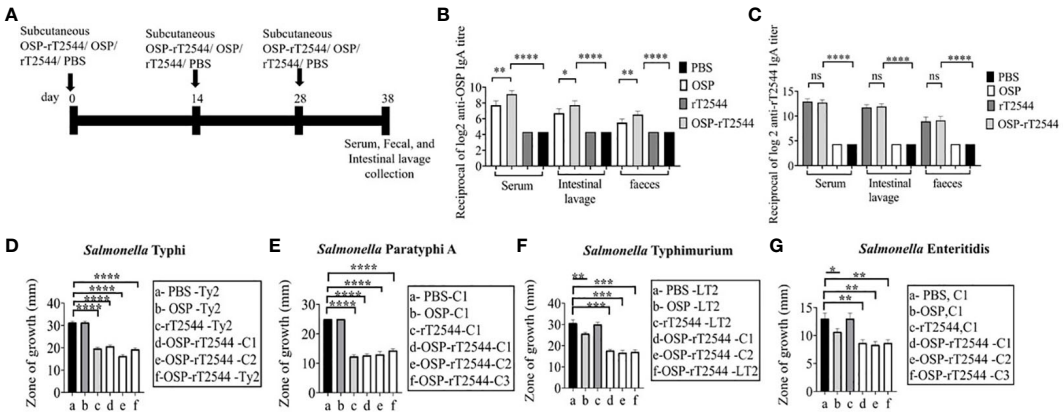

FIGURE 8
Induction of protective mucosal antibodies by OSP-rT2544 immunization. **(A)** Schedule of subcutaneous immunization of C57BL/6 mice at days 0, 14, and 28 with vehicle (PBS), conjugate (OSP-rT2544) (8μg of OSP in conjugate), or unconjugated vaccines (OSP (8 μg), rT2544 (24 μg)). Mice were sacrificed on day 38 and samples were collected. **(B, C)** ELISA showing OSP- and rT2544-specific serum IgA and intestinal sIgA titers in the groups of mice (n=5/group) after immunization with different antigens. Data represent mean ± SEM values from different mice samples (n=5). Statistical analysis was performed using two-tailed Student's *t*-test (**P < 0.01; ***P < 0.001; ****P < 0.0001). **(D–G)** Soft agar motility assay. Bacteria were spotted at the center of the soft agar (LB medium with 0.4% Bacto agar) containing intestinal wash (5%) from the immunized mice collected on day 38. Bacterial migration from the inoculation point to the periphery of the plate was measured after 10h incubation at 37°C. Experiments were repeated three times and mean (± SEM) of the values from all three experiments were plotted. Statistical analysis was performed using two-tailed Student's *t*-test (*p<0.05; **P < 0.01; ***P < 0.001; ****P < 0.0001). Color scheme used is same as above.

concentrations were measured by ELISA. We found significantly elevated, circulating pro-inflammatory/Th1 (IFNγ, TNF-α) and anti-inflammatory/Th2 (IL-4, IL-10, IL-6) cytokines in OSP-rT2544-immunized mice as opposed to only modest elevation in the comparator immunized groups (Figure 9). This result suggested that OSP-rT2544 immunization induces both Th1 and Th2 cytokine response in serum with the latter being predominant.

Immunization with OSP-rT2544 generates protective memory response

To study antigen-specific memory T cells, bone marrow derived dendritic cells (BMDCs) were isolated from the naïve C57BL/6 mice and pulsed *in vitro* with OSP or OSP-rT2544 antigen for 24h. Antigen-pulsed BMDCs were then co-cultured with the experimental mice splenocytes containing $CD4^+$ T cells. IFNγ release in the co-culture supernatants was estimated to be >10 folds higher for the splenocytes from OSP-rT2544 immunized mice compared with the animals that received OSP alone or left unimmunized (13.5 pg/ml), suggesting significant augmentation of T cell memory response by rT2544 when conjugated to OSP (Figure 10A). To determine memory T cell subsets, co-cultured $CD4^+$ T cells, as mentioned above were analyzed by flow cytometry after staining for the surface expression of 'Cluster of differentiation' (CD) markers ($CD4^+CD62L^{low}CD44^{hi}$). Cell subset analysis showed that augmented memory response was largely contributed by the effector memory T cells ($CD62L^{low}CD44^{high}$) (Figure 10B). Further, to analyze memory B cell response, a booster dose was administered to the immunized mice on day 110 of the first immunization and anti-OSP and anti-rT2544 serum antibodies were measured ten days later. A significantly higher secondary antibody response (day 120) compared with the primary response (day 38) was observed (four times for anti-OSP, and eight times for anti-rT2544 antibodies) (Figures 10C, D), suggesting differentiation of memory B cells into plasma cells, producing IgG at the latter time point. Given that the avidity of antibodies for the secondary response is higher than the primary response, anti-rT2544 and anti-OSP IgG immune complexes collected at days 38 and 120 were washed (3 times) with PBS-T, containing 6M urea before the addition of HRP-conjugated secondary antibodies. The avidity index was calculated by multiplying the ratio of the absorbances of the wells that were washed with and without 6M urea-containing buffer by 100. The result showed significantly high avidity indices (60-62%) of the secondary antibodies after booster immunization compared with the primary immunization (18-22%), suggesting a strong memory B cell response (Figures 10E, F). To corroborate functional activities of the higher avidity antibodies, we performed serum bactericidal assay (SBA) with these antibodies and different *Salmonella* strains (Supplementary Table 6). The results showed 50% growth inhibition at dilutions of secondary OSP-rT2544 antisera compared with the dilutions of the primary antisera as follows, 1:3200 vs. 1:1600 for *S.* Typhi Ty2, 1:25600 vs. 1:12800 for *S.* Paratyphi A, 1:12800 vs. 1:6400 for *S.* Typhimurium LT2, 1:3200 vs. 1:1600 for *S.* Enteritidis. The result suggested that inhibition dilution of the secondary OSP-rT2544 antisera was significantly higher than inhibition accompanied by antisera collected on day 38 (Figure 10G; Supplementary Table 8). These results suggested that immunization with OSP-rT2544 might elicit potent, long-lived protective immunity against *Salmonella* infection.

Discussion

We report here development of a glycoconjugate containing O-specific polysaccharide (OSP) from *S.* Typhimurium and an outer membrane protein (T2544) of *S.* Typhi/*S.* Paratyphi that displayed strong potential as a candidate multivalent vaccine against typhoidal and non-typhoidal *Salmonella* serovars in mouse infection models. Subcutaneous immunization of mice with OSP-rT2544 induced rapid seroconversion with high titers of protective antibodies in the serum and intestinal secretions, in addition to memory B and T cell response, conferring high protection of vaccinated animals against *Salmonella* infection.

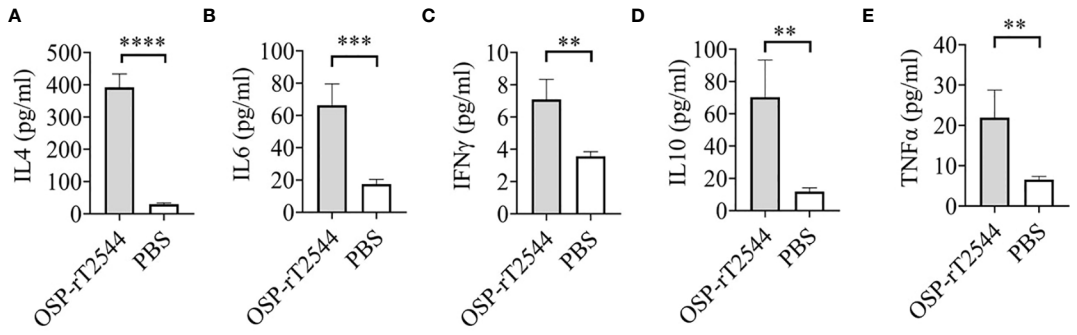

FIGURE 9
OSP-rT2544 induces both Th1 and Th2 serum cytokine response. **(A–E)** C57BL/6 mice were subcutaneously immunized with OSP-rT2544 (8μg of OSP in conjugate) or PBS (vehicle) on days 0, 14, and 28. Ten days after the last immunization (day 38), sera were collected from the immunized mice and cytokine levels in the serum were measured by ELISA. Briefly, Precoated ninety-six well plates were incubated with serum samples along with biotin-conjugate for 2h at room temperature. After three subsequent washes, plates were further incubated for one hour at room temperature with streptavidin-HRP. Following the addition of the TMB substrate, color development was evaluated using spectrophotometry at 450 nm. Statistical analysis was performed using two-tailed Student's *t*-test (**P < 0.01; ***P < 0.001; ****P < 0.0001).

Previous studies reported serotype independent protection against NTS (non-typhoidal *salmonella*) by S. Typhimurium type 3 secretion system tip and translocator proteins and their chimera. However, protection conferred was modest at best (13) as opposed to up to 80% protective efficacy for OSP-T2544. Bacterial surface polysaccharides are attractive candidates for vaccine development and presently constitute many commercially available vaccines. While polysaccharides, being T-independent antigens are poorly immunogenic by themselves and fail to induce immunological memory, they have been efficiently conjugated with carrier proteins to augment immunogenicity (44). Synthesis of glycoconjugate vaccines with a covalent bond between the saccharide and the carrier protein molecules and using different conjugation chemistries were described previously (45–48). The approaches taken fall into two main categories, namely the 'random linkage' along the polysaccharide (PS) chain and 'selective attachment' at the PS terminus. High molecular weight (MW), cross-linked, and generally undefined heterogeneous structures are produced by random chemistry, whereas selective chemistry generates better-defined structures while avoiding chemical alteration of the saccharide chain (45, 49–51). Immunogenicity of glycoconjugate vaccines is significantly influenced by the conjugation chemistry. Studies with OSP from different *Salmonella* strains coupled to multiple carrier proteins, using different chemical methods and diverse linkers suggested that important antigenic epitopes may be sterically protected by the bulky protein when polysaccharides are directly connected to the carrier protein (52). Instead, when a linker joins the polysaccharide to a carrier protein, steric shielding may be reduced and the polysaccharide externally presented to the immune cells, increasing the number of antigenic epitopes that are available to activate antigen-presenting cells (52). In this study, we developed the OSP-rT2544 conjugate using random linkage method where hydroxyl groups along the saccharide were randomly activated by CnBr (cyanogen bromide) chemistry (53–56). Cyanylation is a time-tested method and a simple and quick workflow for sugar-protein conjugation, as described previously for OSP-TT (31), Hib-protein conjugate (56), V. cholerae O:1 serotype Inaba (57), V. cholerae O:1 serotype Ogawa (58), and *Francisella tularensis* (59). Following cyanylation reaction, cyanate esters are formed that further interact with the hydroxyl groups to create cyclic imidocarbonates that can effectively couple to the carboxyl groups

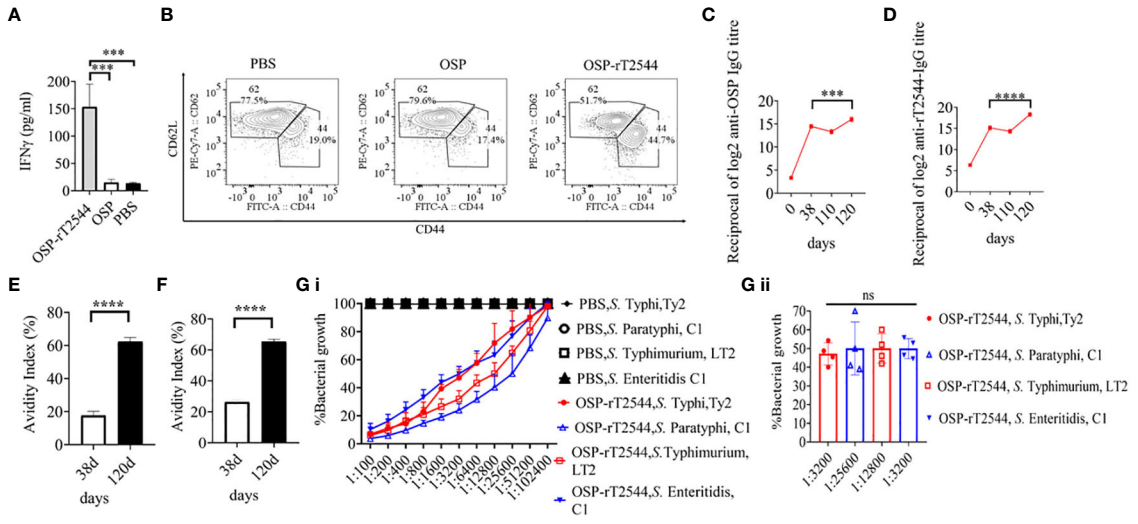

FIGURE 10
Induction of protective memory response. **(A)** C57BL/6 mice were subcutaneously immunized as described above with the antigens indicated in the Figure 6. Antigen-primed memory CD4+ T cells were isolated from the splenocytes of the mice 120 days of the start of the immunization. To evaluate the memory T cells response, cells were converted to effector T cells by presenting the respective antigens to them in association with MHC Class II. To this end, bone marrow derived dendritic cells (BMDCs), isolated from the naïve C57BL/6 mice were pulsed with OSP or OSP-rT2544 for 24h, followed by co-culturing of the cells with the memory T cells. Memory response was analyzed by the quantification of IFNγ released in the co-culture supernatants using ELISA. Statistical analysis was performed using two-tailed Student's *t*-test (***P < 0.001; ****P < 0.0001). Data represents mean (± SEM) of four independent experiments. **(B)** $CD4^+$ T cells, co-cultured with antigen-pulsed BMDCs for 24h, as mentioned under 'Figure 10 A', were analyzed by flow cytometry after staining for the surface expression of 'Cluster of differentiation' (CD) markers for T-effector memory cell determination ($CD4^+CD62L^{low}$ $CD44^{hi}$). Representative images from one out of four experiments are shown. **(C, D)** C57BL/6 mice were subcutaneously immunized on days 0, 14, and 28 with OSP-rT2544 (8µg of OSP and 24 µg of rT2544 in conjugate) and a booster was given with the same antigen on day 110 **(C)** OSP and **(D)** rT2544-specific serum IgG titers were measured by ELISA at the indicated time points. Data represent mean ± SEM values from different mice samples (n=6). Statistical analysis was performed using two-tailed Student's *t*-test (***P < 0.001; ****P < 0.0001). **(E, F)** Antibody avidity assay. Anti-rT2544 **(E)** and anti-OSP **(F)** avidity index were determined in the OSP-rT2544 serum (diluted 1:100 in PBS-T), collected at the indicated time points after washing the immune complex with 6M urea buffer by ELISA. The avidity index was calculated by multiplying the ratio of the absorbances of the wells that were washed with and without urea-containing buffer by 100. Data represent mean ± SEM values from different mice samples (n=3). Statistical analysis was performed using two-tailed Student's *t*-test (****P < 0.0001). **(G)** Serum bactericidal assay. Serial dilutions of heat-inactivated antisera, collected from differentially immunized mice at 120 d of immunization were mixed with 25% guinea pig complement and incubated with the *S.* Typhi, *S.* Paratyphi A, *S.* Typhimurium, LT2 and *S.* Enteritidis as indicated in the figure **(G i)** Bactericidal activity was expressed as the serum dilution at which 50% growth inhibition of the bacteria was noted at T_{180} (3h incubation) compared with T_0. Immunogens that have a 50% growth reduction at a specific serum dilution are indicated in the figure **(G ii)**. Bars represent the percent mean (± SEM) of growth reduction of quadruplicate samples. Color scheme used is same as above.

of the carrier proteins, following 1-ethyl-3-(3-dimethy laminopropyl) carbodiimide (EDC)-mediated condensation (60). For several other glycoconjugates, CDAP replaced CnBr to activate polysaccharides (31, 61). Primary mechanism of CDAP-mediated activation is the creation of isourea linkages between the cyanoesters on the activated carbohydrate and the lysine residues on the carrier protein (55, 58). However, one major drawback associated with CDAP chemistry is over-crosslinking, leading to reduced immunogenicity of the glycoconjugates due to gelling of the carbohydrates and peptides (52). In vaccine production, CnBr activation is commonly accompanied by the use of ADH linker. It was previously reported that conjugation chemistry using ADH linker is more reactive due to shorter reaction time and higher derivatization yield, as was found with the glycoconjugate vaccine for meningococcal serogroup X (62). Similar to OSP-TT (31), Vi-CRM197 (48) and Hib-protein (56) conjugates, we used ADH linker to create a covalent linkage between OSP and T2544 by carbodiimide chemistry.

Several factors, including the molecular weight (MW) of the conjugate and the molar ratio of the sugar and the carrier protein influence vaccine immunogenicity. In our study, very high molecular weight, crosslinked conjugate with partition coefficient (kd) of 0.02 was formed, as there are multiple activation points within OSP and multiple linkage points on the protein (T2544). It was previously reported that immunization with higher MW glycoconjugates results in greater anti-PS antibody response. Thus, larger and more cross-linked Vi-DT and GBS type III-TT conjugate vaccines induced higher anti-Vi and anti-saccharide IgG response, respectively (63, 64). The saccharide-to-protein ratio has a direct relationship with the immunogenicity of glycoconjugates; a larger ratio leads to improved cross-linking and activation of saccharide-specific B cells with increased polysaccharide loading.

For OSP-rT2544 conjugate containing ADH linker and generated by random activation, PS to protein molar ratio of 1.53 elicited significantly higher anti-OSP antibodies compared with OSP alone after three doses of mouse immunization. These features are in agreement with *Salmonella* Typhimurium OSP-TT conjugate with ADH linker and a saccharide to protein ratio of 0.6, produced by random activation. This conjugate was more immunogenic than the molecule generated by selective chemistry with the saccharide to protein ratio (w/w) of 0.1 (61). Further, using ADH linker rather than cystamine or SPDP increased the immunogenicity of *Salmonella* Typhi Vi conjugates, when it was coupled to recombinant Pseudomonas aeruginosa exotoxin A (rEPA) by random chemistry (65). Similar results were obtained with *S.* aureus type 8 capsular PS linked via random chemistry to rEPA or DT, where use of ADH linker yielded higher PS to protein ratio compared with cystamine or SPDP (66, 67). A study using deacylated lipopolysaccharides (LPS) from *Vibrio cholerae* O1 serotype Inaba and cholera toxin (CT) reported that random chemistry and ADH linker produced conjugates with LPS to CT ratio of 0.8 as opposed to 0.72 for single-point attachment using SPDP linker with the former being more immunogenic (68). However, *Salmonella* Enteritidis OSP directly conjugated to flagellin monomers, polymers, or CRM197 by random activation without linkers or with selective aminooxyoxime thioether chemistry using diaminooxy cysteamine and N-(γ-maleimidobutyloxy)- sulfosuccinimide ester linker induced similar IgG response and confers protection against bacterial challenge in mice (65, 69).

Carrier proteins used in the glycoconjugate preparations augment the immune response against the covalently attached polysaccharides, while the immune response specific to the protein largely remains unaltered. T2544 functions as an adjuvant to increase the serum anti-OSP antibody titer by 32 times after subcutaneous immunization of mice, keeping the levels of anti-T2544 antibodies unchanged (Figures 5B, C, 6B, C). Flagellin in a conjugate formulation with *Salmonella* Enteritidis OSP enhanced anti-OSP antibody titers by 10-fold in mice after 3 intramuscular immunization doses, while anti-flagellin antibody response against the conjugate was similar to that of unconjugated flagellin (69). Similar results were observed for *Salmonella* Typhimurium when OSP was conjugated to FliC or CRM197 by random chemistry (42, 70), although anti-CRM197 antibody titer was 100-fold elevated with the conjugate. Surprisingly, much higher anti-OSP antibody response was reported here when conjugation was performed using selective chemistry. This is contrary to most other studies that reported higher antibody response with glycoconjugates developed by random chemistry rather than selective conjugation (61, 65, 68). Intraperitoneal immunization with *S.* Typhimurium OSP-porin conjugate resulted in anti-OSP and anti-porin end-points titers of 1/600 and 1/8500, respectively after 3 doses (71). This contrasts with anti-OSP and anti-T2544 end-point titers of 1/25600 and 1/51200, respectively in our study.

Salmonella conjugate vaccines, including the licensed products and those at the advanced stage of clinical development are largely monovalent, specifically acting against single *Salmonella* serovar. A Vi-TT conjugate vaccine has been licensed for local distribution in India (4–6). For *S.* Typhimurium, 90-100% protection was conferred by OSP-FliC, OSP-CRM197 and OSP-porin conjugates (70, 71) against clinical and reference strains of *Salmonella*. In contrast, OSP-T2544 candidate vaccine conferred 75-80% of protection against *S.* Typhi, *S.* Paratyphi, and *S.* Typhimurium and 55-60% cross-protection against *S.* Enteritidis (Figure 4). While the cause of cross-reactivity to S. Enteritidis is still under investigation, antibodies against common O-Ag epitopes like O:1 and O:12 or the shared core region are most likely to account for (42).

OSP- and rT2544-specific serum antibodies were comprised of both IgG1 and IgG2a sub-classes (Figures 5D, 6D). Polysaccharide antigens have been found to induce IgG2 class switch in the absence of T cell engagement (72). In contrast, T cell-dependent (TD) protein antigens elicit antibodies of IgG1 subclass. Anti-polysaccharide antibodies shifted towards the IgG1 subclass in mice following conjugation to a carrier protein (73, 74). Similarly, OSP-rT2544 conjugate induced higher titers of anti-OSP IgG1 than IgG2a compared with unconjugated OSP (Figure 6D). This corroborates with the other published studies that reported

predominantly IgG1 antibodies specific to OSP in the conjugate immunized group (42, 75). The elevated IgG1 response in conjugate compared to the unconjugated form of saccharide supports the concept that two forms of the saccharide may activate different regulating mechanisms or select B cell clones with different isotype-specificity (30). We also found increased IL4 concentrations in the conjugate antisera (Figure 9) that was previously reported for other glycoconjugate vaccines (29). IL-4 plays an important role in humoral immunity by inducing differentiation of Th0 into Th2 cells and mediating IgG1 antibody release, which may activate the classical complement pathway and provide long-term protection.

We measured protective efficacy of vaccine antigen-specific antibodies by serum bactericidal assay (SBA) titer and soft agar motility inhibition assay using intestinal sIgA. SBA is accepted as an *in vitro* surrogate of vaccine immunogenicity. SBA measured functional *Salmonella*-specific antibodies capable of complement-mediated bacterial killing, resulting in 50% decrease in bacterial count. OSP-rT2544 antisera displayed SBA titer of 1:1600 against *S.* Typhi and *S.* Enteritidis, while similar titers for *S.* Paratyphi A and *S.* Typhimurium attained the values of 1:12800 and 1:6400, respectively (Figures 5E, F, 6E, 7B). Published studies reported comparatively lower values of serum bactericidal titers for OSP-TT (against *S.* Typhi) and OSP-CRM197 (against *S.* Typhimurium and *S.* Enteritidis) (42, 76). We found significant inhibition of bacterial motility in soft agar by intestinal secretory antibodies, but failed to find similar studies in the published literature with other glycoconjugate vaccines. However, 3-fold increased titers of sIgA were reported after immunization with OSP-CRM197 (42) as opposed to 2-fold increase after OSP-rT2544 in the present study (Figures 8D-G). This might correlate with decreased motility of *Salmonella*, pre-incubated with the intestinal wash from the vaccinated mice, as was previously reported for *S.* Typhi and *S.* Paratyphi A ghost cell-based bivalent vaccine candidate (77).

In some studies, functional assays with the conjugate sera was performed by passive transfer into mice. Passive protection conferred by OSP-TT antisera administered through intraperitoneal route suggested functional serum antibodies against *S.* Typhimurium (61), where passively transferred IgM (80-100%) was more protective than IgG (20-30%). However, passive administration of rabbit antisera against OSP-porin conjugate through intravenous route showed 100% protection of mice against intraperitoneal challenge with *S.* Typhimurium (71). In other studies, opsonophagocytosis was performed to determine the functionality of the conjugate antisera. For *S.* Enteritidis COPS-FliC conjugate, pre-incubation with antisera resulted in 5% increase of opsonophagocytosis compared with the vehicle immune sera (69). We, however, did not evaluate OSP-rT2544 antisera by passive immunization or opsonophagocytosis assay.

The ability to generate robust and enduring immune memory is the hallmark of a successful vaccine and critical for the intended public health impact. An antibody recall response was demonstrated with tetrasaccharide-CRM_{197} conjugate after a booster on day 260 when the primary antibody response was reduced by two-fold compared with the titers achieved after the third dose of immunization (day 36) (78). In contrast, following vaccination with OSP-rT2544, sustained OSP- and rT2544-specific primary antibody response was observed at day 110, which further increased after the administration of a booster dose with the production of higher avidity antibodies which is a marker for T-cell dependent affinity maturation. A separate study evaluated B cell memory response by ELISPOT assay after human volunteers received a conjugate vaccine containing *Vibrio Cholerae* O1 Inaba and tetanus toxoid and reported 3.5 OSP-specific and 5 carrier protein-specific IgG spots per 10^5 splenocytes at day 56 day (18).

To further corroborate the antibody recall response, we checked for $CD4^+$ effector memory cells producing IFN-γ in the OSP-rT2544 immunized mice. Generation of recombinant T2544-specific $CD4^+$ T cells was earlier reported earlier by our laboratory (30). Elevated levels of IFN-γ production was found following antigen restimulation of mouse splenocytes in the recipients of OSP-rT2544 (Figures 10A, B). However, similar studies were not reported earlier for glycoconjugate vaccines containing OSP.

Despite convincingly demonstrating activation of different arms of the immune system with protective serum and mucosal antibody response, conferring broad spectrum protection against typhoidal and non-typhoidal *Salmonella* serovars, this study has several limitations. We did not compare immunogenicity of candidate glycoconjugate vaccines, developed using different conjugation chemistries and having diverse linker molecules between OSP and T2544. Given that T2544 is an intrinsic *Salmonella* protein, head-to-head comparison with a different preparation, comprising of OSP linked to a non-*Salmonella* protein would provide further insights into the mechanisms underlying immune activation by glycoconjugate vaccines. Further elaboration of T cell response, including activation of different $CD4^+$ cell subsets (Th9, Th17, follicular helper T cell, resident memory and central memory T cells) as well as cytotoxic T cells (central and effector memory cell) would better characterize the immune response. Finally, studies elaborating the relative contributions of different compartments of the immune system (humoral, cellular and mucosal) would help to develop newer vaccines with improved efficacies.

Data availability statement

The original contributions presented in the study are included in the article/Supplementary Material. Further inquiries can be directed to the corresponding author.

Ethics statement

The animal study was approved by ICMR-National Institute of Cholera and Enteric Diseases. The study was conducted in accordance with the local legislation and institutional requirements.

Author contributions

RH: Conceptualization, Data curation, Formal analysis, Investigation, Methodology, Software, Visualization, Writing – original draft, Writing – review & editing. AD: Methodology,

Writing – review & editing. DG: Methodology, Writing – review & editing. SC: Methodology, Writing – review & editing. AP: Methodology, Writing – review & editing. GB: Methodology, Writing – review & editing. S-iM: Funding acquisition, Writing – review & editing. SD: Conceptualization, Data curation, Formal Analysis, Funding acquisition, Investigation, Methodology, Project administration, Resources, Software, Supervision, Validation, Visualization, Writing – original draft, Writing – review & editing.

Funding

The author(s) declare financial support was received for the research, authorship, and/or publication of this article. This work was supported by extramural grants from Indian Council of Medical Research, Government of India (58/17/2020/PHA/BMS) and the Japan Agency for Medical Research and Development (AMED; Grant No. JP23wm0125004).

Acknowledgments

RH acknowledges the University Grant Commission (UGC) (student ID-191620094970) to get the fellowship for this study. All other authors acknowledge Indian Council of Medical Research (ICMR), National Institute of Cholera and Enteric Diseases (NICED) and Japan Agency for Medical Research and Development (AMED; Grant No. JP23wm0125004).

Conflict of interest

Author GB was employed by company BD Biosciences.

The remaining authors declare that the research was conducted in the absence of any commercial or financial relationships that could be construed as a potential conflict of interest.

Publisher's note

Supplementary material

The Supplementary Material for this article can be found online at: https://www.frontiersin.org/articles/10.3389/fimmu.2023.1304170/full#supplementary-material

References

1. Deen J, von Seidlein L, Andersen F, Elle N, White NJ, Lubell Y. Community-acquired bacterial bloodstream infections in developing countries in south and southeast Asia: a systematic review. *Lancet Infect Dis* (2012) 12(6):480–7. doi: 10.1016/S1473-3099(12)70028-2

2. Marchello CS, Birkhold M, Crump JAVacc-iNTS consortium collaborators. Complications and mortality of non-typhoidal salmonella invasive disease: a global systematic review and meta-analysis. *Lancet Infect Dis* (2022) 22(5):692–705. doi: 10.1016/S1473-3099(21)00615-0

3. MacLennan CA, Stanaway J, Grow S, Vannice K, Steele AD. *Salmonella* combination vaccines: moving beyond typhoid. *Open Forum Infect Dis* (2023) 10 (Suppl 1):S58–66. doi: 10.1093/ofid/ofad041

4. Patel PD, Patel P, Liang Y, Meiring JE, Misiri T, Mwakiseghile F, et al. Safety and efficacy of a typhoid conjugate vaccine in Malawian children. *N Engl J Med* (2021) 385 (12):1104–15. doi: 10.1056/NEJMoa2035916

5. Qadri F, Khanam F, Liu X, Theiss-Nyland K, Biswas PK, Bhuiyan AI, et al. Protection by vaccination of children against typhoid fever with a Vi-tetanus toxoid conjugate vaccine in urban Bangladesh: a cluster-randomised trial. *Lancet* (2021) 398 (10301):675–84. doi: 10.1016/S0140-6736(21)01124-7

6. Shakya M, Voysey M, Theiss-Nyland K, Colin-Jones R, Pant D, Adhikari A, et al. Efficacy of typhoid conjugate vaccine in Nepal: final results of a phase 3, randomised, controlled trial. *Lancet Glob Health* (2021) 9(11):e1561–8. doi: 10.1016/S2214-109X(21)00346-6

7. Black RE, Levine MM, Ferreccio C, Clements ML, Lanata C, Rooney J, et al. Efficacy of one or two doses of Ty21a Salmonella typhi vaccine in enteric-coated capsules in a controlled field trial. *Chilean Typhoid Commit Vaccine* (1990) 8(1):81–4. doi: 10.1016/0264-410x(90)90183-m

8. MacLennan CA, Martin LB, Micoli F. Vaccines against invasive Salmonella disease: current status and future directions. *Hum Vaccin Immunother* (2014) 10 (6):1478–93. doi: 10.4161/hv.29054

9. Kumar VS, Gautam V, Balakrishna K, Kumar S. Overexpression, purification, and immunogenicity of recombinant porin proteins of Salmonella enterica serovar Typhi (S. Typhi). *J Microbiol Biotechnol* (2009) 19(9):1034–40. doi: 10.4014/jmb.0812.675

10. Rolli J, Rosenblatt-Velin N, Li J, Loukili N, Levrand S, Pacher P, et al. Bacterial flagellin triggers cardiac innate immune responses and acute contractile dysfunction. *PloS One* (2010) 5(9):e12687. doi: 10.1371/journal.pone.0012687

11. Xiao Y, Liu F, Yang J, Zhong M, Zhang E, Li Y, et al. Over-activation of TLR5 signaling by high-dose flagellin induces liver injury in mice. *Cell Mol Immunol* (2015) 12(6):729–42. doi: 10.1038/cmi.2014.110

12. Rolli J, Loukili N, Levrand S, Rosenblatt-Velin N, Rignault-Clerc S, Waeber B, et al. Bacterial flagellin elicits widespread innate immune defense mechanisms, apoptotic signaling, and a sepsis-like systemic inflammatory response in mice. *Crit Care* (2010) 14(4):R160. doi: 10.1186/cc9235

13. Martinez-Becerra FJ, Kumar P, Vishwakarma V, Kim JH, Arizmendi O, Middaugh CR, et al. Characterization and Protective Efficacy of Type III Secretion Proteins as a Broadly Protective Subunit Vaccine against Salmonella enterica Serotypes. *Infect Immun* (2018) 86(3):e00473–17. doi: 10.1128/IAI.00473-17

14. Lee SJ, Benoun J, Sheridan BS, Fogassy Z, Pham O, Pham QM, et al. Dual immunization with sseB/flagellin provides enhanced protection against salmonella infection mediated by circulating memory cells. *J Immunol* (2017) 199(4):1353–61. doi: 10.4049/jimmunol.1601357

15. Jneid B, Rouaix A, Féraudet-Tarisse C, Simon S. SipD and IpaD induce a cross-protection against Shigella and Salmonella infections. *PloS Negl Trop Dis* (2020) 14(5): e0008326. doi: 10.1371/journal.pntd.0008326

16. Phalipon A, Tanguy M, Grandjean C, Guerreiro C, Bélot F, Cohen D, et al. A synthetic carbohydrate-protein conjugate vaccine candidate against Shigella flexneri 2a infection. *J Immunol* (2009) 182(4):2241–7. doi: 10.4049/jimmunol.0803141

17. Desalegn G, Kapoor N, Pill-Pepe L, Bautista L, Yin L, Ndungo E, et al. A novel shigella O-polysaccharide-ipaB conjugate vaccine elicits robust antibody responses and confers protection against multiple shigella serotypes. *mSphere* (2023) 8(3):e0001923. doi: 10.1128/msphere.00019-23

18. Sayeed MA, Bufano MK, Xu P, Eckhoff G, Charles RC, Alam MM, et al. A Cholera Conjugate Vaccine Containing O-specific Polysaccharide (OSP) of V. cholerae O1 Inaba and Recombinant Fragment of Tetanus Toxin Heavy Chain (OSP:rTTHc)

Induces Serum, Memory and Lamina Proprial Responses against OSP and Is Protective in Mice. *PloS Negl Trop Dis* (2015) 9(7):e0003881. doi: 10.1371/journal.pntd.0003881

19. Trebicka E, Jacob S, Pirzai W, Hurley BP, Cherayil BJ. Role of antilipopolysaccharide antibodies in serum bactericidal activity against Salmonella enterica serovar Typhimurium in healthy adults and children in the United States. *Clin Vaccine Immunol* (2013) 20(10):1491–8. doi: 10.1128/CVI.00289-13

20. Goh YS, Clare S, Micoli F, Saul A, Mastroeni P, MacLennan CA. Monoclonal antibodies of a diverse isotype induced by an O-antigen glycoconjugate vaccine mediate *in vitro* and *in vivo* killing of African invasive nontyphoidal salmonella. *Infect Immun* (2015) 83(9):3722–31. doi: 10.1128/IAI.00547-15

21. Simon R, Levine MM. Glycoconjugate vaccine strategies for protection against invasive Salmonella infections. *Hum Vaccin Immunother* (2012) 8(4):494–8. doi: 10.4161/hv.19158

22. Micoli F, Ravenscroft N, Cescutti P, Stefanetti G, Londero S, Rondini S, et al. Structural analysis of O-polysaccharide chains extracted from different Salmonella Typhimurium strains. *Carbohydr Res* (2014) 385:1–8. doi: 10.1016/j.carres.2013.12.003

23. Ravenscroft N, Cescutti P, Gavini M, Stefanetti G, MacLennan CA, Martin LB, et al. Structural analysis of the O-acetylated O-polysaccharide isolated from Salmonella Paratyphi A and used for vaccine preparation. *Carbohydr Res* (2015) 404:108–16. doi: 10.1016/j.carres.2014.12.002

24. World Health Organization. *Antigenic formulae of the Salmonella serovars* (2007). Available at: https://www.pasteur.fr/sites/default/files/veng_0.pdf (Accessed 6 November 2022).

25. Perera SR, Sokaribo AS, White AP. Polysaccharide vaccines: A perspective on non-typhoidal. *Salmonella* (2021) 25:691–714. doi: 10.3390/polysaccharides2030042

26. Borrow R, Dagan R, Zepp F, Hallander H, Poolman J. Glycoconjugate vaccines and immune interactions, and implications for vaccination schedules. *Expert Rev Vaccines* (2011) 10(11):1621–31. doi: 10.1586/erv.11.142

27. Findlow H, Borrow R. Interactions of conjugate vaccines and co-administered vaccines. *Hum Vaccin Immunother* (2016) 12(1):226–30. doi: 10.1080/21645515.2015.1091908

28. Dagan R, Poolman J, Siegrist CA. Glycoconjugate vaccines and immune interference: a review. *Vaccine* (2010) 28:5513–23. doi: 10.1016/j.vaccine.2010.06.026

29. Konadu EY, Lin FY, Hó VA, Thuy NT, Van Bay P, Thanh TC, et al. Phase 1 and phase 2 studies of Salmonella enterica serovar Paratyphi A O-specific polysaccharide-tetanus toxoid conjugates in adults, teenagers, and 2- to 4-year-old children in Vietnam. *Infect Immun* (2000) 68(3):1529–34. doi: 10.1128/IAI.68.3.1529-1534.2000

30. Das S, Chowdhury R, Ghosh S, Das S. A recombinant protein of Salmonella Typhi induces humoral and cell-mediated immune responses including memory responses. *Vaccine* (2017) 35(35 Pt B):4523–31. doi: 10.1016/j.vaccine.2017.07.035

31. Konadu E, Shiloach J, Bryla DA, Robbins JB, Szu SC. Synthesis, characterization, and immunological properties in mice of conjugates composed of detoxified lipopolysaccharide of Salmonella Paratyphi A bound to tetanus toxoid with emphasis on the role of O acetyls. *Infect Immun* (1996) 64(7):2709–15. doi: 10.1128/iai.64.7.2709-2715.1996

32. Bastos RC, Corrêa MB, de Souza IM, da Silva MN, da Silva Gomes Pereira D, Martins FO, et al. Brazilian meningococcal C conjugate vaccine: physicochemical, immunological, and thermal stability characteristics. *Glycoconj J* (2018) 35(1):3–13. doi: 10.1007/s10719-017-9787-2

33. Micoli F, Rondini S, Gavini M, Lanzilao L, Medaglini D, Saul A, et al. O:2-CRM (197) conjugates against Salmonella Paratyphi A. *PloS One* (2012) 7(11):e47039. doi: 10.1371/journal.pone.0047039

34. He W, Mazzuca P, Yuan W, Varney K, Bugatti A, Cagnotto A, et al. Identification of amino acid residues critical for the B cell growth-promoting activity of HIV-1 matrix protein p17 variants. *Biochim Biophys Acta Gen Subj.* (2019) 1863 (1):13–24. doi: 10.1016/j.bbagen.2018.09.016

35. Nguyen TK, Selvanayagam R, Ho KKK, Chen R, Kutty SK, Rice SA, et al. Co-delivery of nitric oxide and antibiotic using polymeric nanoparticles. *Chem Sci* (2016) 7 (2):1016–27. doi: 10.1039/c5sc02769a

36. Satpute SK, Banpurkar AG, Dhakephalkar PK, Banat IM, Chopade BA. Methods for investigating biosurfactants and bioemulsifiers: a review. *Crit Rev Biotechnol* (2010) 30(2):127–44. doi: 10.3109/07388550903427280

37. Das S, Chowdhury R, Pal A, Okamoto K, Das S. Salmonella Typhi outer membrane protein STIV is a potential candidate for vaccine development against typhoid and paratyphoid fever. *Immunobiology* (2019) 224(3):371–82. doi: 10.1016/j.imbio.2019.02.011

38. Ghosh S, Chakraborty K, Nagaraja T, Basak S, Koley H, Dutta S, et al. An adhesion protein of Salmonella enterica serovar Typhi is required for pathogenesis and potential target for vaccine development. *Proc Natl Acad Sci U S A.* (2011) 108(8):3348–53. doi: 10.1073/pnas.1016180108

39. Barthel M, Hapfelmeier S, Quintanilla-Martínez L, Kremer M, Rohde M, Hogardt M, et al. Pretreatment of mice with streptomycin provides a Salmonella enterica serovar Typhimurium colitis model that allows analysis of both pathogen and host. *Infect Immun* (2003) 71(5):2839–58. doi: 10.1128/IAI.71.5.2839-2858.2003

40. Rondini S, Micoli F, Lanzilao L, Gavini M, Alfini R, Brandt C, et al. Design of glycoconjugate vaccines against invasive African Salmonella enterica serovar Typhimurium. *Infect Immun* (2015) 83(3):996–1007. doi: 10.1128/IAI.03079-14

41. Hedman K, Rousseau SA. Measurement of avidity of specific IgG for verification of recent primary rubella. *J Med Virol* (1989) 27:288–92. doi: 10.1002/jmv.1890270406

42. Fiorino F, Rondini S, Micoli F, Lanzilao L, Alfini R, Mancini F, et al. Immunogenicity of a bivalent adjuvanted glycoconjugate vaccine against salmonella typhimurium and salmonella enteritidis. *Front Immunol* (2017) 8:168. doi: 10.3389/fimmu.2017.00168

43. Shippy DC, Eakley NM, Mikheil DM, Fadl AA. Role of StdA in adhesion of Salmonella enterica serovar Enteritidis phage type 8 to host intestinal epithelial cells. *Gut Pathog* (2013) 5(1):43. doi: 10.1186/1757-4749-5-43

44. MacLennan CA, Martin LB, Micoli F. Vaccines against invasive Salmonella disease. *Human Vaccines & Immunotherapeutics*. (2014) 10(6):1478–93. doi: 10.4161/hv.29054

45. Pozsgay V. Oligosaccharide-protein conjugates as vaccine candidates against bacteria. *Adv Carbohydr Chem Biochem* (2000) 56:153–99. doi: 10.1016/s0065-2318(01)56004-7

46. Frasch CE. Preparation of bacterial polysaccharide-protein conjugates: analytical and manufacturing challenges. *Vaccine* (2009) 27(46):6468–70. doi: 10.1016/j.vaccine.2009.06.013

47. Costantino P, Rappuoli R, Berti F. The design of semi-synthetic and synthetic glycoconjugate vaccines. *Expert Opin Drug Discovery* (2011) 6(10):1045–66. doi: 10.1517/17460441.2011.609554

48. Micoli F, Rondini S, Pisoni I, Proietti D, Berti F, Costantino P, et al. Vi-CRM 197 as a new conjugate vaccine against Salmonella Typhi. *Vaccine* (2011) 29:712–20. doi: 10.1016/j.vaccine.2010.11.022

49. Wang JY, Chang AH, Guttormsen HK, Rosas AL, Kasper DL. Construction of designer glycoconjugate vaccines with size-specific oligosaccharide antigens and site-controlled coupling. *Vaccine* (2003) 21(11-12):1112–7. doi: 10.1016/s0264-410x(02)00625-4

50. Jones C. Vaccines based on the cell surface carbohydrates of pathogenic bacteria. *Acad Bras Cienc* (2005) 77:293–324. doi: 10.1590/s0001-37652005000200009

51. Lucas AH, Apicella MA, Taylor CE. Carbohydrate moieties as vaccine candidates. *Clin Infect Dis* (2005) 41(5):705–12. doi: 10.1086/432582

52. Bröker M, Berti F, Costantino P. Factors contributing to the immunogenicity of meningococcal conjugate vaccines. *Hum Vaccin Immunother* (2016) 12(7):1808–24. doi: 10.1080/21645515.2016.1153206

53. Chu C, Schneerson R, Robbins JB, Rastogi SC. Further studies on the immunogenicity of Haemophilus influenzae type b and pneumococcal type 6A polysaccharide-protein conjugates. *Infect Immun* (1983) 40(1):245–56. doi: 10.1128/iai.40.1.245-256.1983

54. Lees A, Nelson BL, Mond JJ. Activation of soluble polysaccharides with 1 cyano-4-dimethylaminopyridinium tetrafluoroborate for use in proteinpolysaccharide conjugate vaccines and immunological reagents. *Vaccine* (1996) 14:190–8. doi: 10.1016/0264-410x(95)00195-7

55. Shafer DE, Toll B, Schuman RF, Nelson BL, Mond JJ, Lees A. Activation of soluble polysaccharides with 1-cyano-4-dimethylaminopyridinium tetrafluoroborate (CDAP) for use in protein-polysaccharide conjugate vaccines and immunological reagents. II. Selective crosslinking of proteins to CDAP-activated polysaccharides. *Vaccine* (2000) 18(13):1273–81. doi: 10.1016/s0264-410x(99)00370-9

56. Schneerson R, Barrera O, Sutton A, Robbins JB. Preparation, characterization, and immunogenicity of Haemophilus influenzae type b polysaccharide-protein conjugates. *J Exp Med* (1980) 152(2):361–76. doi: 10.1084/jem.152.2.361

57. Grandjean C, Wade TK, Ropartz D, Ernst L, Wade WF. Acid-detoxified Inaba lipopolysaccharide (pmLPS) is a superior cholera conjugate vaccine immunogen than hydrazine-detoxified lipopolysaccharide and induces vibriocidal and protective antibodies. *Pathog Dis* (2013) 67(2):136–58. doi: 10.1111/2049-632X.12022

58. Ftacek P, Nelson V, Szu SC. Immunochemical characterization of synthetic hexa-, octa- and decasaccharide conjugate vaccines for Vibrio cholerae O:1 serotype Ogawa with emphasis on antigenic density and chain length. *Glycoconj J* (2013) 30 (9):871–80. doi: 10.1007/s10719-013-9491-9

59. Stefanetti G, Okan N, Fink A, Gardner E, Kasper DL. Glycoconjugate vaccine using a genetically modified O antigen induces protective antibodies to *Francisella tularensis*. *Proc Natl Acad Sci U S A.* (2019) 116(14):7062–70. doi: 10.1073/pnas.1900144116

60. Zhu H, Rollier CS, Pollard AJ. Recent advances in lipopolysaccharide-based glycoconjugate vaccines. *Expert Rev Vaccines* (2021) 20(12):1515–38. doi: 10.1080/14760584.2021.1984889

61. Watson DC, Robbins JB, Szu SC. Protection of mice against Salmonella typhimurium with an O-specific polysaccharide-protein conjugate vaccine. *Infect Immun* (1992) 60(11):4679–86. doi: 10.1128/iai.60.11.4679-4686.1992

62. Micoli F, Romano MR, Tontini M, Cappelletti E, Gavini M, Proietti D, et al. Development of a glycoconjugate vaccine to prevent meningitis in Africa caused by meningococcal serogroup X. *Proc Natl Acad Sci U S A.* (2013) 110(47):19077–82. doi: 10.1073/pnas.1314476110

63. An SJ, Yoon YK, Kothari S, Kothari N, Kim JA, Lee E, et al. Physico-chemical properties of Salmonella typhi Vi polysaccharide-diphtheria toxoid conjugate vaccines affect immunogenicity. *Vaccine* (2011) 29(44):7618–23. doi: 10.1016/j.vaccine.2011.08.019

64. Wessels MR, Paoletti LC, Guttormsen HK, Michon F, D'Ambra AJ, Kasper DL. Structural properties of group B streptococcal type III polysaccharide conjugate vaccines that influence immunogenicity and efficacy. *Infect Immun* (1998) 66 (5):2186–92. doi: 10.1128/IAI.66.5.2186-2192.1998

65. Kossaczka Z, Lin FY, Ho VA, Thuy NT, Van Bay P, Thanh TC, et al. Safety and immunogenicity of Vi conjugate vaccines for typhoid fever in adults, teenagers, and 2- to 4-year-old children in Vietnam. *Infect Immun* (1999) 67(11):5806–10. doi: 10.1128/IAI.67.11.5806-5810.1999

66. Fattom A, Shiloach J, Bryla D, Fitzgerald D, Pastan I, Karakawa WW, et al. Comparative immunogenicity of conjugates composed of the Staphylococcus aureus type 8 capsular polysaccharide bound to carrier proteins by adipic acid dihydrazide or N-succinimidyl-3-(2-pyridyldithio)propionate. *Infect Immun* (1992) 60(2):584–9. doi: 10.1128/iai.60.2.584-589.1992

67. Fattom A, Li X, Cho YH, Burns A, Hawwari A, Shepherd SE, et al. Effect of conjugation methodology, carrier protein, and adjuvants on the immune response to Staphylococcus aureus capsular polysaccharides. *Vaccine* (1995) 13:1288–93. doi: 10.1016/0264-410x(95)00052-3

68. Gupta RK, Szu SC, Finkelstein RA, Robbins JB. Synthesis, characterization, and some immunological properties of conjugates composed of the detoxified lipopolysaccharide of Vibrio cholerae O1 serotype Inaba bound to cholera toxin. *Infect Immun* (1992) 60(8):3201–8. doi: 10.1128/iai.60.8.3201-3208.1992

69. Simon R, Tennant SM, Wang JY, Schmidlein PJ, Lees A, Ernst RK, et al. Salmonella enterica serovar enteritidis core O polysaccharide conjugated to H:g,m flagellin as a candidate vaccine for protection against invasive infection with S. enteritidis. *Infect Immun* (2011) 79(10):4240–9. doi: 10.1128/IAI.05484-11

70. Baliban SM, Yang M, Ramachandran G, Curtis B, Shridhar S, Laufer RS, et al. Development of a glycoconjugate vaccine to prevent invasive Salmonella Typhimurium infections in sub-Saharan Africa. *PloS Negl Trop Dis* (2017) 11(4):e0005493. doi: 10.1371/journal.pntd.0005493

71. Svenson SB, Nurminen M, Lindberg AA. Artificial Salmonella vaccines: O-antigenic oligosaccharide-protein conjugates induce protection against infection with Salmonella typhimurium. *Infect Immun* (1979) 25(3):863–72. doi: 10.1128/iai.25.3.863-872.1979

72. Vidarsson G, Dekkers G, Rispens T. IgG subclasses and allotypes: from structure to effector functions. *Front Immunol* (2014) 5:520. doi: 10.3389/fimmu.2014.00520

73. Mäkelä O, Péterfy F, Outschoorn IG, Richter AW, Seppälä I. Immunogenic properties of alpha (1-6) dextran, its protein conjugates, and conjugates of its breakdown products in mice. *Scand J Immunol* (1984) 19(6):541–50. doi: 10.1111/j.1365-3083.1984.tb00965.x

74. Seppälä I, Pelkonen J, Mäkelä O. Isotypes of antibodies induced by plain dextran or a dextran-protein conjugate. *Eur J Immunol* (1985) 15(8):827–33. doi: 10.1002/eji.1830150816

75. Sun P, Pan C, Zeng M, Liu B, Liang H, Wang D, et al. Design and production of conjugate vaccines against S. Paratyphi A using an O-linked glycosylation system in *vivo*. *NPJ Vaccines* (2018) 3:4. doi: 10.1038/s41541-017-0037-1

76. Saxena M, Di Fabio JL. Salmonella typhi O-polysaccharide–tetanus toxoid conjugated vaccine. *Vaccine* (1994) 12(10):879–84. doi: 10.1016/0264-410x(94)90029-9

77. Halder P, Maiti S, Banerjee S, Das S, Dutta M, Dutta S, et al. Bacterial ghost cell based bivalent candidate vaccine against Salmonella Typhi and Salmonella Paratyphi A: A prophylactic study in BALB/c mice. *Vaccine* (2023) 41(41):5994–6007. doi: 10.1016/j.vaccine.2023.08.049

78. Reinhardt A, Yang Y, Claus H, Pereira CL, Cox AD, Vogel U, et al. Antigenic potential of a highly conserved Neisseria meningitidis lipopolysaccharide inner core structure defined by chemical synthesis. *Chem Biol* (2015) 22(1):38–49. doi: 10.1016/j.chembiol.2014.11.016

Revision

Manuscript #	IAI00346-24R1
Current Revision #	1
Other Version	IAI00346-24
Submission Date	2024-10-21 00:00:00
Current Stage	Manuscript Sent to Production
Title	A newly-developed oral infection mouse model of shigellosis for immunogenicity and protective efficacy studies of a candidate vaccine
Manuscript Type	Full-Length Text
Special Section	N/A
Journal Section	Bacterial Infections
Corresponding Author	Dr. Santasabuj Das (National Institute of Cholera and Enteric Diseases)
Contributing Authors	Ms. Risha Haldar , Prolay Halder , Dr. Hemanta Koley , Dr. SHIN-ICHI MIYOSHI , Dr. Santasabuj Das (corr-auth)
Abstract	Shigella infection poses significant public health challenge in the developing world. However, lack of a widely available mouse model that replicates human shigellosis creates a major bottleneck to better understanding of disease pathogenesis and development of newer drugs and vaccines. BALB/c mice pre-treated with streptomycin and iron ($FeCl_3$) plus desferrioxamine intraperitoneally followed by oral infection with virulent Shigella flexneri 2a resulted in diarrhoea, loss of body weight, bacterial colonization and progressive colitis characterized by disruption of epithelial lining, loss of crypt architecture with goblet cell depletion, increased PMN infiltration into the mucosa, submucosal swelling (edema) and raised proinflammatory cytokines and chemokines in the large intestine. To evaluate the usefulness of the model for vaccine efficacy studies, mice were immunized intranasally with a recombinant protein vaccine containing Shigella invasion protein IpaB. Vaccinated mice conferred protection against Shigella, indicating that the model is suitable for testing of vaccine candidates. To protect both Shigella and Salmonella, a chimeric recombinant vaccine (rIpaB-T2544) was developed by fusing IpaB with Salmonella outer membrane protein T2544. Vaccinated mice developed antigen-specific, serum IgG and IgA antibodies and a balanced Th1/Th2 response and were protected against oral challenge with Shigella (S. flexneri 2a, S. dysenteriae, S. sonnei) using our present mouse model and Salmonella (Salmonella Typhi and Paratyphi) using iron overload mouse model. We here describe the development of an oral Shigella infection model in wild type mouse. This model was successfully used to demonstrate the immunogenicity and protective efficacy of a candidate protein subunit vaccine against Shigella.
Tweet	
Editor	Prof. Andreas J Bäumler
Original MS Preferred Reviewers	James B. Kaper (University of Maryland School of Medicine), Edward T. Ryan (Massachusetts General Hospital), Richelle Charles (Massachusetts General Hospital)
Original MS Non-Preferred Reviewers	N/A
Keywords	Oral route, S. flexneri, Shigellosis, Bivalent Subunit vaccine (IpaB-T2544), Mouse model
Research Areas	Bacteriology, Immunology, Vaccines
PubMed Similar Manuscripts	(expand)
Conflict of Interest	No conflict of interest.
Preprint Server	No
Biorxiv Preprint	No
Funding Sources	Indian Council of Medical Research (ICMR) ✔ : Risha Haldar 58/17/2020/PHA/BMS Japan Agency for Medical Research and Development (AMED) ✔ : SHIN-ICHI MIYOSHI JP23wm0125004
Decision	Accept / 2024-11-06
Data Citation	Are the data sets and/or code used in the experiments and studies described in this submission identified and cited in the manuscript and reference list in accord with ASM's Data Citation Policy? Yes
Data Availability	Yes

Manuscript Items

1. Author Cover Letter (last updated: 10/21/2024 13:48:44) PDF (76KB)
2. Author Cover Letter (last updated: 10/21/2024 13:26:29) PDF (103KB)
3. "Response to Reviewer Comments" (last updated: 10/21/2024 12:00:51) PDF (214KB)
4. Manuscript Text File (last updated: 10/21/2024 12:51:09) PDF (543KB)
5. Merged File containing manuscript text and 10 Figure files. (last updated: 10/30/2024 16:52:28) PDF (8568KB)
   a. Manuscript Text File (last updated: 10/21/2024 12:51:09) PDF (543KB)
   b. Figure 1 (last updated: 10/21/2024 13:34:33) PDF (232KB)
   c. Figure 2 (last updated: 10/21/2024 13:34:33) PDF (2155KB)
   d. Figure 3 (last updated: 10/21/2024 13:34:34) PDF (769KB)
   e. Figure 4 (last updated: 10/21/2024 13:34:31) PDF (3488KB)
   f. Figure 5 (last updated: 10/21/2024 13:34:35) PDF (75KB)
   g. Figure 6 (last updated: 10/21/2024 13:34:33) PDF (183KB)
   h. Figure 7 (last updated: 10/30/2024 16:52:28) PDF (224KB)
   i. Figure 8 (last updated: 10/21/2024 13:34:33) PDF (11020KB)
   j. Figure 9 (last updated: 10/21/2024 13:34:35) PDF (438KB)
   k. Figure 10 (last updated: 10/21/2024 13:34:31) PDF (2453KB)
6. Supplemental tables (last updated: 10/21/2024 13:34:31) Supplemental Material
   Tables S1 to S4; Supplementary figure legends and supplementary references.
7. Supplemental figures (last updated: 10/21/2024 13:34:34) Supplemental Material
   Fig. S1 and S2.
8. Fig. S3 (last updated: 10/21/2024 13:34:35) Supplemental Material
   Histology sections of the colon and caecum tissue of uninfected and untreated BALB/c mice.

A newly-developed oral infection mouse model of shigellosis for immunogenicity and protective efficacy studies of a candidate vaccine

Risha Haldar[1], Prolay Halder[2], Hemanta Koley[2], Shin-ichi Miyoshi[3], Santasabuj Das[1,4#]

[1]Division of Clinical Medicine, ICMR-National Institute of Cholera and Enteric Diseases, P-33 CIT Road, Scheme-XM, Kolkata, India.

[2]Division of Bacteriology, ICMR-National Institute of Cholera and Enteric Diseases, P-33 CIT Road, Scheme-XM, Kolkata, India.

[3] Division of Medicine, Dentistry and Pharmaceutical Sciences, Graduate School of Medicine, Dentistry and Pharmaceutical Sciences, Okayama University, Okayama Japan.

[4] Division of Biological Science, Indian Council of Medical Research (ICMR)-National Institute of Occupational Health, Ahmedabad, India

Running title: Oral *Shigella* mice model for vaccine effectivity

Corresponding author; Email; santasabujdas@yahoo.com, dasss.niced@gov.in

Abstract

Shigella infection poses significant public health challenge in the developing world. However, lack of a widely available mouse model that replicates human shigellosis creates a major bottleneck to better understanding of disease pathogenesis and development of newer drugs and vaccines. BALB/c mice pre-treated with streptomycin and iron ($FeCl_3$) plus desferrioxamine intraperitoneally followed by oral infection with virulent *Shigella flexneri 2a* resulted in diarrhoea, loss of body weight, bacterial colonization and progressive colitis characterized by disruption of epithelial lining, loss of crypt architecture with goblet cell depletion, increased PMN infiltration into the mucosa, submucosal swelling (edema) and raised proinflammatory cytokines and chemokines in the large intestine. To evaluate the usefulness of the model for vaccine efficacy studies, mice were immunized intranasally with a recombinant protein vaccine containing *Shigella* invasion protein IpaB. Vaccinated mice conferred protection against *Shigella*, indicating that the model is suitable for testing of vaccine candidates. To protect both *Shigella* and *Salmonella*, a chimeric recombinant vaccine (rIpaB-T2544) was developed by fusing IpaB with *Salmonella* outer membrane protein T2544. Vaccinated mice developed antigen-specific, serum IgG and IgA antibodies and a balanced Th1/Th2 response and were protected against oral challenge with *Shigella* (*S. flexneri* 2a, *S. dysenteriae, S. sonnei*) using our present mouse model and *Salmonella* (*Salmonella* Typhi and Paratyphi) using iron overload mouse model. We here describe the development of an oral S*higella* infection model in wild type mouse. This model was successfully used to demonstrate the immunogenicity and protective efficacy of a candidate protein subunit vaccine against *Shigella.*

Keywords. Oral route, *S. flexneri*, Shigellosis, Bivalent Subunit vaccine (IpaB-T2544), Mouse model

Introduction

Shigella is a gram-negative, human-restricted, bacterial pathogen that is transmitted through the faeco-oral route and creates a replicative niche in the large intestine, leading to severe recto-colitis, known as shigellosis. The global incidence of the disease ranges from 80 to165 million each year with 600,000 deaths, primarily in under 5 children (1). The disease is manifested by mucoid or bloody diarrhoea, fever, abdominal pain and failure to thrive (2). Shigellosis in the endemic zones is mainly caused by *S. flexeneri 2a* and *S. sonnei*, and the colon biopsies show epithelial destruction with edema, capillary congestion, hemorrhage, crypt hyperplasia, goblet cell depletion and mononuclear and polymorphonuclear (PMN) leukocytes cell infiltration (3). Widespread multidrug resistance results in frequent treatment failures for *Shigella* infection, while attempts to develop vaccines have yielded limited success so far.

Shigella is a locally invasive pathogen that replicates in the epithelial cell cytosol after exiting phagosomes and hides from the host immune system by lateral cell-to-cell spread. Bacteria reaching the lamina propria are taken up by the macrophages, wherein *Shigella* could induce pyroptosis, a mode of inflammatory cell death (2). Extensive in vitro and in vivo studies have identified that a type three secretion system (T3SS) and its multiple secreted effectors, such as IpaB, IpaC, IpgD, IpaH7.8 play critical roles in *Shigella* pathogenesis (4). While many targets of these effector proteins have been identified in the cell culture system, in vivo significance of them is largely unknown.

Non-availability of a suitable animal model that mimics the human disease and is genetically manipulable remains a major bottleneck in better understanding of *Shigella* pathogenesis and vaccine development. Several in vivo models, including guinea pig Keratoconjunctivitis, rabbit ileal loop and rectal infection, mouse pulmonary infection and new-born mouse, nonhuman primate and human challenge models have been reported for shigellosis (5, 6, 7, 8, 9, 10, 11, 12, 13, 14). However, high cost, ethical concerns, less available immunological tools, neonate age limit and irrelevant nature of the target organs limit their usefulness. More recently, an intraperitoneal infection model and a genetically-modified (nlrc4-/-) mouse model have been established wherein the relation between *Shigella* infection and intestinal pathology were studied (15, 16). While this is a useful model to study disease pathogenesis,

the genetically modified model may not be widely available and the model's usefulness for vaccine immunogenicity and protective efficacy was not tested.

Shigella colonizes human large intestine which is the body site for the largest number and diversity of resident flora in the mammals that provides protection against pathogenic bacteria. Studies were published on STm enterocolitis in mice after reduction of resident intestinal bacterial load by pre-treatment with streptomycin (17). Varying levels of intestinal inflammation were observed with several other *S.* enterica serovars, but not with *S.* Paratyphi after streptomycin pre-treatment (18).

Iron is an essential micronutrient for intracellular survival and growth of many Gram-negative bacteria, including *S.* Typhi and *Shigella* as it functions as a co-factor of several enzymes involved in basic biological processes such as DNA replication and respiration (19). As a part of the inflammatory response to infection, the host tends to sequester Fe from the bone marrow sites of erythropoiesis to storage, most typically to bind ferritin and induce hypoferremia, reducing the amount of free Fe available for the pathogen. The fact that an excess of free Fe in the system increases the susceptibility of the host to infection in both mice and humans highlights the protective relevance of host sequestration of Fe. The dose of Fe needed to make it susceptible to infection, however, must be given at a level high enough to inhibit neutrophil and macrophage immunological responses as well as the synthesis of TNF-alpha and nitric oxide. While this dose is toxic to the bacterium (20), Fe toxicity in mice can be eliminated with a lower dose of iron, combined with the iron chelator deferoxamine (DFO), keeping the establishment of infection intact as observed for *Salmonella* (21). DFO is a hexadentate chelator, which binds with iron at a 1:1 molar ratio, thereby removing free iron from the bloodstream and enhancing its elimination in the urine (22). Bacteria can bind and take up ferrioxamine group of DFO via the FoxA receptor for utilization of iron, as was reported for *Y. enterocolitica* (23). FoxA is a TonB dependent transporter of ferrioxamines (24) and TonB-dependent receptor delivers the siderophore to the periplasm where it is transported to the cytosol by the FhuBCD, a PBP-dependent ABC transporter (25). Increased iron availability has been associated with decreased abundance of more beneficial bacteria like bifidobacteria and increased infection by enteric pathogens (26). In vitro studies showed heightened bacterial proliferation upon transition from iron-deficient environments to those with elevated iron levels, leading to adhesion, invasion and injury to the epithelium (27). Iron-treated chickens developed small granulomatous lesions in the lamina propria with villus

epithelial shedding of the large intestine after oral challenges with *Yersinia pseudotuberculosis* (28). Further, pre-treatment with iron-dextran resulted in increased susceptibility of mice to yersiniosis, when orally or parenterally challenged with *Y. enterocolitica* (29). We had previously used iron (plus iron chelator desferal) to develop a mouse model of systemic *Salmonella* Typhi infection (30).

Shigella invasion plasmid antigen B (IpaB) is highly conserved among all *Shigella* serotypes (31). IpaB-specific antibody generates phagocytic activity (32, 33) and triggers IFN-γ-mediated immune response (34). Intranasal immunization with IpaB generated robust systemic and mucosal antibodies and T cell-mediated immunity and protected mice against lethal pulmonary infection with *Shigella flexneri* and *Shigella sonnei* (35, 36). Evidence from *Shigella* CHIM (controlled human infection model) studies showed that IpaB-specific serum IgG may also serve as a correlate of protection (37).

We report the development of an oral *Shigella* infection model in mice after combined pre-treatment with streptomycin and iron. This model was successfully used to demonstrate the immunogenicity of a subunit protein candidate vaccine against *Shigella.* We had earlier reported that subcutaneous immunization with a conserved, *S.* Typhi/ *S.* Paratyphi outer membrane protein T2544 induces protective humoral and cell-mediated immune responses in an iron overload mouse model of infection when administered through the subcutaneous route (30, 38). Further, T2544 was successfully incorporated into a glycoconjugate vaccine for multivalent protection (39). Here, to provide a broader coverage against both *Salmonella* and *Shigella*, we have combined T2544 with IpaB to generate a chimeric protein (IpaB-T2544) and showed that immunization with the recombinant chimeric protein protected mice against *Shigella* and typhoidal *Salmonella,* thus acting as a bivalent vaccine candidate.

Materials and Methods

Bacterial strains, growth conditions and plasmid

Salmonella Typhi Ty2 was generous gifts from J. Parkhill, Sanger Institute, Hinxton, UK. *Shigella flexneri 2a* (2457T), and clinical isolates of *Shigella dysenteriae, Shigella sonnei* and *Salmonella* Paratyphi A, were received from IMTECH, Chandigarh. All strains were grown in Hectoen enteric agar BD DIFCO and were maintained in Tryptic soy agar (TSA) BD DIFCO at 37˚C. *Escherichia coli* BL21, a kind gift from Dr. Rupak K. Bhadra (CSIR-IICB, Kolkata, India) was cultured in Luria–Bertani agar at 37 °C. Bacterial culture media and pET-

28a plasmid were purchased from BD Difco and Addgene (USA), respectively. The oligonucleotides used in this study were synthesized from IDT.

Animals

Animal breeding and experimentation were approved by institutional animal ethical committee (PRO/192/-June 2022-25). All the animal experiments were conducted following the statute given by Committee for the Purpose of Control and Supervision of Experiments on Animal (CPCSEA), Ministry of environment and forest, Government of India. Mice were procured from the animal resources of ICMR-NICED, Kolkata, India. Animals were maintained at $25^{\circ} \pm 2^{\circ}$ C with 75 ± 2% humidity and fed sterile food and water. In this study, 6-week-old female BALB/c mice were used for the immunization. All the immunological experiments and protection study was performed at the age of 10 weeks after the completion of immunization.

Murine oral *Shigella* infection model

For the experiments, animals (10-week-old) were housed individually or in groups equipped with steel grid floors. Mice deprived of food and water for 4–6 hr before the oral streptomycin (20 mg/mouse) treatment. Afterward, animals were supplied with water and food ad libitum. 20h later the streptomycin treatment, water and food were withdrawn again and mice were injected with Desferrioxamine (25 mg/Kg body weight) intraperitoneally. Fifteen minutes later the Desferrioxamine treatment, $FeCl_3$ (0.32 mg per gm of body weight) was administered the same route before 4 hours of infection (34, 35). Four hours later, mice were treated with 5% $NaHCO_3$ to neutralize the stomach acids. After 20 minutes of bicarbonate treatment, mice were infected by oral gavage with *Shigella flexeneri 2a* (5×10^7 CFU) resuspended in PBS.

Recovery of *Shigellae* from organs and feces

To enumerate intracellular CFU from the ceca and colons from un-infected, infected, and immunized mice, organs were isolated aseptically at different time points. Tissues were vigorously washed in PBS with gentamicin (50 μg/ml) and mechanically homogenized in 1x

PBS followed by lysed with 1% Triton-X100. Lysates were serially diluted and plated on TSA plates containing 100 µg/ml streptomycin. Colonies were counted after overnight incubation at 37°C.

Fecal pellets were collected and homogenized in 2% FBS in 1 mL of PBS containing protease inhibitors. For CFU determination serial dilutions were made in PBS and plated on TSA plates containing 100 µg/ml streptomycin.

Histopathology

Colon and caecum tissues were excised from mice and preserved in 10% formalin. Formalin-dissolved tissues were then embedded in paraffin blocks. Tissues fixed in paraffin were divided into 5-µm-thick sections. The sections were soaked in xylene twice for 20 minutes at 56°C to deparaffinize and were dehydrated with ethanol (twice at 100%, once at 95%, and once at 75% ethanol) for five minutes. Tissue sections were mounted on glass slides and stained with Hematoxylin and Eosin. Slides were examined under a microscope and evaluated in a blinded fashion by two independent investigators. Different magnifications of images were captured to represent different parameters. 10x - presence of swelling (edema) in the submucosal layer, 20x - degenerative changes in the epithelial lining, 40x - presence of increased infiltration of lymphocytes in the mucosa and submucosa, loss of crypt architecture with loss of goblet cells. Slides were scored for different histological parameters as described in **Supplementary Table 1** and **Supplementary Table 2.**

Cytokine estimation from intestinal tissue

Cecum and colon were isolated from mice at different post-infection time points and rinsed 5 times in PBS to remove fecal contents. Organs were then homogenized in 1 mL of 2% FBS in PBS with protease inhibitors, and spun down at 2000 g. The concentration of IL-1β, TNFα, IFNγ, and CXCL10 were measured in the supernatant using the commercial ELISA kits (R&D) following the manufacturer's protocol. Briefly, ninety-six well plates were incubated overnight with capture antibody in coating buffer. Following three subsequent washes plates were subjected to blocking for one hour at room temperature. Samples were added to the wells following wash and incubated for two hours at room temperature. After three subsequent washes, plates were further incubated for two hours at room temperature

with detection antibody. After three washes plates were further incubated with streptavidin-HRP for twenty minutes at room temperature. Following three washes plates were finally incubated with substrate for thirty minutes at room temperature. The reaction ended with the stop solution and the colour development was evaluated using spectrophotometry at 450 nm.

Cloning expression and purification of rIpaB-T2544

ipab and *t2544* genes were cloned in tandem into the prokaryotic expression vector pET28a. We first amplified the 801 bp domain regions of *ipab* gene by PCR using the genomic DNAs of *Shigella flexeneri 2a* strain as the template and cloned into pET28a vector using the following IpaB primers: IpaB forward primer: CGCGGATCCGGTGGCGGTGGCTCG GATCTTACTGCTAACCAAAAT and IpaB reverse primer: CCGGAGCTC AACACAACCCATTACTCTGTTGAG where BamHI and SacI were used as restriction enzymes (New England Biolabs). Later on, *t2544* along with an upstream linker sequence (GGACCAGGACCA is the gene codon of a non-furin linker containing glycine and proline amino acids) (total sequence length 663bp) was PCR amplified and the PCR product was cloned between SalI and XhoI restriction enzymes (New England Biolabs) of the pET28a-IpaB plasmid (T2544 FP: GCCGTCGACGGACCAGGACCAGAAGGGATCTATATCACCGGG and T2544 RP: GCCCTCGAGTTAAAAGGCGTAAGTAATGCCGAG). After clone confirmation by restriction digestion, followed by sequencing (Agri genome), the recombinant plasmid (rIpaB-T2544) was transformed into *E. coli* BL21 (DE3) pLysS cells. Transformed E. coli BL21 pLysS cells were inoculated into terrific broth (BD Difco) and incubated until the OD_{600} reached 0.5. Transformed cells were induced with 1 mM isopropylthiogalactoside (IPTG) for 4 h at 37°C, followed by centrifugation at 5000g. The resulting pellet was resuspended in lysis buffer containing 8 M urea, 200 mM NaCl, 2 mM imidazole and 50 mM Tris-HCl. Induced bacterial cells were subjected to 5 to 80 cycles of sonication on ice, with each cycle consisting of 5 pulses of 1 sec each and a 1-minute incubation period. The power output was designed to deliver a maximum of 30 watts at a frequency of 20 kHz. The sonicated sample was purified by affinity chromatography using Ni-NTA slurry according to the manufacturer's instructions (Qiagen). Briefly, the sonicated sample was centrifuged at 15000 rpm for 30 minutes at 4°C. The supernatant was collected and used for protein purification. 1ml of Ni-NTA slurry was centrifuged at 1500 × g and the supernatant were removed. The Ni-NTA beads were then mixed with equilibration buffer (20 mM Tris-HCl,

400 mM NaCl, 5 mM imidazole, 8 M urea) for 1 hour at room temperature. 4ml of protein supernatant was added to the equilibrated Ni-NTA beads and incubated at room temperature for 4 hours. The protein-Ni-NTA mixture was loaded into the column (Bio-Rad empty polypropylene column) and column-bound recombinant protein was eluted using elution buffer (20 mM Tris-HCl, 300 mM NaCl, 500 mM imidazole, 8 M urea). After that the protein solution was renatured by gradual removal of urea by dialysis in 20 mM Tris-HCl, 150 mM NaCl, 10% glycerol, 0.5% Triton-X 100 and 2 M urea buffer using a 10 kD membrane (Millipore). The purity of the protein was determined by sodium dodecyl-sulfate polyacrylamide gel electrophoresis (SDS–PAGE).

Circular dichroism (CD)

1.0 ml of rIpaB, rT2544 and rIpaB-T2544 at a concentration of 180 µg/ml was filtered through a 0.45 µm pore-size filter to remove suspended particles, if any and taken in a 0.1 mm path-length quartz cuvette. Circular dichroism (CD) spectrum of the protein sample was captured at the wavelength range of 200 to 300 nm at 25°C on the Jasco-1500 spectrophotometer. A minimum of three spectra were recorded in 1 nm steps at a speed of 50 nm per minute. Baselines were subtracted and data was recorded as ellipticity (CD [mdeg]).

Western blot

In 12% SDS-PAGE, rT2544 (5 µg), rIpaB (7µg) and rIpaB-T2544 (3 µg each) were resolved and then transferred to a PVDF membrane (Millipore). After transfer, membrane was washed with 1X TBS for 5 min at room temperature. After blocking with 5% BSA for 1 h at room temperature, membranes were washed with 1X TBS-T [Tris Buffered Saline pH 7.5, containing 0.1% Tween-20 (v/v)] three times for 5 min at room temperature. Membrane was then incubated with mouse anti His-tag (CST) antibody (1:1000) in 5% BSA, 1X TBS, 0.1% Tween 20 at 4°C with gentle shaking, overnight. Membranes were washed with TBS-T for 5 times and incubated with rabbit anti-mouse IgG antibody (1:10000 dilutions), conjugated to horseradish peroxidase (HRP) for 1 h at room temperature. After 3 washes with TBS-T in an orbital shaker, membranes were developed by chemiluminescent reagents (SuperSignal West Pico, Thermo Fisher) and the signals were captured in ChemiDoc ^{TM} MP imaging system (Bio Rad).

Animal immunization, and infection

Female BALB/c mice (6 weeks old) were immunized intranasally with PBS (vehicle), 40µg of rT2544, rIpaB, or rIpaB-T2544 at 2-weeks intervals for 3 times. On days 0, 14, 28, 38, and 90 after vaccination, blood samples were collected from the mice by tail snip. The samples were then incubated for 30 minutes at 37°C, centrifuged for 15 minutes at 1,200 × g at 4°C, and stored at −80°C. Fecal samples were collected on days 0, 14, 28, and 38, weighed, and thoroughly dissolved in 100 mg/ml of PBS with 1% BSA (SRL). Samples were then centrifuged at 15,000 × g for 10 min at 4°C, and protease inhibitor cocktails (Sigma-Aldrich) were added to the supernatants before being stored at -80°C. Intestinal washes were collected after sacrifice of the mice (on day 38). To this end, the small intestine was removed and washed three times with 1 ml of PBS-1% BSA (BSA, SRL). After centrifuging the samples for 10 minutes at 10,000 × g at 4°C, protease inhibitor cocktails (Sigma-Aldrich) were added to the supernatants and stored at -80°C. Fourteen days after the last immunization, different groups of mice were infected with different bacterial strains (*Shigella* Spp., *Salmonella* Typhi, *Salmonella* Paratyphi A).

For *Shigella* infection, fourteen days after the last immunization (day 42), mice were pretreated with streptomycin sulfate and iron with desferal (desferrioxamine) (as described above) before the oral dosage of different *Shigella* strains [*Shigella flexeneri 2a* (5×10^9 CFU), *Shigella dysenteriae* (5×10^8 CFU), *Shigella sonnei* (5×10^8 CFU)]. Infected mice were monitored for 20 days.

For *Salmonella* infection, on day 42 of first immunization, BALB/c mice were deprived of food and water for 10 hr. Mice were treated with intraperitoneal injection of $Fe3^+$ as $FeCl_3$ (0.32 mg per gm of body weight) along with Desferrioxamine (25 mg/Kg body weight) four hours prior to the bacterial challenge. Four hours later, mice were treated 5% $NaHCO_3$ to neutralize the stomach acids. After 20 minutes of the bicarbonate treatment, mice were orally infected with 5×10^7 CFU (10X LD_{50}) of *S.* Typhi or 5×10^5 CFU (10X LD_{50}) of *S.* Paratyphi A and monitored for 10 days (34, 35).

Cytokine estimation from splenocytes

PBS and rIpaB-T2544 immunized mice were sacrificed on day 38, ten days after the last immunization. Splenocytes were collected from the spleen and 200 µl of splenocytes were cultured in RPMI 1640 medium (1×10^5 cells/well) in 96-well microtiter plates. Cells were incubated with 5µg/ml of rIpaB-T2544 for 48h. Levels of cytokine secretion were measured

(pg/ml) from the supernatants at 48h. Cytokines were estimated by commercial ELISA kits (BD bioscience [IL-4, IL-5, IL-6, IL-12], R&D [IL-4, IFN-γ, TNF-α]) following the manufacturer's instructions.

Enzyme-Linked Immunosorbent Assay (ELISA)

Microtiter plates were coated with 2µg/ml of rT2544, IpaB, or rIpaB-T2544 and incubated at 4°C overnight. After rinsing with PBS-T (Phosphate buffer saline, containing 0.05% Tween 20), the wells were blocked using PBS, containing 1% BSA (SRL) for 1 hour at room temperature. Following further washes, plates were incubated with serum, feces, or intestinal lavage samples, diluted serially (1:200 to 1: 409600 for IgG and 1:20 to 1:25600 for IgA) for 2 hours at room temperature. Subsequently, rabbit anti-mouse IgG (1:10000) or goat anti-mouse IgA (1:5000) antibodies conjugated to HRP were used to incubate the wells for 1 h at room temperature. The immune complex was developed using tetramethyl benzidine (TMB) substrate (BD OptEIA^{TM}) and OD_{450} of the mixture was measured in a spectrophotometer (Shimadzu, Japan).

Details of the reagents are listed in **Supplementary Table 3.**

Statistical analysis

Data related to CD was analyzed using ORIGIN software (2019b). Antibody titers were represented as reciprocal of the log 2 values. GraphPad Prism 8.0.1.244 were used for statistical analyses and for the comparison of two groups student t-test was accompanied (*P, 0.05, **P < 0.01, ***P < 0.001, ****P < 0.0001). One-way ANOVA, Two-way ANOVA with Tukey's post-test were performed for multiple comparisons, *P < 0.05, **P < 0.01, ***P <0.001.

Result

Combined treatment with streptomycin and iron ($FeCl_3$) renders mice susceptible to oral *Shigella* infection and disease development

To establish an oral *Shigella* infection model, different groups of BALB/c mice (10 weeks old, n=6) were pre-treated with various combinations of oral streptomycin and/or injectable

iron ($FeCl_3$) plus iron chelator, desferal ($FeCl_3$/desferal) 24h and 4h, respectively before the oral gavage with different doses of virulent *Shigella flexeneri 2a* as shown in **Figure 1**. All mice that received either streptomycin or $FeCl_3$/desferal survived the bacterial challenge (**Figure 1 A-C**). In contrast, 50% and 100% of the mice that received 5×10^8 CFU (LD_{50}) and 5×10^9 CFU (LD_{100}), respectively after pre-treatment with both streptomycin and $FeCl_3$/desferal succumb to the infection. All the mice similarly pre-treated, but challenged with 5×10^7 CFU (sublethal dose) of *S. flexneri 2a* survived (**Figure 1**). To investigate the difference in the outcome of infection with the lower ($5x10^7$ CFU) and the higher ($5x10^8$ CFU) doses of *S. flexneri 2a*, we measured the body weights daily and fecal shedding of bacteria on alternate days of the infected mice till 14-days post-infection (**Supplementary Figure 1 A, B**). The results showed a sharp decline in the body weights of all the infected mice in the first 2 days after the infection. However, mice infected with the lower dose rapidly gained weights after this time point, while those infected with the higher dose displayed a much slower gain of weight, suggesting greater impact of infection. Comparison of fecal shedding between the two groups of mice showed maximum shedding after 2 days of infection, which was similar for both the groups. This suggests greater (~10-fold) colonization of the intestine by *S. flexneri* for the mice that received the higher dose. This corroborated with more rapid decline of bacterial shedding in the animals infected with the lower bacterial dose to touch the baseline within 10 days. In contrast, mice infected with the higher dose showed a much slower decline of fecal bacterial shedding. Thus, the difference in deaths of mice between the 2 groups may be explained by significantly better and longer infection of the mice that received 10 times more bacteria. The above results underscored that although there was no bottleneck for infection, a threshold of infectious dose was required to cause severe diseases, resulting in death. Given that the higher dose ($5x10^8$ CFU) used here was the LD_{50} dose, only 50% of the mice died and this occurred over a period of time. This difference was most likely related to the success of infection that varies for experiments with live organisms, especially mammals. This is suggested by the fact that bacterial shedding of the surviving mice from this group gradually decreased over time, indicating that mice, which were colonized by fewer no of bacteria or handled the infection better survived longer. Overall, these findings suggested that iron plus streptomycin pre-treatment increases susceptibility of mice to oral *Shigella* infection. Further, LD_{50} and LD_{100} doses for other *Shigella* serovars, such as *S. dysenteriae* and *S. sonnei* in streptomycin plus $FeCl_3$/desferal pre-treated mice were 1 log lower than *S. flexneri 2a* (**Supplementary Figure 2**).

Further, sublethal infection (5×10^7 CFU) with *S. flexneri 2a* led to diarrhoea by 24 hours (**Figure 2A v**) and maximum body weight loss (69%) at 48h p.i. (**Figure 2B v**) in streptomycin and iron pre-treated group. In comparison, mice from the comparator groups, which either received no infection or combined treatment with FeCl3 (plus desferal) and streptomycin had no diarrhoea (**Figure 2A i-iv**) and showed continued gain in body weights (**Figure 2 B i-iv**).

In the infected mice, disease severity correlated with bacterial recovery from the colon and caecum lysates and the feces. We observe peak CFU at 48h p.i. that gradually decreased with time (**Figure 2C**), indicating gradual recovery, which corroborated with the self-limiting *Shigella* gastroenteritis of humans (40). In our study, we have used only virulent strains shed in the stool that were congo red positive, suggesting that they contain virulence plasmid. Together these results suggested that oral challenge with *Shigella spp*. readily causes colonic infection and disease in streptomycin- and iron-pre-treated mice and may be considered as a model for human shigellosis.

Oral *S. flexneri* 2a infection of mice, pre-treated with streptomycin and iron causes colitis

Length of the colon is a widely used indicator of the severity of *Shigella* colitis. We observed maximum shortening of the colon (average length 40 mm) at 48h post-infection only in strep+iron pre-treated animals (**Figure 3 A-B v**) in comparison to >87 mm in the other groups (**Figure 3 A-B i-iv**)).

Colon and caecum morphology were studied by histology of hematoxylin and eosin stained tissues after *Shigella flexeneri 2a* infection (5×10^7 CFU) (**Figure 4**). Tissue sections of the control group (**Figure 4 i-iv, Supplementary Figure 3, Supplementary Figure 4 i-iv, Supplementary Figure 5 i-iv**) showed well-organized histological features with intact intestinal epithelial lining and properly arranged crypts with abundant goblet cells. No abnormal PMN infiltrates and thickening of the mucosal and submucosal layers were observed. In contrast, streptomycin and iron/desferal pre-treated infected mice showed evidence of tissue damage, characterized by disruption of epithelial lining, loss of crypt architecture with decreased goblet cell numbers and increased PMN infiltration into the mucosa of the colon and caecum at 24 and 72 hrs (**Figure 4 v, Supplementary Figure 4 v, Supplementary Figure 5 v**). A submucosal swelling (edema) with PMN infiltration was

observed at 48h of infection. Resolution of these damages was visible after 72h with recovery of crypt structure and goblet cell number, decreased PMN infiltration and repair of the epithelial lining. The process of resolution and repair further progressed and the recovery of the tissue architecture was complete by 7d post-infection (**Supplementary Figure 6 and Supplementary Figure 7**). A blind histological scoring was performed with the infected tissue samples and plotted in a bar diagram **(Supplementary Table 1, Supplementary Table 2, Supplementary Figure 8**).

In our study, visible bacteria within the cells were observed in the pathological specimens (**Supplementary Figure 6-7**, 24-72 h, white arrows, 40X magnification).

Together these data suggested that oral *Shigella* infection caused severe inflammatory damage to the colonic tissues in streptomycin- and iron-pretreated mice. The macroscopic and microscopic features of colonic and caecal inflammation were accompanied by the release of high levels of pro-inflammatory cytokines and chemokines, such as TNF-α, IL-1β, IFN-γ and CXCL10 in the supernatants of the tissue homogenates at different time points with maximum levels recorded after 48h of infection (**Figure 5 A-D**). Together the above results suggested that streptomycin and iron pre-treatment of adult mice rendered them susceptible to oral *Shigella* infection, with rapid colonization of the large intestine and the development of progressive colitis, manifested by diarrhoea, loss of body weights, shortening of the colon with tissue destruction and pro-inflammatory cytokines and chemokines production.

Intranasal immunization with recombinant IpaB augmented humoral immune response and protects mice against oral *Shigella* infections

To determine if the new oral shigellosis model was suitable for vaccine efficacy studies, we generated a recombinant protein (rIpaB)-based subunit vaccine by expressing a gene construct of *Shigella flexneri 2a ipab* (801 bp) in *E. coli*. The recombinant protein (rIpaB, 37 kDa) was purified from *E. coli* BL21 (DE3) PlyS by affinity chromatography using Ni-NTA agarose (**Supplementary Figure 9C)** and its purity and size were confirmed by western blots (**Supplementary Figure 9D).** Secondary structure of rIpaB-T2544 was analyzed by Far-UV CD spectra that showed one negative band, indicating alpha helix and one positive band, suggesting β helical structure at 222.6 nm and 202.3 nm, respectively (**Supplementary**

Figure 9E). To check for the protective efficacy of the candidate vaccine, BALB/c mice were immunized intranasally with three doses of the recombinant protein or the vehicle (PBS) at 14d intervals (**Supplementary Table 4, Figure 6A)**. Analysis of serum antibody endpoint titers showed that immunization with rIpaB induced 2560 times higher IpaB-specific IgG compared with the vehicle (PBS) immunization (**Figure 6B).** Oral infection with $10xLD_{50}$ dose of the *Shigella* spp. killed all the mice that received the vehicle within 11 days of infection, whereas 80-90% of the mice immunized with rIpaB were still alive beyond 20 days (**Figure 6C**). Collectively, the above data indicated that the newly developed oral *Shigella* infection model could be effectively used to evaluate the protective efficacy of vaccine candidates.

Recombinant IpaB immunization reduces colonization of the mouse large intestine by S*higella flexneri 2a* and disease manifestations after oral infection

To investigate if rIpaB could reduce the disease severity of *Shigella flexeneri 2a* infection, immunized mice were challenged orally with a sublethal dose (5×10^7 CFU) of the bacterium that was used for the model development. Vehicle-immunized mice were visibly sick with diarrhoea at 24h post-infection, while the rIpaB vaccine-immunized groups were agile and symptom-free **(Figure 7A**). Mice immunized with rIpaB showed increased body weight as opposed to reduced body weight of the vehicle-immunized, infected group (**Figure 7B**). Significant shortening of the colon was observed in the latter group, while rIpaB-immunized mice displayed normal colon lengths (**Figure 7 Ci-Cii)**. The above manifestations corroborated with *S. flexeneri 2a* colonization of the caecum and colon and shedding in the faeces with significant reduction of the CFU counts in rIpaB- vaccinated mice (**Figure 7D).** Together the above results suggested that the IpaB vaccine candidate might have induced immune response in the large intestine to prevent *Shigella* infection. To further investigate if this led to reduced tissue destruction in rIpaB-vaccinated mice, histopathology of the large intestinal tissues was performed. were observed in. While mice of the unimmunized (PBS treated) group showed destruction of the epithelial lining, loss of crypt architecture with decreased number of goblet cells, increased infiltration of lymphocytes in the mucosa and submucosa, and submucosal edema, the immunized (rIpaB treated) mice had intact epithelial lining and crypt architecture with abundant goblet cells, absence of mucosal or submucosal damage and no abnormal cellular infiltrates (**Figure 8 A-B, Supplementary Figure 10).**

Overall, these results suggested that intranasal immunization with rIpaB prevented *Shigella* from colonizing the large intestine after oral infection, thereby reducing tissue damage and disease manifestations.

Intranasal immunization with recombinant chimeric protein, IpaB-T2544 protects mice against oral *Shigella* and typhoidal *Salmonella* infections

We had previously reported that a candidate vaccine formulation based on T2544, administered subcutaneously induced high levels of serum antibodies and robust effector and memory T cell response, leading to protection from *S.* Typhi challenge (30). Moreover, T2544 used as a carrier protein acted as a vaccine adjuvant and augmented the immunogenicity of *S.* Typhimurium O-specific polysaccharide (39). Hence, to develop a bivalent vaccine formulation against *Shigella* and *Salmonella* spp, a chimeric protein containing T2544 and IpaB was generated. To this end, *Shigella flexneri* 2a *ipab* and *Salmonella* Typhi *t2544* genes were cloned in-frame, which was confirmed by agarose gel electrophoresis of the restriction digestion products (**Supplementary Figure 9A**), followed by nucleotide sequencing (**Supplementary Figure 9B**). The recombinant protein (rIpaB-T2544, 55 kDa) was purified from *E. coli* BL21 (DE3) PlyS by affinity chromatography using Ni-NTA agarose (**Supplementary Figure 9C)** and the purity and size confirmation was by western blots using His-tag antibody (**Supplementary Figure 9D).** The secondary structure of rIpaB-T2544 was analyzed by Far-UV CD spectra that showed one negative band, indicating alpha helix and one positive band, suggesting β helical structure at 222.5 nm and 206 nm, respectively (**Supplementary Figure 9E**).

To check for the protective efficacy of the candidate vaccine against *Shigella* and *Salmonella*, BALB/c mice were immunized intranasally with three doses of the recombinant chimeric protein or the individual proteins that constituted the chimera or the vehicle (PBS) at 14d intervals (**Supplementary Table 4, Figure 9A)**. A 10xLD_{50} oral infection dose of *Shigella* spp. killed all the mice that received either the vehicle or rT2544 within 14 days of infection, whereas 80-90% of the mice immunized with rIpaB-T2544 or rIpaB alone were still alive beyond 20 days (**Figure 9B-D**). Vaccine efficacy against *S.* Typhi and *S.* Paratyphi A, as evaluated in the BALB/c mouse model showed nearly 70% protection following rIpaB-T2544 immunization against 10X LD_{50} doses of *S.* Typhi (5 x 10^7 CFU) or *S.* Paratyphi (5 x 10^5 CFU), while T2544 alone was non-protective with all the immunized mice being dead

within 5-6 days (**Figure 9 E-F)**. This suggested that IpaB acted as an immune adjuvant to T2544 for intranasal vaccination. Moreover, rIpaB-T2544 is a bivalent vaccine candidate against *Shigella* spp. and *Salmonella* (*S.* Typhi and *S.* Paratyphi A), when administered through the intranasal route.

IpaB in the chimeric vaccine candidate augmented serum and mucosal antibody response to T2544, while rIpaB-T2544 induced a balanced T helper cell response

Analysis of serum antibody endpoint titers showed that immunization with rIpaB and rIpaB-T2544 induced similar magnitudes of IpaB-specific IgG, while T2544-specific IgG titers were significantly higher for the chimeric vaccine (**Figure 10 Ai-ii).** The IgG isotypes comprised of IgG1 and IgG2a, indicating induction of both type 1 and type 2 responses, although the latter response was predominant (**Figure 10 Bi-ii).** Serum and intestinal secretory IgA titers followed the same pattern as serum IgG, with identical anti-IpaB titers for rIpaB and rIpaB-T2544 immunizations, but significantly higher anti-T2544 IgA titers for the chimeric protein vaccine (**Figure 10 Ci-ii**). Collectively these results suggested that rIpaB-T2544 was strongly immunogenic and IpaB acted as an immune adjuvant to T2544, significantly boosting the antibody titers in the serum and intestinal secretions.

Cell-mediated immune responses may significantly contribute to vaccine-induced protection, with Th1 response being critical for clear intracellular pathogens and Th2 cells promoting serum antibodies and sIgA production. To assess the cellular immune responses induced by our candidate vaccine, splenocytes isolated from the immunized mice were subjected to mixed leukocyte reaction (MLR) and cultured for 48 h in presence of antigen stimulation. Both Th1 (IL12, IFNγ, TNFα, IL-2) and Th2 (IL-4, IL-5) cytokines, as measured in the culture supernatants were significantly elevated in rIpaB-T2544-immunized mice, as opposed to minimal rise in the vehicle-immunized group (**Figure 10 Di-ii**). These results suggested a balanced T-cell response after immunization with rIpaB-T2544.

Discussion

In this study, we report, to the best of our knowledge, the first murine model of oral *Shigella* infection in a wild-type mouse strain. Iron overload BALB/c mice, pre-treated with streptomycin were susceptible to *S. flexneri 2a* infection of the large intestine, leading to

severe diarrhoea and loss of body weights, colonic inflammation with shortening of the length, neutrophil infiltration, loss of goblet cells, crypt and villus erosions, and enhanced secretion of inflammatory cytokines and chemokines. This model was also useful for the efficacy study of a candidate vaccine against *Shigella*.

Development of an animal model of *Shigella* infection has always been challenging due to the human-restricted nature of the pathogen. Mice being naturally resistant to *Shigella* infection, earlier attempts were directed towards other small animals. Guinea pig keratoconjunctivitis was the first reported model (9), which was useful to differentiate a virulent from a non-virulent strain of *Shigella* and indicated the role of T3SS as the virulence determinant of *Shigella* infection. However, it threw little light on host-pathogen interactions, because of the irrelevant target tissue. Subsequent models that were developed, such as the rabbit ileal loop (8) and rabbit (13) or guinea pig rectal (14) infection model offered more insights into human shigellosis. Especially, the infant rabbit model closely recapitulated the human, commonly observed with *S. dysenteriae* type I infection (rarely found nowadays) and manifested by severe inflammation, massive ulceration of the colonic mucosa, bloody diarrhoea, and marked weight loss, although the authors used more frequently isolated *S. flexneri 2a* for infection (13). Notwithstanding, the above models remained non-physiological due to a different portal of entry for the bacteria. Despite having significant potential to help new drug development, they have limited usefulness for the study of protective host immune responses and development of new vaccines. Attempts were also made by manipulating the mouse intestinal environment or genetic background to establish a *Shigella* infection model. Elimination of the gut microbiota of C57BL/6 mice using an antibiotic cocktail before and after the oral challenge with *Shigella* helped to establish the infection and colitis (41), but the bacteria remained non-invasive, precluding host-pathogen interaction studies. While pre-treatment of mice with a single oral dose of streptomycin was successful to model *S.* Typhimurium colitis (17), similar attempts gave rise to predominantly small intestinal infection with few epithelial lesions and minimal PMN infiltration for oral *Shigella* infection (42), especially with *S. sonnei*. However, susceptibility to shigellosis (*S. flexneri*) dramatically improved for mice genetically deficient in NAIP-NLRC4 inflammasome, giving rise to disease manifestations that follow human infection and the model was used to demonstrate host-protective function for inflammasomes in intestinal epithelial cells (16).

When *Shigella* invades the host cell, it must rapidly adjust to a new environment where it has to derive certain nutrients or metabolic cofactors, such as oxygen, carbon sources and iron,

which are under the host's control. Because free iron is intrinsically toxic, the host has evolved a variety of defence mechanisms, such as the expression of iron-binding proteins to reduce the amount of iron present inside the cells. However, *Shigella* expresses molecules that can take up intracellular iron, including siderophores, heme transporters, and ferric and ferrous iron transport systems (43). *Shigella* use iron for several essential functions, including respiration and DNA replication (19). The role of iron in *Shigella* pathogenesis is underscored by marked upregulation of the iron acquisition systems (Iut, Sit, FhuA, and Feo) and the stress-associated Suf protein in the face of iron starvation by intracellular bacteria (44). In environments where oxygen is scarce, like the gut lumen, feO supplies iron. The Sit system is specifically designed to supply iron to the bacteria growing inside the host cells, since it is expressed in the presence of oxygen and carries ferrous iron (25). The outer membrane receptor needed for aerobactin (siderophore of *Shigella*) import is encoded by the iutA gene. Iron-loaded aerobactin can enter the cell using the general hydroxamate transport system FhuBCD after passing through the outer membrane (45). We established a mouse model of *S. flexneri* in the wild-type background by combining streptomycin pre-treatment with iron overload.

In our study, the pathogenic lesions in the large intestine of the infected mice recovered by day seven, which corresponded to the average disease duration in humans (46). However, other animal models reported faster recovery with more rapid elimination of the bacteria. Rectal biopsy of patients revealed two types of colitis after *Shigella* infection, mild and moderate/severe (47). Histopathological examination of mild colitis showed flattened surface epithelium with erosions, increased cellular infiltration in the lamina propia, absent crypt abscesses, mild mucosal and submucosal edema. In contrast, moderate colitis was characterized by mucosal damage with crypt abscesses and dense neutrophil infiltration into the lamina propria. Histological features in our study were more similar to mild colitis in the human samples. An additional strength of our model was that it worked for multiple pathogenic *Shigella* species. Other mouse models reported are less useful because of the absence of intestinal disease in some cases (48) and the requirement of technical expertise in others (49).

We established productive infection of *S. flexneri* in BALB/c mice. Previous studies reported that intestinal epithelial-specific NAIP-NLRC4 inflammaosome activation protects C57BL/6 mice against *Shigella* infection (16). However, C57BL/6 is a Th1-biased strain, while NLRP3 inflammasome inhibition protects BALB/c mice, which is a Th2-biased strain from human metapneumovirus (50) and Leishmania infection (51, 52). *S. flexneri* type III secretion

603 system effector protein IpaH7.8 E3 ubiquitin ligase plays a pivotal role in NLRP3
604 inflammasome activation in macrophages (53). Studies had shown that Th2 response was
605 associated with the production of IL-4–, IL-5–, and IL-13 cytokines that increased disease
606 susceptibility and persistence in mice (54, 55).
607
608 Our model is a useful adjunct to the existing models, since it is simple, cheap, uses
609 physiological route of infection and appropriate for vaccine efficacy studies . Absence of a
610 suitable animal model has significantly hindered the development of *Shigella* vaccine that is
611 urgently required for the developing world. We report here construction of a subunit vaccine
612 based on the invasin protein IpaB that is conserved across the major pathogenic *Shigella spp.*
613 (*S. flexeneri 2a*, *S. dysenteriae* and *S. Sonnei*) and was incorporated in several vaccine
614 preparations (35, 56). Further, we developed a chimera of IpaB and a conserved outer
615 membrane protein, T2544 from *Salmonella* Typhi and *Salmonella* Paratyphi A (30). We had
616 previously reported that s.c. immunization with recombinant T2544 and a glycoconjugate of
617 T2544 and *S.* Typhimurium OSP conferred protection against multiple *Salmonella* serotypes
618 (39). Serum anti-IpaB endpoint IgG titre (1/ 204800) found in this study was comparable,
619 while serum and fecal IgA titre (1/12800 and 1/1280) were significantly higher compared
620 with the previous reports. Intranasal immunization with a mixture of IpaB and IpaD resulted
621 in IpaB-specific serum IgG and fecal IgA endpoint titres of 1/1000000 and 1/1000,
622 respectively after three doses (35). IpaB specific serum IgG and fecal IgA endpoint titre were
623 found to be 1/1000000 and 1/100 following immunization with chimeric ipaB-IpaD along
624 with dmlt (56). Another study found that when adjuvant rGroEL was added to rIpaB, the
625 resulting IgG and IgA antibody titers increased by 1.5 and 1.3 times, respectively, in
626 comparison to rIpaB alone (57). The mixture of IpaB/IpaD showed 90% and 30% protection
627 against a 11- and 24-median LD_{50} dose of *Shigella flexeneri 2a*, while 80% and 50%
628 protection was observed against a 5- and 9-median LD_{50} dose of *Shigella sonnei* (35). Mice
629 immunized with IpaB-IpaD fusion protein containing double mutant LT (dmLT) confers
630 70%, 100% and 40% protection against lethal dose of *S. flexeneri*, *S. sonnei* and *S.*
631 *dysenteriae* (56). On the other hand, rIpaB+GroEL immunized mice showed 80% protection
632 against the lethal dose of *S. flexeneri*, *S. sonnei*, and *S. boydii* (57). In our study, the vaccine
633 chimera, rIpaB-T2544 was equally efficacious, where 90% protection was found for *S.*
634 *flexeneri* and 80% protection was found for *S. sonnei* and *S. dysenteriae* with 10X LD_{50} dose,
635 which were similar to the protection observed in the pulmonary infection model (35, 57). An

interesting finding for our study was 16-fold increase in T2544-specific IgG antibody titres in the mice immunized with rIpaB-T2544 chimera antigen compared with rT2544 administered as a sole antigen. In addition, T2544-specific IgA titre was 40-fold higher in the serum, and 16-fold higher in the fecal and intestinal washes. In the protection study, rIpaB-T2544-immunized mice showed 70% protection against *Salmonella* Typhi and Paratyphi A, while no protection was found with rT2544 alone. These results suggested that rIpaB acts as an adjuvant that enhances the immunogenicity of T2544.

IFNγ production is required for the protection of mice against *Shigella* infection (58). *Shigella* replicates intracellularly and multiplies further when IFNγ is not present, indicating that an IFNγ-mediated mechanism is in place to limit infection (59). Production of IFNγ-in response to IpaB was demonstrated using peripheral blood mononuclear cells (PBMCs) from infected individuals (60) or other vaccine candidates (57, 35, 56). In our study, mice immunized with rIpaB-T2544 enhanced IFNγ production along with other cytokines (IL-12, TNF-α, IL-2), indicating Th1 lymphocytes activation.

A potential limitation of our mouse model is the requirement for antibiotic pre-treatment, which alters the gut microbiota. Iron further alters the resident microbial population. This indicates that the model is not suitable to study *Shigella* infection in the context of microbial communities. As *Shigella* infection globally occurs due to the predominance of *Shigella flexneri* strain, other strains of Shigella were not used for the model establishment in our study. Furthermore, for the model development and the potential of its use in vaccine-induced protection studies, we used virulent *Shigella spp* only. *Shigella* pathogenesis is attributable to a multitude of virulence factors that enable the bacteria to invade and proliferate within the colonic epithelial cells and evade host immune responses. Most known virulence factors of *Shigella* are encoded by a large (200-kbp) virulence plasmid, which is essential for *Shigella* pathogenicity (11–13). All the strains used in our study contained the virulence plasmid, as revealed by the positive Congo Red stain. Many of the virulence factors of *Shigella*, such as IcsA/VirG are essential for pathogenesis, rendering the mutants avirulent. It would be important to study if the virulence factors that serve non-redundant role during human and some other animal infections (14, 16) are also critical for pathogenesis in the novel mouse model developed by us. This study will inform us if this mouse model could be useful for mechanistic studies into human shigellosis. However, this is out of scope of the current manuscript. We did not examine *Shigella* pathogenesis in terms of vacuolar escape or cell to cell spread in the intestinal epithelium. IpaB is a known immunogenic protein and has been

studied as a candidate vaccine for tests in a lethal pulmonary mouse model; however, we did not repeat the protective efficacy study for IpaB in the mouse lung model. Further, we did not compare the immune cells population activated by IpaB or IpaB-T2544. Instead, we only determined the vaccine efficacy of IpaB and IpaB-T2544 against *Shigella* spp. In our preclinical study, we have used the intranasal route of immunization, since intranasal delivery of IpaB and IpaD were reported to confer better protection in comparison with the intradermal delivery in mice (61). Although intranasal immunization with native invaplex was well tolerated and immunogenic in phase 1 studies (62, 63), one potential limitation was the failure of protection in a CHIM trial (64).

Conflict of interest

The authors have or do not have an association that might pose a conflict of interest (e.g., pharmaceutical stock ownership, consultancy, advisory board membership, relevant patents or research funding).

Author contributions

S.D., S.M., and R.H. had conceptualized the work. R.H. performed all the experiments and analyzed the data. P.H. and H.K. helped in the animal experiment. S.D. and R.H. wrote the paper. S.M. critically read the paper and provided valuable inputs.

Funding

This work was supported by extramural grants from Indian Council of Medical Research, Government of India (58/17/2020/PHA/BMS) and the Japan Agency for Medical Research and Development (AMED; Grant No. JP23wm0125004).

Acknowledgments

Risha Haldar acknowledges the University Grant Commission (UGC) [student ID-191620094970] to get the fellowship for this study. Prolay Halder acknowledges Indian Council of Medical Research to get the fellowship [ICMR fellowship ID No. 3/1/3/JRF-2018/HRD-066(66125)] for this study. We acknowledge Dr. Ashis Debnath, veterinary

pathologist for blind histological score assessment. All other authors acknowledge Indian Council of Medical Research (ICMR), National Institute of Cholera and Enteric Diseases (NICED) and Japan Agency for Medical Research and Development (AMED; Grant No. JP23wm0125004).

Data availability statement

The raw data supporting the conclusions of this article will be made available by the authors, without undue reservation.

References

1. Watkins LKF, Appiah GD: Chapter 4: travel-related infectious diseases-shigellosis. CDC Yellow Book 2020. Oxford University Press; 2020.
2. Mattock E, Blocker AJ. How Do the Virulence Factors of Shigella Work Together to Cause Disease? Front Cell Infect Microbiol. 2017 Mar 24;7:64. doi: 10.3389/fcimb.2017.00064. PMID: 28393050; PMCID: PMC5364150.
3. Mathan MM, Mathan VI. Morphology of rectal mucosa of patients with shigellosis. Rev Infect Dis. 1991 Mar-Apr;13 Suppl 4:S314-8. doi: 10.1093/clinids/13.supplement_4.s314. PMID: 2047656.
4. Schnupf P, Sansonetti PJ. *Shigella* Pathogenesis: New Insights through Advanced Methodologies. Microbiol Spectr. 2019 Mar;7(2). doi: 10.1128/microbiolspec.BAI-0023-2019. PMID: 30953429.
5. Phalipon A, Sansonetti PJ. Shigella's ways of manipulating the host intestinal innate and adaptive immune system: a tool box for survival? Immunol Cell Biol. 2007 Feb-Mar;85(2):119-29. doi: 10.1038/sj.icb7100025. Epub 2007 Jan 9. PMID: 17213832.
6. Shipley ST, Panda A, Khan AQ, Kriel EH, Maciel M Jr, Livio S, Nataro JP, Levine MM, Sztein MB, DeTolla LJ. A challenge model for Shigella dysenteriae 1 in cynomolgus monkeys (Macaca fascicularis). Comp Med. 2010 Feb;60(1):54-61. PMID: 20158950; PMCID: PMC2826086.
7. Islam D, Ruamsap N, Khantapura P, Aksomboon A, Srijan A, Wongstitwilairoong B, Bodhidatta L, Gettayacamin M, Venkatesan MM, Mason CJ. Evaluation of an intragastric challenge model for Shigella dysenteriae 1 in rhesus monkeys (Macaca mulatta) for the pre-clinical assessment of Shigella vaccine formulations. APMIS.

2014 Jun;122(6):463-75. doi: 10.1111/apm.12168. Epub 2013 Sep 13. PMID: 24028276; PMCID: PMC3954967.

8. Arm Hg, Floyd Tm, Faber Je, Hayes Jr. Use Of Ligated Segments Of Rabbit Small Intestine In Experimental Shigellosis. J Bacteriol. 1965 Mar;89(3):803-9. doi: 10.1128/jb.89.3.803-809.1965. PMID: 14273664; PMCID: PMC277540.
9. Mackel Dc, Langley Lf, Venice La. The use of the guinea-pig conjunctivae as an experimental model for the study of virulence of Shigella organisms. Am J Hyg. 1961 Mar;73:219-23. doi: 10.1093/oxfordjournals.aje.a120179. PMID: 13764890.

10. Fernandez MI, Thuizat A, Pedron T, Neutra M, Phalipon A, Sansonetti PJ. A newborn mouse model for the study of intestinal pathogenesis of shigellosis. Cell Microbiol. 2003 Jul;5(7):481-91. doi: 10.1046/j.1462-5822.2003.00295.x. PMID: 12814438.
11. Phalipon A, Kaufmann M, Michetti P, Cavaillon JM, Huerre M, Sansonetti P, Kraehenbuhl JP. Monoclonal immunoglobulin A antibody directed against serotype-specific epitope of Shigella flexneri lipopolysaccharide protects against murine experimental shigellosis. J Exp Med. 1995 Sep 1;182(3):769-78. doi: 10.1084/jem.182.3.769. PMID: 7544397; PMCID: PMC2192169.
12. Sansonetti PJ, Phalipon A, Arondel J, Thirumalai K, Banerjee S, Akira S, Takeda K, Zychlinsky A. Caspase-1 activation of IL-1beta and IL-18 are essential for Shigella flexneri-induced inflammation. Immunity. 2000 May;12(5):581-90. doi: 10.1016/s1074-7613(00)80209-5. PMID: 10843390.
13. Yum LK, Byndloss MX, Feldman SH, Agaisse H. Critical role of bacterial dissemination in an infant rabbit model of bacillary dysentery. Nat Commun. 2019 Apr 23;10(1):1826. doi: 10.1038/s41467-019-09808-4. PMID: 31015451; PMCID: PMC6478941.
14. Shim DH, Suzuki T, Chang SY, Park SM, Sansonetti PJ, Sasakawa C, Kweon MN. New animal model of shigellosis in the Guinea pig: its usefulness for protective efficacy studies. J Immunol. 2007 Feb 15;178(4):2476-82. doi: 10.4049/jimmunol.178.4.2476. PMID: 17277155.
15. Yang JY, Lee SN, Chang SY, Ko HJ, Ryu S, Kweon MN. A mouse model of shigellosis by intraperitoneal infection. J Infect Dis. 2014 Jan 15;209(2):203-15. doi: 10.1093/infdis/jit399. Epub 2013 Jul 31. PMID: 23904297.
16. Mitchell PS, Roncaioli JL, Turcotte EA, Goers L, Chavez RA, Lee AY, Lesser CF, Rauch I, Vance RE. NAIP-NLRC4-deficient mice are susceptible to shigellosis. Elife.

765 2020 Oct 19;9:e59022. doi: 10.7554/eLife.59022. PMID: 33074100; PMCID:
766 PMC7595732.
767 17. Barthel M, Hapfelmeier S, Quintanilla-Martínez L, Kremer M, Rohde M, Hogardt M,
768 Pfeffer K, Rüssmann H, Hardt WD. Pretreatment of mice with streptomycin provides
769 a Salmonella enterica serovar Typhimurium colitis model that allows analysis of both
770 pathogen and host. Infect Immun. 2003 May;71(5):2839-58. doi:
771 10.1128/IAI.71.5.2839-2858.2003. PMID: 12704158; PMCID: PMC153285.
772 18. Suar M, Jantsch J, Hapfelmeier S, Kremer M, Stallmach T, Barrow PA, Hardt WD.
773 Virulence of broad- and narrow-host-range Salmonella enterica serovars in the
774 streptomycin-pretreated mouse model. Infect Immun. 2006 Jan;74(1):632-44. doi:
775 10.1128/IAI.74.1.632-644.2006. PMID: 16369020; PMCID: PMC1346614.
776 19. Wei Y, Murphy ER. Shigella Iron Acquisition Systems and their Regulation. Front
777 Cell Infect Microbiol. 2016 Feb 9;6:18. doi: 10.3389/fcimb.2016.00018. PMID:
778 26904516; PMCID: PMC4746246.
779 20. James A. Imlay et al. Toxic DNA Damage by Hydrogen Peroxide Through the Fenton
780 Reaction in Vivo and in Vitro.Science240,640-
781 642(1988).DOI:10.1126/science.2834821
782 21. JONES, R., PETERSON, C., GRADY, R. et al. Effects of iron chelators and iron
783 overload on Salmonella infection. Nature 267, 63–65 (1977).
784 https://doi.org/10.1038/267063a0
785 22. Mobarra N, Shanaki M, Ehteram H, Nasiri H, Sahmani M, Saeidi M, Goudarzi M,
786 Pourkarim H, Azad M. A. Review on Iron Chelators in Treatment of Iron Overload
787 Syndromes. Int J Hematol Oncol Stem Cell Res. 2016 Oct 1;10(4):239-247. PMID:
788 27928480; PMCID: PMC5139945.
789 23. Autenrieth IB, Bohn E, Ewald JH, Heesemann J. Deferoxamine B but not
790 deferoxamine G1 inhibits cytokine production in murine bone marrow macrophages. J
791 Infect Dis. 1995 Aug;172(2):490-6. doi: 10.1093/infdis/172.2.490. PMID: 7622893.
792 24. Saldaña-Ahuactzi Z, Knodler LA. FoxR is an AraC-like transcriptional regulator of
793 ferrioxamine uptake in Salmonella enterica. Mol Microbiol. 2022 Oct;118(4):369-
794 386. doi: 10.1111/mmi.14970. Epub 2022 Aug 15. PMID: 35970762; PMCID:
795 PMC9804782.
796 25. Mey AR, Gómez-Garzón C, Payne SM. Iron Transport and Metabolism in
797 Escherichia, Shigella, and Salmonella. EcoSal Plus. 2021 Dec

15;9(2):eESP00342020. doi: 10.1128/ecosalplus.ESP-0034-2020. Epub 2021 Dec 13. PMID: 34910574; PMCID: PMC8865473.

26. Abbas M, Hayirli Z, Drakesmith H, Andrews SC and Lewis MC (2022) Effects of iron deficiency and iron supplementation at the host-microbiota interface: Could a piglet model unravel complexities of the underlying mechanisms? Front. Nutr. 9:927754. doi: 10.3389/fnut.2022.927754.
27. Kortman GA, Boleij A, Swinkels DW, Tjalsma H. Iron availability increases the pathogenic potential of Salmonella typhimurium and other enteric pathogens at the intestinal epithelial interface. PLoS One. 2012;7(1):e29968. doi: 10.1371/journal.pone.0029968. Epub 2012 Jan 17. PMID: 22272265; PMCID: PMC3260200.
28. Cork SC, Marshall RB, Fenwick SG. The effect of parenteral iron dextran, with or without desferrioxamine, on the development of experimental pseudotuberculosis in the domestic chicken. Avian Pathol. 1998;27(4):394-9. doi: 10.1080/03079459808419357. PMID: 18484018.
29. Robins-Browne RM, Prpic JK. Effects of iron and desferrioxamine on infections with Yersinia enterocolitica. Infect Immun. 1985 Mar;47(3):774-9. doi: 10.1128/iai.47.3.774-779.1985. PMID: 3972453; PMCID: PMC261386.
30. Ghosh S, Chakraborty K, Nagaraja T, Basak S, Koley H, Dutta S, Mitra U, Das S. An adhesion protein of Salmonella enterica serovar Typhi is required for pathogenesis and potential target for vaccine development. Proc Natl Acad Sci U S A. 2011 Feb 22;108(8):3348-53. doi: 10.1073/pnas.1016180108. Epub 2011 Feb 7. PMID: 21300870; PMCID: PMC3044360.
31. Muthuramalingam M, Whittier SK, Picking WL, Picking WD. The Shigella Type III Secretion System: An Overview from Top to Bottom. Microorganisms. 2021 Feb 22;9(2):451. doi: 10.3390/microorganisms9020451. PMID: 33671545; PMCID: PMC7926512.
32. Shimanovich AA, Buskirk AD, Heine SJ, Blackwelder WC, Wahid R, Kotloff KL, Pasetti MF. Functional and Antigen-Specific Serum Antibody Levels as Correlates of Protection against Shigellosis in a Controlled Human Challenge Study. Clin Vaccine Immunol. 2017 Feb 6;24(2):e00412-16. doi: 10.1128/CVI.00412-16. PMID: 27927680; PMCID: PMC5299116.
33. Bernshtein B, Ndungo E, Cizmeci D, Xu P, Kovác P, Kelly M, Islam D, Ryan ET, Kotloff KL, Pasetti MF, Alter G. 2022. Systems approach to define humoral

correlates of immunity to Shigella. Cell Rep 40:111216. https://doi .org/10.1016/j.celrep.2022.111216.

34. WaySS, Borczuk AC, Dominitz R, Goldberg MB. 1998. An essential role for gamma interferon in innate resistance to Shigella flexneri infection. Infect. Immun. 66:1342–1348.
35. Martinez-Becerra FJ, Kissmann JM, Diaz-McNair J, Choudhari SP, Quick AM, Mellado-Sanchez G, Clements JD, Pasetti MF, Picking WL. Broadly protective Shigella vaccine based on type III secretion apparatus proteins. Infect Immun. 2012 Mar;80(3):1222-31. doi: 10.1128/IAI.06174-11. Epub 2011 Dec 27. PMID: 22202122; PMCID: PMC3294653.
36. Heine SJ, Diaz-McNair J, Martinez-Becerra FJ, Choudhari SP, Clements JD, Picking WL, Pasetti MF. Evaluation of immunogenicity and protective efficacy of orally delivered Shigella type III secretion system proteins IpaB and IpaD. Vaccine. 2013 Jun 19;31(28):2919-29. doi: 10.1016/j.vaccine.2013.04.045. Epub 2013 May 2. PMID: 23644075; PMCID: PMC3718310.
37. Ndungo E, Randall A, Hazen TH, Kania DA, Trappl-Kimmons K, Liang X, Barry EM, Kotloff KL, Chakraborty S, Mani S, Rasko DA, Pasetti MF. A Novel Shigella Proteome Microarray Discriminates Targets of Human Antibody Reactivity following Oral Vaccination and Experimental Challenge. mSphere. 2018 Aug 1;3(4):e00260-18. doi: 10.1128/mSphere.00260-18. PMID: 30068560; PMCID: PMC6070737.
38. Das S, Chowdhury R, Pal A, Okamoto K, Das S. Salmonella Typhi outer membrane protein STIV is a potential candidate for vaccine development against typhoid and paratyphoid fever. Immunobiology. 2019 May;224(3):371-382. doi: 10.1016/j.imbio.2019.02.011. Epub 2019 Mar 22. PMID: 30952553.
39. Haldar R, Dhar A, Ganguli D, Chakraborty S, Pal A, Banik G, Miyoshi SI, Das S. A candidate glycoconjugate vaccine induces protective antibodies in the serum and intestinal secretions, antibody recall response and memory T cells and protects against both typhoidal and non-typhoidal Salmonella serovars. Front Immunol. 2024 Jan 9;14:1304170. doi: 10.3389/fimmu.2023.1304170. PMID: 38264668; PMCID: PMC10804610.
40. Orenstein R. Gastroenteritis, Viral. Encyclopedia of Gastroenterology. 2020:652–7. doi: 10.1016/B978-0-12-801238-3.65973-1. Epub 2019 Nov 1. PMCID: PMC7173604

41. Q S Medeiros PH, Ledwaba SE, Bolick DT, Giallourou N, Yum LK, Costa DVS, Oriá RB, Barry EM, Swann JR, Lima AÂM, Agaisse H, Guerrant RL. A murine model of diarrhea, growth impairment and metabolic disturbances with *Shigella flexneri* infection and the role of zinc deficiency. Gut Microbes. 2019;10(5):615-630. doi: 10.1080/19490976.2018.1564430. Epub 2019 Feb 3. PMID: 30712505; PMCID: PMC6748602.
42. Martino MC, Rossi G, Martini I, Tattoli I, Chiavolini D, Phalipon A, Sansonetti PJ, Bernardini ML. Mucosal lymphoid infiltrate dominates colonic pathological changes in murine experimental shigellosis. J Infect Dis. 2005 Jul 1;192(1):136-48. doi: 10.1086/430740. Epub 2005 May 31. PMID: 15942903.
43. Payne SM, Wyckoff EE, Murphy ER, Oglesby AG, Boulette ML, Davies NM. Iron and pathogenesis of Shigella: iron acquisition in the intracellular environment. Biometals. 2006 Apr;19(2):173-80. doi: 10.1007/s10534-005-4577-x. PMID: 16718602.

44. Killackey SA, Sorbara MT and Girardin SE (2016) Cellular Aspects of Shigella Pathogenesis: Focus on the Manipulation of Host Cell Processes. Front. Cell. Infect. Microbiol. 6:38. doi: 10.3389/fcimb.2016.00038.
45. Fecker L, Braun V.1983.Cloning and expression of the fhu genes involved in iron(III)-hydroxamate uptake by Escherichia coli. J Bacteriol156:.https://doi.org/10.1128/jb.156.3.1301-1314.1983
46. Clements D, Ellis CJ, Allan RN. Persistent shigellosis. Gut. 1988 Sep;29(9):1277-8. doi: 10.1136/gut.29.9.1277. PMID: 3058558; PMCID: PMC1434353.
47. Anand BS, Malhotra V, Bhattacharya SK, Datta P, Datta D, Sen D, Bhattacharya MK, Mukherjee PP, Pal SC. Rectal histology in acute bacillary dysentery. Gastroenterology. 1986 Mar;90(3):654-60. doi: 10.1016/0016-5085(86)91120-0. PMID: 3510937.
48. pulmonary (Mallett CP, VanDeVerg L, Collins HH, Hale TL. Evaluation of Shigella vaccine safety and efficacy in an intranasally challenged mouse model. Vaccine. 1993;11(2):190-6. doi: 10.1016/0264-410x(93)90016-q. PMID: 8438617.
49. Zhang Z, Jin L, Champion G, Seydel KB, Stanley SL Jr. Shigella infection in a SCID mouse-human intestinal xenograft model: role for neutrophils in containing bacterial dissemination in human intestine. Infect Immun. 2001 May;69(5):3240-7. doi: 10.1128/IAI.69.5.3240-3247.2001. PMID: 11292746; PMCID: PMC98282.

50. Lê VB, Dubois J, Couture C, Cavanagh MH, Uyar O, Pizzorno A, Rosa-Calatrava M, Hamelin MÈ, Boivin G. Human metapneumovirus activates NOD-like receptor protein 3 inflammasome via its small hydrophobic protein which plays a detrimental role during infection in mice. PLoS Pathog. 2019 Apr 9;15(4):e1007689. doi: 10.1371/journal.ppat.1007689. PMID: 30964929; PMCID: PMC6474638.
51. Lima-Junior DS, Costa DL, Carregaro V, Cunha LD, Silva AL, Mineo TW, Gutierrez FR, Bellio M, Bortoluci KR, Flavell RA, Bozza MT, Silva JS, Zamboni DS. Inflammasome-derived IL-1β production induces nitric oxide-mediated resistance to Leishmania. Nat Med. 2013 Jul;19(7):909-15. doi: 10.1038/nm.3221. Epub 2013 Jun 9. PMID: 23749230.
52. Gurung P, Karki R, Vogel P, Watanabe M, Bix M, Lamkanfi M, Kanneganti TD. An NLRP3 inflammasome-triggered Th2-biased adaptive immune response promotes leishmaniasis. J Clin Invest. 2015 Mar 2;125(3):1329-38. doi: 10.1172/JCI79526. Epub 2015 Feb 17. PMID: 25689249; PMCID: PMC4362229.
53. Suzuki S, Mimuro H, Kim M, Ogawa M, Ashida H, Toyotome T, Franchi L, Suzuki M, Sanada T, Suzuki T, Tsutsui H, Núñez G, Sasakawa C. Shigella IpaH7.8 E3 ubiquitin ligase targets glomulin and activates inflammasomes to demolish macrophages. Proc Natl Acad Sci U S A. 2014 Oct 7;111(40):E4254-63. doi: 10.1073/pnas.1324021111. Epub 2014 Sep 22. PMID: 25246571; PMCID: PMC4210038.
54. Scott P, Natovitz P, Coffman RL, Pearce E, Sher A. Immunoregulation of cutaneous leishmaniasis. T cell lines that transfer protective immunity or exacerbation belong to different T helper subsets and respond to distinct parasite antigens. J Exp Med. 1988 Nov 1;168(5):1675-84. doi: 10.1084/jem.168.5.1675. PMID: 2903212; PMCID: PMC2189120.
55. Heinzel FP, Sadick MD, Mutha SS, Locksley RM. Production of interferon gamma, interleukin 2, interleukin 4, and interleukin 10 by CD4+ lymphocytes in vivo during healing and progressive murine leishmaniasis. Proc Natl Acad Sci U S A. 1991 Aug 15;88(16):7011-5. doi: 10.1073/pnas.88.16.7011. PMID: 1908085; PMCID: PMC52223.
56. Martinez-Becerra FJ, Chen X, Dickenson NE, Choudhari SP, Harrison K, Clements JD, Picking WD, Van De Verg LL, Walker RI, Picking WL. Characterization of a novel fusion protein from IpaB and IpaD of Shigella spp. and its potential as a pan-

Shigella vaccine. Infect Immun. 2013 Dec;81(12):4470-7. doi: 10.1128/IAI.00859-13. Epub 2013 Sep 23. PMID: 24060976; PMCID: PMC3837967.

57. Chitradevi, S., Kaur, G., Uppalapati, S. et al. Co-administration of rIpaB domain of Shigella with rGroEL of S. Typhi enhances the immune responses and protective efficacy against Shigella infection. Cell Mol Immunol 12, 757–767 (2015). https://doi.org/10.1038/cmi.2014.86.
58. Le-Barillec K, Magalhaes JG, Corcuff E, Thuizat A, Sansonetti PJ, Phalipon A, Di Santo JP. Roles for T and NK cells in the innate immune response to Shigella flexneri. J Immunol. 2005 Aug 1;175(3):1735-40. doi: 10.4049/jimmunol.175.3.1735. PMID: 16034114.
59. Raqib R, Qadri F, SarkEr P, Mia SM, Sansonnetti PJ, Albert MJ, Andersson J. Delayed and reduced adaptive humoral immune responses in children with shigellosis compared with in adults. Scand J Immunol. 2002 Apr;55(4):414-23. doi: 10.1046/j.1365-3083.2002.01079.x. PMID: 11967124.
60. Way SS, Borczuk AC, Dominitz R, Goldberg MB. An essential role for gamma interferon in innate resistance to Shigella flexneri infection. Infect Immun. 1998 Apr;66(4):1342-8. doi: 10.1128/IAI.66.4.1342-1348.1998. PMID: 9529051; PMCID: PMC108058.
61. Heine SJ, Diaz-McNair J, Andar AU, Drachenberg CB, van de Verg L, Walker R, Picking WL, Pasetti MF. Intradermal delivery of Shigella IpaB and IpaD type III secretion proteins: kinetics of cell recruitment and antigen uptake, mucosal and systemic immunity, and protection across serotypes. J Immunol. 2014 Feb 15;192(4):1630-40. doi: 10.4049/jimmunol.1302743. Epub 2014 Jan 22. PMID: 24453241; PMCID: PMC3998105.
62. Tribble D, Kaminski R, Cantrell J, Nelson M, Porter C, Baqar S, Williams C, Arora R, Saunders J, Ananthakrishnan M, Sanders J, Zaucha G, Turbyfill R, Oaks E. Safety and immunogenicity of a Shigella flexneri 2a Invaplex 50 intranasal vaccine in adult volunteers. Vaccine. 2010 Aug 23;28(37):6076-85. doi: 10.1016/j.vaccine.2010.06.086. Epub 2010 Jul 7. PMID: 20619378.
63. Riddle MS, Kaminski RW, Williams C, Porter C, Baqar S, Kordis A, Gilliland T, Lapa J, Coughlin M, Soltis C, Jones E, Saunders J, Keiser PB, Ranallo RT, Gormley R, Nelson M, Turbyfill KR, Tribble D, Oaks EV. Safety and immunogenicity of an intranasal Shigella flexneri 2a Invaplex 50 vaccine. Vaccine. 2011 Sep

16;29(40):7009-19. doi: 10.1016/j.vaccine.2011.07.033. Epub 2011 Jul 23. PMID: 21787825.

64. Harro, C.R.; Riddle, M.S.; Kaminski, R.; Turbyfill, K.R.; Gormley, R.; Porter, C.; Ranallo, R.T.; Kordis, A.; Buck, M.; Jones, A. Shigella flexneri 2a Invaplex 50 intranasal vaccine phase 2b challenge study. In Proceedings of the Vaccines for Enteric Diseases, Malaga, Spain, 9–11 September 2009.

Figure legends

Figure 1. Survival assay with different doses of *Shigella flexeneri 2a*. Kaplan-Meyer plot of cumulative mortality of BALB/c mice (n=6). Different groups of mice were infected (A, B, C, E) with *Shigella flexeneri 2a* with different doses while one group remained uninfected (D). The mortality of mice was observed for 20 days. The color scheme used to mark different bacteria doses are as follows; green-5×10^7 CFU; black- 5×10^8 CFU; and red- 5×10^9 CFU.

Figure 2. Adult mice were susceptible to oral infection with *S. flexneri 2a* strain at a dose of 5×10^7. BALB/c mice were orally infected with 5×10^7 dose of *S. flexneri 2a*. (A) Photographs of the anal region of BALB/c mice of different groups at different post-infection time points. A representative image from three independent experiments (n=4 mice per group) is shown. (B) Body weight changes post-infection. Data represent mean ± SEM values of multiple animals (n=4 mice per group) at each time point. Statistical analyses were performed by one-way ANOVA and Tukey's post-test for multiple comparisons, *P < 0.05, **P < 0.01, ***P <0.001. (C) Colony forming units (CFU) of *S. flexneri 2a* in the colon, cecum, and feces of infected and control mice at different post infection time points. All the tissue homogenates were cultured overnight on TSA plate. Data represent mean ± SEM of the values from multiple animals (n=6 mice per group). Statistical analyses were performed by one-way ANOVA and Tukey's post-test for multiple comparisons, *P < 0.05, **P < 0.01, ***P <0.001.

Figure 3. Susceptible adult mice showed decreased colon length after oral infection with *S. flexneri 2a* strain at a dose of 5×10^7. (A) Colonic shortening after the infection. Caecum and ascending colon isolated from the infected and uninfected mice, sacrificed at different time points post-infection. A representative image from three independent experiments (n=6 mice per group) is shown. (B) Graphical representation of Colon length. Data represent mean ± SEM of the values from multiple animals (n=6 mice per group). Statistical analyses were performed using one-way ANOVA and Tukey's post-test for multiple comparisons; *P < 0.05, **P < 0.01, ***P <0.001.

Figure 4. Histology sections of the colon and caecum tissue of BALB/c mice after different treatments. Different groups of mice (n=6 mice per group) were infected with 5×10^7 CFU *Shigella flexeneri 2a* and sacrificed at the indicated time points. Colon and caecum were excised, fixed, and embedded in paraffin. Tissue sections were stained with Hematoxylin & Eosin and observed in a microscope (40x magnification, Scale bar =10 μm). The images are the magnified form of the 10X images (areas of green box) presented in supplementary information. Intact crypt architecture with abundant records of goblet cells, intact mucosa and submucosa without abnormal infiltrates were observed in the control group of mice (i-iv). Streptomycin-iron with infected group (v) showed loss of crypt architecture with decreased goblet cells, increased infiltration of lymphocytes in the mucosa and submucosa. Black round dotted circles represent intact crypt architecture and blue round dotted circles represent loss of crypt architecture. Different colors of arrow indicate different parameters as follows; yellow arrow- abundant goblet cells; green arrow- loss of goblet cells; red arrow- lymphocyte infiltration in the mucosa; blue arrow- lymphocyte infiltration in the submucosa.

Figure 5. Proinflammatory cytokine and chemokine induction after *Shigella flexeneri 2a* infection. Streptomycin and iron pre-treated BALB/c mice (n=4) were infected with 5×10^7 CFU *Shigella flexeneri 2a.* ELISA performed with the colonic tissue homogenates for the proinflammatory cytokines (A-C) and chemokines (D). Data represent mean ± SEM values from different mice samples (n=4). Statistical analyses were performed with two-tailed Student's t-test (**P < 0.01, ***P < 0.001, ****P <0.0001) between two different groups.

Figure 6. Intranasal immunization with recombinant IpaB augmented humoral immune response and protects mice against oral *Shigella* infections. (A) Experimental schedule of Immunization, sample collection and bacterial challenge of BALB/c mice. (B) Time kinetics of antigen-specific total IgG in the mouse serum as measured by ELISA. Data represent mean ± SEM values from different mice samples (n=5). X-axis indicate the time points after the start of the immunization when samples were collected. Statistical analysis was performed using two-way ANOVA and Tukey's post-test for multiple comparisons, ****P < 0.0001. The colour scheme used to mark different experimental groups are as follows: PBS-black; rIpaB-red. (C) Kaplan-Meyer plot of cumulative mortality of the mice immunized intranasally with vehicle or the recombinant protein. Ten days after the last immunization (38d), immunized mice were pre-treated with streptomycin and iron followed by oral infection with different *Shigella* spp. (*Shigella flexeneri 2a* (5×10^9 CFU, n= 10), *Shigella* dysenteriae (5×10^8 CFU, n= 10), *Shigella* sonnei (5×10^8 CFU, n= 10) and monitored for 20 days. The colour scheme used to mark different experimental groups are as follows: PBS-black; rIpaB-red.

Figure 7. rIpaB immunized mice were not susceptible to infection following oral administration of *S. flexneri 2a*. BALB/c mice were immunized intranasally with Vehicle (PBS) and rIpaB (40µg/mouse) on days 0, 14, and 28. Ten days after the last immunization (38d), immunized mice were pre-treated with Streptomycin and iron followed by oral infection with 5×10^7 CFU bacteria. (A) Photos of the anal region of immunized groups at 24 hours of post-infection. Experiment was repeated three times and one image out of three independent experiments (n=6) is shown. (B) Body weight changes were monitored between infected and uninfected groups at different post-infection time points. Data represent mean ± SEM values from different mice samples (n=5). Statistical analyses were performed with two-tailed Student's t-test (****P<0.0001). (C) Mice were sacrificed at the indicated time points and the colon length of the respective groups were observed. (C i), Representative photograph of the colon length of different groups of mice. Experiment was repeated three times and one image out of three independent experiments is shown. (C ii), Bar representing the comparison of the colon length between two groups of mice. Data represent mean ± SEM values from different mice samples (n=3). Statistical analyses were performed with two-tailed Student's t-test (**P < 0.01, ***P < 0.001, ****P<0.0001). (D) Colony forming units (CFU) in homogenates of colon, cecum, and feces. Data represent mean ± SEM of the values from

multiple animals (n=3). Statistical analyses were performed by one-way ANOVA and Tukey's post-test for multiple comparisons, *P < 0.05, **P < 0.01, ***P <0.001.

Figure 8. Histology sections of colon and caecum of immunized and unimmunized BALB/c mice after infection. BALB/c mice (n=10) were immunized intranasally with Vehicle (PBS) and rIpaB (40µg/mouse) on days 0, 14, and 28. Ten days after the last immunization (38d), immunized mice were pre-treated with streptomycin and iron followed by oral infection with 5× 10^7 CFU bacteria. Mice were sacrificed at the indicated time points. Colon and caecum were excised, fixed, and embedded in paraffin. Tissue sections were stained with Hematoxylin & Eosin and observed in a microscope (40x magnification, Scale bar =10 µm). The images are the magnified form of the 10X images (areas of green box) presented in supplementary information. Intact crypt architecture with abundant records of goblet cells, intact mucosa and submucosa without abnormal infiltrates were observed in the control group of mice (i-iv). Streptomycin-iron with infected group (v) showed loss of crypt architecture with decreased goblet cells, increased infiltration of lymphocytes in the mucosa and submucosa. Black round dotted circles represent intact crypt architecture and blue round dotted circles represent loss of crypt architecture. Different colors of arrow indicates different parameters as follows; yellow arrow- abundant goblet cells; green arrow- loss of goblet cells; red arrow- lymphocyte infiltration in the mucosa; blue arrow- lymphocyte infiltration in the submucosa.

Figure 9. Intranasal immunization with recombinant chimeric protein, IpaB-T2544 protects mice against oral *Shigella* and typhoidal *Salmonella* infections. (A) Experimental schedule of Immunization, sample collection and bacterial challenge of BALB/c mice. (B-F) Kaplan-Meyer plot of cumulative mortality of the mice immunized intranasally with vehicle, chimeric (rIpaB-T2544) or the recombinant proteins (rIpaB, rT2544). One set of immunized mice were pre-treated with Streptomycin and iron followed by oral infection with *Shigella* flexeneri 2a (5 x 10^9 CFU, n= 10) (B), *Shigella* dysenteriae (5 x 10^8 CFU, n= 10) (C), *Shigella* sonnei (5 x 10^8 CFU, n= 10) (D) and monitored for 20 days. Other sets of immunized mice were pre-treated with iron followed by oral infection with S. Typhi (5 x 107 CFU, n= 10) (E) and S. Paratyphi A (5 x 105 CFU, n=10) (F) and monitored

for 10 days. The colour scheme used to mark different experimental groups are as follows: PBS-black; rT2544-green; rIpaB-red; rIpaB-T2544-blue.

Figure 10. Humoral and mucosal adjuvanticity of rIpaB and balanced TH1 and TH2 cytokine production from splenocytes of intranasal rIpaB-T2544 immunized mice. BALB/c mice were immunized intranasally with Vehicle (PBS) and rIpaB-T2544 (40µg/mouse) on days 0, 14, and 28. (A) Time kinetics of antigen-specific total IgG in the mouse serum as measured by ELISA. Data represent mean ± SEM values from different mice samples (n=5). X-axis indicate the time points after the start of the immunization when samples were collected. Statistical significance between the titer values from rIpaB-T2544 and rT2544 vaccine recipients is shown. Statistical analysis was performed using two-way ANOVA and Tukey's post-test for multiple comparisons, ****P < 0.0001. The colour scheme used to mark different experimental groups are as follows: PBS-black; rT2544-green; rIpaB-red; rIpaB-T2544-blue. (B) Serum IgG isotypes measured by ELISA at day 38. Data represent mean ± SEM values from different mice samples (n=5). Statistical analysis was performed using two-tailed Student's t-test. ****P < 0.0001. (C) ELISA showing serum IgA and intestinal sIgA titers after immunization with different antigens. Mice were sacrificed on day 38 and samples were collected. Data represent mean ± SEM values from different mice samples (n=5). Statistical analysis was performed using two tailed Student's t-test. ****P < 0.0001. (D) Immunized mice were sacrificed on day 38 and splenocytes were isolated and cultured in the presence of antigen stimulation for 48 h. (i-ii), T cell cytokines were measured from the culture supernatants by ELISA. Data represent mean ± SEM values from different mice samples (n=4). Experiment was replicated three times, and data from a representative experiment are shown. Statistical analysis was performed using two tailed Student's t-test (*P < 0.05; ***P < 0.001; ****P < 0.0001).

Supplementary Figure legends

Supplementary Figure 1. Oral infection with 5×10^8 cfu doses of *S. flexneri 2a* increases body weight loss, and stool shedding. BALB/c mice were orally infected with 5×10^7 cfu and 5×10^8 cfu doses of *S. flexneri 2a.* (**A**) Body weight changes post-infection. Data represent mean ± SEM values of multiple animals (n = 12 for the lower dose group; n ≥ 6 for the higher dose group) at each time point. Statistical analyses were performed by two-way ANOVA,

****P < 0.0001. (**B**) Colony forming units (CFU) of *S. flexneri 2a* in the feces of infected mice. Fecal homogenates were cultured overnight on TSA plates. Data represent mean ± SEM of the values from multiple animals (n=6). Statistical analyses were performed by two-way ANOVA, *P < 0.05, **P < 0.01, ***P <0.001, ****P <0.0001. Statistical analyses were performed by student t-test (*P < 0.05, **P < 0.01, ***P <0.001).

Supplementary Figure 2. Survival assay. Kaplan-Meyer plot of cumulative mortality of infected mice. Streptomycin and iron pre-treated BALB/c mice (n=10) were infected with different doses of *Shigella* serovars and observed for 20 days. The colour scheme used to mark different experimental groups are as follows: uninfected-black; *Shigella flexeneri 2a*-green; *Shigella dysenteriae*-red; *Shigella sonnei*-blue.

Supplementary Figure 3. Histology sections of the colon and caecum tissue of uninfected and untreated BALB/c mice. Un treated (without strep+ without iron) + uninfected (without infection) mice (n=4) were sacrificed at 0h. Colon and caecum were excised, fixed, and embedded in paraffin. Tissue sections were stained with Hematoxylin & Eosin and observed in a microscope. Intact epithelial lining, intact crypt architecture with abundant records of goblet cells, intact mucosa and submucosa without abnormal infiltrates were observed in the group of mice. Yellow boxes represent the 20X (Scale bar =50 µm) and green boxes represent 40X (Scale bar =10 µm) magnification of the 10X (Scale bar =100 µm) image. Black round dotted circles represent intact crypt architecture, yellow arrow represents-abundant goblet cells.

Supplementary Figure 4. Histology sections of the colon tissue of BALB/c mice after different treatments. Different groups of mice (n=6 mice per group) were infected with 5×10^7 CFU *Shigella flexeneri 2a* and sacrificed at the indicated time points. Colon was excised, fixed, and embedded in paraffin. Tissue sections were stained with Hematoxylin & Eosin and observed in a microscope. Intact epithelial lining was observed in the control group of mice (i-iv, 20X magnification). Streptomycin-iron with infected group (v) showed degenerative changes in the epithelial lining (20X magnification), and submucosal swelling (edema) (10X magnification). Yellow boxes represent the 20X (Scale bar =50 µm)

magnification of the 10X (Scale bar =100 µm) image. Green boxes indicate the region selected for presentation in Figure 4 (colon). Double-headed black arrow indicates submucosal swelling (edema); single black arrow indicates the changes in the epithelial lining.

Supplementary Figure 5. Histology sections of the caecum tissue of BALB/c mice after different treatments. Different groups of mice (n=6 mice per group) were infected with 5×10^7 CFU *Shigella flexeneri 2a* and sacrificed at the indicated time points. Caecum was excised, fixed, and embedded in paraffin. Tissue sections were stained with Hematoxylin & Eosin and observed in a microscope. Intact epithelial lining was observed in the control group of mice (i-iv, 20X magnification). Streptomycin-iron with infected group (v) showed degenerative changes in the epithelial lining (20X magnification), and submucosal swelling (edema) (10X magnification). Yellow boxes represent the 20X (Scale bar =50 µm) magnification of the 10X (Scale bar =100 µm) image. Green boxes indicate the region selected for presentation in Figure 4 (caecum). Double-headed black arrow indicates submucosal swelling (edema); single black arrow indicates the changes in the epithelial lining.

Supplementary Figure 6. Histology sections of the colon tissue of BALB/c mice after infection. Mice (n=12) were pretreated with streptomycin and iron and infected with 5×10^7 CFU *Shigella flexeneri 2a.* Infected mice were sacrificed at the indicated time points. Colon was excised, fixed, and embedded in paraffin. (A) Tissue sections were stained with Hematoxylin & Eosin, observed in a microscope and (B) histological scores were blindly assessed. Streptomycin-iron with infected group showed degenerative changes in the epithelial lining (20X magnification), loss of crypt architecture with decreased goblet cells (40X magnification), increased infiltration of lymphocytes in the mucosa and submucosa (20X magnification), and submucosal swelling (edema) (10X magnification). Yellow boxes represent the 20X (Scale bar =50 µm) and green boxes represent 40X (Scale bar =10 µm) magnification of the 10X (Scale bar =100 µm) image. Black round dotted circles represent intact crypt architecture and blue round dotted circles represent loss of crypt architecture. Different colors of arrow indicate different parameters as follows; yellow arrow- abundant goblet cells; green arrow- loss of goblet cells; red arrow- lymphocyte infiltration in the

mucosa; blue arrow- lymphocyte infiltration in the submucosa; double headed black arrow- submucosal swelling (edema); single black arrow indicates the changes in the epithelial lining; white arrow-bacteria.

Supplementary Figure 7. Histology sections of the caecum tissue of BALB/c mice after infection. Mice (n=12) were pretreated with streptomycin and iron and infected with 5×10^7 CFU *Shigella flexeneri 2a.* Infected mice were sacrificed at the indicated time points. Caecum was excised, fixed, and embedded in paraffin. Tissue sections were stained with Hematoxylin & Eosin, observed in a microscope and (B) histological scores were blindly assessed. Streptomycin-iron with infected group showed degenerative changes in the epithelial lining (20X magnification), loss of crypt architecture with decreased goblet cells (40X magnification), increased infiltration of lymphocytes in the mucosa and submucosa (40X magnification), and submucosal swelling (edema) (10X magnification). Yellow boxes represent the 20X (Scale bar =50 µm) and green boxes represent 40X (Scale bar =10 µm) magnification of the 10X (Scale bar =100 µm) image. Black round dotted circles represent intact crypt architecture and blue round dotted circles represent loss of crypt architecture. Different colors of arrow indicate different parameters as follows; yellow arrow- abundant goblet cells; green arrow- loss of goblet cells; red arrow- lymphocyte infiltration in the mucosa; blue arrow- lymphocyte infiltration in the submucosa; double headed black arrow- submucosal swelling (edema); single black arrow indicates the changes in the epithelial lining; white arrow-bacteria.

Supplementary Figure 8. Histological scores of the colon and caecum tissue from BALB/c mice after infection. Mice (n=12) were pretreated with streptomycin and iron and infected with 5×10^7 CFU *Shigella flexeneri 2a.* Infected mice were sacrificed at the indicated time points. (A) Colon and (B) Caecum were excised, fixed, and embedded in paraffin. Tissue sections were stained with Hematoxylin & Eosin and histological scores were blindly assessed. The experiment was repeated three times and one representative data is shown. The scoring parameters were mentioned in the supplementary table 1 and supplementary table 2.

Supplementary Figure 9. Cloning and purification of rIpaB-T2544. (A) 1% Agarose gel electrophoresis of pET28a-*ipab-t2544* clone, after restriction digestion with BamHI, and

SacI, SalI and XhoI. Lane M1: 1 kb DNA ladder, M2: 100bp DNA ladder, 1: Undigested clone, 2: Restriction enzymes digested clone. (B) Sequencing of the rIpaB-T2544 clone using pET forward and reverse primers. *A,* The FASTA file format of the sequences is provided. Yellow and green colors code for the recognition sites of the restriction enzyme BamHI and linker sequence (GS linker), respectively, whereas the blue color codes for the open reading frame (ORF) of IpaB. *B,* Yellow, sky, and red colors code for the recognition sites of the restriction enzymes XhoI, SalI and SacI. The green color codes for the linker sequence (GP linker), whereas the magenta color code for the open reading frame (ORF) of t2544 and the blue color code for the open reading frame (ORF) of IpaB. (C) 12% SDS–PAGE of recombinant purified proteins (5µg of each). Molecular mass markers (kDa) are on the left. (D) Western blot probed with anti-His antibody after resolving the recombinant purified proteins (rT2544, 5 µg, rIpaB, 7 µg, rIpaB-T2544, 3 µg) in 12% SDS-PAGE. Molecular mass markers (kDa) are on the left. The experiment was repeated three times and a representative blot is shown here. (E) Far-UV circular dichroism spectra of protein samples (180 µg/ml) captured at the wavelength range of 200 to 350 nm at 25°C in PBS (pH 7.4) on the Jasco-1500 spectrophotometer. Data presented as ellipticity (CD [mdeg]) after subtracting the baseline values. Different lines are describesd as follows; upper line- rT2544, middle line-rIpaB and lower line- rIpaB-T2544. Experiment was replicated three times, and data from a representative experiment are shown.

Supplementary Figure 10. Histology sections of colon and caecum of immunized and unimmunized BALB/c mice after infection. BALB/c mice (n=10) were immunized intranasally with Vehicle (PBS) and rIpaB (40µg/mouse) on days 0, 14, and 28. Ten days after the last immunization (38d), immunized mice were pre-treated with streptomycin and iron followed by oral infection with 5×10^7 CFU bacteria. Mice were sacrificed at the indicated time points. Colon and caecum were excised, fixed, embedded in paraffin, and tissue sections were stained with Hematoxylin & Eosin. Intact epithelial lining was observed in the control group of mice (i-iv, 20X magnification). Streptomycin-iron with infected group (v) showed degenerative changes in the epithelial lining (20X magnification), and submucosal swelling (edema) (10X magnification). Yellow boxes represent the 20X (Scale bar =50 µm) magnification of the 10X (Scale bar =100 µm) image. Green boxes indicate the region selected for presentation in Figure 8. Double-headed black arrow indicates submucosal swelling (edema); single black arrow indicates the changes in the epithelial lining.

Figure 1

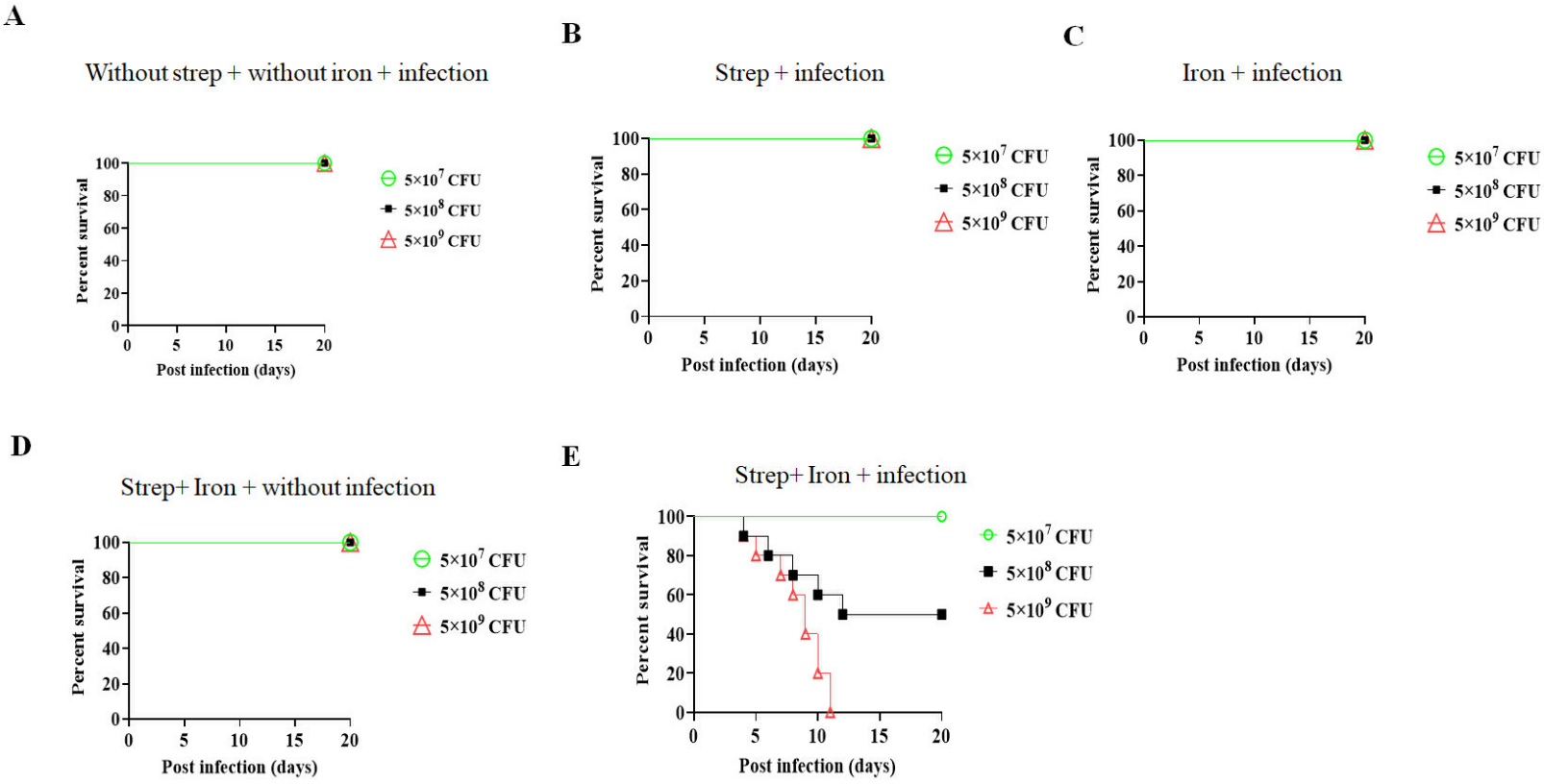
A
Without strep + without iron + infection
Percent survival
Post infection (days)
5×10^7 CFU
5×10^8 CFU
5×10^9 CFU
B
Strep + infection
C
Iron + infection
D
Strep+ Iron + without infection
E
Strep+ Iron + infection

Figure 2

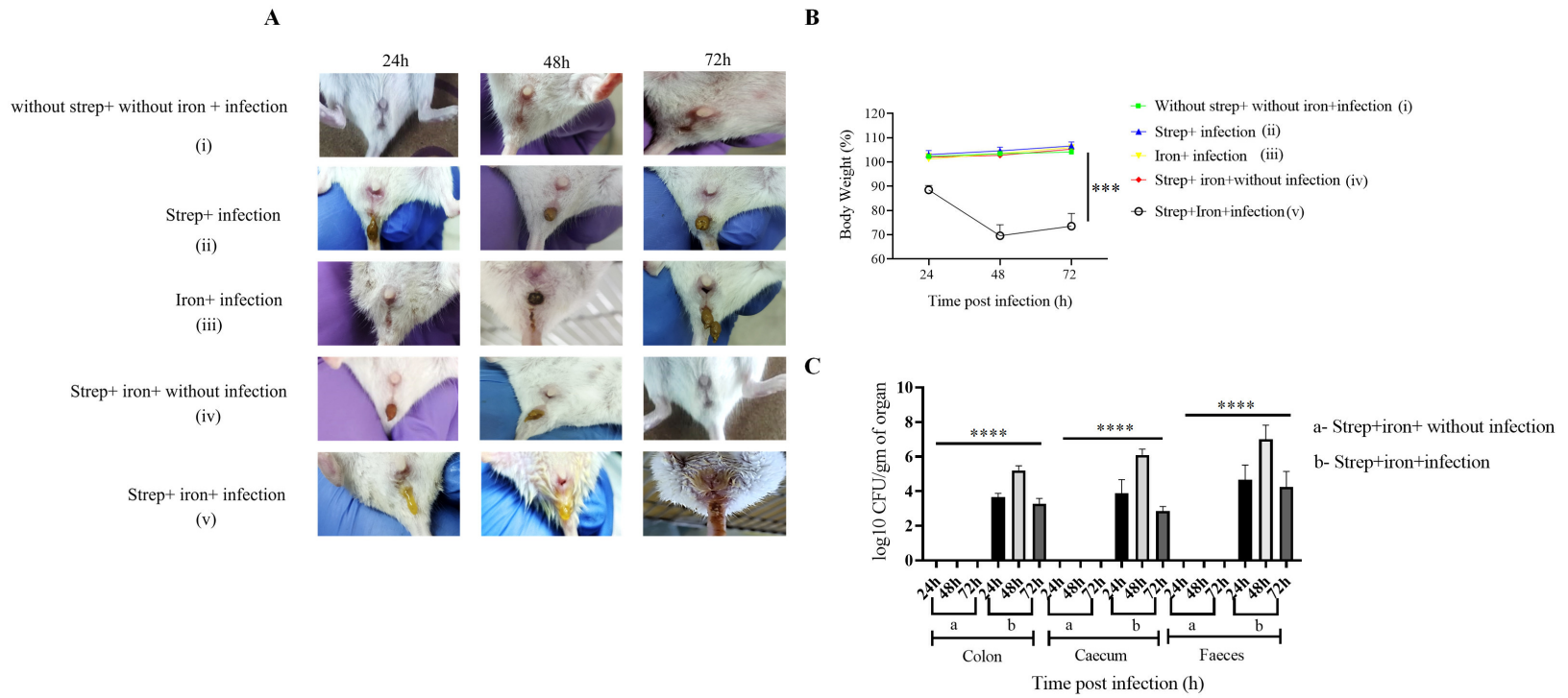
A
24h
48h
72h
without strep+ without iron + infection
(i)
Strep+ infection
(ii)
Iron+ infection
(iii)
Strep+ iron+ without infection
(iv)
Strep+ iron+ infection
(v)
B
Body Weight (%)
120
110
100
90
80
70
60
24
48
72
Time post infection (h)
***
Without strep+ without iron+infection (i)
Strep+ infection (ii)
Iron+ infection (iii)
Strep+ iron+without infection (iv)
Strep+Iron+infection(v)
C
log10 CFU/gm of organ
10
8
6
4
2
0
****
****
****
24h
48h
72h
a
b
Colon
Caecum
Faeces
Time post infection (h)
a- Strep+iron+ without infection
b- Strep+iron+infection

Figure 3

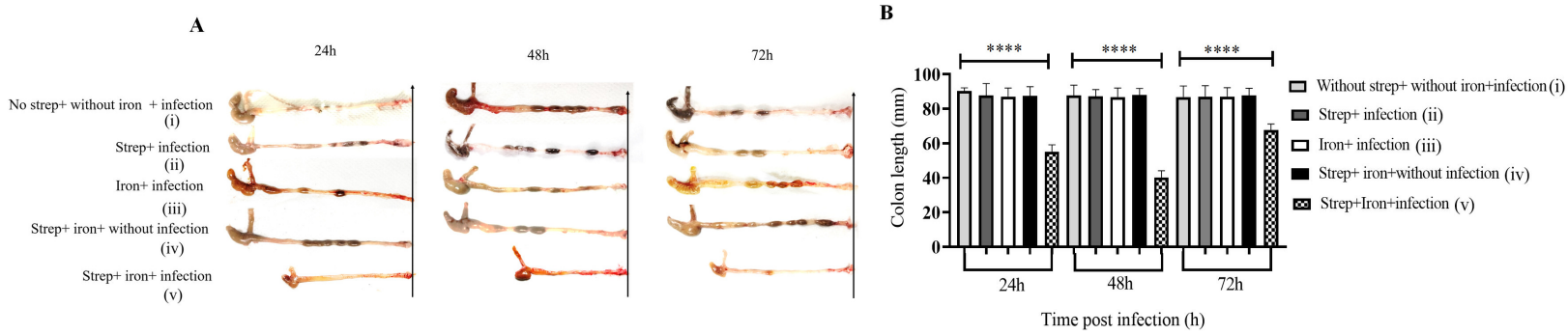
A
24h
48h
72h
No strep+ without iron + infection (i)
Strep+ infection (ii)
Iron+ infection (iii)
Strep+ iron+ without infection (iv)
Strep+ iron+ infection (v)
B
****
****
****
Colon length (mm)
100
80
60
40
20
0
24h
48h
72h
Time post infection (h)
Without strep+ without iron+infection (i)
Strep+ infection (ii)
Iron+ infection (iii)
Strep+ iron+without infection (iv)
Strep+Iron+infection (v)

Figure 4

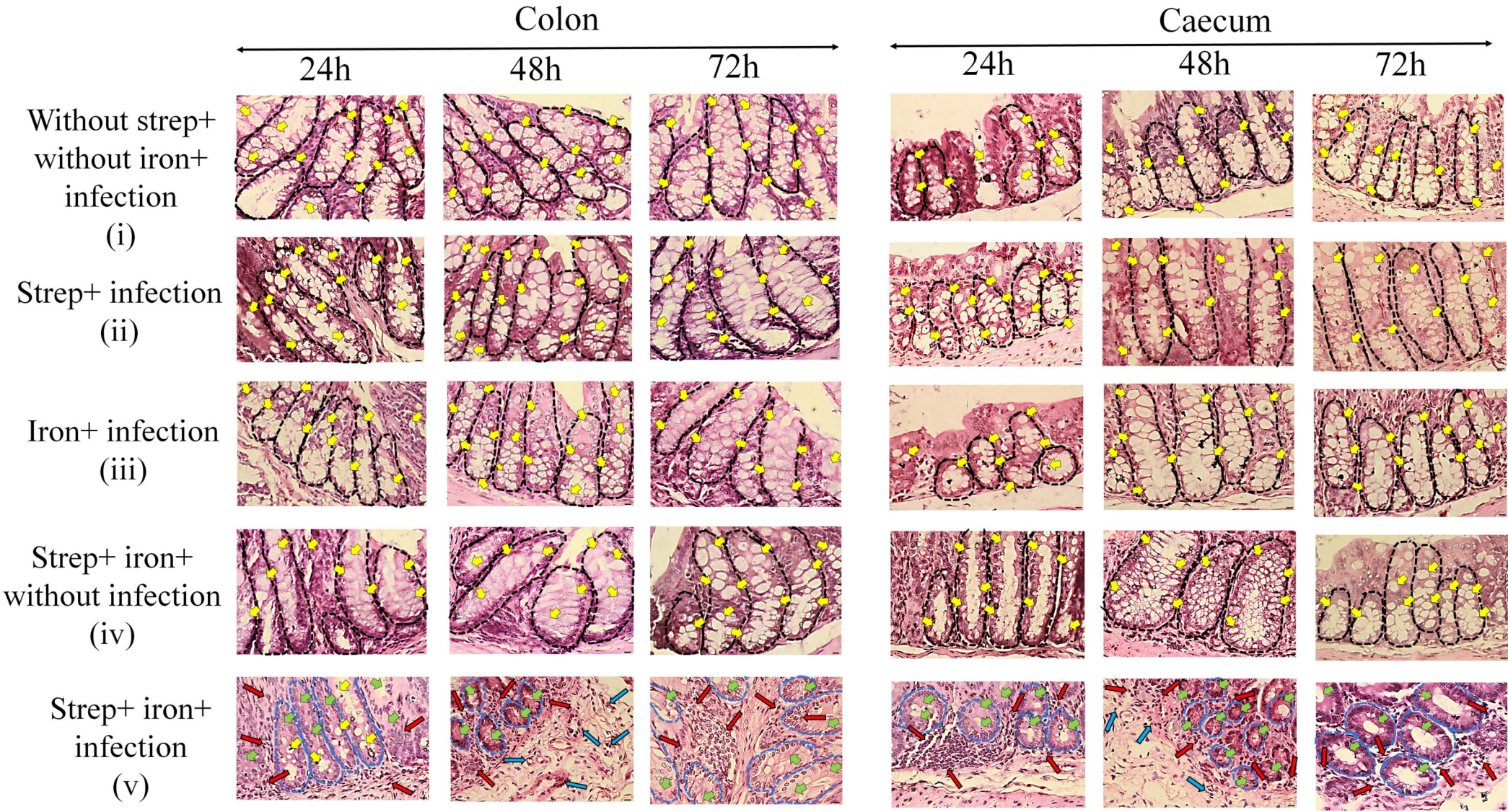
Colon
Caecum
24h
48h
72h
24h
48h
72h
Without strep+ without iron+ infection (i)
Strep+ infection (ii)
Iron+ infection (iii)
Strep+ iron+ without infection (iv)
Strep+ iron+ infection (v)

Figure 5

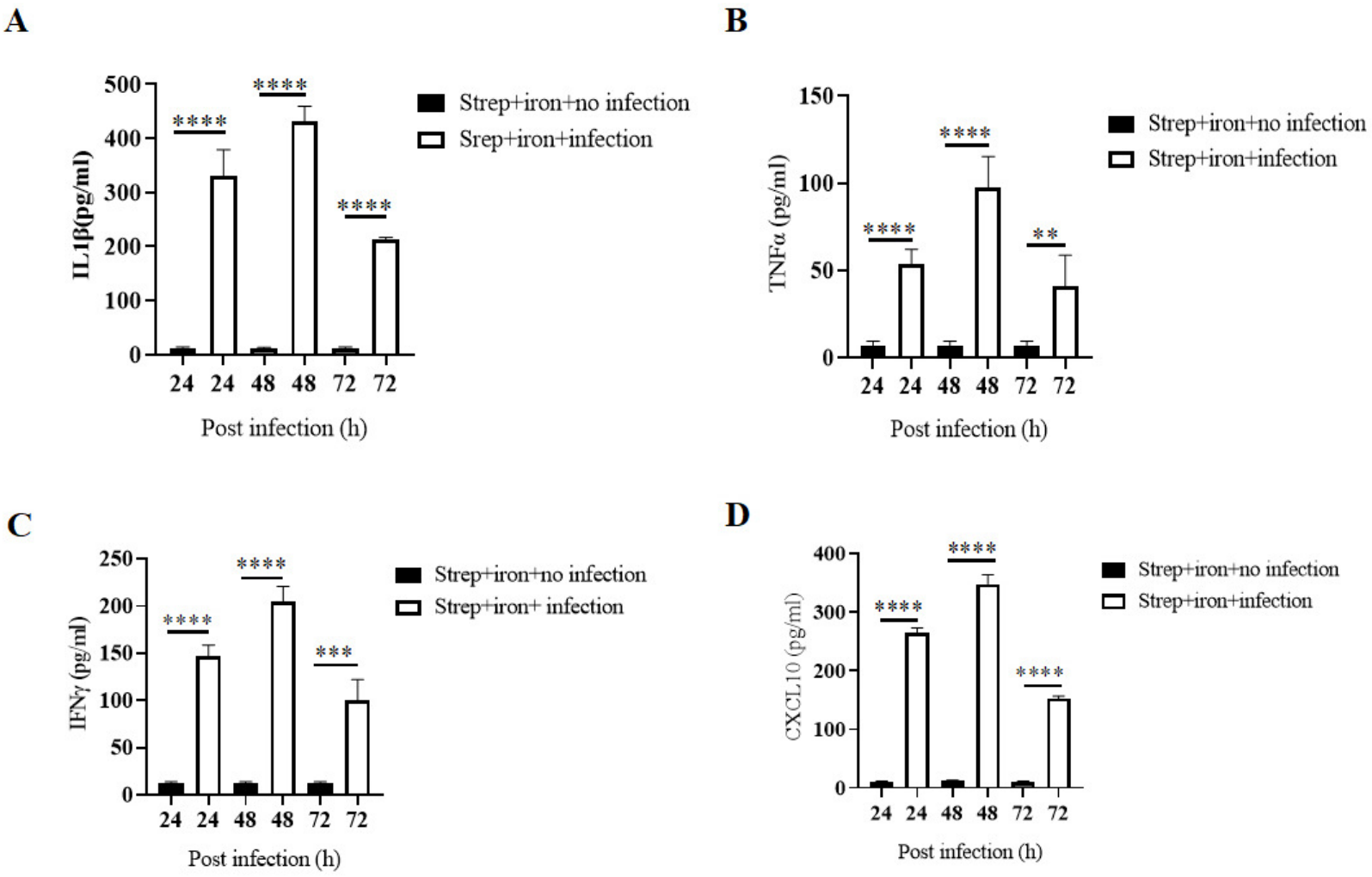
A
IL1β(pg/ml)
500
400
300
200
100
0
****
****
****
Strep+iron+no infection
Srep+iron+infection
24 24 48 48 72 72
Post infection (h)
B
TNFα (pg/ml)
150
100
50
0
****
****
**
Strep+iron+no infection
Strep+iron+infection
24 24 48 48 72 72
Post infection (h)
C
IFNγ (pg/ml)
250
200
150
100
50
0
****
****
***
Strep+iron+no infection
Strep+iron+ infection
24 24 48 48 72 72
Post infection (h)
D
CXCL10 (pg/ml)
400
300
200
100
0
****
****
****
Strep+iron+no infection
Strep+iron+infection
24 24 48 48 72 72
Post infection (h)

Figure 6

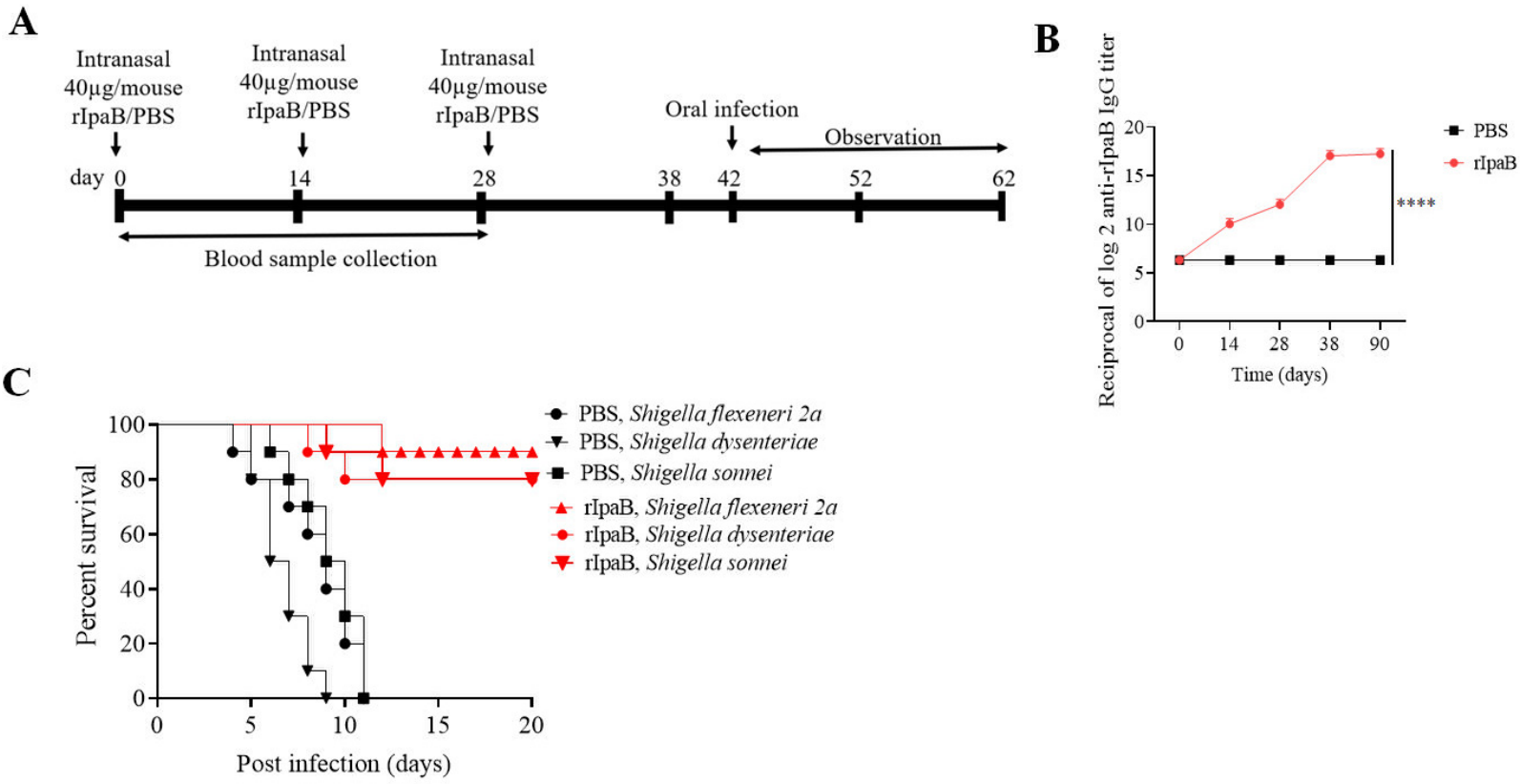
A
Intranasal
40μg/mouse
rIpaB/PBS
Intranasal
40μg/mouse
rIpaB/PBS
Intranasal
40μg/mouse
rIpaB/PBS
Oral infection
Observation
day 0
14
28
38
42
52
62
Blood sample collection
B
Reciprocal of log 2 anti-rIpaB IgG titer
20
15
10
5
0
****
PBS
rIpaB
0
14
28
38
90
Time (days)
C
Percent survival
100
80
60
40
20
0
0
5
10
15
20
Post infection (days)
PBS, Shigella flexeneri 2a
PBS, Shigella dysenteriae
PBS, Shigella sonnei
rIpaB, Shigella flexeneri 2a
rIpaB, Shigella dysenteriae
rIpaB, Shigella sonnei

Revised Figure 7

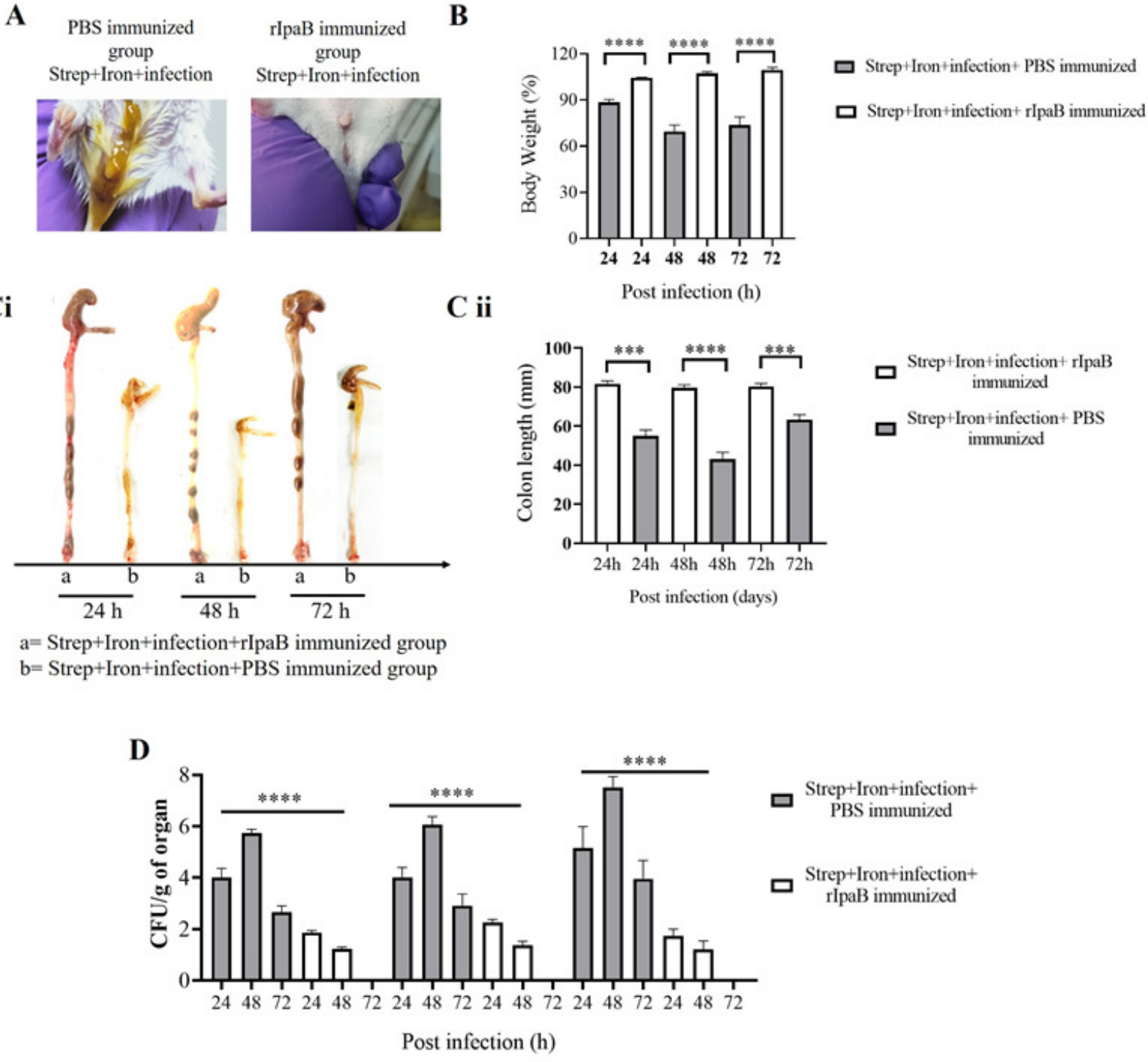

Figure 8

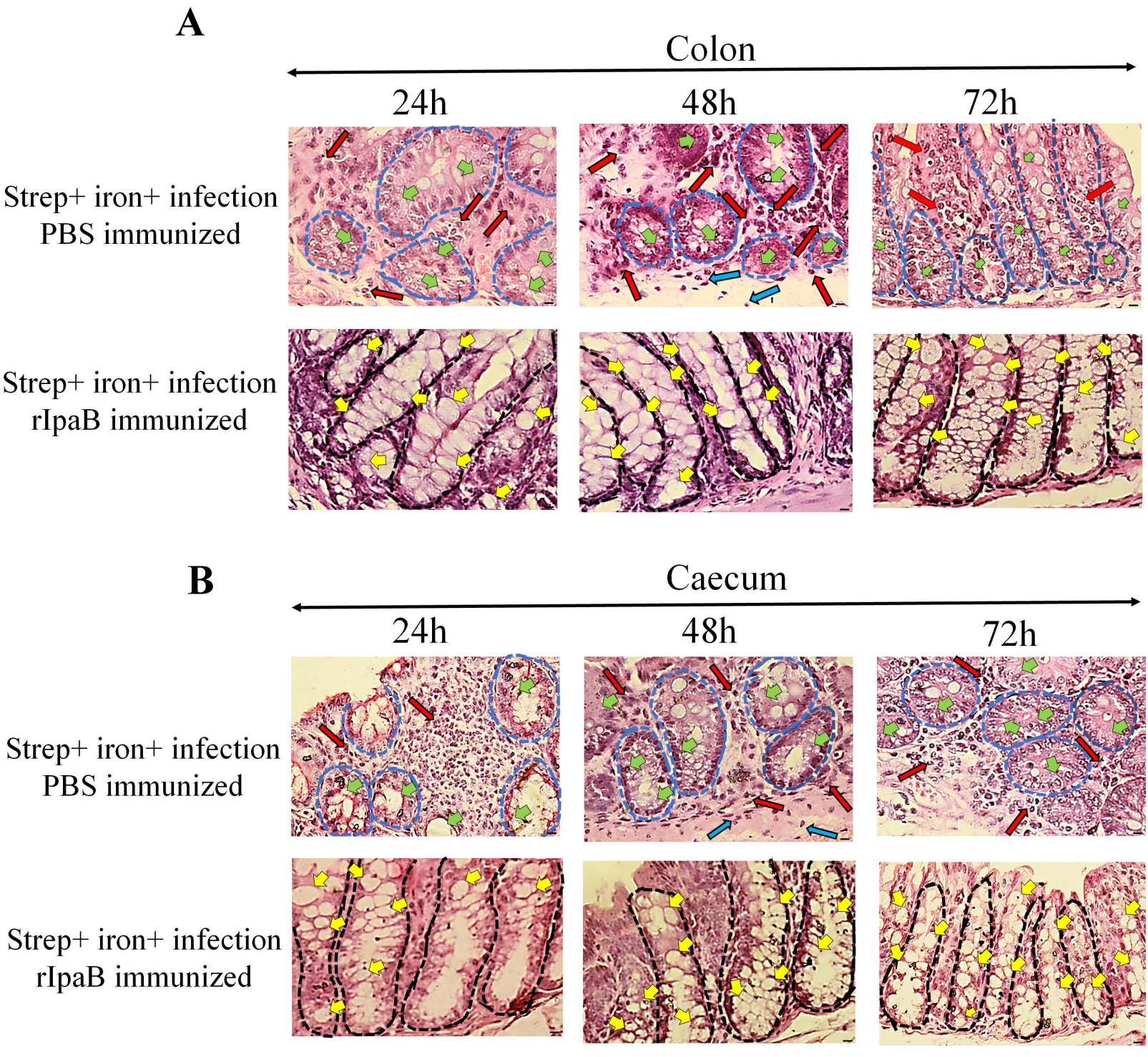
A
Colon
24h
48h
72h
Strep+ iron+ infection
PBS immunized
Strep+ iron+ infection
rIpaB immunized
B
Caecum
24h
48h
72h
Strep+ iron+ infection
PBS immunized
Strep+ iron+ infection
rIpaB immunized

Figure 9

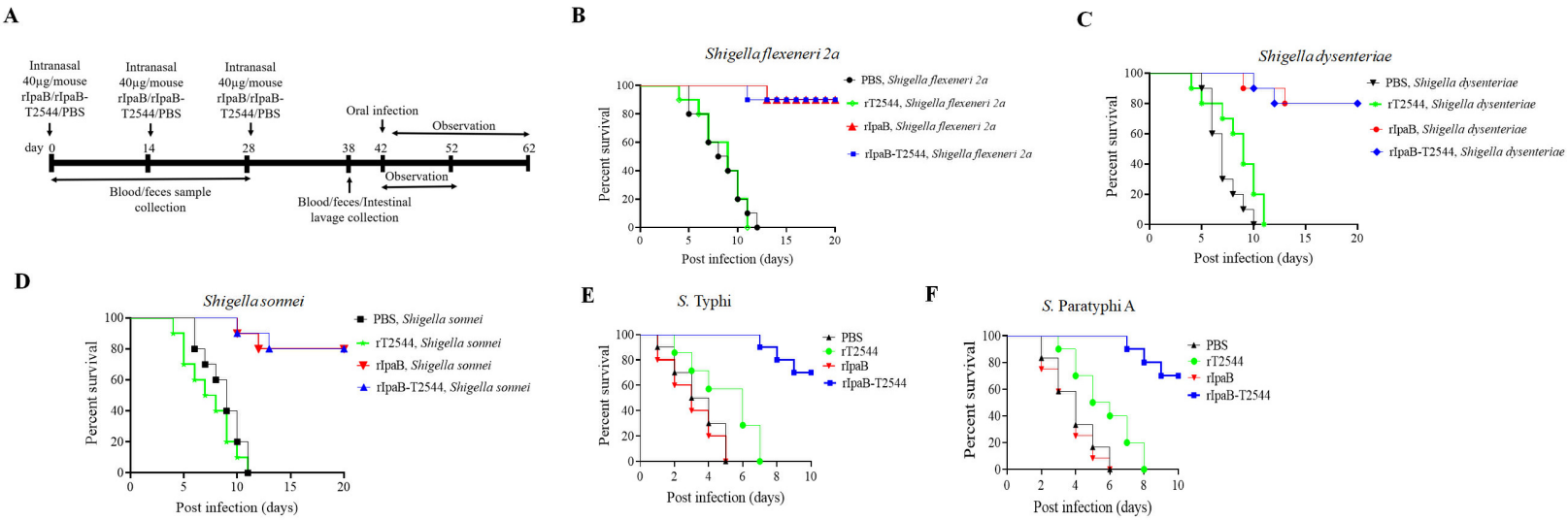
A
Intranasal 40μg/mouse rIpaB/rIpaB-T2544/PBS
Intranasal 40μg/mouse rIpaB/rIpaB-T2544/PBS
Intranasal 40μg/mouse rIpaB/rIpaB-T2544/PBS
Oral infection
Observation
day 0 14 28 38 42 52 62
Observation
Blood/feces sample collection
Blood/feces/Intestinal lavage collection
B
Shigella flexeneri 2a
PBS, Shigella flexeneri 2a
rT2544, Shigella flexeneri 2a
rIpaB, Shigella flexeneri 2a
rIpaB-T2544, Shigella flexeneri 2a
Percent survival
Post infection (days)
C
Shigella dysenteriae
PBS, Shigella dysenteriae
rT2544, Shigella dysenteriae
rIpaB, Shigella dysenteriae
rIpaB-T2544, Shigella dysenteriae
Percent survival
Post infection (days)
D
Shigella sonnei
PBS, Shigella sonnei
rT2544, Shigella sonnei
rIpaB, Shigella sonnei
rIpaB-T2544, Shigella sonnei
Percent survival
Post infection (days)
E
S. Typhi
PBS
rT2544
rIpaB
rIpaB-T2544
Percent survival
Post infection (days)
F
S. Paratyphi A
PBS
rT2544
rIpaB
rIpaB-T2544
Percent survival
Post infection (days)

Figure 10

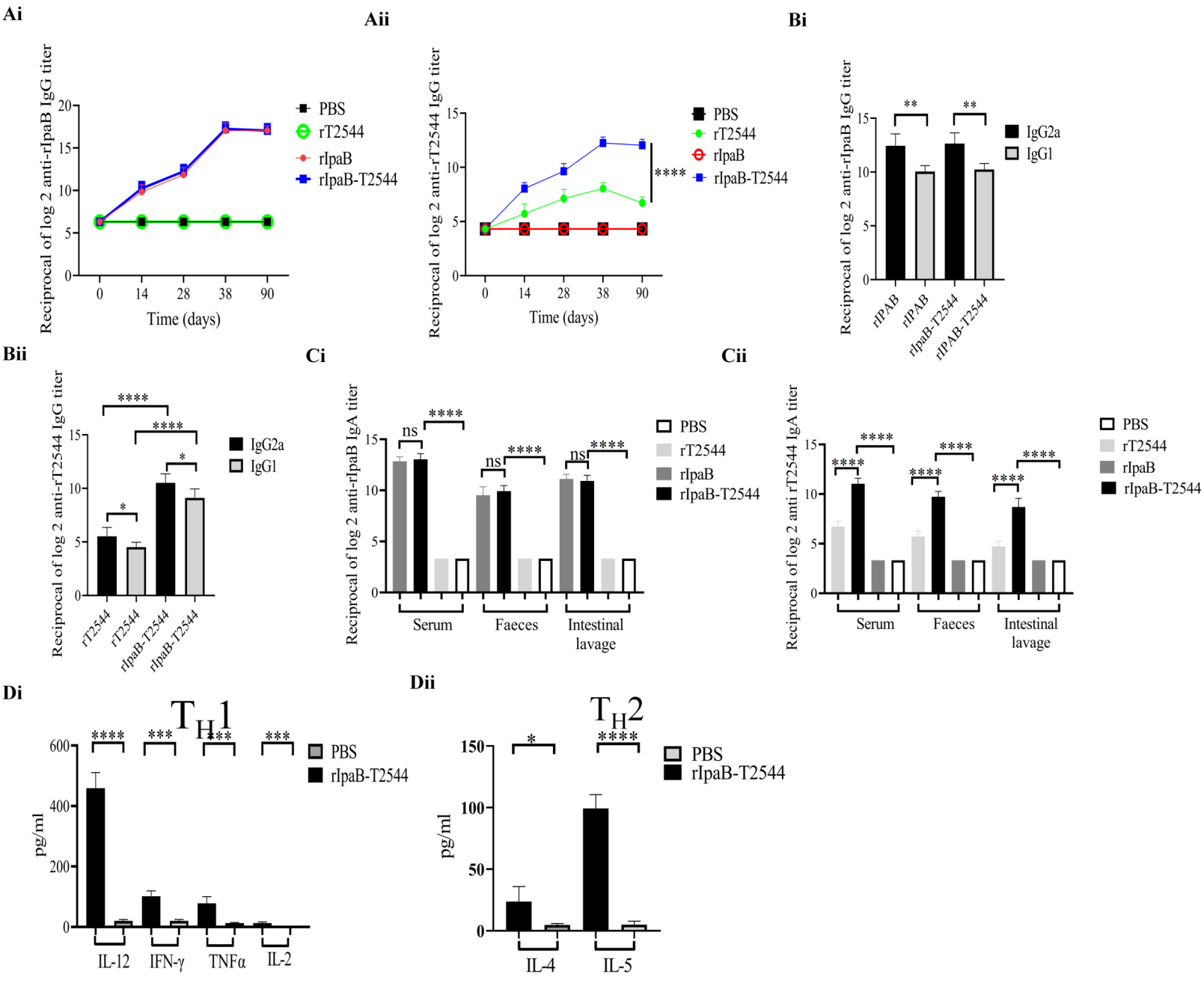
Ai
Reciprocal of log 2 anti-rIpaB IgG titer
Time (days)
PBS
rT2544
rIpaB
rIpaB-T2544
Aii
Reciprocal of log 2 anti-rT2544 IgG titer
Time (days)
****
Bi
Reciprocal of log 2 anti-rIpaB IgG titer
IgG2a
IgG1
rIPAB
rIpaB-T2544
Bii
Reciprocal of log 2 anti-rT2544 IgG titer
rT2544
Ci
Reciprocal of log 2 anti-rIpaB IgA titer
ns
Serum
Faeces
Intestinal lavage
Cii
Reciprocal of log 2 anti rT2544 IgA titer
Di
TH1
pg/ml
IL-12
IFN-γ
TNFα
IL-2
Dii
TH2
IL-4
IL-5